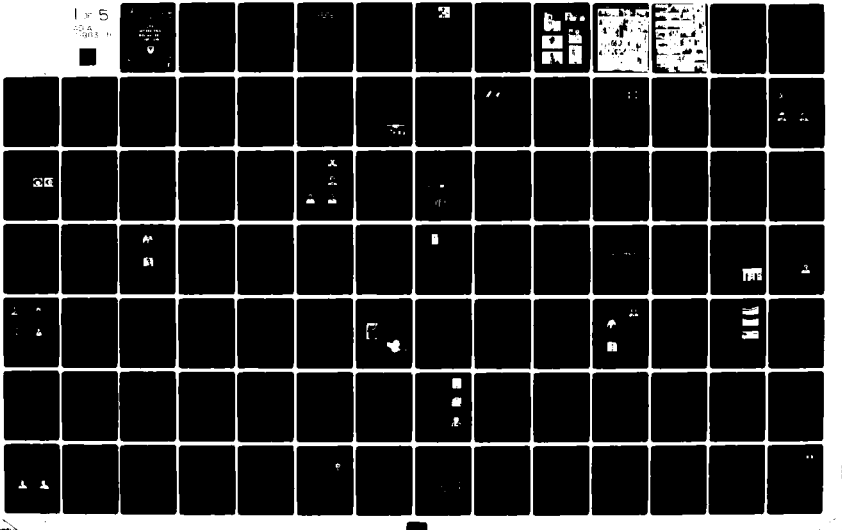
AD-A096 308 ARMY COMMUNICATIONS RESEARCH AND DEVELOPMENT COMMAND --ETC F/G 9/1
PROCEEDINGS OF THE INTERNATIONAL WIRE AND CABLE SYMPOSIUM (29TH--ETC(U)
NOV 80 E F GODWIN

UNCLASSIFIED

NL



LEVEL II

(12)

AD A096308

# PROCEEDINGS of the 29th. INTERNATIONAL WIRE and CABLE SYMPOSIUM

**NOVEMBER 18-20 1980**




This document has been approved for public release and sale; its distribution is unlimited.

**SPONSORED BY THE**

**U S Army Communications Research and Development Command**

**Fort Monmouth, New Jersey**

81 3 13 104

SECURITY CLASSIFICATION OF THIS PAGE (When Data Entered)

## REPORT DOCUMENTATION PAGE

READ INSTRUCTIONS BEFORE COMPLETING FORM

| | |
|---|---|
| 1. REPORT NUMBER: N/A | 2. GOVT ACCESSION NO.: AD-A096308 |
| 3. RECIPIENT'S CATALOG NUMBER: (12) 4776 | |
| 4. TITLE (and Subtitle): (6) Proceedings of the ~~25th~~ International Wire and Cable Symposium 1980 (29th) Held at Cherry Hill New Jersey on November 18, 19 and 20, 1980 | 5. TYPE OF REPORT & PERIOD COVERED: Final - November |
| | 6. PERFORMING ORG. REPORT NUMBER: N/A |
| 7. AUTHOR(S): Various; Director: (10) Elmer F. Godwin | 8. CONTRACT OR GRANT NUMBER(s): None (16) |
| 9. PERFORMING ORGANIZATION NAME AND ADDRESS: Fiber Optic Team (DRDCO-COM-RM-1), Multichannel Transmission Division, CENCOMS, CORADCOM, Ft Monmouth 07703 | 10. PROGRAM ELEMENT, PROJECT, TASK AREA & WORK UNIT NUMBERS: Proj. # 1LI 627Ø1 AH92; AMC Code 612701.H92.MA.11.21 |
| 11. CONTROLLING OFFICE NAME AND ADDRESS: Fiber Optic Team (DRDCO-COM-RM-1), Multichannel Transmission Division, CENCOMS, CORADCOM, Ft Monmouth, NJ 07703 (11) | 12. REPORT DATE: November 1980; 13. NUMBER OF PAGES: 456 |
| 14. MONITORING AGENCY NAME & ADDRESS (if different from Controlling Office): Same as 11 above. (9) Final rept. | 15. SECURITY CLASS. (of this report): UNCLASSIFIED; 15a. DECLASSIFICATION/DOWNGRADING SCHEDULE |

16. DISTRIBUTION STATEMENT (of this Report)

APPROVED FOR PUBLIC RELEASE: DISTRIBUTION UNLIMITED.

17. DISTRIBUTION STATEMENT (of the abstract entered in Block 20, if different from Report)

18. SUPPLEMENTARY NOTES

Proceedings of technical papers presented at 29th International Wire and Cable Symposium sponsored annually by US Army Communications Research and Development Command (CORADCOM).

19. KEY WORDS (Continue on reverse side if necessary and identify by block number)

Aerospace electronics, cable design, cable evaluation, cable manufacture, cable materials, cable performance, cable testing, electronic wiring, fiber optics, interconnections, military electronics, telephone communications, wire insulation, wire materials, wire testing.

20. ABSTRACT (Continue on reverse side if necessary and identify by block number)

The International Wire and Cable Symposium is the only symposium of its kind in the world. The proceedings include papers in the field of electrical and electronic wire and cable, materials, testing, evaluation, connections, splicing, installation, applications, fire retardancy, fiber optics, manufacturing, processing, wire/cable design and manufacturing.

DD FORM 1 JAN 73 1473 EDITION OF 1 NOV 65 IS OBSOLETE

UNCLASSIFIED 410 489

SECURITY CLASSIFICATION OF THIS PAGE (When Data Entered)

## INSTRUCTIONS FOR PREPARATION OF REPORT DOCUMENTATION PAGE

RESPONSIBILITY. The controlling DoD office will be responsible for completion of the Report Documentation Page, DD Form 1473, in all technical reports prepared by or for DoD organizations.

CLASSIFICATION. Since this Report Documentation Page, DD Form 1473, is used in preparing announcements, bibliographies, and data banks, it should be unclassified if possible. If a classification is required, identify the classified items on the page by the appropriate symbol.

### COMPLETION GUIDE

General. Make Blocks 1, 4, 5, 6, 7, 11, 13, 15, and 16 agree with the corresponding information on the report cover. Leave Blocks 2 and 3 blank.

Block 1. Report Number. Enter the unique alphanumeric report number shown on the cover.

Block 2. Government Accession No. Leave Blank. This space is for use by the Defense Documentation Center.

Block 3. Recipient's Catalog Number. Leave blank. This space is for the use of the report recipient to assist in future retrieval of the document.

Block 4. Title and Subtitle. Enter the title in all capital letters exactly as it appears on the publication. Titles should be unclassified whenever possible. Write out the English equivalent for Greek letters and mathematical symbols in the title *(see "Abstracting Scientific and Technical Reports of Defense-sponsored RDT/E," AD-667 000)*. If the report has a subtitle, this subtitle should follow the main title, be separated by a comma or semicolon if appropriate, and be initially capitalized. If a publication has a title in a foreign language, translate the title into English and follow the English translation with the title in the original language. Make every effort to simplify the title before publication.

Block 5. Type of Report and Period Covered. Indicate here whether report is interim, final, etc., and, if applicable, inclusive dates of period covered, such as the life of a contract covered in a final contractor report.

Block 6. Performing Organization Report Number. Only numbers other than the official report number shown in Block 1, such as series numbers for in-house reports or a contractor/grantee number assigned by him, will be placed in this space. If no such numbers are used, leave this space blank.

Block 7. Author(s). Include corresponding information from the report cover. Give the name(s) of the author(s) in conventional order *(for example, John R. Doe or, if author prefers, J. Robert Doe)*. In addition, list the affiliation of an author if it differs from that of the performing organization.

Block 8. Contract or Grant Number(s). For a contractor or grantee report, enter the complete contract or grant number(s) under which the work reported was accomplished. Leave blank in in-house reports.

Block 9. Performing Organization Name and Address. For in-house reports enter the name and address, including office symbol, of the performing activity. For contractor or grantee reports enter the name and address of the contractor or grantee who prepared the report and identify the appropriate corporate division, school, laboratory, etc., of the author. List city, state, and ZIP Code.

Block 10. Program Element, Project, Task Area, and Work Unit Numbers. Enter here the number code from the applicable Department of Defense form, such as the DD Form 1498, "Research and Technology Work Unit Summary" or the DD Form 1634, "Research and Development Planning Summary," which identifies the program element, project, task area, and work unit or equivalent under which the work was authorized.

Block 11. Controlling Office Name and Address. Enter the full, official name and address, including office symbol, of the controlling office. *(Equates to funding/sponsoring agency. For definition see DoD Directive 5200.20, "Distribution Statements on Technical Documents.")*

Block 12. Report Date. Enter here the day, month, and year or month and year as shown on the cover.

Block 13. Number of Pages. Enter the total number of pages.

Block 14. Monitoring Agency Name and Address *(if different from Controlling Office)*. For use when the controlling or funding office does not directly administer a project, contract, or grant, but delegates the administrative responsibility to another organization.

Blocks 15 & 15a. Security Classification of the Report: Declassification/Downgrading Schedule of the Report. Enter in 15 the highest classification of the report. If appropriate, enter in 15a the declassification/downgrading schedule of the report, using the abbreviations for declassification/downgrading schedules listed in paragraph 4-207 of DoD 5200.1-R.

Block 16. Distribution Statement of the Report. Insert here the applicable distribution statement of the report from DoD Directive 5200.20, "Distribution Statements on Technical Documents."

Block 17. Distribution Statement *(of the abstract entered in Block 20, if different from the distribution statement of the report)*. Insert here the applicable distribution statement of the abstract from DoD Directive 5200.20, "Distribution Statements on Technical Documents."

Block 18. Supplementary Notes. Enter information not included elsewhere but useful, such as: Prepared in cooperation with . . . Translation of *(or by)* . . . Presented at conference of . . . To be published in . . .

Block 19. Key Words. Select terms or short phrases that identify the principal subjects covered in the report, and are sufficiently specific and precise to be used as index entries for cataloging, conforming to standard terminology. The DoD "Thesaurus of Engineering and Scientific Terms" *(TEST)*, AD-672 000, can be helpful.

Block 20. Abstract. The abstract should be a brief *(not to exceed 200 words)* factual summary of the most significant information contained in the report. If possible, the abstract of a classified report should be unclassified and the abstract to an unclassified report should consist of publicly- releasable information. If the report contains a significant bibliography or literature survey, mention it here. For information on preparing abstracts see "Abstracting Scientific and Technical Reports of Defense-Sponsored RDT&E," AD-667 000.

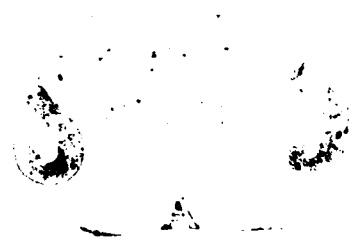
★ U.S. GPO: 1974—540-847/9052

# PROCEEDINGS OF 29TH INTERNATIONAL WIRE AND CABLE SYMPOSIUM

Sponsored by
US Army Communications Research and Development Command
(CORADCOM) Fort Monmouth, N.J.

Cherry Hill, New Jersey
November 18, 19 and 20, 1980

APPROVED FOR PUBLIC RELEASE: DISTRIBUTION UNLIMITED



# 29th INTERNATIONAL WIRE AND CABLE SYMPOSIUM

## SYMPOSIUM COMMITTEE

Elmer F. Godwin, Director, GEF Associates - (201)741-8864
Winnie Conti, Secretary, USA CORADCOM - (201)544-2770
Adolf Asam, ITT Electro-Optical Products Division
Ken Bow, Dow Chemical USA
John Brazee, Continental Telephone Service Corporation
Leo M. Chattler, DCM International Corporation
Michael DeLucia, David W. Taylor Naval Ship R&D Center
Marta Farago, Northern Telecom Ltd.
Irving Kolodny, General Cable Company
William Korcz, Shell Development Company
Joseph McCann, USA CORADCOM
Frank Short, Belden Corporation
George Webster, Bell Laboratories

### ADVISORY

Joe Neigh, AMP, Inc.

### TECHNICAL SESSIONS

**Tuesday, 18 November 1980**

| | |
|---|---|
| 9:30 a.m. Session I | Tutorial - Outlook For Voluntary Standards In U.S.A. |
| 2:00 p.m. Session II | Cable Design I |
| 2:00 p.m. Session III | Material |

**Wednesday, 19 November 1980**

| | |
|---|---|
| 9:00 a.m. Session IV | Cable Design II |
| 9:00 a.m. Session V | Connectors |
| 2:00 p.m. Session VI | Fiber Optics I |
| 2:00 p.m. Session VII | Fire Considerations |

**Thursday, 20 November 1980**

| | |
|---|---|
| 9:00 a.m. Session VIII | Fiber Optics II |
| 9:00 a.m. Session IX | Testing |
| 2:00 p.m. Session X | Fiber Optics III |
| 2:00 p.m. Session XI | Cable Applications |

PAPERS

Responsibility for the contents rests upon the authors and not the symposium committee or its members. After the symposium, all the publication rights of each paper are reserved by their authors, and requests for republication of a paper should be addressed to the appropriate author. Abstracting is permitted, and it would be appreciated if the symposium is credited when abstracts or papers are republished. Requests for individual copies of papers should be addressed to the authors.



Accession For
NTIS GRA&I
DTIC TAB
Unannounced
Justification
By
Distribution/
Availability Codes
Dist | Avail and/or Special
A

## MESSAGE FROM THE DIRECTOR

On behalf of CORADCOM and the symposium committee, welcome to the 29th Annual International Wire and Cable Symposium (IWCS). It is indeed gratifying to report that the symposium continues to attract world-wide attention from scientists, consultants, manufacturers, material suppliers and end product users of cables/wires. Many favorable comments were received on the technical contents and timely relevance of the papers presented during last year's symposium. Last year's attendance of 1583 included representatives from 404 U.S. companies, 30 foreign countries and 10 U.S. government agencies.

This year, the committee is also looking forward to a very exciting and enthusiastic meeting with many excellent papers scheduled for presentation. The technical program will begin with a tutorial session, entitled "Outlook For Voluntary Standards in U.S.A.", followed by ten individual sessions. The three sessions on fiber optics should be of special interest since twelve of the eighteen papers will contrast various developments and applications of fiber optics in seven foreign countries.

Committee members, Adolf Asam, ITT Electro Optical Products Division, Ken Bow, Dow Chemical U.S.A., Marta Farago, Northern Telecom Ltd., Irv Kolodny, General Cable Company, and Frank Short, Beldon Corporation, are retiring from the committee. Each member was extremely dedicated and contributed significantly to the success of the committee's objectives. On behalf of the committee, I wish to thank each one for their valuable contributions and wish them success in their future activities.

The committee recognizes the inconveniences encountered and concern expressed by many attendees with respect to the number of hotels/motels used for housing accommodations and their location or distance from the Hyatt. However, before another location can be selected, it must be approved by CORADCOM, the symposium sponsor. CORADCOM has stipulated that any location selected for the symposium must be within a reasonable distance of Fort Monmouth, preferably less than 100 miles, which limits the number of facilities with adequate accommodations.

The symposium cannot prosper without the sustained participation and attendance of representatives of the various industrial organizations and government activities. Therefore, the committee solicits the continued support of all members of the wire and cable industry. Again, I wish to express my appreciation to each committee member for their support, dedicated effort and cooperation. A very special thanks to Ms. Conti for her sincere dedication to the symposium objectives, her support and cooperation.

Elmer F. Godwin

ELMER F. GODWIN
Director, IWCS

# PROCEEDINGS

# INTERNATIONAL WIRE & CABLE SYMPOSIUM

# BOUND—AVAILABLE AT CORADCOM

23rd International Wire & Cable Symposium Proceedings — 1974 — 7.00
24th International Wire & Cable Symposium Proceedings — 1975 — 7.00
25th International Wire & Cable Symposium Proceedings — Not Available
26th International Wire & Cable Symposium Proceedings — Not Available
27th International Wire & Cable Symposium Proceedings — 1978 — 8.00
28th International Wire & Cable Symposium Proceedings — 1979 — 8.00
*29th International Wire & Cable Symposium Proceedings — 1980 — $10.00
*Extra Copies 1-3 $10.00; next 4-10 $8.00; next 11 and above $5.00 each

Make check or bank draft PAYABLE in US dollars to the INTERNATIONAL WIRE & CABLE SYMPOSIUM and forward request to:

International Wire & Cable Symposium
US Army Communications R&D Command
ATTN: DRDCO-COM-RM-1 (W. Conti)
Fort Monmouth, NJ 07703
USA

## PHOTOCOPIES—AVAILABLE AT DEPARTMENT OF COMMERCE

Photocopies are available for complete sets of papers for 1964 and 1966 thru 1979 Information on prices and shipping charges should be requested from the:

US Department of Commerce
National Technical Information Service
Springfield, Virginia 22151
USA

Include Title, Year and "AD" Number

13th Annual Wire & Cable Symposium (1964) — AD 787164
15th Annual Wire & Cable Sumposium (1966) — AD A006601
16th International Wire & Cable Symposium (1967) — AD 787165
17th International Wire & Cable Symposium (1968) — AD 787166
18th International Wire & Cable Symposium (1969) — AD 787167
19th International Wire & Cable Symposium Proceedings 1970 — AD 714985
20th International Wire & Cable Symposium Proceedings 1971 — AD 733399
21st International Wire & Cable Symposium Proceedings 1972 — AD 752908
22nd International Wire & Cable Symposium Proceedings 1973 — AD 772914
23rd International Wire & Cable Symposium Proceedings 1974 — AD A003251
24th International Wire & Cable Symposium Proceedings 1975 — AD A017787
25th International Wire & Cable Symposium Proceedings 1976 — AD A032801
26th International Wire & Cable Symposium Proceedings 1977 — AD A047609
27th International Wire & Cable Symposium Proceedings 1978 — AD A062322
28th International Wire & Cable Symposium Proceedings 1979 — AD A081428

Kwix Index of Technical Papers, International Wire & Cable Symposium (1952 - 1975) — AD A027558

**Highlights of the 28th**
**International Wire and Cable Symposium**
**November 13, 14 & 15, 1979**
Cherry Hill Hyatt House, Cherry Hill, NJ



Banquet Guest Speaker - Mr. Bohumil Jerabek, Canada's Leading Industrial Research Analyst and Consumer Advocate.



Greetings by COL E.R. Weidner, Chief of Staff, CORADCOM, Fort Monmouth, NJ



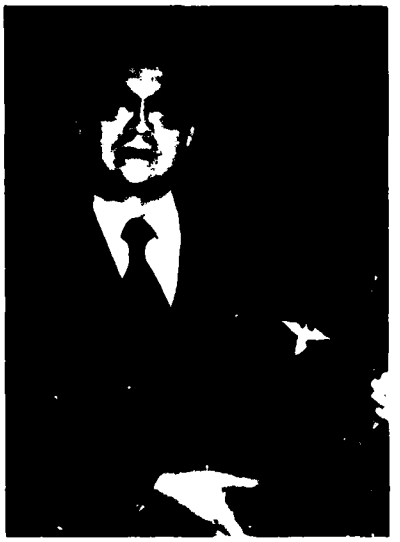
Dr. James Soos, Director, Communications Systems Center, CORADCOM, offering greetings from Commanding General, CORADCOM.



Panel Members - Tutorial Session (left to right), J. Kessler, President, Kessler Marketing Intelligence; R. Callahan, Editor/Publisher, Wire Technology & Wire Industry News; I. Kolodny, Session Chairman, General Cable Company and J. Morris, News Editor of Electrical Marketing News Letter for McGraw-Hill. Not shown - L. Perlman, Director, Commodities Research Unit Ltd.



Richard C. Mondello, Bell Labs, receiving Award for Best Presentation.



Fumio Suzuki, Sumitomo Electric Industries, Ltd., Japan, receiving Award for Outstanding Technical Paper. Co-authors were S. Sato, A. Mori and Y. Suzuki.





# AWARDS

| *Outstanding Technical Paper* | | *Best Presentation* |
|---|---|---|
| H. Lubars and J.A. Olszewski, General Cable Corp—"Analysis of Structural Return Loss in CATV Coaxial Cable" | 1968 | N. Dean, B.I.C.C.—"The Development of Fully Filled Cables for the Distribution Network" |
| J.P. McCann, R. Sabia and B. Wargotz, Bell Laboratories—"Characterization of Filler and Insulation in Waterproof Cable" | 1969 | J.D. Kirk, Alberta Government Telephones—"Progress and Pitfalls of Rural Buried Cable" |
| D.E. Setzer and A.S. Windeler, Bell Laboratories—"A Low Capacitance Cable for the T2 Digital Transmission Line" | 1970 | Dr. O. Leuchs, Kable and Metalwerke—"A New Self-Extinguishing Hydrogen Chloride Binding PVC Jacketing Compound for Cables" |
| R. Lyenger, R. McClean and T. McManus, Bell Northern Research—"An Advanced Multi-Unit Coaxial Cable for Toll PCM Systems" | 1971 | S. Nordblad, Telefonaktiebolaget L.M. Ericsson—"Multi-Paired Cable of Nonlayer Design for Low Capacitance Unbalance Telecommunication Network"<br><br>N. Kojima, Nippon Telegraph and Telephone—"New Type Paired Cable for High Speed PCM Transmission" |
| J.B. Howard, Bell Laboratories—"Stabilization Problems with Low Density Polyethylene Insulations" | 1972 | S. Kaufman, Bell Laboratories—"Reclamation of Water-Logged Buried PIC Telephone Cable" |
| Dr. H. Martin, Kabelmetal—"High Power Radio Frequency Coaxial Cables, Their Design and Rating" | 1973 | R.J. Oakley, Northern Electric Co., Ltd.—"A Study into Paired Cable Crosstalk" |
| D. Doty, AMP Inc.—"Mass Wire Insulation Displacing Termination of Flat Cable" | 1974 | G.H. Webster, Bell Laboratories—"Material Savings by Design in Exchange and Trunk Telephone Cable" |
| T.S. Choo, Dow Chemical U.S.A.—"Corrosion Studies on Shielding Materials for Underground Telephone Cables" | 1975 | J.E. Wimsey, United States Air Force—"The Bare Base Electrical Systems" |
| N.J. Cogelia, Bell Telephone Laboratories and G.K. Lavoie and J.F. Glahn, US Department of Interior—"Rodent Biting Pressure and Chemical Action and Their Effects on Wire and Cable Sheath" | 1976 | Michael DeLucia, Naval Ship Research and Development Center—"Highly Fire-Retardant Navy Shipboard Cable" |
| Thomas K. McManus, Northern Telecom Canada Ltd. and R. Beveridge, Saskatchewan Telecommunications, Canada—"A New Generation of Filled Core Cable" | 1977 | William L. Schmacher, AMP Inc.—"Design Considerations for Single Fiber Connector" |
| Fumio Suzuki, Shizuyoshi Sato, Akinori Mori and Yoichi Suzuki; Sumitomo Electric Industries, Ltd., Japan—"Microcoaxial Cables Insulated with Highly Expanded Polyethylene By Chemical Blowing Method" | 1978 | Richard C. Mondello, Bell Labs.—"Design and Manufacture of An Experimental Lightguide Cable For Undersea Transmission Systems" |
| S. Masaki, Y. Yamazaki and T. Ideguchi, Nippon Telegraph and Telephone Public Corporation, Japan,—"New Aluminum Sheath Cable Used For Electromagnetic Shielding" | 1979 | I. Wadehra, IBM Corporation—"Performance of Polyvinyl Chloride Communication Cables in Modified Steiner Tunnel Test" |

# CONTRIBUTORS

**Abbey Plastics Corporation**
Hudson, MA
**Abbott Industries, Inc.**
Leominster, MA
**AEG Telefunken Kabelwerke AG**
Moenchengladbach 2, W. GERMANY
**AFA Industries/Arnold Field Associates**
Hackensack, NJ
**Alambres Y Cables Venezolanos C.A.**
Caracas/Venezuela
**Alcoa Conductor Products Company**
Pittsburgh, PA
**Allied Chemical**
Hopewell, VA
**Allied Chemical-Fibers & Plastics Co.**
Morristown, NJ
**Alpha Wire Corp.**
Elizabeth, NJ
**Amercable Corporation**
El Dorado, Arkansas
**American Hoechst Corporation**
Somerville, NJ
**AMP Inc.**
Harrisburg, PA
**The Anaconda Company-Aluminum Div.**
Louisville, KY
**The Anaconda/Continental Wire & Cable**
York, PA
**Andrew Corporation**
Orland Park, IL
**Anixter Bros. Inc.**
Skokie, Illinois
**Arco Chemical Company**
Philadelphia, PA
**Arvey Corporation**
Cedar Grove, NJ
**Associated Lead Inc.**
Philadelphia, PA
**Astro Wire & Cable Corp.**
Worcester, MA
**Austral Standard Cables Pty. Ltd.**
Victoria, AUSTRALIA
**Baker Industries, Inc.**
Hartselle, AL
**BASF Wyandotte Corp.**
Parsippany, NJ
**Belden Corporation**
Geneva, Illinois
**Belding Corticelli Thread Co.**
Putnam, CT
**Bell Canada (Ontario Region)**
Toronto, Ontario, CANADA
**Berkshire Electric Cable Co.**
Leeds, MA
**BF Goodrich Chemical Group**
Independence, OH
**BICC Telecommunication Cables Ltd.**
Prescot, Merseyside, ENGLAND
**Borden Chemical**
Columbus, OH
**Boston Insulated Wire and Cable Co.**
Hamilton, Ontario, CANADA
**Brand-Rex Company**
Willimantic, CT
**Breen Color Concentrates, Inc.**
Lambertville, NJ
**The Bridge Mfg. Co.**
Enfield, Conn.
**Burgess Pigment Company**
Sandersville, GA
**Cable Consultants Corp.**
Larchmont, NY
**Cables de Comunicaciones, S.A.**
Zaragoza, SPAIN
**Cabot Corporation**
Boston, MA
**Camden Wire Co. Inc.**
Camden, NJ
**Canada Wire and Cable Ltd.**
Winnipeg, Manitoba, CANADA
**R. E. Carroll, Inc.**
Trenton, NJ
**Cary Chemicals Inc.**
Edison, NJ
**Central Telephone Company**
Las Vegas, Nevada
**Central Tool & Machine Co.**
Bridgeport, CT
**Chase & Sons, Inc.**
Randolph, Mass.
**Ciba-Geigy**
Ardsley, NY
**C-I-L Inc.**
Brampton, Ontario, CANADA
**Clinton Instrument Company**
Clinton, CT
**C.N.E.T.**
Paris, France
**Colonial Rubber Works**
Dyersburg, TN
**Comm/Scope Company**
Catawba, NC
**Communications Technology Corp.**
Los Angeles, CA
**Conductores Monterrey, S.A.**
Monterrey, N.L. Mexico
**Copperweld Bimetallic Group**
Pittsburgh, PA
**Corning Glass Works**
Corning, NY
**The Dainichi-Nippon Cables, Inc.**
Itami, JAPAN

**Davis-Standard Division**
Pawcatuck, Conn.
**Delphi Wire & Cable**
Folcroft, PA
**Diamond Shamrock Alberta Gas Ltd.**
Toronto, Ontario, CANADA
**Diamond Shamrock Corp.**
Cherry Hill, NJ
**Disco, Inc.**
Ringwood, NJ
**Dow Corning Corp.**
Midland, MI
**Duncan M. Gillies Co., Inc.**
West Boylston, MA
**Dussek Brox. (Canada) Ltd.**
Belleville, Ontario, CANADA
**Dussek Campbell Ltd.**
Crayford, Kent, England
**Eastman Chemical Products, Inc.**
Kingsport, Tenn.
**Ebasco Services, Inc.**
New York, NY
**The Electric Wire and Cable Co. of Israel**
Haifa, Israel
**Electrical Conductors, Inc.**
North Chicago, IL
**Electroconductores, C.A.**
Caracas, Venezuela
**Electronic Drives & Controls**
Randolph, NJ
**Engineered Wire & Cable Inc.**
Winsted, Conn.
**Essex Group**
Decatur, IL
**Felten & Guilleaume Carlswerk AG**
Cologne, W. Germany
**Firestone Plastics Company**
Pottstown, PA
**Firestone Synthetic Fibers Co.**
Hopewell, MA
**Fluorglas Division, Oak Materials Grp.**
Hoosick Falls, NY
**FMC Corporation**
Philadelphia, PA
**Formulabs Industrial Inks, Inc.**
Escondido, CA
**Freeport Kaolin Company**
New York, NY
**The Fujikura Cable Works, Ltd.**
Tokyo, JAPAN
**The Furukawa Electric Co., Ltd.**
Chiyoda-ku, Tokyo, JAPAN
**Gavitt Wire and Cable Co., Inc.**
Brookfield, MA
**Gavlick Machinery Corporation**
Bristol, CT
**Gem Gravure Co., Inc.**
West Hanover, MA
**General Cable Company**
Greenwich, CT
**General Electric Co.**
Waterford, NY
**General Engineering USA, Ltd.**
South Windsor, CT
**G.M. Gest Inc.**
Toronto, Ontario, CANADA
**W.L. Gore & Associates, Inc.**
Newark, Delaware
**Great American Chemical Corp.**
Fitchburg, MA 01420
**GTE Service Corporation**
Stamford, CT
**Guill Tool & Engineering Co.**
West Warwick, RI
**Hercules Inc.**
Wilmington, DE
**HiTemp Wires Inc.**
Hauppauge, NY
**Hooker Chemical/Ruco Division**
Hicksville, NY
**Hudson Wire Company**
Ossining, NY
**Ibaraki Electrical Communication Lab**
Tokai, Ibaraki, JAPAN
**ICI Americas Inc.**
Wilmington, DE
**Indeco Peruana S.A.**
Lima, Peru
**International Wire Products Inc.**
Wyckoff, NJ
**ITT Electro-Optical Products Div.**
Roanoke, VA
**ITT Surprenant Division**
Clinton, MA
**ITW/DEVCON Corp.**
Danvers, MA
**Jonathan Temple, Inc.**
Hackensack, NJ
**Judd Wire Division**
Turners Falls, MA
**LaBarge Inc., Electronics Division**
Irvine, CA
**Lamart Corporation**
Clifton, NJ
**Librascope, Division of Singer**
Glendale, CA
**S.A. Lignes Telegraphiques et Telephoniques**
Conflans St. Honorine, France
**Litton/Ingalls Shipbuilding**
Pascagoula, MS
**Lowe Associates, J.J. Inc.**
Bedford Hills, NY
**Maillefer Company**
South Hadley, MA
**Mark-Mor Tool & Die, Inc.**
Allenwood, NJ
**Micro-Tek Corp.**
Cinnaminson, NJ

**Sumitomo Electric Industries, Inc.**
Yokohama, JAPAN
**Sun Chemical Company**
Paterson, NJ
**Sun Petroleum Products Company**
Philadelphia, PA
**Superior Cable Corporation**
Hickory, NC
**The Swiss Insulating Works, Ltd.**
Breitenbach, Switzerland
**Syncro Machine Company**
Perth Amboy, NJ
**Taconic Plastics, Inc.**
Petersburg, NY
**Tamaqua Cable Corp.**
Schuylkill Haven, PA
**Technical Coatings Co.**
Nutley, NJ
**Teknor Apex Co.**
Pawtucket, RI
**TelComm Products/3M**
St. Paul, MN
**Telecom Australia**
Melbourne, Australia
**Teledyne Thermatics**
Elm City, NC
**Teledyne Western Wire & Cable**
Los Angeles, CA
**Telephone Cables Ltd.**
Dagenham, Essex, England
**Tenneco Chemicals Inc.**
Piscataway, NJ
**Tensolite Company, Div. of Carlisle Corp.**
Buchanan, NY
**Thermax Wire Corp.**
Flushing, NY
**Times Fiber Commmunications, Inc.**
Wallingford, CT
**Torpedo Wire & Strip, Inc.**
Pittsfield, PA
**Trea Industries**
No. Kingston, RI
**Ube Industries, Ltd.**
New York, NY
**Unifos Kemi AB**
Stenungsund, SWEDEN
**Union Carbide Corporation**
New York, NY
**USS Chemicals, Div. of US Steel Corp.**
Pittsburgh, PA
**Ware Chemical, Div. of Dart Ind.**
Stratford, Conn.
**Weber & Scher Mfg. Co. Inc.**
Newark, NJ
**Whitmor Wire & Cable Corp.**
N. Hollywood, CA
**Wilcom Products Inc.**
Laconia, NH
**Wilson Products Co.**
Neshanic, NJ, Assesse, Belgium
**Wyre Wynd Inc.**
Jewett City, CT
**Wyrough and Loser, Inc.**
Trenton, NJ
**The Zippertubing Co.**
Los Angeles, CA

**Monsanto Industrial Chemicals Co.**
St. Louis, MO
**The Montgomery Company**
Windsor Locks, CT
**Montrose Products Co.**
Auburn, MA
**M&T Chemicals Inc.**
Woodbridge, NJ
**H. Muehlstein & Co., Inc.**
Montvale, NJ
**National Wire and Cable Corporation**
Los Angeles, CA
**NEPTCO-New England Printed Tape Co.**
Pawtucket, RI
**The New Brunswick Telephone Co., Ltd.**
Saint John, New Brunswick
**Nippon Telegraph & Telephone Public Corp.**
Tokyo, JAPAN
**Nokia Cable Machinery**
Helsinki, Finland
**Nokia, Inc.**
Atlanta, GA
**Nonotuck Manufacturing Company**
South Hadley, MA
**Northern Petro Chemical Co.**
Des Plaines, IL
**Northern Telecom Canada Ltd.**
Montreal, Quebec, CANADA
**The Okonite Company**
Ramsey, NJ
**Olex Cables Ltd.**
Melbourne, Australia
**Omega Wire Inc.**
Camden, NY
**Pacific Electric Wire & Cable Co.**
Taiwan, Rep. of China
**Pantsote Inc.-Film/Compound Div.**
Passaic, NJ
**Penn Color, Inc.**
Doylestown, PA
**Pennwalt Corp.**
Philadelphia, PA
**Penreco**
Butler, PA
**A.E. Petsche Co., Inc.**
Arlington, TX
**Phalo Corporation**
Shrewsbury, MA
**Phelps Dodge Communications Co.**
White Plains, NY
**Phelps Dodge Communications Co.**
Yonkers, NY
**Phelps Dodge International Corp.**
Coral Gables, FL
**Philadelphia Insulated Wire Co.**
Morristown, NJ
**Phillips Cables Ltd.**
Vancouver, B.C. Canada
**Phillips Chemical Co.**
Pasadena, TX
**Pirelli Cables Ltd.**
St. Jean, Quebec, CANADA
**Pirelli-Cimco Corp.**
Allendale, NJ
**Plastoid Corporation**
New York, NY
**Plymouth Rubber Co., Inc.**
Canton, MA
**Polymer Services, Inc.**
E. Brunswick, NJ
**Porth Textiles, Ltd.**
Wales, U.K.
**PPG Industries, Inc.**
Chicago, IL
**Prestolite Wire Division, an Eltra Co.**
Port Huron, MI
**Prodelin, Inc.**
Highstown, NJ
**Products Research & Chemical Corp.**
Burbank, CA
**Radiation Dynamics, Inc.**
Melville, NY
**Radix Wire Co.**
Euclid, OH
**Raychem Corporation**
Menlo Park, CA
**Reichhold Chemicals, Inc.**
Hackettstown, NJ
**Reliable Electric Company**
Franklin Park, IL
**Remtek Corporation**
San Jose, CA
**RJR Archer, Inc.**
Winston-Salem, NC
**The Rochester Corporation**
Culpeper, VA
**The Rockbestos Company**
New Haven, Conn.
**John Royle and Sons**
Pompton Lakes, NJ
**Santech, Inc.**
Toronto, Ont., CANADA
**Saytech, Inc.**
East Brunswick, NJ
**Shell Chemical Company**
Houston, Texas
**Siemens AG**
Munich, Germany
**Siemens AG**
Neustadt bei Coburg, GERMANY
**Societe Anonyme de Telecommunications (SAT)**
Paris, France
**Southwest Chemical & Plastics Co.**
Seabrook, TX
**Southwire Company**
Carrollton, GA
**Sterling Davis Electric**
Wallingford, Conn.
**Sterling Davis Electrical**
Wallingford, CT

# TABLE OF CONTENTS


**Tuesday, November 18, 1980—9:30 A.M.-12:00 P.M.**
**Hunterdon and Cumberland Rooms**

SESSION I: *Tutorial*—Outlook for Voluntary Standards in U.S.A.

*Chairperson:* I. Kolodny, General Cable Company
*Panel Members:* S. I. Sherr, Staff Director Standards, IEEE
D. L. Peyton, Executive Vice President, ANSI
D. Abelson, Office of the STR, Department of Commerce
H. Collins, Washington Representative, Underwriters Laboratories

**Tuesday, November 18, 1980—2:00-5:00 P.M.**
**Gloucester Room**

SESSION II: Cable Design 1

*Chairperson:* G. Webster, Bell Laboratories

IMPROVED PULP INSULATION FOR TELECOMMUNICATIONS CABLE, *H. E. Durr, R. C. Bevers. R. O. Koch, W. M. Flegal, Western Electric Co.* ..... 1
A COMPARISON OF PEF AND FOAM-SKIN CORES, *A. Tsujikawa, H. Yasuhara, H. Suzuki, T. Ohnuma, The Fujikura Cable Works, Ltd., Chiba-ken, Japan* ..... 9
DEVELOPMENT, CHARACTERIZATION, AND PERFORMANCE OF AN IMPROVED CABLE FILLING COMPOUND, *D. M. Mitchell, R. Sabia, Bell Laboratories* ..... 15
COAXIAL LINE WITH THE HIGHEST ELECTRICAL LENGTH STABILITY, *Y. Saito, S. Furuya, H. Sugawara, Y. Asano, S. Kato, Sumitomo Electric Industries, Ltd., Yokohama, Japan* ..... 26
SOLUTION TO CORE GROWTH IN CONNECTORIZED CABLE, *M. R. Reynolds, G. M. Yanizeski, Bell Laboratories, and R. N. McIntyre, Western Electric* ..... 38
CABLE SHEATH BUCKLING STUDIES AND THE DEVELOPMENT OF A BONDED STALPETH SHEATH, *G. M. Yanizeski, E. L. Johnson, Bell Laboratories, and R. G. Schneider, Western Electric* ..... 48

**Tuesday, November 18, 1980—2:00-5:00 P.M.**
**Hunterdon Room**

SESSION III: Material

*Chairperson:* K. Bow, Dow Chemical USA

A NEW LOW DIELECTRIC CONSTANT FILLING COMPOUND FOR TELECOMMUNICATIONS CABLE, *L. E. Davis, N. I. Patel, Superior Cable Corp.* ..... 59
PLASTICIZER EVAPORATION FROM VINYL INSULATED WIRES, *P. C. Warren, Bell Laboratories* ..... 66
CARBOXYLATED NITRILE/PVC FLUXED BLENDS FOR EXTRA-HEAVY-DUTY-CABLE JACKET COVERS, *H. F. Schwarz, Polysar Limited, Sarnia, Ontario, Canada* ..... 76
COMPARISON OF THE RELATIVE COST EFFECTIVENESS OF BROMINATED AND CHLORINATED FLAME RETARDANTS IN EPDM, *J. M. Lesniewski, Saytec, Inc.* ..... 90
PERFLUOROALKOXY FLUOROCARBON RESIN PROPERTIES RELATING TO ELECTRICAL AND ELECTRONIC APPLICATIONS, *M. I. Bro, D. I. McCane, D. B. Allen, J. C. Reed, E. I. DuPont de Nemours* .. 94

**Wednesday, November 19, 1980—9:00 A.M.-12:00 P.M.**
**Gloucester Room**

SESSION IV: Cable Design II

*Chairperson:* F. Short, Belden Corp.

APPLICATION OF SPACER FORMING TECHNIQUE TO COMMUNICATION CABLES, *S. Yonechi, H. Horima, S. Tanaka, Sumitomo Electric Industries, Yokohama, Japan and K. Ishihara, Ibaraki Electrical Communication Laboratory, Ibaraki, Japan* ..... 101
MEAN POWER SUM FAR-END CROSSTALK OF PIC CABLES AS A FUNCTION OF AVERAGE TWIST HELIX ANGLE, *J. J. Refi, Bell Laboratories* ..... 111
GENERAL CROSSTALK MODEL FOR PAIRED COMMUNICATION CABLES, *P. Kish, Y. LeBorgne, Northern Telecom Canada Ltd., Montreal, Canada* ..... 117
INSULATION RESISTANCE PROBLEMS AND ITS RELATIONSHIP TO TRANSMISSION, *V. Abadia, J. Z. Avalos, Cables de Comunicaciones, S. A., Zaragoza, Spain* ..... 128
THE USE OF TEST DATA AND FIELD DATA IN DESIGNING SPLICE CLOSURES, *M. Moisson, Raychem Corporation, Raychem, Belgium* ..... 136
NON-COATED BONDABLE POLYIMIDE/FLUOROCARBON TAPE INSULATION FOR LIGHTWEIGHT ELECTRICAL WIRE, *A. J. Sheppard, Martin Marietta Aerospace* ..... 145

**Wednesday, November 19, 1980—9:00 A.M.-12:00 P.M.**
**Hunterdon Room**

SESSION V: Connectors

*Chairperson:* J. Neigh, AMP, Inc.

TELECOMMUNICATION CABLE SPLICING METHOD USING A NEW HEAT SHRINKABLE SLEEVE, *K. Yokoyama, The Tokyo Electric Power Co., Tokyo, Japan, N. Sato, S. Goto, M. Makiyo, The Fujikura Cable Works, Inc., Chibaken, Japan, S. Mase, The Fujikura Cable Works, Tokyo, Japan* ..... 151
LOW PRESSURE MOLDING FOR ENCAPSULATION OF CABLE SPLICING, *L. J. Charlebois, F. A. Huszarik, Bell Northern Research, Ottawa, Ontario, Canada* .. 159

APPLICATIONS FOR MODULAR AND DISCRETE WIRE CABLE SPLICING, *R. Young, AMP, Inc.* ..... 164
MODULAR HARDWIRE BLOCK WITH SWITCHING CAPABILITY, *G. B. Matthews, 3M Company* ..... 168
AUTOMATIC CONNECTORIZATION OF 25 PAIR CABLE, *R. G. Ebrey, H. A. Sckerl, Western Electric and G. G. Seaman, Western Electric* ..... 178
CONNECTOR PERFORMANCE MONITORING IN THE OUTDOOR CROSS CONNECT ENVIRONMENT, *I. E. Martin, A. N. Satar, Bell-Northern Research, Ottawa, Ontario, Canada and C. D. Gupta, Bell Canada, Toronto, Ontario, Canada* ..... 188

**Wednesday, November 19, 1980—2:00-5:00 P.M.**
**Gloucester Room**

SESSION VI: Fiber Optics I

*Chairperson:* L. Chattler, DCM International Corp.

FIBER OPTIC CABLE COIL PACKS FOR AIR DEPLOYMENT, *R. E. Thompson, X. G. Glavas, V. E. Kalomiris, ITT and H. Wichansky, CORADCOM* .... 194
AN OPTICAL FIBRE LINK IN A MOUNTAINOUS ENVIRONMENT, *J. R. Osterfield, S. R. Norman, Pirelli General Cable Works Ltd., Hants, United Kingdom, D. N. McIntosh, A. J. Rodgers, Central Electricity Research Laboratories, Surrey, United Kingdom and R. Castelli, M. Tamburello, Telettra S.P.A., Milan, Italy* . 202
OUTSIDE PLANT HARDWIRE FOR USE IN FT3 LIGHTWAVE SYSTEMS, *N. E. Hardwick, J. L. Baden, Bell Laboratories* ..... 212
SPLICING TECHNIQUES FOR TACTICAL FIBER OPTIC SYSTEMS, *S. F. Large, Mitre Corp.* ..... 221
A MILITARY SIX FIBER HERMAPHRODITIC CONNECTOR, *J. G. Woods, M. Hodge, J. Ryley, TRW Philadelphia Research Labs.* ..... 229

**Wednesday, November 19, 1980—2:00-5:00 P.M.**
**Hunterdon Room**

SESSION VII: Fire Considerations

*Chairperson:* M. DeLucia, David W. Taylor Naval Ship R & D Center

INDEXING METHOD FOR CABLE CLASSIFICATION USING THE FM LABORATORY-SCALE COMBUSTIBILITY APPARATUS, *J. L. Lee, A. Tewarson, R. F. Pion, Factory Mutual Research Corp.* ..... 236
FLAME RESISTANT COMMUNICATION CABLE WITH LEAD SCREEN TAPE COATED WITH POLYMER, *K. Yoshioka, Y. Amano, G. Morikawa Sumitomo Electric Industries, Ltd., Yokohama, Japan* ..... 240
DEVELOPMENT OF A FLAME RESISTANT NONCONTAMINATING PVC JACKET FOR COAXIAL CABLE, *J. T. Loadholt, S. Kaufman, Bell Laboratories* ..... 245
NEW GENERATION OF NONHALOGENATED, FLAME RETARDANT COMPOUNDS AND CABLES, *H. A. Mayer, G. Hög, AEG-Telefunken Kabelwerke AG, Mönchengladbach, West Germany* ..... 253
NEW FLAME RETARDANT HALOGEN-FREE CABLES FOR NUCLEAR POWER PLANTS, *H. Harbort, SEL (Standard Elektrik Lorenz AG), Stuttgart, West Germany* ..... 263
A NEW NON-HALOGENATED FLAME RETARDANT WIRE INSULATION BASED ON POLYPHENYLENE OXIDE, *H. de Munck, General Electric Plastics BV, Holland, W. E. Simpson, J. R. Bury, Standard Telecommunication Laboratories Ltd., Harlow, England and J. A. Devoldere, Bell Telephone Manufacturing Co., Ghent, Belgium* ..... 268

**Thursday, November 20, 1980—9:00 A.M.-12:00 P.M.**
**Gloucester Room**

SESSION VIII: Fiber Optics II

*Chairperson:* A. Asam, ITT Electro-Products Division

OPTICAL ATTENUATION TESTING IN FIELD AND FACTORY, *J. E. G. Chapman, BICC Telecommunication Cables Ltd., Prescott, England, D. Cheng, BICCOTEST Ltd., Cheshunt, England and D. R. Cronin, BICC Telecommunication Cables Ltd., Prescott, England* ..... 279
WATERBLOCKING IN OPTICAL CABLES, *O. R. Bresser, A. J. H. Leenen, S. H. K. in't Veld, NKF Kabel B.V., Waddinxveen, The Netherlands* ..... 290
INNOVATIVE METHODS FOR INSTALLING FIBER OPTIC CABLES, *J. B. Masterson, General Cable Co.* .. 299
FABRICATION AND TEST OF OPTICAL FIBER CABLES FOR MILITARY AND PTT APPLICATIONS, *W. Shmidt, U. Zwick, SEL (Standard Elektrik Lorenz AG), Stuttgart, W. Germany* ..... 306
COMPOSITE FIBER-OPTIC OVERHEAD GROUND WIRE, *M. Igarashi, J. Yokoyama, H. Iwamura, The Tokyo Electric Power Co., Inc., Tokyo, Japan and N. Mori, I. Matsubara, Y. Saito, Sumitomo Electric Industries, Ltd., Tokyo, Japan* ..... 312
DESIGN, MANUFACTURE, PERFORMANCE AND INSTALLATION OF A RUGGEDIZED FIBER-ELEMENT OPTICAL CABLE, *P. Scadding, Times Fiber Communications* ..... 322

**Thursday, November 20, 1980—9:00 A.M.-12:00 P.M.**
**Hunterdon Room**

SESSION IX: Testing

*Chairperson:* M. Farago, Northern Telecom Canada Ltd.

COPPER INHIBITOR AND ANTIOXIDANT LEVELS IN HIGH DENSITY POLYETHYLENE: THEIR MEASUREMENT BY HIGH PERFORMANCE LIQUID CHROMATOGRAPHY AND RELATION TO INSULATION LIFE, *J. Fech, A. DeWitt, General Cable Co.* ..... 327
IDENTIFICATION OF PARTICLES IN HIGH DENSITY POLYETHYLENE THAT CAUSE SPARK FAILURES DURING HIGH SPEED EXTRUSION, *G. A. Schmidt, L. A. Bopp, General Cable Co.* ..... 331
COMPUTERIZED STATISTICAL QUALITY CONTROL OF TELEPHONE CABLES, *L. M. Chattler, DCM International Corp.* ..... 350
LIGHTNING SURGE WAVES INDUCED IN TRANSMISSION LINES, *H. Koga, T. Motomitsu, M. Taquchi, Ibaraki Electrical Communication Laboratory and N.T.T. Tokai, Ibaraki, Japan* ..... 363

MEASURING TRANSMISSION LINE TRANSFER FUNCTIONS USING A FOURIER TECHNIQUE, *N. H. Gholson, Naval Ocean Research and Development Activity* ..... 375

**Thursday, November 20, 1980—2:00-5:00 P.M.**
**Gloucester Room**

SESSION X: Fiber Optics III

*Chairperson:* B. Korcz, Shell Development Co.

EVALUATION OF TRANSMISSION LOSS IN OPTICAL FIBER CABLES BY MEANS OF THE BACKSCATTERING TECHNIQUE, *M. Eriksrud, S. Lauritzen, N. Ryen, Norwegian Institute of Technology, Trondheim, Norway* 380
DESIGN AND PRACTICAL CONSIDERATION FOR MANUFACTURING A NON-METALLIC FIBER OPTIC CABLE FOR AERIAL APPLICATION, *M. M. Rahman, H. K. Eastwood, P. Rivett, M. Herrera, Canstar, Montreal, Quebec, Canada* ..... 386
FIBER OPTIC CABLES FOR AERIAL APPLICATIONS, *U. Oestreich, G. Zeidler, Siemens AG, Munich, W. Germany and P. R. Bark, D. O. Lawrence, Siecor Optical Cables, Inc.* ..... 394
OPTICAL FIBERS IN OVERHEAD POWER TRANSMISSION SYSTEMS FOR COMMUNICATION AND CONTROL, *B. J. Maddock, C.E.R.L., Surrey, England, K. L. Lawton, BICC Telecommunication Cables Ltd., Manchester, England and K. H. Pickup, BICC Metals Ltd., Merseyside, England* ..... 402
INSTALLATION OF A TRIAL FIBER CABLE DESIGNED FOR TRANSOCEANIC SUBMARINE TELECOMMUNICATION SYSTEMS, *P. Worthington, ITT-Standard Telephones and Cables Ltd., Southampton, England* 410
OPTICAL CABLE NETWORK FOR 150 SUBSCRIBERS, *F. Krahn, Felten & Guilleaume Carlswerk AG, Koln, W. Germany* ..... 418

**Thursday, November 20, 1980—2:00-5:00 P.M.**
**Hunterdon Room**

SESSION XI: Cable Applications

*Chairperson:* J. Brazee, Continental Telephone Service Corp.

PREVENTION OF CABLE PRESSURE DAM FAILURES, *C. D. Gupta, Bell Canada, Toronto, Ontario, Canada and W. P Trumble, Bell Northern Research, Nepean, Ontario, Canada* ..... 424
THEORETICAL ANALYSIS AND REDUCTIONAL COUNTERMEASURE OF DANCING PHENOMENA ON SELF-SUPPORTING CABLE, *M. Iwazaki, K. Katagiri, A. Sekiguchi and S. Masaki, NTT Engineering Bureau, Tokyo, Japan* ..... 432
IRRADIATED POLY (VINYL CHLORIDE) INSULATED WIRE USED IN TELEPHONE EQUIPMENT, *E. A. Burek, Western Electric* ..... 439
PROVISION OF 30 CHANNEL PCM SYSTEMS USING TWO PRECONNECTORIZED 10 PAIR DISTRIBUTION TYPE CABLES INSTALLED IN PARALLEL, *H. J. Spencer, B.P.O. Telecommunications Headquarters, London, England and C. E. Wilbud, B. J. Symmons, Standard Telephones & Cables Ltd., Gwent, England* ..... 443
A MEANS FOR MONITORING AND PROTECTING OUTSIDE CABLE PLANT AGAINST MOISTURE, *D. E. Vokey, Canada Wire, Winnipeg, Manitoba, Canada* ..... 452

# IMPROVED PULP INSULATION FOR TELECOMMUNICATIONS CABLE

Helmut E. Durr, Robert C. Bevers
Robert O. Koch and William M. Flegal

Western Electric Co., Inc.
2000 Northeast Expressway
Norcross, GA. 30071

## ABSTRACT

Since its introduction in the 1930's, no significant changes in the pulp insulating process had occurred. In 1979, a new, improved process was introduced by Western Electric Company. This new insulation, which is used in TUFPULP* Cable, was developed to meet the requirements of the telephone companies for pulp insulated conductors with improved durability and handleability. In addition, the increased strength of the insulation has resulted in fewer defects throughout the entire manufacturing process.

In the new insulating process, a thin layer of adhesive is applied to the bare copper conductor. The adhesive is partially dried in an oven prior to the application of the pulp. The adhesion of the pulp to the conductor is greatly enhanced resulting in a tougher insulation. No degradation in the electrical performance or the water migration and pneumatic resistance values of TUFPULP cables has been observed.

*Trademark of Western Electric Company.

## INTRODUCTION

The very early telephone conductors were bare wires having no insulation. As the number of lines began to increase, it became necessary to group wires into a cable and insulation of the individual conductors was therefore required. From 1880 to 1891, two layers of cotton were used as the insulating material. Paper ribbon replaced the cotton in 1891 and continued in use until 1930 when the paper pulp insulating process was developed. This development permitted the mass production of pulp insulated conductors at low cost and entirely replaced paper ribbon for exchange area cables.

## PULP MANUFACTURING PROCESS

The pulp insulation of conductors involves a unique process of forming a paper tube about a conductor using a type of paper-making equipment. As shown in Figure 1, copper wire centered in a wet paper ribbon is mechanically spun about the wire to form a tube. It is dried in an electric furnace and taken up on reels for subsequent operations. With this insulating process 60 wires are insulated simultaneously on each machine. The insulating machine itself is composed of several major and minor units combined into a single in-line manufacturing facility approximately 120 feet long and 15 wide. The function of each unit shown in Figure 2 is described below.

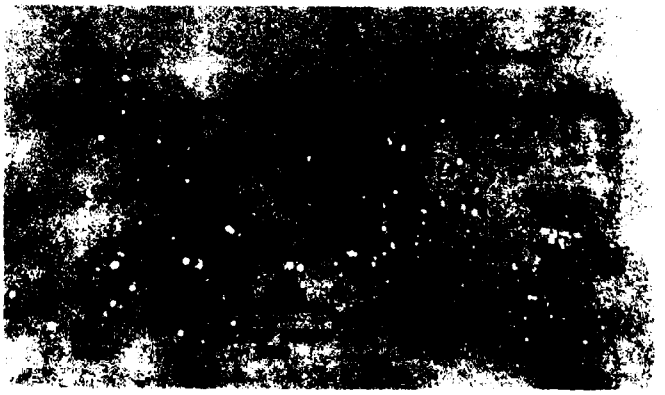
### Supply Stand

The insulating process begins with 60 bare wire supply positions. The individual supply position consists of a stem-pack which holds about 1000 pounds of annealed copper wire. Since the insulating machine runs continuously, the supply end must furnish wire in unbroken continuity. A method has been developed to shift from an empty to a full package of supply wire without stopping the machine or interrupting the continuity of the wire. Devices are also provided on the supply stand to straighten and properly tension the wire for the insulating process.

### Electrolytic Cleaner

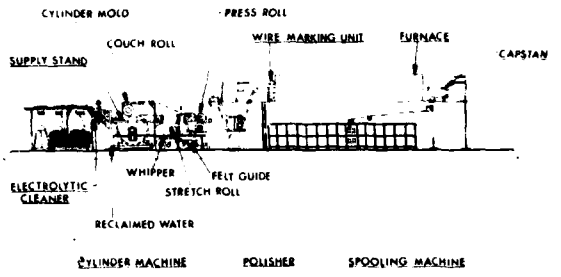
After the supply stand, the wires are passed through a two section electrolytic cleaner. A caustic solution of sodium orthosilicate is contained in the first stage and the second stage has a water rinse. Cleaning of the copper wires was more necessary when batch annealing of the conductor was used.

FIGURE 1



*TYPICAL SECTION THROUGH WIRE*

FIGURE 2




***STANDARD PULP INSULATING PROCESS***

Paper Forming Machine

The copper wires then enter the single-cylinder paper forming machine where the refined pulp is continuously being metered into the vat or forming section of the machine. In the vat, the pulp is diluted with water to a low consistency and formed into ribbons by the conventional paper-making technique of straining the pulp fibers from the water suspension as it flows through a wire screen under slight pressure.

The rotating cylinder mold or forming screen is divided into 60 narrow, uniform sections running around the circumference by painting alternate strips of a plastic material onto the surface. The flow of water through these areas is blocked and the deposition of fibers is thus prevented. Ribbons of paper are formed only in the unpainted strips on the cylinder mold and the copper wires are guided so that one wire is embedded in the center of each ribbon. After forming, the wet paper pulp ribbons with the embedded wires are transferred from the cylinder mold to an endless fabric belt called a felt and are passed through a pair of rubber covered press rolls where the excess water is removed.

Polisher

After leaving the paper machine, the wet ribbon is formed around the wire by passing it through high speed rotating polishers to produce a tight cylindrical wrap of the ribbon around the wire.

Furnace

The wet insulation is then dried by passing it through an electrically heated furnace which is approximately 30 feet long, has a maximum entrance temperature of up to 1600°F and a maximum exit temperature of about 900°F.

Capstan

The capstan pulls the wires through the furnace and passes them onto the take-up unit. It is specially designed to minimize crushing and to control wire tension.

Take-Up

At the take-up unit, the wires are put onto reels for further processing. Each position holds two reels that can be operated independently, permitting the continuous spooling of the insulated wire. A bare wire detector is located on the take-up to inform the operator automatically when incomplete insulation occurs.

Few changes have occurred in this basic pulp insulating process since its introduction in 1930. Pulp cable has been a good product because of its low cost, high pair density and desirable water blocking properties. Even with the penetration of plastic insulations, pulp still comprises about 40% of Western Electric cable production. With the increasing cost and decreasing availability of oil-based plastics, the use of replenishable pulp insulation has assumed new importance.

Although pulp cable has many favorable attributes, problems do arise in both its manufacture and use. Defect levels are higher with standard pulp than with plastic insulation. These defects can be categorized as follows (Figure 3):

1) Insulation unraveling to expose the conductor

2) Bare wire

3) Insulation being crushed against connectors and splice cases

4) Insulation deteriorating due to repeated handling

The introduction of factory connectorization further highlighted the problems with standard pulp insulation.

FIGURE 3 ***TYPICAL DEFECTS***

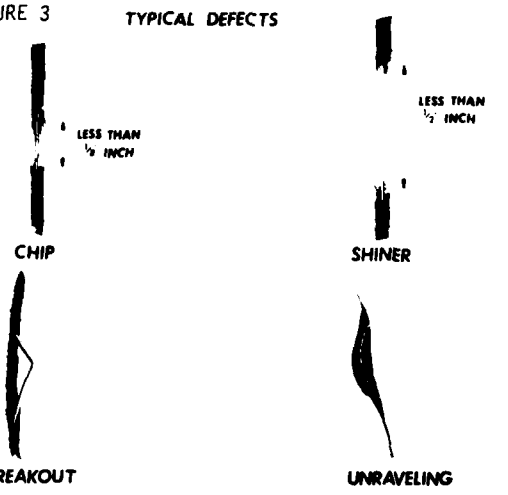
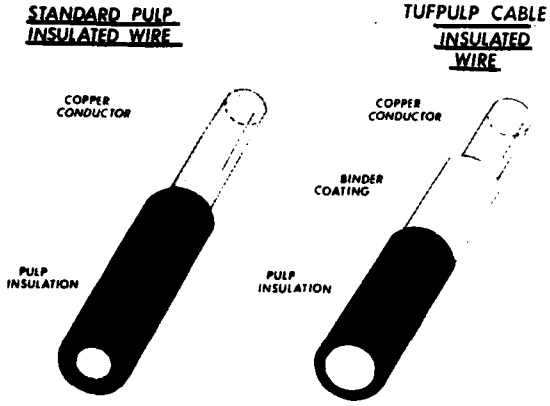


FIGURE 4




TUFPULP CABLE PROCESS DEVELOPMENT

To meet the need for an improved pulp cable, development work was initiated to evaluate acrylic binders for improving the adhesion of the pulp insulation to the copper conductor. These successful efforts culminated in the conversion of all pulp insulating facilities at Western Electric to the improved process by mid-1980. Recognizing the improvement achieved by the new process, the product has been named TUFPULP cable.

The new insulated conductors appear identical to standard pulp-insulated wire. The difference becomes obvious, however, when attempting to remove the insulation from the wire. The process applies the binder to the wire before the insulation is added, "gluing" the pulp to the wire (Figure 4). This increased adhesion lowers defects throughout the cable manufacturing processes and reduces exposure of bare wire during handling of the cable at splicing. Although breaks in the pulp insulation can still occur, the insulation no longer slips on the wire to expose eighth-inch (or longer) lengths of bare copper as standard pulp tended to do.

## Material

The binder presently used in the process is a water-based emulsion of nonionic, acrylic polymers which is diluted with water prior to use. Because this material necessarily forms "tacky" films upon drying, a potential problem with the binder is film buildup in the equipment used to handle it. Equipment design must minimize exposure of the emulsion to air and avoid free-fall and splashing since the emulsion easily foams. Because the emulsion is acidic, stainless steel or plastic materials are required.

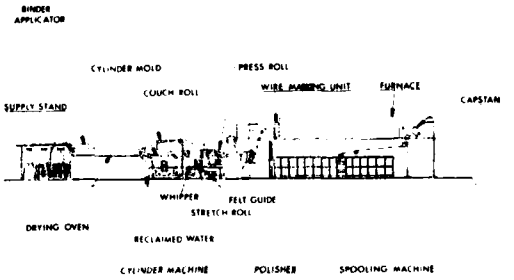
## Applicator

The key to the new process is the application of a uniform coating of the binder emulsion on the conductors followed by drying to a tacky condition prior to formation of the pulp ribbon around the conductors. The applicator and oven have been installed in the space formerly occupied by the electrolytic cleaner as shown in Figure 5. The cleaner is not required for the new process.

In the applicator, conductors pass through a bath of emulsion and then through sizing dies which wipe off excess binder (Figure 6). Binder is pumped to an applicator tube which is enclosed except for sixty narrow slots on the top side for the conductors. The applicator tube is located so that each wire passes through its slot without dragging against the tube. The wires moving through the applicator tube pick up binder which is carried to the sizing dies. Binder pumped out of the tube slots also runs down the tube and to the bottom of the applicator, but the flow rate is adjusted to cause most binder to be carried with the wires. This design minimizes the amount of binder exposed to air and therefore film buildup on the tube.

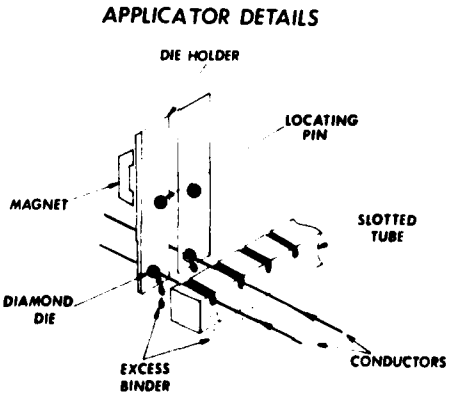
The sizing dies are diamonds to reduce wear from contact with the moving conductors. The diameter of the opening is slightly greater than the conductor diameter. Because the wires entering the dies are carrying more binder than the annulus between the wire and die can accommodate, the faces of the dies are flooded with excess binder which runs down the die holders to the bottom of the applicator. This flooding of the die entrance assures a uniform liquid coating over the entire surface of the wires.

FIGURE 5




*TUFPULP CABLE INSULATING PROCESS*

FIGURE 6



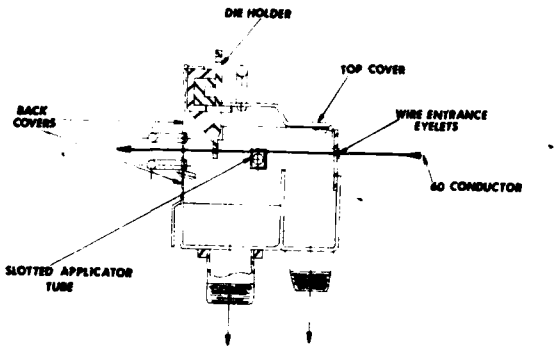
The bottom of the applicator is a trough which collects the excess binder from the applicator tube and die holders. This emulsion flows by gravity through a strainer to remove debris and into the supply tank. It is recirculated to the applicator along with fresh make-up which replaces the liquid removed by the wires.

The die holders are placed in the applicator on locating pins and held by magnets. This allows easy replacement of a die when necessary because of plugging. To change a die, the wire is cut, the die holder changed, and the wire strung through the new die.

To minimize film buildup, the entire applicator is covered to reduce exposure to air, and the parts are Teflon® plastic coated to provide a smooth surface (Figure 7). Because binder is continuously flowing over the surfaces and being exposed to air, however, film buildup is an inherent problem. Every 8 hours film is removed from the applicator tube slots, the face of the dies and the exit side of the dies. This can be done while the machine is running. During scheduled shutdowns every one or two weeks, the applicator tubes and dies are removed for more complete cleaning.

FIGURE 7

***APPLICATOR CROSS-SECTIONAL VIEW***

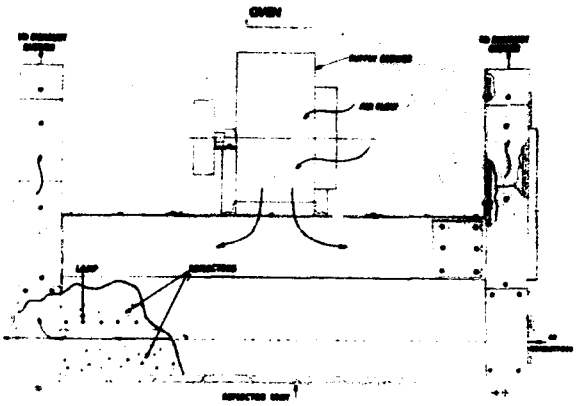



## Oven

The next step in the process is the drying of the binder. Since the binder is applied as an aqueous emulsion, the water must be removed before the coated conductor enters the pulp insulating machine. Any undried binder will be washed off the wire and may result in defective product.

The oven selected consists of many lamps mounted above the wires (Figure 8), with ceramic reflectors above and below the lamps. In order to keep the lamps and ceramic reflectors at reasonable temperatures, air is forced through the oven by a blower. This air flow contributes to the drying process but studies indicate that no more than 10 to 20% of the total heat transfer occurs in the convective mode. Since the air flow is the primary source of energy loss from the oven, the flow rate should be no greater than that required to maintain safe operating temperatures of the lamps and ceramics.

FIGURE 8




## TUFPULP CABLE CHARACTERISTICS

### Insulation Adhesion

The bond between the pulp insulation and the conductor is the primary characteristic that differentiates the improved insulation from standard pulp insulation. This bond or adhesion results in superior handleability which is of primary importance in splicing operations. Also, this bond contributes significantly toward the reduction in the quantity of chips and bare wire during manufacturing operations where excessive stress can result in broken insulation and the exposure of bare wire. The manufacturing stages where this generally occurs are insulating, twisting, and stranding.

Adhesion is defined as the force required to pull the conductor from a known insulated length. A test instrument designed by Western Electric is used to measure the adhesion. Results are expressed in pounds per linear inch.

Average insulation adhesion values of the most common wire gauges (26, 24, 22) are shown in Figure 9. TUFPULP cable adhesions are significantly higher than those of standard pulp. Since adhesion is a function of contact surface area between insulation and conductor, results could alternatively be expressed in pounds per square inch to eliminate dependence on conductor diameter.

### Elongation

The elongation of TUFPULP cable conductors

as measured is reduced from that of standard pulp as shown in Figure 10. As the load increases, both the insulation and the conductor start to elongate until the pulp breaks at about 2%. This peak defines the combined tensile strength of the insulated conductor.

The load drops after the insulation breaks and the conductor continues to elongate until failure. The ultimate tensile strength and elongation are defined by this point.

The lower elongation values for TUFPULP cable are explained by examination of Figure 11. After an insulation break, the stress is concentrated at the point of the break because the cross-sectional area for load distribution is reduced relative to the remainder of the specimen. With standard pulp, the conductor is not restrained by the insulation after it breaks, permitting the load to be distributed equally over the entire specimen length.

FIGURE 9

**ADHESION VS. GAUGE**

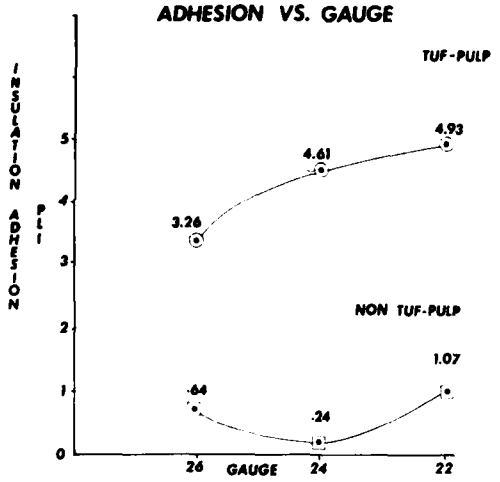



FIGURE 10

**26 GAUGE TENSILE ELONGATION CURVES**

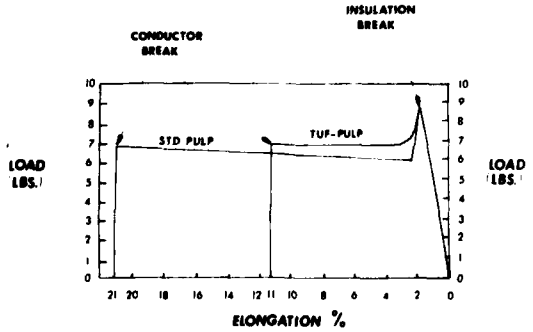
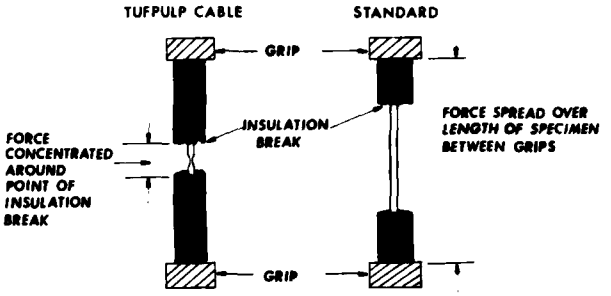



FIGURE 11

**DIFFERENCES IN ELONGATION TESTING**




Low elongation has caused problems primarily with 26 gauge. Excessive wire breaks during reel transfer at the insulating machines and during twisting can occur if high tensile forces are experienced. Such wire breaks also occurred with standard product but less frequently. To minimize this problem the adhesive film thickness has been controlled to allow more elongation and improve manufacturability. Low elongation has not caused any problems in the installation or splicing of cables.

## Electrical Characteristics

Some concern was expressed initially that the high dielectric constant of the acrylic binder would result in unacceptable mutual capacitance in the finished cable. Production results have demonstrated that these concerns were unwarranted. The average mutual capacitance of all pulp cables manufactured over periods of 4 to 5 months is shown in Figure 12. The specification limit and desired average are also shown. As shown, excellent mutual capacitance results have been achieved.

The average conductor resistance for the same periods are shown in Figure 13. No significant change in average resistance has been observed.

Improved manufacturability has made possible a reduction in insulation thickness. With standard pulp a corresponding increase in defects would be observed. Because of the superior properties of TUFPULP cable, however, low defect levels can be maintained and mutual capacitance remains at or below the targeted values. With smaller insulated conductor diameters, cable diameters can be reduced with significant savings in sheathing materials. Alternatively, more pairs can be placed in the same cable diameter. Higher pair densities can reduce installation costs for operating companies.

FIGURE 12

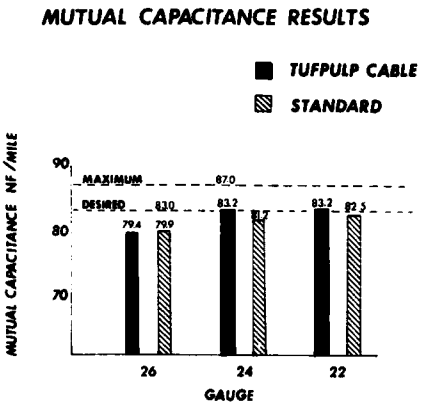
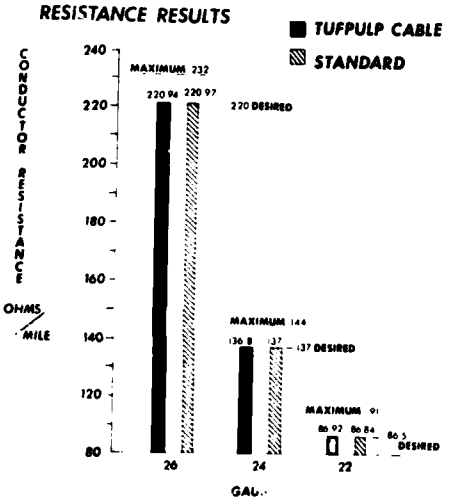



FIGURE 13




## TUFPULP CABLE RESULTS

### Manufacturing Defect Levels

Historically, one of standard pulp's major disadvantages has been its high percentage of defective pairs which require repair. Defects identified by testing after twisting, stranding, cabling and sheathing include shorts, opens, and crosses. Since the conversion to the new process, overall defect levels have been reduced by at least 40% in each manufacturing operation with corresponding reduction in repair effort. For TUFPULP cables which have factory-installed connectors, the final test area can be by-passed because of the low defect level and final testing done after connectorization. This reduction in testing is not possible with standard pulp.

### Cable Evaluations

In addition to the cable manufacturing results previously discussed, additional evaluations have been conducted in conjunction with Bell Laboratories. One of the first evaluations was a duct pull test to determine if the apparent conductor elongation reduction resulted in increased opens when pulling cables in ducts.

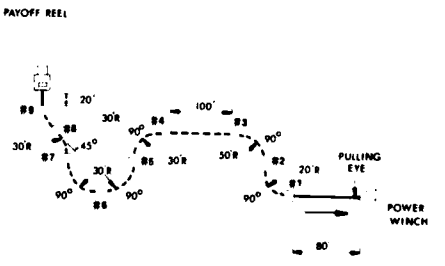
The first 2700 pair-26 gauge cable made with 100% of the new insulation was tested at the BTL field installation test site at Chester, N.J. The defect-free cable was first pulled into a 3 1/2" concrete duct of typical configuration (one 90° bend and two 45° bends) where no opens were generated. An unplanned test occurred when removing the cable from this duct for subsequent tests. Forces far in excess of the 10,000 pound full-scale indication were required for removal. This step generated two opens while the subsequent installation in a 4" torture run with five 90° bends and two 45° bends (See Figure 14) gave no additional opens. Since the only problem was in the unintended severe abuse of removal, it was concluded that elongation was not a problem.

TUFPULP cable was extensively tested by Bell Laboratories. Table 1 is a partial listing of the many properties checked. TUFPULP cable is clearly superior or equivalent to standard pulp in every area except elongation, which has been shown to be no problem.

### Field Results

In addition to the detailed evaluation of experimental cables, field trials were conducted. The extent of the field trials are shown in Table 2. These 98 cables, ranging in size from 900 to 3600 pairs, were installed by 14 different telephone operating companies over a period of two years. About one-third of these installations were observed by Western Electric or Bell Laboratories engineers.

FIGURE 14



The field trials established the superiority of the new insulation over standard pulp. From the field trial cables, it was demonstrated that the new insulation has improved handleability, fewer factory defective pairs, and reduced tendency for split pairs from pairs untwisting. Reduced splicing time was often reported with faster turn-up of cables than normal. The new product was readily accepted by the participating operating companies.

## CONCLUSIONS

The development of the new insulating process has resulted in an improved pulp cable. Most of the shortcomings of standard pulp have been eliminated by the new process and economies have been achieved in both the manufacture and installation of TUFPULP cables. Because of the favorable response by operating telephone companies, pulp cable will remain an important product offering for the foreseeable future.


## ACKNOWLEDGEMENTS

The success of this project would not have been possible without the assistance of the design, development, and plant engineers at Western Electric's Hawthorne, Phoenix and Atlanta Works. The contributions of the BTL Transmission Media Laboratory to the development, evaluation and introduction of TUFPULP cable are gratefully acknowledged.


TABLE 1

BTL EVALUATIONS
Characteristics Checked

| | Standard Pulp Cable | TUFPULP Cable |
|---|---|---|
| **PHYSICAL** | | |
| Water Migration (Flow Ratio)* | 1.00 (normal) | 0.85 |
| Pneumatic Resistance "R"* | 2.25 - 3.75 | 2.80 |
| Insulation Crush (26 Ga.) | 14 - 27 pounds | 17 - 42 pounds |
| Durability (Wind-Up) (26, 24, 22 Ga.) | 3 - 5 cycles | 11 - 12 cycles |
| Dielectric Strength Avg. (26 Ga.) | 793V | 945V |
| Elongation - Avg. (26 Ga.) | 21% | 6% |
| High Temperature Aging | No Degradation | |
| Wire Handling - Wet and Dry | No Problems | |
| Gas Plugging | No Leaks | |
| Corrosion | None | |
| **ELECTRICAL** | | |
| Capacitance/Diameter | Comparable | |
| Dielectric Constant | Comparable | |
| Insertion Loss (22 Ga.) | 5.25 dB/kf | 5.17 dB/kf |
| **HEALTH** | | |
| Burning | No Problem | |
| Fungus Growth | None | |

*900 Pair, 26 Gauge Cable

TABLE 2

FIELD TRIALS

| GAUGE | NO. OF CABLES | TLF[1] | MCF[2] |
|---|---|---|---|
| 26 | 47 | 29 | 182 |
| 24 | 22 | 19 | 68 |
| 22 | 29 | 21 | 43 |
| | 98 | 69 | 293 |

[1]TLF - Thousand Linear Feet of Cable

[2]MCF - Million Conductor Feet



HELMUT E. DURR
Western Electric Co., Inc.
2000 Northeast Expressway
Norcross, GA. 30071

Helmut E. Durr is a Senior Staff Engineer with the Western Electric Cable and Wire Product Engineering Control Center. He received a Bachelor of Science degree in Mechanical Engineering from the Institute of Technology of Cologne, Germany. He is a member of the Wire Association and TAPPI. Mr. Durr was Chief Project Engineer for this development.



ROBERT C. BEVERS
Western Electric Co., Inc.
2000 Northeast Expressway
Norcross, GA. 30071

Robert C. Bevers is a Development Engineer with the Western Electric Cable and Wire Product Engineering Control Center. He holds Bachelor of Science in Chemistry and Bachelor of Chemical Engineering degrees from the Georgia Institute of Technology. Since joining Western Electric in 1969, Mr. Bevers has worked on various pulp cable development projects.



ROBERT O. KOCH
Western Electric Co., Inc.
2000 Northeast Expressway
Norcross, GA. 30071

Robert O. Koch is a Development Engineer in the Western Electric Cable and Wire Product Engineering Control Center. He holds a Bachelor of Science in Chemistry degree from Millsaps College and a certificate in Pulp and Paper Engineering from Georgia Tech. Before joining Western Electric, he worked on the Saturn V project.



WILLIAM M.FLEGAL
Western Electric Co., Inc.
2000 Northeast Expressway
Norcross, GA. 30071

William M. Flegal received the Doctor of Philosophy degree from the Georgia Institute of Technology. In 1970, he joined Western Electric's Cable and Wire Product Engineering Control Center as a Senior Development Engineer with primary assignments in plastic insulating development. He is a Professional Engineer and a member of NSPE and ASME. He is a previous contributor to the Wire and Cable Symposium.

# A COMPARISON OF PEF AND FOAM-SKIN CORES

Akira Tsujikawa  Hikaru Yasuhara  Hideo Suzuki  Toshio Ohnuma

The Fujikura Cable Works, Ltd., Sakura-shi, Japan

## ABSTRACT

This paper reports on the comparison of PEF* and foam-skin cores in some mechanical properties of the quad type air core telephone cable.

We found the fact that the mechanical properties of PEF and foam-skin cores are nearly equal in case of the same conductor size, insulation diameter, and volume expansion rate. A choice of the foam-skin core on the cable design requires a little larger amount of PE weight under the same mutual capacitance as PEF. Therefore, the foam-skin core is slightly stronger than PEF. But the difference is small and the material cost of foam-skin must be a little higher than PEF. It is also true for the reverse which the foam-skin can reduce the insulation diameter with the same PE weight as PEF, but it causes serious difficulties to the manufacturing extremely thinner foam and skin layers than PEF because the quad type air core has essentially very thin wall thickness.

So, we may conclude from the facts described above that PEF is more suitable than foam-skin for the quad type air core telephone cable.

## 1. INTRODUCTION

In the recent decade the cellular insulation with high density polyethylene have been rapidly being improved from the solid insulation with low density PE, which had taken place of the paper insulation, for the sake of the material saving[2], the high pair density[3], and the mechanical toughness in the multi-paired telephone cable. There are two types of cellular insulations. The first is PEF which is mainly applied for the pressurized air core cable and the second is foam-skin which is generally used for the jelly filled cable.

Many people studied in various ways about the characteristics of PEF and foam-skin, but those studies were done as the object for the jelly filled cable. This paper reports on the comparison of PEF and foam-skin in some mechanical characteristics. And the quad type air core telephone cable was chosen as the subject of this study, because the cellular insulation cable are widely used in the gas pressurized system in Japan. We dealt with the tensile test and the NEMA type abrasion resistance test of the insulation because these tests could be considered to be mostly basic in mechanical characteristics of cable cores.

* PEF means Foamed Poly-Ethylene[1]

## 2. TEST METHOD

### 2.1 SAMPLES

Uncabled single cores after being extruded are put to the following tests. The insulation material is high flow HDPE[1]. It is used for both skin and foam in case of foam-skin core. Photo 1 and 2 by a scanning electron microscope show respectively the photomicrographs of PEF and foam-skin cores. They are the two of samples applied in this study.

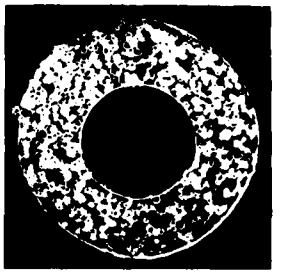


Photo 1 : PEF



Photo 2 : foam-skin

### 2.2 TENSILE TEST

Specimens were only insulated PE about 150 mm long removed from conductors and had just 20 mm gauge lengths marked for measuring the elongation. Each 50 mm of both ends was chucked and the lower chuck was separated from the upper one with a speed of 50 mm/min.

The tensile strength can be calculated by equation (1) using the measured maximum value of pulling force, and in the same way the elongation percentage can be obtained by equation (2) using the measured value which is the stretched gauge length

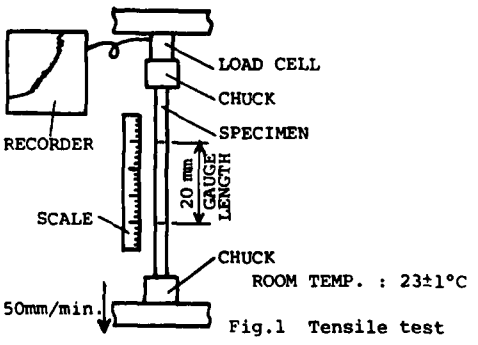



Fig.1 Tensile test

at breaking.

$$\sigma = \frac{P}{A} \quad - - - - - - - - - \quad (1)$$

$$\delta = \frac{(L-20)}{20} \times 100 \quad - - - \quad (2)$$

where :

| | | |
|---|---|---|
| $\sigma$ | : tensile strength | ($kg/mm^2$) |
| P | : maximum pulling force | (kg) |
| A | : cross sectional area of only insulation | ($mm^2$) |
| $\delta$ | : elongation percentage | ( % ) |
| L | : final gauge length at breaking | ( mm ) |

2.3 ABRASION RESISTANCE TEST[4]

Fig.2 shows the manner of NEMA type abrasion resistance test. One end of core sample with conductor about 1 m long was fixed and the tension T was constantly given to the core at the other end. The reasonable tension T is shown in table 1.

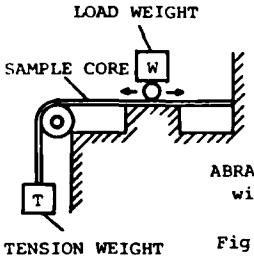



Table 1

| conductor (mmϕ) | 0.4 | 0.5 | 0.65 |
|---|---|---|---|
| tension T ( g ) | 80 | 125 | 210 |

STROKE : 10 mm
SPEED : 1 Hz
ROOM TEMP. : 23±1°C
ABRASION ROD : 4 mmϕ
with extremely smooth surface

Fig.2 Abrasion resistance test

A number of scrape times till the abrasion rod contacting with the conductor was obtained correspondingly to a proper load weight W. As it is well known that the scattering of the measurements by this method tends to be very large for the reason of the unbalance of wall thickness, the oily surface of the core by finger grease, and others, we carried out the following original manner. The sample core was put on the equipment after wiping the grease on its surface with alcohol. The average value was calculated at every measurement, and the specimen was rotated by 90 degrees and advanced 30 mm after each time. The test was repeated till the scattering was within 5 % of that average value and the convergent value was considered the desirable one. The abrasion resistance curve of one sample as in Fig.3 is obtained if those several desirable values against various load weights were plotted in a semi-logarism graph.

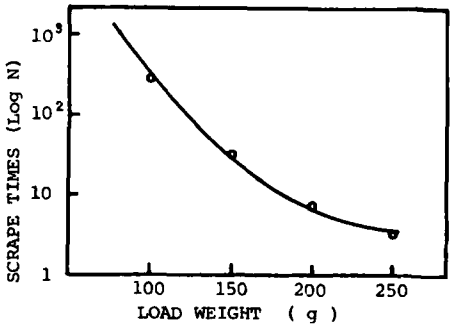



Fig.3 Typical curve of the abrasion resistance characteristic

## 3. AN EXAMINATION OF CONSTANT CONDUCTOR SIZE AND INSULATION DIAMETER

In the beginning, single cores which had a constant conductor size 0.65 mmϕ, a constant insulation diameter 1.05 mmϕ, and various expansion rates were put to the tests in the mechanical characteristics above mentioned. Samples of foam-skin cores had not only various expansion rates of foam layer but also 30, 40, and 50 μm of skin thicknesses. Fig.4 shows the relation between the volume expansion rate and the tensile strength. By the way, the volume expansion rate means the geometrical content of cells in PE insulation defined by the following equation (3). In the case of foam-skin core it means the overall expansion rate including both skin and foam layers.

$$\eta_V = [1 - \frac{W}{\frac{\pi}{4}(D^2 - d^2)\rho}] \times 100 \quad - - - - \quad (3)$$

where :

| | | |
|---|---|---|
| $\eta_V$ | : volume expansion rate | ( % ) |
| W | : PE weight per unit core length | ( g/m ) |
| D | : overall insulation diameter | ( mmϕ ) |
| d | : conductor diameter | ( mmϕ ) |
| $\rho$ | : PE density | ($g/cm^3$) |

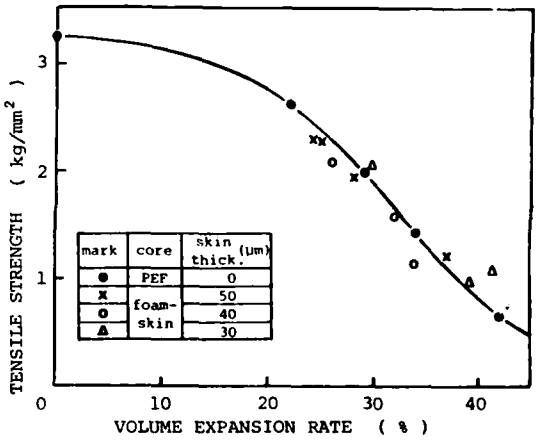



Fig.4 Relation between tensile strength and volume expansion rate

It can be read from Fig.4 that the tensile strength of insulation becomes weaker as increasing of the expansion rate. It is still more interesting that PEF and foam-skin have almost the same tensile strength.

Now Fig.4 could be rewrited by the PE weight per unit core length instead of the volume expansion rate, because the PE weight is equivalent to the expansion rate on the occasion of a constant conductor size and insulation diameter.

Fig.5, Fig.6, and Fig.7 show respectively the tensile strength, the elongation percentage, and the number of scrape times at W=800 g against PE weight per unit core length. It makes more clear that the difference between PEF and foam-skin cannot be observed in these figures.

From above results, we could get the assumption that the mechanical properties of single core

on the tensile test and the abrasion resistance test have respectively relationships with the PE weight per unit core length and with no difference between PEF and foam-skin.

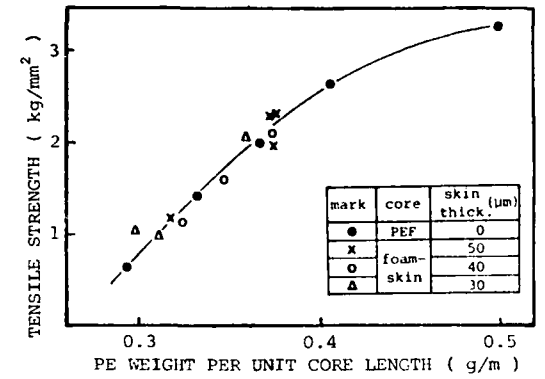



Fig.5 Relation between tensile strength and PE weight per unit core length

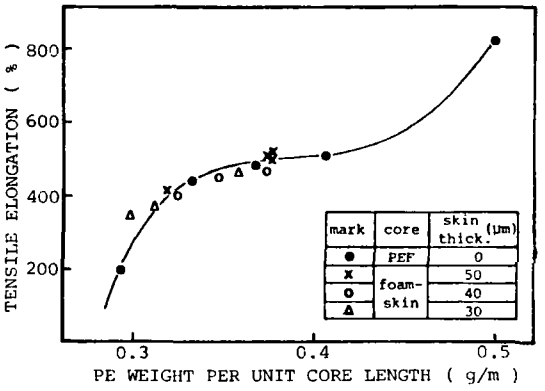



Fig.6 Relation between tensile elongation and PE weight per unit core length

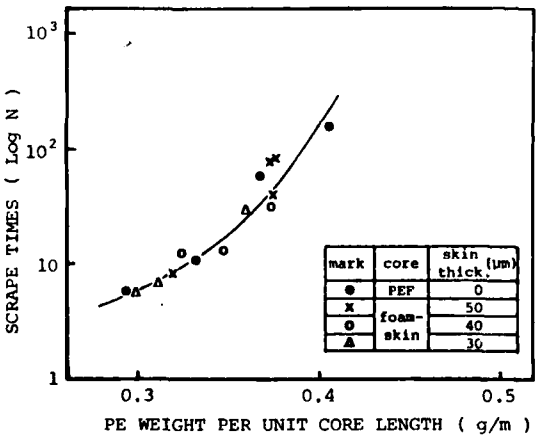



Fig.7 Relation between number of scrape times at W=800 g and PE weight per unit core length

## 4. AN EXAMINATION OF VARIOUS CONDUCTOR SIZES, INSULATION DIAMETERS, AND EXPANSION RATES

PEF and foam-skin cores which had 0.4, 0.5, and 0.65 mmϕ of conductor sizes and 0.56～1.05 mmϕ of insulation diameters and 20, 30, and 40 % of volume expansion rates were put to the same tests as before for the purpose of the extension of this study. Fig.8 shows the tensile strength and elongation v.s. PE weight in one graph. It can be read from these curves that both strength and elongation are nearly unchangeable against the variation of PE weight if the volume expansion rate was kept constant. In other words the tensile strength and elongation depend on not PE weight but volume expansion with no difference between PEF and foam-skin. However, the curves depending on the PE weight by the parameter of the expansion can be obtained if the maximum pulling force was adopted to the vertical axis instead of the tensile strength as in Fig.9.

Next, the result of abrasion resistance test is shown in Fig.10. The horizontal axis is PE weight per unit core length and the vertical axis is

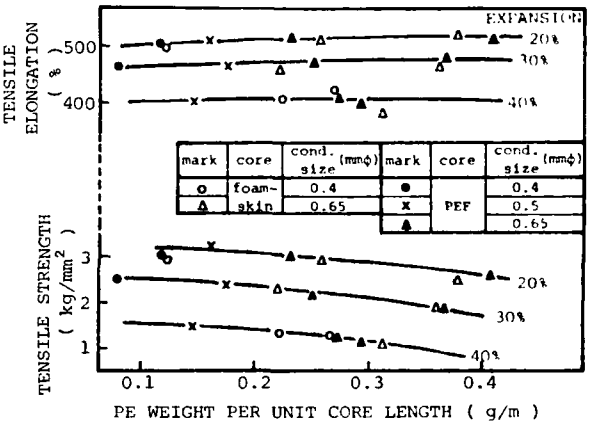



Fig.8 Curves of tensile strength and tensile elongation v.s. PE weight per unit core length

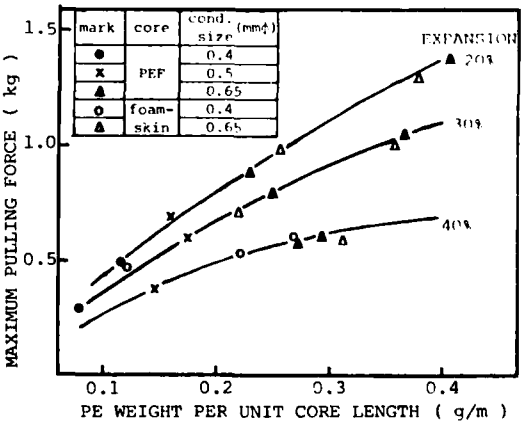



Fig.9 Relation between maximum pulling force and PE weight per unit core length

the load weight on which the number of scrape times comes to 100. The reason why the load weight is scaled on the vertical axis is as follows. Several curves in Fig.11 could be obtained when various samples were put to the NEMA type abrasion resistance test. In the figure, the curves covering any sample core are sought in the range of scrape times N=10～100. Therefore, the load weights are convenient to the evaluation of the abrasion resistance characteristic of many sample cores. So, we compared them by the load weights $W_1$, $W_2$, $W_3$ --- which the number of scrape times N=100.

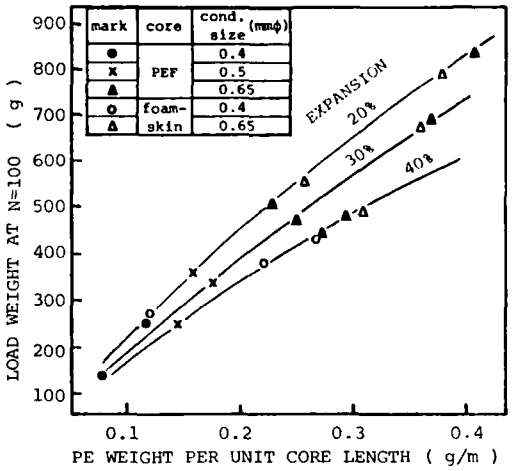



Fig.10 Relation between load weight at N=100 and PE weight per unit core length

It can be read from Fig.10 that the abrasion resistance characteristic has no difference between PEF and foam-skin and has a relation with PE weight and without conductor size and insulation diameter, same as pulling force in Fig.9.

As above results, the forementioned assumption in chapter 3 can be developed into the following theory. The mechanical properties of single core on the tensile and abrasion resistance tests have respective relations with PE weight per unit core length by the parameter of the volume expansion rate without regard of conductor size and insulation diameter and have no difference between PEF and foam-skin.

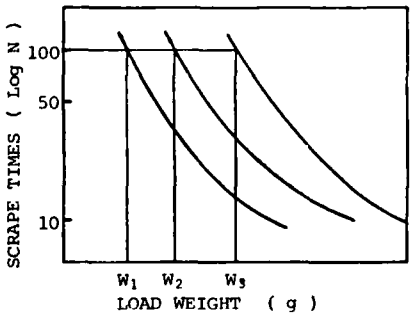
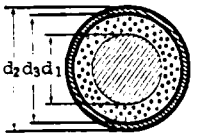



Fig.11 Curves of abrasion resistance characteristic for explanation

## 5. A DISCUSSION OF PEF AND FOAM-SKIN IN CASE OF SAME CAPACITANCE

### 5.1 IN CASE OF THE SAME CAPACITANCE OF SINGLE CORE

Let's examine the relation between the capacitance of single core and the expansion rate making a comparison of PEF and foam-skin.




We assume that :

$d_1$ : conductor diameter (mmφ)
$d_2$ : overall insulation diameter (mmφ)
$d_3$ : foam layer diameter (mmφ)
$\eta_f$ : expansion rate in only foam layer ( % )
$\eta_v$ : volume expansion rate ( % )
$C$ : capacitance of single core (pF/m)
$\varepsilon_f$ : dielectric constant of only foam layer
$\varepsilon_b$ : dielectric constant of original PE
$\varepsilon$ : equivalent dielectric constant of a core
$W_s$ : PE weight of skin layer (g/m)
$W_f$ : PE weight of foam layer (g/m)
$\rho$ : PE density of original PE (g/cm³)

$$C = \frac{\varepsilon}{18 \cdot \ln(d_2/d_1)} \times 10^3$$

$$\varepsilon = \frac{\varepsilon_f \cdot \varepsilon_b \cdot \ln(d_2/d_1)}{[\varepsilon_f \cdot \ln(d_2/d_3) + \varepsilon_b \cdot \ln(d_3/d_1)]}$$

$$\frac{(\varepsilon_b - \varepsilon_f)}{(\varepsilon_b - 1)} \approx \frac{3 \cdot \varepsilon_f}{(2 \cdot \varepsilon_f + 1)} \times \frac{\eta_f}{100}$$

$$W_S = \frac{\pi}{4}(d_2^2 - d_3^2)\rho$$

$$\eta_f = \left[1 - \frac{W_f}{\frac{\pi}{4}(d_3^2 - d_1^2)\rho}\right] \times 100$$

$$\eta_v = \left[1 - \frac{W_S + W_f}{\frac{\pi}{4}(d_2^2 - d_1^2)\rho}\right] \times 100$$

from above equations

in case of foam-skin

$$\eta_f = \frac{[E - 18 \cdot C \cdot \ln(d_3/d_1)][36 \cdot \varepsilon_b \cdot C \cdot \ln(d_3/d_1) + E]}{54 \cdot E(\varepsilon_b - 1)C \cdot \ln(d_3/d_1)} \times 100$$

$$\eta_v = \frac{d_3^2 - d_1^2}{d_2^2 - d_1^2} \times \eta_f$$

where : $E = \varepsilon_b \times 10^3 - 18 \cdot C \cdot \ln(d_2/d_3)$

in case of PEF, substitute $d_3 = d_2$ into above equations

$$\eta_f = \frac{[E - 18 \cdot C \cdot \ln(d_2/d_1)][36 \cdot \varepsilon_b \cdot C \cdot \ln(d_2/d_1) + E]}{54 \cdot E(\varepsilon_b - 1)C \cdot \ln(d_2/d_1)} \times 100$$

$$= \eta_v$$

where : $E = \varepsilon_b \times 10^3$

Now let's calculate the expansion rate assuming the capacitance of single core to be 200 pF/m. If $d_1$=0.65 mmφ, $d_2$=1.05 mmφ, skin thickness=50 μm, $\varepsilon_b$=2.33, then $\eta_f$, $\eta_v$, PE weight are obtained in table 2.

Table 2

| | $\eta_f$ (%) | $\eta_v$ (%) | PE weight (g/m) |
|---|---|---|---|
| PEF | — | 39.0 | 0.307 |
| foam-skin | 46.9 | 33.1 | 0.337 |

As above, we got the fact that the volume expansion rate of foam-skin core is lower than that of PEF, in other words the foam-skin core needs more amount of PE than PEF on such assumption as a constant insulation diameter and a constant capacitance of single core. We can save the materials about 10 % if PEF core would be chosen.

On the other hand, foam-skin core has higher mechanical strength. read from Fig.9 and Fig.10 and tabled in table 3.

Table 3

| | pulling force ( kg ) | load weight of abrasion test(g) |
|---|---|---|
| PEF | 0.65 | 500 |
| foam-skin | 0.88 | 590 |

5.2 IN CASE OF THE SAME MUTUAL CAPACITANCE OF TELEPHONE CABLE

We compared between PEF and foam-skin about the dimensional structures when the mutual capacitance in the quad type air core cable was 50 nF/km. Fig.12 shows the relations of the expansion rate and the PE weight against to the various overall insulation diameters in the case of 0.4 mmϕ conductor size.

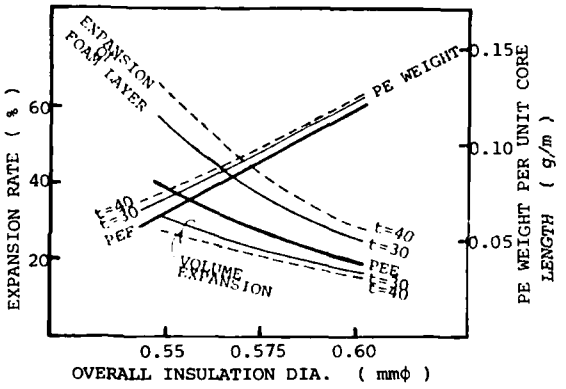



Fig.12 Relations of expansion rate and PE weight against to various overall insulation diameters

This graph could be obtained from the manufacturing data of PEF cables made in Fujikura Cable Works and the partial calculative data. Examples are shown in table 4, in which the insulation diameter is 0.58 mmϕ[5] in Fig.12.

Table 4

| | wall thick. ( μm ) | | expansion ( % ) | | PE weight ( g/m ) |
|---|---|---|---|---|---|
| | foam | skin | foam | overall | |
| PEF | 90 | — | — | 26 | 0.096 |
| foam-skin 1 | 60 | 30 | 34 | 21.5 | 0.102 |
| foam-skin 2 | 50 | 40 | 39 | 20 | 0.104 |

It become clear from table 4 that the foam-skin requires about 6 % heavier PE weight than PEF in this case.

Taking it the other way round, foam-skin can reduce the insulation diameter with the same PE weight as PEF. This is very important for a cable design because the limited dimension of underground cable ducts demands the higher pair density. However, one serious problem comes out. We shall discuss this problem a little further. We can rearrange into table 5 from Fig.12 in the condition that PE weight per unit core length is 0.096 g/m.

Table 5

| | wall thick. ( μm ) | | expansion ( % ) | | PE weight ( g/m ) | overall dia. (mmϕ) |
|---|---|---|---|---|---|---|
| | foam | skin | foam | overall | | |
| PEF | 90 | — | — | 26 | 0.096 | 0.580 |
| foam-skin3 | 57 | 30 | 38 | 23 | 0.096 | 0.574 |
| foam-skin4 | 46 | 40 | 45 | 22 | 0.096 | 0.572 |

The insulation diameter will be surely made small, therefore the foam-skin will possively reduce the cable diameter as about 1 % as PEF. But nobody can commercially produce such a core because it is very difficult to get a good cell structure and a good concentricity for such thin thickness in both foam and skin layers according to many experiances.

So, foam-skin must be disadvantageous by the restriction on manufacturing techniques in the condition of such thin thickness.

## 6. CONCLUSION

It became clear that the mechanical properties of single core on the tensile and abrasion resistance tests have respectively relationships with the PE weight per unit core length and with no difference between PEF and foam-skin by the first examination of a constant conductor size 0.65 mmϕ and a constant insulation diameter 1.05 mmϕ.

*Next, by the second examination of* various conductor sizes 0.4～0.65 mmϕ, and various expansion rate 20～40 %, it became also clear that the tensile strength and elongation depend on not the PE weight per unit core length but the volume expansion rate. And the maximum pulling force in the tensile test and the abrasion resistance depend on the PE weight per unit core length by the parameter of volume expansion rate, and no difference between PEF and foam-skin in this examination.

It was derived from the calculation of some equations that a foam-skin core requires more amount of PE weight if both PEF and foam-skin cores have same capacitance, conductor size, and insulation diameter. Taking it the other way round, a foam-skin can reduce the insulation diameter with the same PE weight as PEF. However, as for a fine gauge conductor like 0.4 mmϕ, it is very difficult to get a good cell structure and a good concentricity because of very thin thickness in both foam and skin layers in the case of quad type air core cable.

These above mentioned are summarized again as follows. A choice of foam-skin core on the cable design requires a little larger amount of PE weight under the same mutual capacitance as PEF. Therefore, the foam-skin core is slightly stronger than PEF. But the difference is very small and also the material cost of foam-skin must be a little higher than PEF. It is also true for the reverse which the foam-skin can reduce the cable diameter, but it causes serious difficulties to the manufacturing for the very thin thickness in both foam and skin

layers because the insulation core of the quad type air core cable has essentially thin wall thickness.

So, we may conclude from the facts described above that PEF is more suitable than foam-skin for the quad type air core telephone cable, though foam-skin has many advantages as reported by other persons.

## ACKNOWLEDGEMENT

Many members in Fujikura Cable Works have made important contributions to our study. The authors wish to acknowledge them and especially express deep appreciations for much advice of manager Mr. M. Ishibashi and Mr. K. Nakano with whom the authors had many discussions at the early stage of this study.

## REFERENCES

1. K. Ogawa, S. Tanaka, A. Tsujikawa, H. Ishihara "A NEW FOAMED POLYETHYLENE INSULATED JUNCTION CABLE FOR TELECOMMUNICATION" 1971 20th IWCS
2. D. M. Mitchell and G. H. Webster "MATERIAL SAVING BY DESIGN IN EXCHANGE AND TRUNK TELEPHONE CABLE 1974 23rd IWCS
3. T. D. Nantz "AN INCREASED PAIR DENSITY UNDERGROUND FEEDER CABLE" 1978 27th IWCS
4. J. Takizawa, K. Ohshima, K. Nishimura, and K. Ohgaki "A PEF-LAP CABLE JUST BEGUN TO BE GENERALLY USED INTO LOCAL JUNCTION NETWORK" April 1974 Shisetsu
5. M. Tokuoka and T. Nakajima "LOCAL PEC CABLE — LOCAL MULTI-PAIR CABLE FULLY COLOUR CODED" April 1980 Shisetsu



Toshio Ohnuma
Engineer

Telecommunication Cable Research & Development Department. The Fujikura Cable Works, Ltd. Sakura-shi, Chiba-ken, Japan.

Mr. Ohnuma was born in 1948. He received the B.E. degree in mechanical engineering from Tokyo Institute of Technology in 1972 and joined The Fujikura Cable Works, Ltd. He is taking charge of the development of insulating and jacketing techniques.



Akira Tsujikawa
Manager

Telecommunication Cable Research & Development Department. The Fujikura Cable Works, Ltd. Sakura-shi, Chiba-ken, Japan.

Mr. Tsujikawa was born in 1937. He received the B.E. degree in electrical engineering from Keio University in 1961 and joined The Fujikura Cable Works, Ltd. He is responsible for Telecommunication Cable R. & D. Dept. He is a member of the Institute of Electronics and Communication Engineers of Japan.



Hikaru Yasuhara
Chief

Telecommunication Cable Research & Development Department. The Fujikura Cable Works, Ltd. Sakura-shi, Chiba-ken, Japan.

Mr. Yasuhara was born in 1942. He received the B.E. degree in electronics engineering from Tokyo University in 1966 and joined The Fujikura Cable Works, Ltd. He is responsible for the development and engineering of telephone cables. He is a member of Electronics and Communication Engineers of Japan.



Hideo Suzuki
Engineer

Telecommunication Cable Research & Development Department. The Fujikura Cable Works, Ltd. Sakura-shi, Chiba-ken, Japan.

Mr. Suzuki was born in 1948. He received the B.E. degree in polymer chemistry from Gunma University in 1971 and joined The Fujikura Cable Works, Ltd. He is responsible for the development of plastic materials and polymer processings. He is a member of The Society of Polymer Science Japan.

# DEVELOPMENT, CHARACTERIZATION, AND PERFORMANCE OF AN IMPROVED CABLE FILLING COMPOUND

D. M. Mitchell
R. Sabia

Bell Laboratories
Norcross, Georgia

## ABSTRACT

Multipair telephone cable containing waterblocking material is widely used for buried feeder and distribution service. Compounds based on petrolatum have been used successfully to protect the cable core from water entry. A new filling compound has been developed that retains the waterblocking reliability of petrolatum and offers the following improvements:

- Facilitates cable splicing.
- Eliminates the need for removing filling compound from cable core prior to the application of selected encapsulants.
- Improves cable flexibility at low temperatures.
- Reduces soiling and staining due to handling filled cable.

Exhaustive laboratory and field tests have characterized the physical and chemical properties of the material and confirmed its performance in cable. The results indicate that the characteristics of filled cable are improved significantly by the new compound.

## 1. INTRODUCTION

A new filling compound, FLEX-GEL has been developed to replace petrolatum based materials for use in waterproof cables. Performance tests on FLEX-GEL filled cables compared to results on petrolatum filled cables show that we can expect continued reliability of the buried filled cable plant and, additionally:

- Reduced time for cable splicing.
- Elimination of need for cleaning cable splices prior to encapsulation.
- Improved low and high temperature properties.
- Reduced soiling and staining of craftspersons handling the filled cable core.

In presenting this development:

- Section 2 reviews the evolution of filled cable and lists requirements for an improved filling compound.
- Section 3 highlights materials properties critical to a new compound.
- Section 4 discusses classes of materials considered and their limitations.
- Section 5 identifies an oil extended thermoplastic rubber, FLEX-GEL, as a compound that exhibits properties suitable for use as a filling compound.
- Section 6 covers preferred FLEX-GEL compositions.
- Section 7 compares the performance of insulation materials exposed to FLEX-GEL and petrolatum.
- Section 8 reports performance data on cable filled with FLEX-GEL and petrolatum.

## 2. BACKGROUND

A multipair telephone cable consists of insulated conductors grouped in units to form a core and enclosed within a protective sheath. The conductors occupy approximately half of the volume within the core; the remainder is distributed in the interstitial space between conductors.

When a cable is buried, it may be literally immersed in water. Experience has shown that water can enter the core due to damage to the sheath, or accidental leaks can occur at prepared sheath openings.

Plastic insulation alone is not sufficient protection against the effects of water in telephone cable. On the contrary, although the plastic insulation may prevent an immediate indication of water in the cable core, that very insensitivity poses a serious maintenance problem. As water travels along the cable, the transmission properties deteriorate as:

- The air in the interstices is displaced by water.
- Pinholes in the insulation, harmless when dry, are bridged by water, causing noise or crosstalk.
- Open circuits occur due to corrosion.

Furthermore, a trouble indication may be remote from the point of water entry, making location and repair of the leak difficult. The filled cable design, Figure 1, was developed to overcome the shortcomings of plastic insulated cables. In a filled cable, all interstitial spaces are filled and all sheath layers are flooded with hydrophobic compounds.

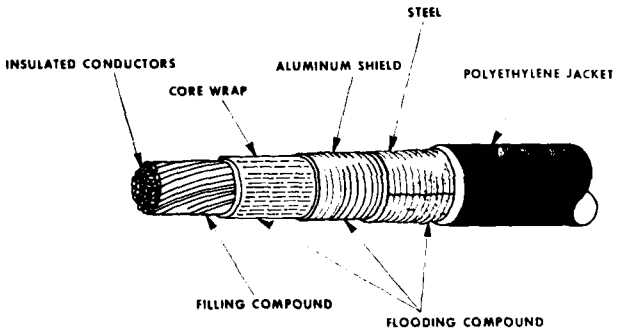



**FIGURE 1. WATERPROOF CABLE WITH ASP SHEATH**

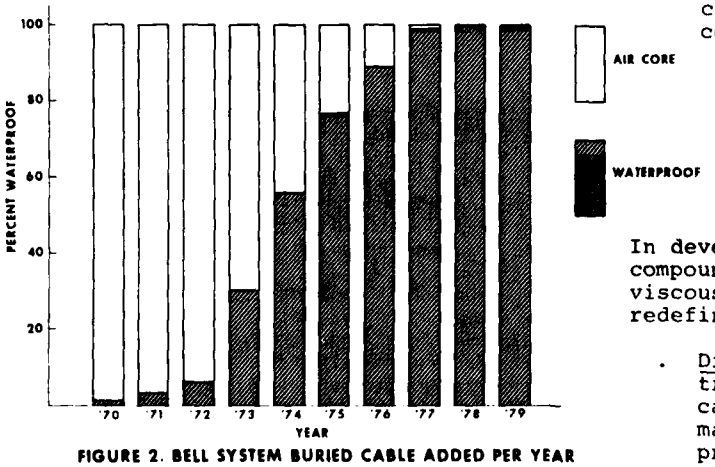



**FIGURE 2. BELL SYSTEM BURIED CABLE ADDED PER YEAR**

From its introduction[1] to the Bell System over eleven years ago, the use of waterproof cable on buried distribution and feeder routes has grown dramatically, Figure 2. Sealed connectors, encapsulated splices, and filled service wires and stubs were developed[2] to provide a waterproof system. Maintenance records indicate that upkeep is less than one-tenth that involving buried air core cable. This success has been due to the use of petrolatum as the filling compound. The economy and effectiveness of petrolatum have made the search for a material offering the same performance reliability with improved characteristics a difficult one.

A successful candidate was required to meet a restrictive set of selection criteria:

- Be compatible with design requirements for telephone cable.
- Retain the performance reliability of present waterproof cable.
- Meet strict safety standards.
- Be compatible with present cable manufacturing methods.
- Be compatible with other materials in the outside plant.
- Be economical.
- Permit reliable encapsulated splices without the necessity for compound removal in the splice area.
- Reduce splicing time.
- Improve low temperature flexibility.
- Resist high temperature displacement and drip.
- Reduce the soiling and staining associated with handling waterproof cable cores.

## 3. MATERIALS CONSIDERATIONS

In developing an improved cable filling compound the dielectric, thermal and viscous requirements were reexamined and redefined where necessary.

- Dielectric Properties - A low dielectric constant is desirable to minimize cable cost. Petrolatum, a hydrocarbon material, exhibits acceptable properties.

- Thermal Properties - In order to exhibit more uniform properties in the field environment, the compound should not exhibit thermal transitions from about -20 to +60C. Petrolatum undergoes continuous melting from about -10 to 80C. Thus, it is continuously changing from a hard wax to an oil.

- Viscous Properties - Since cables are filled as units or as cores, the viscosity-temperature profile of the filling compound is limited by the thermal properties of the insulation. The viscosity-temperature profile of petrolatum is compatible with high density polyethylene and polypropylene. Other manufacturing considerations are line speed and filling pressure.

## 4. CLASSES OF MATERIALS

In this section various classes of potential filling compounds are discussed. Where pertinent, desirable properties are identified.

a. Microcrystalline Gels - Petrolatum is classical example of a microcrystalline gel. Synthetic microcrystalline gels have been investigated by Sabia and Kaufman[3] and by McReynolds and Mitacek[4] using polyethylene and mineral oils. Other combinations are possible. For example, a blend of polybutene and polyethylene has been used widely by the Bell System.[5] These gels, compared to petrolatum can exhibit desirable properties, but, as greases, they would not be considered by cable splicers to be an improvement in cable filling compounds.

b. Modified Petrolatum - Many cable filling compounds are modified petrolatum. The additive may be polyethylene[6] in combination with "amorphous" polypropylene, polybutene, polyisobutylene,[7] etc. These additives improve the high temperature properties by increasing the melting range (with polyethylene) or by increasing the viscosity (with polyisobutylene). However, the low temperature properties and other handling characteristics are degraded.

c. Greases - This broad class of materials may be classified in three types. Soap greases consist of mineral oils and metal soaps. Nonsoap greases consist of mineral oils gelled with agents derived from clays. Synthetic greases consist of synthetic oils thickened with inert materials, such as fine silica. Materials from this class have been commercially introduced in filled closures[8] and filled connectors. Although they can exhibit desirable physical properties, these materials were not considered as cable filling compounds because of their high dielectric constants and "greasy" nature.

d. Foams - Two foam filled cable designs have been evaluated but are not commercially available.

One system consisted of a foamed polyurethane.[9] An extensive critique of this system is outside the scope of this paper, but the resulting cable was very stiff and did not appear to offer any advantage over petrolatum.

A more promising system consisted of hollow beads in a matrix.[10] Depending on the matrix chosen and pending the solution of several processing challenges, such a system could meet several of our objectives. A variation is to use hollow fibers in an organic matrix. Hollow fibers occur in nature and may be inorganic (chrysotile) or organic (the fur of polar bears). The former has been the subject of patents on the gelling of oils.[11] These hollow fibers were considered early in our developments of water blocking compounds but presented several technical challenges based on our study of oils gelled with 3 denier polypropylene fibers.[12]

e. Hydrophilic Materials - These are materials which form a gel in the presence of water. They may be derived from protein (e.g., gelatin) or polysaccharides (e.g., methylcellulose) or may be synthetic (e.g., acrylamides). Many patents and various cable designs[13] have been based on these materials.[14] A critique of these materials is outside the scope of this paper. A major objection is that a filled cable design based on these materials (continuous or as blocks) allows a significant change of the transmission characteristics if the cable is violated in the presence of water.

f. Reactive, Two Part Systems - This class includes polyurethane and epoxy systems. As discussed below, these materials exhibit poor dielectric properties. Yet, their physical properties (see below) are very desirable in an improved cable filling compound.

Two part polyurethanes are being used to fill cables. One low viscosity (~20 cps) compound is currently used to reclaim water logged PIC cables.[15] Another, medium viscosity (~300 cps) polyurethane, developed for filling closures,[16] is currently also used to fill stubs for coils and repeaters.

These compounds, although highly oil extended, exhibit high dielectric properties. Thus, reclamation of a water logged cable, with carrier or loaded systems, is restricted to about 350 feet between repeaters or load points.[17] It follows that the dielectric properties of polyurethanes are acceptable for stubs since they are 50 feet or less. Although it is possible to design a filled cable to accommodate the dielectric properties of these materials, the cost would be prohibitive.

These polyurethanes do not exhibit any transitions from -20 to +60°C. They are flexible at low temperatures, and exhibit low tear strength. Water resistance performance in the field has been excellent.[18] The reaction of craft in handling the filled stub during splicing has been very favorable. For these reasons, the polyurethane system developed for filling splices[16] was set up as a model compound in terms of handling and splicing.

The physical properties of an oil extended thermoplastic rubber have been discovered to parallel those of the oil extended polyurethane discussed in (f) but with excellent dielectric properties as well. The resulting compounds have been found to meet all requirements listed in Section 2.

## 5. FLEX-GEL CONSTITUENTS

This section will briefly discuss the properties of the oil and rubbers utilized in the compounding of FLEX-GEL.

a. Oils - The criteria for ASTM compounding oils are shown in Table I. There are five compounding oils, depending on the percent saturates. Oils high in aromatic content cause stress cracking of polycarbonates commonly used in splicing connectors and exhibit high dielectric constants. As a class, ASTM Type 101, 102 and 103 oils are not acceptable. In contrast, selected naphthenic and paraffinic oils (ASTM Types 104A and 104B) exhibit acceptable dielectric properties, and do not crack polycarbonates.

b. Rubbers - Styrene block copolymers in which the polystyrene blocks sandwich a rubber block, Figure 3, constitute an unique class of thermoplastic rubbers. Variations include branched or "star" structures. Three basic types have been commercialized, distinguished by the rubber block. The rubber block may be polybutadiene (coded SBS), polyisoprene (SIS) or an ethylene/butylene copolymer (SEBS). The thermoplastic properties arise from the incompatibility at use temperatures between the polystyrene and rubber blocks. The aggregation of the styrene blocks results in domains[19] that act as cross links, Figure 4.

TABLE I

THE CRITERIA FOR ASTM COMPOUNDING OIL TYPES

ASTM D-2226

| ASTM Type | % Saturates |
|---|---|
| 101 | 20 max |
| 102 | 20.1-35 |
| 103 | 35.1-65 |
| 104 A (naphthenic)[1] | 65.1 min. |
| 104 B (paraffinic)[2] | 65.1 min. |

1. Exhibit a viscosity-gravity constant greater than 0.820, ASTM D-2501.
2. Exhibit a viscosity-gravity constant of 0.820 maximum, ASTM D-2501.

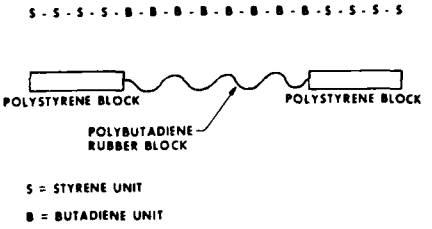



FIGURE 3. DIAGRAMMATIC REPRESENTATION OF A THERMOPLASTIC RUBBER CHAIN

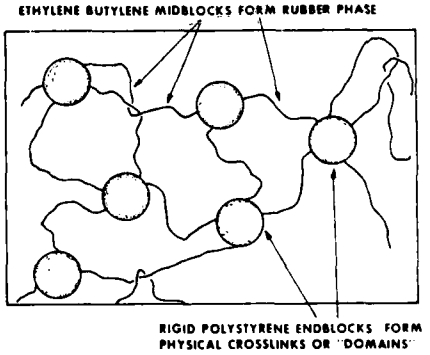



FIGURE 4. DIAGRAMMATIC REPRESENTATION OF A THERMOPLASTIC RUBBER STRUCTURE

Similarly, compatibility of extender oils and the rubber block is necessary for compounding. For example, only aromatic oils will dissolve the SBS copolymers.

The SIS copolymers dissolve with some difficulty in naphthenic oils at high temperatures. On cooling, the styrene blocks come out of solution and associate. The resulting products exhibit desirable properties. One compound based on SIS is used in the Bell System as a water blocking material.[20] This copolymer was not selected for the improved cable filling compound because:

- The limited compatibility with naphthenic/paraffinic oils requires extensive mixing.
- High blending temperatures (140°C) can result in degradation of the polyisoprene block.
- The polyisoprene block is highly susceptible to oxidative degradation at lower temperatures.
- Commercial SIS grades in compositions of interest exhibit tack.

The SEBS copolymers overcome the objections to the SIS copolymers:

- The copolymers dissolve readily in naphthenic and/or paraffinic oils.
- At the low blending temperatures (120-130°C) the copolymer exhibits adequate stability.
- The saturated rubber block can be adequately stabilized.
- The compositions of interest do not exhibit tack.

## 6. PREFERRED COMPOSITIONS

The phase diagram in Figure 5 delineates the composition. The improved cable filling compound is constituted of three major components, a rubber, and extender oil and polyethylene.[21] Minor components are a stabilizer and a compatibilizer.[22] The oil is added to lower the viscosity and the tear strength of the rubber. Polyethylene is added to improve the slump (sag) properties at high temperatures without increasing the viscosity. Compounds based on Figure 5 have been termed FLEX-GEL.

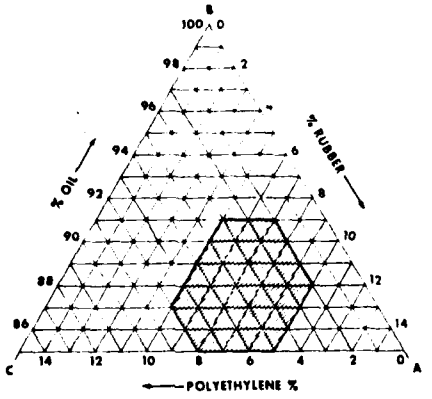



**FIGURE 5. PHASE DIAGRAM OF PREFERRED COMPOSITIONS**

Properties for a typical FLEX-GEL formulation are given in Table II. The striking feature when compared to petrolatum is that FLEX-GEL compositions exhibit tensile properties rather than being "greasy."



Compared to the oil extended polyurethane identified earlier as a "model" compound, the tensile and tear strengths of the FLEX-GEL compound listed in Table II are approximately 1/5 their value. In contrast to the polyurethane, the new compound exhibits low dielectric values and is a thermoplastic.

The thermograms of a FLEX-GEL composition and the petrolatum currently used by Western Electric are compared in Figure 6. Petrolatum exhibits a broad endothermic (melting) transition from about -6 to +80°C. In this range, the petrolatum changes from a hard wax to an oil. In contrast, the FLEX-GEL composition exhibits a transition at -72°C probably associated with the extended rubber. A second transition at about 62°C is associated with glass transition of the polystyrene domains. The melting endotherm peak at about 98°C is associated with melting of the polyethylene. Thus, the objective of designing a compound which does not undergo a transition in the range of -20 to +60°C has been attained.

The differences in the thermal properties between the FLEX-GEL composition and the petrolatum in Figure 6 are very evident in Figure 7. Here the storage and loss moduli, G' and G", at 1 Hz are plotted versus temperatures. The storage modulus, G' between 0 and 60°C of petrolatum changes by a factor of $10^6$. In contrast G' for FLEX-GEL changes by a factor of 30.

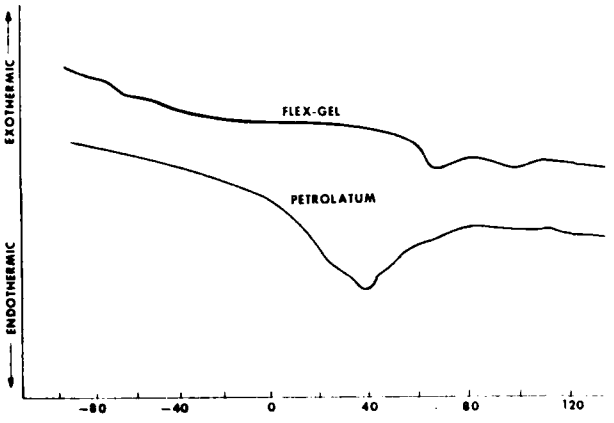



**FIGURE 6. THERMOGRAMS OF FLEX-GEL AND PETROLATUM**

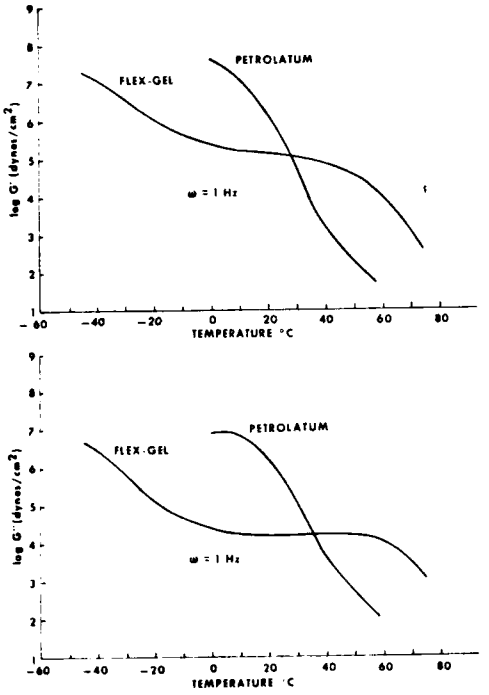



**FIGURE 7. DYNAMIC MECHANICAL PROPERTIES OF FLEX-GEL AND PETROLATUM**

Similarly, the loss modulus, G", which reflects the viscous properties changes significantly with petrolatum. In contrast, G" of the FLEX-GEL formulation is nearly constant in the temperature range of interest, -20 to +60°C.

The conclusion from examination of Figures 6 and 7 is that FLEX-GEL will exhibit improved low and high temperature properties in comparison to petrolatum. How these differences are reflected in cable performance will be discussed in Section 8.

## 7. INTERACTIONS WITH INSULATION MATERIALS

The compatibility of insulation materials with the oils in FLEX-GEL is a primary consideration. Studies outlined below show that insulation materials perform satisfactorily after exposure to FLEX-GEL.

In one study, insulation grade materials were milled and compression molded. Microtensile bars were then immersed in petrolatum and various oils at various temperatures. Typical results are reported in Table III. The weight gains after 3,000 hours at 70°C in various oils are comparable to the gain in petrolatum. Similarly, the loss in tensile properties is comparable.

TABLE III

AGING OF INSULATION GRADE MATERIALS

| Insulation Grade Polymer | Environment | % Change After 3070 hrs at 70°C Weight Gain | Loss in Ultimate Elongation | Loss in Tensile Strength |
|---|---|---|---|---|
| High density ethylene copolymer | Shellflex 310 | 9.3 | 15 | [illegible] |
| | Shellflex 371 | 12.0 | 19 | 32 |
| | Drakeol 35 | 8.1 | 11 | 18 |
| | Petrolatum | 7.3 | 44 | 35 |
| | Air | -3.6 | 16 | 17 |
| Propylene copolymer | Shellflex 310 | 24 | 0 | 11 |
| | Shellflex 371 | 26 | 0 | 17 |
| | Drakeol 35 | 23 | 0 | 23 |
| | Petrolatum | 18 | 15 | 4 |
| | Air | 0.6 | 25 | 0 |

In another study, 22 gauge conductors with plastic skin/foam insulation (DEPIC)[23] were exposed at 70°C to petrolatum and to a FLEX-GEL formulation. The stripping force after various intervals is reported in Table IV. The data (which are relevant, for example, if the cable is terminated on binding posts) show no degradation on exposure to FLEX-GEL.

TABLE IV

STRIPPING FORCE OF DEPIC INSULATION

| Time at 70°C, Hours | Average Force, lb/inch Environment: Petrolatum | FLEX-GEL |
|---|---|---|
| 0 | 0.26 | 0.26 |
| 1 | 0.29 | 0.22 |
| 24 | 0.19 | 0.20 |
| 192 | 0.13 | 0.21 |
| 256 | 0.16 | 0.23 |

In a third study, still in progress, the oxidative stability of insulation exposed to FLEX-GEL insulation is being determined. Initially, the oxidation time at 120°C and 140°C was measured for DEPIC insulation retrieved from filled cables. The data in Table V for petrolatum and FLEX-GEL exposed insulation are comparable. In long term tests, FLEX-GEL filled cables are undergoing aging in laboratory accelerated pedestal environments[24] and in an outdoor exposure test site in Yuma, Arizona. Again, data gathered show comparable performance between petrolatum and FLEX-GEL filled cable.

TABLE V

OXIDATIVE STABILITY AS DETERMINED BY OXYGEN UPTAKE

| DEPIC (High Density Polyethylene) | Oxidation Times,* Hours, At | |
|---|---|---|
| Insulation From | 130°C | 120°C |
| (a) Petrolatum Filled Cable | 300 | 1450 |
| (b) FLEX-GEL Filled Cable | 260 | 1540 |

*Time to absorb 10cc of $0_2$ per gram of insulation.

## 8. PERFORMANCE TESTING OF WATERPROOF CABLE WITH FLEX-GEL FILLING COMPOUND

### a. Background

Experimental cables containing FLEX-GEL were produced by the Western Electric Company, Product Engineering Control Center, in the Development Capabilities Laboratory at the Atlanta Works. DEPIC insulation was used in all cables. Except as noted, performance test data are presented for 200-pair, 22-gauge cable with ASP sheath. Control specimens filled with petrolatum were tested concurrently.

### b. Dielectric Tests

Transmission characteristics are shown in Table VI. The values obtained for each cable "as received" are typical for waterproof DEPIC design. Thermal cycling was used to simulate the effect of heating and cooling due to outdoor storage, without a thermal shield, prior to burial; it consisted of at least 60 excursions from 70°F to 160°F with sufficient dwell time to achieve equilibrium at the upper and lower limits. The effect of thermal cycling was to increase the levels of attenuation and mutual capacitance in the cable containing FLEX-GEL while lowering those of cables containing petrolatum. In addition to the effects of compound permeation which have been reviewed by previous investigators,[25-27] another mechanism may contribute to the observed differences. FLEX-GEL is much less mobile at elevated temperatures than unmodified petrolatum and is therefore less susceptible to migration and internal re-distribution, thereby reducing the effect of thermal cycling. The change in mutual capacitance, to the extent observed in these tests, does not have a significant effect on transmission properties.

Dielectric strength values, shown in Table VII exceed manufacturing requirements. The presence of a filling compound having good dielectric properties and applied uniformly enhances the dielectric strength of primary insulation; this is true of petrolatum as well as of FLEX-GEL. A possible advantage of FLEX-GEL is that its rubbery texture may provide a more effective and durable incremental improvement.

TABLE VI

TRANSMISSION CHARACTERISTICS AT 772 kHz

| | As Received | | Percent Change After Thermal Cycling* | |
|---|---|---|---|---|
| | FLEX-GEL | PJ | FLEX-GEL | PJ |
| a dB/mi | 22.6 | 22.7 | 0.49 | -0.88 |
| $C_m$ μF/mi | 83.7 | 84.1 | 1.19 | -1.31 |

a: Attenuation

$C_m$: Mutual Capacitance

*60-cycles from 70°F to 160°F

TABLE VII

DIELECTRIC STRENGTH OF
FLEX-GEL FILLED CABLE WITH DEPIC INSULATION

| | Dielectric Strength, Kv | | | |
|---|---|---|---|---|
| | As Received | | After Thermal Cycling | |
| | $\bar{X}$ | σ | $\bar{X}$ | σ |
| Wire-to-wire | 25.5 | 7.7 | 23.1 | 5.9 |
| Pair-to-pair | 17.8 | 4.2 | 23.7 | 0.3 |
| Core-to-shield | 21.2 | 2.5 | 24.6 | 0.3 |

### c. Water Resistance Tests

Cables were tested for water resistance before and after thermal cycling. The results are shown in Figure 8. In these tests, specimens of completed cable, 20 feet long, were prepared by drilling 1/8-inch holes and penetrating all sheath layers down to the core wrap. Successive holes, one foot apart, were rotated 90-degrees. Mutual capacitance values were measured for a selected number of innermost pairs and the same number of outermost pairs. The cable was then immersed in water to a depth of 3-feet with the ends kept dry. Mutual capacitance was remeasured immediately after immersion and at intervals thereafter. Normal good product is expected to show less than 1% change within 30-days and to approach an equilibrium level near 3% with increased exposure. Both petrolatum and FLEX-GEL filled cables are capable of meeting this criterion "as received." It is noted, however, that waterproofness of the petrolatum-filled cable, has been significantly degraded after thermal cycling, whereas the effect on the FLEX-GEL filled cable, while significant, is still below the 3% equilibrium level.

Water resistance was also measured by applying a 3-foot head of water to the end of a measured length of cable positioned horizontally. It is essential that the cable ends be carefully prepared to avoid compressing the sheath layers or core. Failure is indicated when persistent leaks occur in either the core or sheath layers. Specimens were started at a length of 6-feet and successively

cut back in 1-foot increments until leaking occurred or the test was terminated. At least one week was allowed at each test condition. The water contained 1% fluoroscein dye to permit the tracing of any leak path (by dissection of the specimen and examination under ultraviolet illumination) and to provide evidence of leaking (by residual strain) in the event of evaporation of effluent between observations. Typical results are summarized in Table VIII. The post thermal cycle results again indicate resistance to redistribution of FLEX-GEL, since cables filled with petrolatum frequently fail this condition. The reverse bending of the mechanical cycle applies shear to the compound within the core; the rubber-like consistency of FLEX-GEL apparently imparts resistance to separation or the formation of fissures which could cause leakage paths within the filled matrix.

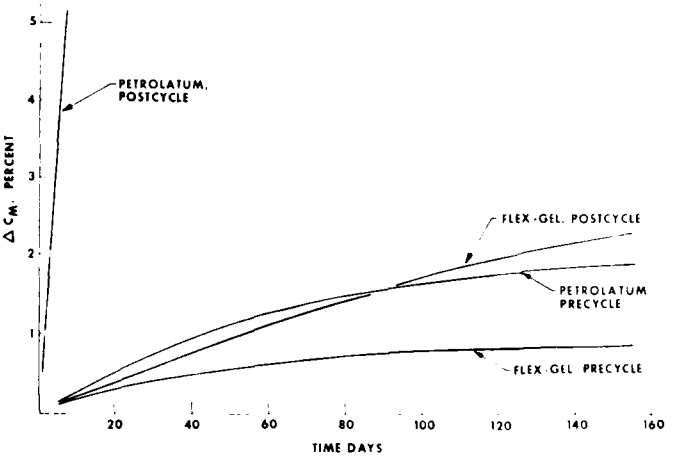



**FIGURE 8. CHANGE IN MUTUAL CAPACITANCE**

## d. Closure Tests

The water resistance of buried cable systems as a whole is strongly dependent upon the integrity of buried splice closures. That need has been addressed through the introduction of sealed connectors which block water entry at individual conductor joints and encapsulants intended to protect the complete splice bundle. It is essential for complete water tightness that an interfacial seal be formed between the insulation of each conductor and the encapsulant.

The test procedures have been outlined. For convenience these are briefly reviewed in Appendix A. Cables containing FLEX-GEL pass this test without removal of the compound coating the individual conductors, when encased in D Encapsulant, the Bell System reenterable compound.[16]

Further indication of the seal between D Encapsulant and conductor insulation coated with FLEX-GEL is given in Table IX. The results shown are averages of repeated tests. In the procedure used, insulated conductors were removed from cables containing the respective filling compounds, prepared with straight ends and minimum curvature, and embedded in D Encapsulant. "Uncleaned" conductors were embedded with the filling compound still in place, "cleaned" conductors were thoroughly wiped with absorbent tissue. Uncleaned FLEX-GEL coated conductors perform much better than those coated with petrolatum.

TABLE VIII

WATER FLOW IN CABLE CORE

FLEX-GEL FILLED CABLE WITH PIPIC INSULATION

| | Length, Feet | | | |
|---|---|---|---|---|
| | 6 | 3 | 2 | 1 |
| 22½ Hr, 22 Da | | | | |
| Pre Thermal Cycle | NL | NL | NL | Leak |
| Post Thermal Cycle* | NL | NL | NL | NL |
| 900 Hr, 26 [illegible] | | | | |
| Pre Mechanical Cycle | NL | NL | NL | NL |
| Post Mechanical Cycle† | NL | NL | NL | NL |

*60 excursions [illegible]

†Three reversals [illegible]

NL = No Leak

TABLE IX

PULL-OUT STRENGTH OF INDIVIDUAL CONDUCTORS IMBEDDED IN D-ENCAPSULANT

Specimens: 22 ga PIPIC, 3 inches Long

| Filling Compound | Pull-out Strength, lbs | |
|---|---|---|
| | Uncleaned | Cleaned |
| FLEX-GEL | 2.43 | 2.84 |
| Petrolatum | 0.27 | 3.96 |

## e. Thermal Tests

In addition to the thermal cycle tests already described, a "cable drip test" is commonly used to measure the high temperature performance of a filled cable. In this test 12-inch specimens with 2-inches of sheath cut back and the cores flared are vertically suspended in a circulating air oven with the flared ends down and positioned so that all drip is collected. The test results depend on the number of pairs and conductor gage of the cable under test. Test results are shown in Table X. The greatly reduced drip from FLEX-GEL filled cable correlates with the reduced sensitivity to thermal cycling reported above from transmission measurements and core flow tests.

TABLE X

HIGH TEMPERATURE CABLE DRIP DATA

Specimen: 200 pr, 22 ga cable, 12 inches long

| Filling Compound | Drip After 7 Days at Temperature, gms 60°C | 70°C |
|---|---|---|
| FLEX-GEL | 6.4 | 8.4 |
| Petrolatum | 37.5 | 56.7 |

## f. Handling Tests

As deduced from Figures 5 and 6, petrolatum solidifies to a waxy solid at low temperatures, causing filled cables to become stiff and making core access and pair separation difficult. FLEX-GEL, on the other hand, remains a soft rubber. The relative bending stiffness at 30°F for cables containing the two compounds is shown in Figure 9.

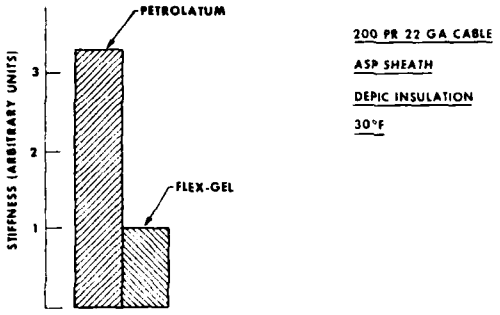



FIGURE 9. RELATIVE STIFFNESS ON BENDING

In addition, studies have indicated that time savings up to 50% can be achieved in performing typical splicing operations at low temperature using FLEX-GEL rather than petrolatum filled cable.

## 9. CONCLUSION

A new family of cable filling compounds has been developed. The compounds are thermoplastic rubbers highly extended with mineral oils. Performance tests show that the characteristics of filled cable are improved significantly by a preferred composition. Cables filled with the new composition are now available to the operating companies.


## ACKNOWLEDGEMENT

This work was made possible with the support of many individuals and organizations. We acknowledge the contributions of the Western Electric Company, Product Engineering Control Center, Atlanta, and members of Bell Laboratories, Atlanta. The Michigan, Mountain, South Central, Southwestern, and Southern Bell System Operating Companies participated in product evaluations and field trials. The following individuals have contributed the data presented here: S. R. McAnally, F. J. Mullin, B. J. Overton, R. R. Ross, R. W. Tarwater, and J. L. Williams.


## REFERENCES


1. Biskeborn, M. C. and Dobbin, D. P., Seventeenth International Wire and Cable Symposium, 1968.
2. Collins, R. P. and Apen, J. R., International Symposium on Subscriber Loop and Services, May 1976.
3. Sabia, R. and Kaufman, S., unpublished studies.
4. McReynolds, L. A. and Mitacek, B., National Transportation, Power Plant and Fuels and Lubricants Meeting, 1964.
5. Western Electric Specification MS 58432.
6. McCann, J. P., Sabia, R., and
7. U. S. Patent 3,775,548.
8. S. Compound, Lube Products Corporation, Mineola, New York.
9. Falke, H., Seventeenth International Wire and Cable Symposium, 1968.
10. Mildner, R. C. et al, Eighteenth International Wire and Cable Symposium, 1969.
11. British Patent 1,175,850.
12. Sabia, R., unpublished studies.
13. McManus, T. K. and Beveridge, R., Proceedings of the Twenty-sixth International Wire and Cable Symposium, p. 204, 1977.
14. U. S. Patent 3,347,974.

15. Kaufman, S. and Sabia, R., Proceedings of the Twenty-first International Wire and Cable Symposium, p. 64, 1972.

16. Brauer, M. and Sabia, R., Proceedings of the Twenty-fourth International Wire and Cable Symposium, p. 104, 1975.

17. Pesto, W. G., unpublished studies.

18. Kaufman, S. et al, Proceedings of the Twenty-sixth International Wire and Cable Symposium, p. 24, 1977.

19. Haws, J. R. and Wright, R. F., Handbook of Thermoplastic Rubbers (B. M. Walker, Editor) Van Nostrand Reinhold Co., 1979.

20. U. S. Patent 3,879,575.

21. U. S. Patent 4,176,240.

22. Sabia, R., U. S. Patent, pending.

23. Mitchell, D. M., Proceedings of the Twenty-third International Wire and Cable Symposium, p. 216, 1974.

24. Gilroy, H. M., Proceedings of the Twenty-third International Wire and Cable Symposium, p. 42, 1974.

25. Aloisio, C. J. and Nelson, E. D., Proceedings of the Twenty-second International Wire and Cable Symposium, p. 261, 1973.

26. Mangaraj, E. et al, Proceedings of the Twenty-seventh International Wire and Cable Symposium, p. 139, 1978.

27. Garmon, J. P. and Davis, L. E., Proceedings of the Twenty-eighth International Wire and Cable Symposium, p. 232, 1979.

## APPENDIX A

### OUTLINE OF WATERPROOF TESTS FOR ENCAPSULATED SPLICES

SERIES I

- Prepare encapsulated splices according to practice. Western Electric's 710 SB Connectors (unsealed), which leave the terminated conductors exposed, are used.
- Immerse the encapsulated splice in a 3-foot depth of water at room temperature and apply, one foot from the splice, an 8-foot head of water (5-foot net head on splice) to the cable. The cable ends shall be kept dry and accessible for measurement.
- Periodically monitor conductor resistance to ground and to mate for 50 days.
- Remove the splice, re-enter, and examine.
- Reencapsulate the splice according to predetermined practice and seal water entry port.
- Place reencapsulated splice in wet sand and cycle from 0 to 100°F for 25 days using 12 hour cycles.
- Insulation readings less than $10^9$ ohms are cause for failure.

SERIES II

- Using similarly prepared splices, immerse and cycle in wet sand for 50 days from 0 to 100°F.
- Monitor insulation resistance.
- Reenter and examine.
- Reencapsulate and apply eight foot head of water for 25 days as in Series I.
- Insulation readings less than $10^9$ ohms are cause for failure.



D. M. Mitchell is a graduate of Newark College of Engineering (now New Jersey Institute of Technology), BS-ME. He joined Bell Laboratories in 1954. Much of his early career was devoted to ocean cable development. Since 1971 he has been associated with the Transmission Media Laboratory with principal responsibilities in the development and application of multipair waterproof cable.



Raffaele Sabia, a graduate of St. Francis College of Brooklyn (B.S.) and Polytechnic Institute of Brooklyn, (Ph.D.), was employed by the Polymer Chemical Division of W. R. Grace prior to joining Bell Telephone Laboratories in 1963. Since 1963 he has been active in the research and development of materials for application in the wire and cable area and in the preparation of the text in the series "Physical Design of Electronic Systems" published by Prentice Hall. Since 1967 he has been supervisor of the Chemical Engineering Group in the Transmission Media Laboratory.

# COAXIAL LINE WITH THE HIGHEST ELECTRICAL LENGTH STABILITY

Y. Saito, S. Furuya, H. Sugawara, Y. Asano, S. Kato

Sumitomo Electric Industries, Ltd.

Yokohama, Japan

## Summary

This paper deals with newly developed techniques for providing a coaxial line with the highest possible electrical length stability, in which both the coaxial cable and the gas pressure control equipment are designed to minimize the variation in the electrical length of the cable brought about by changes in temperature and pressure of the gas filled in the cable. A coaxial cable with an electrical length-temperature coefficient less than $\pm 1$ PPM/°C can be obtained by merely applying a new direct extrusion technique to a specially designed insulator of helical string with an external pipe. The pressures of dry gas, which is sealed seperately in the insulating space of each coaxial cable using gas-tight coaxial connectors, can be controlled individually with a system accuracy of $\pm 1$ g/cm$^2$ by utilizing gas density control equipment with a built-in micro-processor.

## 1. Introduction

Recently, observation systems have been employed in specific fields such as radio astronomy in which a large antenna, such as an interferometer or a radioheliograph, is formed by connecting with coaxial cables a number of antenna elements which are spaced apart from each other. In such systems, the electrical length of the system must be kept constant for long observation periods such as more than several months while reception of intercepted signals from space is conducted.

A coaxial cable with an air-dielectric insulator for such systems was designed to considerably reduce the electrical length, or phase, variation due to temperature variation in order to eliminate the necessity of intricate operations to maintain the system at a constant temperature or of providing phase control devices.

The coaxial cable must have dry gas sealed in the insulating space in order to be operated at stable conditions during high-frequency transmission. A gastight coaxial connector and gas density control equipment have also been developed in order to minimize variation of the electrical length of the coaxial cable.

The new coaxial line is applicable to highly phase-sensitive electronic systems such as an interferometer and a radioheliograph in the field of radio astronomy and sampling lines in AM broadcast arrays.

## 2. Electrical Length Stabilization

When a cable is exposed to temperature variations, its electrical length is affected by changes in the physical length of the conductors and by changes in the permittivity of the insulator. The physical length of the coaxial cable increases with a rise in temperature at the same rate as the linear expansion coefficient of the conductors, causing the electrical length to increase. On the other hand, the permittivity of the insulating material decreases with a rise in temperature, causing the electrical length to decrease. Consequently, the electrical-length stabilization of the coaxial cable can be realized essentially by counterbalancing the change in physical length and the change in effective permittivity of the cable.

### 2.1 Theory

#### 2.1.1 Electrical Length-Temperature Coefficient

The electrical length-temperature coefficient of a coaxial cable is given by the sum of the phase constant-temperature coefficient and the physical length-temperature coefficient of the cable and is defined by

$$K_T = \frac{1}{Le}\frac{\Delta Le}{\Delta T} = \frac{1}{\beta}\frac{\Delta \beta}{\Delta T} + \frac{1}{L}\frac{\Delta L}{\Delta T} \qquad (1)$$

where $K_T$: electrical length-temperature coefficient of the cable (/°C)

$\beta$: phase constant of the cable (rad./km)

L: physical length of the cable (km)

Le: electrical length of the cable (rad.)

T: operating temperature (°C)

The phase constant, $\beta$, of the coaxial cable is well known to be given by the following equations:

$$\beta = Af + B\sqrt{f}$$

$$A = \frac{20}{3}\pi\sqrt{\varepsilon}$$

$$B = \frac{\sqrt{\varepsilon}}{60\ell n\, D/d}\left(\frac{\sqrt{\rho_1}}{d} + \frac{\sqrt{\rho_2}}{D}\right) \qquad (2)$$

where f: frequency (MHz)

$\varepsilon$: effective permittivity of the cable

$\rho_1$, $\rho_2$: specific resistances of the inner and outer conductors, respectively ($n\Omega$-cm)

d, D: outer diameter of the inner conductor and inner diameter of the outer conductor, respectively (mm)

The change in phase constant with temperature, which can be derived from formula (2), is as follows:

$$\frac{1}{\beta}\frac{\Delta\beta}{\Delta T} = \frac{1}{2}\frac{1}{\varepsilon}\frac{\Delta\varepsilon}{\Delta T} + \left\{\frac{1}{100\pi D\ell n\frac{D}{d}\sqrt{f}}\left(\frac{\frac{D}{d}\sqrt{\rho_1}}{\sqrt{\rho_1}\left(1+\frac{D}{d}\sqrt{\frac{\rho_1}{\rho_2}}\right)}\right)\left(\frac{1}{2}\frac{\Delta\rho_1}{\rho_1}\frac{1}{\Delta T}\right) + \frac{1}{2(1+\frac{D}{d}\sqrt{\frac{\rho_2}{\rho_1}})}\frac{\Delta\rho_2}{\rho_2}\frac{1}{\Delta T}\right\}$$

$$-\left\{\left(\frac{1}{\ell n D}\frac{1}{d}+\frac{1}{1+\frac{D}{d}\sqrt{\frac{\rho_1}{\rho_2}}}\right)\frac{1}{D}\frac{\Delta D}{\Delta T} - \left(\frac{1}{\ell n D}\frac{1}{d}-\frac{\frac{D}{d}\sqrt{\frac{\rho_1}{\rho_2}}}{1+\frac{D}{d}\sqrt{\frac{\rho_1}{\rho_2}}}\right)\frac{1}{d}\frac{\Delta d}{\Delta T}\right\} \qquad (3)$$

Equation (3) above shows that the rigorous phase constant-temperature coefficient is a function of frequency because of the temperature dependence of both specific resistances and dimensions of the inner and outer conductors. The term in braces in equation (3), however, is small enough to be neglected compared to the first term, which shows the effective permittivity-temperature coefficient. In the case of an air-dielectric coaxial cable, the effective permittivity-temperature coefficient can be evaluated by the following equation:

$$\frac{1}{\varepsilon}\frac{\Delta\varepsilon}{\Delta T} \approx \frac{1-\frac{1}{\varepsilon}}{1-\frac{1}{\varepsilon_m}}\left\{\frac{1}{\varepsilon_m}\frac{\Delta\varepsilon_m}{\Delta T} + \left(1-\frac{1}{\varepsilon_m}\right)\left[\alpha_m - \alpha_1\frac{1+\left(\frac{\alpha_2}{\alpha_1}\right)\left(\frac{D}{d}\right)}{1+\left(\frac{D}{d}\right)}\right]\right\} \qquad (4)$$

where $\varepsilon_m$ and $\alpha_m$ are the inherent permittivity and the coefficient of linear expansion of the insulating material, respectively, and $\alpha_1$ and $\alpha_2$ are the coefficients of linear expansion of the inner and outer conductors, respectively. Because the coefficient of thermal expansion of an insulator is generally larger than that of a conductor, it is assumed that the inner and outer conductors restrain the thermal expansion of the insulating material in the radial direction.

It is well known that the change in physical length of a cable with temperature can be represented by the following equation in the case where the inner and outer conductors are rigidly secured to the insulator:

$$\frac{1}{L}\frac{\Delta L}{\Delta T} = \alpha_1\frac{1+\left(\frac{\alpha_2}{\alpha_1}\right)\left(\frac{E_2}{E_1}\right)\left(\frac{S_2}{S_1}\right)}{1+\left(\frac{E_2}{E_1}\right)\left(\frac{S_2}{S_1}\right)} \qquad (5)$$

where $S_1$, $S_2$: sectional areas of the inner and outer conductors, respectively

$E_1$, $E_2$: Young's modulus of the inner and outer conductors, respectively

From equations (1) through (5), the electrical length-temperature coefficient of air-dielectric coaxial cables in which both the inner and outer conductors are made of the same material is then:

$$K_T = \alpha + \frac{1}{2}\frac{\left(1-\frac{1}{\varepsilon}\right)}{\left(1-\frac{1}{\varepsilon_m}\right)}\left\{\frac{1}{\varepsilon_m}\frac{\Delta\varepsilon_m}{\Delta T} + \left(1-\frac{1}{\varepsilon_m}\right)(\alpha_m-\alpha)\right\} \qquad (6)$$

where $\alpha$ is the coefficient of linear expansion of the conductor material. Further, the effective permittivity of air-dielectric coaxial cables is approximated as a function of the space factor, R, of the insulator. For a coaxial cable insulated with a helical string, the space factor of the insulator is expressed by the following formula:

$$R \approx \frac{\varepsilon - 1}{\varepsilon_m - 1} \qquad (7)$$

For a coaxial cable insulated with a helical string with an outer pipe, however, the space factor of the insulator and the effective permittivity of the cable are related to each other as functions of cable dimensions, as follows:

$$R = \frac{D^2-(D-2t)^2+\frac{2W}{\pi}(D-d-2t)}{D^2-d^2} \qquad (8)$$

$$\varepsilon \approx \frac{\ell n\, D/d}{\frac{1}{\varepsilon_m}\ell n\frac{D}{D-2t}+\ell n\frac{\pi(D-2t)+(\varepsilon_m-1)W}{\pi d+(\varepsilon_m-1)W}} \qquad (9)$$

where t and W are thicknesses of the outer pipe and the helical string of the insulator, respectively. Consequently, from equations (6) through (9) it can be seen that the electrical length stability of coaxial cables can be greatly increased by selecting the space factor of the insulator so that the electrical length-temperature coefficient given by equation (6) above is zero. The inherent permittivity-temperature coefficient, $\frac{1}{\varepsilon_m}\frac{\Delta\varepsilon_m}{\Delta T}$, of the insulating material is negative in the range of ordinary operating

temperatures (-50 to +100°C) with the absolute value slightly larger than the coefficient of linear expansion, $\alpha_m$, of the insulating material. Further, the coefficient of linear expansion, $\alpha_m$, of the insulating material is larger by one order than that, $\alpha$, of the conducting material. Accordingly, it is evident that the electrical length-temperature coefficient, $K_T$, in equation (6) can be made to be zero. However, since the inherent permittivity of the insulating material and its temperature coefficient are, in general, functions of both temperature and frequency, in order to obtain the highest electrical length stability it is necessary to select the space factor of the insulator after first determining by other means the effect of operating temperature and frequency on these constants.

The electrical length-temperature coefficient of a foamed plastic-insulated coaxial cable is also calculated by using the relation (well known as the Wagner-Rayleigh's equation) between the effective permittivity of the cable and the expansion ratio of the foamed insulator, and is expressed as follows:

$$K_T \approx \alpha + \frac{1}{2} \frac{\left(\frac{1}{\varepsilon_m} + 2\frac{\varepsilon_m}{\varepsilon}\right)(1-V)}{\left(2+\frac{1}{\varepsilon_m}\right)+\left(1-\frac{1}{\varepsilon_m}\right)V} \frac{1}{\varepsilon_m} \frac{\Delta\varepsilon_m}{\Delta T} \qquad (10)$$

where V is the expansion ratio of the foamed insulator.

2.1.2 Electrical Length-Pressure Coefficient

Air-dielectric coaxial cables normally contain pressurized gas in order to achieve high quality transmission. Because variation in the density of the gas will cause a change in the effective permittivity of the cable, the pressure of the sealed gas should be precisely controlled to maintain constant gas density, and gastightness of the connectors fitted at both ends of the cable should be maintained. Therefore, in order to carry out the control operation satisfactorily, it is necessary to determine whether a pressure variation is caused by leakage of the pressurized gas or by temperature variation. Accordingly, the pressure of the dry gas sealed in the electrical length-stabilized coaxial cable is appropriately controlled by checking the actual gas pressure with the expected gas pressure value at a given temperature, which is determined by the following equation:

$$P(T) = P(T_o)\left\{1 + \frac{T-T_o}{273+(T-T_o)}\right\} \qquad (11)$$

where $T_o$ is a predetermined reference temperature, P(T) is the pressure of the gas, T is the temperature of the cable, and $P(T_o)$ is the absolute pressure of the gas sealed in the cable at the reference temperature. It should be noted that degree of variation of the gas pressure brought about by temperature variations is of the order of 4 to 8 $(g/cm^2)/°C$ if the sealed gas pressure is selected to be 0.1 to 1 $kg/cm^2$ with respect to atmospheric pressure, as is the customary usage.

The electrical length-pressure coefficient of the air-dielectric coaxial cable is expressed by the following approximation, with the assumption that the change in dimensions of the cable brought about by the change in the gas pressure is too small to be taken into consideration:

$$K_P \approx \frac{1}{2} \frac{1-R}{1+\left(\frac{\varepsilon_m}{\varepsilon_o}-1\right)R} \frac{1}{\varepsilon_o} \frac{\Delta\varepsilon_o}{\Delta P} \qquad (12)$$

where $K_P$ is the electrical length-pressure coefficient and $\varepsilon_o$ is the inherent permittivity of the sealed gas. The permittivity-pressure coefficient of the gas can be easily derived by differentiating the well-known Clausius-Mosotti's equation with respect to the pressure, as follows:

$$\frac{1}{\varepsilon_o} \frac{\Delta\varepsilon_o}{\Delta P} \approx \frac{3}{P} \frac{(\varepsilon_o-1)}{(\varepsilon_o+2)} \qquad (13)$$

The electrical length-pressure coefficient of a coaxial cable in which, for example, dry nitrogen gas is pressurized, can be estimated to be $1.97 \times 10^{-4}/(kg/cm^2)$. Consequently, it becomes necessary to control the gas pressure appropriately in accordance with the relation between the gas pressure and the temperature, which is shown by equation (11). The gas pressure should be controlled with high accuracy, for example, less than $\pm 5$ $g/cm^2$, in order to maintain the value of electrical length variation within $\pm 1$ PPM (Parts Per Million = $10^{-6}$).

2.2 Cable Design

The new coaxial cable with air-dielectric insulation was designed to considerably reduce the electrical length, or phase, variation due to temperature variation. A cross-sectional view and partial cutaway view of the new coaxial cable are shown in Figure 1. The insulator is composed of helical polyethylene string on the inner conductor and a polyethylene pipe over the helical string.

Figure 2 shows a nomograph of relations calculated from equations (6), (8) and (9), that can be used in determining the optimum design of

electrical length-stabilized, 1-inch coaxial cable. It shows that the optimum space factor of the insulator can be easily changed by choosing an appropriate value for the pipe thickness of the insulator. In order to obtain an electrical length-temperature coefficient less than ±1 PPM/°C, the space factor should be controlled within error of about 3% around the optimum value so that the deviation of the effective permittivity is less than 0.5%. In Figure 2 the relation between the space factor of the insulator and the effective permittivity for foamed polyethylene insulation type coaxial cable is also shown.

Table 1 gives a comparison of cable constructions between the new and the conventional stabilized coaxial cables. The two conventional cables are 2/5-inch cables composed of foamed polyethylene insulator with expansion ratios of about 80% (type-A) and 50% (type-B), solid copper inner conductors, and aluminum-pipe outer conductors. The new design permits the use of softened aluminum wire, bringing about the advantages of not only lighter weight and greater flexibility but also greater economy. The characteristic impedance of the new cable is 50 Ω, and that of both conventional cables is 75 Ω.

Figure 3 shows a photograph of the new stabilized 1-inch coaxial cable.

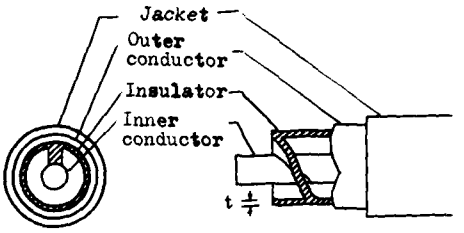



Fig. 1 Cable structure of new stabilized COAX

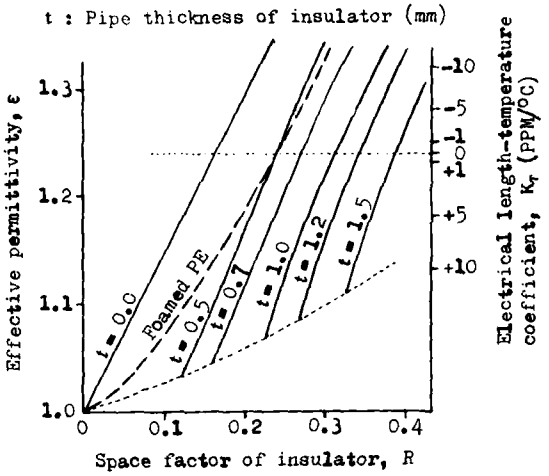



Fig. 2 Optimum design for stabilization

Table 1. Cable construction of stabilized COAX

| Description \ Type | | New Stabilized COAX | Conventional Stabilized COAX | |
|---|---|---|---|---|
| | | | A | B |
| Inner Conductor | Material | Softened Aluminum Wire | Softened Copper Wire | |
| | Outer Diameter, mm | 8.0 | 2.9 | 2.2 |
| Insulator | Material | Polyethylene (Specially Designed) | | |
| | Construction | Helical String with External Pipe | Foamed (80%) | Foamed (50%) |
| | Outer Diameter, mm | 20 | 11 | 10 |
| Outer Conductor | Material | Softened Aluminum Pipe | | |
| | Outer Diameter, mm | 22 | 12 | 11 |
| Jacket | Material | Ethylene Copolymer with M.I. 0.2 | | |
| | Outer Diameter, mm | 26 | 15 | 14 |
| Cable Weight, kg/m | | 0.49 | 0.20 | 0.19 |



Fig. 3 View of new stabilized COAX

2.3 Extrusion Technique

Because the insulator is formed by welding the helical polyethylene string around the inner conductor to the outer polyethylene pipe by the direct extrusion technique [1][2], the space factor of the insulator can be finely controlled during formation of the insulator at an optimum value predetermined in accordance with the new cable design method mentioned above for getting the highest electrical length stability irrespective of temperature. Consequently, an electrical length-temperature coefficient less than $\pm 1$ PPM/°C over a temperature range of 20°C has been achieved without any particular efforts.

Figure 4 shows a cutaway view of the direct extrusion apparatus. In this process both the helical polyethylene string around the inner conductor and the polyethylene pipe over the helical string are simultaneously formed into a single insulator, as is shown in Figure 1. This process offers the following advantages compared with all other existing techniques and thus produces the highest quality coaxial cable.

(1) It is possible to produce cables with a very long unit-length under stable conditions.

(2) Since there is no residual stress in the helical string, dimensional and thermal stability of the insulator are high, giving this cable extremely high electrical length stability.

(3) Usage of a polyethylene pipe, whose outer wall is in contact with the inner wall of the outer conductor, raises the reliability in relation to corrosion of the conductors and leakage of the gas sealed in the cable.

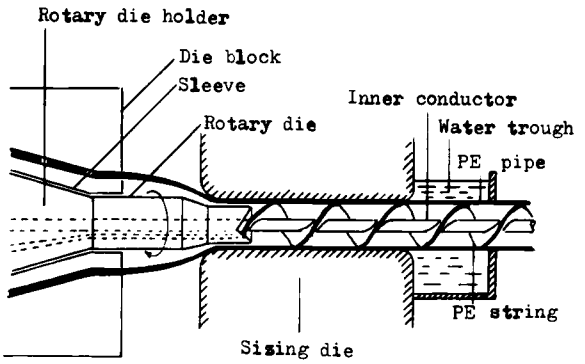



Fig. 4 Extrusion apparatus

2.4 Electrical Length Measurement

The technique for measuring electrical length variation is essential for evaluating the quality of electrical length-stabilized coaxial cable. The transmission method, which is superior to the reflection method with regard to detecting sensitivity, especially in conditions when the cable is very long and is operated at very high frequency, should be used.

The electrical length measuring setup for the transmission method is shown in Figure 5. The test signal is divided into two signals, direct and indirect. The direct signal is fed to a vector voltmeter, and the indirect signal is fed to a coaxial switch which alternately

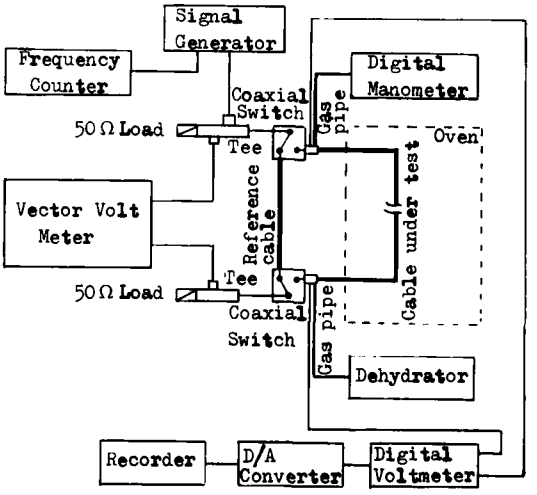



Fig. 5 Electrical length measuring setup

changes the direction of the signal toward the reference cable and the cable under test. The electrical length of the cable can be determined from the difference between phases of the two indirect signals, both of which can be calibrated with the direct signal. Because comparative measurement is conducted without replacement of probes during measurement, this new method has an advantage of minimum error. The resistance of the inner conductor of the test cable and the pressure of the gas filled in the cable are recorded automatically to detect ever-changing temperatures and gas pressures, respectively.

## 3. Properties of Stabilized Coaxial Cable

### 3.1 Electrical Length-Temperature Coefficient

Figure 6 shows the comparison of the electrical length variations versus temperature between the new stabilized coaxial cable and the two conventional stabilized coaxial cables insulated with foamed polyethylene. The electrical length variation of the new coaxial cable is greatly reduced in comparison with the conventional cables even though the new cable has the same effective permittivity as the A-type cable does. The new stabilized coaxial cable is designed so that the electrical length variation with temperature is minimized at a temperature of 20°C and at a frequency of 500 MHz.

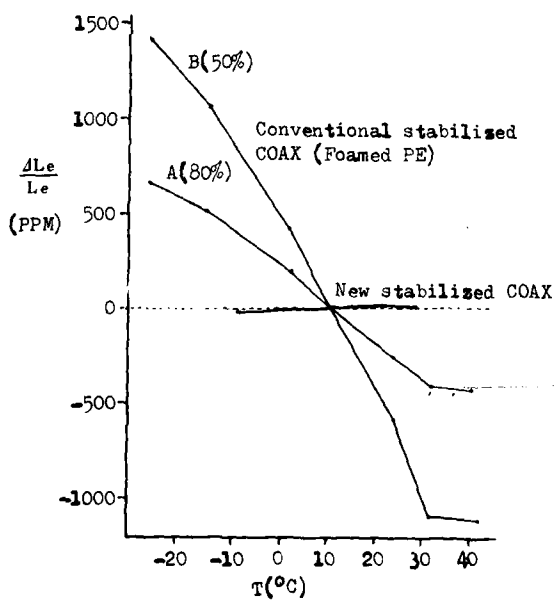



Fig. 6 Electrical length variation vs. temperature

Also shown, in Figure 7, is the comparison of the electrical length-temperature coefficients versus temperature between these stabilized coaxial cables. The electrical length-temperature coefficient of the new cable is smaller by at least one order in comparison with that of the conventional cables over a wide range of temperatures. The electrical length-temperature coefficient of the new cable in the very high frequency range decreases as temperature rises, becomes zero at temperature of 20°C, and then increases in absolute value after changing its sign from positive to negative at the optimum

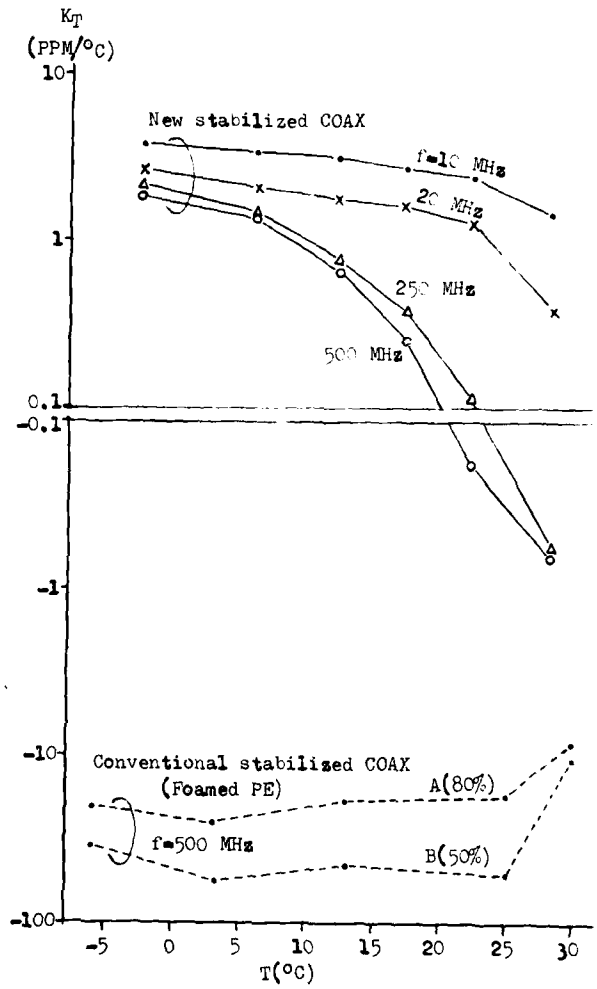



Fig. 7 Electrical length-temperature coefficient variation vs. temperature

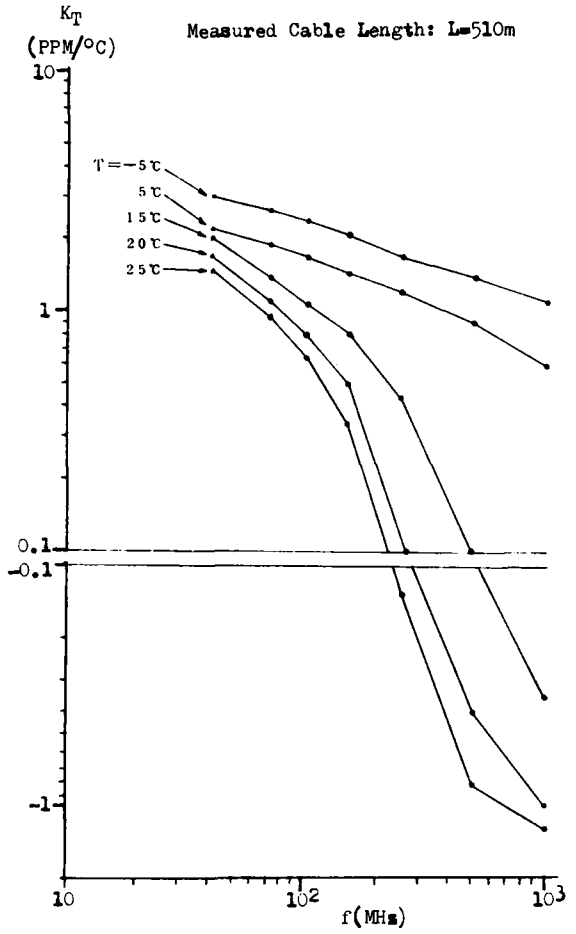



Fig. 8 Electrical length-temperature coefficient variation vs. frequency

temperature. It was confirmed through repeated heat cycle tests that the change in electrical length-temperature coefficient follows the same plot in the reverse process. It shows that the new coaxial cable has excellent stability brought about by the absense of distortion of the insulator compared with all other existing stabilized coaxial cables, which must receive repeated heat treatment during production in order to have stable temperature characteristics.[3]

Figure 8 shows measured electrical length-temperature coefficients versus frequency of another new stabilized coaxial cable designed to have maximum stability at a temperature of 15°C and at a frequency of 500 MHz. The measurement shows the tendency for the electrical length-temperature coefficient to decrease as frequency rises, become zero at an optimum frequency, and then increase in absolute value after changing its sign from positive to negative at the optimum frequency.

The detailed data shown in Figures 7 and 8 reveals that the electrical length-temperature coefficient of the coaxial cable is affected by both temperature and frequency.

### 3.2 Electrical Properties

General transmission parameters of coaxial cables such as characteristic impedance, transmission loss, impedance uniformity, and temperature dependencies of these parameters are shown in Table 2.

Reflection within the cable due to impedance irregularities, which are caused by imperfections in manufacture, must be reduced to enable wide-band transmission with high quality. The most common method used for testing coaxial cables involves measurement of the structural return loss (SRL) of a length of the cable as a func-

Table 2 Typical electrical properties

| Item | | Remark |
|---|---|---|
| Characteristic Impedance ( Ω at 100 MHz) | | 50.0 |
| Attenuation Constant (dB/km at 15°C) | f = 100 MHz | 16.5 |
| | f = 500 MHz | 38.5 |
| | f = 1000 MHz | 56.3 |
| Structural Return Loss | (dB at f < 1000 MHz) | > 30 |
| Temperature Coefficient (at PPM/°C, 5 ~ 25°C) | Electrical Length | ±(0 ~ 1) |
| | Capacitance | -(10 ~ 15) |
| | Characteristic Impedance | +(15 ~ 30) |
| | Attenuation | + 2000 |

tion of frequency. A typical record measured over the frequency range of 10 - 1000 MHz by the swept-frequency method using an impedance bridge is shown in Figure 9. The measured SRL is above 32 dB in the entire frequency band and, as a result, good connection of the new coaxial cable to electronic equipment is possible.

Figure 10 shows the relation of, transmission loss vs. frequency characteristics measured by the swept-frequency method using a Ratio Meter. The dimensional uniformity of the cable is so good that the loss curve is smooth enough for high quality transmission.

### 3.3 Mechanical Properties

Figure 11 illustrates the electrical length variation with bending. The figure reveals that the electrical length of the new cable, after increasing slightly when bending diameter is over 30 times the outer diameter of the cable, graqually decreases. The amount of change in electrical length with bending is extremely reduced compared with existing coaxial cables because the flexibility of the cable is greatly increased; consequently, the advantages of smaller cable drum, easier cable installation, and space saving can be obtained.

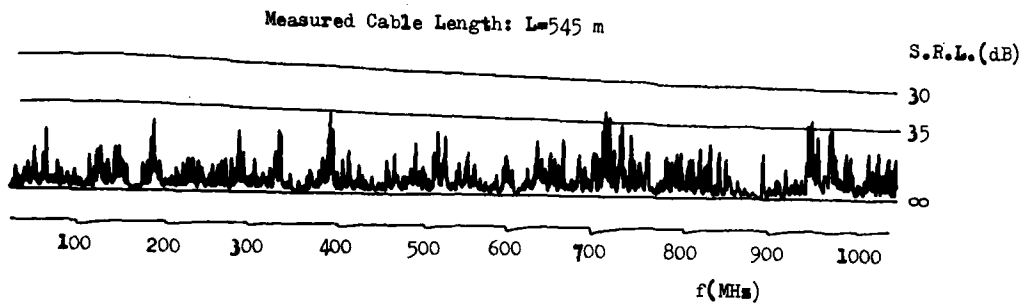



Fig. 9 Typical structural return-loss curve

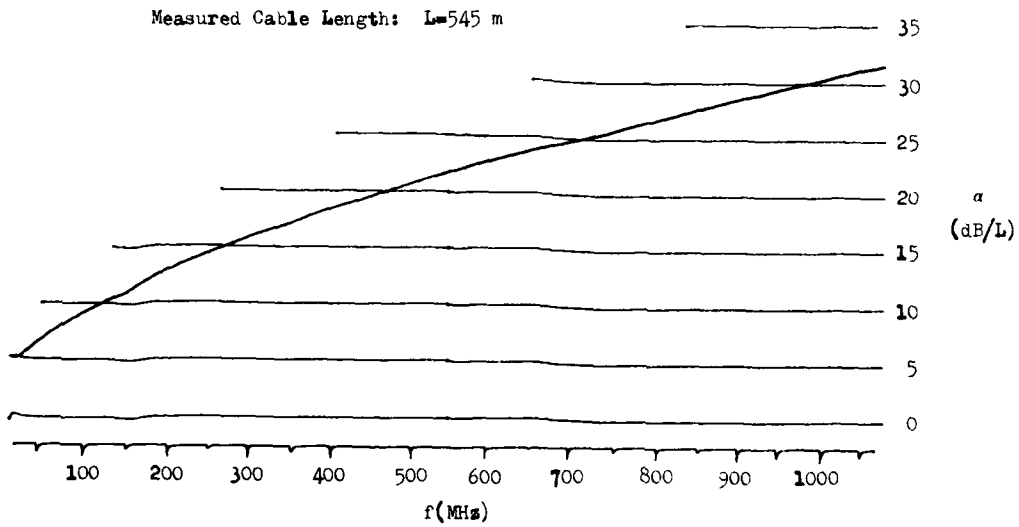



Fig. 10 Typical transmission-loss curve

Figure 12 shows the measured change in electrical length with tension. A gradual increase of the electrical length with tension occurs, which will be valuable for the installation of the cable on racks or in troughs.

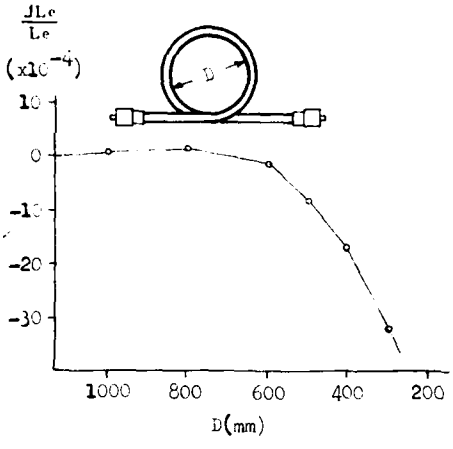



Fig. 11 Change in electrical length with bending

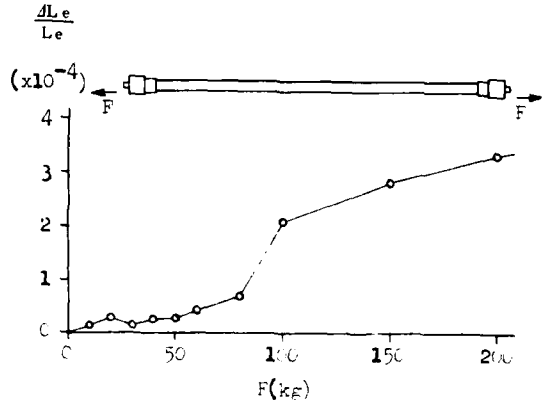



Fig. 12 Change in electrical length with tension

## 4. Gas Control System

### 4.1 Electrical Length-Pressure Coefficient

A gastight coaxial connector and a gas control system have also been developed in order to minimize variation in the electrical length of the cables brought about by variations in the permittivity of the sealed gas due to variation in the density of the gas rather than directly by the gas pressure itself.

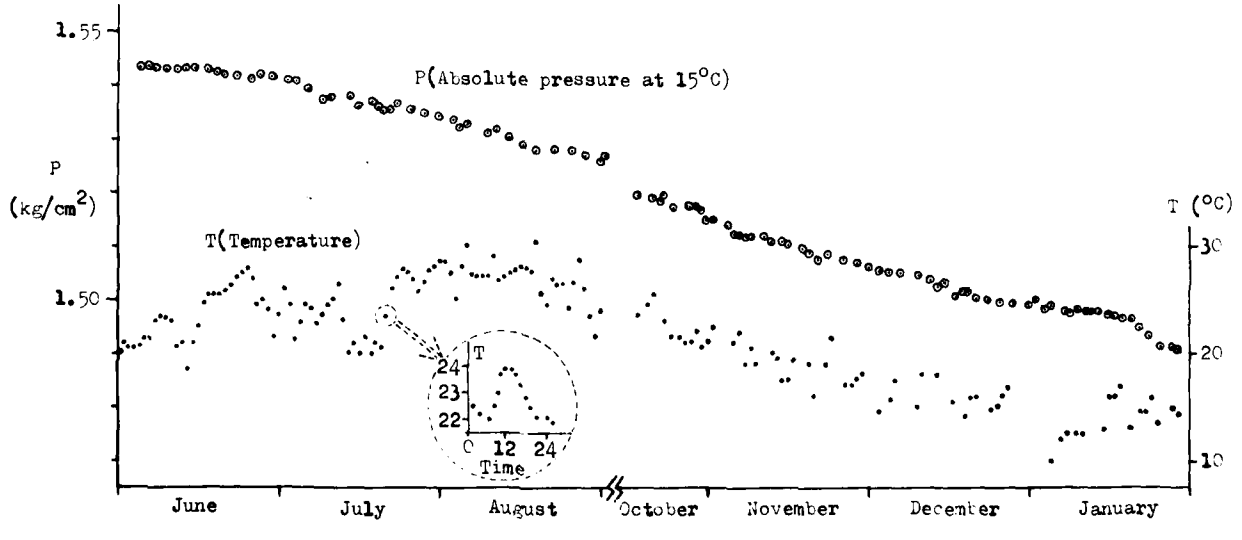



Fig. 13 Long-term gastightness of coaxial connectors

The coaxial connector was designed to guarantee not only good impedance matching with the coaxial cable at high frequencies but also such good gastightness that gas leakage is less than 0.5 $g/cm^2$ per day, which means the electrical length decrease will be below 0.1 PPM per day. Figure 13 shows a long-term measurement of gas leakage from the connectors equipped at both ends of a 500-m-long coaxial cable. The gas pressures measured were converted into absolute pressures with respect to a mean temperature of 15°C according to equation (11) in order to accurately detect the leakage of gas. Gastightness of the coaxial connectors was so good that the leakage of gas sealed in the cable was less than 0.3 $g/cm^2$ per day irrespective of temperature variations over a range of 20°C during the period from June to January.

Figure 14 shows the relation between the pressure of dry nitrogen gas and the electrical length variation of a pressurized coaxial cable. Good agreement of the electrical length-pressure coefficients with the calculated value of $1.97 \times 10^{-4}/(kg/cm^2)$ and measured value of $1.9 \times 10^{-4}/(kg/cm^2)$ was obtained.

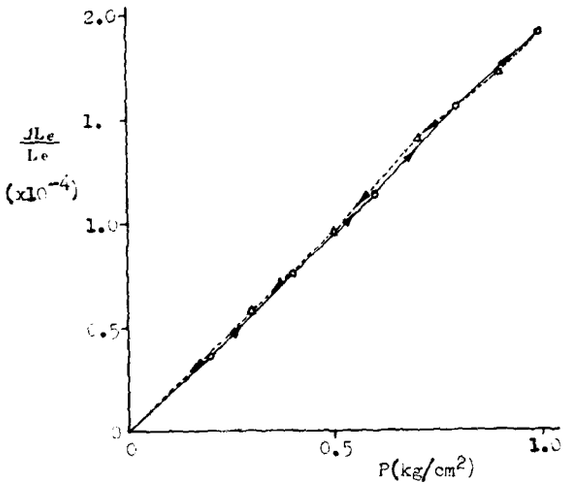



Fig. 14 Electrical length variation vs. gas pressure

## 4.2 Gas Density Control Equipment

The gas density control equipment is composed of a dehydrator, a gas density controller, a gas distribution unit, and sensors to measure gas pressure and temperature in each of the coaxial cables. In this system, the gas supply pressures are controlled individually by utilizing the measured temperatures and gas pressures so that the gas densities of all cables are kept at a constant predetermined value.

Figure 15 shows the block diagram of the gas density control system. The gas density controller with a built-in micro-processor has the functions of monitoring gas pressures and cable temperatures, computing the gas density of each coaxial cable, and controlling the gas distribution unit. The gas distribution unit consists of a DC motor, gear trains, a regulator, and electromagnetic valves. When a change in gas density of one cable is detected, the corresponding electromagnetic valve is opened and the DC motor is activated to drive the regulator at a speed proportional to the magnitude of the error and to regulate the gas pressure under classical feedback control. The prototype gas density control equipment is shown in Figure 16. The system accuracy of the gas pressure has been

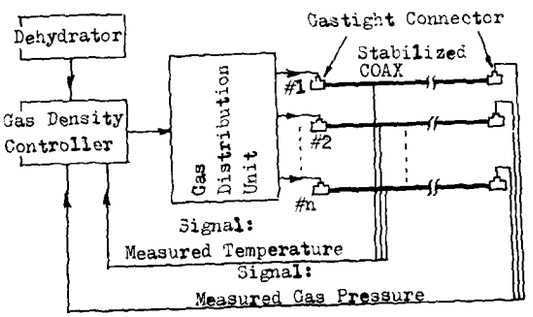



Fig. 15 Block diagram of gas control equipment

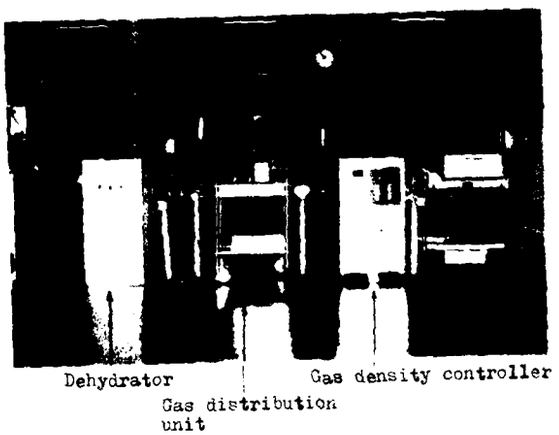



Fig. 16 Prototype gas density control equipment

improved to within $\pm 1$ g/cm$^2$ irrespective of temperature even under the harsh conditions when the initial gas pressure is being raised from zero to a set point, for example 0.5 kg/cm$^2$.

Figure 17 shows the long-term (10 months) phase measurements of the new stabilized coaxial cable. Gas sealed in a 510-m-long cable has been Controlled successfully by utilizing the gastight coaxial connectors and the prototype gas density control equipment shown in Figure 16. An Electrical length-temperature coefficient of less than $\pm 1$ PPM/°C has been established over a temperature range of 20°C.

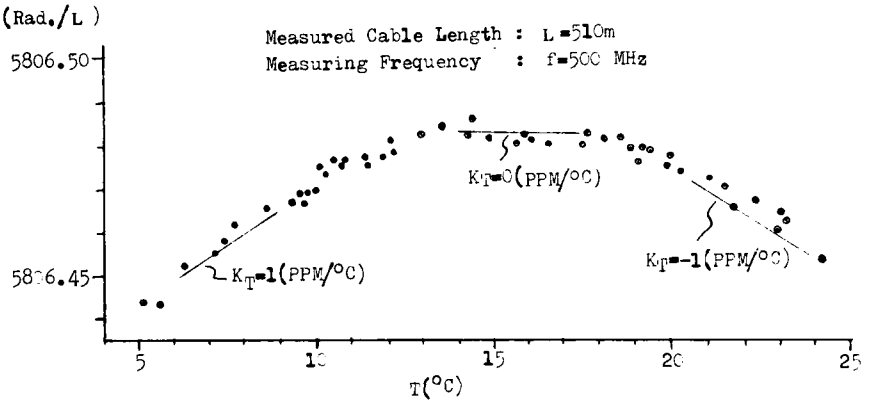



Fig. 17 Long-term electrical length stability of new COAX.

## 5. Conclusion

New techniques to produce a coaxial line with extremely stabilized electrical length have been developed. The coaxial line can be successfully applied to highly phase-sensitive electronic systems such as interferometers, radioheliographs, and sampling lines without the necessity of intricate operations to maintain the system at a constant temperature or of providing phase control devices.

## References


(1) Y. Saito, H. Kumamaru, K. Sakamoto, S. Shimada: LEAKY COAXIAL CABLE WITH HELICAL MEMBRANE POLYETHYLENE INSULATION BY DIRECT EXTRUSION, Proc. 26th IWCS, 1977.

(2) U.S. Patent 4,181,486

(3) F. Mysliwiec: PHASE STABILITY OF COAXIAL CABLE, Broadcast Engineering, August 1967.





Yasunori Saito
Sumitomo Electric Industries, Ltd.
1, Taya-cho,
Totsuka-ku,
Yokohama, Japan


Yasunori Saito received his B.S. degree in Electrical Communication Engineering from Tohoku University in 1969. He then joined Sumitomo Electric Industries and has been engaged in research and development of communication cables such as superconducting cable, leaky coaxial cable, phase stabilized coaxial cable and optical fiber cable.

Mr. Saito is a senior engineer of Communication R & D Group, and a member of the Institute of Electronics & Communication Engineers of Japan.



Shuji Furuya
Sumitomo Electric
Industries, Ltd.
1, Taya-cho,
Totsuka-ku,
Yokohama, Japan

Shuji Furuya received his B.S. and M.S. degrees both in mechanical engineering from Kyoto University in 1970 and 1972, respectively. He then joined Sumitomo Electric Industries and has been engaged in development of various kinds of computer application systems.
Mr. Furuya is a member of Communication R & D Group.



Yasuo Asano
Sumitomo Electric
Industries, Ltd.
1, Taya-cho,
Totsuka-ku,
Yokohama, Japan

Yasuo Asano received his B.S. degree in Mechanical Engineering from Waseda University in 1968. He joined Sumitomo Electric Industries in 1971 and has been engaged in development and design of connectors for coaxial cables such as CATV coaxial cable and leaky coaxial cable.
Mr. Asano is now a member of Communication Division, and a member of the Japan Society of Mechanical Engineers.



Hirokazu Sugawara
Sumitomo Electric
Industries, Ltd.
1, Taya-cho,
Totsuka-ku,
Yokohama, Japan

Hirokazu Sugawara received his B.S. and M.S. degrees both in electrical engineering from Hokkaido University in 1970 and 1972, respectively. He then joined Sumitomo Electric Industries and has been engaged in design of microcomputer application systems.
Mr. Sugawara is now a member of Communication Division.



Shuji Kato
Sumitomo Electric
Industries, Ltd.
1, Taya-cho,
Totsuka-ku,
Yokohama, Japan

Shuji Kato received his B.S. degree in Electrical Engineering from Tokyo University in 1971. He then joined Sumitomo Electric Industries and has been engaged in development and design of communication systems.
Mr. Kato is now a member of Communication Division, and a member of the Institute of Electronics & Communication Engineers of Japan.

# SOLUTION TO CORE GROWTH IN CONNECTORIZED CABLE

M. K. Reynolds and G. M. Yanizeski
Bell Laboratories
Norcross, Georgia

R. N. McIntyre
Western Electric
Norcross, Georgia

## ABSTRACT

An excess of exposed core may be generated during an underground cable installation. This problem is termed "core growth." The solution of this problem was found using a procedure that simulated the in-plant and field operations which cause core growth. Most core growth results from bending the first 20 or 30 feet of the cable at the connectorized end and is strongly dependent on the helical cabling lay in the core. The solution developed is that of clamping the sheath to the core. This method is inexpensive, employs "off-the-shelf" hardware, and does not damage the cable core. It is effective in reducing core growth from values as large as 1.7" to a maximum of only 0.35".

## 1. INTRODUCTION

When cables are connectorized in the factory, the length of wire between the sheath opening and the connector modules must be carefully controlled to ± 1/2 inch.[1] However, splicers working with cables installed in ducts have found that the exposed wire lengths have changed up to 2 and 3 inches after placing. This change in length has been termed "core growth." It is a problem on large connectorized cables because there is limited space in the splice closure to accommodate the extra wire. Early attempts to control the problem by carefully folding and dressing wire units in the splice closure were unsatisfactory. This procedure is quite time consuming for the splicer, and there is a danger of wire damage if the extra wire is not properly distributed to avoid compression as the case is closed and sealed.

A solution that would eliminate core growth and enable normal wire handling was needed. Our goals were to develop an inexpensive, effective solution that could be easily implemented in manufacturing and that would not damage the cable.

The solution to the core growth problem was obtained empirically. The key to our program was a testing procedure that simulated the in-plant and field operations producing core growth. The testing procedure enabled quick, controlled, quantitative feedback on proposed solutions. This simulation has been validated by comparison of results to actual field measurements. While core growth has not been completely eliminated, the simulation has been used to develop a clamping method which significantly reduces the problem.

Field measurements establishing the magnitude of the core growth problem are presented in Section 2. Despite the empirical approach used in our program, much was learned about the core growth mechanism. Thus, an analysis is presented in Section 3. The testing procedure, the clamping solution, and experimental results are presented in Sections 4, 5 and 6. Field measurements giving final verification of the solution are given in Section 7; factory implementation is discussed in Section 8, and an overall summary is given in Section 9.

## 2. CORE GROWTH FIELD MEASUREMENTS

Unit lengths, between the sheath opening and the connectors, were measured in the factory after connectorizing and in the field after the cables were completely installed and ready for final splicing. Core growth measurements are presented in Table I for four 1800 pair, 24 gauge pulp-insulated cables and for sixteen 2700 pair, 26 gauge pulp-insulated cables.

These cables have 100 pair units, and all the unit lengths were measured on all of the cables. In Table I, the maximum unit growth and the minimum unit growth are presented for each of the cables along with the "skew," which is the maximum minus the minimum growth. Clearly there is a large difference in unit growth within each cable as indicated by the large skews. These variations and how they are generated will be discussed and analyzed in the next section. Because these measurements were made after connectorizing, they do not include normal manufacturing variations within the allowed ± 1/2-inch tolerance on wire length. Thus, "core growth" as measured by a splicer relative to expected wire length could be larger than indicated in Table I.

Table I: Core Growth Field Measurements

| | MAX | MIN | SKEW |
|---|---|---|---|
| | 2 1/2 | -1/2 | 3 |
| 1800-24 | 1 5/8 | -5/8 | 2 1/4 |
| | 2 1/8 | -3/4 | 2 7/8 |
| | 1 3/4 | -3/8 | 2 1/8 |
| Average | 2.0 | -0.6 | 2.6 |
| Std. Dev. | 0.4 | 0.2 | 0.4 |
| | 1 | -3/4 | 1 3/4 |
| | 1 3/4 | -1 1/2 | 3 1/4 |
| | 1 | -1/2 | 1 1/2 |
| | 1 3/8 | -5/8 | 2 |
| | 1 1/8 | -3/8 | 1 1/2 |
| | 1/2 | -3/4 | 1 1/4 |
| | 1 1/2 | -1 3/8 | 2 7/8 |
| 2700-26 | 5/8 | -1/2 | 1 1/8 |
| | 3/8 | -3/8 | 3/4 |
| | 1 1/2 | -1 1/8 | 2 5/8 |
| | 1 1/8 | -1/2 | 1 5/8 |
| | 1 3/4 | -3/4 | 2 1/2 |
| | 1 3/4 | 3/8 | 1 3/8 |
| | 1 1/2 | -1 1/8 | 2 5/8 |
| | 1 3/4 | 0 | 1 3/4 |
| | 1 1/2 | -3/4 | 2 1/4 |
| Average | 1.3 | -0.7 | 1.9 |
| Std. Dev. | 0.5 | 0.5 | 0.7 |

## 3. UNDERSTANDING CORE GROWTH

There are two mechanisms which account for the final core growth seen by the splicer. The first mechanism produces a uniform increase in length across the core. The second mechanism produces both unit growth and retraction, an effect we call "skew." As shown in Figure 1, it is a combination of uniform growth and skew, in varying proportions, which yields the final core growth with which the splicer must deal.

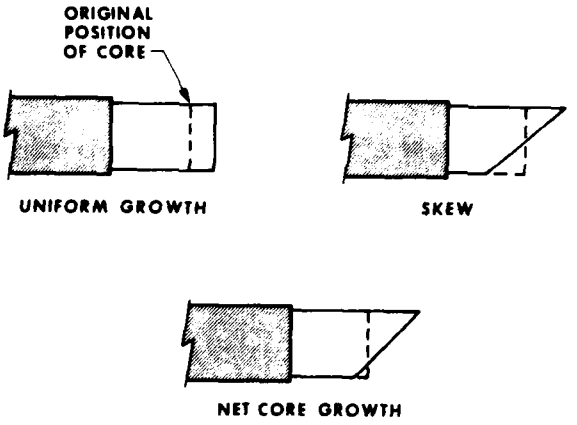



**FIGURE 1. COMPONENTS OF CORE GROWTH**

Uniform growth results from the bending the connectorized end of the cable experiences whenever it is free of the reel. The core is "pumped out" in decreasing amounts with each consecutive bend. The pumping mechanism is attributed to the working out of extra length in the core and to the releasing of possible residual stresses from manufacturing. These factors are subtle and difficult to measure or analyze. For these reasons, characterization of uniform growth was limited to the experimental results presented in Section 6.

The mechanism which causes skew is well understood and has been analyzed. Skew is caused by forming or "racking" the connectorized cable end against the manhole wall. As shown in Figure 2, this creates an "S" bend in the cable as it is forced into the corner of the manhole.

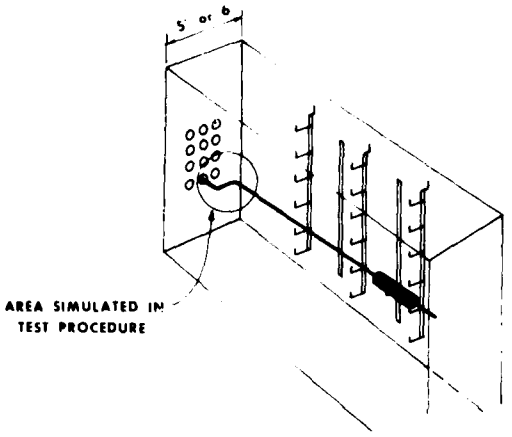



FIGURE 2. RACKED CABLE IS SHARPLY BENT TO CONFORM WITH MANHOLE WALLS

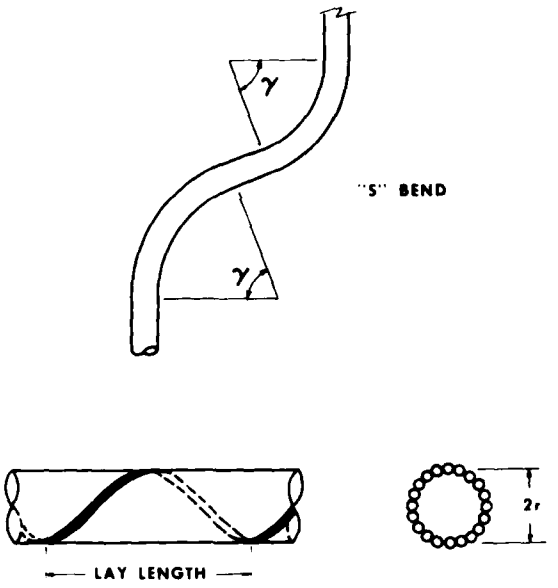



FIGURE 3. RACKED CABLE AND CORE MODELS

The varying radii from the centers of curvature force the units in the core to take paths of different length when the cable is bent. The helical lay can result in a unit being on the compression side or the tension side of both bends. The net result at the sheath opening is an almost linear variation in unit length as shown in Figure 1.

A simple kinematic analysis is helpful in understanding skew. Consider a long cylinder formed of helically wound units at a fixed radius as shown in Figure 3. We can approximate the "S" shape by bending this cylinder into two connected arcs of opposite sense with the same angle. Assume that the circular cross-section is retained and that the units are free to slide relative to each other. We can predict the amount of skew produced after computing the lengths of the paths taken by each unit as it conforms to the two arcs.

To compute the total path lengths, first bend the cylinder into one arc of given angle and radius. Figure 4 shows this geometry along with a ground reference system (X,Y,Z) and a cable reference system (x,y,z). The equation for the path of a helically wound unit with respect to the cable is:

$$\bar{P}_{/C} = r \cos\left(\theta + \frac{2\pi}{l}\rho\alpha\right)\bar{I} + r \sin\left(\theta + \frac{2\pi}{l}\rho\alpha\right)\bar{J} \qquad (1)$$

where l is the lay length of the helix.

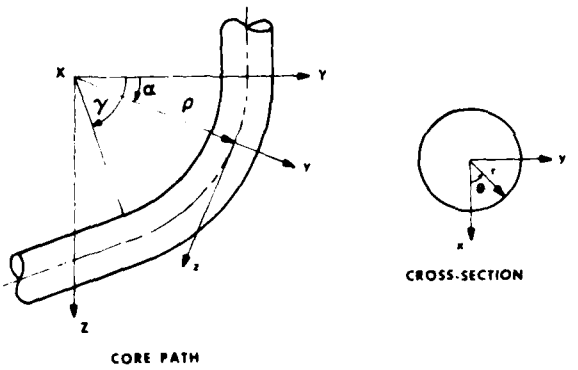



FIGURE 4. REFERENCE FRAMES FOR SKEW ANALYSIS

The path of the cable with respect to the ground reference system is:

$$\bar{C}_{/G} = \rho \cos\alpha\,\bar{J} + \rho \sin\alpha\,\bar{K} \qquad (2)$$

Writing the unit position with respect to the ground yields:

$$\bar{P}_{/G} = r \cos\left(\theta + \frac{2\pi}{\ell}\theta\alpha\right)\bar{I} + \left[r \sin\left(\theta + \frac{2\pi}{\ell}\rho\alpha\right) + \rho\right]\cos\alpha\,\bar{J} + \left[r \sin\left(\theta + \frac{2\pi}{\ell}\rho\alpha\right) + \rho\right]\sin\alpha\,\bar{K} \quad (3)$$

We may now find the arc length of a given unit by integrating the incremental length dS, expressed as a function of $\alpha$, over the angle $\gamma$; i.e.,

$$ds = \sqrt{\left(\frac{dx}{d\alpha}\right)^2 + \left(\frac{dy}{d\alpha}\right)^2 + \left(\frac{dz}{d\alpha}\right)^2}\,d\alpha$$

$$S = \int_o^{\gamma} \left[r^2 \sin^2\left(\theta + \frac{2\pi}{\ell}\rho\alpha\right) + 2r\rho \sin\left(\theta + \frac{2\pi}{\ell}\rho\alpha\right) + \frac{\left(4\pi^2 r^2 + \ell^2\right)\rho^2}{\ell^2}\right]^{1/2} d\alpha \quad (4)$$

Thus we may compute S1, the path length of a unit through one arc of the "S" bend. To compute the length through the rest of the "S" bend, adjustments to the value of $\theta$ must be made to account for the change in unit position at the beginning of the second arc. With these changes in mind, the integral may be used to compute S2, the unit path length through the second arc for the same unit. However, before summing the path lengths of different units to compute the skew, one final adjustment is made.

The skew effect propagates in both directions from a bend when not restricted. We assume only half the path length change from the first turn is reflected in skew at the cable end. All the effect from the second turn is included since the core is "locked up" in the first turn. Therefore to compute skew, we compare, for different units (expressed as different initial values of $\theta$), the sum

$$\text{SKEW} = 1/2\ S1 + S2. \quad (5)$$

The parameters in Eq. 4 are set to agree with values representative of the typical connectorized cable and the racking simulation described in Section 4, i.e.,

$\ell$ = 48 in.; r = 1.15 in.; $\gamma$ = 70°

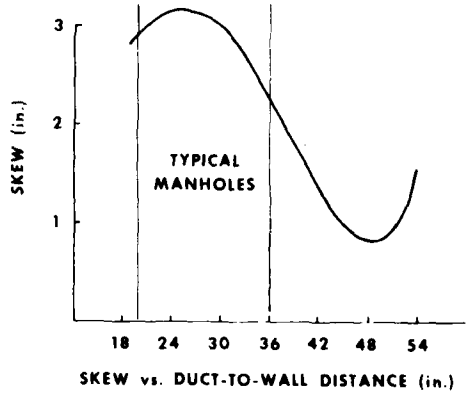
$\rho$ = 12.5 in. in arc 1

$\rho$ = 16.5 in. in arc 2

$\theta = \frac{\pi n}{4}$ rad., n = 0, 1, ...8

After solving the integrals, Eq. 5 predicts a skew value of 3.2". This value is somewhat larger than those values found in Section 6 on Experimental Results, which range from 1.6" to 2.2". Such a discrepency is understandable since the model does not include such effects as ovalization of the cross-section, buckling of units, and shifting of units away from their original position, all of which tend to reduce skew.

As shown in Figure 5, the model is most useful in showing the dependence of skew



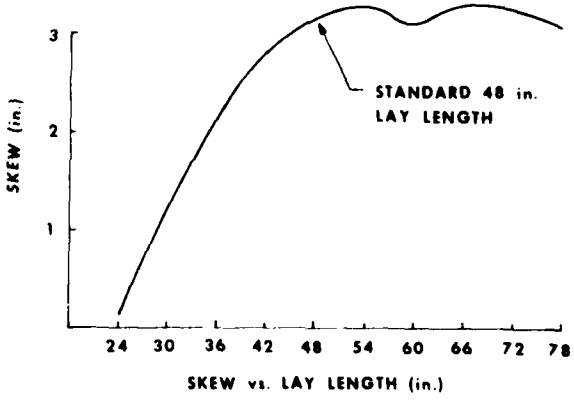




**FIGURE 5.**

upon racking geometry and lay length of the core. The plots indicate that both the duct-to-wall distance and the cable lay length currently in use are near worst case conditions. The common duct-to-wall distance of 24" is half the cable lay length. Thus units on the outside or inside of the first turn also tend to lie on the outside or inside respectively of the second turn. The contribution of skew to core growth could be significantly reduced by using either wider manholes or cables with a shorter lay length. However, the expense involved with making either of these changes is prohibative. Even were manhole dimensions enlarged, nothing can be done about those already in place.

## 4. CORE GROWTH SIMULATION PROCEDURE

### 4.1. Cable Samples

Cables chosen for the simulation test had never been handled or re-reeled. This insured that any inherent potential for growth had not been worked out of the cable. It also insured that each cable had experienced the same history.

The cables chosen for the simulation testing program are 1200 pair, 22 gauge; 1800 pair, 24 gauge; and 2700 pair, 26 gauge pulp insulated cables with a stalpeth sheath. These are typical of the large cables installed in ducts.

### 4.2. Test Procedure

The test procedure simulates four phases of cable handling:

1) in-plant handling prior to shipping,
2) installation of the cable,
3) racking the cable against the walls of the manhole after installation,
4) splicer handling.

#### In-Plant Handling

The simulation of in-plant handling begins at thd connectorizing operation. The end of the cable is unreeled onto a bench and tied down in the same manner as in the factory. An 18-inch length of sheath is removed, a protective polyester film is inserted a minimum of 2 inches between the sheath and the core, and a bond clamp is installed by cutting a 1/8-inch wide slot in the sheath. The polyester film and the bond clamp are standard on connectorized cable. This point in the simulation procedure represents that point in the factory when the connectors have been installed. However, no connectors are installed in the simulation.

Four marks are made on the core 90 degrees apart and 2.0 inches from the sheath opening. It is the measured movement of these marks that indicates core movement in the simulation.

Cables were tested with and without clamps applied to the sheath. Those cables receiving clamps are clamped at this point in the simulation.

After marking, the core is enclosed in a protective bag, tied with twine, and re-reeled. In the plant, the reel would be transported to another location, and the splice bundle would be sealed in a protective container. This "sealing" operation is simulated by unreeling and re-reeling twenty feet of cable at the connectorized end. After re-reeling, the end of the cable is tied to the flange of the reel. At this point, the in-plant simulation is complete. It has been a near one-to-one reproduction of the actual factory handling procedures that produce core growth.

#### Field Installation

Installation of the cable from the reel down through the manhole opening into the duct could not be directly reproduced without undue effort and cost. Instead, the cable was subjected to a series of controlled bending and looping operations. It was found that bending is the most important mechanism contributing to uniform core growth. Indeed, during an actual installation, the cable undergoes considerable bending as the connectorized bundle is freed from the end of the reel and worked into the manhole.

To simulate installation, the leading end of the cable is attached to a powered take-up reel, and the entire cable (approximately 60 feet) is unreeled. The connectorized end of the cable is taken almost completely up to the take-up reel, and then approximately 30 feet of cable is pulled back off the take-up reel. At this point, the connectorized end of the cable is looped as shown in Figure 6. The length and height of the loop are controlled to insure consistant cable-to-cable testing. The cable is then re-reeled, unreeled, looped, and re-reeled two more times to complete simulation of the installation procedure.

#### Racking

A near one-to-one simulation of racking is used in the test procedure. As shown in Figure 7, the connectorized end of the cable is fed through a 4-inch diameter steel pipe. It is then pulled into the

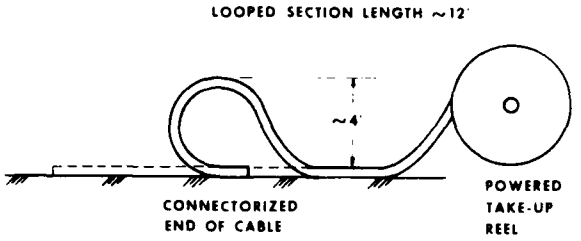



**FIGURE 6. LOOPING CABLE SIMULATES MECHANICAL CHARACTER OF CABLE INSTALLATION**

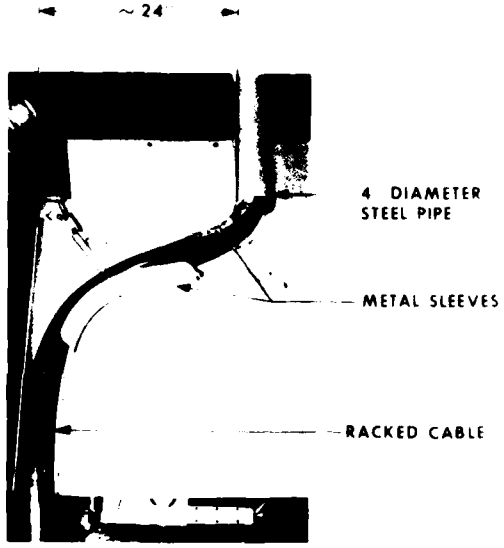



**FIGURE 7. PHOTO OF SIMULATED RACKING GEOMETRY**

corner of the simulated manhole geometry with a wire rope and winch. Metal sleeves are used at the pipe and where the wire rope contacts the cable to prevent severe kinking.

Splicer Handling

After racking, the exposed core is "worked" in a controlled manner to simulate splicing. That is, the core is bent three times in a vertical, 180 degree arc, and then it is bent three times in a horizontal, 180 degree arc.

4.3. Core Movement Measurements

Core movement is determined by measuring the position of the four marks made on the core after the connectorizing step in the simulation. Measurements are made at the following three points in the simulation:

1) before racking (after the end of the cable has been fed through the pipe),
2) after racking,
3) after working the core.

## 5. DEVELOPMENT OF CLAMPING SOLUTION

Initially, several techniques to dissipate potential core growth by tensioning, twisting, and bending ten to twenty feet of the cable end were tried. Although effective in reducing average growth, these methods did not significantly improve the skew performance. Instead a solution was sought which would prevent core growth rather than dissipate it.

The final design uses a single adjustable hose clamp over the sheath and core just behind the sheath opening as shown in Figure 8. Figure 8 shows a clamped cable with the standard end plate in place. With proper positioning, the clamp is completely compatible with the end plate hardware of the standard Bell System closure.

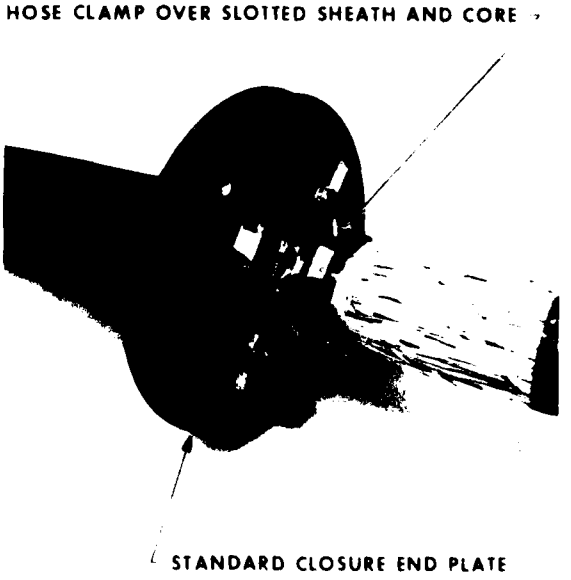



**FIGURE 8. PHOTO OF CLAMPED CABLE**

The sheath is prepared before clamping with longitudinal slots. The slots, which are evenly spaced, are required to allow the otherwise rigid sheath cylinder to be uniformly compressed onto the core by the hose clamp, locking the sheath and core together. Polyester film is used between sheath and core under the clamp to protect the core.

The slots are placed in the sheath by means of a special tool. The tool cuts an entire slot in one operation in such a manner that the edges of the metal layers of the sheath are turned away from the core. This is an important part of protecting the core from damage because the sheath tabs are compressed onto the core by the hose clamp. The clamp is sized to reduce the cable diameter by approximately 12% at a final bolt torque of 50 in-lb.

Figure 9 shows the correspondence between bolt torque and reduction in cable diameter for three cable sizes. Each curve is the average of two cables. The similarity of the curves demonstrate the uniform manner in which compression is applied to the cores.

The clamp failed consistently at 70 in.-lb. when the bolt began to slip. The 50 in.-lb. torque was chosen to leave some margin of safety and yet provide a firm clamping force without damaging the core. Tests showed that a polyester film protective layer is more than adequate for core protection at this level. This is the same film that is normally used to protect the core from the sharp edges of the metal layers in the sheath on connectorized cable.

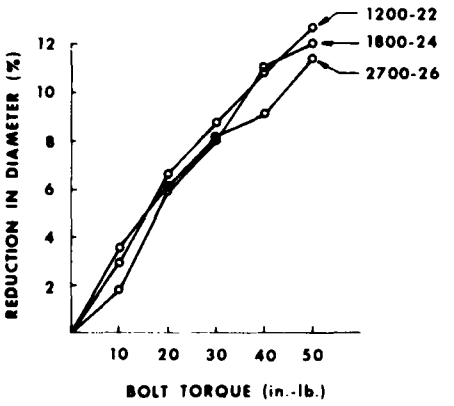



**FIGURE 9. CORRESPONDENCE BETWEEN CLAMP BOLT TORQUE AND REDUCTION IN DIAMETER**

## 6. EXPERIMENTAL RESULTS

The effectiveness of the clamping solution was determined by subjecting the sample cables described in Section 4.1 to the full simulation test. Two lengths of each sample cable type were tested with clamps, and two of each were tested without. Core movement was measured at three stages in the simulation procedure as described in Section 4.3.

Core movement results measured after installation but before racking are presented in Table II. Only the largest values are presented from each type of cable tested.

Table II: Before Racking Values of Maximum Growth and Skew (in.)

| Cable: | 1200-22 | 1800-24 | 2700-26 |
|---|---|---|---|
| Max. Growth | | | |
| Unclamped | 0.7 | 1.0 | 0.5 |
| Clamped | 0.1 | 0.2 | 0.1 |
| Skew | | | |
| Unclamped | 0.3 | 0.4 | 0.2 |
| Clamped | 0.1 | 0.2 | 0.2 |

Note that before racking, the solution works to reduce maximum unit growth from between 0.5 - 1.0 inches to no more than 0.2 inches. Skew is also reduced although it is not a factor before racking.

Table III below shows again the larger values from each pair of cables, but in this case the cables have been both looped and racked, but not given final splicer handling.

Table III: After Racking Values of Maximum Growth and Skew (in.)

| Cable: | 1200-22 | 1800-24 | 2700-26 |
|---|---|---|---|
| Max. Growth | | | |
| Unclamped | 1.2 | 1.4 | 1.1 |
| Clamped | 0.2 | 0.2 | 0.2 |
| Skew | | | |
| Unclamped | 1.9 | 2.0 | 1.7 |
| Clamped | 0.6 | 0.5 | 0.8 |

The clamping solution continues to hold the maximum growth to 0.3 inches or less after racking while unclamped cables average more than 1.0 inch. The solution limits the skew to less than half the amount experienced with unclamped cables.

The results of the final measurements after racking and splicer working are presented in graphical form in Figure 10. The complete range of measurements for each cable is indicated by the vertical bar in each graph. The region above each horizontal line represents positive unit growth and the region below is negative. Skew is represented by the length of the bar.

From examination of Figure 10 it is clear that both skew and uniform growth are substantially reduced by the clamping solution. Maximum growth is reduced from values as high as 1.7 inches to less than 0.4 inches in all cases. Skew is reduced from as much as 2.2 inches to 0.9 inches or less. These results after the complete simulation are quite consistent with the initial data from the field presented in Table I.

It should be noted from Figure 10 that the clamp is more effective against core growth than core retraction. The reason is that growth occurs when units under compression are pushed out. The clamp restricts their movement and the units buckle. However, retraction occurs when the units are in tension. Buckling is not a factor and the tension is large enough to overcome the resistance created by the clamp.

Additional experimental work was performed to determine how an originally clamped core will behave if the clamp is removed before splicing. Such a necessity might arise if the units of the two cables to be joined must be rotated within the sheath to be properly aligned. Two 1200 pair, 22 gauge and two 2700 pair, 26 gauge cables were clamped and run through the simulation. After racking, the clamps were removed and the cores were worked by bending (see Section 4) and by rotating them clockwise and counterclockwise. The larger values from each pair of cables are presented in Table IV below.

Table IV: Core Growth Values Before and After Clamp Removal and Working (in.)

| | MAX. GROWTH | SKEW |
|---|---|---|
| 1200 PAIR 22 GA. | | |
| Before Removal | 0.1 | 1.0 |
| Clamp Removed | 0.1 | 1.0 |
| After Working | 0.5 | 1.4 |
| 2700 PAIR 26 GA. | | |
| Before Removal | 0.1 | 0.4 |
| Clamp Removed | 0.2 | 0.7 |
| After Working | 0.7 | 1.6 |

As expected, some recovery of unclamped core growth occurs when the clamp is removed. This is especially true if the core is worked considerably after clamp removal. For best results, the clamp should be left on the cable through the splicing operation.

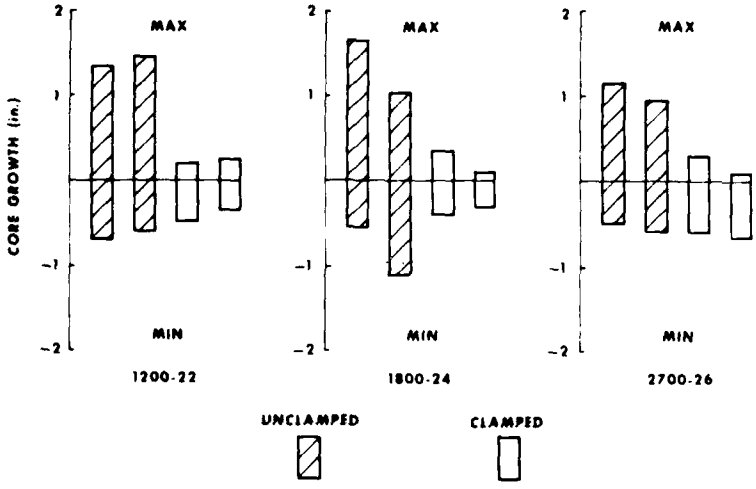



FIGURE 10. AFTER RACKING CORE GROWTH - STALPETH PULP

## 7. FIELD TRIAL

Three connectorized 1200 pair, 22 gauge pulp insulated cables were prepared with the clamps and reference marks as described earlier. Unit lengths from the sheath opening to the connector modules were also recorded. The cables were shipped to Orlando, Florida and installed by operating company personnel using standard installation procedures for connectorized cable. However, the racking normally required to position the connectorized end against the side wall was not performed on two of the cables because they were installed in "splayed" ducts. In a splayed duct system, the ducts form an "S" bend near the manhole so that the cable enters the manhole near the wall. Average measured core movements after final positioning are summarized in Table V.

Table V: Orlando Field Trial

| | Duct Type | Max. Growth | Skew |
|---|---|---|---|
| 1 | Standard | 0.1 | 0.1 |
| 2 | Splayed | 0.2 | 0.5 |
| 3 | Splayed | -2.2 | 0.4 |

The results for cables 1 and 2 demonstrate the effectiveness of the clamping solution. With regard to Cable No.3, such negative movement had not been reported previously, and did not fit the distribution of data presented in Section 2 on cables measured in the field. A possible explanation for the behavior is the installation of the cable in a splayed duct. The additional drag force exerted on the plastic sheath, as the cable leaves the manhole in the "S" bend path, may cause the sheath to be milked over the trailing end's exposed core.

Conversations with the Florida splicing crew revealed that they have previously seen unit lengths as much as 5 inches shorter than normal. Central Florida has proportionately more splayed ducts than other areas. Hence it is suggested that the core growth solution may have acted to reduce core retraction.

Three connectorized 3600 pair, 26 gauge pulp insulated cables were also factory prepared with the clamping solution and reference marks. They were installed in Fresno, California in standard ducts. Table VI shows the average core growth results. Note that two of the three cables exhibited retraction rather than growth. Neither the core growth or retraction was large enough to cause any concern, demonstrating again the success of the clamping solution.

Table VI: Fresno Field Trial

| | Max. Growth | Skew |
|---|---|---|
| 1 | 0.5 | 0.3 |
| 2 | -0.5 | 0.8 |
| 3 | -0.3 | 0.1 |

## 8. FACTORY IMPLEMENTATION

Application of the clamp can be conviently accomplished during the normal sheath preparation stage that the cable goes through when the bond clamp is applied, prior to connectorization. In fact, the tabbing tool design is being utilized to produce a quicker and improved method of tabbing for application of the bond clamp in both the factory and field. The protective polyester collar is already a standard requirement in pre-connectorization, so no additional labor is needed to place this layer. The implementation of the clamping solution will cause little disruption of the product flow and a minimal time penalty.

## 9. SUMMARY

Our original goals were to develop a core growth solution that is effective, inexpensive, easily implemented in manufacturing, and not damaging to the core. All of these goals have been met. Core growth has been restricted to only 0.35 inches and skew has been cut in half. Material costs are small because the only hardware is an inexpensive hose clamp. Tabbing the sheath and applying the clamp are easily accomplished during the sheath preparation operation of the present pre-connectorization process. Finally, the polyester film already used on connectorized cable provides sufficient protection to prevent core damage.

## 10. ACKNOWLEDGEMENTS

The authors wish to express their appreciation to the following people whose efforts contributed to the completion of this project: A. S. Hamilton, R. D. Farley, P. T. Nunn, G. Snyder and D. Sahm.

## 11. REFERENCES

1. D. R. Frey and A. G. Hardee, "CONnectorized Exchange Cable Splicing (CONECS)," Proceedings of the 25th International Wire and Cable Symposium, November, 1976.



Mickey Reynolds is a member of the Cable and Wire Department, Bell Laboratories, Norcross, Georgia. He received his M.S. from Georgia Institute of Technology in 1979. Since joining Bell Laboratories in 1978, he has been involved with mechanical characterization of cable core and sheath.



George Yanizeski is a mamber of the Cable and Wire Department, Bell Laboratories, Norcross, Georgia. He received his Ph.D. from Carnegie-Mellon University in 1968. He joined Bell Laboratories in 1972, and since 1976 he has been involved in cable sheath mechanical characterization studies and new design development.



Bob McIntyre is a memeber of the Cable and Wire Product Engineering Control Center, Western Electric, Norcross, Georgia. He received his Bachelors Degree in Mechanical Engineering from Georgia Institute of Technology in 1974. He joined Western Electric in 1974 and has been involved in cable testing and termination processes.

# CABLE SHEATH BUCKLING STUDIES AND THE DEVELOPMENT OF A BONDED STALPETH SHEATH

G. M. Yanizeski and E. L. Johnson
Bell Laboratories
Norcross, Georgia

R. G. Schneider
Western Electric
Norcross, Georgia

## Abstract

In recent years, the increased popularity of jumbo size duct cables, the necessity of mid-winter installations and the introduction of high production placing equipment have dictated improved performance by cable sheaths. Theoretical and experimental studies have pointed the way to modest improvements in standard stalpeth, and they have also established the need for a new sheath design. Utilizing advances in bonding technology, a bonded stalpeth sheath having greatly improved buckling resistance has been developed and tested. Advantages of the bonded stalpeth design are that it can be made by a one-pass operation, it eliminates core exposure to the high temperature of soldering, it exhibits high diffusion resistance, and it can withstand the rigors of cold weather installation without buckling. Field experience and laboratory evaluations have substantiated the bonded stalpeth's superiority.

## I. Introduction

In recent years, several factors have necessitated improved buckling performance for stalpeth cable sheath. Large pair size cables have increased in popularity; improved jacketing compounds have enabled colder installation temperatures without cracking,[1] and telephone operating companies have been employing high production placing equipment. As a result, cable sheath buckling emerged as a problem in the 1977-1978 winter season. The buckles form irregularities in the cable surface and are a problem during duct installation because they can snag or abrade.

Our first efforts were directed at improving standard stalpeth. Experimental and theoretical results on the buckling of standard stalpeth are presented in Section II. Through modest improvements in performance and special care taken during installation, the incidence of failure has been controlled. However, it has been concluded that a new design with a greater margin of safety is needed. The new design is bonded stalpeth, in which the steel is adhesively bonded to the outer plastic jacket. Bonded stalpeth is described in Section III, and a full range of performance results is presented. A summary of all results and conclusions is presented in Section IV.

## II. Buckling Performance of Standard Stalpeth

### Description of Standard Stalpeth

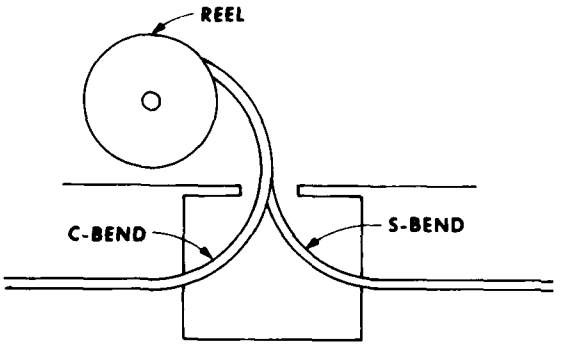
Stalpeth sheath consists of a corrugated 8-mil aluminum tape over the core, a corrugated 6-mil steel tape with a soldered, longitudinal seam, a flooding compound over the steel, and a black outer jacket of low density polyethylene. The flooding compound can be either a tar-like thermoplastic cement or an amorphous atactic polypropylene.

### Installation Methods and Modes of Buckling

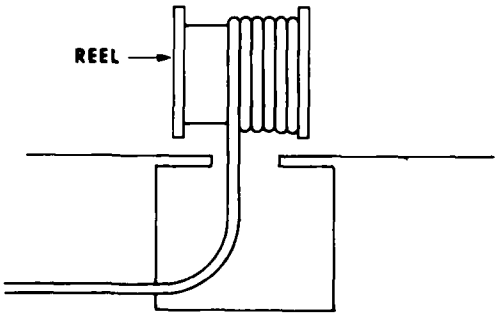
Figure 1 shows the three basic configurations for installing cables in ducts. In the C-bend configuration, the compressive strains causing buckling are generated as the cable is straightened and reel set is overcome. In the S-bend configuration, the cable sustains bending beyond that needed to straighten the cable, and additional compressive strains are generated. In the side payout configuration, the cable undergoes bending and torsion as the cable comes off the top of the reel and then turns to enter the duct. Side payout is used in high production placing methods in which several reels are mounted on a flat bed tractor trailer. Side payout is the most severe configuration for buckling, and C-bend is the least severe.

Figure 2 shows the three modes of sheath buckling. The rippling mode and the kinking mode occur during simple bending. The torsional mode is due to torsional loading during side payout. In the rip-

pling mode, the jacket initially forms a sine wave; however, as shown in Figure 2a, a few buckles often grow much larger than neighboring buckles when the cable is bent beyond initial buckling. In the kinking mode, the cross section collapses. This is the mode of buckling seen when bending a hollow tube. Indeed, the sheath sample in Figure 2b contains an undersized core and is nearly hollow. The torsional buckle, as shown in Figure 2c, is oriented approximately 45° to the cable axis. By far, the most common form of buckling seen on standard stalpeth is the rippling mode.




1a C AND S–BEND CONFIGURATIONS




1b SIDE PAYOUT CONFIGURATION

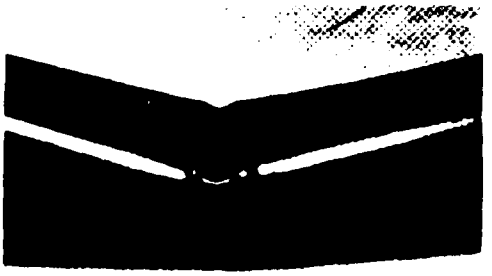
**FIGURE 1 THREE CONFIGURATIONS FOR PULLING CABLES INTO DUCTS**

## Testing Methods

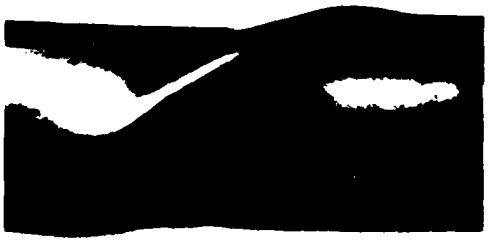
Buckling performance in bending is critical because all configurations for installing cable in ducts involve bending. For this reason, initial testing was devoted to bending.



2a RIPPLING MODE OF BUCKLING



2b KINKING MODE OF BUCKLING



2c TORSIONAL BUCKLE ORIENTED ~45° TO CABLE AXIS

**FIGURE 2 THREE MODES OF CABLE SHEATH BUCKLING**

Two types of buckling tests were utilized: 1) bend tests on 6-foot cable samples, and 2) re-reeling tests on 600 to 900-foot lengths of cable. The "6-foot" test was used to quickly test a variety of cables and thus gain quantitative knowledge on buckling. The "re-reeling" test closely simulates actual installation conditions and was used to verify results from the 6-foot test and to prove-in design changes.

Figure 3 is a diagram of the 6-foot test. A 6-foot length of cable is bent until the incipiency of buckling. The cord C, the cord height H, and the cable diameter D are measured, and the radius of curvature

is calculated from the following:

$$\rho = \frac{4H^2 + C^2}{8H} + \frac{D}{2}, \qquad (1)$$

which was derived using the Pythagorean theorem.[2]

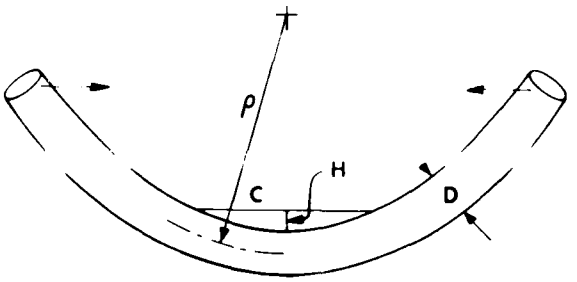



**FIGURE 3 SIX-FOOT BEND TEST**

Figure 4 is a diagram of the re-reeling test. Reels of cable are stored a minimum of 24 hours in a temperature-controlled chamber usually set at 15°F. The reels of cable are removed and within 20 minutes re-reeled using in-plant re-reeling facilities. Re-reeling rates are in the 100 feet per minute range, and as shown in Figure 4, an S-bend configuration is used. Results reported in this paper are for those lengths of cable known to be manufactured under stable conditions exclusive of start up transients.

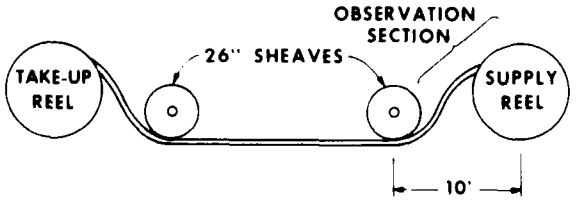



**FIGURE 4 RE-REELING TEST**

An important parameter affecting buckling performance is the "cross-sectional stiffness." In this test, a 1-foot length of cable is compressed between 6-inch plates in an Instron testing machine. The stiffness K is the slope of the force-deflection plot measured between $\Delta D = 0.02$ and 0.08 inches. Thus, K is close to the initial slope; however, by starting at $\Delta D = 0.02$ inches, small random fluctuations at the beginning of the plot are avoided.

Results from the 6-Foot Test

The cable samples used in the 6-foot test had initial curvatures due to reel set. As shown in Reference 2, the strain generated when bending an initially curved member is

$$\epsilon = y\left(\frac{1}{\rho_2} - \frac{1}{\rho_1}\right), \qquad (2)$$

where y is the distance from the neutral (unstrained) surface, $\rho_1$ is the initial radius of curvature and $\rho_2$ is the final radius of curvature. The "change in curvature" is defined as

$$\Delta \frac{1}{\rho} = \frac{1}{\rho_2} - \frac{1}{\rho_1}. \qquad (3)$$

All results from the 6-foot test are presented in terms of the critical change in curvature needed to initiate buckling.

As shown in Figure 5, the critical change in curvature decreases sharply with increasing cable size for stalpeth-sheathed cable with a pulp core. In part, this is due to the dependence of strain on cable diameter. However, between 2.8 and 3.4 inches, $(\Delta\ 1/\rho)_c$ decreases by a factor of 2.4 while the diameter increases by a factor of only 1.2. A more important effect is cross-sectional stiffness, which also changes with cable size.

Figure 6 is a plot of the critical change in curvature needed to cause buckling versus cross-sectional stiffness for cables between 3.20 and 3.41 inches. This narrow size range minimizes the strain effect. All of the cable samples represented in Figure 6 have conventional, unbonded sheaths and thus buckle in the same mode. This means that the strong effect of stiffness on buckling seen in Figure 6 is applicable to pulp-stalpeth cable over a range of cable sizes. As shown in Figure 7, the cross-sectional stiffness of pulp-stalpeth decreases with increasing size. Applying the linear, least-squares data fit in Figure 7 to the linear fit in Figure 6 gives $(\Delta\ 1/\rho)_c$ values of 0.086 and 0.042 $in^{-1}$ for pulp-stalpeth cables with 2.8 and 3.4-inch diameters. From the linear fit in Figure 5, the directly measured $(\Delta\ 1/\rho)_c$ values for pulp-stalpeth are 0.095 and 0.039 $in^{-1}$. The agreement is excellent, and probably better than should be expected in light of the experimental scatter in the data. Nonetheless,

decreasing cross-sectional stiffness is clearly the dominant reason buckling resistance degrades with increasing size.

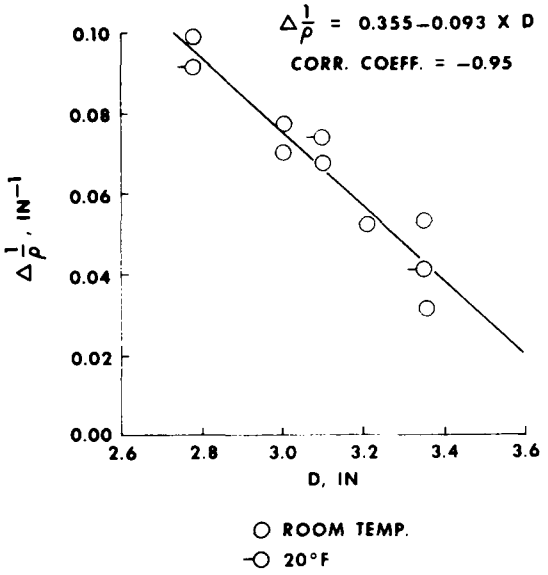



FIGURE 5 BUCKLING PERFORMANCE OF PULP STALPETH CABLE DEGRADES WITH INCREASING CABLE SIZE

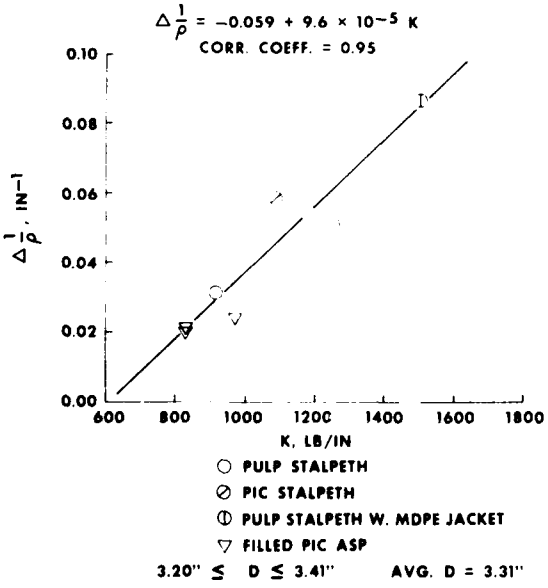



FIGURE 6 BUCKLING PERFORMANCE IMPROVES WITH INCREASING CROSS-SECTIONAL STIFFNESS FOR CABLES OF NEARLY THE SAME SIZE

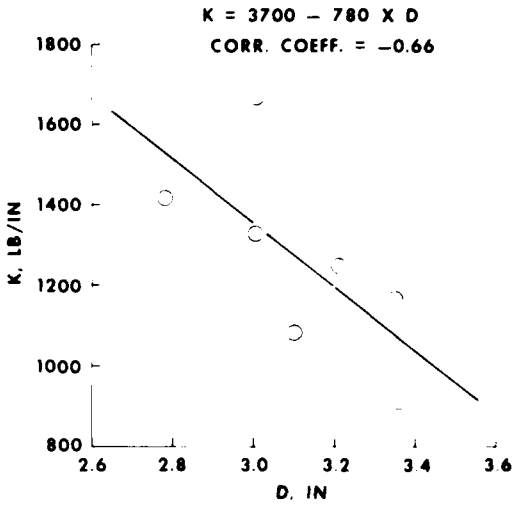



FIGURE 7 CROSS-SECTIONAL STIFFNESS DECREASES WITH INCREASING SIZE FOR PULP STALPETH CABLE

## Theory Compared with Test Results

The critical change in curvature at which a filled, thin-walled cylinder buckles in the rippling mode (Figure 2a) is well approximated by*

$$\left(\Delta\frac{1}{\rho}\right)_c = \frac{1 + \frac{9}{4}\frac{E_c}{E_s}\left(\frac{b}{h}\right)^{3/2}}{1.8\ b^2/h} \qquad (4)$$

where

$h$ = thickness of the cylinder wall

$b$ = radius of the cylinder, measured to the center of the cylinder wall

$E_s$ = modulus of the cylinder wall

and

$E_c$ = plane strain modulus for the material inside the cylinder.

*Equation (4) was developed by G. S. Brockway (Bell Laboratories) from a result by P. Seide[3] using an approximation suggested by P. Seide. A full development of this equation is being prepared for publication.

Although (4) was not derived for the complex geometry of multipair cable with a multilayer sheath, it can be adjusted for cable applications by using cross-sectional stiffness measurements to calculate $E_c$. For an infinitely long, solid cylinder compressed between two, nondeformable flat plates, the change in diameter is given by[4]

$$\Delta D = \frac{4p}{\pi E_c}\left(1/3 + \ell n\ \frac{5}{4}\sqrt{\frac{DE_c}{p}}\right) \qquad (5)$$

where

p = force per unit length

D = diameter

Differentiating (5) with respect to $\Delta D$ and solving for $k = dp/d(\Delta D)$ yields

$$k = \frac{\frac{\pi}{4}E_c}{\ell n\left[\frac{5}{4}\sqrt{\frac{DE_c}{p}}\right] - \frac{1}{6}} \qquad (6)$$

where k is the cross-sectional stiffness per unit length.

As described earlier, the cross-sectional stiffness is measured between $\Delta D = 0.02$ inches and $\Delta D = 0.08$ inches. Substituting an average $\Delta D = 0.05$ inches into (5), iterating (5) to obtain $E_c/p$ and substituting the numerical result for $E_c/p$ into (6) yields

$$E_c = 3.65\ k\ , \qquad (7)$$

which is independent of cable diameter for cables between 3.0 and 3.5 inches. The stiffness per unit length (k) is obtained by dividing the equation in Figure 7 by 6 inches, which is the length of the flat plate in the Instron testing machine. Substituting k into (7) and the resulting $E_c$ into (4) yields the following for the critical change in curvature to initiate buckling:

$$\Delta\left(\frac{1}{\rho}\right)_c = h/b^2\left[0.56 + \left(\frac{2760-1190b}{E_s}\right)\left(\frac{b}{h}\right)^{3/2}\right]$$

(for pulp-stalpeth) , (8)

where $\Delta\ 1/\rho$ is in $in.^{-1}$, $E_s$ is in psi, b is in inches, and from the definition of the radius b,

$$b = (D-h)/2\ . \qquad (9)$$

The modulus for low density polyethylene jacketing compound measured at 110 Hz is 45,000 psi at 72°F and 115,000 psi at 15°F. The curves obtained by substituting these moduli for $E_s$ into (8) are plotted in Figure 8 along with the 6-foot test results from Figure 5. The agreement between theoretical and experimental results is surprisingly good in light of the simplifications inherent in (4).

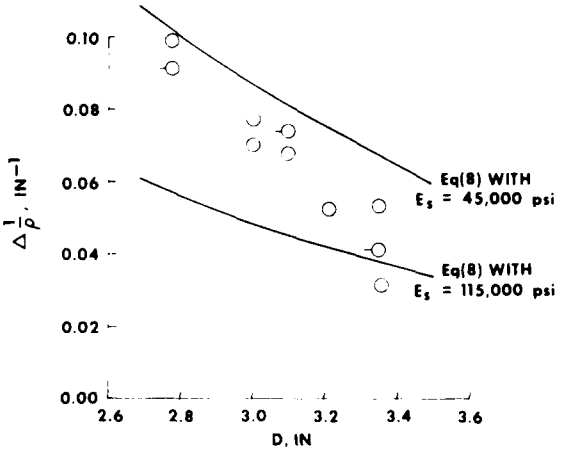



FIGURE 8 AGREEMENT BETWEEN THEORY AND EXPERIMENTAL RESULTS FOR THE BUCKLING OF PULP-STALPETH CABLE

As indicated by the two curves plotted in Figure 8, increasing the modulus of the jacketing compound decreases buckling resistance. The $E_s$ values in Figure 8 represent modulus changes due to temperature. Indeed, field experience confirms that cable jackets buckle more easily at low temperatures. The temperature effect was not evident in the 6-foot test. A possible explanation is that the 6-foot test was conducted at a low strain rate, which did not produce a strong temperature effect.

The modulus effect indicated in Equation (8) can be used to evaluate candidate jacketing compounds for buckling performance. For example, at 15°F and at 100 Hz, jacketing grade medium density polyethylene has a modulus of 130,000 psi while low density polyethylene at 15°F and 110 Hz has a modulus of 115,000 psi. The difference in moduli is small, and at 15°F the two compounds should give similar buckling performance.

Figure 9 is a plot of the change in curvature at buckling, from Equation (8), versus jacket thickness for two cable sizes and two jacket moduli. For these cable sizes, jacket thickness has only a negligible effect on buckling resistance.

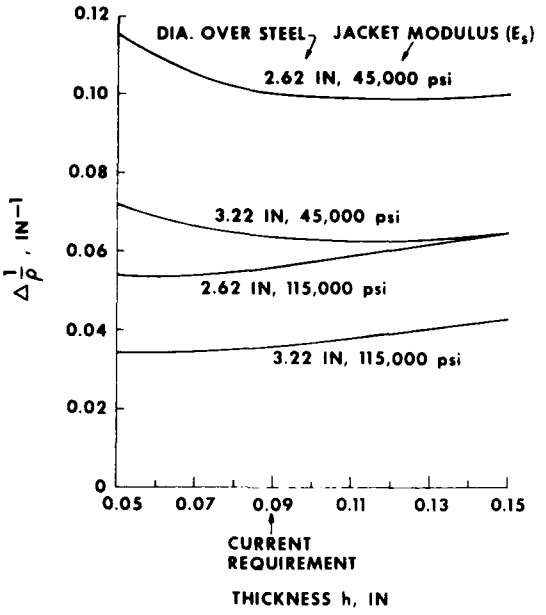



**FIGURE 9 JACKET THICKNESS HAS NEGLIGIBLE EFFECT ON BUCKLING OVER A RANGE OF CABLE SIZES AND JACKET MODULI**

## Re-Reeling Test Results for Pulp-Stalpeth

Table I contains test results for 6 reels of pulp-stalpeth cable listed in order of increasing cross-sectional stiffness and increasing $(\Delta\ 1/\rho)_c$ from the 6-foot test. Cables 5 and 6 had the highest stiffnesses and also performed best in the re-reeling tests. In the re-reeling tests, the change in curvature is approximately $\Delta\ 1/\rho = 0.06$ in$^{-1}$, and cables with $(\Delta\ 1/\rho)_c > 0.06$ in$^{-1}$ passed the re-reeling test without buckling.

Cable 2 in Table I has a flooding of atactic polypropylene (APP) over the steel and the others have thermoplastic cement (TPC). Changing between these two compounds does not significantly affect buckling.

The core in cable 3 has a new, thinner, tougher pulp insulation that enables smaller diameters without sacrificing electrical performance. Despite the smaller diameter, it buckled during the re-reeling test. Cable 3 was not subjected to the 6-foot test. However, another length of cable of the same design was tested. It was 3.11 inches in diameter; it had a cross-sectional stiffness of 1080 lb/in and a $(\Delta\ 1/\rho)_c$ of 0.034 in$^{-1}$. Thus, the new core is smaller, but the cross-sectional stiffness and consequently the buckling performance is comparable to standard core cable.

TABLE I

RE-REELING TEST RESULTS AT 15°F FOR PULP-STALPETH CABLES

| Cable | Flooding | Dia. in. | K lb/in | $\left(\Delta \frac{1}{\rho}\right)_c$ in$^{-1}$ | Buckled? |
|---|---|---|---|---|---|
| 1. 3600-26 | TPC | 3.36 | 920 | 0.032 | Yes |
| 2. 1200-22 | APP | 3.11 | 920 | - | Yes |
| 3. 3600-26 | TPC | 3.18 | 1040 | - | Yes |
| 4. 3600-26 | TPC | 3.24 | 1250 | 0.051 | Yes |
| 5. 1200-22 | TPC | 3.08 | 1580 | 0.068 | No |
| 6. 1800-24 | TPC | 3.03 | 1670 | 0.077 | No |

Cable 4 was manufactured by tightening a standard core without regard to electrical performance. Average mutual capacitance reached 0.094 μf/mile. Although the overall cross-sectional stiffness increased relative to cable 1, it did not increase sufficiently to prevent buckling.

## Efforts to Improve Stalpeth

Summarizing the results from this section, the potentially most effective method for improving the buckling performance of standard stalpeth is to increase cross-sectional stiffness by tightening the cable cross section. Changing jacket thickness, changing flooding compounds, or changing from low to medium density polyethylene do not significantly improve performance. Buckling performance was improved on production cables by tightening the sheath layers in order to increase cross-sectional stiffness. However, the degree to which cross-sectional stiffness can be increased is limited by electrical performance requirements in the core unless a new, more expensive core design with thicker insulation is introduced. Thus, it was concluded that a new sheath design is needed.

## III. Bonded Stalpeth Sheath

### Description of Bonded Stalpeth

Bonded stalpeth contains the same basic components as standard stalpeth - corrugated aluminum, corrugated steel, and a low density polyethylene jacket. However, bonded stalpeth does not have a soldered steel seam or a flooding compound, and the steel is adhesively bonded to the polyethylene jacket.

The steel used in bonded stalpeth has a copolymer adhesive coating that bonds to the polyethylene jacket during extrusion. It employs the same basic technology as copolymer-coated aluminum.[5,6] Although bonded aluminum sheaths have been manufactured since the 1960's, bonded steel sheaths are relatively new. One development that enables bonded steel sheaths is the use of tin-plated or chrome-coated steels. The tin or chrome prevents corrosion of the steel and thus enables good bond life under moisture conditions.

Bonded steel sheath provides the same traditional advantages as bonded aluminum sheath in the areas of diffusion resistance, corrosion resistance, and crack resistance of the metal layer. However, our primary incentive in pursuing bonded stalpeth was to eliminate buckling of the polyethylene jacket during cold weather installation.

### Buckling Performance of Bonded Stalpeth

Table II contains a list of the bonded stalpeth-sheathed cables subjected to re-reeling tests. Cable 1 is a full size 3600 pair, 26 gauge, 3.4-inch diameter pulp core cable. In separate tests, it was subjected to both S-bend and side payout re-reeling at 18°F without any sign of buckling. By contrast, all three 3600 pair, 26 gauge pulp cables with standard stalpeth sheaths listed in Table I buckled. These standard stalpeth-sheathed cables exhibited some buckling along most of their lengths although most of the buckles were not large enough to cause installation problems. The complete absence of buckles on cable 1 in Table II demonstrates a significant increase in buckling resistance.

Cable 2 in Table II is relatively small, but it has a very soft core. It was re-reeled without buckling. Even in the start up section of the cable, where the core was especially loose and lumpy, there were no buckles except for one slight dent.

TABLE II

BONDED STALPETH-SHEATHED CABLES SUBJECTED TO RE-REELING TESTS

| | Cable | Dia. in. | Test Config. | Temp. °F | Length ft. |
|---|---|---|---|---|---|
| 1. | 3600-26 pulp | 3.4 | S-Bend | 18 | 800 |
| | | | Side payout | 18 | |
| 2. | 616-24 plastic | 2.7 | S-bend | 9 | 600 |
| 3. | 3600-26 pulp | 3.4 | S-bend | 15 | 275 |
| 4. | 924-24 plastic | 3.2 | S-bend | 15 | 940 |

Cable 3 is a full-size 3600 pair, 26 gauge pulp cable that was manufactured with varied metal overlap forming and corrugating along its length. Even though most of the metal forming and corrugating was below normal factory standards, it was re-reeled without serious buckling.

Cable 4 is relatively large (3.2-in diameter) and has a very soft, plastic-insulated core. As a result, its cross-sectional stiffness is only 510 lb/in. This is well below the cross-sectional stiffness of any of the pulp-stalpeth cables in Table I. For this reason, cable 4 represents the worst case condition for testing the buckling resistance of bonded stalpeth sheath. Cable 4 was re-reeled at 15°F without buckling except for one small buckle near the inside end that would have survived installation.

A field trial installation of two 3600 pair, 26 gauge pulp-insulation cables with bonded stalpeth sheaths was conducted in Detroit, Michigan on April 16, 1979. Unfortunately, the trial was delayed, and worst case, winter temperatures were missed. According to the U.S. Weather Bureau, hourly temperatures ranged between 41°F and 46°F for the 24-hour period leading up to the installation. The first cable was successfully installed in a tight S-bend configuration, and the second was successfully installed in the side payout configuration.

### Why Bonded Stalpeth Resists Buckling

A key to the improved buckling resistance attained with bonded stalpeth is a change in the mode of buckling. As shown in Figure 2a and 2b, cable sheath subjected to bending can buckle in the rippling mode or the kinking mode. Standard stalpeth is more susceptible to rippling than to kinking. That is, the polyethylene

jacket ripples before the cable is bent sufficiently to kink. The jacket cannot ripple on bonded stalpeth because it is adhesively joined to the corrugated steel. Consequently, bonded stalpeth can sustain additional bending until it kinks.

In the kinking mode, the theoretical critical change in curvature is approximated by*

$$\left(\Delta \frac{1}{\rho}\right)_c = \frac{t}{2b^2} \sqrt{\frac{\hat{E}_c}{E_L}} \qquad (10)$$

where

$t$ = composite sheath thickness

$b$ = radius of the sheath

$E_L$ = longitudinal (axial) modulus of sheath

$\hat{E}_c$ = composite circumferential modulus of sheath and core

Equation (10) has not been developed in detail yet for cable or verified experimentally. However, it does indicate two reasons why bonded stalpeth resists buckling. The first is due to the corrugated steel, which is compliant in the longitudinal cable direction and stiff in the circumferential direction. Thus, the corrugated steel increases the $\hat{E}_c/E_L$ ratio and correspondingly increases $(\Delta\ 1/\rho)_c$. The second reason is due to the cable core. It contributes to $\hat{E}_c$ and further increases $\hat{E}_c/E_L$. An additional effect of the core is to minimize the severity of any kink, once initiated, by resisting any large collapse of the sheath cross section.

At this time, it is not certain whether bonded stalpeth resists kinking significantly better than standard stalpeth. Both have corrugated steel and are supported by a core of wire pairs. Nonetheless, the switch from rippling to kinking has been observed and seems to be the main reason bonded stalpeth is more resistance to buckling.

*Equation (10) was developed by G. S. Brockway (Bell Laboratories) from theoretical results for orthotropic cylindrical shells by Reissner and Weinitschke.[7]

## Manufacturing Bonded Stalpeth

Unlike the two step operation of soldering and jacketing previously employed in the manufacture of stalpeth sheath, the new bonded stalpeth sheath lends itself to being manufactured on a single-pass sheathing line equipped with ASP-type metal forming equipment. The copolymer-coated steel is corrugated to a prescribed depth as a function of cable diameter and then formed with the corrugated aluminum in cone formers using ASP technology. The overlapped edge of the steel is preshaped to facilitate seam bonding. The steel overlap seam can be sealed for additional diffusion resistance by injecting an adhesive into the overlap just prior to the final forming fingers.

The reduction in heat required to seal the bonded seam (steel temperature of 200°F) versus the previous soldered seam (steel temperature 600-700°F) allows for an elimination of the longitudinal heat barrier tape in the stalpeth design as well as for the elimination of water cooling and air wiping employed in soldering. As a result, insulation resistance and core to sheath failures in pulp cable attributable to water entering the seam after the soldering operation has been eliminated. Additionally, the new bonded stalpeth sheath can be safely applied to all plastic-insulated underground cables due to the elimination of the soldering operation, which can create conductor-to-conductor or core-to-sheath electrical faults due to melting of the plastic insulation.

The final operation in the manufacture of the bonded stalpeth sheath involves tubing the polyethylene jacketing compound over the metal-sheathed core. By using vacuum on the extruder crosshead, the polyethylene can be completely pulled into the corrugation valleys to effect a diffusion resistant sheath capable of sustaining low temperature bending due to the high bond strength between the steel and polyethylene.

## Life Testing of Bonded Stalpeth

Adhesive bonds in cable sheaths can be degraded by humidity and by mechanically generated forces. In a humid environment, moisture diffuses through the polyethylene jacket and can degrade the adhesive bonds or weaken the metal substrate by corrosion. In pressurized cable, gas pressure can exert a peel force between the polyethylene jacket and the steel if pressure comes into contact with the jacket. The rate of degradation by both humidity and pressure is highest at elevated temperatures.

Figure 10 shows average peel test results for laboratory-prepared laminates aged in water at 158°F (70°C).[8] Although some initial degradation takes place, both the chrome-coated and tin-plated steels show good long-term bond strength to black jacketing compound.

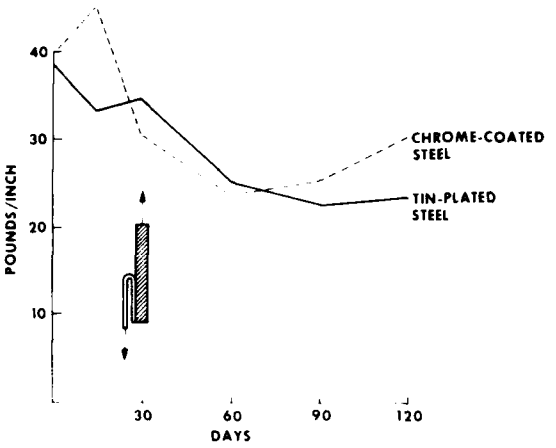



**FIGURE 10 PEEL TEST RESULTS FOR COATED STEEL-BLACK JACKET LAMINATES AGED IN 158°F WATER (PLOTTED FROM DATA IN REF. 8)**

Figure 11 shows minimum point peel strength results for bonded stalpeth sheath samples aged at 140°F in 100% relative humidity. The peel tests were conducted on 0.5-inch wide by 10-inch long longitudinal samples. Samples were numbered 1 through 6 and located on the cable as indicated in Figure 11. Two-foot lengths of cable with end caps and 10-inch by 1-1/2-inch cut sections of sheath were subjected to the high humidity, high temperature test environment. Due to edge exposure, the cut sections of sheath were exposed to a higher rate of aging than the cables with end caps. As indicated in Figure 11, the cut sheath samples show some bond degradation (within the experimental fluctuations) while the cable samples indicate no bond degradation. Results from the cut sheath samples confirm results obtained from laboratory-prepared laminates. Results from the cable samples indicate a near complete immunity to degradation by moisture as long as the plastic jacket is intact.

All of the results in Figure 11 are from the same cable, which contains tin-plated steel. However, the results from Figures 10 and 11 together indicate good long-term bond life in moisture for both tin-plated and chrome-coated steel.

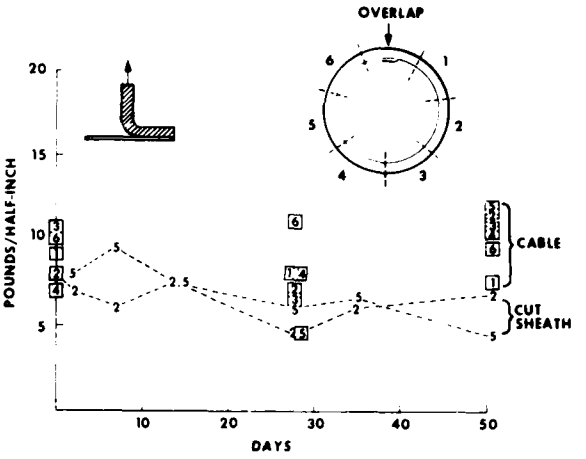



**FIGURE 11 MINIMUM POINT PEEL TEST RESULTS FOR SHEATH SAMPLES AND CABLE SAMPLES AT 140°F AND 100% R.H.**

Table III is a summary of the aging results on two-foot lengths of pressurized cables. The overlap seams were not bonded on any of these cables; therefore, air pressure had access to the jacket at the seam. Failure was initially determined by pressing the jacket to detect any local delamination. Final verification was determined from diameter measurements, which were made throughout the test. None of the cables that failed delaminated more than about a third of their circumference.

TABLE III

CABLE AGING RESULTS FOR BONDED SHEATH CABLE PRESSURIZED AT 10 PSI

| Cable | Dia. in. | Sample | Temp. °F | Time to Failure Days |
|---|---|---|---|---|
| 1. 3600-26 pulp | 3.4 | 1 | 120 | >83 |
| 2. 4200-26 plastic | 3.2 | 1 | 160 | 18 to 24 |
| | | 2 | 160 | 18 to 24 |
| | | 3 | 170 | 7 to 8 |
| | | 4 | 170 | 7 to 8 |
| 3. 4200-22 pulp | 3.1 | 1 | 160 | 18 to 24 |
| | | 2 | 170 | 7 to 8 |
| 4. 616-24 plastic | 2.7 | 1 | 120 | >60 |
| | | 2 | 160 | >60 |
| | | 3 | 170 | 5 to 18 |

Cables stored in the sun on reels can reach 160°F and occasionally 170°F. From Table III, bonded steel sheath can survive 160°F for 18 days and 170°F for 7 days of continuous exposure. Although this might be sufficient time to survive most reel yard storage, it was decided that a thermal reflective wrap would be

applied to reels of bonded stalpeth cable. With the wrap, temperatures stay below about 120°F and there is no danger of delamination. Further tests are now underway under actual reel yard conditions to determine whether the wrap can be safely eliminated.

## Diffusion Resistance

The high degree of diffusion resistance attained with bonded aluminum sheaths is well established and is one of the primary reasons bonded aluminum sheaths are popular.[6,9] Bonded steel sheaths have the same potential diffusion resistance. The only question is whether adequate bonding can be attained with the corrugated steel geometry. The approach used here to answer this question is to compare the measured diffusion rate with the ideal, theoretical diffusion rate.

Moisture diffusion through bonded sheaths can take several weeks to reach steady state. However, helium diffusion can reach steady state in a few hours. For this reason, steady-state helium diffusion rates were measured and compared for bonded stalpeth sheath and a polyethylene tube.

From theoretical results presented in Reference (6), the diffusion resistance of the bonded sheath is

$$R_{sheath} = \frac{0.81(h/L)^{0.17}}{P} \qquad (11)$$

where h is the thickness of the polyethylene jacket, 2L is the gap between underlap and overlap of the steel seam, and P is the permeation coefficient. For a thin tube of diameter D, the diffusion resistance is

$$R_{tube} = \frac{h}{\pi DP} . \qquad (12)$$

From Equations (11) and (12), the bonded sheath should be 140 to 200 times more resistant to diffusion than the polyethylene tube for a seam gap (2L) ranging from 0.01 to 0.001 inches. The measured ratio between the bonded sheath and the tube is 90. Considering that the theoretical results are based on ideal, complete jacket-to-steel bonding, the 90 times improvement indicates overall good diffusion resistance for the corrugated steel sheath.

## Sheath Joining

Standard electrical bonding hardware can be used with bonded stalpeth. The aluminum is bare and makes direct contact with the bottom shoe of the bond clamp. Measurements show that there is effectively no resistance between the aluminum and steel due to point contacts created through the copolymer coating during extrusion of the hot polyethylene. Thus, the steel is not isolated electrically, and overall shielding is equivalent to standard stalpeth.

# IV. Summary and Conclusions

The buckling performance of standard stalpeth is most effectively improved by increasing the overall cross-sectional stiffness of the cable. Neither changing the flooding compound, changing the jacketing compound (from low to medium density), or increasing the jacket thickness significantly improves buckling resistance. Since increasing the cross-sectional stiffness is limited by electrical performance, only modest improvements in buckling resistance can be attained with standard stalpeth sheath.

Bonded stalpeth provides the needed improvements in buckling resistance. Re-reeling tests and field experience show that large cables with a bonded stalpeth sheath can be installed at 15°F without difficulty. The bonded stalpeth has good long-term life under service conditions; it provides good resistance to moisture diffusion, and it can be manufactured without damaging plastic-insulated cores. Bonded stalpeth has been in production since the first half of 1980, and it is expected that eventually most pulp-insulated and all plastic-insulated duct cables manufactured by Western Electric will have bonded stalpeth sheaths.

## Acknowledgements

We thank the following people whose help and contributions were instrumental to our program and paper: W. D. Bohannon, R. D. Farley, E. L. Franke, A. S. Hamilton, M. D. Kinard, D. J. Meskell, Jr., P. T. Nunn, A. D. Patel, W. R. Sanders, and R. W. Williams.

## References


1. G. M. Yanizeski, E. D. Nelson, and C. J. Aloisio, "Predicting Fracture, Creep and Stiffness Characteristics of Cable Jacket from Material Properties," Twenty-fifth International Wire and Cable Symposium, 1976.

2. M. R. Santana and G. M. Yanizeski, "Bending Performance of Fiber-Optic Cable Sheaths: First Application of New Apparatus and Techniques," paper to be published.

3. P. Seide, "The Stability Under Axial Compression and Lateral Pressure of a Circular-Cylindrical Shell and an Elastic Core," EM10-1 STL/TR-60-000-09032, Space Technology Laboratories, Inc., 1960.

4. R. J. Roark, Formulas for Stress and Strain, 4th Ed., McGraw-Hill, New York, 1965.

5. G. E. Clock, G. A. Klumb and R. C. Mildner, "Adhesive Thermoplastic Polymers for the Wire and Cable Industry," Twelfth International Wire and Cable Symposium, 1963.

6. R. C. Mildner, W. E. Ropp and J. H. Snow, "The Evolution of Sheath Constructions for Communications Cable," Fifteenth International Wire and Cable Symposium, 1966.

7. Eric Reissner and H. J. Weinitschke, "Finite Pure Bending of Circular Cylindrical Tubes," Quarterly of Applied Mathematics, Vol. 20, 1963.

8. K. E. Bow (Dow Chemical), letter to A. C. Levy (Bell Laboratories), January 3, 1980.

9. E. D. Metcalf, "A Bonded, Non-Corrugated Aluminum/Polyethylene Sheathing System for Telephone Cable," Twenty-first International Wire and Cable Symposium, 1972.





George Yanizeski is a member of the Cable and Wire Department, Bell Laboratories, Norcross, Georgia. He received his Ph.D. from Carnegie-Mellon University in 1968. He joined Bell Laboratories in 1972, and since 1976 he has been involved in cable sheath mechanical characterization studies and new design development.





Randy Schneider is a department chief at the Western Electric Cable and Wire Product Engineering Control Center in Norcross, Georgia. He joined Western Electric at the Baltimore location in 1969 after receiving his B.S. degree in Chemical Engineering from the University of Maryland. His department does development engineering on cable sheaths and final cable preparation.





Ernest Johnson joined Bell Laboratories in 1972 after receiving his AAS degree in Electronics Engineering from Fayetteville Tech. He is now a member of the Cable and Wire Department engaged in multipair transmission measurements.

# A NEW LOW DIELECTRIC CONSTANT FILLING COMPOUND FOR TELECOMMUNICATIONS CABLE

Lawrence E. Davis
Naren I. Patel

Superior Cable Corporation
Hickory, North Carolina

## ABSTRACT

Telecommunications cable filling compounds containing petroleum-derived materials and an inorganic filler are discussed. Their properties such as dielectric constant, dissipation factor, and density are examined. Performance data for compound flow, water penetration, low temperature flexibility, attenuation, and mutual capacitance of cables filled with these materials are also presented.

From the data presented, it is concluded that use of the new compound exhibiting a low dielectric constant would allow a significant reduction in the thickness of conductor insulations without impairing the electrical properties or performance characteristics of filled communications cable. Hence, the cable would be smaller and lighter.

## INTRODUCTION

Over the past few years, the costs of petroleum-derived compounds have risen sharply primarily due to OPEC price increases. As a result, the costs of most of the raw materials employed in the manufacture of communications cable have increased, including that of filler. In order to contain cost increases, inorganic compounds which are not directly affected by crude oil price changes were investigated as additives for filling compounds. Costs of inorganic additives would presumably rise more slowly than costs of petroleum-derived products such as petrolatum and particularly some of the petroleum jelly modifiers utilized in commercially available cable fillers.

Any component employed to extend or modify cable grade petroleum jelly should exhibit a dielectric constant of 2.2, or preferably less, and be compatible with cable and splicing components without degrading other desirable properties of filling compound. With these criteria in mind, a number of inorganic insulating materials were investigated as possible additives. Hollow inorganic microspheres were found to have acceptable chemical and electrical properties. Microspheres exhibit a dielectric constant of 1.2 [1]. Further investigation indicated that the balloons could be incorporated into filling compounds in sufficient quantities to significantly reduce the dielectric constant of petrolatum below that of commercially available filling materials. Since reducing the dielectric constant of the filler lowers the effective dielectric constant of watertight cable in a similar manner as does foamed insulation, cables of smaller diameter are theoretically possible.

The penalties associated with filled cable designs as compared to air core construction with respect to increased material usage, cost, size and weight are well known in the industry. Previously, other investigators have examined the use of organic thermoplastic hollow microspheres [2] as a means of reducing the effective dielectric constant of filling compound. These thermoplastic microspheres were reported to be susceptible to thermal degradation and mechanical damage which was partly responsible for the failure of this early material in gaining acceptance by the industry. In contrast, the inorganic microballoons are thermally stable and less susceptible to deformation or breakage under load than were the organic microspheres.

The potential of reducing the effective dielectric constant of cable led to a comprehensive research and development program to determine to what extent insulation diameters for watertight cables could be lowered by utilizing hollow microballoons.

## LABORATORY EVALUATION AND TEST METHODS

### Electrical Properties

Compounds can be tailored, by adjusting the hollow microsphere content, to have a dielectric constant as low as 1.6. This is approximately half way between the dielectric constant of air and that of petrolatum.

Test samples for the determination of electrical characteristics of laboratory formulations containing various percentages of microspheres were prepared by pouring a flat slab approximately 3/16 of an inch thick in a 3 x 5 inch mold. After cooling to room temperature, the slab was removed from the mold and placed in a liquid displacement cell. The electrodes of the cell were brought into contact with the surfaces of the

compound by adjusting the micrometer. The capacitance between the electrodes at 1 kHz was then determined by using a 3 electrode measurement system. The ratio of the capacitance across the slab to that obtained for air between the electrodes with the same micrometer setting gave the dielectric constant of the sample.

The dielectric constants obtained experimentally are in good agreement with the theoretical values calculated from the equation: [3]

$$\frac{\varepsilon - \varepsilon_p}{3\varepsilon} = V \frac{\varepsilon_g - \varepsilon_p}{\varepsilon_g + 2\varepsilon}$$

where, $\varepsilon$ = composite dielectric constant

$\varepsilon_p$ = dielectric constant of petrolatum

$\varepsilon_g$ = dielectric constant of microspheres

$V$ = volume fraction

The dissipation factor was simultaneously measured along with the dielectric constant. A typical value of $5 \times 10^{-4}$ was obtained at 1 kHz for material exhibiting a dielectric constant of 1.6.

Drip Temperature

Elevated drip temperature characteristics of laboratory formulations with various percentages of microspheres and petroleum jelly modified with additives were determined by repeatedly dipping a bundle of ten 24 gauge insulated conductors four inches in length into a molten mixture until a coating approximately 1/8 inch thick was applied to the wires. The bundles of coated wires were then placed into a forced draft oven maintained at 71°C for 24 hours. During the test period, the samples were observed for any oil separation or drip. To establish relative performance, formulations which did not exhibit loss of material from the wire at 71°C were retested at 75°C and 80°C. Freshly coated wire bundles were used for each test temperature. Several formulations have been found which meet or exceed the 71°C drip temperature.

## CABLE TRIALS

Subsequent to laboratory investigation of several possible cable filling formulations containing hollow microspheres, a three-phase program for evaluation of compounds in cables was established. The first phase consisted of designing and building equipment for handling and mixing the balloons as well as for pressure filling a core with the experimental material. The second phase was to evaluate the prototype equipment by filling standard production cores and to use these cores to examine the physical and electrical properties of the experimental compound within a cable. In Phase III, cores containing pairs with reduced insulation thickness were to be filled with the new material to determine design parameters. Additionally, cables were to be filled under plant conditions and evaluated.

In Phase I, a device for mixing experimental compounds and for pressure filling cores was designed and constructed in the laboratory. The primary concern during the design was to obtain a flow system which could handle the materials without damaging the balloons. To evaluate the system, a microsphere formulation exhibiting a dielectric constant of 1.65 was mixed with the new applicator and recirculated for four days at 220°F. The dielectric constant of the grease was measured immediately following mixing and after the recirculating period. No change in the dielectric constant of the compound was detected.

Subsequent to determining how to handle microspheres, Phase II of the project was conducted. During this phase, the six cables listed in Table I were constructed and subjected to electrical and physical testing to investigate the performance of the formulation. The tests conducted included REA PE-39 qualification procedures for heat aging, humidity cycling, and temperature cycling, followed by water penetration. The REA compound flow procedure for filled cables was also conducted for each specimen at 65°C, 71°C, and 75°C. Low temperature cable flexibility and compound cracking were also evaluated utilizing sample number 6.

Electrical Measurements

An initial concern in using grease containing microspheres in pressure filling applications was the possibility of filtering or straining of balloons by the core during the application process. Examination of individual pair mutual capacitance values with respect to the cable average was employed to investigate this phenomenon. If filtering occurred during filling, a higher concentration of bubbles would surround the outside pairs of the cable while the interior would contain a higher concentration of petroleum jelly. In the event of such a segregation, a pattern of increasing mutual capacitance toward the center of the cable would be manifested. However, variations noted in 100 pair constructions were random with respect to the location of a pair in the core, and no filtration during pressure filling of the cable was detected.

The possibility of a frequency dependent surface polarization effect [4] due to the presence of microspheres in the water blocking compound was also investigated by measuring the mutual capacitance at 1 kHz, 100 kHz, 772 kHz, and at 1576 kHz for the first three cables only (Table I). No polarization effects were detected by these measurements.

Water Penetration

REA PE-39 water penetration procedure was

conducted for samples of each cable prior to environmental conditioning and following heat aging at 65°C for 14 days, humidity cycling at 95% relative humidity between 52°C and 57°C for 100 cycles, and temperature cycling between -40°C and 60°C for 10 cycles. Twenty-two of the twenty-four specimens met the REA requirement after a three-foot head of water was applied to one end of the sample for one hour. The failure path for the temperature cycling specimen for cable number 1 and the heat aging specimen for cable number 2 was between the core wrap and the shield. These failures do not appear to be related to use of the new compound. Another material, a commercially available filling compound being evaluated by the plant, was used to flood over the core during a separate jacketing operation. Since short lengths (300 ft.) were employed for the trials, the possibility also exists that optimum flooding conditions were not obtained. Therefore, unusual end-condition effects may have contributed to these failures.

Since the cores appeared to be watertight for all cables, the compound was considered an effective cable filling material.

Low Temperature Flexibility

To investigate compound fracture and cable flexibility under low temperature conditions, the 50 pair 19 gauge cable was selected for testing. The larger interstitial areas in the 19 gauge construction are more susceptible to compound fissuring and will have larger voids if cracking occurs.

A six-foot section of cable number 6 was cooled to -20°C and bent around a mandrel 15 times the diameter of the cable. The specimen was then reverse bent and removed from the mandrel. After allowing the cable to stabilize at room temperature, one and one-half feet were removed from both ends of the specimen and the three-foot center portion of the sample subjected to the REA PE-39 water penetration procedure.

The cold bend sample passed the water penetration test indicating that no significant fracturing of the grease containing microspheres occurs when the cable is bent at low temperatures.

The effort required to deflect the cold bend sample was subjectively judged to be no more difficult than that for conventionally filled cable.

Compound Flow Test

The REA PE-39 compound flow procedure was carried out at temperatures of 65°C, 71°C and 75°C. Of the six cables constructed during Phase II of the development program, five exhibited compound flow at 65°C while one did not fail at 75°C. The failures may have resulted from significant fluctuations in application temperatures for the various cables as well as changes in compound temperatures during an individual cable filling operation. The apparent compound sensitivity to application temperature caused by thermal instability in the equipment required changes in equipment and compound formulation before proceeding to Phase III of the program.

CABLES WITH REDUCED INSULATION DIAMETERS

Since the addition of microspheres to petrolatum lowers the dielectric constant of the filling compound, the effective dielectric constant of watertight cables is reduced, thus permitting a reduction in insulation thickness while maintaining the industry specified mutual capacitance of 52 nanofarads per kilometer. Twenty-five pair cables of 26, 24, 22, and 19 gauge conductors with reduced insulation dimensions (Table II) were filled in the laboratory to ensure that calculated changes in physical dimensions would provide the correct capacitance value for the samples. Cables 7 through 10 met the required mutual capacitance value within manufacturing variance. While production runs will be required to determine the exact DOD dimensions of pairs in cables filled with the experimental grease, the values provided in Table II should be reasonably accurate. Depending on gauge, DOD reductions of from 1.6 mils to 4.2 mils can be obtained by employing hollow microspheres as an additive in petrolatum.

Due to the amount of particulate matter in the experimental compound, some concern was expressed with respect to filling 100 pair 26 gauge cables even though 50 pair 26 gauge air core constructions had been successfully made. To evaluate the ability to fill 26 gauge cable, a 100 pair foam core with reduced insulation dimensions was obtained for laboratory trials.

The smaller interstices resulting from DOD reduction (1.5 mils below air core size) required a change in the pressure filling setup. Higher pressures and compound temperatures were employed to fill the 100 pair 26 gauge reduced dimension foam core. To ensure that this core was watertight, several water penetration samples were evaluated along the length of the core. All of these samples met the water penetration requirement as have all reduced dimension cables filled with the experimental compound. However, the mutual capacitance value is below specification requirements,and further design changes resulting in smaller cores may be utilized to obtain the desired electrical parameters.

By utilizing the low dielectric filling compound in conjunction with cellular insulation, smaller cable sizes employing less material than any conventional watertight construction of equivalent gauge can be manufactured. Such a construction could provide for reduced cable weights, smaller installation loads, and greater duct space utilization per pair while maintaining the advantages of a filled cable.

The cores of cables 7 through 11 were filled in the laboratory and then transferred to the plant for jacketing. As a result, the compound used to flood over the core wrap did not contain hollow microspheres and had a different cooling history than would have occurred if in-line filling during the jacketing operation had been employed. Therefore, a 5000 foot core of 50 pair 22 gauge cable with reduced solid insulation thickness was obtained for a plant trial. The mixing and filling apparatus,along with additional equipment for flooding over the core wrap with the experimental compound,was moved into the plant. Cable number 12 (Table II) filled in the plant exhibited the same performance with respect to compound flow and water penetration as the previous samples containing the same formulation. The laboratory results agree with those obtained from the plant trial and appear to be representative of production cable.

The drip temperature of the preferred compound formulation is in excess of 85°C. With the increasing utilization of filled cable for aerial installation, increased drip temperatures above the REA requirement of 65°C may be desirable in regions of the country where daily highs in the summer can exceed 100°F for prolonged periods.

Water penetration tests conducted on all samples demonstrate that the advantages gained by incorporating hollow microspheres in cable filler can be obtained without any loss of moisture protection. Protection is maintained even after the cable is subjected to bending under low temperature conditions (-20°C) as was demonstrated by subjecting the 19 gauge low temperature bend samples (Cables 6 and 10) to water penetration.

The core and cable diameters of Sample 12 are 40 mils below those of standard filled cable. This provides a reduction of approximately 4% in the total volume of material utilized in the construction of the cable. Due to the lower density of the filler, the weight of Cable 12 was 14% below that of standard filled product.

## COMPOUND AND CABLE CHARACTERISTICS

The hollow microsphere compound exhibits a density of 0.51 grams per cubic centimeter (40% lighter than conventional compounds) as well as a low dielectric constant (1.6). The use of this new material results in cables which are lighter than conventionally filled cable. Reducing the weight of the cable has advantages with respect to selecting support strand size and span length for filled cables in aerial installations. This could hasten the switch from air core to filled cables employed in aerial applications which is already gaining in popularity.

The petrolatum-microsphere formulations are non-tacky and are not as greasy as conventional compounds. Therefore, the new material is easily removed from the conductors and cleaned from hands, tools, and equipment. The individual pairs of a core can be separated with less effort. This is particularly apparent at low temperatures where conventional compounds are stiff.

The hollow inorganic microspheres employed as an additive are chemically inert with respect to the plastic components of cables and splice materials. Therefore, the potential for reducing the total amount of oil in a filling compound which migrates into plastic components by replacing a portion of the petrolatum with microspheres was recognized as a means of obtaining increased compatibility between conventional cable filling materials and plastic insulation.

Transmission data for reduced dimension cable (Table III) at 1 kHz, 100 kHz, 150 kHz, 772 kHz, and 1576 kHz indicate that there is negligible change in the attenuation or conductance of filled cable due to the presence of hollow microspheres in the petrolatum. However, reduced dimension filled cables should exhibit an attenuation intermediate between conventional watertight and air core constructions. This should occur due to changes in inductance caused by closer pair spacing. Additional cable trials are planned to resolve this discrepancy.

Hollow microspheres have a lower coefficient of thermal expansion than petroleum jelly and do not undergo a phase change during the filling operation as does the petrolatum component. Therefore, less compound shrinkage occurs with the new formulation and a higher percentage of fill can be obtained.

## CONCLUSIONS

A low dielectric constant filling material can be produced by employing hollow microspheres as an additive. The advantage of producing smaller and lighter watertight cables without adversely affecting their properties can be gained by using the hollow microsphere formulation of lower dielectric constant.

The hollow microsphere formulations are non-tacky and can be easily cleaned from cables, hands, clothing and tools.

## ACKNOWLEDGMENTS

The authors wish to express thanks to M. Stearns, P. Garmon, C. Stewart, D. Coleman, S. Parikh, and K. Lail for their work in preparing experimental mixtures, cable trials and conducting measurements. The efforts of D. Sinnett and K. Johnson required to design and construct experimental apparatus employed to evaluate the new compound are also appreciated. Also, the cooperation of numerous Hickory Plant personnel in arranging for and construction of experimental cores is acknowledged. Finally, thanks are due to J. Lail and R. Bickel for typing the manuscript.

## REFERENCES


[1] Harry S. Katz and John M. Milewski, HANDBOOK OF FILLERS AND REINFORCEMENTS FOR PLASTICS, Van Nostrand Reinhold Company, 1978.

[2] R. C. Mildner, K. F. Nacke, E. W. Veazey, and P. C. Woodland, "New Approaches to Fluid Blocking", Eighteenth Wire and Cable Symposium, December 1969.

[3] A. S. Windeler, "Polyethylene-Insulated Telephone Cable", Fourth Annual Wire and Cable Symposium of the Signal Corps Engineering Laboratories, December 1955.

[4] P. D. Ritchie, PHYSICS OF PLASTICS, D. Van Nostrand Company, Inc., 1965.

TABLE I

DATA FOR PHASE II CABLES CONTAINING MICROSPHERE FORMULATED FILLING COMPOUND

| CABLE | CORE TYPE | MUTUAL CAPACITANCE µF/Mile | | | | DRIP TEMPERATURE °C (1) | WATER PENETRATION (2) | | | |
|---|---|---|---|---|---|---|---|---|---|---|
| | | 1 kHz | 100 kHz | 772 kHz | 1576 kHz | | Unaged | Aged 65°C 14 Days | Humidity 52 to 57°C 100 Cycles | Temperature -40 to +60°C 10 Cycles |
| 1 | 100 x 22 WT-Core | .076 | .077 | .077 | .077 | <65 | Pass | Pass | Pass | Failed |
| 2 | 50 x 24 WT-Core | .080 | .079 | .079 | .079 | >75 | Pass | Failed | Pass | Pass |
| 3 | 100 x 24 WT-Core | .079 | .078 | .078 | .079 | <65 | Pass | Pass | Pass | Pass |
| 4 | 100 x 24 WT-Core | .077 | .077 | .077 | - | <65 | Pass | Pass | Pass | Pass |
| 5 | 50 x 26 Air-Core | .095 | .095 | .095 | - | <65 | Pass | Pass | Pass | Pass |
| 6 | 50 x 19 WT-Core | .078 | .077 | .077 | - | <65 | Pass | Pass | Pass | Pass |

NOTES: (1) Temperature of the system found to be unstable, resulting in changes in compound application temperature.

(2) The water path for both failures was between the mylar and shield which was filled with commercially available cable filling compound. Since short lengths were filled, the failures may be due to start-up conditions.

TABLE II

DATA FOR PHASE III CABLES CONTAINING MICROSPHERE FORMULATION

FILLING COMPOUND

| Cable Number | WT-Core | Insulation DOD (Inches) | Solid Insulation DOD Reduction from Cable filled with Conventional Compound (Inches) | Mutual Capacitance at 1 kHz in nF/km (µF/Mile) | Drip Temperature °C (1) | Water Penetration |
|---|---|---|---|---|---|---|
| 7 | 25 x 26 Solid | 0.0330 | 0.0016 | 51.9 (0.0835) | >85 | Pass |
| 8 | 25 x 24 Solid | 0.0414 | 0.0018 | 51.5 (0.0828) | 71 | Pass |
| 9 | 25 x 22 Solid | 0.0514 | 0.0024 | 52.1 (0.0838) | >85 | Pass |
| 10 | 25 x 19 Solid | 0.0727 | 0.0042 | 51.8 (0.0834) | >85 | Pass |
| 11 | 100 x 26 Foam | 0.0273 | 0.0073 | 49.1 (0.0790) | >85 | Pass |
| 12 | 50 x 22 Solid | 0.0514 | 0.0024 | 50.3 (0.0809) | >85 | Pass |

NOTE: (1) Cable number 8 was filled with an alternate filling compound. Cables number 7, 9, 10, 11, and 12 were filled with the same formulation.

TABLE III

*TRANSMISSION DATA FOR SAMPLE 12*

| Frequency kHz | Attenuation dB/km | | Conductance ℧/km | | Mutual Capacitance nF/km | |
|---|---|---|---|---|---|---|
| | Conventionally Filled Cable (1) | Microsphere Filled Cable | Conventionally Filled Cable (1) | Microsphere Filled Cable | Conventionally Filled Cable (1) | Microsphere Filled Cable |
| 1 | 1.12 | 1.12 | 0.13 | 0.03 | 51.6 | 50.3 |
| 100 | 4.80 | 4.97 | 12.96 | 11.58 | 51.6 | 50.2 |
| 150 | 5.48 | 5.54 | 19.44 | 14.55 | 51.6 | 50.3 |
| 772 | 12.35 | 12.33 | 100.03 | 98.66 | 51.6 | 50.3 |
| 1576 | 17.39 | 17.52 | 203.5 | 275.0 | 51.4 | 50.2 |

Note: (1) Conventionally filled cable data was converted from tables in Lee's abc of the Telephone, Volume 7, "Understanding Transmission".






**Lawrence Davis is the Materials Engineering Manager for Technical Staff, Superior Cable Corporation. He received his B.S. degree in physics from Appalachian State University in 1969 and graduated with a Master's degree in physics from the University of Wisconsin, Milwaukee in 1974. Prior to joining Superior Cable, he was a Materials Engineer for Continental Telephone Laboratories.**

Naren Ishwarbhai Patel is a Materials Engineer for Technical Staff, Superior Cable Corporation. He received a B.Sc. degree in chemistry from the University of Gujarat, a B.Sc. (Tech.) degree in textile chemistry from the University of Bombay, India, and was awarded a Ph.D. degree by the University of Leeds, England in 1969. Prior to joining Superior Cable Corporation in 1979, he had served as a Director of Quality Control and Director of Research and Development in the textile industry.

# PLASTICIZER EVAPORATION FROM VINYL INSULATED WIRES

P. C. Warren

Bell Laboratories
Murray Hill, N.J.

## Abstract

One mechanism that governs the longevity of plasticized PVC wire insulation is the rate of volatile loss of plasticizer. The activation energy of this process was determined to be 15-20 kcal/mole. Other factors that influence evaporative loss besides temperature include surface area and thickness, as well as air flow and orientation of the wire to that flow. The properties of thermally aged vinyl were shown to be similar to those of unaged, equivalently plasticized material. The predicted time to a given plasticizer loss must take all these factors into account, and are summarized in a simple calculator program.

## Introduction

As electronics technology proliferates in the telecommunications industry, increasing thermal demands will be continually placed on nearby wire insulations and cable jackets. The higher heat outputs can occur at relatively steady temperatures or they may result because of air conditioning or forced air cooling breakdowns, which can integrate to substantial lengths of time over the life of the equipment. A traditional guideline used to select the proper insulation is the UL 83 "Thermoplastic-Insulated Wires"[1] standard, which defines maximum temperatures the insulations may be exposed to, but says little about their gradual degradation at service temperatures over a design time of, say, 40 years. The purpose of this work is to be able to predict exactly how the wires will endure over any length of time, given a reasonably well defined thermal stress.

Most inside wire insulation in buildings and switching installations consists of plasticized poly(vinyl chloride) (PVC). The thermal deterioration of this material occurs primarily by two independent routes, evaporative loss of plasticizer and/or dehydrochlorination of the base resin. This paper will concentrate on the first of the two mechanisms only. Care was taken to monitor any PVC instability to ensure that the second route did not interfere with the plasticizer loss measurements.

## Experimental

Semirigid PVC insulation compounds were formulated with a variety of plasticizers to equal efficiencies and are described in Table 1. The components were homogenized in a Henschel dry blender, fluxed in a Banbury mixer, sheeted on a two-roll mill and diced into pellets. The pellets were then remilled and subsequently molded into tensile bars or extruded onto 26 AWG wire.

## Plasticizer Loss Measurements

Tensile bars or 26 AWG vinyl insulated wires were each weighed and then aged in ASTM E-145 Type IIB forced air ovens at 85°, 105° and/or 121°C. A tensile bar was removed after a given interval of time, reweighed to determine plasticizer loss and then measured for ultimate tensile strength and elongation. Vinyl insulated wires were aged in a similar fashion but were measured for plasticizer loss only. In all cases weight loss was assumed to be solely plasticizer related when (1) little or no color change occurred in the unpigmented sample and (2) no weight was lost from a similarly shaped, unplasticized control that was always included in the oven during the test period.

## Effect of Air Movement

A special apparatus shown in Figure 1 was constructed to measure the effect of air movement on plasticizer loss from vinyl wire insulation. Five 12" x 1" ID tubes were mounted vertically in the oven and individually fed with metered air through the bottom. Each tube was filled one-third with 1/8" glass beads to help equilibrate temperature as well as provide laminar flow up the tube. The individual rotometers were calibrated with a

wet test meter and corrected to 85°C to give five flow rates: 3.2, 7.4, 23.7, 48.4 and 122 linear ft/min.

A three inch length of 26 AWG vinyl insulated wire was hung inside each tube with a simple V hook in one of two orientations, either vertical and linear (parallel to flow) or as a horizontal spiral (perpendicular to flow). Identical lengths and configurations of wire were hung in the oven itself as controls. These latter samples were oriented opposite from those in the sample tubes, i.e., the horizontal draft in the forced air ovens rendered the vertical sample perpendicular and the spiral one parallel to flow. The wire samples were periodically removed, weighed to 0.1 mg and then returned for further aging. At the end of the experiment, the exact amount of original vinyl insulation was determined by dissolving off the insulation, weighing the bare copper wire and subtracting the result from the weight of the original sample.

## Results

Vinyl wire insulation may fail in service in a number of ways, depending on how failure is defined. To better characterize gradual degradation to failure, a 26 AWG di-2-ethylhexyl phthalate (DOP) plasticized insulated wire was aged at 120°C and regularly observed; a schematic diagram summarizes the results in Figure 2. Several obvious changes occurred in the wire: (1) Within one day, room temperature elongation dropped from >200% to ∿20% (2) The insulation also lost volume as plasticizer was lost. (3) After five days, the wire failed a prewrap test. Wires that had been initially installed in the oven in the hangman's noose configuration were allowed to cool for 15 minutes and then unwrapped. This test was shown to be an extremely sensitive test for cracking. (4) Formation of gel next to copper, as evidence by insolubility in tetrahydrofuran, occurred in about ten days. Copper appeared to play a significant role since the outer portion of insulation was still quite soluble. (5) After twenty days the wire darkened to a deep brown and the insulation was now totally insoluble in THF. (6) After a period of approximately 40 days, the wire failed a traditional hangman's noose test, using a #70 drill shaft (.028" OD) as the mandrel. (7) Lastly, after fifty days the wire spewed a white powder which was easily wiped off, exposing the black degraded plastic underneath. The residue was not identified but assumed to be lead chloride.

DOP-plasticized PVC (28 phr) insulation compounds in the shape of .075" thick tensile bars were aged in a forced air circulation oven at 105°C, and loss of plasticizer and room temperature elongation were monitored with time, shown in Figure 3. Plasticizer loss was essentially linear during the early stages of evaporation but began to decrease at about one-third total plasticizer lost and finally leveled off at approximately two-thirds total plasticizer volatilized. The rate of removal of plasticizer at the latter point was about an order of magnitude less than the original rate of evaporation. Room temperature elongation rapidly plummetted with loss of plasticizer, leveling at about 10% of the original value. Figure 4 shows the results of an identical experiment with a slightly less volatile plasticizer, diisodecyl phthalate (DIDP). Again, relatively little change in elongation was noted until about one-third plasticizer was lost, after which the results were identical to the DOP case. Weight loss and elongation experiments at several temperatures with the other compounds listed in Table 1 all gave results similar to the above but over different time spans.

Some properties of the aged materials were briefly examined by comparing them with freshly prepared controls at equal plasticizer concentration. Calibration materials were prepared with DIDP plasticizer in 0-35 phr concentrations in PVC in 5 phr increments. Tensile strength, elongation, glass transition (Tg) and specific gravity were measured and plotted in Figures 5, 6, 7 and 8, respectively. Thirty phr DIDP samples were then oven aged to attain lower plasticizer concentrations, measured for the same properties and compared with the calibration curves. In all four cases, the properties fell sufficiently close to the controls that one can infer that the materials have similar structures regardless of how the plasticizer content is arrived at.

Vinyl insulated wires were hung in forced air ovens at 85°C and weight loss was followed with time, the results of several experiments being listed in Table 2. Clearly the results are qualitatively identical to earlier testing on tensile bars, but weight loss of course occurred much faster because of the greater surface/volume ratio.

Figure 9 shows the effect of air flow on evaporation of DOP from the 26 AWG wires in the parallel orientation. The following observations are noted. (1) The rate of loss is clearly dependent on air

flow, going from an initial rate of 3%/day at 3 ft/min to 7%/day at 122 ft/min. (2) The efficiency of plasticizer removal was much higher in the forced air oven (at an initial rate of 20%/day) than in any of the flow tubes. (3) A zero flow sample showed extremely low evaporation rate, albeit this effect may be exaggerated since plasticizer may have built up inside the tube resulting in abnormally low weight loss. (4) Regardless of the initial rate of weight loss, all experiments leveled off at exactly the same point (about two-thirds loss of total plasticizer) and proceeded at a much slower and steadier evaporation rate of about 0.35%/day.

Shown in Figure 10 is the identical experiment except that wire spirals were used to attain a perpendicular orientation to flow. (1) Again the rate of air flow significantly affected the weight loss experiment, even more so than in the case of parallel orientation. For example, initial loss of 5%/day at 3 ft/min flow increased to 20%/day at 120 ft/min. (2) Unlike the parallel case, the perpendicular alignment at higher flows gave plasticizer losses identical to those in the forced air oven. (3) The forced air oven gave the same weight loss results regardless of orientation. (4) Again, the loss rate abruptly declined at about two-thirds total plasticizer removed.

## Discussion

There are several modes of failure that are possible for vinyl materials. Loss of elongation due to plasticizer volatility is usually the first change encountered in conventional vinyl insulations. For jackets and thick insulations this is probably the most serious failure because it can lead to cracking (but usually not embrittlement) where a sharp bend occurs in the wire; for thin insulations and ones that are not ordinarily moved once placed in service this may not present a catastrophic problem. Loss of plasticizer is accompanied by a proportionate reduction in volume, however, and this mechanism may lead to a degradation of the transmission properties of vinyl jacketed optical fiber because of compressive stresses on the glass. Plasticizer evaporation also implies condensation of the oil on nearby equipment, resulting in possible contamination of exposed electrical contacts. Eventually, of course, dehydrochlorination of the base PVC resin will occur when the thermal stabilizer is depleted, giving two further failure modes - loss of color coding due to light absorption by conjugated double bonds and finally embrittlement because of heavy crosslinking.

For the purposes of this discussion, however, failure of the PVC insulation is defined as the percent loss of plasticizer that results in a sharp (>50%) reduction in elongation relative to the original unaged value. Since plasticizer was originally added to PVC to reduce Tg below room temperature, evaporation of the diluent reverses the effect and Tg is raised as material is lost. Measurements of several properties (tensile strength, elongation, specific gravity and Tg) of aged and unaged materials at equal plasticizer concentrations suggest that the final plasticizer/PVC polymer morphology is independent of how it is attained. When enough plasticizer has been removed from the polymer, Tg passes through room temperature and the material rapidly changes from a rubber to a glass, causing the elongation to drop about an order of magnitude. A thirty phr phthalate-plasticized insulation, for example, will reach this point when approximately one-third total plasticizer is lost. Thus the rapid reduction in elongation is a convenient endpoint because not only does it have physical significance but is relatively sharp and easy to measure.

Study of the evaporation rate of a typical plasticizer from PVC clearly reveals two distinct regimes, one controlled by the vapor pressure of the plasticizer and one by the diffusion of the plasticizer through the polymer.[2] Diffusion-controlled loss is not important in conventional insulations because it does not predominate until plasticizer concentration is ∿10 phr or less. In most commercial vinyl compounds, plasticizer volatility determines the rate of removal of plasticizer, as most materials are amply stabilized so they can endure high temperature processing. Unfortunately, measurement of the vapor pressure of pure plasticizer is considerably more difficult than determining the weight loss of a compounded vinyl, so in this case an understanding of the loss mechanism does not aid in performing a simpler experiment.

Arrhenius plots of the various samples are shown in Figures 11 and 12, utilizing both one-third weight loss and 50% reduction in elongation as the respective end points. The graphs were drawn to determine the activation energies of plasticizer removal, to compare the relative volatilities of the various plasticizers and to be able to extrapolate to evaporation rates of lower temperatures. Absolute times to failure are not relevant since the tensile bar geometry or air

movement over the samples are not typical of wire or its environment. Figure 12 suggests that a second mechanism may be coming into play at higher temperatures, but this is not disturbing since it occurs in a highly impractical temperature region for vinyl. It does, however, raise questions about determining service lives of vinyl materials by measuring percent reduction in elongation at extraordinarily high temperatures ($\geq$ 120°C) for short lengths of time.

Table 3 lists the activation energies of the samples and compares them with heats of vaporization of some plasticizers. Based on the plot in Figure 11, the activation energies of semirigid plasticized PVC appear to be 15-20 kcal/mole, somewhat lower than the heats of vaporization of the pure plasticizer (20-30 kcal/mole) which were calculated from published vapor pressure values found in the literature.[3,4] The scatter in these numbers emphasizes the difficulty in determining the vapor pressure of nonvolatile liquids, as mentioned earlier. The less-than-perfect agreement between the activation energies of plasticized PVC and heats of vaporization suggests that other factors besides simple evaporation may play a role (such as plasticizer interaction with the PVC resin, for instance) that have a different dependence on temperature. Table 2 lists the relative volatilities of several plasticizers at 85°C, the standard being DOP; the agreement between the die cut tensile bar and insulated wire experiments is very good.

Air movement over the insulation surface clearly increases the rate of evaporation of plasticizer from the PVC matrix in the vapor pressure controlled regime. One measure of the extent of acceleration is to compare times to the predefined "failure" point of one-third plasticizer loss for different flow rates and sample orientations. Figures 13 and 14 show the dependence of plasticizer loss on air flow for DOP and DIDP plasticizer, respectively. The general shape of all three curves shows that for very little air movement any change in flow has a large effect. Above a certain point, however, plasticizer evaporation is relatively insensitive to variable flow; in all experiments this point corresponded to a linear flow of 30-40 ft/min. Below this point, volatile molecules are swept away after they depart from the surface, shifting the liquid/vapor equilibrium to the right. Above that point, however, the draft scavenges molecules so efficiently that few will return to the surface and higher flow rates will have little further effect.

Orientation of the wire plays a minor but real role in plasticizer evaporation. In the DOP experiment shown in Figure 13, the parallel alignment was less severe than the perpendicular one by a range of 1.5-2, depending somewhat on the flow rate. Furthermore, the higher flow rates in a parallel mode could not approach forced air oven rates, whereas the other orientation did easily. The more efficient sweep in the perpendicular mode is probably due to local turbulence as well as "one pass" exposure to uncontaminated air. There was no difference at all between orientations in the forced air oven, presumably because the high turbulence within the chamber overwhelmed any effect of geometry.

The numbers in Table 4 were gleaned from Figures 13 and 14, and are multipliers to calibrate forced air oven aging results for several different air currents. Note that the forced air oven is the "worst case" and therefore all calibrated data will be less conservative. For example, a factor of 1 would predict an insulation longevity exactly identical to that predicted by the forced air oven; a factor of 2 would forecast a lifetime twice as long. Two general conclusions can be drawn from the data in the table: (1) Both DOP and DIDP gave similar results in the parallel orientation, ranging from factors of 4-5 at 3 ft/min to about 2 for 100 + ft/min drafts. (2) The perpendicular alignment removed plasticizer about twice as fast as the parallel one.

It is possible to predict the service life of a vinyl insulation to any failure point desired, i.e., any plasticizer loss in the linear portion of the weight loss curve. As previously discussed, a convenient failure point for 30 phr phthalate plasticized PVC is one-third plasticizer lost, approximately equal to 50% retained elongation. The necessary parameters for such predictions include (1) average temperature at which the wire will reside for its lifetime, (2) a rough decision as to what will be the average air flow over the wires, (3) the surface to volume ratio of the wire insulation, and (4) the activation energy for plasticizer loss, about 15-20 kcal/mole. A single experimental point of the rate of plasticizer loss at one temperature is necessary, in this case the time to lose one-third plasticizer from 26 AWG insulated wire at 85°C; these values are summarized in Table 5.

A short RPN program written for a Hewlett-Packard HP 25 calculator was used to

extrapolate this data to arbitrary temperatures, failure points, wire sizes and flow conditions, listed in Figure 15. Several examples help illustrate the utility of this program. For instance, a 22 AWG DOP-plasticized PVC wire at 40°C will lose 5% plasticizer in a low flow environment in about one-half year, but an identical 26 AWG wire will survive only about one-quarter year under similar failure criteria. A 26 AWG trimellitate-plasticized vinyl insulation, however, will endure well in excess of one hundred years under the same conditions. Or, in another example, the same trimellitate wire may be sporadically exposed to 80°C for two years due to air conditioning shutdowns, in which case it would lose 3% plasticizer.

Since most wire and cable manufacturers and customers rely on UL 83 classifications to determine the appropriate materials on insulations, a 20 kcal/mole activation energy was applied to the time/temperature criterion for meeting the specification. Table 6 shows the results for T, THW and THH (60°, 75° and 90° maximum temperature) wires. All these wires would last about 0.5 year at the maximum specified temperature assuming the 20 kcal/mole activation energy. This may be a poor assumption because the activation energies at these high test temperatures are apparently changing rapidly, as shown in Figure 12. In any case, it is felt that while the UL standards may be sufficient for quality control, they do not provide enough information to design insulations subjected to stringent thermal conditions; hopefully the concepts presented in this paper might be better directed to that end.

Acknowledgement

The author would like to thank J. E. Adams for the tensile bar measurements and S. Kaufman for providing the PVC compounds as well as the 26 AWG wire samples. The measurement of Tg of the various DIDP-plasticized PVC samples by H. E. Bair is also appreciated.

References

1. UL 83 "Standard for Thermoplastic-Insulated Wires", Sixth Edition, Underwriters Laboratories, Inc. December 1975.

2. H. M. Quackenbos, Jr., Ind. Eng. Chem., 46, 1335 (1954).

3. Monsanto Plasticizer Data Bulletin, 1975.

4. W. J. Frissell, Ind. Eng. Chem., 48, 1096 (1956).



Paul C. Warren is a Member of Technical Staff at Bell Laboratories, Murray Hill, N.J. He received an A.B. degree in chemistry from Wesleyan University and a Ph.D. in organic chemistry from Cornell in 1969. His current interests at Bell Labs have focused on understanding structure/property relationships of plasticized PVC in order to optimize wire and cable insulation and jacket materials.

TABLE 1

| | | | | | | | | | |
|---|---|---|---|---|---|---|---|---|---|
| **Resin** | | | | | | | | | |
| Poly (vinyl chloride) | (GP-4) | 100 | 100 | 100 | 100 | 100 | 100 | 100 | 100 |
| **Plasticizer** | | | | | | | | | |
| Di-2-ethylhexyl phthalate | (DOP) | 28 | - | - | - | - | - | - | - |
| Mixed alkyl phthalate | (711) | - | 27 | - | - | - | - | - | - |
| Linear alkyl phthalate | (810) | - | - | 12 | - | - | - | - | - |
| Diisononyl phthalate | (DINP) | - | - | - | 29 | - | - | - | - |
| Diisodecyl phthalate | (DIDP) | - | - | - | - | 30 | - | - | - |
| Diundecyl phthalate | (DUP) | - | - | - | - | - | 27 | - | - |
| Ditridecyl phthalate | (DTDP) | - | - | 13 | - | - | - | 30 | - |
| Mixed alkyl trimellitate | (7, 9 TM) | - | - | - | - | - | - | - | 30 |
| **Stabilizer** | | | | | | | | | |
| Tribasic lead sulfate | | 7 | 7 | 7 | 7 | 7 | 7 | 7 | 7 |
| **Lubricant** | | | | | | | | | |
| Dibasic lead stearate | | 0.4 | 0.4 | 0.4 | 0.4 | 0.4 | 0.4 | 0.4 | 0.4 |
| Ethylene bis-stearamide | | 0.4 | 0.4 | 0.4 | 0.4 | 0.4 | 0.4 | 0.4 | 0.4 |
| **Fire Retardant** | | | | | | | | | |
| Antimony trioxide | | 2 | 2 | 2 | 2 | 2 | 2 | 2 | 2 |

TABLE 2

Relative Times to One-Third Plasticizer Loss From Vinyl Compound of 85°C

| Plasticizer | .075" Thick Slabs | Wire Insulation |
|---|---|---|
| DOP | 1.0 | 1.0 |
| 711 | 1.4 | - |
| DINP | 1.8 | - |
| DIDP | 5.5 | 5.8 |
| 50/50 810/DTDP | 6.8 | 6.7 |
| DUP | - | 50 |
| 7,9 TM | - | 400 |

TABLE 3

| Plasticizer | Activation Energy in kcal/mole (Semirigid Compound) | Heat of Vaporization in kcal/mole (Pure Plasticizer) | |
|---|---|---|---|
| | | Monsanto[3] | Frissel[4] |
| DOP | 17 | 26.6 | 23.6 |
| 711 | 16.5 | 30.6 | - |
| DINP | 15 | - | 24.5 |
| DIDP | 20 | 19.5 | 28.2 |
| DUP | - | 22.3 | - |

TABLE 4

Acceleration of Plasticizer Evaporation[a] In Forced Air Oven Relative To Several Air Velocities at 85°C

| Air Flow (ft/min.) | DOP Plasticizer ∥ Orientation | DOP Plasticizer ⊥ Orientation | DIDP Plasticizer ∥ Orientation |
|---|---|---|---|
| 3 | 4.2 | 2.6 | 4.7 |
| 10 | 3.3 | 2.2 | 4.2 |
| 30 | 2.3 | 1.5 | 3.3 |
| 100 | 1.8 | 1.0 | 2.2 |

[a] Based on an endpoint of one-third total plasticizer loss from a 3" length of 26 gauge vinyl insulated wire in a laminar flow environment.

TABLE 5

Times to Failure[a] of Vinyl Insulation Materials at 85°C

| Plasticizer, 30 phr (26 Ga. Vinyl Insulation) | Worst Case (⊥, Forced Flow) |
|---|---|
| DOP | 3.0 days |
| DIDP | 17.5 |
| 810/DTDP | 20 |
| DTDP | 160 |
| DUP | 180 |
| 7,9 TM | 1300 |

[a] Failure is defined as loss of >50% original elongation due to plasticizer evaporation only.

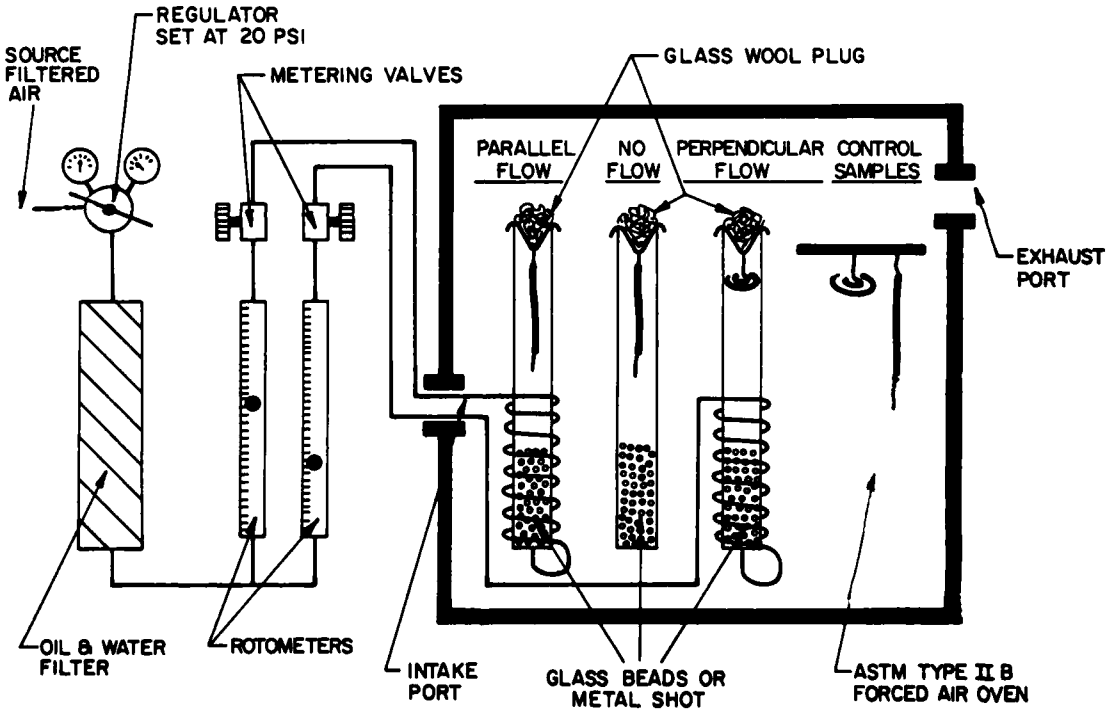
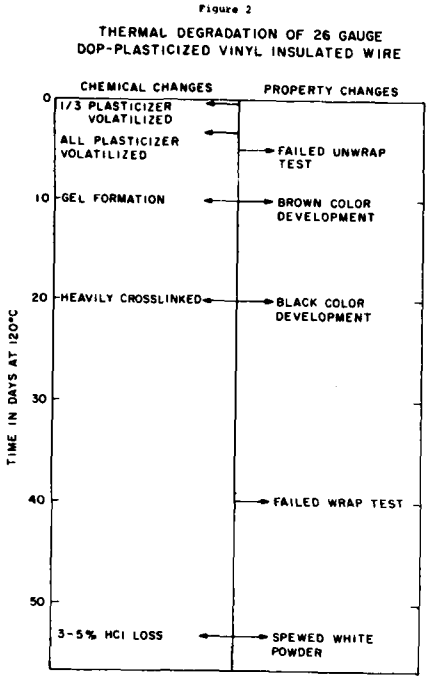



Figure 1

Figure 2



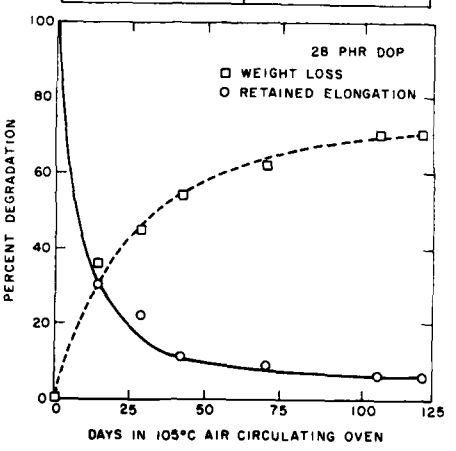




Figure 3

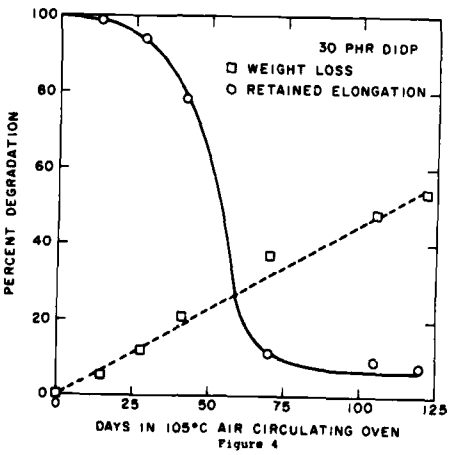



Figure 4

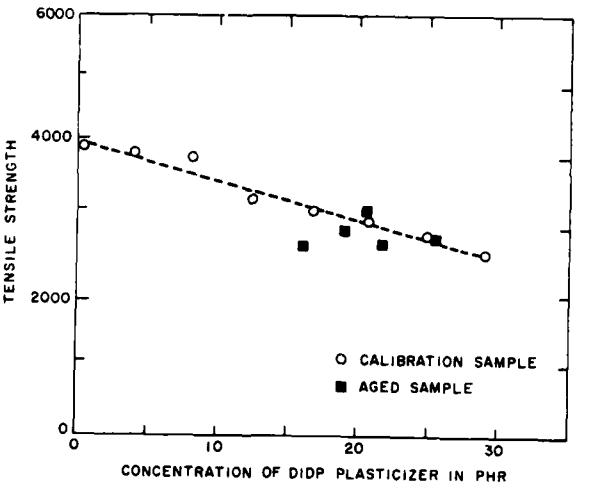



Figure 5

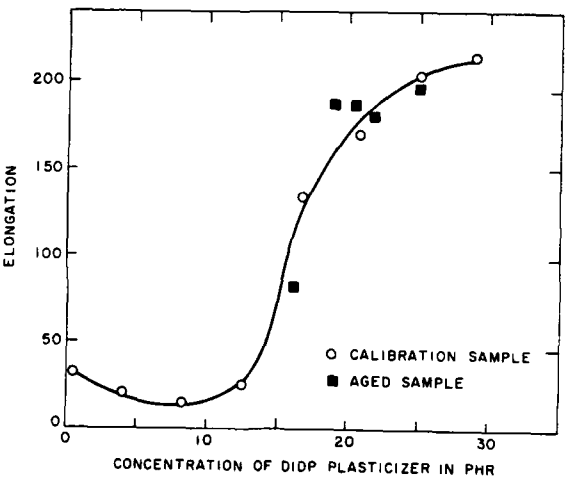



Figure 6

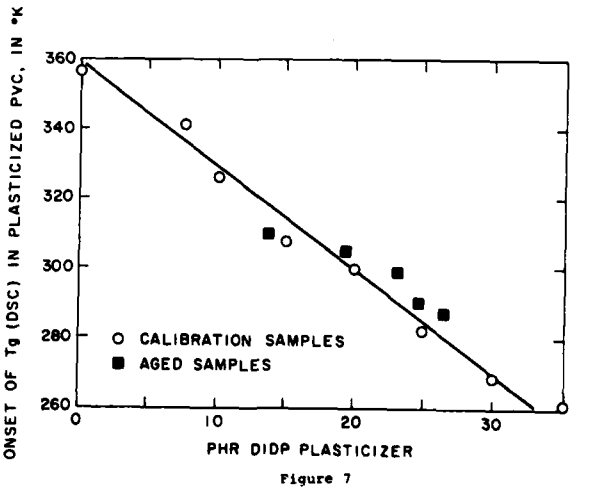



Figure 7

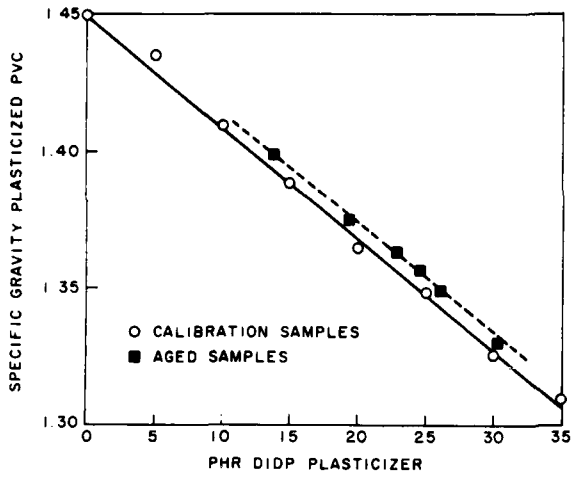



Figure 8

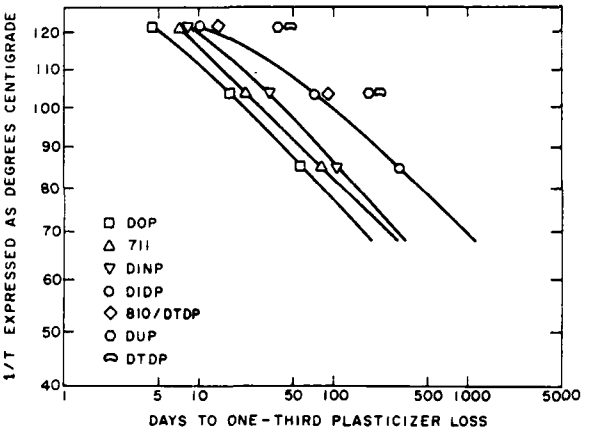



Figure 11

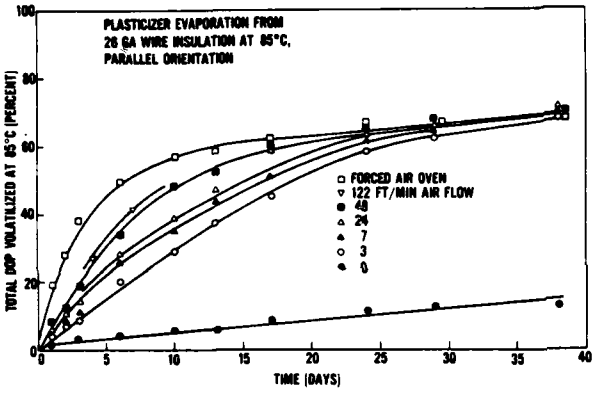



Figure 9

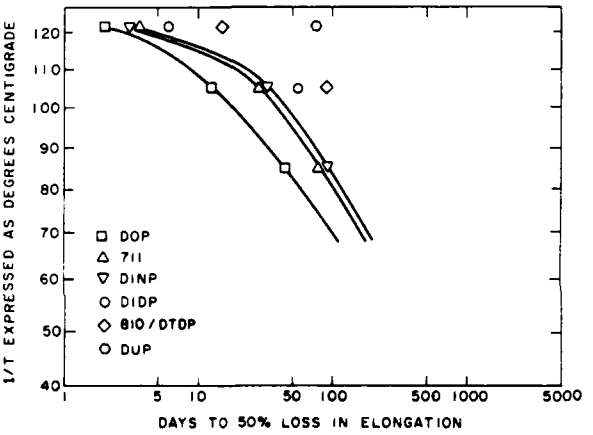



Figure 12

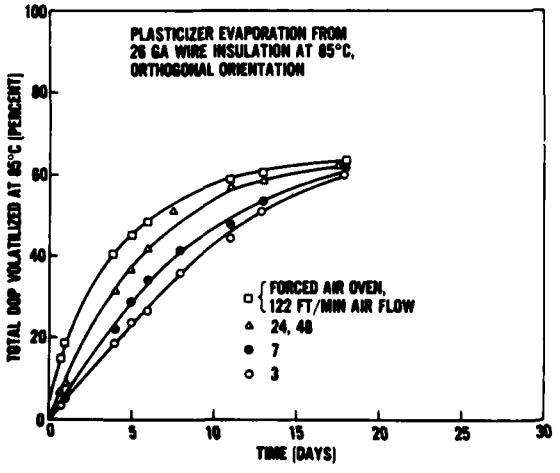



Figure 10

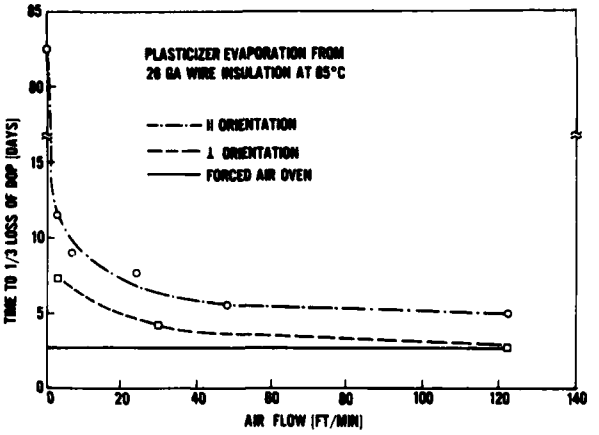



Figure 13

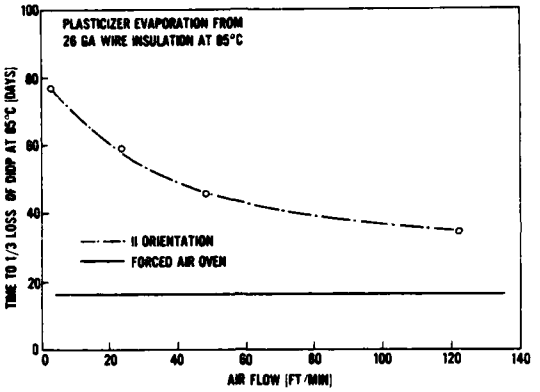



Figure 14

Figure 15

HP-25 Program to Predict Time to Given Plasticizer Loss[a]

Input

| | | |
|---|---|---|
| Measurement: | Surface area/volume of insulation[b], $in^{-1}$ | STO 0 |
| | Temperature of oven, °C | STO 1 |
| | Time to measured plasticizer loss[c], yr. | STO 2 |
| | Amount of plasticizer lost, % | STO 3 |
| | Activation energy[d], kcal $mole^{-1}$ | STO 4 |
| Prediction: | Surface area/volume of insulation[b], $in^{-1}$ | STO 5 |
| | Maximum loss of plasticizer tolerated[e], % | STO 6 |
| | Air flow calibration factor | STO 7 |
| | Temperature of predicted loss, °C | X register |

RPN Program (35 steps)

| | | | |
|---|---|---|---|
| Enter | 3 | RCL 6 | RCL 7 |
| GSB 30 | : | RCL 3 | X |
| RCL 1 | RCL 4 | : | GTO 00 |
| GSB 30 | X | X | 273 |
| - | $10^X$ | RCL 0 | + |
| 4.57 | RCL 2 | RCL 5 | 1/X |
| EEX | X | : | RTN |
| CHS | | X | |

Output

Displayed in X-register, time to given plasticizer loss, yr.

[a] Percent loss must be <33% to stay within the linear regime of plasticizer evaporation curve

[b] Calculator program to determine this quantity shown in Figure 16

[c] Table 3 can be used for those plasticizers listed

[d] 15-20 kcal/mole

[e] Table 4

Figure 16

HP-25 Program to Determine Surface Area/Volume of Wire Insulation

Input

| | |
|---|---|
| OD of wire insulation, in | STO 0 |
| OD of copper wire, in | STO 1 |

RPN Program (10 steps)

| |
|---|
| RCL 1 |
| 4 |
| X |
| RCL 1 |
| $x^2$ |
| RCL 2 |
| $x^2$ |
| - |
| : |
| GTO 00 |

Output

Displayed in X register, surface area/volume, $in^{-1}$

# CARBOXYLATED NITRILE/PVC FLUXED BLENDS FOR EXTRA-HEAVY-DUTY-CABLE JACKET COVERS

SCHWARZ, HERBERT F

POLYSAR LIMITED, SARNIA, ONTARIO, CANADA

Tough, durable vulcanizates for applications demanding excellent resistance not only to oils and fuels, but also to ozone and exacting weather conditions, can be made from compounds based on fluxed blends of regular NBR and PVC. The technology is well established and widely used.

Carboxylated nitrile rubber (XNBR) produces very much greater modulus, tensile strength and abrasion resistance than regular NBR, but early attempts to exploit that advantage in XNBR/PVC blends were thwarted by the tendency of XNBR to crosslink during fluxing. This obstacle has now been overcome.

The study reported here compares XNBR/PVC with NBR/PVC in a range of polymer ratios, in both black-filled and silica-filled compounds, and using several different curing systems. The results show very substantial performance advantages with XNBR, especially in strength and abrasion resistance.

This paper presents formulations and associated data for extra-heavy-duty-cable jacket applications. The data illustrate the exceptional strength and durability achievable in the fluxed XNBR/PVC vulcanizates.

## INTRODUCTION

Throughout the mechanized world there is a growing need for rubber products capable of withstanding extremely harsh service conditions. In many applications, for example, rubber products are required to be highly resistant not only to oils and fuels, but also to ozone, abrasion, heat, flame and weather. Products that must resist some or all of these conditions include cable jackets for the mining, quarrying, transportation and oil industries.

NBR/PVC fluxed blends are widely used - and with notable success - in many of these cable cover applications, but there is an increasing incidence of applications whose performance criteria are very difficult to meet with NBR/PVC compounds. Blending carboxylated nitrile rubber (XNBR) with PVC has been recognized as a possible route to satisfying the more demanding criteria because XNBR was known to produce much higher modulus, tensile strength and abrasion resistance. However, attempts to exploit those advantages have been thwarted, until recently, by the tendency of XNBR to crosslink during fluxing. That obstacle has now been overcome, and proprietary XNBR/PVC blends containing a suitable non-staining, non-discoloring stabilizer system are now on the market.

This paper compares XNBR/PVC and NBR/PVC fluxed blends in both black and light-coloured compounds; at different blend ratios; and in a heavy duty cable jacket compound that meets relevant IPCEA specifications. It also presents development formulations and test data for compositions that merit evaluation in various extra-heavy-duty applications.

## EXPERIMENTAL

XNBR alone, NBR alone, and fluxed XNBR/PVC blends in three blend ratios, prepared as indicated in Table I, were compounded in the simple black and light-coloured compound formulations shown in Table II. They were tested by ASTM procedures, where applicable, to produce the data recorded in Tables III and IV.

Proprietary fluxed blends of NBR and XNBR with PVC (70/30 : rubber/PVC) were compounded in the cable jacket shown in Table V to provide a comparison under laboratory mixing and testing conditions. The XNBR/PVC compound was then evaluated in a plant trial, with the results shown in Table VI.

Further formulations developed for extra-heavy-duty cable jacket applications were compounded and tested in the laboratory (Tables VII to X).

## RESULTS

### Black-Filled and Silica-Filled Compounds

As shown in Tables III and IV, the scorch time of all of the NBR based compounds exceeded 25 minutes,

irrespective of PVC level. They were shorter in the XNBR compounds; decreased with increasing PVC level in the black XNBR compounds; but remained constant at 13-14 minutes in the white XNBR compounds.

Compound Mooney viscosity was higher with XNBR than with NBR in both the black and white compounds. The effect of increased PVC level on compound viscosity can be summarized as follows:

Viscosity
- -decreased in the black compounds, the effect being slightly less pronounced in the XNBR compounds;
- -decreased slightly in the white XNBR compounds;
- -increased slightly in the white NBR compounds.

The Mooney viscosity results have been confirmed in Monsanto Rheometer initial viscosity data (not shown).

Despite their higher viscosities, the XNBR compounds (both black and white) extruded at least as well as - and in many cases, significantly better than - the NBR compounds. At low PVC levels, however, the NBR extrudates were slightly smoother. Increasing the PVC level produced significant improvements in extrusion rate and die swell.

Modulus and tensile strength were always higher, and elongation at break lower, with XNBR. In all cases, tensile strength and elongation at break decreased, and modulus increased, with increased PVC content.

In tear strength, at all blend levels, XNBR equalled NBR in the black vulcanizates and surpassed it in the white. Tear strength increased with PVC level in both the black and white vulcanizates.

The compression set results were interesting for several reasons:

- At both test temperatures, the set values were lower with XNBR in the black vulcanizates and higher in the white;
- At 70°C, the set increased with increasing PVC level;
- At 100°C, the set of the black compounds increased with increased PVC content (the NBR compounds somewhat irregularly). With the white compounds, the set decreased sharply with the addition of 15 parts of PVC, then increased with further increases in the PVC level;
- The set values at 100°C were lower than those obtained at 70°C in all vulcanizates containing 30 parts PVC, and in white vulcanizates containing 45 parts PVC. The reasons for these anomalies are not yet understood.

Abrasion resistance was much better with XNBR. In general, it increased as the PVC content was increased to 30 parts, then decreased (black) or levelled off (white).

XNBR vulcanizates were stiffer than corresponding NBR vulcanizates at low temperatures, and low-temperature flexibility decreased with increasing PVC level.

The air aging data indicate good heat resistance in both black and white compounds at both 70 and 100°C. The black 100% XNBR compound stiffened more (modulus increased more) than the corresponding NBR compound, an effect that was reversed in the compounds containing 30 and 45 parts of PVC. In the white compounds, the relatively large increase shown by the 100% XNBR compound persisted across the entire blend range.

The oil and fuel resistance of all compounds was excellent, increasing with increasing PVC content and, as indicated by linear measurement of volume swell, showing a slight advantage for XNBR.

The ozone resistance of the black NBR based vulcanizates increased with PVC content until there was no detectable cracking, an interesting result considering the severity of the test. The black XNBR based vulcanizates showed the same trend up to 30 parts PVC content, at which point XNBR gave slightly better ozone resistance than NBR despite its higher modulus. With a further increase in PVC level, however, the high modulus of the XNBR based vulcanizate was sufficient to cause a decline.

Extra-Heavy-Duty Cable Jacket Compounds

The merits of XNBR/PVC fluxed blends in extra-heavy-duty cable jacket compounds are illustrated by the examples shown in Tables V - X.

When comparing the NBR/PVC and XNBR/PVC test results shown in Table V, note particularly the advantages in modulus, tensile strength, tear strength and abrasion resistance achieved with XNBR/PVC, and the excellent oil and air aging performance of both types of blend.

Plant trial data for the same XNBR/PVC formulation (Table VI) confirm the findings of the laboratory evaluation and show how the vulcanizate properties relate to IPCEA specifications for extra-heavy-duty cable jackets.

Tables VII to X present additional formulations for extra-heavy-duty cable jacket applications.

A premium quality jacket compound is shown in Table VII. The XNBR/PVC version is compared with two standard 70/30 : NBR/PVC blends. In this comparison, the XNBR/PVC compound again gives very high tensile, modulus, tear and abrasion properties,

and excellent low temperature properties.

Table VIII shows compounds designed for the lead cure process. Two XNBR/PVC based formulations are compared with similar compounds based on a 75/25: NBR/PVC blend containing a low ACN (26%) NBR for improved low temperature flexibility. The tensile strength achieved with XNBR/PVC is approximately 15 per cent above the minimum specification requirements, and its excellent low temperature properties are again noteworthy.

A compound suitable for CV (steam cure) is shown in Table IX. It features a tensile strength of 21 MPa and good modulus, abrasion and low temperature properties.

Table X describes a black cable jacket compound suitable for the lead cure process. The previously observed superior properties of the XNBR/PVC fluxed blend are re-confirmed in this compound.

## CONCLUSIONS

The data presented here show that suitably stabilized XNBR/PVC blends can be fluxed satisfactorily, and can provide outstanding strength and abrasion resistance in cable jacket applications that demand high levels of resistance to oils, fuels, ozone, and weather.


## ACKNOWLEDGEMENTS

The author wishes to thank W.D. Gunter and W.S. Edwards for editoral assistance; and Polysar Limited for permission to publish.





Herbert F. Schwarz is a Development Specialist, Emulsion Rubbers, with Polysar Ltd., Sarnia, Ontario, Canada. He graduated from Swansea Technical College and studied Rubber Technology at the Bridgend Technical College, U.K. Currently, he is involved in Product and Application Developments within the Technical Development Division and is also responsible for NBR-PVC Blend Products and Powder NBR.



POLYSAR KRYFLEX KRYLENE KRYMIX KRYNAC KRYNOL TAKTENE THANS PIP and SS 250 are registered trade marks of Polysar Limited Sarnia Ontario Canada

Information given herein is furnished in good faith without warranty representation inducement or a license of any kind. Polysar does not assume any legal responsibility for use of the information given herein. No warranty or representation is given that Polysar products described will be suitable in purchasers formulations or processes for any particular end use. No representation is given as to freedom from patent infringement.

Materials not manufactured or supplied by Polysar may present hazards in handling and use. Reference should be made to the manufacturer or supplier for all information relating to such materials.

AD-A096 308 ARMY COMMUNICATIONS RESEARCH AND DEVELOPMENT COMMAND --ETC F/G 9/1
PROCEEDINGS OF THE INTERNATIONAL WIRE AND CABLE SYMPOSIUM (29TH--ETC(U)
NOV 80 E F GODWIN

UNCLASSIFIED NL

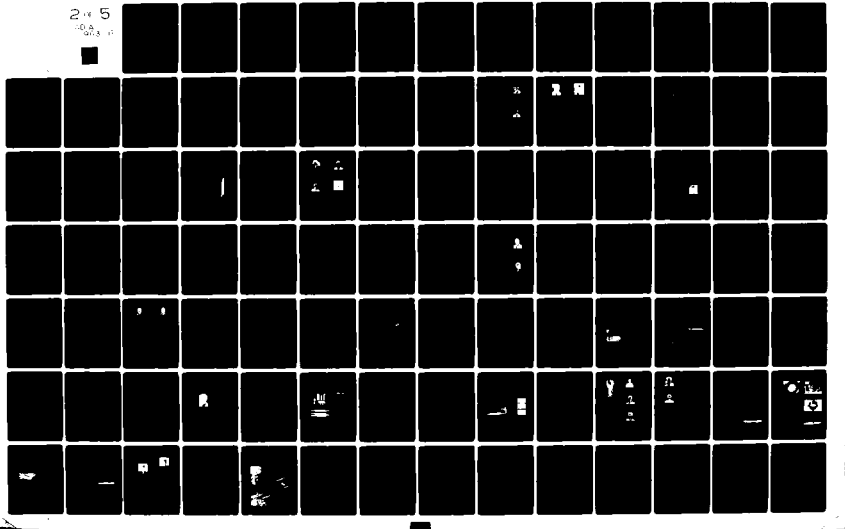


TABLE 1. FLUXED BLEND MASTERBATCHES

| | | | | | | |
|---|---|---|---|---|---|---|
| NBR* | 85 | - | 70 | - | 55 | - |
| XNBR** | - | 85 | - | 70 | - | 55 |
| PVC (medium MW) | 15 | 15 | 30 | 30 | 45 | 45 |
| Plasticizer | 5 | | 10 | | 15 | |
| Stabilizer | 2 | | 2 | | 2 | |
| Lubricants | 1.75 | | 2.5 | | 3.25 | |
| Antioxidant | 1.2 | | 1.2 | | 1.2 | |
| Viscosity | | | | | | |
| (ML-1+4' at 100°C) | 46 | 57 | 46 | 55 | 50 | 53 |
| (ML-1+4' at 125°C) | 28 | 36 | 29 | 35 | 32 | 35 |

Stocks fluxed for 2 minutes at 155 - 160°C in an internal mixer, then sheeted off a warm (~60°C) mill.

* Bound ACN-34%, ML-1+4' at 100°C-50 (KRYNAC 34.50)
** Medium ACN, highly carboxylated grade (KRYNAC 221)

TABLE II. BASE COMPOUNDS

| | Black | White |
|---|---|---|
| Fluxed blend masterbatch (Table I) | 100 | 100 |
| Sulfur | 1.25 | 0.3 |
| Stearic acid | 1 | 1 |
| N-550 (FEF) carbon black | 40 | - |
| HiSil EP (silica) | - | 50 |
| Santocure MOR | - | 3 |
| TMTM | 0.5 | - |
| TMTD | - | 0.5 |
| TETD | - | 0.5 |
| XNBR curative* | 10 | 10 |

Compounds mixed in a 4-minute, upside-down cycle; Model B Banbury; 77 rpm; 80°C at start; cold water on full. XNBR curative and accelerators added on the sheet-off mill.

* 50/50: NBR/$ZnO_2$ (KRYNAC PA50)

TABLE III. BLACK COMPOUND

| Rubber/PVC ratio (see Table 1) | 100:0 | | 85:15 | | 70:30 | | 55:45 | |
|---|---|---|---|---|---|---|---|---|
| | NBR | XNBR | NBR | XNBR | NBR | XNBR | NBR | XNBR |
| Viscosity (ML-1 + 4' at 100°C) | 67 | 103 | 61 | 93 | 58 | 83 | 62 | 74 |
| Mooney scorch ($t_5$ at 125°C) | 25 | 16.5 | 25 | 15.2 | 25 | 13.7 | 25 | 9.2 |
| Monsanto Rheometer at 165°C, 900 cpm, 3° arc, 60 s preheat | | | | | | | | |
| ML (dN.m) | 26 | 36 | 21 | 30.5 | 18 | 31.5 | 15.5 | 25 |
| MH (dN.m) | 78 | 99 | 59 | 86 | 50 | 78 | 42 | 64 |
| ts5 (min) | 3.7 | 3.1 | 4.6 | 2.6 | 5.1 | 2.8 | 5.7 | 3.5 |
| t'90 (min) | 7.6 | 9.7 | 8.6 | 10.3 | 9.6 | 10.6 | 10.5 | 10.6 |
| Extrusion, ½ Royle, 70 rpm, 104°C | | | | | | | | |
| Rate (cm/min) | 80 | 93 | 94 | 108 | 121 | 119 | 135 | 143 |
| Die swell (%) | 137 | 121 | 106 | 92 | 60 | 67 | 44 | 36 |
| Appearance rating | A5 | A5 | A10 | A9 | A10 | A9 | A10 | A10 |
| Cure time at 166° (min) | 8 | 10 | 10 | 12 | 10 | 10 | 12 | 12 |
| Specific gravity | 1.14 | 1.14 | 1.17 | 1.18 | 1.20 | 1.20 | 1.23 | 1.26 |
| Hardness, Shore A | 63 | 76 | 69 | 80 | 73 | 82 | 82 | 88 |
| Modulus at 100% elong. (MPa) | 2.0 | 5.1 | 3.1 | 6.5 | 4.6 | 9.4 | 7.5 | 13.4 |
| Modulus at 300% elong. (MPa) | 10.1 | 20.6 | 10.5 | 19.2 | 12.0 | 20.6 | 13.5 | - |
| Tensile strength (MPa) | 22.3 | 22.3 | 20.2 | 21.8 | 17.3 | 21.6 | 15.8 | 19.5 |
| Elongation at break (%) | 600 | 350 | 600 | 360 | 530 | 340 | 460 | 260 |
| Tear strength, Die C (kN/m) | 51 | 46 | 55 | 55 | 62 | 62 | 70 | 70 |
| Compression set, ASTM B (%) | | | | | | | | |
| 22 h at 70°C | 21 | 19 | 41 | 31 | 59 | 51 | 60 | 57 |
| 22 h at 100°C | 37 | 34 | 54 | 41 | 48 | 46 | 65 | 61 |
| Gehman (°C) $T_2$ | -16 | -6 | -10 | +3 | -10 | +8 | +1 | +12 |
| $T_5$ | -20 | -14 | -17 | -6 | -15 | -2 | -5 | + 3 |
| $T_{10}$ | -22 | -16 | -20 | -10 | -18 | -7 | -9 | -2 |
| $T_{100}$ | -28 | -24 | -28 | -22 | -30 | -29 | -20 | -24 |
| NBS Abrasion (%) | 157 | 536 | 287 | 587 | 441 | 1032 | 352 | 387 |
| Aged in Air, 168 h at 70°C | | | | | | | | |
| Hardness, Shore A | 65 | 75 | 71 | 80 | 76 | 87 | 80 | 90 |
| Modulus at 100% elong. (MPa) | 2.4 | 6.5 | 3.1 | 8.4 | 5.3 | 13.0 | 8.0 | 14.2 |
| Modulus at 300% elong. (MPa) | 13.1 | 24.6 | 12.5 | 23.1 | 14.9 | - | 16.2 | - |
| Tensile strength (MPa) | 21.2 | 28.1 | 19.4 | 23.2 | 18.3 | 23.5 | 17.2 | 20.4 |
| Elongation at break (%) | 460 | 320 | 500 | 310 | 450 | 250 | 360 | 250 |

| | | | | | | | | |
|---|---|---|---|---|---|---|---|---|
| **Aged in Air, 168 h at 100°C** | | | | | | | | |
| Hardness, Shore A | 65 | 79 | 68 | 83 | 76 | 85 | 84 | 90 |
| Modulus at 100% elong. (MPa) | 3.6 | 11.0 | 4.1 | 14.4 | 8.0 | 13 | 12.5 | 21.3 |
| Modulus at 300% elong. (MPa) | 18.9 | - | 16.8 | - | 19.2 | - | - | - |
| Tensile strength (MPa) | 20.6 | 23.5 | 20.1 | 26.5 | 19.2 | 26.1 | 19.3 | 24.6 |
| Elongation at break (%) | 330 | 200 | 370 | 210 | 300 | 170 | 220 | 150 |
| **Aged in ASTM Oil #2, 168 h at 100°C** | | | | | | | | |
| Hardness, Shore A | 60 | 78 | 62 | 82 | 75 | 91 | 86 | 95 |
| Modulus at 100% elong. (MPa) | 2.2 | 8.5 | 2.7 | 10.8 | 5.9 | 18.1 | 11.2 | 22.0 |
| Modulus at 300% elong. (MPa) | 13.4 | - | 13.3 | - | 17.4 | - | 20.1 | - |
| Tensile strength (MPa) | 20.2 | 25.7 | 20.1 | 25.0 | 20.7 | 27.1 | 20.2 | 25.1 |
| Elongation at break (%) | 430 | 270 | 460 | 260 | 410 | 220 | 320 | 190 |
| Volume change (%) | 9.2 | 9.2 | 6.1 | 4.5 | 3.0 | 1.5 | - | - 3.0 |
| **Aged in ASTM Fuel B, 168 h at RT** | | | | | | | | |
| Hardness, Shore A | 41 | 52 | 43 | 57 | 55 | 64 | 63 | 70 |
| Modulus at 100% elong. (MPa) | 1.4 | 2.5 | 1.6 | 3.0 | 2.5 | 4.4 | 3.7 | 4.6 |
| Modulus at 300% elong. (MPa) | 9.0 | 13.9 | 7.5 | 12.8 | 8.4 | 15.4 | 9.6 | 11.9 |
| Tensile strength (MPa) | 9.0 | 15.0 | 9.3 | 15.8 | 12.9 | 16.4 | 11.6 | 13.2 |
| Elongation at break (%) | 300 | 330 | 380 | 370 | 500 | 320 | 400 | 370 |
| Volume change (%) | 29.5 | 31.3 | 24.2 | 22.5 | 19.1 | 15.8 | 15.8 | 9.2 |
| **Dynamic Ozone Resistance, 50 pphm, 40°C, 0-20% extension, 32 cpm** | | | | | | | | |
| Rating after 24 h | 1 | 1 | 1 | 1 | 0 | 0 | 0 | 1 |
| 48 h | 2 | 2 | 3 | 2 | 2 | 0 | 0 | 2 |
| 72 h | 3 | 3 | 4 | 3 | 2 | 2 | 0 | 2 |
| 100 h | 3 | 3 | 4 | 3 | 2 | 2 | 0 | 3 |
| 120 h | 3 | 3 | 5 | 3 | 3 | 2-3 | 0 | 3 |
| 144 h | 3 | 4 | 5 | 3 | 3 | 3-4 | 0 | 3 |
| 168 h | 5 | 5 | 5 | 4-5 | 4-5 | 3-4 | 0 | 4 |

TABLE IV. WHITE COMPOUND

| Rubber/PVC ratio | 100:0 | | 85:15 | | 70:30 | | 55:45 | |
|---|---|---|---|---|---|---|---|---|
| | NBR | XNBR | NBR | XNBR | NBR | XNBR | NBR | XNBR |
| Viscosity (ML-1+4' at 100°C) | 68 | 92 | 76 | 90 | 81 | 90 | 86 | 90 |
| Mooney scorch ($t_5$ at 125°C) | 25 | 12.5 | 25 | 14 | 25 | 13 | 25 | 14 |
| Monsanto Rheometer at 165°C, 900 cpm, 3° arc, 60 s preheat | | | | | | | | |
| ML (dN.m) | 22 | 38 | 22 | 35 | 20 | 32 | 19 | 31 |
| MH (dN.m) | 57 | 88 | 57 | 88 | 59 | 81 | 55 | 69 |
| ts5 (min) | 5 | 4 | 4.7 | 3.2 | 4.6 | 3.5 | 4.5 | 3.5 |
| t'90 (min) | 11.2 | 7.7 | 10.5 | 7.8 | 9.3 | 7.7 | 8.5 | 6.7 |
| Extrusion, ½ Royle, 70 rpm, 104°C | | | | | | | | |
| Rate (cm/min) | 84 | 93 | 98 | 93 | 118 | 118 | 128 | 131 |
| Die swell (%) | 132 | 135 | 93 | 95 | 56 | 59 | 41 | 36 |
| Appearance rating | A7 | A10 | A8 | A10 | A10 | A10 | A10 | A10 |
| Cure time at 166°C (min) | 12 | 8 | 12 | 8 | 10 | 10 | 10 | 10 |
| Specific gravity | 1.18 | 1.17 | 1.21 | 1.20 | 1.25 | 1.25 | 1.28 | 1.29 |
| Hardness, Shore A | 62 | 75 | 70 | 82 | 75 | 85 | 82 | 93 |
| Modulus at 100% elong. (MPa) | 1.4 | 3.9 | 2.2 | 6.5 | 4.2 | 11.0 | 6.4 | 13.8 |
| Modulus at 300% elong. (MPa) | 3.3 | 11.4 | 5.5 | 14.4 | 8.0 | 17.8 | 8.9 | - |
| Tensile strength (MPa) | 16.0 | 19.2 | 15.9 | 18.4 | 14.0 | 17.9 | 11.4 | 16.3 |
| Elongation at break (%) | 940 | 500 | 740 | 400 | 600 | 320 | 480 | 260 |
| Tear strength, Die C (kN/m) | 52 | 53 | 53 | 58 | 60 | 65 | 61 | 109 |
| Compression set, ASTM B (%) | | | | | | | | |
| 22 h at 70°C | 27 | 29 | 34 | 38 | 46 | 49 | 54 | 56 |
| 22 h at 100°C | 46 | 49 | 37 | 38 | 41 | 46 | 47 | 53 |
| Gehman (°C) $T_2$ | -18 | -8 | -15 | +1 | -5 | +7 | 0 | +10 |
| $T_5$ | -22 | -15 | -19 | -8 | -11 | -2 | -7 | 0 |
| $T_{10}$ | -23 | -17 | -21 | -12 | -15 | -8 | -11 | -6 |
| $T_{100}$ | -29 | -27 | -29 | -25 | -25 | -25 | -28 | -25 |
| NBS Abrasion (%) | 81 | 362 | 84 | 315 | 101 | 268 | 108 | 263 |
| Aged in Air, 168 h at 70°C | | | | | | | | |
| Hardness, Shore A | 65 | 80 | 67 | 86 | 82 | 89 | 80 | 89 |
| Modulus at 100% elong. (MPa) | 1.7 | 5.9 | 2.5 | 10.3 | 5.1 | 19.5 | 7.5 | 19.6 |
| Modulus at 300% elong. (MPa) | 5.0 | 11.7 | 6.9 | 20.7 | 9.4 | - | 10.3 | - |
| Tensile strength (MPa) | 16.8 | 22.7 | 14.3 | 21.7 | 13.5 | 21.6 | 11.3 | 21.6 |
| Elongation at break (%) | 720 | 420 | 640 | 340 | 520 | 200 | 420 | 220 |
| Aged in Air, 168 h at 100°C | | | | | | | | |
| Hardness, Shore A | 66 | 80 | 69 | 85 | 75 | 90 | 82 | 93 |
| Modulus at 100% elong. (MPa) | 2.0 | 7.0 | 2.9 | 12.0 | 4.5 | 17.1 | 6.9 | 22.2 |
| Modulus at 300% elong. (MPa) | 5.9 | 21.1 | 7.3 | 23.4 | 9.6 | - | 10.4 | - |
| Tensile strength (MPa) | 15.8 | 22.3 | 14.0 | 23.4 | 13.4 | 22.4 | 11.3 | 23.3 |
| Elongation at break (%) | 660 | 310 | 600 | 300 | 480 | 220 | 350 | 230 |

| | | | | | | | | |
|---|---|---|---|---|---|---|---|---|
| **Aged in ASTM Oil #2, 168 h at 100°C** | | | | | | | | |
| Hardness, Shore A | 59 | 76 | 60 | 83 | 71 | 90 | 84 | 94 |
| Modulus at 100% elong. (MPa) | 1.5 | 6.4 | 2.0 | 11.0 | 4.4 | 17.9 | 7.5 | 22.8 |
| Modulus at 300% elong. (MPa) | 5.4 | 19.8 | 6.3 | 23.7 | 9.8 | - | 10.8 | - |
| Tensile strength (MPa) | 18.0 | 26.1 | 15.8 | 25.0 | 15.3 | 23.3 | 12.4 | 23.4 |
| Elongation at break (%) | 700 | 400 | 630 | 310 | 510 | 260 | 350 | 200 |
| Volume change (%) | 8 | 6 | 6 | 3 | 3 | - | -3 | -6 |
| **Aged in ASTM Fuel B, 168 h at RT** | | | | | | | | |
| Hardness, Shore A | 35 | 47 | 44 | 61 | 54 | 65 | 64 | 76 |
| Modulus at 100% elong. (MPa) | 0.6 | 1.9 | 1.5 | 3.5 | 2.5 | 5.0 | 3.6 | 7.5 |
| Modulus at 300% elong. (MPa) | 3.4 | 7.8 | 4.7 | 10.9 | 6.1 | 12.8 | 6.5 | - |
| Tensile strength (MPa) | 8.4 | 11.0 | 8.9 | 13.1 | 10.0 | 13.5 | 8.8 | 13.7 |
| Elongation at break (%) | 650 | 420 | 640 | 360 | 590 | 320 | 500 | 280 |
| Volume change (%) | 30 | 30 | 23 | 26 | 17 | 16 | 13 | 9 |
| **Dynamic ozone resistance, 50 pphm, 40°C, 0-20% extension, 32 cpm** | | | | | | | | |
| Rating after 24 h | 1 | 1 | 2 | 1 | 0 | 0 | 0 | 0 |
| 48 h | 2 | 2 | 3 | 2 | 1 | 2 | 0 | 1 |
| 72 h | 3 | 2 | 3 | 3 | 2 | 2 | 0 | 2 |
| 100 h | 4 | 3 | 4-5 | 3 | 3 | 2 | 0 | 2 |
| 120 h | 5 | 3 | 5 | 3 | 4 | 3 | 2 | 4 |
| 144 h | 5 | 4-5 | 5 | 4-5 | 4-5 | 3 | 3 | 5 |
| 168 h | 5 | 5 | 5 | 5 | 5 | 4 | 4 | 5 |

TABLE V. CABLE JACKETS - COMPARISON OF NBR AND XNBR

(70/30 RUBBER/PVC RATIO)

Parts by weight

| | |
|---|---|
| Fluxed blend (Table II) | 100 |
| Uvinul D-49 | 0.2 |
| NBC | 1 |
| Silane A-189 | 1.5 |
| Polygard | 0.5 |
| Irganox 1076 | 0.3 |
| Triphenyl phosphite | 1 |
| Antimony trioxide | 3 |
| Titanium dioxide | 10 |
| HiSil 233 | 15 |
| Laminar | 45 |
| Di-tridecyl phthalate | 15 |
| Dioctyl sebecate | 10 |
| Stearic acid | 1 |
| Morfax | 1.5 |
| Sulfads | 1.5 |
| TMTD | 1 |
| MC sulphur | 0.15 |

| | NBR * | XNBR ** |
|---|---|---|
| Zinc oxide | 3.0 | -- |
| XNBR curative (Table II) | -- | 6.0 |
| Viscosity (ML-1 + 4' at 100°C) | 20 | 22 |
| Mooney scorch (t5 at 125°C) | 5.3 | 7.3 |
| Monsanto Rheometer at 165°C, 900 cpm, 3° arc, 60 s preheat | | |
| ML (dN.m) | 11 | 16 |
| MH (dN.m) | 42 | 57 |
| ts5 (min) | 1.6 | 1.6 |
| t'90 (min) | 5.5 | 6.6 |
| Cured 8 minutes at 166°C | | |
| Hardness, Shore A | 56 | 70 |
| Modulus at 100% elong. (MPa) | 1.9 | 3.0 |
| Modulus at 300% elong. (MPa) | 6.9 | 10.4 |
| Tensile strength (MPa) | 13.9 | 17.2 |
| Elongation at break (%) | 450 | 400 |
| Tear strength, Die C (kN/m) | 29 | 36 |
| Compression set, ASTM B (%) | | |
| 22 h at 70°C | 36 | 37 |
| 22 h at 100°C | 37 | 41 |
| NBS Abrasion (%) | 69 | 83 |
| Gehman (°C) $T_2$ | -14 | +5 |
| $T_5$ | -20 | -12 |
| $T_{10}$ | -23 | -18 |
| $T_{100}$ | -32 | -34 |
| Set, IPCEA (%) | 4.5 | 8 |
| Aged in Air, 168 h at 100°C | | |
| Hardness, Shore A | 53 | 77 |
| Modulus at 100% elong. (MPa) | 1.9 | 5.1 |
| Modulus at 300% elong. (MPa) | 9.2 | 18.1 |
| Tensile strength (MPa) | 12.7 | 18.1 |
| Elongation at break (%) | 350 | 310 |

| | NBR | XNBR |
|---|---|---|
| Aged in Air, 168 h at 120°C | | |
| Hardness, Shore A | 66 | 81 |
| Modulus at 100% elong. (MPa) | 2.8 | 7.8 |
| Tensile strength (MPa) | 10.7 | 16.8 |
| Elongation at break (%) | 260 | 220 |
| Aged in Air, 336 h at 100°C | | |
| Hardness, Shore A | 62 | 76 |
| Modulus at 100% elong. (MPa) | 2.1 | 5.7 |
| Modulus at 300% elong. (MPa) | 10.3 | -- |
| Tensile strength (MPa) | 11.3 | 15.9 |
| Elongation at break (%) | 320 | 260 |
| Aged in ASTM Oil #2, 22 h at 121°C | | |
| Volume change (%) | -9.2 | -9.2 |
| Aged in ASTM Oil #2, 18 h at 121°C | | |
| Hardness, Shore A | 82 | 81 |
| Modulus at 100% elong. (MPa) | 2.0 | 5.9 |
| Modulus at 300% elong. (MPa) | 8.6 | 17.4 |
| Tensile strength (MPa) | 12.5 | 19.4 |
| Elongation at break (%) | 380 | 340 |
| Oxygen Bomb, 2.1 MPa, 168 h at 80°C | | |
| Hardness, Shore A | 54.5 | 68.5 |
| Modulus at 100% elong. (MPa) | 2.0 | 3.6 |
| Modulus at 300% elong. (MPa) | 9.3 | 14.1 |
| Tensile strength (MPa) | 13.7 | 17.2 |
| Elongation at break (%) | 370 | 340 |
| Aged in Air Bomb, 0.55 MPa, 20 h at 127°C | | |
| Hardness, Shore A | 54 | 72 |
| Modulus at 100% elong. (MPa) | 1.8 | 1.8 |
| Modulus at 300% elong. (MPa) | 8.9 | -- |
| Tensile strength (MPa) | 11.7 | 15.3 |
| Elongation at break (%) | 350 | 280 |
| Dynamic ozone resistance, 50 pphm, 40°C 0-20% extension, 32 cpm | | |
| Hours to first cracks (10X lens) | 144 | 120 |

* 70/30 NBR/PVC, 60 Mooney

** 70/30 XNBR/PVC, 90 Mooney, Table I

TABLE VI. EXTRA HEAVY DUTY CABLE JACKET - PLANT TRIAL

(XNBR COMPOUND FROM TABLE V)

| | Laboratory Mix | Plant Mix | Specification* |
|---|---|---|---|
| Modulus at 200% elong. (MPa) | 6.4 | 7.1 | 4.8 min. |
| Tensile strength (MPa) | 17.2 | 17.8 | 16.56 min. |
| Elongation at break (%) | 400 | 400 | 300 min. |
| Tear strength, Die C (kN/m) | 36 | 42 | 7 min. |
| Set, IPCEA (%) | 8 | not tested | 30 max. |
| Aged in Air, 168 h at 100°C | | | |
| Tensile strength (% retained) | 105 | 102 | 50 min. |
| Elongation at break (% retained) | 78 | 63 | 50 min. |
| Aged in ASTM Oil #1, 18 h at 121°C | | | |
| Tensile strength (% retained) | 113 | 100 | 60 min. |
| Elongation at break (% retained) | 85 | 70 | |
| Gehman (°C) | | | serviceability |
| $T_{10}$ | -18 | -17 | at -10°C |
| $T_{100}$ | -34 | -34 | |

* IPCEA S-19-81, NEMA WC 3, 7.6.20.1.3
and S-68-516, NEMA WC 8, 7.2.18.1.3

TABLE VII. EXTRA-HEAVY-DUTY JACKET - NON BLACK, PREMIUM QUALITY

| | (parts by weight) | | | |
|---|---|---|---|---|
| XNBR/PVC fluxed blend* | 95 | - | - | |
| NBR/PVC fluxed blend** | - | 100 | - | |
| NBR/PVC fluxed blend*** | - | - | 100 | |
| Silane A-189 | 0.5 | 0.5 | 0.5 | |
| Naugard 445 | 1 | 1 | 1 | |
| Antimony trioxide | 5 | 5 | 5 | |
| Titanium dioxide | 5 | 5 | 5 | |
| HiSil 215 | 40 | 40 | 40 | |
| Dioctyl adipate | 20 | 20 | 20 | |
| Cadmium stearate | 1.4 | 1.4 | 1.4 | |
| Zinc oxide | - | 5 | 5 | |
| Tetrone A | 0.7 | 0.7 | 0.7 | |
| Santocure NS | 1.5 | 1.5 | 1.5 | |
| XNBR curative (Table II) | 10 | - | - | |
| Viscosity (ML- 1 + 4'at 100°C) | 82 | 70 | 55 | |
| Mooney scorch (t5 at 125°C) | 9.5 | 21.5 | 24.0 | |
| | | | | Specification (1) |
| Modulus at 200% elong. (MPa) | 10.0 | 4.5 | 3.5 | 4.83 min. |
| Tensile strength (MPa) | 20.7 | 16.5 | 13.5 | 16.56 min. |
| Elongation at break (%) | 470 | 750 | 720 | 300 min. |
| Tear strength, Die C (kN/m) | 74 | 41 | 38 | |
| Set, IPCEA (%) | 7 | 6 | 6 | 30 max. |
| NBS Abrasion (%) | 760 | 179 | 126 | --- |
| Brittle point (°C) | -54 | -41 | -31 | --- |
| Aged in Air Bomb, 0.55 MPa, 20 h at 127°C | | | | |
| Tensile strength (% retained) | 96 | 109 | 110 | 50 min. |
| Elongation at break (% retained) | 58 | 75 | 82 | 50 min. |
| Aged in Oxygen Bomb, 2.1 MPa, 168 h at 80°C | | | | |
| Tensile strength (% retained) | 97 | 102 | 111 | 50 min. |
| Elongation at break (% retained) | 81 | 72 | 88 | 50 min. |
| Aged in ASTM Oil #2, 18 h at 121°C | | | | |
| Tensile strength (% retained) | 116 | 112 | 122 | 60 min. |
| Elongation at break (% retained) | 70 | 72 | 88 | 60 min. |

*70/30 rubber/PVC, 90 Mooney, Table I
**70/30 rubber/PVC, 75 Mooney, Table I
***70/30 rubber/PVC, 60 Mooney

(1) IPCEA S-19-81, NEMA WC 3, 7.6.20.3.1

TABLE VIII. EXTRA-HEAVY-DUTY JACKET - NON BLACK, LEAD CURE

| | | | (parts by weight) | | |
|---|---|---|---|---|---|
| XNBR/PVC fluxed blend* | 97 | - | 100 | - | |
| NBR.PVC fluxed blend** | - | 100 | - | 100 | |
| Silane A-189 | - | - | 0.5 | 0.5 | |
| Naugard 445 | 1 | 1 | 1 | 1 | |
| Antimony trioxide | 5 | 5 | 5 | 5 | |
| Titanium dioxide | 2 | 2 | 2 | 2 | |
| HiSil 215 | 40 | 40 | 30 | 30 | |
| Mistron Vapor | - | - | 10 | 10 | |
| Dioctyl phthalate | 9 | 9 | 9 | 9 | |
| Dioctyl sebecate | 14 | 14 | 14 | 14 | |
| Cadmium stearate | 1.4 | 1.4 | 1.4 | 1.4 | |
| Zinc oxide | - | 3 | - | 3 | |
| Tetrone A | 0.7 | 0.7 | 0.7 | 0.7 | |
| Santocure NS | 1.5 | 1.5 | 1.5 | 1.5 | |
| XNBR curative (Table II) | 6 | - | 6 | - | |
| | | | | | |
| Viscosity (ML - 1+4' at 100 C) | 91 | 69 | 60 | 52 | |
| Scorch time (t5 at 125 C) | 10.0 | 16.0 | 9.0 | 19.0 | |
| | | | | | Specification (1) |
| Modulus at 200% elong. (MPa) | 7.5 | 2.8 | 9.0 | 4.5 | 4.83 min. |
| Tensile strength (MPa) | 18.8 | 14.4 | 18.9 | 15.0 | 16.56 min. |
| Elongation at break (%) | 560 | 770 | 520 | 640 | 300 min. |
| Tear strength, Die C (kN/m) | 22 | 34 | 17 | 18 | 7.04 min. |
| | | | | | |
| Set, IPCEA (%) | 6 | 7 | 9 | 6 | 30 max. |
| NBS abrasion (%) | 580 | 89 | 272 | 97 | -- |
| Brittle point ($^{o}$C) | -46 | -51 | -51 | -53 | -- |
| | | | | | |
| Aged in Air Bomb, 0.55 MPa, 20 h at 127$^{o}$C | | | | | |
| Tensile strength (% retained) | 104 | 103 | 114 | 93 | 50 min. |
| Elongation at break (% retained) | 68 | 90 | 77 | 84 | 50 min. |
| | | | | | |
| Aged in Oxygen Bomb, 2.1 MPa, 168 h at 80$^{o}$C | | | | | |
| Tensile strength (% retained) | 84 | 116 | 103 | 100 | 50 min. |
| Elongation at break (% retained) | 75 | 91 | 88 | 86 | 50 min. |
| | | | | | |
| Aged in ASTM Oil #2, 18 h at 121$^{o}$C | | | | | |
| Tensile strength (% retained) | 108 | 120 | 130 | 93 | 60 min. |
| Elongation at break (% retained) | 66 | 91 | 79 | 97 | 60 min. |

*70/30 rubber/PVC, 90 Mooney, Table I.
**75/25 rubber PVC, rubber ACN content - 26%, rubber Mooney - 65

(1) IPCEA S-19-81, NEMA WC 3, 7.6.20.1.3

TABLE IX. EXTRA HEAVY DUTY JACKET - NON BLACK, CV CURE

| | (parts by weight) | | |
|---|---|---|---|
| XNBR/PVC fluxed blend* | 100 | - | |
| NBR/PVC fluxed blend** | - | 100 | |
| Silane A-189 | 0.5 | 0.5 | |
| Naugard 445 | 1 | 1 | |
| Antimony trioxide | 5 | 5 | |
| Titanium dioxide | 2 | 2 | |
| HiSil 215 | 30 | 30 | |
| Mistron Vapor | 10 | 10 | |
| Dioctyl phthalate | 9 | 9 | |
| Dioctyl adipate | 14 | 14 | |
| Zinc oxide | - | 3 | |
| MBTS | 2.5 | 2.5 | |
| TMTD | 1.5 | 1.5 | |
| TETD | 1.5 | 1.5 | |
| XNBR curative (Table II) | 6 | - | |
| MC sulfur | 0.5 | 0.5 | |
| Viscosity (ML- 1 + 4' at 100°C) | 51 | 50 | |
| Mooney scorch (t5 at 125°C) | 25.0 | 14.0 | |
| | | | Specification (1) |
| Modulus at 200% elong. (MPa) | 7.9 | 6.6 | 4.83 min. |
| Tensile strength (MPa) | 21.0 | 16.5 | 16.56 min. |
| Elongation at break (%) | 530 | 450 | 300 min. |
| Tear strength, Die C (kN/m) | 13 | 5 | 7.04 min. |
| Set, IPCEA (%) | 9 | 5 | 30 max. |
| NBS abrasion (%) | 245 | 186 | --- |
| Brittle point (°C) | -46 | -56 | --- |
| Aged in Air Bomb, 0.55 MPa, 20 h at 127°C | | | |
| Tensile strength (% retained) | 97 | 100 | 50 min. |
| Elongation at break (% retained) | 62 | 80 | 50 min. |
| Aged in Oxygen Bomb, 2.1 MPa, 168 h at 80°C | | | |
| Tensile strength (% retained) | 97 | 100 | 50 min. |
| Elongation at break (% retained) | 81 | 78 | 50 min. |
| Aged in ASTM Oil #2, 18 h at 121°C | | | |
| Tensile strength (% retained) | 110 | 118 | 60 min. |
| Elongation at break (% retained) | 75 | 96 | 60 min. |

*70/30 rubber/PVC, 90 Mooney, Table I
**70/30 rubber PVC, rubber ACN-26%, rubber Mooney - 65

(1) IPCEA S-19-81, NEMA WC 3, 7.6.20.1.3

TABLE X. EXTRA-HEAVY-DUTY JACKET - BLACK, LEAD CURE

| | | | |
|---|---|---|---|
| XNBR/PVC fluxed blend* | 100 | - | |
| NBR/PVC fluxed blend** | - | 100 | |
| Naugard 445 | 3 | 3 | |
| Antimony trioxide | 5 | 5 | |
| HiSil 215 | 21 | 21 | |
| Mistron Vapor | 10 | 10 | |
| N-326 (HAF-LS) black | 25 | 25 | |
| Dioctyl phthalate | 9 | 9 | |
| Dioctyl adipate | 10 | 10 | |
| Paraplex G-54 | 10 | 10 | |
| Stearic acid | 0.5 | 0.5 | |
| Zinc oxide | - | 3 | |
| MBTS | 2 | 2 | |
| Sulfasan R | 2 | 2 | |
| TMTD | 1.5 | 1.5 | |
| XNBR curative (Table II) | 6 | - | |
| Viscosity (ML - 1+4' at 100°C) | 49 | 56 | |
| Scorch time ($t_5$ at 125°C) | 10.5 | 12.0 | |
| | | | Specification (1) |
| Modulus at 200% elong. (MPa) | 8.1 | 6.6 | 4.83 min. |
| Tensile strength (MPa) | 18.5 | 17.3 | 16.56 min. |
| Elongation at break (%) | 510 | 490 | 300 min. |
| Tear strength, Die C (kN/m) | 19 | 12 | 7.04 min. |
| Set, IPCEA (%) | 11 | 7 | 30 max. |
| NBS abrasion (%) | 104 | 86 | -- |
| Brittle point (°C) | -36 | -41 | -- |
| Aged in Air Bomb, 0.55 MPa, 20 h at 127°C | | | |
| Tensile strength (% retained) | 105 | 94 | 50 min. |
| Elongation at break (% retained) | 61 | 71 | 50 min. |
| Aged in Oxygen Bomb, 2.1 MPa, 168 h at 80°C | | | |
| Tensile strength (% retained) | 105 | 90 | 50 min. |
| Elongation at break (% retained) | 73 | 78 | 50 min. |
| Aged in ASTM Oil #2, 18 h at 121°C | | | |
| Tensile strength (% retained) | 105 | 104 | 60 min. |
| Elongation at break (% retained) | 75 | 88 | 60 min. |

*70/30 rubber/PVC, 90 Mooney
**75/25 rubber/PVC, rubber ACN content 26%, rubber Mooney -65

(1) IPCEA S-19-81, NEMA WC 3, 7.6.20.1.3

# Comparison of the Relative Cost Effectiveness of Brominated and Chlorinated Flame Retardants in EPDM

*Joseph M. Lesniewski*

Saytech Inc., Division of Ethyl Corporation
East Brunswick, New Jersey

## Abstract

The usefulness of flame retarded EPDM for wire and cable applications has been presented. These presentations demonstrate the merits of the compound when either a chlorinated or brominated additive is incorporated as a flame retardant agent. Generally, those demonstrations are based on equal weight substitution of the chlorinated or brominated flame retardant agent into a standard formula. This paper attempts to illustrate the relative effectiveness of the fire retardant agents. Relative cost comparisons as well as relative flame resistance of the diadduct of hexachlorocyclopentadiene and cyclooctadiene or an imide of tetrabromcphthalic anhydride is made. The flame test portion of the UL-44 standard is used to obtain the relative effectiveness of the additives as fire retardants.

## Introduction

An alicyclic chlorinated flame retardant, the Diels-Alder diadduct of hexachlorocyclopentadiene and cyclooctadiene, and a brominated flame retardant, an imide of tetrabromophthalic anhydride, have been shown to give the desired combination of good physical properties, VW-1 type flame performance, stable wet electricals, heat resistance and acceptable cost in EPDM wire and cable compounds. Evaluation had been performed by direct weight substitution of one flame retardant for the other in a standard formula.[1] Since it is generally accepted that I>Br>Cl>F in the flame retardant efficiencies, a survey of the standard compound using lower amounts of flame retardant appeared warranted. A series of compounds were prepared, each incorporating smaller amounts of either the chlorinated or brominated flame retardant. The object is to evaluate the effects that reduction has on the fire resistance, physical properties and cost of the final product. The polymer to additive ratio of the standard compound was maintained by either adding make up EPDM and/or calcined clay, the major filler in the formula. That was necessary not only because of the removal of the fire retardant component, but in order to insure the best opportunity for the best dispersion, certain of the ingredients were added in masterbatch form. In addition to the flame retardant ingredients (halogen and antimony oxide) the dibasic lead phthlate, peroxide, and antioxidant were masterbatched.

## Compounding

All compounds were prepared using conventional equipment. A Banbury, with a forty pound capacity, was charged to approximately eighty two percent of its capacity, with all of the ingredients except the peroxide. A five minute cycle was maintained, and drop temperatures kept below 290°F (143°C). The drop was then passed onto a mill, sheeted and strained through an extruder containing a twenty-two mesh screen package. The strained material was then recharged to the Banbury, along with the peroxide masterbatch. A three minute Banbury cycle was maintained, and the drop temperature was kept below 250°F (121°C). The drop was then sheeted from a mill in ribbon form. That ribbon was then fed to an extruder with an L/D of 20/1, and forty-five mils in insulation was placed on 14 awg solid copper wire and crosslinked in the CV tube. Temperature in the extruder and screw rpm were maintained to assure proper processing (seventy-five fpm at 240°F (116°C).

All compounds were subjected to the same extrusion temperatures and rates necessary to prepare the forty five mils insulation. Good adhesion was obtained, and all ran exceptionally well. Approximately one thousand feet of wire was prepared from each compound.

## Formulation

The "standard" formula used as the base from which all flame evaluations were made is the Revised NDX 5117. The flame retardant component of the formula was removed in discrete amounts until seventy percent of the original remained. Specific formula contain either a 0%, 10%, 15% or 20% removal of the fire retarding agents and in one instance for the imide (bromine) a thirty percent removal was made. The total part loading was maintained by adding EPDM and calcined clay. (Table XI)

Table I

Concentrate Compositions

80% Dibasic lead phthalate on EPDM
40% Dicumyl peroxide on EPDM

Flame Retardant Concentrates

60% Flame Retardant
20% Antimony Oxide
20% EPDM

Table II

Revised NDX 5117 (2)

| Ingredient | Wt. Parts |
|---|---|
| EPDM | 80.0 |
| Low Density polyethylene | 20.0 |
| Dibasic lead phthlate | 4.0 |
| Oligemeric 2,2,4-trimethyl-1,2 dihydroquinoline | 1.0 |
| Calcined Clay | 65.0 |
| Vinylsilane | 1.5 |
| Dicumyl peroxide | 4.0 |
| 2:1 Complex of Alkylated Phenol Phosphonate with Nickel | 0.7 |
| Halogenated FR | 30.0 |
| Antimony Oxide | 10.0 |

## Physical Properties

Tensile strength and elongation data were obtained from the cured insulation. This illustrates the reinforcing characteristic of the imide of tetrabromophthalic anhydride. Modulus at 200% is higher and elongation slightly lower. Tensile strength for each set of comparable loadings of flame retardant are essentially equivalent with the exception of those formula which contain twenty percent less than the standard amount of flame retardant. Here, the formula containing the brominated flame retardants starts to indicate higher tensile strength than the counterpart formula containing the chlorinated flame retardant. Similar results were obtained from samples of each compound when cured in a press for forty minutes at 355°F(177°C).

Table III

Physical Properties (Diadduct Variation)

| % Removal of FR | 0 | 10 | 15 | 20 |
|---|---|---|---|---|
| Tensile psi | 1628 | 1623 | 1702 | 1658 |
| Elongation % | 360 | 297 | 353 | 317 |
| $M_{200}$ | 1213 | 1347 | 1337 | 1406 |

Table IV

Physical Properties (Imide Variation)

| % Removal of FR | 0 | 10 | 15 | 20 | 30 |
|---|---|---|---|---|---|
| Tensile psi | 1692 | 1776 | 1618 | 1810 | 1917 |
| Elongation % | 260 | 220 | 257 | 353 | 183 |
| $M_{200}$ | 1515 | 1663 | 1461 | 1728 | - |

Rheometer cure studies were also performed for each compound. Results indicate comparable scorch times, higher stiffness and a slightly higher cure rate for the brominated flame retarded compounds.

Table V

Rheometer Cure Study at 177°C
(Diadduct Variation)

| | (4) | (3) | (2) | (1) |
|---|---|---|---|---|
| % Removal of FR | 0 | 10 | 15 | 20 |
| Min. Torque | 10 | 10 | 10 | 10 |
| Scorch-Sec. | 60 | 60 | 60 | 60 |
| Cure Angle ° | 37 | 39 | 39 | 39 |
| 10' Max. Torque | 100 | 104 | 108 | 110 |

Table VI

Rheometer Cure Study at 117°C
(Imide Variation)

| | (8) | (7) | (6) | (5) | (9) |
|---|---|---|---|---|---|
| % Removal of FR | 0 | 10 | 15 | 20 | 30 |
| Min. Torque | 10 | 10 | 10 | 10 | 12 |
| Scorch-Sec. | 45 | 55 | 55 | 55 | 45 |
| Cure Angle ° | 47 | 47 | 44 | 44 | 60 |
| 10' Max. Torque | 128 | 124 | 122 | 124 | 176 |

## Flame Tests

Oxygen Index, UL-94 and VW-1 type fire tests were performed for each formula. Part of the ribbon stock used to fabricate the wire was cured in a press to the suitable thickness for the UL-94 and oxygen index tests (1/8 inch). The VW-1 type fire test (FR-1) was performed on the wire with 45 mils of insulation. Results from the UL-94 test indicate that only the standard formula and the one with 10% removal of the imide of tetrabromphthalic anhydride obtain a 94-VO rating. The formula containing the diadduct burned under UL-94 testing. Ratings from the oxygen index test clearly indicate a better response from the imide of tetrabromophthalic anhydride than the chlorinated flame retardant in all formulations.

Table VII

Flame Test Results
(Diadduct Variation)

| % Removal FR | 0 | 10 | 15 | 20 |
|---|---|---|---|---|
| Oxygen Index | 27.8 | 27.8 | 27.2 | 27.2 |
| UL-94 | Burn | Burn | Burn | Burn |
| FR-1 (wire) | Pass | Fail | Fail | Fail |

Table VIII

Flame Test Results
(Imide Variation)

| % Removal FR | 0 | 10 | 15 | 20 | 30 |
|---|---|---|---|---|---|
| Oxygen Index | 31.6 | 29.5 | 28.9 | 28.9 | 29.9 |
| UL-94 | 94VO | 94VO | Burn | Burn | Burn |
| FR-1 (wire) | Pass | - | Pass | Pass | Fail |

Since oxygen index and UL-94 tests do not take into account the geometry of the wire, VW-1 type tests were performed on the extruded insulation on wire. Samples of wire, 45 mils on 14 awg wire, were subjected to testing. The VW-1 tests were performed at Saytech Incorporated's Laboratory in East Brunswick, New Jersey and verified by the Underwriter's Laboratory at Melville, Long Island, New York. Those results illustrate the efficiency of the imide of tetrabromophthalic anhydride over the chlorinated flame retardant. The results strongly indicate that the standard loading for the diadduct of hexachlorocyclopentadiene and cyclooctadiene is at its optimum loading for this system and that a further lowering results in failure of the VW-1 test.

The amount of the imide of tetrabromophthalic anhydride may be lowered by twenty percent, perhaps even by twenty-five percent, before the system will fail the VW-1.

## Cost Evaluation

The cost of each compound was calculated to determine the cost per pound and pound volume value. It is pointed out that the original formulae containing the diadduct (chlorine) and the imide (bromine) have cost per pound values which differ by 0.7 cents ($1.166 vs. $1.159), but their pound volume cost differs by 4 cents ($1.511 vs. $1.551). Since the flame test and other testing indicate that a twenty percent removal of the imide flame retardant component still performs satisfactorily, its values become a valid indicator of the savings one may obtain. By removing twenty percent of the imide flame retardant component, a 10.9 cents per pound and 10 cents per pound volume may be obtained. This, or course, translates to more wire insulation at lower cost.

Table IX

Cost Comparison of
Flame Retarded Formula

| Cost/lb. $ | 1.166 | 1.159 | 1.108 | 1.082 | 1.057 | 1.016 |
|---|---|---|---|---|---|---|
| Spec. Grav. | 1.296 | 1.338 | 1.336 | 1.335 | 1.334 | 1.332 |
| Lb-Volume $ | 1.511 | 1.551 | 1.480 | 1.445 | 1.410 | 1.353 |
| % Rem. FR | * | 0 | 10 | 15 | 20 | 30 |

*Diadduct all others based on imide

Table X

Ingredient Cost 8/80

| | Price/lb. | Sp. Gr. |
|---|---|---|
| EPDM | 0.89 | 0.86 |
| Low Density Polyethylene | 0.49 | 0.92 |
| DiBasic Lead Phthalate(Conc) | 1.57 | 2.40 |
| Oligemeric 2,2,4 trimethyl-1,2 dihydroquinoline | 1.45 | 1.06 |
| Calcined Clay | 0.1375 | 2.63 |
| Vinylsilane | 3.75 | 1.04 |
| DiCumyl Peroxide (Conc) | 2.97 | 1.05 |
| 2:1 Complex of Alkyated Phenol Phosphonate with Nickel | 7.15 | 1.30 |
| Diadduct/$Sb_2O_3$ (Conc) | 2.59 | 1.68 |
| Imide/$Sb_2O_3$ (Conc) | 2.56 | 2.05 |

Table XI

Variation of the Flame Retardant Components

| | | | | | | | | | | | | | |
|---|---|---|---|---|---|---|---|---|---|---|---|---|---|
| EPDM | 70.0 | 70.0 | 71.0 | 71.0 | 71.5 | 71.5 | 72.0 | 72.0 | 73.0 | | | | |
| Low Density Polyethylene | 20.0 | 20.0 | 20.0 | 20.0 | 20.0 | 20.0 | 20.0 | 20.0 | 20.0 | | | | |
| Dibasic lead phthalate conc. | 5.0 | 5.0 | 5.0 | 5.0 | 5.0 | 5.0 | 5.0 | 5.0 | 5.0 | | | | |
| Oligeneric 2,2,4-trimethyl 1,2 dihydroquinoline | 1.0 | 1.0 | 1.0 | 1.0 | 1.0 | 1.0 | 1.0 | 1.0 | 1.0 | | | | |
| Calcined Clay | 65.0 | 65.0 | 69.0 | 69.0 | 71.0 | 71.0 | 73.0 | 73.0 | 77.0 | | | | |
| Vinyl Silane | 1.5 | 1.5 | 1.5 | 1.5 | 1.5 | 1.5 | 1.5 | 1.5 | 1.5 | | | | |
| Dicumyl peroxide conc. | 10.0 | 10.0 | 10.0 | 10.0 | 10.0 | 10.0 | 10.0 | 10.0 | 10.0 | | | | |
| 2:1 Complex of alkylated phenol phosphonate with Nichel | | | | | | | | | | | | | |
| Brominated FR conc. containing $Sb_2O_3$ | 50.0 | - | 45.0 | - | 42.5 | - | 40.0 | - | 35.0 | | | | |
| Chlorinated FR conc. containing $Sb_2O_3$ | - | 50.0 | - | 45.0 | - | 42.5 | - | 40.0 | - | | | | |
| % Removal of FR agent | 0 | 0 | 10 | 10 | 15 | 15 | 20 | 20 | 20 | | | | |

## Conclusions

The effectiveness of the imide of tetrabromophthalic anhydride over the diadduct of hexachlorocyclopentadiene and cyclooctadine is advantageous in producing compounds with acceptable physical properties and superior flame resistance. Formula based on that effectiveness overcome the higher specific gravity of the brominated compound and yield higher pound volume savings without sacrificing the flame resistant requirements.

## Acknowledgements

The author wishes to express his thanks to the personnel of Triangle PWC, Inc. and Wyrough and Loser, Inc. for their assistance in preparing the compounds and for providing the physical test data.

## References

(1) V.I. Vaidya, "Flame Retarded EPDM Integral Insulation Jacket Composition with Excellent Heat Resistance and Electrical Stability" 114th Meeting of the Rubber Division of the American Chemical Society, Boston, Oct. 1978

(2) Source E. I. du Pont de Nemours & Co., Inc.

# PERFLUOROALKOXY FLUOROCARBON RESIN PROPERTIES RELATING TO ELECTRICAL AND ELECTRONIC APPLICATIONS

M. I. BRO, D. I. MC CANE, D. B. ALLEN, AND J. C. REED

E. I. DU PONT DE NEMOURS

A review of the properties of perfluoroalkoxy fluorocarbon resin as they pertain to the electrical and electronics industry is presented.

Thermal exposure of wire insulation of perfluoroalkoxy fluorocarbon resin (PFA) at 285°C (545°F) for 20,000 hours in air produced no deterioration in the electrical, physical, or mechanical properties measured.

This unusual behavior, at temperatures only 15°C below the melt temperature of the resin, could not be adapted to the usual Arrhenius relationship commonly used to determine a temperature rating for the continuous use of such materials.

In light of the test data presented, it is proposed that Teflon® perfluoroalkoxy fluorocarbon resin insulations can be used continuously at 285°C and that the product be given such a rating for electrical uses.

## INTRODUCTION

Teflon® PFA fluorocarbon resins represent a combination of mechanical, physical, and electrical properties over a range of temperatures that make them uniquely suitable for a wide variety of electrical and electronic applications. Typical physical and mechanical properties of the two grades of Teflon® PFA resin produced for this application area are shown in Table I.

Teflon® 340 is a general purpose resin designed for melt extrusion on wire and for injection molding where maximum melt flow is required. Teflon® 350 is designed for use in extremes of chemical and thermal environments where maximum resistance to stress is required.

This paper describes those properties which are useful to the engineer in designing components for the electrical and electronic industry. Applications for this material include extruded coatings for hook-up wire, heater cables, heavy wall conduit, jacketing for multiconductor cable, geophysical cables, jacketing for fiber optics, and insulation for aircraft engine wires. It has also been injection molded into electrical switch components, connector inserts, insulating bushings and standoff insulators

## THE DIELECTRIC CONSTANT

The dielectric constant of Teflon® PFA fluorocarbon resins is approximately 2 over a wide range of frequencies, temperatures and densities. The minor changes which occur with changes in these conditions are shown in Figure 1. The values for density of Teflon® PFA vary only slightly, 2.13-2.17, and the dielectric constant varies about 0.03 units over this range, among the lowest of all solid materials. There is no measurable effect of humidity on the dielectric constant of PFA.

FIGURE I

*DIELECTRIC CONSTANT OF TEFLON® PFA FLUOROCARBON RESINS AT VARIOUS FREQUENCIES AND TEMPERATURES (BY ASTM D-150)*

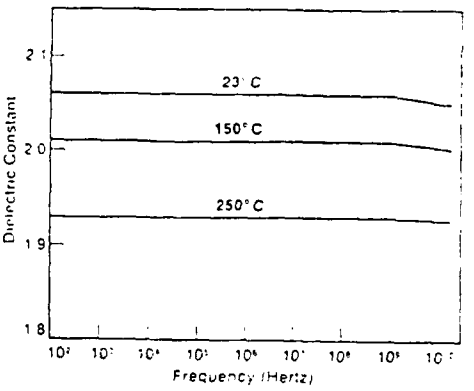


TABLE I

TYPICAL PROPERTIES OF TEFLON® PFA

| Property | ASTM Method | Teflon® 340 | Teflon® 350 |
|---|---|---|---|
| Nominal Melting Point, °C(°F) | | 302-306<br>(575-590°) | 302-306<br>(575-590°) |
| Specific Gravity | | 2.13-2.16 | 2.13-2.16 |
| Melt Flow Rate, Gms/10 min. | D-3307 | 11.0 | 2.0 |
| Tensile Strength | D-1708 | | |
| Megapascals 23°C(73°F) | | 28 | 31 |
| (lbs./sq. in.) | | (4000) | (4500) |
| 250°C (482°F) | | 12 | 14 |
| | | (1800) | (2000) |
| Tensile Yield | D-1708 | | |
| Megapascals 23°C (73°F) | | 14 | 15 |
| (lbs./sq. in.) | | (2000) | (2200) |
| 250°C (482°F) | | 3 | 4 |
| | | (500) | (600) |
| Ultimate Elongation | D-1708 | | |
| 23°C (73°F) | | 300 | 300 |
| 250°C (482°F) | | 480 | 500 |
| Flexural Modulus | D-790 | | |
| Megapascals 23°C (73°F) | | 655 | 689 |
| (lbs./sq. in.) | | (95,000) | (100,000) |
| 250°C (482°F) | | 58 | 70 |
| | | (8000) | (10,000) |
| Creep Resistance* | D-695 | | |
| Tensile Modulus | | | |
| Megapascals RT | | 276 | 276 |
| (lbs./sq. in.) | | (40,000) | (40,000) |
| 250° C (482°F) | | 41 | 41 |
| | | (6000) | (6000) |
| Hardness Durometer | D-2240 | D-60 | D-60 |
| MIT Folding Endurance Cycles (7-8 mils) | | 50,000 | 500,000 |
| Water Absorp., % | D-570 | 0.03 | 0.03 |
| Coefficient of Linear Thermal Expansion | D-696 | | |
| M/M-Kelvin, 20°C-100°C (70°F-212°F) | | $1.2 \times 10^{-5}$ | $1.2 \times 10^{-5}$ |
| (in./in./°F) | | $(6.7 \times 10^{-5})$ | $(6.7 \times 10^{-5})$ |
| 100°C-150°C (212°F-300°F) | | $1.7 \times 10^{-5}$ | $1.7 \times 10^{-5}$ |
| (in./in./°F) | | $(9.4 \times 10^{-5})$ | $(9.4 \times 10^{-5})$ |
| 150°C-210°C (300°F-408°F) | | $2.0 \times 10^{-5}$ | $2.0 \times 10^{-5}$ |
| (in./in./°F) | | $(11.1 \times 10^{-5})$ | $(11.1 \times 10^{-5})$ |

*10 hour apparent modulus stress = 7 MPa (1000 psi) at RT, 07 MPa (100 psi) at 250°C (482°F)

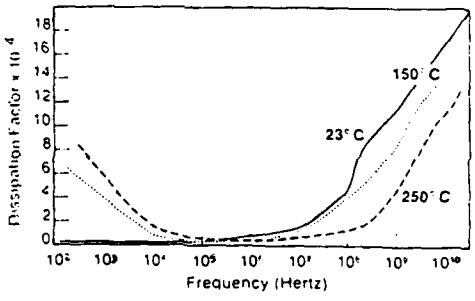
## DISSIPATION FACTOR

The dissipation factor of PFA varies with frequency and temperature. This is shown in Figure 2.

The dissipation factor at low frequency ($10^2$ - $10^4$ Hertz) increases at higher temperatures. It has been suggested that this observed increase is due ionic impurities present in the resin. Little difference is seen in dissipation factor with temperature in the range of $10^4$ - $10^7$ Hertz.) At higher frequencies to $10^{10}$ Hertz, there is a steady increase in dissipation factor with increasing frequency. Increases are greatest when measured at room temperature. There is also an indication that a maximum exists at about 3 x $10^9$ Hertz. This higher dissipation factor with increasing frequency may preclude the use of this product as a core material for coaxial cable which operates at radar frequencies.

FIGURE 2

DISSIPATION FACTOR OF TEFLON® PFA FLUOROCARBON RESIN AT VARIOUS FREQUENCIES AND TEMPERATURES (BY ASTM D-150)




## ELECTRICAL RESISTIVITY OF TEFLON® PFA

The volume and surface resistivities of fluorocarbon resins are high and are unaffected by time or temperature. Measurements of the volume resistivity of Teflon® PFA by the method outlined in ASTM D257 gave a value greater than $10^{18}$ohm-cm. The surface resistivity was greater than $10^{18}$ohm sq.

## ARC TRACKING

When Teflon® PFA was tested by the method described in ASTM-D495 using stainless steel electrodes, no tracking was observed for the duration of the test — i.e. 180 seconds, indicating that the resin does not form a carbonized conducting path. Similar performance was observed when Teflon® FEP or TFE fluorocarbon resins were tested.

## PERFORMANCE IN FIRE SITUATIONS

Teflon® PFA, like FEP and TFE fluorocarbon resin is among the safest of all plastics in fire situations. It passes the U/L83 vertical flame test and is classified 94VE-O according to U/L94. The OI (Oxygen Index) by ASTM-2863 is greater than 95% and the smoke density rating in the NBS smoke chamber is 4.

As in the case of other fluorocarbons, Teflon® PFA contributes little in fuel value in case of exposure to fire. A comparison of fuel values of typical materials is shown below.

TABLE II

FUEL VALUES OF VARIOUS MATERIALS*

| FUELS | HEAT CONTRIBUTED | |
|---|---|---|
| Fuel Oil | 42MJ/kg | (18,000 BTU/lb.) |
| Coal | 23-33MJ/kg | (10-14,000 BTU/lb.) |
| Wood | 19-23MJ/kg | (8-10,000 BTU/lb.) |
| **INSULATING MATERIALS** | | |
| Polyethylene | 47MJ/kg | (20,000 BTU/lb.) |
| PVC | 21-30MJ/kg | (9-13,000 BTU/lb.) |
| Rubber | 23-33MJ/kg | (10-14,000 BTU/lb.) |
| Teflon® | 5MJ/kg | (2,200 BTU/lb.) |

*Per ASTM D-240 and D-2015 heat of combustion

## PERFORMANCE ON PROLONGED THERMAL EXPOSURE

Long-term heat treatment of PFA plaques, tensile bars, and coated wires at 285°C (545°F) indicates that the resin can be used continuously at this temperature without deterioration of its mechanical or electrical properties.

In Figure 3, the change in the tensile strength of wire coatings as measured at room temperature is plotted versus hours of thermal treatments in air at 230°C and 285°C. The tensile strength measured at room temperature of coatings made from Teflon® 340 resin show a gradual increase with time of about 15% after 20,000 hours at 285°C. Similar increases were observed when the tensile measurements were made at 200°C. The room temperature elongation of the tensile specimens increased about 25% with thermal treatment at 285°C as shown in Figure 4.

The increase in tensile properties is attributed to an increase in molecular weight as indicated by a decrease in melt flow as shown in Figure 5. The precise mechanism of the observed increase is not known at present. End-linking of the polymer chains appears to be the predominant reaction since there is no observable increase in melt elasticity as typified by cross-linking of polymer chains to establish a branched structure.

FIGURE 3

TENSILE STRENGTH OF TEFLON® PFA WIRE COATINGS AFTER PROLONGED THERMAL TREATMENT IN AIR

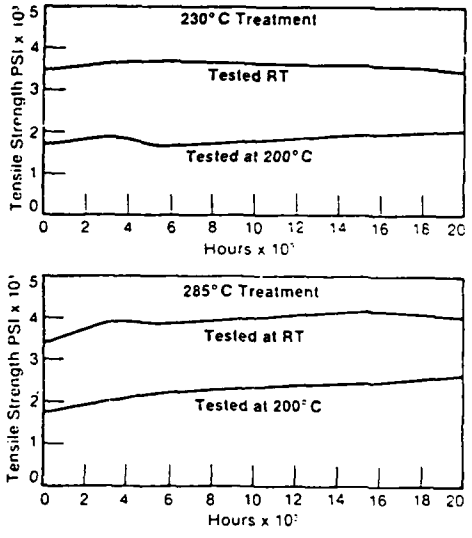



FIGURE 4

TENSILE ELONGATION OF TEFLON® PFA WIRE COATINGS AFTER PROLONGED THERMAL TREATMENT IN AIR

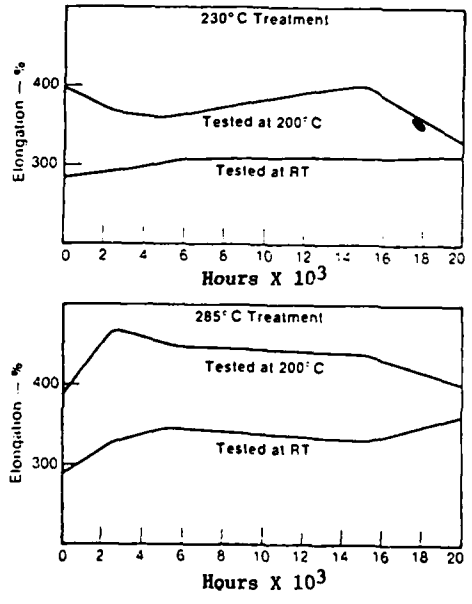
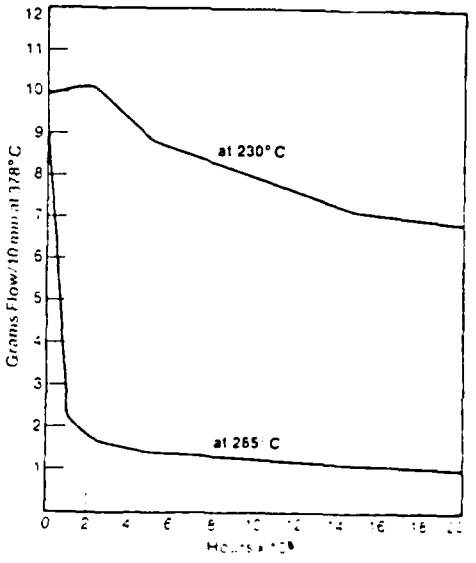



FIGURE 5

CHANGE IN MELT FLOW DURING PROLONGED THERMAL TREATMENT OF TEFLON® PFA FLUOROCARBON RESINS AT 250°C AND 285°C



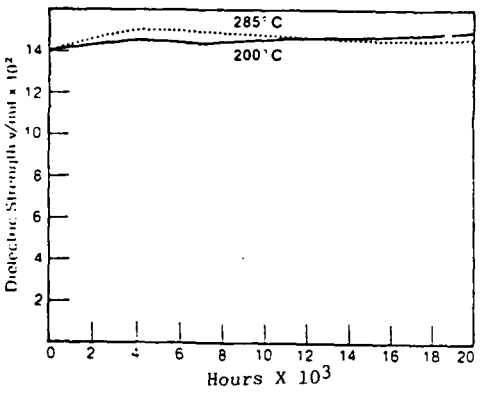

*The intent of the thermal treatment* was to establish a temperature rating for the continuous use of the resin in electrical applications. The method based upon the Arrhenius relationship following the IEEE standard No. 1 Underwriters' uses a temperature at which 50% of a given physical property is retained after 20,000 hours. (Polymeric Materials -- Long Term -- UL-746B).

Temperatures of 230°C (440°F) and 285°C (545°F) were used in early exploratory tests to bracket the temperature range for study. The high temperature is only 15°C below the melting point listed for Teflon® PFA (ASTM-3307-74). It became clear from this work that 285°C had to be the lowest of the four temperatures required for the study test. Since it is impossible, from a practical point of view, to select four test temperatures between 285°C and 302-306°, and considering that PFA is obviously improving in tensile properties at 285°C, this approach toward establishing a continuous use temperature rating was abandoned.

Further tests were performed to identify weaknesses which might preclude the use of this material at these temperatures. Changes in dielectric strength are plotted versus heating time at 285°C in Figure 6. No significant change in dielectric constant was observed. This again is typical of TFE and FEP fluorocarbon resins.

FIGURE 6

CHANGE IN DIELECTRIC STRENGTH OF TEFLON® PFA ON PROLONGED HEATING AT 285°C AND 230°C




THE 1X MANDREL WRAP TEST

A 1X mandrel wrap was employed to gain an insight into the mechanical performance of these wire constructions after prolonged thermal exposure. This severe treatment tests the ability of a wire to withstand bending abuse after prolonged heat exposure. The test is a slight modification of the wrap-back test in MIL Specification 22759. A straight sample of wire is placed in an oven at a specified temperature for three hours; it is then removed and visually inspected for any cracks. If crack-free, the sample is wrapped on itself (1X) and replaced in the oven for three hours. The sample is removed and visually inspected for cracks. If crack-free, the wrapped sample is soaked in salt water for at least four hours and then tested dielectrically at 2.5 KV for five minutes. Those samples which survive are unwrapped and again dielectrically tested at 2.5KV for five minutes. The results of such tests are shown in Table III.

TABLE III

1X MANDREL WRAP TEST AFTER 3 HOURS AT 285°C

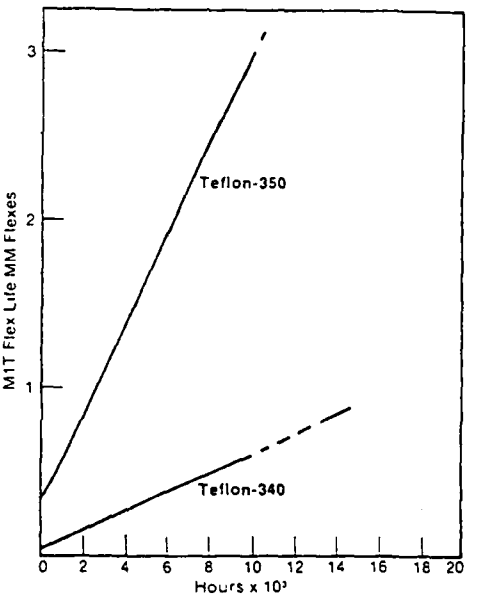
| TIME IN HRS. AT 285°C | NUMBER PASSING TEST | |
|---|---|---|
| | WRAP | UNWRAP |
| 0 | 3/3 | 0/3 |
| 2.500 | 3/3 | 2/3 |
| 10.000 | 3/3 | 3/3 |
| 20.000 | 3/3 | 3/3 |

The wire specimens passed the wrap portion of the 1X mandrel test at all thermal treatments. While the untreated samples could not pass the unwrap portion of the test, as the thermal treatment progressed, more and more of the specimens passed. This is consistent with the decrease in melt flow number observed, indicating an increase in molecular weight.

It parallels the improvement in flex life observed on thermal treatment shown in Figure 7.

FIGURE 7

CHANGE IN FLEX LIFE OF TEFLON® PFA ON LONG TERM THERMAL TREATMENT




The excellent performance of wires coated with Teflon® PFA on heating at 285°C (15°C below melt temperature) in air for 20,000 hours led to the conclusion that wire constructions coated with this resin should be given a temperature rating of 285°C provided the conductor itself can withstand such thermal environments.

PERFORMANCE OF PIGMENTED WIRE COATINGS OF TEFLON® PFA UNDER PROLONGED THERMAL TREATMENT

As a companion study, pigment-coated wire constructions using six common colors were also submitted to the prolonged heat treatment. The colors were blue, red, green, yellow, orange, and brown. The tensile properties, tensile strength, and elongation increased in a manner consistent with the unpigmented constructions described in Figures 1 and 2. The melt flow numbers decreased as expected. The dielectric strength values showed little difference in performance from the unpigmented samples, showing a decrease as heat treatment was prolonged. A modest improvement was noted in the 1X mandrel test as heat treatment progressed.

The most significant observation was a gradual color fading with time as the test continued. However, all colors were still recognizable after the 20,000 hour test at 285°C in air.

SUMMARY AND CONCLUSIONS

The electrical properties of Teflon® PFA fluorocarbon resins are described in parameters useful to this general field of applications.

The dielectric constant (Ca 2), dielectric strength (2,000 v/mil), surface and volume resistivity ( $>10^{18}$ ohms), arc tracking ( > 180 sec) and flammability (94V-0) are typical of the fluorocarbon resins.

The dissipation factor at room temperature remains essentially constant at 0.00003 from $10^2$ - $10^6$ Hertz and increases gradually to 0.012 at $10^{10}$ Hertz. The dissipation factor varies at elevated temperatures in a similar manner. This may preclude its use as a primary insulation in stringent applications involving radar frequencies.

Thermal treatment at 285°C (545°F) for 20,000 hours caused no deleterious effects on the electrical properties. Indeed, improvements in the tensile properties, flex life, and "mandrel wrap" performance were observed. This was accompanied by an increase in the melt viscosity of the material. The resin did not follow the usual behavior adaptable to an Arrhenius plot. The tests indicate that Teflon® PFA fluorocarbon resin can be used continuously at 285°C as wire insulation, as well as in other electrical applications such as switch components, bushings, and stand-off insulators. Although it is noted that this is only 15°C below its melting point, this is the highest continuous use temperature proposed for any fluorocarbon resin. While the tests performed were prototype constructions. actual use of the resin under these conditions has not been observed in the industry to date.



**MANVILLE I. BRO**

Dr. Bro received his PhD in Organic Chemistry from the State University of Iowa. He joined the Du Pont Company in 1951. He has worked in various technical positions supervising Research and Development of fluorocarbon polymers. His present position as Marketing Programs Manager of new fluoropolymer products involves the analysis of markets and introduction of new, high and low temperature, corrosion resistant polymers with superior electrical properties.



**DONALD I. McCANE**

Dr. McCane received his PhD in Organic Chemistry from the University of Michigan. He joined Du Pont in 1953. He has held various positions in Du Pont Research groups conducting and supervising experiments toward new fluorocarbon polymers. He holds a number of patents in these areas. At present, he is a consultant in Du Pont's Fluoropolymer Products Division providing technical support for their melt fabricable fluoropolymers.



**JOSEPH C. REED**

Mr. Reed received a BSEE and a MS degree from Virginia Polytechnic Institute. He joined the Du Pont Company in 1948 and has worked in various positions in manufacturing and technical operations. He is a member of ASTM Subcommittee on Fluoroplastics and Chairman of the Fluoropolymers Section.



**DAVID B. ALLEN**

Mr. Allen received his BS in chemistry from Georgetown University. He joined Du Pont in 1954 and has been involved in various technical and marketing assignments. His present assignment involves development of new markets and uses for wire and cable made from fluoropolymers. Mr. Allen is a member of the Society of Automotive Engineers, NEMA, Electronics Industry Association and the Underwriters Laboratories Ad Hoc Committee on Large Scale Fire Testing.

# APPLICATION OF SPACER FORMING TECHNIQUE TO COMMUNICATION CABLES

by

S. Yonechi*, H. Horima*, S. Tanaka* and K. Ishihara**

* Sumitomo Electric Industries, Ltd.
1, Taya-cho, Totsuka-ku, Yokohama, 244 Japan

** Ibaraki Electric Communication Laboratory
Nippon Telegraph and Telephone Public Corporation
Tokai, Ibaraki-Ken, 319-11 Japan

Abstract

A new spacer forming technique has been developed. Flat plastic or laminated tapes are formed into V-shaped or U-shaped spacers and then stranded with each other in the stranding process. These spacers can accommodate optical fibers or star quads of insulated copper conductors, or can be used as the insulator of a coaxial core.

The technique was developed for optical cable in order that the spacers might preserve transmission characteristics and protect the optical fibers. It was then studied how to apply this technique to fabrication of coaxial cores and screened pair-type units. In coaxial cores, six V-shaped polyester spacers were used as the insulators between the inner conductor and outer conductor. A screened pair-type unit was formed by stranding five V-shaped spacers of polyester-laminated aluminum tape, and each spacer accommodated a star quad.

All of these cables which adopted the new spacer forming technique had sufficient transmission and mechanical properties, and a considerable number of spacer-type optical cables, in particular, have been put into actual use.

## 1. Introduction

A structure with spacers is supposed to be useful for avoiding microbending and preserving transmission characteristics of optical cables. In many reported cases, optical fibers are embeded in a groove spacer preformed by extrusion before fiber stranding.(1) The fabrication of these cables which use grooved spacers has generally two difficulties: preparation of the spacer, and synchronization between the spacer and fibers.

On the other hand, the spacer described here is constructed simultaneously with the fiber stranding process. Hence, a preformed spacer and special synchronization are not needed, and these advantages make it possible to use a conventional stranding machine. Moreover, this technique has another advantage in that arbitrary stranding pitches can be easily designed as far as the stranding machine permits.

This paper describes the principle of spacer forming, the fabrication of optical cables, and their characteristics. Applications of this technique to coaxial and screened pair-type cables are also described.

## 2. Manufacturing Method (2)

The manufacturing method is shown in Fig. 1. In the stranding process, flat tapes are folded into the desired V-shaped or U-shape spacers by passing the tape through spacer formers located just before the assemblage die, and are then stranded with each other. A rather thick tape is considered to be preferable as the spacer from the point of view of tape forming and mechanical strength of the cable, and the spacer formers play an important role in this technique. The formers should precisely fold the flat tapes into the designated spacer configuration, which corresponds to the slit shape of the spacer formers. That is, V-shaped spacers can be obtained by passing the tape through a narrow rectangular slit, and U-shaped spacers, through a triangular slit. These mechanisms are shown in Fig. 2. The spacer forming tension should be as small as possible and should be almost equal for all of the spacers being stranded simultaneously. Maintaining uniformity in the tension and dimensions of spacers ensures a round, firm cable core. The use of a rotary assemblage die synchronized with the cage of the stranding machine is better than that of an ordinary stationary die, for precise settlement of spacers in the cable core can thus be assured.

After stranding of the spacers, the cable core is wrapped in some tapes. These wrapping

tapes also make the core rigid and tight in this technique. Each compartment defined by spacers can accommodate optical fibers, and also pairs or quads, and the spacers can be used as the insulator of the coaxial core.

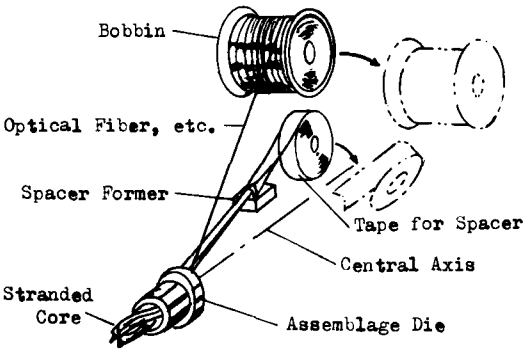



Fig. 1 Manufacturing Method

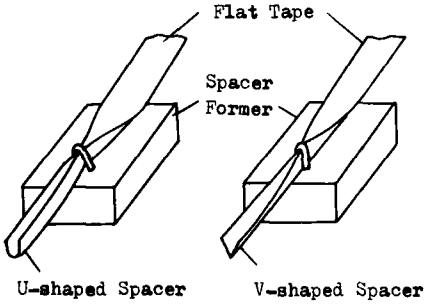



Fig. 2 Spacer Forming Mechanisms

## 3. Optical Cables with Spacers

### 3.1 Cable structure

The new spacer forming technique was first developed for optical cable. In general, lateral forces which arise due to microbending tend to increase the transmission loss of optical fibers.[3] In order to avoid microbending, it is effective to accommodate the optical fibers in the cable in a loosely fitting manner. When the V-shaped or U-shaped spacers are large enough to accommodate optical fibers, the fibers are no longer susceptible to external forces in the cabling processes and installation work.

After various investigations, it became clear that polyester tape with a thickness of 0.075mm to 0.2mm was adequate for the spacers of optical cable. Buckling load of the spacer is calculated by the following equation:

$$P = \frac{\pi^2 E t^3 B}{48 \ell^2}$$

where P : buckling load (kg)
t : thickness of spacer (mm)
E : Young's modulus of spacer ($kg/mm^2$)
l : height of spacer (mm)
B : length of spacer (mm)

Polyester tape possesses a large Young's modulus, about 500 $kg/mm^2$, compared with other plastic tapes, which contributes to increase the buckling load given by the above equation. When two spacers are in contact with each other, as illustrated in Fig. 3, buckling load of 2kg, 8 times as large as that in the case of a single spacer, is derived from the equation. The value is sufficient for the cable core to withstand any lateral force caused throughout the cable manufacturing processes.

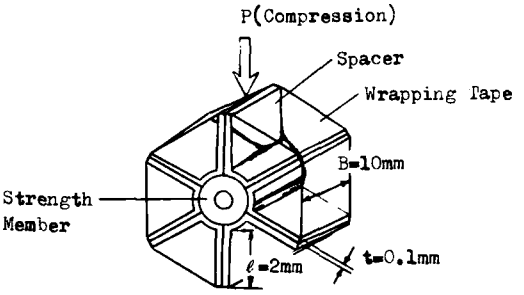



Fig. 3 Compression on Spacer

The typical structures of optical cables with spacers are shown in Fig. 4. The individual fiber can be easily identified by coloring the spacers rather than by employing colored fibers. The spacers accommodating individual fibers are stranded together around the central strength member. By adopting a larger size spacer, several fibers can be accommodated in one spacer. Use of the spacers easily leads to combining optical fibers with copper conductor pairs or quads, which are often included in optical cable, without additional loss increase.[4] Figure 5 shows the structures of various spacer-type optical

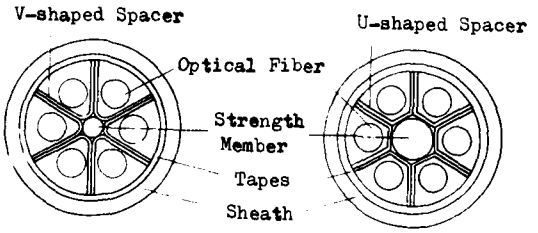
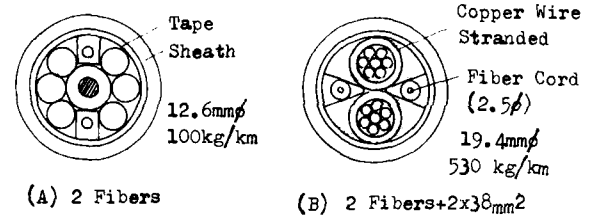
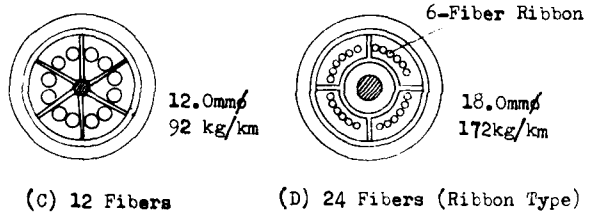



Fig. 4 Typical Structures of Spacer-Type Optical Fiber Cables



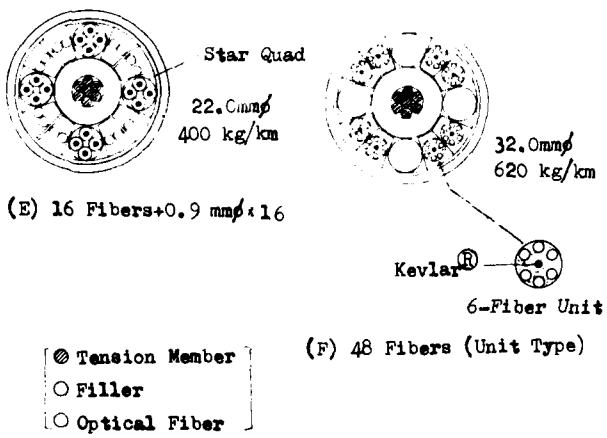




Fig. 5 Various Examples of Spacer-Type Optical Cables

cables. These cables have been put into actual use for optical communication lines at home and abroad.[5][6]

### 3.2 General properties of spacer type optical cable

#### 3.2.1 Transmission properties

In the cabling processes of optical cables, it is most important to conserve the inherent transmission characteristics of the optical fiber. The spacers contribute to making the optical fibers free from microbending. Figure 6 shows the average transmission loss change throughout the cabling processes for the fibers in cables(C) and (F) in Fig. 5, and almost the same results were confirmed for the other optical cables with spacers in Fig. 5. The fibers used had a core diameter of 50 $\mu$m and a cladding diameter of 125 $\mu$m with silica-type graded index profile, and were doubly coated with silicone and nylon.[3] The stability of transmission characteristics is primarily caused by the spacers, which isolate the optical fibers from all external forces.

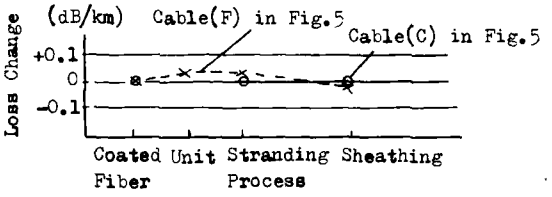



Fig. 6 Loss Change of Fibers in Cabling Processes

#### 3.2.2 Mechanical properties

Table 1 shows the mechanical test conditions for cables (A), (C), and (F) in Fig. 5; no loss change and no fiber break were observed. The deformation of spacer-type optical cables under mechanical forces is generally less than that of non-spacer type optical cables.[7] This effect is the result of the reactional forces yielded by the spacers and of the round, tight structure produced by using spacers to sturdily combine cable elements such as the strength member, wrapping tapes, etc. The results indicate that conventional installation techniques can be satisfactorily used for these optical cables with spacers.

Table 1 Mechanical Test Conditions

| Item / Cable | Tension | Bending | Compression | Impact |
|---|---|---|---|---|
| (A) | 150 kg | R=200mm (R:Bending Radius) 10 times | 100kg / 50mm Width | Weight 0.45kg x Hight 1.0m |
| (C) | 150 kg | R=70mm 10 times | 100kg / 50mm Width | Weight 0.45kg x Hight 1.0m |
| (F) | 1400 kg | R=100mm 10 times | 500kg / 50mm Width | Weight 2.3kg x Hight 0.9m |

3.2.3 Temperature property

The transmission loss of the optical fiber in the spacer also shows stability even when temperature changes. Figure 7 shows the results of transmission loss change versus temperature for cable (C) in Fig. 5. The transmission loss change is less than 0.05dB/km ranging from -40°C to 60°C. This stability depends on the central strength member and the polyester spacer, both of which have coefficients of linear expansion smaller than that of coated fiber.

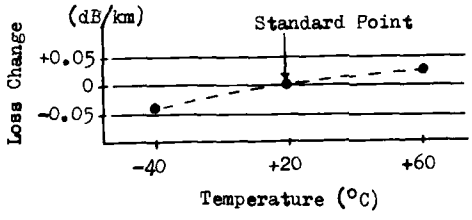



Fig. 7 Loss Change vs. Temperature for Cable (C) in Fig. 5

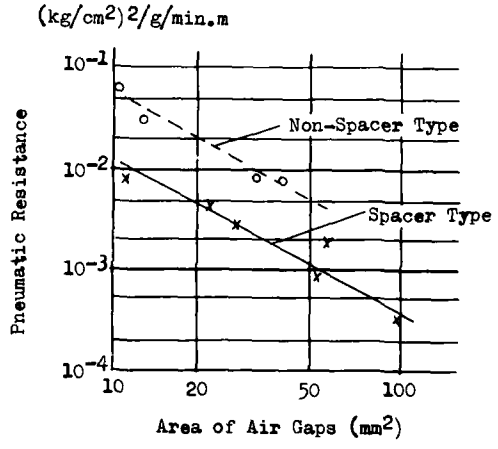



Fig. 8 Pneumatic Resistance vs. Area of Air Gaps

3.2.4 Penumatic property

It has been confirmed that the spacers, by increasing the air gaps in the cable, contribute to decreasing pneumatic resistance. Figure 8 shows the pneumatic resistances measured for fabricated spacer and non-spacer type optical cables.[8] It can be clearly seen that the pneumatic resistance of spacer type optical cable is less than that of non-spacer type even in the case of equal cross-sectional area of gaps in the cable, since the air gaps in individual elements in the spacer type is larger than that in the non-spacer type.

3.2.5 Optical fiber unit with spacers

The fiber units with spacers shown in Fig. 9 were designed and manufactured. They can be easily used for optical cables with a relatively large number of fibers. Their unit structures are summarized in Table 2. The average transmission loss change between fiber coating and unit making was 0.05dB/km and 0.0dB/km for unit (A) and unit (B), respectively.

A compression test using unit (A) was carried out as illustrated in Fig. 10. After the unit was crushed, the optical fiber was pulled out. The tension necessary to remove the fiber was measured by a spring balance; the

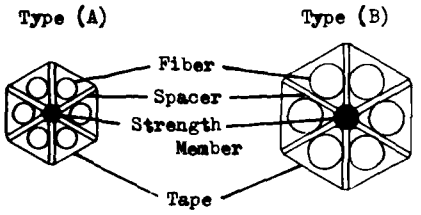



Fig. 9 6-Fiber Units with V-Spacers

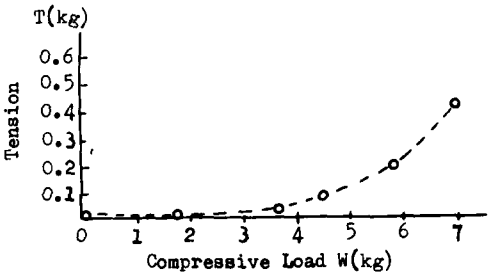



Fig. 11 Results of Compression Test

Table 2 Construction of Units

| Item \ Unit | (A) | (B) |
|---|---|---|
| Fiber | Core : 50 m $\phi$<br>Cladding : 125 m $\phi$<br>Buffer : 350 m $\phi$<br>Silica-Type Graded Index Profile | |
| Jacket of Fiber | Nylon 0.7 mm$\phi$ | Nylon 0.9 mm$\phi$ |
| Strength Member | 0.4 mm$\phi$ steel wire | 1.0 mm$\phi$ steel wire |
| Spacer | Polyester<br>0.075mm(T) x 3.5mm(W) | Polyester<br>0.1mm(T) x 3.5mm(W) |
| Unit Diameter | 3.7 mm$\phi$ | 4.1 mm$\phi$ |

results are shown in Fig. 11. It can be clearly seen that the fiber is not subjected to any compressive stress below a load of 3kg/110mm width. There is no compressive stress left on the fiber even if wrapping tapes are strongly wound. After the unit with spacers is fabricated, it is possible to use the conventional cabling techniques for the unit without any particular need for concern.

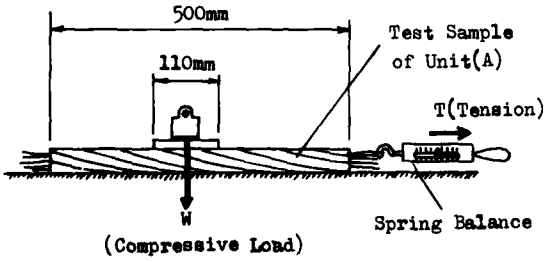



Fig. 10 Compression Test on Unit (A)

Another fiber-pulling test was done for unit (B). The relation between the maximum pulling tension of fiber removal and the length of the sample unit was investigated without lateral compressive load on the unit. From the results in Fig. 12, it can be seen that the fiber can be pulled out when the length of the unit is less than about 10m. Beyond 10m length, the fiber cannot be pulled out without damaging it. It was concluded that the fibers in the unit with spacers are sectionally free and are irremovable when they have longer lengths.

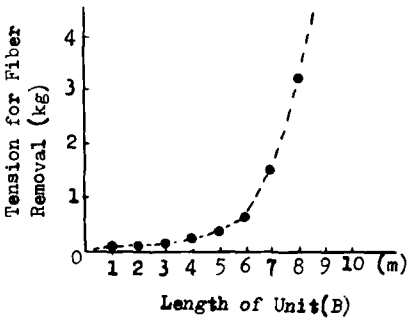



Fig. 12 Results of Fiber Pulling Test

## 4. Coaxial Core with Spacers

Application of the spacer forming technique to coaxial cores was investigated. Polyester spacers were included as the insulator between the inner conductor and outer conductor. The large amount of air included with the spacers was considered to decrease the equivalent dielectric constant of the insulation. Two coaxial cores with different sizes, as shown in Fig. 13 and Table 3, were designed and fabricated. The coaxial cores were fabricated at the same time by stranding six V-shaped polyester spacers around an inner conductor, forming an outer conductor of copper tape, and wrapping in laminated tape. Polyester tape was wound under the outer conductor to make the core tight. By the selection of the spacer stranding pitch, the electrical properties of the coaxial core can be finely controlled, because the lay length affects the volume of polyester contained as the insulator.

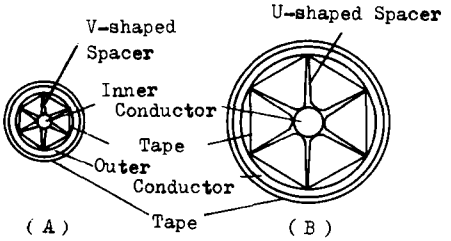



Fig. 13 Structures of Spacer Type Coaxial Cores

Electrical properties of the coaxial cores are given in Table 4. The measured values of capacitance and characteristic impedance were reasonable in view of the values of the equivalent dielectric constant derived from the construction. Attenuation constant versus frequency was measured for both coaxial cores in the range from 10 to 100MHz, as shown in Fig. 14. The structural return loss (SRL) of both coaxial cores was less than 26dB in the frequency region from 10 to 300MHz. Figure 15 shows SRL characteristics of coaxial core (A). This figure indicates good uniformity in the manufacturing process.

Various sizes of coaxial cores with spacers can be easily produced by changing spacer sizes. Moreover, it is possible to insert as many optical fibers as desired into the coaxial core with spacers.

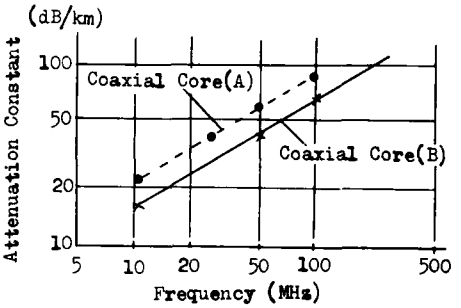



Fig. 14 Attenuation Constant vs. Frequency

Table 3 Construction of Coaxial Cores

| Item \ Type | (A) | (B) |
|---|---|---|
| Inner Conductor | 1.1 mmφ Copper Clad Steel | 2.06 mmφ Copper |
| Spacer (Insulator) | Polyester Tape 0.125mm(T) x 3.5mm(W) | 0.15mm(T) x 8mm(W) |
| Wrapping Tape of Spacer | 0.025mm Thickness Polyester | 0.025mm Thickness Polyester |
| Outer Conductor | Copper Tape 0.15mm(T) x 16mm(W) | Copper Tape 0.085mm(T) x 30mm(W) |
| Wrapping Tape of Core | Polyester (T:0.025mm) Laminated Aluminum (T:0.02mm) | Polyester (T:0.025mm) Laminated Aluminum (T:0.02mm) |
| Outer Diameter | 5.0 mmφ | 10 mmφ |

Table 4 Electrical Properties of Coaxial Cores

| Item \ Type | | (A) | (B) |
|---|---|---|---|
| Insulation Resistance | | 825 kMΩ•km | 1400 kMΩ•km |
| Dielectric Strength | | Insulation capable of withstanding for 1 minute DC test potential of 2000 V | |
| Conductor Resistance | Inner | 56.29 Ω/km | 5.06 Ω/km |
| | Outer | 7.42 Ω/km | 6.18 Ω/km |
| Capacitance | | 57.68 nF/km | 51.11 nF/km |
| Characteristic Impedance | | 70.8 Ω | 75.5 Ω |
| Attenuation Constant (at 10 MHz) | | 22.4 dB/km | 16.2 dB/km |

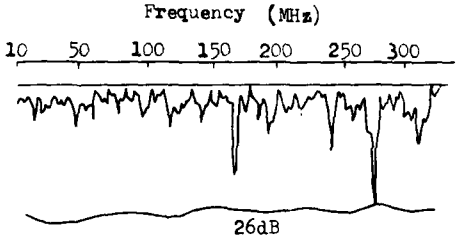



Fig. 15 Structural Return Loss of Core (A)

5. Screened Pair-type Unit with Spacers

V-shaped or U-shaped spacers with metal can also be used as a screen of electromegnetic field. Polyester-laminated aluminum tape is suitable for this purpose. The structures of screened units with spacers are shown in Fig. 16 and Table 4. Five star quads and spacers were assembled with each other in an assemblage die, and then were wrapped in laminated tapes by a stranding machine without injuring the quads. Thus the quads were almost screened mutually regarding electromagnetic interferences.

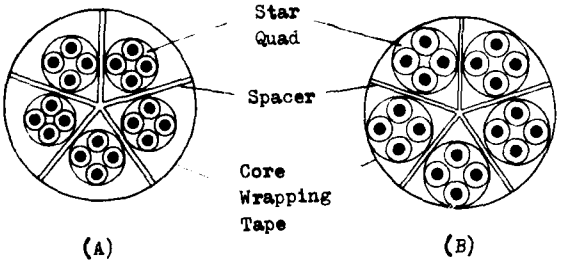



Fig. 16 Structures of Screened Units with Spacers

To clarify the improvement in crosstalk characteristics, far end crosstalk of screened units was measured in the frequency range from 100 KHz to 5 MHz together with that of non-screened units having no spacers. The results are shown in Fig. 17. The improvement of crosstalk characteristics was simply accomplished by using the spacer forming technique without any increase in the cabling process. When designed like unit (B), the unit diameter is almost equal to that of non-screened units.

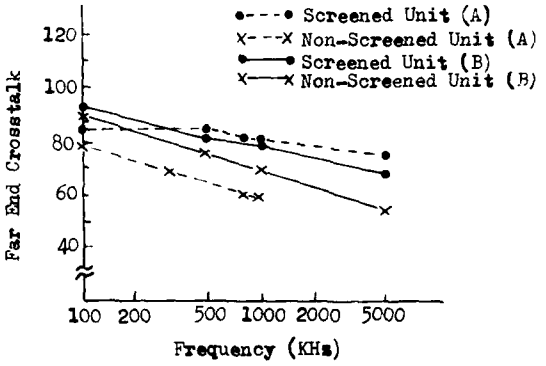



Fig. 17 Frequency Property of Far End Crosstalk within Unit

6. Complete Spacer-type Composite Cable

Optical fiber units of type (A) in Fig. 9, coaxial cores of type (A) in Fig. 13, and screened units of type (A) in Fig. 16 were assembled together by a conventional large-size stranding machine, and then were commonly sheathed as a complete spacer-type composite cable. Figure 18 shows the cross-sectional structure of the cable. Transmission loss of the fibers was almost un-

Table 5 Construction of Screened Units

| Item \ Type | (A) | (B) |
|---|---|---|
| Conductor Diameter | 0.5mm | 0.65mm |
| Insulation Diameter | 0.74mm | 1.20mm |
| Blowing Degree | 20% | 30% |
| Spacer | Polyester (T: 0.1 mm) Laminated Aluminum Tape (T:0.025mm) | Polyester (T: 0.1 mm) Laminated Aluminum Tape (T:0.025 mm) |
| Core Wrapping Tape | Polyester (T:0.025mm) Laminated Aluminum Tape (T: 0.02mm) | Polyester (T:0.025mm ) Laminated Aluminum Tape (T: 0.02mm ) |
| Unit Diameter | 9mm | 9mm |

changed throughout the cabling processes, as shown in Fig. 19, and electrical characteristics of coaxial cores and screened units were also stable. From this, the mechanical properties of each core were considered to be strong enough to withstand the considerable mechanical loads imposed on each core by the stranding and taking up operations. A general view of the composite cable is shown in Fig. 20.

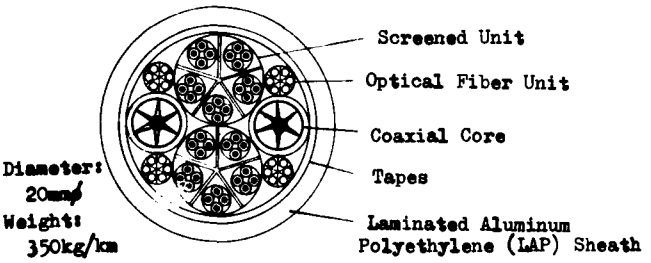



Fig. 18 Structure of Composite Cable

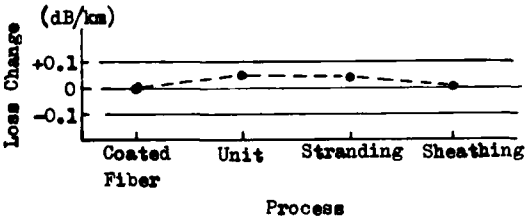



Fig. 19 Loss Change of Fibers in the Cabling Processes

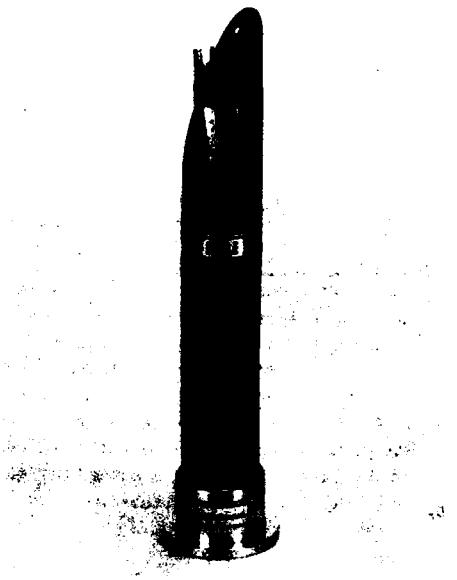


Fig. 20 General View of Composite Cable

## 7. Conclusion

Various kinds of optical cables utilizing the spacer forming technique were manufactured. These optical cables with spacers have excellent transmission and mechanical properties and have put into actual use at home and abroad.

By using this forming technique, it was seen that coaxial cables and screened pair-type cables could be easily manufactured and had outstanding electrical properties.

This technology will be further developed in the future to increase the range of applications.

Acknowledgements

The authors wish to thank Dr. N. Uchida of Ibaraki Electrical Communication Laboratory of N.T.T. and M. Hoshikawa and Y. Kameo of Sumitomo Electric Industries, Ltd. for their helpful comments and suggestions.

References

(1) T.S. Swiecicki, F.D. King, and F.P. Kapron, "UNIT CORE STRUCTURES FOR OPTICAL COMMUNICATION SYSTEMS," 27th I.W.C.S., Nov., 1978.

(2) S. Yonechi, H. Horima, S. Tanaka, and K. Ishihara, "DEVELOPMENT OF SPACER TYPE OPTICAL FIBER CABLES AND THEIR APPLICATION," IECE Japan, CS78-214, March, 1979 (in Japanese).

(3) K. Ishihara, S. Mochizuki, N. Nakatani, N. Uchida, H. Hondo, H. Horima, and S. Sugawara, "Determination of Optimum Structure in Coated Optical Fiber and Cable Unit," The Optical Communication Conference, September, 1979, Amsterdam.

(4) K. Ishihara, M. Tokuda, and S. Seikai, "48-Core Optical Fiber Cable Design and Characteristics," Review of The Electrical Communication Laboratories, Vol. 27, November-December, 1979.

(5) Y. Ohashi, "APPLICATION OF FIBER OPTICS," Proceedings of the 2nd Conference on Fiber Optics and Communications, Chicago, September, 1979.

(6) S. Suzuki, T. Yamanishi, T. Nakahara, K. Aoto, T. Hashimoto, H. Horima, K. Furuta, T. Kadota, H. Kumamaru, and K. Sakamoto, "COMPOSITE CABLE FOR OPTICAL COMMUNICATION AND POWER TRANSMISSION," Proceedings of the 2nd Conference on Fiber Optics and Communications, Chicago, September, 1979.

(7) S. Yonechi, O. Nishi, T. Yamanishi, and T. Toda, "DESIGN AND CHARACTERISTICS OF OPTICAL FIBER CABLE AND JOINT," Proceedings of the 1st Conference of Fiber Optics and Communications, Chicago, September, 1978.

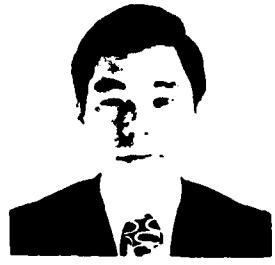
(8) S. Yonechi, S. Tanaka, T. Nakahara, H. Kumamaru, M. Hoshikawa and K. Ishihara, "Characteristics of Optical Fiber Cables with Spacers," Proceeding of the Topical Meeting on Optical Fiber Communication, Washington DC, March, 1979.

AUTHORS



Shin-ichi Yonechi

Shin-ichi Yonechi was born in 1945 and received a B.S. in 1966 from Tohoku University. He joined Sumitomo Electric Industries, Ltd. in 1971, and has been engaged in research and development of communication cables. He is Engineer in Optical Fiber Cable Department, and is a member of the Institute of Electronics and Communication Engineers of Japan.



Shigeru Tanaka

Shigeru Tanaka was born in 1951 and received a M.S. in 1976 from Tokyo University. He joined Sumitomo Electric Industries, Ltd. in 1976, and has been engaged in research and development of optical fiber cable. He is a member of Institute of Electronics and Communication Engineers of Japan.



Hiroaki Horima

Horoaki Horima was born in 1947 and received a M.S. in 1972 from Osaka University.
He joined Sumitomo Electric Industries, Ltd. in 1972, and has been engaged in research and development of multi-pair communication cable, CATV coaxial cable and optical fiber cable.
He is Engineer in Optical Fiber System Department, and is a member of the Institute of Electronics and Communications Engineers of Japan.



Koushi Ishihara

Koushi Ishihara was born in 1943, received a M.S. degree from Yamanashi University in 1969, and joined the Electrical Communication Laboratory in 1969, and has been engaged in research and development of cable structure, and now designing optical fiber cable.
Mr. Ishihara is Assistant Chief of Optical Transmission Line Section in Ibaraki ECL, and a member of the Institute of Electronics and Communication Engineers of Japan.

# MEAN POWER SUM FAR-END CROSSTALK OF PIC CABLES AS A FUNCTION OF AVERAGE TWIST HELIX ANGLE

*J. J. Refi*

Bell Laboratories
Norcross, GA 30071

*ABSTRACT*

The mean power sum far-end crosstalk (FEXT) of the various designs of plastic insulated conductor (PIC) cables used in the Bell System (air core and waterproof, solid and expanded insulations, 19 through 26-gauge, 83 nF/mile and low capacitance) is a function of their average twist helix angle. Cables with small helix angles have stronger crosstalk coupling than cables with large helix angles. Consequently, 26-gauge solid insulation air core cable which has the smallest helix angle of any standard PIC cable also has the strongest (worst) mean FEXT coupling. At the other extreme, 19-gauge solid insulation waterproof cable which has the largest helix angle also has the weakest (best) mean FEXT coupling. The crosstalk spread between these two designs is as much as 6 dB.

Frequency scaling of mean FEXT is also a function of twist helix angle. The dependence, however, is slight—ranging from 5.7 dB per octave of frequency for 26-gauge air core to 6.2 dB per octave for 19-gauge solid insulation waterproof. This is from 0.3 dB less to 0.2 dB more than the classical 6 dB per octave rule.

Equations are presented which can be used to calculate the expected mean power sum FEXT performance of any copper PIC cable used in the Bell System. In addition, as long as pair twist schemes are judiciously chosen, these equations can also be used to predict the crosstalk performance of new cable designs.

## 1. INTRODUCTION

The maximum utilization of digital carrier systems on multipair cable depends to a large degree on the cable's crosstalk performance. Consequently, it has become increasingly desirable to know the crosstalk characteristics of the various cable designs. One way of obtaining this information is by actually measuring crosstalk on each cable design and, in fact, many such measurements have been made. However, knowledge of how crosstalk varies among these designs would allow predictions of not only the crosstalk performance of existing designs which have not been measured, but also of new designs which have yet to be manufactured.

A number of authors have examined the theoretical and practical aspects of modeling crosstalk in multipair cable.[1,2] Such investigations are extremely useful for examining the effect of twist length selection, manufacturing tolerances, and other parameters on crosstalk. The present paper will not attempt to delve into similar analytical detail. Instead, simple empirical data on various Bell System cable designs will be examined and their crosstalk performance related to readily identifiable cable design parameters.

## 2. CROSSTALK MEASUREMENTS

Over the years a number of Bell System cables have been measured for crosstalk on a Computer Operated Transmission Measurement Set (COTMS).[3] Normally, 50 consecutive pairs are connected to a pair fan-out and the 1225 pair-to-pair crosstalk combinations among those pairs measured at a number of frequencies. The power sum crosstalk of a specific pair is then calculated by summing the pair-to-pair couplings into that pair on a power basis. Statistical parameters such as means and standard deviations can then be computed and reported for both the pair-to-pair and the power sum crosstalk distributions.

## 3. CROSSTALK TYPE EXAMINED

The highest bit rate digital carrier systems used on multipair cable (T2[4] and T1C[5]) use power sum crosstalk rather than pair-to-pair crosstalk in the design of their repeatered lines. Consequently, *power sum* crosstalk data were examined. Power sum means were accumulated at five standard measurement frequencies—0.15, 0.772, 1.6, 3.15 and 6.3 MHz. Not all cables were measured at all five frequencies and so the number of measurements in the data base may change with frequency.

Depending on whether unidirectional or bidirectional carrier transmission is employed, either FEXT or NEXT (near end crosstalk) is important. This paper concentrates specifically on mean power sum FEXT.

As mentioned in Section 2, COTMS measurements are normally made on 50 pair groupings. All of the data presented here are therefore for 50 pair groups except for 25 pair cables. In these cases, the data are for all 25 pairs.

## 4. CABLE TYPES EXAMINED

Cable designs in the data base represent almost all standard 83 nF/mile copper PIC cables, i.e., air core and waterproof, solid and DEPIC (dual expanded plastic insulated conductor)[6] insulations, and 19 through 26-gauge conductors. In addition to these standard cables, data were also examined on some "special" cables such as T2 LOCAP* cable (22-gauge DEPIC, 39 nF/mile for air core, and 46 nF/mile for waterproof)[7], ICOT* cable (24-gauge DEPIC, 52 nF/mile for air core, and 60 nF/mile for waterproof)[8], MAT* cable (25-gauge DEPIC, 64 nF/mile, air core)[9], DUCTPIC* cable (26-gauge DEPIC, 83 nF/mile, air core)[10] and an experimental 28-gauge cable (28-gauge solid insulation, 83 nF/mile, air core). These cables are termed "special" because they utilize shorter twist lengths and have a basically different twist spectrum than the standard cables. In addition, T2 LOCAP, ICOT and MAT cables have lower mutual capacitances than the standard 83 nF/mile.

## 5. CORRELATION OF MEAN FEXT WITH DIAMETER OVER DIELECTRIC

### 5.1 Standard Cables

Table 1 shows the number of FEXT measurements† and the average of the power sum FEXT means of each standard cable design at 0.15 MHz.

---

* Trademark of Western Electric.

† The term "measurements" will be used instead of "cables" because several measurements may have been made on different units in a single cable.

**Table 1**
**Number of Measurements and Average of the Power Sum FEXT Means for Standard Cables at 0.15 MHz**

| | air core | | waterproof | | | | | |
|---|---|---|---|---|---|---|---|---|
| | solid | | DEPIC | | solid | | totals | |
| AWG | n | avg(dB/kft) | n | avg(dB/kft) | n | avg(dB/kft) | n | avg(dB/kft) |
| 19 | 0 | - | 2 | 66.4 | 3 | 69.2 | 5 | 68.1 |
| 22 | 7 | 64.9 | 2 | 65.8 | 5 | 66.4 | 14 | 65.6 |
| 24 | 3 | 63.6 | 1 | 64.2 | 4 | 66.2 | 8 | 65.0 |
| 26 | 3 | 62.8 | 1 | 63.4 | 2 | 64.8 | 6 | 63.6 |
| Totals | 13 | 64.1 | 6 | 65.3 | 14 | 66.7 | 33 | 65.4 |

Note from this table that for any particular core/insulation type, crosstalk improves in going vertically from 26 to 19-gauge. Also note that for any particular gauge, crosstalk improves in going horizontally from air core to solid waterproof. Because all of these cables have the same 83 nF/mile mutual capacitance, DOD (diameter over dielectric) increases in moving up the table, and also in moving across the table to the right. Consequently, it appears that crosstalk improves with increasing DOD. To test this possibility, Figure 1 shows a plot of the 33 mean power sum FEXT values vs. DOD. A simple linear regression fit to these values correlates very well (correlation coefficient, $\rho$, =0.875), thereby supporting the hypothesis that crosstalk improves with increasing DOD.

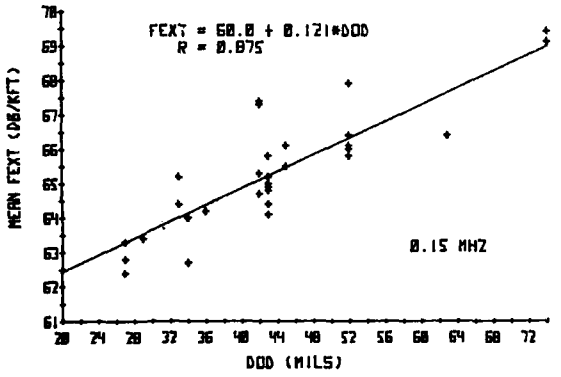



**Figure 1**—Mean power sum FEXT vs. diameter over dielectric (DOD) for 33 standard cable measurements at 0.15 MHz.

### 5.2 Standard and Special Cables

Figure 1 showed that the mean FEXT of standard 83 nF/mile cables correlates strongly with DOD ($\rho$=0.875). As mentioned in Section 4, FEXT data were also examined for a number of "special" cables, viz., T2 LOCAP, ICOT, MAT, and DUCTPIC cables and an experimental 28-gauge cable. Because these special cables have different mutual capacitances and/or twist length schemes than the standard cables, they provide a good basis for testing the validity of DOD as a basic measure of the mean FEXT performance of both standard and "special" cables.

Figure 2 shows the same plot as in Figure 1 but with the addition of several special cables superimposed (crosstalk data were not available at 0.15 MHz for T2 LOCAP cable).

Note from this figure that the FEXT performance of all the special cables (especially MAT and ICOT cable) is better than that predicted by the regression line for the standard cables. Recalling that all of these special cables have shorter twists than the standard cables, perhaps a new parameter which combines the effects of both DOD and twist might be a more suitable independent variable.

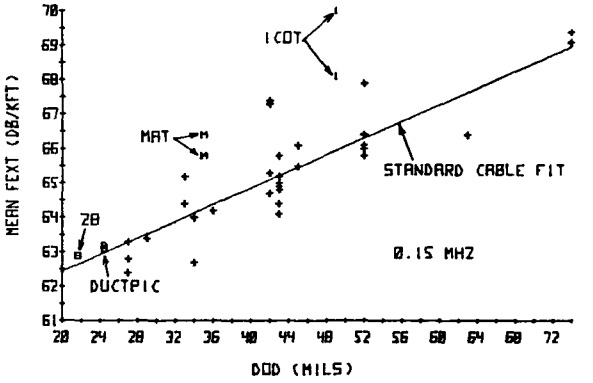



**Figure 2**—Mean power sum FEXT vs. diameter over dielectric (DOD) for 33 standard and 7 "special" cable measurements at 0.15 MHz.

### 6. TWIST HELIX ANGLE

At this point, it is worthwhile to speculate as to why crosstalk should improve as DOD increases.

DOD controls the size of the insulated single, the spacing between the conductors of a pair, and the spacing between pairs in a cable. As the spacing between pairs increases, their coupling decreases and so mean FEXT improves. This explanation, however, oversimplifies the actual situation. Although large DOD's do increase pair separation, they also increase the spacing between the conductors of a pair. This latter effect *increases* coupling. Consequently, two forces are at work—an *interpair* spacing and an *intrapair* spacing—and these forces tend to counteract each other. If the *interpair* spacing effect dominates, then crosstalk should improve as DOD increases and this would explain the observed DOD dependence.

Pair separation is not exclusively a function of DOD. Intuition plus empirical observations indicate that for a given DOD, long twists allow adjacent pairs to get very close to one another whereas short twists force adjacent pairs farther apart. For instance, Figure 3(a) shows that the interaxial distance between two adjacent nontwisted pairs can be as little as DOD. On the other hand, when the pairs are tightly twisted, they tend to circumscribe an imaginary cylinder about them (Figure 3(b)) which keeps the pairs farther apart. A measure of the effectiveness of twist length in keeping pairs separated is the twist helix angle, $\theta$, shown in Figure 4. This figure shows that $\theta$ is proportional to the product of DOD and twist frequency (TF) where TF is the reciprocal of twist length. Consequently, if FEXT improves with increasing DOD because DOD increases pair separation, then since helix angle is a better measure of pair separation, FEXT should correlate even more strongly with helix angle.

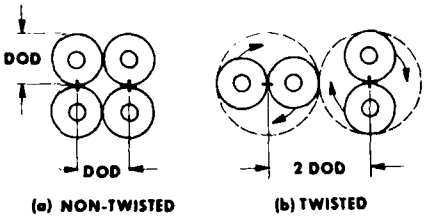



**Figure 3**—The effect of twisting on pair separation for: (a) non-twisted pairs, and (b) twisted pairs.

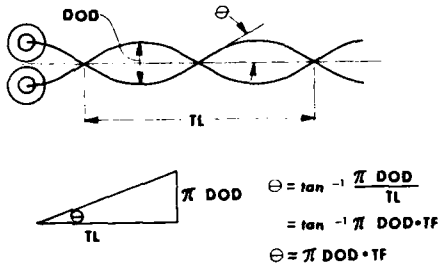



**Figure 4**—The helix angle, $\theta$, of a twisted pair is proportional to the product of diameter over dielectric (DOD) and twist frequency (TF).

A second possible explanation as to why FEXT should improve as DOD increases relates to twist uniformity. Twists with large helix angles require more mechanical energy to deform than do twists with small helix angles. Consequently, large helix angle twists have greater mechanical stability and can better resist deformation during subsequent stages of manufacture. Because of their more perfect twists, these large helix angle pairs are more likely to produce better crosstalk. In fact, Mr. Strakhov concludes in his paper that: "The fundamental causes of observed crosstalk levels appears to be small and random deviations from perfect formation of the twisted pair."[1] Mr. Holte concludes similarly in his paper.[2]

Since both the pair separation theory and the twist uniformity theory point toward twist helix angle as a fundamentally better measure of crosstalk performance than DOD, the following section examines this possibility.

## 7. CORRELATION OF MEAN FEXT WITH AVERAGE TWIST HELIX ANGLE

Although all the pairs in a given cable have the same DOD, they have several different (usually 25) twist frequencies. Insofar as *mean* power sum FEXT is the average of the crosstalk in each of these differently twisted pairs, *mean* FEXT should be related to the *average* twist helix angle of the pairs. *For a given design, this average* twist helix angle is simply proportional to the product of the DOD and the *average* twist frequency (TF) of that design.

### 7.1 Standard Cables

Table 2 lists the DOD, average TF and helix angle* for each standard cable design used in the Bell System. The four gauges have three different average twist frequencies, and these span only a 16% range (from 0.2827 to 0.3270 twists/inch). Contrastingly, the DOD's span a 174% range (from 27 to 74 mils). Consequently, the twist frequency effect in these cables is small compared to the DOD effect, and so the correlation coefficient should improve only slightly when helix angle is used instead of DOD as the independent variable.

* Although helix angle equals π x DOD x TF, the term "helix angle" will be used more loosely in this paper to mean "DOD x TF".

**Table 2**
**Average Twist Frequency, Diameter over Dielectric and Helix Angle for Standard Cables**

| | | air core | | waterproof | | | |
|---|---|---|---|---|---|---|---|
| | | solid | | DEPIC | | solid | |
| AWG | average TF (twists/in) | DOD (mils) | DOD x TF | DOD (mils) | DOD x TF | DOD (mils) | DOD x TF |
| 19 | 0.2827 | 60 | 17.0 | 63 | 17.8 | 74 | 20.9 |
| 22 | 0.3007 | 43 | 12.9 | 45 | 13.5 | 52 | 15.6 |
| 24 | 0.3270 | 34 | 11.1 | 36 | 11.8 | 42 | 13.7 |
| 26 | 0.3270 | 27 | 8.8 | 29 | 9.5 | 33 | 10.8 |

Figure 5 shows the same FEXT data as in Figure 1, but plotted against average twist helix angle instead of DOD. As expected, the correlation has improved slightly from 0.875 to 0.898. While this improvement of itself may not be significant, Section 7.2 shows that the effect of using helix angle is quite substantial when the "special" cables are included.

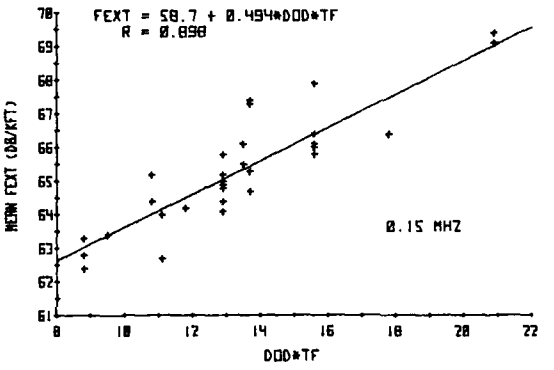



**Figure 5**—Mean power sum FEXT vs. the product of diameter over dielectric (DOD) and twist frequency (TF) for 33 standard cable measurements at 0.15 MHz.

So far, the investigations have been at a single frequency—0.15 MHz. As mentioned in Section 3, however, four other frequencies were also examined. Table 3 summarizes the linear regression equations for the standard cables at all five frequencies.

**Table 3**
**Linear Regression Equations for Mean Power Sum FEXT of Standard Cables**

| frequency | FEXT(dB/kft) = $a + b$ x DOD(mils) x TF(twists/inch) | | |
|---|---|---|---|
| (MHz) | $a$ | $b$ | $\rho$ |
| 0.15 | 58.7 | 0.494 | 0.898 |
| 0.772 | 46.9 | 0.375 | 0.8[illegible] |
| 1.6 | 41.0 | 0.348 | 0.854 |
| 3.15 | 35.5 | 0.321 | 0.813 |
| 6.3 | 29.2 | 0.308 | 0.796 |

### 7.2 Standard and Special Cables

Table 4 lists the DOD, average TF and helix angle for each special cable design. Except for T2 LOCAP cable, all of the cable designs have 25 unique twist lengths and 25-pair unit construction. T2 LOCAP cable differs in that it has 22 unique twists and uses 7, 14 and 30-pair units depending on cable pair size.

**Table 4**
**Average Twist Frequency, Diameter Over Dielectric and Helix Angle of "Special" Cables**

| Cable | AWG | average TF (twists/inch) | air core DEPIC DOD (mils) | air core DEPIC DOD x TF | air core solid DOD (mils) | air core solid DOD x TF | waterproof DEPIC DOD (mils) | waterproof DEPIC DOD x TF |
|---|---|---|---|---|---|---|---|---|
| T2 LOCAP | 22 | 0.5164 | 79 | 40.8 | - | - | 79 | 40.8 |
| ICOT | 24 | 0.4018 | 49 | 19.7 | - | - | 49 | 19.7 |
| MAT | 25 | 0.4018 | 35 | 14.1 | - | - | - | - |
| DUCTPIC | 26 | 0.4018 | 24.5 | 9.8 | - | - | - | - |
| 28 AWG | 28 | 0.4018 | - | - | 21.6 | 8.7 | - | - |

Figure 6 shows the same FEXT data as in Figure 2. but plotted against average twist helix angle instead of DOD. Note that the special cables (which in Figure 2 performed better than that predicted simply on the basis of their DOD's) now fall reassuringly on either side of the helix angle regression line.

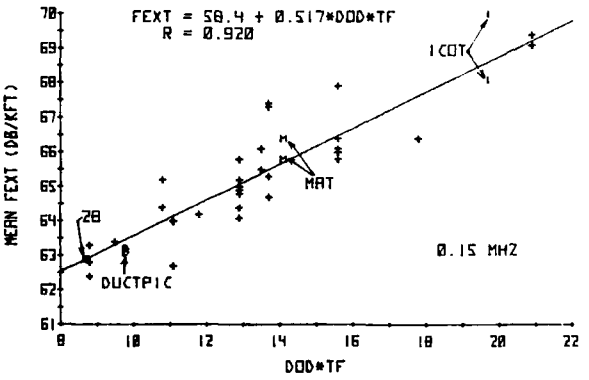



**Figure 6**—Mean power sum FEXT vs. the product of diameter over dielectric (DOD) and twist frequency (TF) for 33 standard and 7 "special" cable measurements at 0.15 MHz.

Table 5 summarizes the linear regression equations at all five frequencies for the standard and special cables taken together. Because T2 LOCAP cable's helix angle is by far the largest of any design (almost twice as large as any other cable), and because crosstalk data on T2 LOCAP cable were only available at 3.15 MHz, two regressions were performed at 3.15 MHz—one without T2 LOCAP cable and one with.

**Table 5**
**Linear Regression Equations for Mean Power Sum FEXT of Standard and "Special" Cables**

| frequency (MHz) | FEXT(dB/kft) = $a+b$ x DOD(mils) x TF(twists/inch) without T2 LOCAP $a$ | $b$ | $\rho$ | with T2 LOCAP $a$ | $b$ | $\rho$ |
|---|---|---|---|---|---|---|
| 0.15 | 58.4 | 0.517 | 0.920 | - | - | - |
| 0.772 | 46.6 | 0.398 | 0.872 | - | - | - |
| 1.6 | 40.7 | 0.369 | 0.872 | - | - | - |
| 3.15 | 35.2 | 0.342 | 0.842 | 34.9 | 0.370 | 0.968 |
| 6.3 | 29.0 | 0.331 | 0.840 | - | - | - |

Comparing the results in Table 5 to the results for the standard cables alone in Table 3 reveals that by combining the standard cables with the special cables, the correlation coefficients have improved. This confirms that helix angle serves as a basic parameter that can be used to determine the mean FEXT of all copper cable designs—be they standard or "special".

Because crosstalk data did not exist at 0.15 MHz on T2 LOCAP cable, its crosstalk performance was not shown in Figure 6. However, data on this cable do exist at 3.15 MHz, and Figure 7 shows its performance. Notice that all of the special cables fit the regression line extremely well.

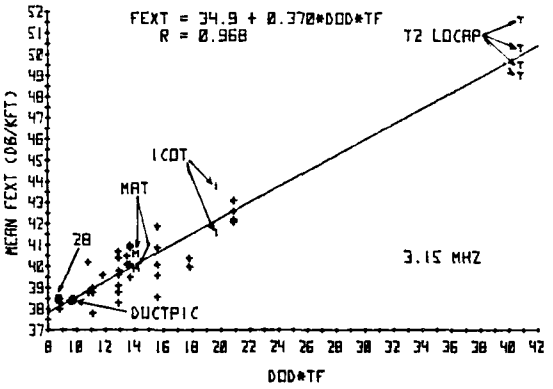



**Figure 7**—Mean power sum FEXT vs. the product of diameter over dielectric (DOD) and twist frequency (TF) for 34 standard and 11 "special" cables at 3.15 MHz.

#### 8. Effect of Helix Angle on Frequency Scaling

The regression slopes, $b$, in both Tables 3 and 5 decrease with increasing frequency. This suggests the radical notion that FEXT frequency scaling is not simply a constant for all cables, but that it is a function of the cable's average twist helix angle! The Appendix (Equation A-9) shows that the scaling is given by:

$$\Delta \text{ MEAN FEXT} = (18.03 + 0.117 \times \text{DOD} \times \text{TF}) \log_{10}\frac{f_1}{f_2} \qquad (1)$$

For FEXT to scale at the classical 6 dB per octave of frequency rate, the term in parentheses should equal 20. Instead, the coefficient is equal to a constant term, 18.03, plus another term that is proportional to helix angle. This indicates that mean FEXT scales more rapidly with frequency for large helix angles than for small. From Table 2, the DOD x TF product ranges from about 9 for 26-gauge air core to about 21 for 19-gauge solid insulation waterproof. Substituting these values into Equation (1) yields a frequency scaling of from 5.7 dB to 6.2 dB per octave. Consequently, the frequency scalings for standard cables are from 0.3 dB less to 0.2 dB more per octave than the classical 6 dB per octave

rule. Although this perturbation is slight, it is indeed an interesting and unexpected phenomenon.

### 9. A General Mean Power Sum FEXT Equation

The five regression equations listed in Table 5 under the heading "without T2 LOCAP" can be combined into a single general equation which expresses the mean power sum FEXT of all copper PIC cables (except for T2 LOCAP cable) at any frequency as a simple function of DOD and average TF. This equation, derived in the Appendix (Equation A-13), is as follows:

$$\text{MEAN FEXT} = 44.02 + 0.405 \times \text{DOD} \times \text{TF} - (18.03 + 0.117 \times \text{DOD} \times \text{TF}) \log_{10} f \quad (2)$$

90% of the 189 mean FEXT copper measurements in the data base fall within ±1.5 dB of the value calculated using Equation (2).

## 10. CONCLUSIONS

The analyses in this paper show that:

- Twist helix angle is a basic parameter that can be used to express the mean power sum FEXT of a wide variety of cable designs—air core and waterproof, solid and DEPIC insulations, 19 through 26-gauge, 83 nF/mile and low capacitances.
- Mean power sum FEXT frequency scaling is a function of twist helix angle with actual scalings ranging from 5.7 dB per octave for 26-gauge solid insulation air core cable to 6.2 dB per octave for 19-gauge solid insulation waterproof cable. These scalings are from 0.3 dB less to 0.2 dB more per octave than the classical 6 dB per octave rule.

A general equation was presented in Section 9 which can be used to calculate the expected mean power sum FEXT of any standard or "special" copper cable (except for T2 LOCAP cable) at any frequency from 0.15 to 6.3 MHz. Alternately, rather than use this general equation, the regression equations in Table 5 can be used to calculate crosstalk at each of the five standard frequencies.

In addition to being used to calculate the mean power sum FEXT performance of existing Bell System cable designs, the equations presented here can be used to predict the crosstalk performance of *new* designs. As long as pair twists are judiciously chosen and spaced within the twist spectrum, one can use these equations to predict the mean power sum crosstalk of new cable designs simply on the basis of DOD and average TF.

## REFERENCES


[1] Strakhov, N. A., "Crosstalk on Multipair Cable—Theoretical Aspects," National Telecommunications Conference, *Conference Record*, pp. 8B-1 through 8B-7, November 1973.

[2] Holte, N., "Calculation of Crosstalk in Balanced Pair Cables by Means of Simulation," 26th International Wire and Cable Symposium, *Proceedings*, pp. 428-439, November 1977.

[3] Anderson, R. E., "Computer Controlled Cable Measurements," 21st International Wire and Cable Symposium, *Proceedings*, pp. 188-192, December 1972.

[4] Bobsin, J. H. and Forman, L. E., "The T2 Digital Line—Extending the Digital Network," *Bell Laboratories Record*, September 1973.

[5] Lombardi, J. A., Maurer, R. E. and Michaud, W. P., "The T1C System," 11th International Conference on Communication, *Conference Record*, pp. 39-1 to 39-9, 1975.

[6] Mitchell, D. M., "Material Savings by Design in Exchange and Trunk Telephone Cable, Part I: Waterproof Cable with Dual Insulation," 23rd International Wire and Cable Symposium, *Proceedings*, pp. 216-221, November 1974.

[7] Durham, R. L., Nutt, W. G. and Refi, J. J., "LOCAP: A Low Capacitance Cable for a High-Capacity System," *Bell Laboratories Record*, July/August 1974.

[8] Nutt, W. G. and Savage, J. P., "Multipair Cables for Digital Transmission," National Telecommunications Conference, *Conference Record*, pp. 21.1.1 through 21.1.5, December 1978.

[9] Webster, G. H., "Material Savings by Design in Exchange and Trunk Telephone Cable, Part II: Metropolitan Area Trunk Cable," 23rd International Wire and Cable Symposium, *Proceedings*, pp. 222-225, November 1974.

[10] Nantz, T. D., "An Increased Pair Density Underground Feeder Cable," 27th International Wire and Cable Symposium," *Proceedings*, pp. 187-190, November 1978.


## Appendix

### An Equation for Mean Power Sum FEXT at Any Frequency as a Function of Twist Helix Angle

Mean FEXT varies with frequency as follows:

$$y = c_0 + c_1 x \quad (A\text{-}1)$$

where:

$y$ = MEAN FEXT
$x = \log_{10} f$

The parameters $c_0$ and $c_1$ can be estimated by the method of least squares which involves minimizing the sum of squares of the residuals $R$ where:

$$R = \sum_{i=1}^{i=N} (y_i - c_0 - c_1 x_i)^2 \quad (A\text{-}2)$$

Taking the partial derivative with respect to $c_0$, setting to 0 and solving for $c_0$:

$$\frac{\partial R}{\partial c_0} = \sum_{i=1}^{i=N} (y_i - c_0 - c_1 x_i) = 0$$

$$\sum_{i=1}^{i=N} y_i - N c_0 - c_1 \sum_{i=1}^{i=N} x_i = 0$$

$$c_0 = \frac{\sum_{i=1}^{i=N} y_i - c_1 \sum_{i=1}^{i=N} x_i}{N} \quad (A\text{-}3)$$

Similarly, taking the partial derivative of (A-2) with respect to $c_1$, setting to 0 and solving for $c_0$:

$$\frac{\partial R}{\partial c_1} = \sum_{i=1}^{i=N} (y_i - c_0 - c_1 x_i)(x_i) = 0$$

$$\sum_{i=1}^{i=N} y_i x_i - c_0 \sum_{i=1}^{i=N} x_i - c_1 \sum_{i=1}^{i=N} x_i^2 = 0$$

$$c_0 = \frac{\sum_{i=1}^{i=N} y_i x_i - c_1 \sum_{i=1}^{i=N} x_i^2}{\sum_{i=1}^{i=N} x_i} \quad (A\text{-}4)$$

Equations (A-3) and (A-4) express $c_0$ in terms of $c_1$. Equating these two equations to one another, and solving for $c_1$:

$$\frac{\sum_{i=1}^{i=N} y_i x_i - c_1 \sum_{i=1}^{i=N} x_i^2}{\sum_{i=1}^{i=N} x_i} = \frac{\sum_{i=1}^{i=N} y_i - c_1 \sum_{i=1}^{i=N} x_i}{N}$$

$$c_1 = \frac{N \sum_{i=1}^{i=N} y_i x_i - \sum_{i=1}^{i=N} x_i \sum_{i=1}^{i=N} y_i}{N \sum_{i=1}^{i=N} x_i^2 - \left[\sum_{i=1}^{i=N} x_i\right]^2} \qquad \text{(A-5)}$$

$c_1$ is the frequency scaling coefficient and it's numeric value can be found by substituting the appropriate crosstalk values, $y_i$, at given frequency values, $x_i$, into (A-5).

Table 5 gave mean FEXT equations as a function of helix angle at five frequencies. These equations have the form:

$$y_i = a_i + b_i z \qquad \text{(A-6)}$$

where:

$$z = \text{DOD x TF}$$

Substituting (A-6) into (A-5):

$$c_1 = \frac{z\left[N \sum_{i=1}^{i=N} b_i x_i - \sum_{i=1}^{i=N} x_i \sum_{i=1}^{i=N} b_i\right] + N \sum_{i=1}^{i=N} a_i x_i - \sum_{i=1}^{i=N} x_i \sum_{i=1}^{i=N} a_i}{N \sum_{i=1}^{i=N} x_i^2 - \left[\sum_{i=1}^{i=N} x_i\right]^2} \qquad \text{(A-7)}$$

where:

$$x_i = \log f_i$$

Substituting the values of $a_i$, $b_i$ and $\log f_i$ from Table 5 into (A-7) yields:

$$c_1 = -0.117z - 18.03 \qquad \text{(A-8)}$$

where:

$$z = \text{DOD x TF}$$

Substituting (A-8) into (A-1):

$$y = c_0 + (-0.117z - 18.03) \log_{10} f$$

Consequently, the change in crosstalk in going from $f_1$ to $f_2$ is:

$$\Delta \text{ MEAN FEXT} = (18.03 + 0.117 \text{ x DOD x TF}) \log_{10} \frac{f_1}{f_2} \qquad \text{(A-9)}$$

So far we have found $c_1$, the frequency scaling coefficient. We can also solve for $c_0$, the intercept. Substituting (A-8) into (A-3):

$$c_0 = \frac{1}{N} \sum_{i=1}^{i=N} y_i - \frac{1}{N} \sum_{i=1}^{i=N} x_i (-0.117z - 18.03) \qquad \text{(A-10)}$$

Substituting (A-6) for the $y_i$ into (A-10):

$$c_0 = \frac{1}{N}\left[\sum_{i=1}^{i=N} a_i + z \sum_{i=1}^{i=N} b_i\right] + \frac{1}{N} \sum_{i=1}^{i=N} x_i (0.117z + 18.03) \qquad \text{(A-11)}$$

To obtain a numeric value for $c_0$, we substitute the values of $a_i$, $b_i$ and $\log f_i$ from Table 5 into (A-11) and obtain:

$$c_0 = 44.02 + 0.405z \qquad \text{(A-12)}$$

Substituting (A-12) and (A-8) into (A-1):

$$y = (44.02 + 0.405z) - (0.117z + 18.03)x$$

or

$$\text{MEAN FEXT} = 44.02 + 0.405 \text{ x DOD x TF} - (18.03 + 0.117 \text{ x DOD x TF}) \log_{10} f \qquad \text{(A-13)}$$

Equation (A-13) combines the five equations from Table 5 into one general equation which expresses the MEAN FEXT of all copper PIC cables (except T2 LOCAP cable) at any frequency from 0.15 MHz to 6.3 MHz. 90% of the crosstalk values in the data base fall within ±1.5 dB of the value calculated using this equation.



James J. Refi
Bell Laboratories
2000 N.E. Expressway
Norcross, GA 30071

Mr. Refi began work with Bell Laboratories in 1966 at the Baltimore Laboratory as a Member of Technical Staff. He has worked on land coaxial and multipair cables and has authored papers on T2-LOCAP cable, pair unbalance phenomena, and lightning surges in telephone cable.

Mr. Refi received his B.S.E.E. from Villanova University in 1966 and the M.S.E.E. from the Polytechnic Institute of Brooklyn in 1968. He is a member of I.E.E.E., Tau Beta Pi, and Eta Kappa Nu.

# GENERAL CROSSTALK MODEL FOR PAIRED COMMUNICATION CABLES

by

P. Kish Y. Le Borgne

Northern Telecom Canada Limited
Montreal, Quebec

## *ABSTRACT*

A valuable tool for characterization of paired communication cables is developed in the form of a general crosstalk model at VF and carrier frequencies. Parameters analyzed in the model are:- pair to pair capacitance unbalance - inductive couplings - terminating impedances - propagation effects expressed as a function of frequency and cable length - conductor size - type of insulation - and cable construction.

A comparison between experimental and theoretical results is presented, illustrating the impact of each parameter on crosstalk performance. It is shown that the model gives excellent accuracy over a wide range of conditions, and it can be used to simulate actual installation to predict the transmission quality.

## *INTRODUCTION*

Because of the complex nature of interwire couplings in paired communication cables, traditionally, it has been impractical to formulate exact analytical solutions in a general model for predicting crosstalk behaviour. In this paper, we have come a step closer to the desired objective by following a straightforward network modelling approach.

A detailed development of the theoretical model is presented in the Appendices. In Appendix 1, a general set of network equations is derived for an elemental cable section. These include the effects of direct metallic couplings between pairs as well as indirect longitudinal couplings. In Appendix 2, the equations are solved for a simplified case considering direct couplings only with balanced terminations. Good agreement is obtained with experimental crosstalk measurements at low frequencies (up to 100 kHz) for a wide range of terminating impedances.

Previous crosstalk models have been developed by different authors in the literature. Some of these are based on traditional assumptions limiting their use. For example, the model developed in Ref. (1) does not consider the effect of terminating impedances on NEXT and FEXT. A more sophisticated model was developed later by Nantz et al(2),(3). However, it too has some drawbacks, namely:

- The computation of crosstalk is dependent on measurements which we wish to avoid in a general model.
- The model is not related to basic cable parameters such as R, L, G, C.

Since available models were not suitable for our purposes, we proceeded in developing a general crosstalk model for two coupled transmission lines with shield return. The theory, as developed in the Appendices, is based on a straightforward application of network theory and matrix analysis of simultaneous equations.

## *MODELLING APPROACH*

Essentially, the cable is represented by a finite number of elemental $\Pi$ networks cascaded together. The network equations for each elemental cable section are defined in terms of the basic resistive, capacitive and inductive couplings within the cable. The network equations are then further simplified by defining all voltages and currents in terms of their metallic and longitudinal components, and also by choosing a convenient frame of reference. In so doing, it is possible to segregate the general network equations (16) in two distinct parts. The first part defines the network response for metallic excitation.

$$[\frac{I_m}{2}] = [Y_m][V_m] + [Y_{m\ell}][V_\ell]$$

the second part defines the network response for longitudinal excitation,

$$[2I_\ell] = [Y_\ell][V_\ell] + [Y_{\ell m}][V_m]$$

The interaction between metallic and longitudinal components is defined by the

coupling matrix [$Y_{\ell m}$]. These coupling terms are usually neglected in traditional derivations. However, they can have a significant effect on crosstalk behaviour at high frequencies on long lengths of cable.

The last step in the development involves solving the network equations for a full cable length comprised of "n" elemental sections. In Appendix 2, we chose to study a simplified case considering metallic couplings only at low frequencies. However, the same procedure can be used in developing solutions for the extended model.

Having defined the transmission equations for a single cable section, the transmission equations for "n" sections are obtained by matrix multiplication. In the process, considerable simplification is achieved by assuming weak couplings between pairs and by assuming approximately equal propagation constants for each pair.

Far End Crosstalk (I/O FEXT) and Near End Crosstalk (NEXT) are then obtained by solving the transmission equations for node voltages in terms of the boundary conditions at the input and output of the cable. These are given by equations (30) to (33) of Appendix 2.

The above equations were programmed on the computer and were used to determine crosstalk behaviour on some standard types of PIC cables in the frequency range between 1 kHz to 100 kHz. Some of these results are presented below.

## *CROSSTALK RESULTS*

### *Low Frequencies*

Crosstalk measurements were performed on standard lengths of 22 gauge PIC cable at a test frequency of 1 kHz. The cable pairs were approximately terminated in their characteristic impedance ($Z_o \simeq 600$ ohms).

A comparison between the measurement data and the theoretical results is given in Fig. 1.

From the graph, a strong correlation is evident between Far End Crosstalk at 1 kHz and capacitance unbalance pair-to-pair. For low values of capacitance unbalance, there is a larger spread in measured results about the theoretical curve. This spread is due, in large part, to measurement inaccuracies. Overall, a very good agreement is obtained between the predicted results from the model (dashed line) and the experimental data. The results also agree with the simplified formulae developed in Ref. (1).

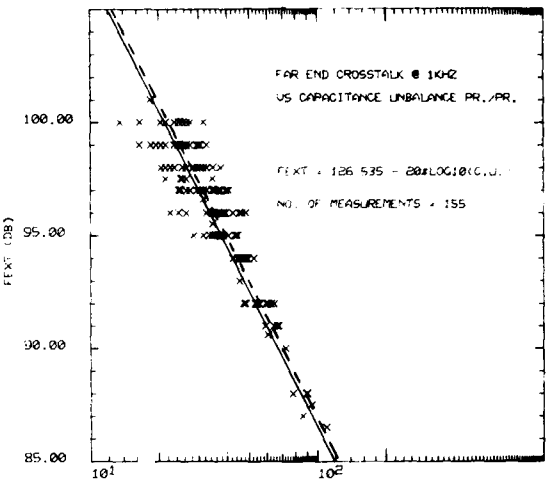



FIG. 1 CAPACITANCE UNBALANCE PR./PR. (PF)

In the second part of the test program, crosstalk measurements were performed on some representative pair combinations over a wide frequency range from 1 kHz to 100 kHz. The test pairs were terminated in a variable set of impedances ranging from short circuit to open circuit. Throughout the testing, the level generator and level receiver impedance was fixed at 135 ohms. The measured results for Far End Crosstalk are presented in Fig. 2.

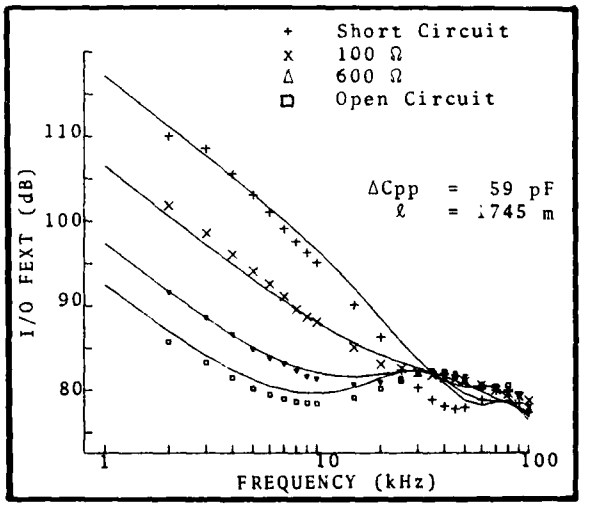



FIG. 2 I/O FEXT VS. FREQUENCY FOR VARIOUS TERMINATING IMPEDANCES

A large variation in measured crosstalk behaviour is evident over the frequency range and for the terminating impedances selected. These variations can be explained from the effects of propagation in the cable and from reflections due to unmatched terminations. The predicted results from the model are also plotted on the same graph. These track very closely with the observed behaviour.

From these and other analyses performed on the model, the following comments can be made on its accuracy and limitations.

- For most cases the model compares with measurements to within 3 dB.
- Its performance in following the variation of crosstalk behaviour versus frequency and terminating impedance is excellent.
- Use of the general low frequency model is limited to a maximum frequency of 100 kHz.

*High Frequencies*

Although complete solutions are not developed in a general model at high frequencies, nevertheless, some insight can still be gained by examining measured crosstalk behaviour on cables with varying degrees of longitudinal unsymmetry. The average crosstalk behaviour for two typical 25-pair, 22 gauge PIC cables is presented in Fig. 3. One of the cables was manufactured under inferior conditions and has a higher pair unbalance with respect to ground. The other cable was manufactured with tighter controls on insulated conductor dimensions. All crosstalk results were obtained by initially measuring a long length of cable and by successively cutting back and remeasuring shorter lengths of the same cable.

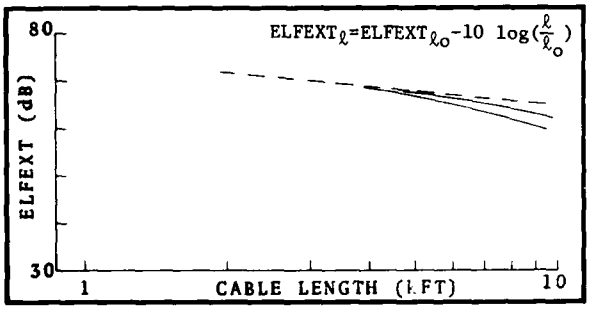



FIG. 3 EQUAL LEVEL FAR END CROSSTALK @ 772 kHz

From the measured results, it is observed that the Far End Crosstalk performance is significantly degraded for long lengths at high frequencies. The degradation is much worse than expected according to classical theory[1]. We have carried out some experiments which indicate that the crosstalk degradation correlates with pair dimensional unsymmetry. For example, good results have been achieved on cables manufactured with mated conductors and/or where the insulated conductors were manufactured under computer control.

*Appendix 1*

*Development of a General Crosstalk Model for Paired Communication Cables*

Theory:

*1.0 General*

The crosstalk coupling between two pairs in a multipair cable is modelled in terms of the simplified structure of Fig. A1. In this model all the unused pairs in the cable are tied together and grounded to the cable shield.

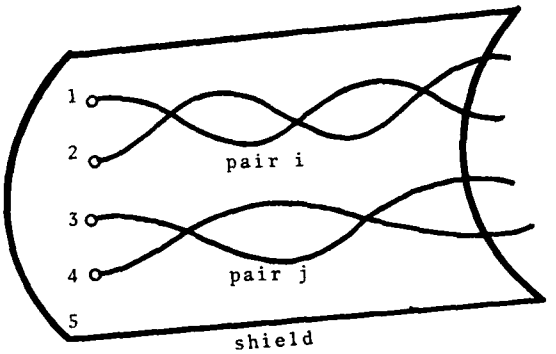



FIG. A1

The basic resistive, capacitive and inductive couplings within the cable can be represented by a lumped network where the length of cable is short compared to the wavelength. In the subsequent development, a $\Pi$ network is used to model a short section of cable of length $\ell \approx \ell_{sect}$. Where the length of cable is long compared to wavelength (i.e. effects of propagation cannot be ignored), the total length is modelled in terms of a series of $\Pi$ sections cascaded together.

The first step in the development is to obtain the network representation for an elemental section of cable.

Consider the Π model shown in Fig. A2.

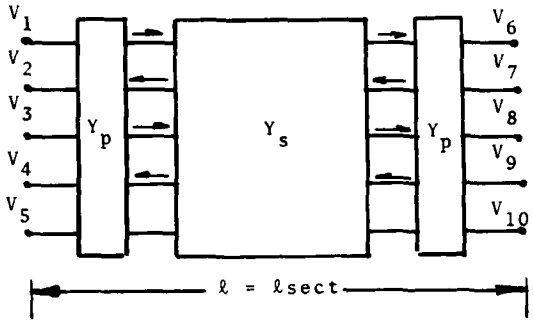



FIG. A2

Nodes (1,2) and (6,7) represent the input and output ports for pair i respectively.

Nodes (3,4) and (8,9) represent the input and output ports for pair j respectively.

Nodes (5,10) represent the cable shield at the input and output respectively.

Note: All node voltages and currents are defined with respect to a distant reference node.

$Y_p$ represents all the shunt admittances between wires and wires to shield for a half section length.

$Y_s$ represents all the series admittances for each wire including mutual couplings between wires and wires-to-shield for a full section length.

The detailed interconnection between network components including all capacitive and inductive couplings is illustrated in Fig. A3.

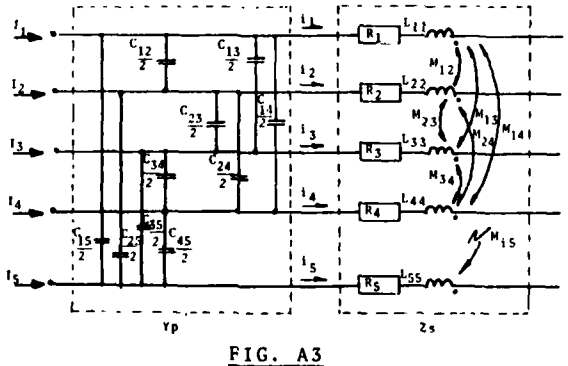



FIG. A3

*1.1 Network Equations for $Y_p$*

The nodal equations for network $[Y_p]$ are determined with reference to Fig.A3 as follows:

$$I_1 = Y_{11}V_1 - Y_{12}V_2 - Y_{13}V_3 - Y_{14}V_2 - Y_{15}V_5 + i_1 \quad (1)$$

$$I_2 = Y_{21}V_1 + Y_{22}V_2 - Y_{23}V_3 - Y_{24}V_4 - Y_{25}V_5 + i_2 \quad (2)$$

$$I_3 = Y_{31}V_1 - Y_{32}V_2 + Y_{33}V_3 - Y_{34}V_4 - Y_{35}V_5 + i_3 \quad (3)$$

$$I_4 = Y_{41}V_1 - Y_{42}V_2 - Y_{43}V_3 + Y_{44}V_4 - Y_{45}V_5 + i_4 \quad (4)$$

$$I_5 = Y_{51}V_1 - Y_{52}V_2 - Y_{53}V_3 - Y_{54}V_4 + Y_{55}V_5 + i_5 \quad (5)$$

where,

$$Y_{11} = Y_{12}+Y_{13}+Y_{14}+Y_{15} = j\omega \frac{C_{12}+C_{13}+C_{14}+C_{15}}{2}$$

$$Y_{22} = Y_{21}+Y_{23}+Y_{24}+Y_{25} = j\omega \frac{C_{21}+C_{23}+C_{24}+C_{25}}{2}$$

$$Y_{33} = Y_{31}+Y_{32}+Y_{34}+Y_{35} = j\omega \frac{C_{31}+C_{32}+C_{34}+C_{35}}{2}$$

$$Y_{44} = Y_{41}+Y_{42}+Y_{43}+Y_{45} = j\omega \frac{C_{41}+C_{42}+C_{43}+C_{45}}{2}$$

$$Y_{55} = Y_{51}+Y_{52}+Y_{53}+Y_{55} = j\omega \frac{C_{51}+C_{52}+C_{53}+C_{54}}{2}$$

In obtaining a solution for the above set of equations, it is more instructive to redefine the node voltages and currents in terms of their metallic and longitudinal components.

By definition,

$$I_1 = I\ell_1 + Im_1/2 \qquad i_1 = i\ell_1 + im_1/2$$

$$I_2 = I\ell_1 - Im_1/2 \qquad i_2 = i\ell_1 - im_1/2$$

$$I_3 = I\ell_2 + Im_2/2 \qquad i_3 = i\ell_2 + im_2/2$$

$$I_4 = I\ell_2 - Im_2/2 \qquad i_4 = i\ell_2 - im_2/2$$

$$I_5 = Is \qquad i_5 = is$$

$$V_1 = V\ell_1 + Vm_1/2$$

$$V_2 = V\ell_1 - Vm_1/2$$

$$V_3 = V\ell_2 + Vm_2/2$$

$$V_4 = V\ell_2 - Vm_2/2$$

$$V_5 = Vs$$

The above definitions are substituted directly into equations (1) to (5) to obtain a new network representation for $[Y_p]$ in terms of metallic and longitudinal components, i.e.

$$\begin{bmatrix} Im_1/2 \\ Im_2/2 \\ 2I\ell_1 \\ 2I\ell_2 \\ Is \end{bmatrix} = j\omega \begin{bmatrix} \frac{Cm_1}{2} & -\frac{\Delta Cpp}{8} & \frac{\Delta Cpg_1}{4} & -\frac{\Delta Cp2_1}{4} & -\frac{\Delta Cps_1}{4} \\ -\frac{\Delta Cpp}{8} & \frac{Cm_2}{2} & -\frac{\Delta Cp1_2}{4} & \frac{\Delta Cpg_2}{4} & -\frac{\Delta Cps_2}{4} \\ \frac{\Delta Cpg_1}{4} & -\frac{\Delta Cp1_2}{4} & \frac{Cpg_1}{2} & -\frac{Cpp}{2} & -\frac{Cps_1}{2} \\ -\frac{\Delta Cp2_1}{4} & \frac{\Delta Cpg_2}{4} & -\frac{Cpp}{2} & \frac{Cpg_2}{2} & -\frac{Cps_2}{2} \\ -\frac{\Delta Cps_1}{4} & -\frac{\Delta Cps_2}{4} & -\frac{Cps_1}{2} & -\frac{Cps_2}{2} & \frac{Ccs}{2} \end{bmatrix} \begin{bmatrix} Vm_1 \\ Vm_2 \\ V\ell_1 \\ V\ell_2 \\ Vs \end{bmatrix} + \begin{bmatrix} \frac{im_1}{2} \\ \frac{im_2}{2} \\ 2i\ell_1 \\ 2i\ell_2 \\ i_s \end{bmatrix} \quad \ldots(6)$$

where,

$Cm_i = C_{12} + \frac{C_{13}+C_{14}+C_{15}}{4} + \frac{C_{23}+C_{24}+C_{25}}{4}$

= mutual capacitance of pair i.

$Cpg_i = (C_{13}+C_{14}+C_{15}) + (C_{23}+C_{24}+C_{25})$

= capacitance of pair i to ground where its tip and ring are tied together and where the other pair(s) are tied to shield and grounded.

$Cpp = (C_{13}+C_{14}) + (C_{23}+C_{24})$

= capacitance between pairs, where the tip and ring of each pair are tied together but floating with respect to shield.

$Cps_i = C_{15}+C_{25}$

= capacitance of pair i to shield where its tip and ring are tied together and where the other pair(s) are floating with respect to shield.

$Ccs = C_{15}+C_{25}+C_{35}+C_{45}$

= capacitance of all the pairs tied together (core) with respect to shield.

$\Delta Cpp = (C_{13}+C_{24}-C_{14}-C_{23})$

= capacitance unbalance between pairs (metallic coupling).

$\Delta Cpj_i = (C_{13}+C_{14}) - (C_{23}+C_{24})$

= capacitance unbalance of pair i to pair j, where the tip and ring of pair j are tied together and floating with respect to shield.

$\Delta Cpg_i = (C_{13}+C_{14}+C_{15}) - (C_{23}+C_{24}+C_{25})$

= capacitance unbalance of pair i to ground where all the other pair(s) are tied together and grounded to the shield.

$\Delta Cps_i = C_{15}-C_{25}$

= capacitance unbalance of pair i to shield where all the other pair(s) are floating with respect to shield.

### 1.2 *Network Equations for $Z_s$*

The next step in the procedure is to determine the network equations for the series network $[Z_s]$. These are obtained with reference to Fig. A3, as follows:

$$\begin{bmatrix} R_1+j\omega L_{11} & j\omega M_{12} & j\omega M_{13} & j\omega M_{14} & j\omega M_{15} \\ j\omega M_{21} & R_2+j\omega L_{22} & j\omega M_{23} & j\omega M_{24} & j\omega M_{25} \\ j\omega M_{31} & j\omega M_{32} & R_3+j\omega L_{33} & j\omega M_{34} & j\omega M_{35} \\ j\omega M_{41} & j\omega M_{42} & j\omega M_{43} & R_4+j\omega L_{44} & j\omega M_{45} \\ j\omega M_{51} & j\omega M_{52} & j\omega M_{53} & j\omega M_{54} & R_s+j\omega L_s \end{bmatrix} \begin{bmatrix} i_1 \\ i_2 \\ i_3 \\ i_4 \\ i_5 \end{bmatrix} = \begin{bmatrix} V_1 \\ V_2 \\ V_3 \\ V_4 \\ V_5 \end{bmatrix} - \begin{bmatrix} V_6 \\ V_7 \\ V_8 \\ V_9 \\ V_{10} \end{bmatrix} \quad \ldots(7)$$

Expressing series currents and node voltages in terms of their metallic and longitudinal components and substituting into equation (7), we obtain:

$$\begin{bmatrix} Zs_{11} & Zs_{12} & Zs_{13} & Zs_{14} & Zs_{15} \\ Zs_{21} & Zs_{22} & Zs_{23} & Zs_{24} & Zs_{25} \\ Zs_{31} & Zs_{32} & Zs_{33} & Zs_{34} & Zs_{35} \\ Zs_{41} & Zs_{42} & Zs_{43} & Zs_{44} & Zs_{45} \\ Zs_{51} & Zs_{52} & Zs_{53} & Zs_{54} & Zs_{55} \end{bmatrix} \begin{bmatrix} \frac{im_1}{2} \\ \frac{im_2}{2} \\ 2i\ell_1 \\ 2i\ell_2 \\ i_s \end{bmatrix} = \begin{bmatrix} Vm_{1i} \\ Vm_{2i} \\ V\ell_{1i} \\ V\ell_{2i} \\ V_{si} \end{bmatrix} - \begin{bmatrix} Vm_{1o} \\ Vm_{2o} \\ V\ell_{1o} \\ V\ell_{2o} \\ V_{so} \end{bmatrix} \quad \ldots(8)$$

where,

$Zs_{11} = (R_1+R_2) + j\omega\,(L_{11}+L_{22}-M_{12}-M_{21})$

$Zs_{22} = (R_3+R_4) + j\omega\,(L_{33}+L_{44}-M_{34}-M_{43})$

= self impedance for pair i and pair j (metallic excitation).

$$Zs_{33} = \tfrac{1}{4}[R_1+R_2 + j\omega\ (L_{11}+L_{22}+M_{12}+M_{21})]$$

$$Zs_{44} = \tfrac{1}{4}[R_3+R_4 + j\omega\ (L_{33}+L_{44}+M_{34}+M_{43})]$$

= self impedance for pair i and pair j (longitudinal excitation).

$$Zs_{34} = Zs_{43} = \tfrac{1}{4}\ j\omega\ (M_{13}+M_{14}+M_{23}+M_{24})$$

= mutual impedance between pairs (longitudinal excitation).

$$Zs_{12} = Zs_{21} = j\omega\ (M_{13}+M_{24}-M_{14}-M_{23})$$

= mutual impedance between pairs (metallic excitation).

$$Zs_{13} = \tfrac{1}{4}[(R_1-R_2) + j\omega\ (L_{11}-L_{22})]$$

$$Zs_{24} = \tfrac{1}{4}[(R_3-R_4) + j\omega\ (L_{33}-L_{44})]$$

= self impedance unbalance (longitudinal to metallic conversion).

$$Zs_{14} = \tfrac{1}{4}[M_{13}+M_{14}-M_{23}-M_{24}]$$

$$Zs_{23} = \tfrac{1}{4}[M_{31}+M_{32}-M_{41}-M_{42}]$$

= mutual impedance unbalance between pairs (longitudinal to metallic conversion).

$$Zs_{55} = Rs + j\omega Ls$$

= self impedance of cable shield.

$$Zs_{35} = Zs_{53} = \tfrac{1}{4}\ j\omega\ (M_{15}+M_{25}) = j\omega Ls$$

$$Zs_{45} = Zs_{54} = \tfrac{1}{4}\ j\omega\ (M_{35}+M_{45}) = j\omega Ls$$

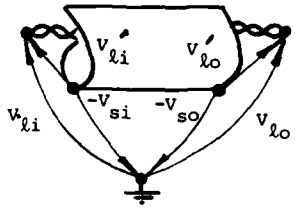
= mutual impedance pair to shield.

$$Zs_{15} = j\omega\ (M_{15}-M_{25}) = 0$$

$$Zs_{25} = j\omega\ (M_{35}-M_{45}) = 0$$

= mutual impedance unbalance pair to shield.

Thus far, all the network equations have been defined with respect to some distant reference node at a reference potential equal to zero. It would be more meaningful to redefine the node voltages with respect to a new reference frame which corresponds to the cable shield at each point along the cable. An illustration is provided below:




$$V\ell'_i = V\ell_i - V_{si}$$

$$V\ell'_o = V\ell_o - V_{so}$$

$$Vm' = Vm$$

In addition, all external currents entering into the cable at the input and output ports are constrained to return via the cable shield:

Thus,

$$i_s = -\ (2i\ell_1 + 2i\ell_2)$$

$$I_s = -\ (2I\ell_1 + 2I\ell_2)$$

Under the above conditions, the network equations relating shield currents and shield voltages become redundant. The remaining network equations for [Zs] are rewritten with respect to the new reference frame as follows:

$$\begin{bmatrix} Zs_{11} & Zs_{12} & (Zs_{13}-Zs_{15}) & (Zs_{14}-Zs_{15}) \\ Zs_{21} & Zs_{22} & (Zs_{23}-Zs_{25}) & (Zs_{24}-Zs_{25}) \\ (Zs_{31}-Zs_{51}) & (Zs_{32}-Zs_{52}) & (Zs_{33}-2Zs_{35}+Zs_{55}) & (Zs_{34}-Zs_{35}-Zs_{54}+Zs_{55}) \\ (Zs_{41}-Zs_{51}) & (Zs_{42}-Zs_{52}) & (Zs_{43}-Zs_{45}-Zs_{53}+Zs_{55}) & (Zs_{44}-2Zs_{45}+Zs_{55}) \end{bmatrix} \begin{bmatrix} \frac{im_1}{2} \\ \frac{im_2}{2} \\ 2i\ell_1 \\ 2i\ell_2 \end{bmatrix} = \begin{bmatrix} Vm_{1i} \\ Vm_{2i} \\ V\ell'_{1i} \\ V\ell'_{2i} \end{bmatrix} - \begin{bmatrix} Vm_{1o} \\ Vm_{2o} \\ V\ell'_{1o} \\ V\ell'_{2o} \end{bmatrix} \quad \ldots(9)$$

For each of the new terms above, it can be shown that the same physical interpretation would apply according to previous definitions, except:

a) All self and mutual inductances are now redefined as <u>loop</u> inductances with shield return.

b) All longitudinal self impedances now include the resistance of the cable shield.

For illustration, a detailed example is worked out below.

By definition,

$$Zs'_{33} = Zs_{33}-2Zs_{35}+Zs_{55}$$

$$= \tfrac{1}{2}[(R_1+R_2) + j\omega (L_{11}+L_{22}+M_{12}+M_{21})]$$

$$-2[\tfrac{1}{2} j\omega (M_{15}+M_{25})]$$

$$+[Rs+j\omega Ls]$$

Since the self inductance of cable shield ($L_S$) equals the mutual inductance pair-to-shield $\frac{1}{2}$ [$M_{15}+M_{25}$], we can rewrite the above equation for $Zs'_{33}$ by setting:

$$j\omega Ls - \tfrac{1}{2}j\omega (M_{15}+M_{25}) = 0$$

Thus,

$$Zs'_{33} = \tfrac{1}{2}[R_1+R_2] + Rs +$$

$$\tfrac{1}{2}[j\omega(\underbrace{L_{11}-M_{15}}_{\mathcal{L}_{11}}+\underbrace{L_{22}-M_{25}}_{\mathcal{L}_{22}}+\underbrace{M_{12}-M_{15}}_{\mathcal{M}_{12}}+\underbrace{M_{21}-M_{25}}_{\mathcal{M}_{21}})]$$

where,

$\mathcal{L}_{11}$ and $\mathcal{L}_{22}$ represent the self inductance of Tip and Ring conductors respectively with shield return.

$\mathcal{M}_{12}$ and $\mathcal{M}_{21}$ represent the mutual inductance between Tip and Ring conductors with shield return.

In a like manner, it can be shown that the network equations for [Yp] remain unaffected by the transformation into the new reference frame. All the terms involving shield voltages conveniently drop out of the equations.

In addition, the last equation defining the current flowing into the cable shield (Is) becomes linearly dependent and hence redundant. Accordingly, the network equations for [Yp] are now given by:

$$\begin{bmatrix} \frac{Im_1}{2} \\ \frac{Im_2}{2} \\ 2I\ell_1 \\ 2I\ell_2 \end{bmatrix} = \begin{bmatrix} Yp_{11} & Yp_{12} & Yp_{13} & Yp_{14} \\ Yp_{21} & Yp_{22} & Yp_{23} & Yp_{24} \\ Yp_{31} & Yp_{32} & Yp_{33} & Yp_{34} \\ Yp_{41} & Yp_{42} & Yp_{43} & Yp_{44} \end{bmatrix} \begin{bmatrix} Vm_1 \\ Vm_2 \\ V\ell'_1 \\ V\ell'_2 \end{bmatrix} + \begin{bmatrix} \frac{im_1}{2} \\ \frac{im_2}{2} \\ 2i\ell_1 \\ 2i\ell_2 \end{bmatrix} \quad \ldots(10)$$

where,

$Yp_{ij}$ terms are as previously defined by equations (6).

*1.3 <u>Complete Network Equations for an Elemental Π Section</u>*

The interconnection between the parallel [Yp] networks and the series [Zs] network can be expressed as follows:

$$[I_i] = [Yp][V_i] + [i_s] \quad (11)$$

$$[Zs][i_s] = [V_i] - [V_o] \quad (12)$$

$$[I_o] = [Yp][V_i] - [i_s] \quad (13)$$

where [Yp] matrix elements are defined by equations (10).

[Zs] matrix elements are defined by equations (9).

Solving equation (12) for series currents [$i_s$], we obtain:

$$[i_s] = [Ys][V_i] - [Ys][V_o] \quad (14)$$

where

$$[Ys] = [Zs]^{-1} \qquad (15)$$

Combining equations (11), (13) and (14), we obtain:

$$\begin{bmatrix} I_i \\ I_o \end{bmatrix} = \begin{bmatrix} Yp+Ys & -Ys \\ -Ys & Yp+Ys \end{bmatrix} \begin{bmatrix} V_i \\ V_o \end{bmatrix} \qquad (16)$$

The above set of equations (16) completely define the behaviour of two coupled transmission lines with shield return for an elemental section of cable. For clarity, they are reproduced below in terms of their constituent metallic and longitudinal components:

$$\begin{bmatrix} \frac{Im_i}{2} \\ \frac{Im_o}{2} \end{bmatrix} = \begin{bmatrix} (Yp_m+Ys_m) & -Ys_m \\ -Ys_m & (Yp_m+Ys_m) \end{bmatrix} \begin{bmatrix} Vm_i \\ Vm_o \end{bmatrix} + \begin{bmatrix} (Yp_{\ell m}+Ys_{\ell m}) & -Ys_{\ell m} \\ -Ys_{\ell m} & (Yp_{\ell m}+Ys_{\ell m}) \end{bmatrix} \begin{bmatrix} V\ell'_i \\ V\ell'_o \end{bmatrix} \qquad \ldots(17)$$

$$\begin{bmatrix} 2I\ell_i \\ 2I\ell_o \end{bmatrix} = \begin{bmatrix} (Yp_{m\ell}+Ys_{m\ell}) & -Ys_{\ell m} \\ -Ys_{\ell m} & (Yp_{\ell m}+Ys_{\ell m}) \end{bmatrix} \begin{bmatrix} Vm_i \\ Vm_o \end{bmatrix} + \begin{bmatrix} (Yp_\ell+Ys_\ell) & -Ys_\ell \\ -Ys_\ell & (Yp_\ell+Ys_\ell) \end{bmatrix} \begin{bmatrix} V_{\ell i} \\ V_{\ell o} \end{bmatrix} \qquad \ldots(18)$$

Each of the coupling terms contained in the above expressions can be related to some physical unsymmetry in a twisted pair structure. Some of the terms, for example, capacitance unbalance between pairs and mutual inductance between pairs have been defined previously[3],[4] for the case of metallic excitation. Generally these are the dominant coupling modes. However, it has been found experimentally that the other terms involving indirect couplings via longitudinal circuits can be significant on long lengths of cable at carrier frequencies.

Within the general model as defined herein, the effect of <u>indirect</u> crosstalk couplings are embodied in the admittance matrix $[Y_{\ell m}]$ which defines the longitudinal to metallic conversion. The <u>direct</u> crosstalk couplings and the transmission constants for metallic excitation are defined by the admittance matrix [Ym]. The transmission constants for longitudinal excitation are defined by the admittance matrix $[Y\ell]$

where,

$$[\frac{Im}{2}] = [Ym][Vm] + [Y_{\ell m}][V\ell]$$

$$[2I\ell] = [Y_{m\ell}][Vm] + [Y\ell][V\ell]$$

are given by equations (17) and (18).

*Appendix 2*

*General Low Frequency Crosstalk Model*

*2.0 Network Equations for a Full Cable Length*

A general low frequency crosstalk model is developed for any arbitrary length of cable which is comprised of "n" elemental sections of length $\ell = \ell_{sect}$. For simplicity, the effect of longitudinal couplings is excluded from the derivation. This assumption is valid at low frequencies where the longitudinal coupling terms can be considered of second order.

Taking these assumptions into account, equations (17) and (18) for an elemental section are reduced to:

$$\begin{bmatrix} \frac{Im_i}{2} \\ \frac{Im_o}{2} \end{bmatrix} = \begin{bmatrix} Yp_m+Ys_m & -Ys_m \\ -Ys_m & Yp_m+Ys_m \end{bmatrix} \begin{bmatrix} Vm_i \\ Vm_o \end{bmatrix} \qquad (19)$$

After expanding and rearranging terms, equations (19) become:

$$\begin{bmatrix} \frac{Im_{1i}}{2} \\ \frac{Im_{1o}}{2} \\ \frac{Im_{2i}}{2} \\ \frac{Im_{2o}}{2} \end{bmatrix} = \left[\begin{array}{cc:cc} yp_1+ys_1 & -ys_1 & -(\Delta yp+\Delta ys) & \Delta ys \\ -ys_1 & yp_1+ys_1 & \Delta ys & -(\Delta yp+\Delta ys) \\ \hdashline -(\Delta yp+\Delta ys) & \Delta ys & yp_2+ys_2 & -ys_2 \\ \Delta ys & -(\Delta yp+\Delta ys) & -ys_2 & yp_2+ys_2 \end{array}\right] \begin{bmatrix} Vm_{1i} \\ Vm_{1o} \\ Vm_{2i} \\ Vm_{2o} \end{bmatrix} \qquad \ldots(20)$$

where,

$$yp_1 = j\omega\frac{Cm_1}{2}$$

$$yp_2 = j\omega\frac{Cm_2}{2}$$

$$ys_1 = 1/Zm_1 = 1/[(R_1+R_2)+j\omega(\mathcal{L}_{11}+\mathcal{L}_{22}-\mathcal{M}_{12}-\mathcal{M}_{21})]$$

$$ys_2 = 1/Zm_2 = 1/[(R_3+R_4)+j\omega(\mathcal{L}_{33}+\mathcal{L}_{44}-\mathcal{M}_{34}-\mathcal{M}_{43})]$$

$$\Delta yp = j\omega\Delta\frac{Cpp}{8} = j\omega\left[\left(\frac{C_{13}+C_{24}-C_{14}-C_{23}}{8}\right)\right]$$

$$\Delta ys = j\omega\Delta\mathcal{M}_{pp}/Zm_1 Zm_2$$

$$= j\omega(\mathcal{M}_{13}+\mathcal{M}_{24}-\mathcal{M}_{14}-\mathcal{M}_{23})Ys_1 Ys_2$$

Note: In deriving the above equations (20) and in subsequent derivations, all unbalance terms of second order or higher are neglected. This approximation is valid for elemental sections where the unbalance terms are of small magnitude and where "$\ell_{sect}$" is short compared to wavelength ($\ell_{sect} < \lambda/10$).

A full cable length can be represented by "n" elemental $\Pi$ sections cascaded together. From network theory, it can be shown that the overall network response is given by:

$$\begin{bmatrix} V_i \\ I_i \end{bmatrix} = \left[T\right]^n \begin{bmatrix} V_o \\ -I_o \end{bmatrix}$$

where [ T ] is the transmission matrix for each section.

The transmission matrix [ T ] for an elemental cable section is obtained from equations (20) as follows:

$$\begin{bmatrix} Vm_{1i} \\ \frac{Im_{1i}}{2} \\ Vm_{2i} \\ \frac{Im_{2i}}{2} \end{bmatrix} = \left[\begin{array}{cc:cc} A & B & -\Delta A & -\Delta B \\ C & D & -\Delta C & -\Delta D \\ \hdashline -\Delta A & -\Delta B & A & B \\ -\Delta C & -\Delta D & C & D \end{array}\right] \begin{bmatrix} Vm_{1o} \\ -\frac{Im_{1o}}{2} \\ Vm_{2o} \\ -\frac{Im_{2o}}{2} \end{bmatrix} \quad \ldots(21)$$

In deriving equations (21), it has been assumed that the propagation constant for pair i and pair j are approximately equal. Hence the matrix is symmetrical.

Accordingly,

$yp_1 \simeq yp_2 = yp$

$ys_1 \simeq ys_2 = ys$

$$A = \frac{yp + ys}{ys} \qquad \Delta A = \frac{ys(\Delta yp+\Delta ys) - (yp+ys)\Delta ys}{ys^2}$$

$$B = \frac{1}{ys} \qquad \Delta B = \frac{-\Delta ys}{ys^2}$$

$$C = \frac{(yp+ys)^2}{ys} - ys$$

$$\Delta C = \frac{2ys(yp+ys)(\Delta yp+\Delta ys)}{ys^2} \; \frac{-(yp+ys)^2\Delta ys \;\; -ys^2\Delta ys}{ys^2}$$

$$D = \frac{yp+ys}{ys}$$

$$\Delta D = \frac{ys(\Delta yp+\Delta ys) - (yp+ys)\Delta ys}{ys^2}$$

For simplicity, we define:

$$\left[X\right] = \begin{bmatrix} A & B \\ C & D \end{bmatrix} \; ; \; \left[\Delta X\right] = \begin{bmatrix} \Delta A & \Delta B \\ \Delta C & \Delta D \end{bmatrix}$$

from which

$$\left[T\right] = \begin{bmatrix} X & -\Delta X \\ -\Delta X & X \end{bmatrix} \quad \text{and} \quad \left[T\right]^n = \prod_{i=1}^{n}\left[T_i\right] \qquad \ldots(22)$$

Assuming weak couplings ($\Delta X << X$), it can be shown that the transmission matrix for a full cable length ($\ell = n \cdot \ell_{sect}$) is given by:

$$\left[T\right] = \begin{bmatrix} X^n & -\sum_{j=0}^{n-1} X^{n-j-1}\Delta X \cdot X^j \\ -\sum_{j=0}^{n-1} X^{n-j-1}\Delta X \cdot X^j & X^n \end{bmatrix} \qquad \ldots(23)$$

where,

$$X^n = \begin{bmatrix} A' & B' \\ C' & D' \end{bmatrix} \qquad \ldots(24)$$

define the transmission parameters of pair i and pair j

and,

$$\sum_{j=0}^{n-1} X^{n-j-1}\Delta X \cdot X^{j} = \begin{bmatrix} \Delta A' & \Delta B' \\ \Delta C' & \Delta D' \end{bmatrix} \quad \ldots(25)$$

define the crosstalk couplings between pair i and pair j.

The crosstalk model is now complete for a full cable length including propagation effects. Given any arbitrary set of input/output conditions, the overall network response of pair i and pair j are determined from the transmission equations below:

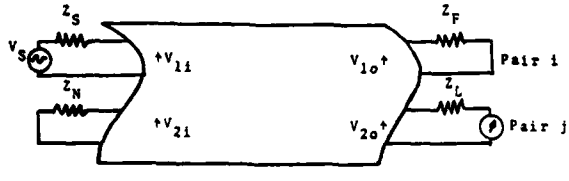
$$\begin{bmatrix} V_{1i} \\ I_{1i} \end{bmatrix} = \begin{bmatrix} A' & B' \\ C' & D' \end{bmatrix} \begin{bmatrix} V_{1o} \\ -I_{1o} \end{bmatrix} + \begin{bmatrix} -\Delta A' & -\Delta B' \\ -\Delta C' & -\Delta D' \end{bmatrix} \begin{bmatrix} V_{2o} \\ -I_{2o} \end{bmatrix} \quad \ldots(26)$$

$$\begin{bmatrix} V_{2i} \\ I_{2i} \end{bmatrix} = \begin{bmatrix} -\Delta A' & -\Delta B' \\ -\Delta C' & -\Delta D' \end{bmatrix} \begin{bmatrix} V_{1o} \\ -I_{1o} \end{bmatrix} + \begin{bmatrix} A' & B' \\ C' & D' \end{bmatrix} \begin{bmatrix} V_{2o} \\ -I_{2o} \end{bmatrix} \quad \ldots(27)$$

## 2.1 *Definitions for FEXT and NEXT*

### 2.1.1 *FEXT*

The cable configuration for Far End Crosstalk measurements is illustrated below:




where, by definition,

$$\text{I/O FEXT} = 20 \log_{10}\left[\frac{V_S}{2V_{2o}}\right] \quad \ldots(28)$$

The final step in the procedure will be to solve for equations (26) and (27) and obtain $V_{1i}$, $V_{2i}$, $V_{1o}$, $V_{2o}$ in terms of source voltage $V_s$ and the boundary conditions defined below:

$$\frac{V_S - V_{1i}}{I_{1i}} = Z_S \qquad \frac{V_{1o}}{-I_{1o}} = Z_F$$

$$\frac{-V_{2i}}{I_{2i}} = Z_N \qquad \frac{V_{2o}}{-I_{2o}} = Z_L \quad \ldots(29)$$

It can be shown that the solutions to the above equations are given by:

$$V_{1i} = \left[\left(A' + \frac{B'}{Z_F}\right)/\left(A' + \frac{B'}{Z_F} + C'Z_S + D'\frac{Z_S}{Z_F}\right)\right]V_S \quad \ldots(30)$$

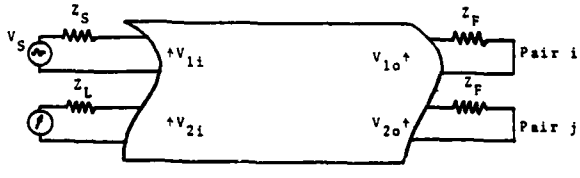
$$V_{2o} = \left[1/\left(A' + \frac{B'}{Z_F} + C'Z_S + D'\frac{Z_S}{Z_F}\right)\right]V_S \quad \ldots(31)$$

$$V_{2i} = \frac{-\left[\left(C'Z_N + D'\frac{Z_N}{Z_L}\right)\left(\Delta A' + \frac{\Delta B'}{Z_F}\right) + \left(A' + \frac{B'}{Z_L}\right)\left(\Delta C'Z_N + \Delta D'\frac{Z_N}{Z_F}\right)\right]V_S}{\left(A' + \frac{B'}{Z_F} + C'Z_S + D'\frac{Z_S}{Z_F}\right)\left(A' + \frac{B'}{Z_L} + C'Z_N + D'\frac{Z_N}{Z_L}\right)} \quad \ldots(32)$$

$$V_{2o} = \frac{\left[\left(\Delta A' + \frac{\Delta B'}{Z_F} + \Delta C'Z_N + \Delta D'\frac{Z_N}{Z_F}\right)V_S\right.}{\left(A' + \frac{B'}{Z_F} + C'Z_S + D'\frac{Z_S}{Z_F}\right)\left(A' + \frac{B'}{Z_L} + C'Z_N + D'\frac{Z_N}{Z_L}\right)} \quad \ldots(33)$$

### 2.1.2 *NEXT*

The cable configuration for Near End Crosstalk measurements is illustrated below:




where, by definition,

$$\text{NEXT} = 20 \log_{10}\left[\frac{V_S}{2V_{2i}}\right] \quad \ldots(34)$$

It can be shown that the solution for NEXT is determined by equations (30) and (32) after setting

$$Z_L = Z_F$$

$$Z_N = Z_L$$

## CONCLUSION

The low frequency crosstalk characteristics of paired cables have been modelled as a function of frequency, cable length, pair-to-pair unbalances and terminating impedances. A distinctive approach was used to develop a general model which takes into account all significant factors influencing crosstalk behaviour. This approach combines transmission line theory and network theory to provide a consistent set of equations for an elemental cable section. From these, complete solutions were obtained for a full cable length at low frequencies. Far End Crosstalk measurements performed on test cables with variable terminations have shown excellent correlation with theoretical results.

The advantages for having such a model are numerous, but can be summarized as follows:

- Since crosstalk varies so much at low frequencies (more than 10 dB variations for different terminations at a single frequency), it becomes impractical to measure and store data for all possible terminations. This model can be used along with a minimal number of measurements ($\Delta$Cpp) to predict accurately crosstalk behaviour under a wide range of conditions.

- Since the effective crosstalk can be calculated for any set of complex terminating impedances, the model can be used to evaluate the performance of new types of paired cable systems.

## ACKNOWLEDGEMENTS

The authors wish to express their gratitude to their colleagues in the cable development laboratory who assisted in the experimental work. In particular, we are grateful for the valuable assistance provided by Drew McDade in the model development.

## References

1. Transmission Systems for Communications, 4th edition, Bell Telephone Laboratories, February 1970, pp. 283-290.

2. T.D. Nantz et al. Characterisation of Crosstalk in Twisted Pair Telephone Cables with non-matched Terminations. Proceedings of 25th IWCS, pp. 100-107.

3. T.D. Nantz & J. Kreutzberg. Precision Insertion Loss Measurements and Data Analysis on Multi-paired Cable. Proceedings of 24th IWCS, November 1975.

4. "Dr. G.A. Campbell's Memoranda of 1907 and 1912", Bell Systems Technical Journal, vol. 14 (Oct. 1935), pp.558-572.



Paul P. Kish received a B.A.Sc. degree in electrical engineering in 1971 and a M.A.Sc. degree in 1972, both from the University of Waterloo, Ontario. He joined Bell-Northern Research and later Northern Telecom Canada Limited as member of Cable Research and Development Staff. He has been working primarily on the design and development of paired communication cables for analog and digital carrier applications. He is presently Manager of Lachine Cable Design, Research and Development, Cable Division.



Yves Le Borgne received a B.Ing. degree in electrical engineering in 1976 from McGill University, Montreal, Quebec. He joined Northern Telecom Canada Limited, Cable Division in April 1978 as member of Research and Development Staff. He has worked on engineering projects related to cable measurement techniques and cable characteristics and has been responsible for the design of pulp insulated exchange cables. In August 1980, he left the company and is presently working with Quantum Management Services Limited in Montreal.

# INSULATION RESISTANCE PROBLEMS AND ITS RELATIONSHIP TO TRANSMISSION

V. Abadía and J.Z. Avalos

CABLES DE COMUNICACIONES, S.A.

## ABSTRACT

A good number of studies have been made concerning the various problems and improvements on capacitance unbalance, crosstalk, control of mutual capacitance, and other critical electrical parameters of telephone cables. However, very few studies have been made about the insulation resistance parameter and its controversial minimum required value on finished telephone cables. In this paper we will attempt to clarify concepts by presenting the insulation resistance (IR) problems expected by different insulating materials, the effect which large IR variations may have on present telephone transmission systems, and the influence, which temperature, voltage, electrification time, water and cable length may have on the obtained value.

## INTRODUCTION

Although the target values of most of the basic transmission parameters have been standardized for a given system, Insulation Resistance values are yet to be standardized. Like most cable manufactures, we have been required to meet widely different IR minimum values, and consequently been exposed to what it seems as many interpretations or criteria of the insulation resistance characteristic. For example, some Administrations place considerable emphasis on requiring high IR values on insulating materials with relatively low volume resistivity, or which because of their processability have undergone a structural change, or just because theoritical calculations show it. On the other hand, other world known telephone institutions have either established a low insulation resistance level or/and make a distinction between filled and unfilled cables as well as on paper pulp, PVC, Nylon, and combination of materials (Dual Insulations). Table 1 shows typical comparative IR values required by some instituions.

TABLE 1

INSULATION RESISTANCE REQUIRED BY SOME SPECIFICATIONS

| COMPANY | MINIMUM INSULATION RESISTANCE AT 20°C - MΩ -Km. | | | |
|---|---|---|---|---|
| | POLYETHYLENE CABLES | | PVC | |
| | AIR CORE | FILLED | CABLES | PAPER |
| A | 16,000 | 1,600 | 1,200 | 1,600 |
| B | 1,600 | 1,600 | | 1,600 |
| C | 6,500 | 1,500* | 50 | |
| D | 10,000 | 5,000 | 100 | |
| E | 16,000 | 1,600 | 600 | |
| F | 35,000 | 35,000 | 150 | |
| G | 1,600 | | | |
| H | 20,000 | 20,000 | 250 | 6,500 |

* Cellular

We can observe that these required minimum values cover a wide range. Moreover, as it will be explain later, IR values lower than those shown above will not necessarily affect the performance of the modern telephone system. But, is there any problem in meeting these values? Obviously, the answer is no. It is not a problem in most cases. With presently available materials and processing methods or techniques, these values are more than exceeded in most cases. However, the values obtained in any given cable or a production run vary in such a way that a few readings may be around 50,000 MΩ-Km. while others around 400,000 MΩ-Km. We have also seen that, under the same environmental conditions, one production plant may report readings on one side of this range while another would yield quite different readings. In any event, although these requirements are usually met, some users are very concerned as to how these widely scattered values would affect their transmission system. One of the attempts of this study is to obtain some possitive information regarding this concern. It should be, of course, possible to process conductors with uniform IR values, however a cable manufacturer would have to implement special processing and quality control methods besides those already implemented

to obtain and control the basic transmission parameters. Taking this extreme step would not only hinder production but would also affect the cable cost.

It should not be construed from the preceeding that we are proposing a radical change in the already established limits. However we would like to make clear that at the present time IR is to some degree unpredictable and that low values or even an occasional failure is not near as alarming as a capacitance or resistance unbalance failure. Of course a reasonable value must be expected because it indicates something about the manufacturer's process and material quality, nevertheless, as it will be explained, drastic changes of insulation resistance do not seem to affect service performance.

## THEORITICAL BACKGROUND

It has already been shown [1,2] that the component which makes IR such a complex parameter to measure is the actual final current. The initial current flowing in the dielectric is made up of 3 components and their sum gradually decays to a steady state value. These three basic components are known as:

a) The charging current - which arises from the material's polarization and is proportional to the cable capacitance or length.

b) The absorption current - which is directly proportional to the insulation losses. The better the dielectric, the higher it is.

c) The leakage current - caused by the materials free ions.

While the first two components decay with time depending on the electrification time, the leakage current remains unchanged from its initial value and will determine the final insulation resistance. A typical set of curves is shown on figure 1.

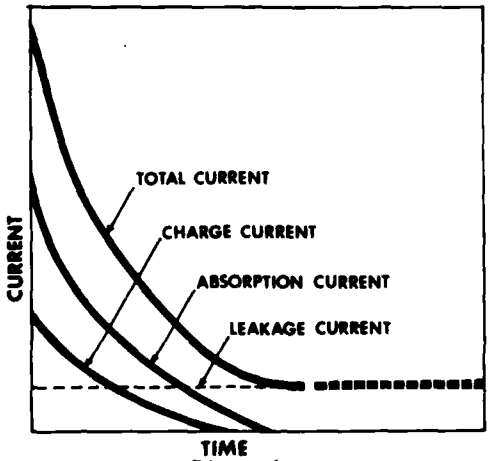



*Figure 1*

*Current Vs. Time*

From these curves, it can be deduced that some materials may need a longer electrification time in order to reach the steady state leakage current to obtain the actual insulation resistance value.

Another useful information is the following expression which sometimes is used to obtain the material's approximated IR value:

$$R_{20} = K \log \frac{D}{d}$$

Where: $R_{20}$ = DC I.R. in MΩ-Km. at 20°C

$K$ = Material constant in MΩ-Km. at 20°C.

$D$ = Diameter over the dielectric

$d$ = Diameter over the conductor

More precisely this expression is derived from the following:

$$R_{20} = \frac{1}{2\pi L} \rho_v \int_{d/2}^{D/2} \frac{dx}{x}$$

$$R_{20} = \frac{1}{2\pi L} \rho_v \ln \frac{D}{d}$$

$$R_{20} = 3.67 \times 10^{-12} \rho_v \log \frac{D}{d}$$

Where: $\rho_v$ = Volume resistivity in Ohms-cm.

As can be observed I.R. is inversely proportional to length. Also since I.R. decreases with increasing temperature, the following expression can be used to obtain values at 20°C.

$$R_{20} = R_t \times 10^{-(20-t)K_1}$$

Where: $R_t$ = I.R. at test temperature t.

$K_1$ = Temperature coefficient of insulating material.

## INSULATION RESISTANCE INFLUENCE ON TRANSMISSION

### 1. THEORICAL ANALYSIS

Whenever there is an insulation resistance problem a question often asked is: How low its value should be before its effects can be detected in a telephone transmission system. To answer this question we developed a simple program to simulate the following insulation resistance failures but keeping all other parameters constant:

- Failure in a cable length
- Failure in a cable splice
- Failure at every splice assuming an equal distance $l$ between splices.

In the first case the pair IR value was decreased until a change on the pair attenuation was detected. Since the conductance losses can be expressed by the following formula, it is possible to increase the conductance by decreasing the insulation resistance.

$$G = \frac{1}{R} + \omega \; pf \; C$$

Where: G = Conductance in micromhos/Km.
R = Insulation resistance in Mohms-Km.
$\omega$ = $2\Pi f$
f = Frecuency en Hertz
C = Mutual capacitance in microfarads/Km.
pf = Power factor of insulating material.

We can see that in order to increase the pair attenuation by 1% at 800 Hz the insulation resistance would have to be much below one MΩ-Km. At higher frequencies the IR would have to be even lower to observe the same effect. Table 2 shows some computed values.

TABLE 2

| MINIMUM IR (MΩ-Km) NECESSARY TO INCREASE THE ATTENUATION VALUE BY 1% | | | | |
|---|---|---|---|---|
| DIAMETER mm. | FREQUENCY IN KHz | | | |
| | 0.8 | 150 | 772 | 1024 |
| 0.405 | 0.192 | 0.004 | 0.002 | 0.002 |
| 0.64 | 0.196 | 0.008 | 0.003 | 0.003 |
| 0.91 | 0.204 | 0.011 | 0.005 | 0.004 |

This data indicates that the IR level would have to be extremely low before the transmission system can be affected.

On the second case we simulated a failure at a "splice point" between two equal lengths of pair. Figure 2 shows the circuit under test.

We first calculated the attenuation increase and then actual measurements were made to verify these values at frequencies of 800 Hz, 150, 772, and 1024 Khz. The shunt resistance was varied from - 10 KΩ to 15 MΩ and the pair length l was 300 meters.

The attenuation did not show any significant increase in any of these configurations.

The third case was a repetition of the second except that five more lengths were spliced with their corresponding resistances to simulate failing conditions. Figure 3 shows the circuit used.

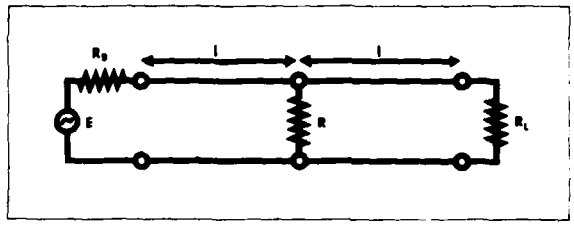



Figure 2

*Circuit to simulate a localized IR failure*

Test results were practically the same, the attenuation was affected when the IR dropped below 10 KΩ. From the foregoing we can say that insulation resistance may cause transmission problems only at very low IR values. In general, IR by itself is a negligible component in transmission if it is not triggered by external agents in which case other parameters will also be affected.

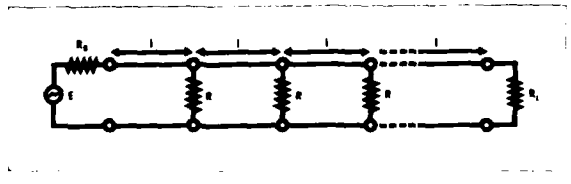



Figure 3

*Circuit to simulate IR failures at several consecutive points.*

*E = Generator*
*l = Cable length*
*Rg = Generator Internal Resistance*
*R = Shunt Variable Resistance*
$R_L$ = *Load Resistance*

## 2. FIELD REPORT

Field data supports to some extent the above conclusions. For example, the insulation resistance of a cable assigned to transmit PCM signals was found to have an extremely low value and there was not any deleterious effect on the transmission quality. Likewise voice frequency transmission cables with IR below 500 MΩ-Km. can be found in service and at the present time no problems have been reported.

However when a transmission problem is reported insulation resistance is the first parameter to be measured. In most of these cases it was found that the IR was very low but mainly due to the high moisture content in the splice case. Of course, other transmission parameters like capacitance and conductance may be also affected. In any event IR is regarded mainly as an alarm system. Therefore, some telephone companies have arbitrarly established a minimum of 1000 MΩ-Km. in their cable maintenance program not because it is an absolute minimum below which transmission problems will occur but because, in our opinion, there is an unknown gap before a low IR, caused by the material or external agents, will affect their transmission system.

## INSULATION RESISTANCE MEASUREMENTS

All the measurements presented in this study were made with a Hewlett Packard Megohmeter type 4329A. Tests were performed to find or ascertain the effect of:

1. Temperature
2. Electrification time
3. Voltage variation
4. Guard terminal conexion
5. Cable length
6. Accelerated aging
7. Water

1. Temperature Cycling: For this test seven cables were placed in a temperature control chamber and tested at temperatures from -30°C to + 70°C at 500 volts and a electrification time of one minute. The insulation types of these cables with lengths varying from 150 to 400 meters were:

   - Solid H.D. Polyethylene filled cable
   - Solid L.D. Polyethylene air core
   - Foam-skin filled cable
   - Cellular filled cable
   - PVC connector cable
   - PVC dumbell drop wire
   - PVC - Nylon Jumper wire

Since our initial and final temperature was 20°C, three readings were actually taken at this temperature. Most materials yielded the same reading when returning to this temperature. As can be observed on figures 4 and 5, all the materials were very much affected when exposed to high temperatures.

It can be seen on Figure 5 that the PVC cables suffer the greatest variations with temperature but were more predictable than the polyethylene insulated cables. Beyond 40°C measurements had to be made at 250 or 100 volts since at the 500 volt setting the pair read like a short circuit. The PVC-Nylon Jumper wire showed the greatest gradient with temperature. This behaviour was expected since nylon tends to absorb moisture more rapidly. At high temperatures it was necessary to drop the test voltage to 50 volts in order to obtain meaningful readings.

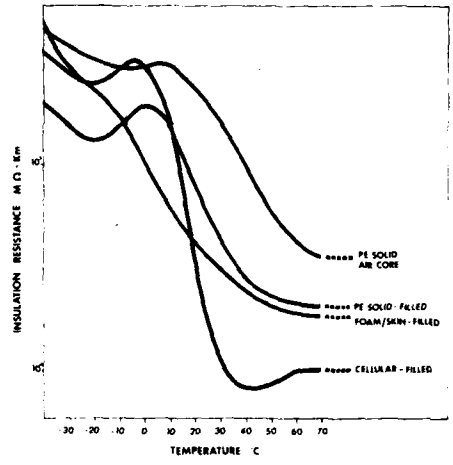



Figure 4

*Insulation Resistance Vs. Temperature for Polyethylene Cables*

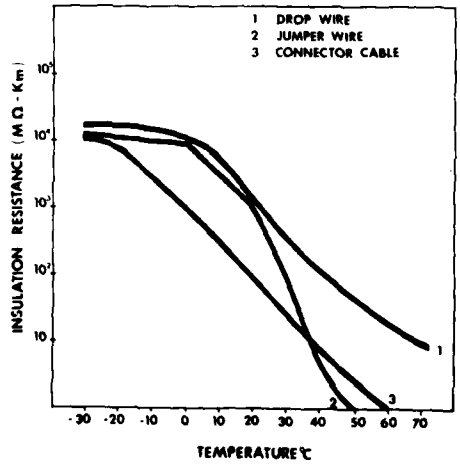



Figure 5

*Insulation Resistance Vs. Temperature for PVC Cables*

On the other hand, the polyethylene cables, except for the foam-skin, had a strange behaviour at temperatures around -5°C. At much lower temperatures the IR began to increase again although at a slower rate. However at temperatures greater than 5°C, the IR decreased as expected and seems to reach a constant value. The reason,on these filled cables, may be that the petroleum jelly absorption is reaching a saturation point and actually approaching the PJ resistivity value. Nonetheless all the polyethylene cables retain a relatively high insulation resistance level at these temperatures. It should be noted that the cellular cables has the lowest IR value while the air core has the highest.

2. Electrification Time: This test was performed in accordance to ASTM D-257 except for the electrification time. We observed that the effect of electrification time is much less pronounced on the raw material than on the finished cable. Figure 6 shows these results on some raw material slabs.

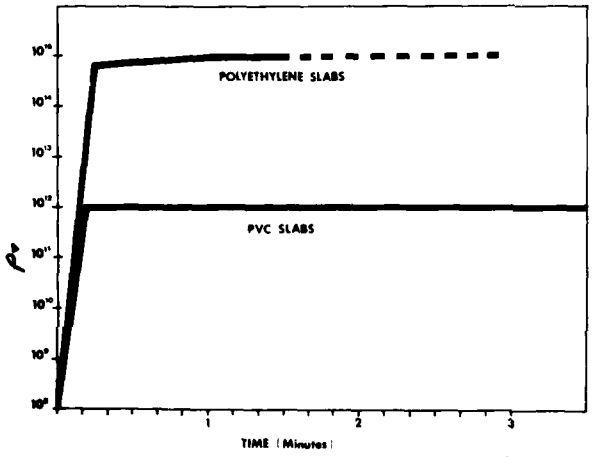



Fig. 6

*Electrification Time Vs. Volume Resistivity on Raw Material Slabs*

As can be observed, the slab specimens reach the steady state leakage current in less than a minute since the relative volume and surface contact are very small if compared to that of an insulated pair. On the other hand, the effect of electrification time on finished cables is slightly more pronounced as shown in Figure 7.

This means that on some materials or type of cables, especially when the requirement to meet is relatively high, there may be a substantial difference on IR value if one can afford the luxury of time. We are not proposing a change on the one minute electrification time but, once again, as it has already been mentioned in our reference 1, it should be understood that electrification time may be an appreciable factor in IR measurements.

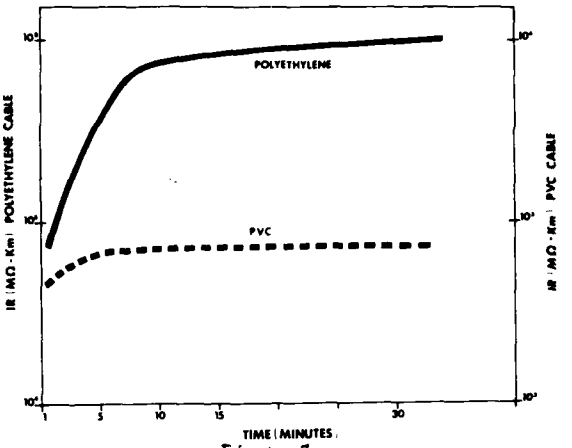



Figure 7

*Electrification Time Vs. Insulation Resistance on Insulated Conductors*

3. Voltage Variation: Insulating materials do not always obey the general definition of Ohm's law because the volume resistivity of most materials depends on the voltage at which it is measured. Our test results seem to ascertain this fact. Any voltage between 100 and 500 volts yields practically the same reading. This is also in agreement with most specifications which require an IR testing voltage of 100 volts minimum and 500 maximum. However at 25 or 50 volts there is an appreciable change in the IR value.

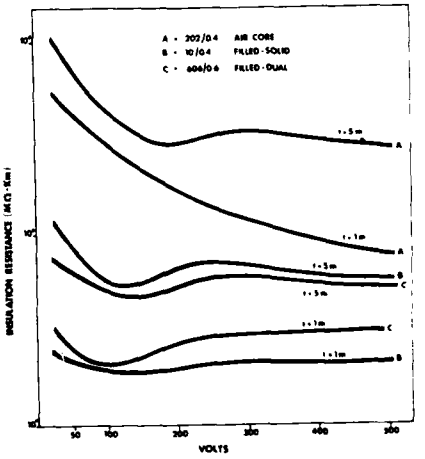



Figure 8

*Insulation Resistance Vs. Voltage*

4. Guard Terminal Conexion: Several ways of guard to insulation conexions were performed with no visible difference on our readings. We concluded that, for telephone cables, insulation resistance measurements would not be affected by leaving this terminal floating.

5. Cable Length: To investigate the effect of cable length, conductor to conductor insulation resistance tests were performed on several pairs. After each test, these pairs were spliced to other pairs in the same cable in order to increase their testing length. Figure 9 shows that when the capacitance of the pair under test is increased the IR decreases. It appears that a saturation charge current is reached after a few lengths have been apliced. The electrification time on each test was one minute. It can be observed that the IR of the air core cable is higher than the filled cables as was expected. However of the two filled cables tested, the 0.6 mm. conductors yields a better IR value than the 0.4 mm. conductors because of the larger space between the conductors.

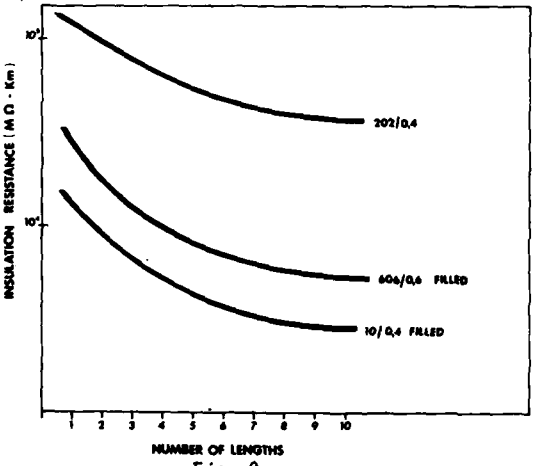



Fig. 9

*Insulation Resistance Vs. Cable Length*

6. Accelerated Aging: One purpose of this test was to find a relationship between aged physical characteristics (Tensile strength, elongation, and melt index) and insulation resistance. Data evaluation shows that such a relationship is very unlikely. However, we observed a substantial IR change after the aged period of 15 days at 80°C. Table 3 shows the average conductor to conductor IR values

Although there was a substantial IR decrease on the immersed samples, the IR of the dry aged samples was hardly affected. It is obvious that the filling compound absorption greatly affects the insulation original IR level. It should be noted that the filling compound volume resistivity is in the order of $10^{13}$ Ω-cm. while polyethylene insulating compounds are greater than $10^{17}$ Ω-cm.

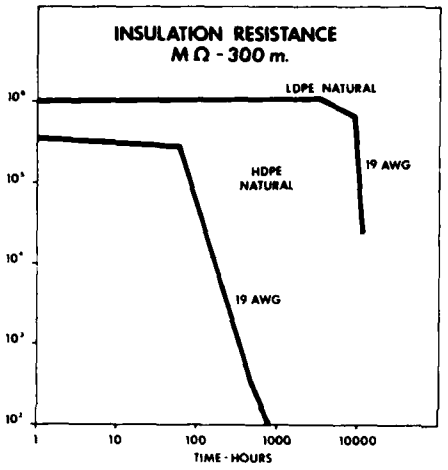
7. Water Effect: Several articles [3,4,5] have already been written on the effects which water and humidity have on insulation resistance. Likewise many kinds of tests were developed to study the IR behaviour under these conditions especially on power cables in which the insulation is under continuous stress. In one of these tests, required on telephone cables, a length of insulated conductor is submerged in water at 75°C while a 600 volt a.c. potential is applied between the conductor and water for 48 hours. At the end of this period the a.c. potential is removed and the insulation resistance measured. Typical curves of this type of test for high and low density polyethylenes can be seen on figure 10. Test results have shown that there is a substantial difference in the IR value depending on the polarity connection. Some specifications require that the positive terminal be connected to the conductor while others specify just the opposite. In some cases, it may mean a passing or failing IR value. We have found that the best IR readings are obtained when the negative lead is connected to the conductor.

In a different type of test, a short length of a dry cable with the core exposed every 20 cm. was submerged in tap water at room temperature alongside a similar length of a filled cable which had been in water for over 18 months. The dry cable

TABLE 3

INSULATION RESISTANCE AFTER AGING

| INSULATION RESISTANCE IN (MΩ-Km.) x 1000 | | | | | |
|---|---|---|---|---|---|
| | | | 15 DAYS AT 80°C | | |
| INSULATION TYPE | ORIGINAL READING IN AIR | AFTER 24 h. IN P.J. | DRY | IMMERSED IN P.J. | PERCENT GAIN IN WEIGHT |
| DUAL | 120 | 50 | 90 | 20 | 16 |
| SOLID | 150 | 45 | 145 | 28 | 9 |




*Water Test at 600 Volt.*

*Fig. 10*

was tested for insulation resistance daily during 50 days. We did not observe and IR change worth mentioning. Although we do not have initial IR data on the filled cable its present level is 30,000 MΩ-Km. In this test, we just verified that monitoring a cable IR may not tell us that water has entered until it is too late and by then other parameters have already triggered the alarm. For example, the mutual capacitance of the air core cable raised to 105 nF/Km. while the conductance measured 2 μυ/Km. in a very few days. Therefore, unless there is a great deal of moisture in a splice case or pedestal, a low IR should not affect the cable life or service performance. However a high level of moisture combined with elevated ambient temperatures will have a detrimental effect on IR. We understand that telephone companies are checking these enviromental harmful agents by properly choosing special cable protections and/or splice closure design.

## CONCLUSIONS

In this study we have been able to verify and/or ascertain the following:

1. The IR level of filled cables is much lower than air core cables because of the PJ absorption. It is more pronounced on cellular than solid insulation.

2. Testing temperature is more critical on filled than on air core cable.

3. Electrification time is an appreciable factor especially on long testing lengths which have more capacitance load. It should be considered on disputable cases.

4. When water enters a polyethylene insulated cable its effect will immediately be felt in the capacitance and conductance values. On the other hand, insulation resistance will remain unchanged during a long time. If very low IR values are found in an installed cable it will probably be caused by water in the splice case.

5. In a normal telephone system and if the amount of moisture is not excessive, low IR values do not seem to affect transmission performance. Of course, a reasonal value should and must be expected but as we have shown there are no solid basis to believe that a pair with a high IR level will yield a better transmission performance than another pair with an IR of less than a thousand megohms.

We understand that there are several other factors affecting IR such as amount of color concentrates, dirt, metallic dust, inclusion of foreign materials, etc. However we have not been able to study their effect.

Lastly, we have seen that Insulation Resistance, a parameter whose value is taken for granted in the normal telephone manufacturing process, remains, to some degree, a complex and unpredictable parameter.

## ACKNOWLEDGEMENT

The authors gratefully acknowledge the colaboration of the C.C.S.A. personnel especially to Messrs. José M. Buil and José Monreal for all the tests performed as well as to a number of people who have kindly helped in this study. We also wish to express our thanks to Miss Maria Luisa Simón for her patience in typing this document.

## REFERENCES

1. "Insulation Resistance Measurements" by E.W. Greenfield, Electrical Engineering, July 1947.

2. "Insulation Resistance and High Potential Testing: Advantages and Limitations" by Harold N. Miller, IEEE Transaction, May/June 1969.

3. "What Moisture Resistance Means in Cable Insulation" by R.C. Graham, Industry and Power, April 1953.

4. "Insulation Resistance Changes in Polyethylene when exposed to high temperature and Humidity" by W.D. Paist, Wire, October 1961.

5. "Insulation Resistance of Polyethylene on Wire-Effect of Heat, Water and Electrical Stress" by C.A. Liddicoat and Benjamin F. Brown, Wire, December 1963.

6. "Investigations of Water Effects on Degradation of Crosslinked Polyethylene Insulated Conductors" by ToshioTabata, Teruo Fukuda, and Zensuke Iwata - IEEE Trans. Power App. and Syst., July/August 1972.



V. Abadía obtained his degree in Telecommunication Engineering in 1974 at the Universidad Politécnica de Madrid. He joined Cables de Comunicaciones S.A. in Zaragoza, Spain, soon after his graduation and is now Manager of the Cable Desing and Engineering Department.



Juan Z. Avalos received his Bachelor in Electrical Engineering and Master in Mechanical Engineering from the City College of New York. Prior to joining Cables de Comunicaciones S.A., Mr. Avalos worked 12 years for General Cable Corp. He is presently working in the Cable Design and Engineering Department in Zaragoza. Mr. Avalos is an IEEE Member.

# THE USE OF TEST DATA AND FIELD DATA IN DESIGNING SPLICE CLOSURES

by Marc Moisson

Telecommunications Division
Raychem Corporation
Kessel-Lo, Belgium

## SUMMARY

Heat shrinkable splice closures have become widely used in telecommunications networks in recent years. The design of a new heat shrinkable splice closure was undertaken, and three major factors were included in its design : existing specifications, predictions of product durability, and field trial data. This paper evaluates existing specifications and includes specific recommendations for improving them. The importance of additional tests to determine product longevity is emphasized, and the significant contribution of field trial data to product design is described.

## INTRODUCTION

The use of heat shrinkable splice closures in telecommunication cable networks has increased several fold in recent years. This overwhelming success is due primarily to the long life, performance and flexibility of heat shrinkable splice closures in an area where reliability is a major concern.

Three major factors influence the design of a durable, reliable, flexible splice closure : specifications, field utility and longevity prediction. Since specifications tend to vary from one country to another depending on local network practices, specifications cannot be the only criteria used in product design. Furthermore, the present American (References 1, 2 and 3), Canadian (Reference 4) and European (Reference 5) specifications tend to emphasize different test methods. In addition, the specifications generally do not include the requirement (Reference 6) for consistent easy installation under field conditions. The product designer also has to take into account the complex relationships between the effects of time and the environment on the strength of the materials he uses. No accepted scientific method exists which enables extrapolation from short duration test results to accurate prediction of a 30-year expected product life.

Considerable effort is being spent to understand the worldwide performance criteria for splice closure systems. This paper reviews the influence of these three factors on the design of a new splice closure system. The paper begins with a presentation of field requirements and the attempts of specifications to reflect those requirements. The implication is that the current specifications are generally inadequate for the prediction of product life. The paper then presents test data generated to predict product lifetime. Next it describes the influence of field trials on product design. Finally it draws a series of conclusions on the relative importance of these three factors.

## SPECIFICATIONS

When a splice closure is put into service in the field, it is exposed to numerous hazardous conditions which it must withstand in order to be a successful product. This portion of the paper describes some of these conditions and their relationship to the existing specifications. The specification requirements which attempt to predict product life are briefly discussed, and other types of tests to predict product life are indicated.

## FIELD CONDITIONS

A splice closure in the field is exposed to hazardous conditions which may be divided into four main sources : (1) the craftsman during the installation of the closure, (2) the craftsman when he is working on other cables in the area, (3) the environment in terms of traffic vibrations and cable travel and (4) the environment in terms of climate. Each of these four sources presents different hazards for the splice closure. When a splice in a manhole, handhole or trench is moved from its assembly location to its permanent location during installation, it subjects the cables at the outlets to a combination of torsion and bending stresses, and it is subjected to tensile and compressive stresses from the cables. The craftsman who is repairing adjacent cables often inadvertently subjects the splice closure to mechanical abuse conditions by standing on the closure or dropping objects onto the closure.

Under these conditions, the closure can be subjected to static bending loading and impact on the case body. Under continuous mechanical stress conditions due to traffic vibration and to cable longitudinal travel, the splice closure often experiences vibration of the system and static load on the cable. Seasonal changes in the environment cause thermal and hydrostatic stresses on the closure system.

## TESTS EMPLOYED

Specifications have been established to attempt to predict the success of a product under field conditions. References 1 through 5 present specifications for splice closure systems. Table 1 provides a comparison of the test requirements of the five specifications. Please note that details on material testing have been omitted from the table; interested readers can consult the references. Representative requirements are given in the specifications REA PE 74 and FTZ 736 627 TV1. Almost all of the tests are aimed at short-term conditions, and they do not test the splice closure's long-term properties. The most notable exception is the temperature cycling test.

The temperature cycling test is apparently the method most favoured for evaluating the long-term behaviour of splice closures. The test is useful in establishing comparative performance trends. Unfortunately, it gives little quantitative guidance regarding the product performance (aging) after exposure to a complex combination of loads over 25 to 30 years.

The relationships between the effects of vibration, temperature variations and other stresses and strains on the product can be very complex. But broad qualitative correlations can be made to give a quantitative prediction of the long-term functionality of the product at static load conditions. The generation of data such as creep and stress-rupture curves at relevant stresses and temperatures in the appropriate media, creep modulus, and impact and tensile strength (Reference 7), are often useful in the engineering design of the closure.

While the tests required by the existing specifications do provide qualitative data for a comparison of candidate splice closures, they do not provide useful engineering data which can be used to predict product life. A number of additional tests have been conducted which do provide the basis for meaningful predictions of long-term product performance under field conditions. Our experimental studies have concentrated on two major areas : the influence of thermal and pressure cycling on the longevity of the closure, and the influence of loads generated by thermal contraction and expansion on the durability of the closure. These tests are discussed below.

## DURABILITY PREDICTIONS

The properties which most heavily influence product life appear to be thermal fatigue and thermal stress. Considerable work has been done in these two areas, and some results of these tests are presented in this section of the paper.

## THERMAL FATIGUE

During the subsequent discussions of these tests, the splice closure will be referred to in terms of the following definitions. The sleeve material will be called the superstrate, the adhesive will be called the bondline and the cable (or, in the case of the tests, the aluminum pipe) will be called the substrate.

In the evaluation of the influence of fatigue testing on the longevity of sleeve material (superstrate) and adhesive (bondline), virgin polyethylene with a density of 0,955 g/cm3 and a polyamide hotmelt were used. These materials were arranged in configurations as shown in Figures 1 and 2. The materials were installed onto aluminum pipes (substrates). Aluminum was chosen because of the highly reproducible nature of its surface with repeated grid blasting and degreasing. Surface oxidation of the aluminum occurs rapidly to form a stable surface. In order to allow pressurization of the samples, slots were made into the pipe.

Since the life expectancy under moderate temperature conditions would impose excessively long test times, the tests were conducted at elevated temperatures. This normal test procedure encounters special problems when used with polymers because polymers tend to have at least one temperature range in which the material does not respond in a predictable manner. This irregularity is caused by one or more of the components of the polymer undergoing a change of state. Earlier test programs on product longevity indicated that if the tests were conducted at temperatures below the susceptible range for that polymer, a consistent relationship existed between temperature and time to failure at a given stress condition. Some results of these tests are shown in Figure 3.

Thermal fatigue data and endurance data at high temperatures (70° C) have also been produced. The data where time at maximum temperature prior to failure for cycled samples is compaired with static temperature failure data for an equivalent high temperature is shown in Figure 4.

In Figure 5 the curve compairing time at maximum stress with fatigue data at an equivalent high stress is presented. It was observed that superstrates fail preferentially during the high temperature part of the cycle, whereas bondline samples failed during the cold part of the cycle.

The data suggests that static failure times at 70° C and cumulative time at 70° C for cycled specimens are similar. From which it can be concluded that time at maximum temperature is the important factor for superstrates. An identical conclusion can be drawn for the stress fatigue samples.

Although bondlines survive longer than superstrates at fixed temperature conditions, in cycling they have failed more rapidly, and as said previously they failed during the cold part of the cycle. This suggests that stress arising from differential thermal expansion and contraction is responsible for bondline failure.

## THERMAL STRESS

Having investigated the behaviour of the superstrate and bondline under thermal fatigue, a further series of tests were conducted to determine the level of stresses occurring at the interfaces of superstrate to adhesive and of adhesive to substrate.

When materials are heated, they usually expand. The temperature coefficient of expansion for most plastics is some ten times greater than that of most metals, and it is not usually linear with temperature. Because of the different properties of the superstrate, adhesive and substrate (e.g. level of cristalinity, moduli, isotropic versus anisotropic behaviour etc.) it is necessary for the design engineer to understand and quantify the level to which thermally generated interfacial stresses are the limiting factor governing product life. To determine this, a given substrate/adhesive/superstrate combination was equipped with strain gauges (Figure 6). Such samples were subsequently subjected to temperature excursions between - 30° C and + 70° C.

The magnitudes of the axial and hoop strains at the three interfaces in the region of the bondline i.e. substrate/adhesive, adhesive/superstrate and superstrate/air are reported in Figures 7 and 8. According to these results, only the adhesive experiences strain (extension/compression).

Further developmental research was performed in the field of material aging, compatibility and design (Reference 10). Results verified that sound material combinations exhibit high performance levels in aging, fatigue and thermal stress testing (References 8 and 9).

From the data it can be concluded that, although there is a sound case for including temperature cycling requirements in a specification, these requirements are insufficient for determining the longevity of a product. The value of the thermal cycling test lies in the fact that it accentuates possible incompatibilities of materials used in a particular product configuration.

From the experimental evidence it is suggested that specifications be completed with additional provisions to ensure that the materials used in manufacturing vital cable accessories comply fully with the standards of the cable material itself.

The following section describes the influence of field trial data on product design.

## FIELD DATA

A specification establishes significant product design parameters, but, as has been noted elsewhere (Reference 11), a specification does not describe all of the conditions which the product must meet. The principal aim of a specification is to reflect field conditions, but the specification cannot indicate the ability of a wide variety of craftsmen to install a product as intended by the designer.

Field trials are very revealing tools for a product designer because the craftsman in the field approaches the product differently than a technician in a laboratory does. Unless the product works under field application conditions, the product will not be successful.

In 1977 the Deutsche Bundespost started a field trial comparison of various splice closure systems. The objective was to find a system which provided improved technical and economic performance. The field trial was conducted in various areas of Germany with numerous craftsmen. The evaluation matrix for these trials is presented in Table II.

## NEW PRODUCT DESIGN

Several significant factors were revealed by these tests. The craftsmen favoured a design which was easy to install. The technical observers favoured a design which was structurally stronger, but which was more difficult to install. This difference of approach led to the development of a new system which was structurally sound and yet which provided flexibility and ease of installation by means of a new branch-off system. This system involves the use of clips with a metal core partially surrounded by hotmelt adhesive. These clips enable the craftsmen in the field to establish up to five branches in the splice, as needed.

## NEW INSTALLATION INSTRUCTIONS

The field trial observations revealed that different craftsmen used a variety of flame lengths, distances of the flame from the product and directions of the flame when applying the splice closure. The most successful flame length, distance from the product and direction of heating were noted.

Computer modelling was later used to determine the optimum heat pattern for the product. Figures 9 and 10 show the different heat diffusion patterns established by heating from different angles.

This combination of field trial observation and computer modelling led to the establishment of uniform installation instructions. These specific and improved installation techniques and the improved product design would not have occurred without the extensive field trials. Thus the field trial input was combined with the specification requirements and the test data to yield a creative solution to the splice closure problem. Figure 11 shows the resulting splice closure.

## CONCLUSION

Three major factors influence the design of a durable, reliable, flexible splice closure : field utility, specifications and longevity predictions. Each of these factors must be considered in the product design. The needs of the craftsman in the field must be met for the product to be a success. Existing specifications include tests designed to measure the product's ability to withstand the conditions it will be exposed to in the field. Although there is a sound case for including temperature cycling requirements in a specification, these requirements are insufficient for determining the longevity of a product. Additional tests must be conducted to determine (1) the influence of thermal and pressure cycling on the longevity of the closure, and (2) the influence of loads generated by thermal contraction and expansion on the durability of the closure. The thermal cycling test can be very valuable in determining possible incompatibilities of materials which would not otherwise be revealed.

## REFERENCES


1. REA specification for encapsulations, splice closures and pressure blocks.
2. GTE specification GTS 8518 for aerial, buried and underground non-metallic splice closures.
3. Product criteria for splice closures AT & T engineering - transmission facilities.
4. Bell northern research document CM 75-2250 test program for buried cable encapsulation systems.
5. Deutsche Bundespost - Verbindungs- und Abzweigmuffen; technische Vorschriften 736 627 TV 1
6. Evolution of direct buried splice closures, W.T. Smith - Telephone engr. and management, September 1979
7. Prediction of fracture, creep and stiffness, characterizations of cable jackets from material properties - M. Yanizeski, Ed Nelson and C.J. Alorsio, I.W.C.S. 1976
8. Raychem document : "Functional testing of VASM closures" - KTR 0069
9. Raychem document : "Cycling performance of VASM closures" - KTR 0114
10. Combined stress aging of adhesive composites - B.J. Lyons - Internal Raychem Corp. document.
11. Laboratory evaluation of buried splice closures N.A. Gac, I.W.C.S. 1978.
12. Heat shrinkable splice cases in the distribution network of the Deutsche Bundespost - G. Schweiger, Proceedings of Intercom 1979.





RAYCHEM N.V.
Diestsesteenweg 692
3200 Kessel-Lo
Belgium
Tel. 016/25 25 44


Mr. Moisson is head of the Telecom Product Development Group and is responsible for the development of cable accessories.

## ACKNOWLEDGEMENTS


The author wishes to express his gratitude for all the people who contributed to the development of this paper. In particular he expresses appreciation to D. Thomas for providing computer data and to M. Keeley for her help in the preparation of the manuscript.

TABLE I

COMPARISON OF INTERNATIONAL REQUIREMENTS FOR UNPRESSURIZED SPLICE CLOSURES

| | BNR TEST PROGRAM | REA SPECIFICATION | GTE SPECIFICATION | AT & T CRITERIA | DBP SPECIFICATION |
|---|---|---|---|---|---|
| Temperature cycle | - 40° C to + 60° C for 10 cycles | Depth 18 in. or more : - 23.3° to 43.3° C<br>For all depths : - 28.9° to 48.9° C<br>Number of cycles : 25 | All closures - 40° to 60° C<br>Number of cycles : 25 | Samples are to be buried under 1 ft of water saturated sand - cycling from - 18° C to 38° C | - 30° to 60° C for 10 cycles while internally pressurized to 40 KPa (5.7 psi.) |
| Insulation resistance (I.R.) | Less than 20% drop in I.R. using an applied voltage of 50 VDC<br>Lowest I.R. value being $8.10^7$ ohms | Not less than $5.10^9$ ohms using an applied voltage of 500 VDC | Not less than $5.10^9$ ohms using an applied voltage of 500 VDC | Not less than $1.10^9$ ohms using an applied voltage of 50 VDC | Relative humidity inside splice case below 30 % after 25 years of exposure in 100 RH environment at 10° C |
| Vibration test | None | 5 - 20 - 5 Hz (in 2 min.) 0.118 in. (2.99 mm) peak amplitude, five times | 10 - 55 - 10 Hz (in 1 min.) 0.03 in. (0.76 mm) peak amplitude, 45 times | None | 10 Hz frequency, 6 mm (0.236 in.) amplitude for 10 days while internally pressurized to 40 KPa (5.7 psi.) |
| Tensile load | None | Tensile load equal to 1/2 the ultimate strength of the cable sheath up to max. load of 250 pounds (1112 N) | Tensile load equal to 1/2 the yield strength of the cable sheath up to max. 250 pounds (1112 N) | A weight of 150 pounds (667 N) shall be placed on each cable for a period of 30 minutes | Force of 1000 N (224 pounds) for cables $\geqslant$ 100 pairs and 750 N (168 pounds) for cables $<$ 100 pairs, this for a period of 5 minutes while internally pressurized to 40 KPa (5.7 psi.) |
| Water submerge | Submerge closure in 3 ft (990 mm) of water at 20° C Apply potential of 50 VDC between tip and ring. | Submerge in water for 48 hours then temperature cycle. | Submerge in 5 in. (127 mm) of water for 20 days. A second test requires submerging the assembly in cool water for 4 hours with one cable end vented. | Submerge closure in 3 in. (76.2 mm) of water and provide a water entrance into the closure with a 5 in. (127 mm) head of water acting on the splice encapsulant. Immersion period : 30 days. | Submerge closure in water at 23° C for 15 minutes while pressurized internally at 40 KPa (5.7 psi.) |
| Impact | None | None | 1 pound (0.445 kg) weight with a diameter of 1 in. (25.4 mm) dropped onto the closure from a height of 3 ft (990 mm) at a temperature of - 40° C | Weight of 5 pounds (2.23 kg) dropped onto the closure from a height of 24 in. (610 mm) at temperatures of - 18° C and 38° C | Weight of 0.5 kg (1.12 pounds) dropped onto closure from 2 m (6.06 ft) at 23° C Sample is internally pressurized to 40 KPa (5.7 psi.) |
| Static load | None | None | None | 200 pounds (89 kg) for 15 min., weight is distributed over total length of closure. Temperatures - 18° C and 38° C | A load of 1000 N (224 pounds) on 25 cm2 (9.8 sq. in.) while splice case is internally pressurized to 40 KPa (5.7 psi.) |
| Axial compression | None | None | None | None | 700 N (157 pounds) for cables $\geqslant$ 100 pairs and 50 N (112 pounds) for cables $<$ 100 pairs for 5 minutes while internally pressurized to 40 KPa (5.7 psi.) |
| Flexure | None | None | None | None | 45° for 5 min. in each of 2 directions while internally pressurized to 40 KPa (5.7 psi.) |
| Torsion | None | None | None | None | 90° for 5 min. in each of 2 directions while internally pressurized to 40 KPa (5.7 psi.) |

TABLE II

EVALUATION MATRIX FOR THE EXPERIMENTS OF SPLICE CLOSURES

| | | Items | A * | B | C | D | E | F | G |
|---|---|---|---|---|---|---|---|---|---|
| 1 | Cable installation | Preparation | | | | | | | |
| 2 | | Jacket cutting | | - | | | | | |
| 3 | | Cable sealing | | | | | | | |
| 4 | | Vacuum seal | | | | | | | |
| 5 | | Cable support | | | | | | | |
| 6 | | Time consumption | | | | | | | |
| | | Block marking & sequencing | | | | | | | |
| 1 | Capacity | AVH | | | | | | | |
| 2 | | Twisting | | | | | | | |
| 3 | | Combination | | | | | | | |
| | | Block marking & sequencing | | | | | | | |
| 1 | Overlapping | A-PM2Y | | | | | | | |
| 2 | | A-PWE2Y | | | | | | | |
| 3 | | A-2YF(L)2Y | | | | | | | |
| 4 | | Time consumption combination 1 or 2 with 3 | | | | | | | |
| 5 | Cut length | A-PM2Y | | | | | | | |
| 6 | | A-PWE2Y | | | | | | | |
| 7 | | A-2YF(L)2Y | | | | | | | |
| 8 | | Time consumption combination 5 or 6 with 7 | | | | | | | |
| | | Block marking & sequencing | | | | | | | |
| 1 | Closure install. | Sealing material | | | | | | | |
| 2 | | Installation | | | | | | | |
| 3 | | Tooling, energy | | | | | | | |
| 4 | | Sealing control | | | | | | | |
| 5 | | Time consumption | | | | | | | |
| | | Block marking & sequencing | | | | | | | |
| 1 | Re-entry | Re-opening | | | | | | | |
| 2 | | Tooling, energy | | | | | | | |
| 3 | | Cleaning | | | | | | | |
| 4 | | Technical concept - necessary spare parts | | | | | | | |
| 5 | | Time consumption | | | | | | | |
| | | Block marking & sequencing | | | | | | | |
| | | Sequencing - total marking | | | | | | | |
| 1 | Generally | Handling | | | | | | | |
| 2 | | Installation instructions | | | | | | | |
| 3 | | Number of types | | | | | | | |
| | | Total time for installation | | | | | | | |

* A - G : indicate seven different types of splice closures

Estimation notes :

1 = very good 2 = good 3 = satisfactory 4 = sufficient 5 = insufficient

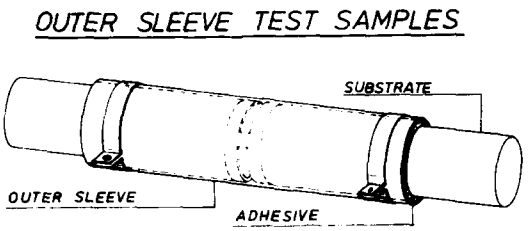



Fig. 1 : Test sample configuration for outer sleeve (superstrate), thermal and hydraulic fatigue and constant temperature testing

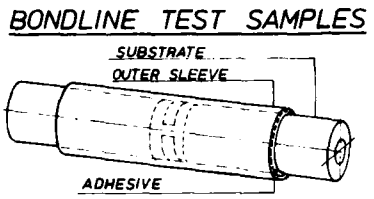



Fig. 2 : Test sample configuration for adhesive (bondline), thermal fatigue and constant temperature testing

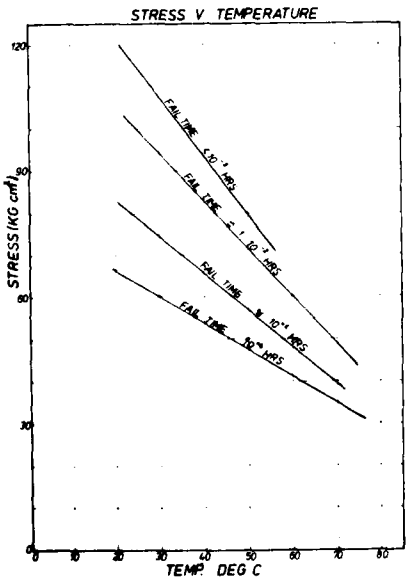



Fig. 3 : Relation between temperature and time to failure for outer sleeve (superstrate) samples

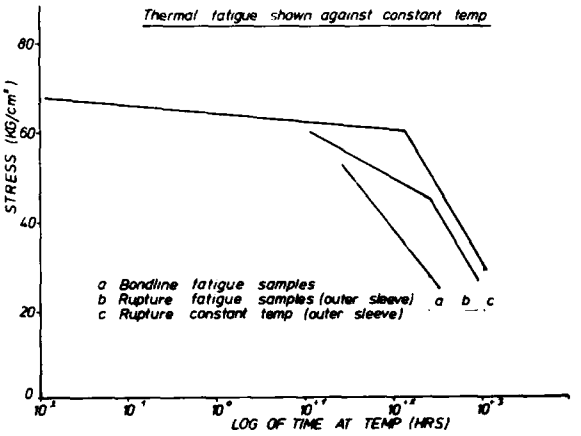



Fig. 4 : Comparison of constant temperature and fatigue data

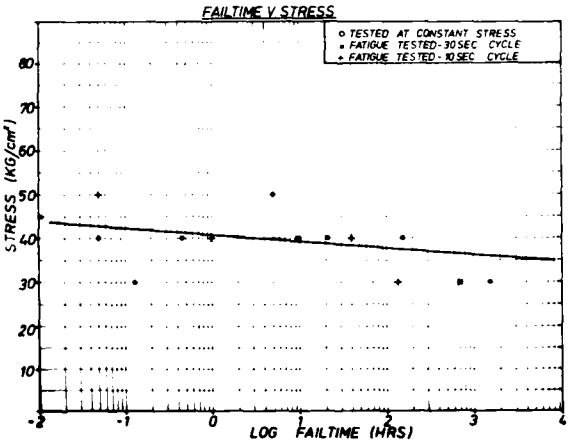
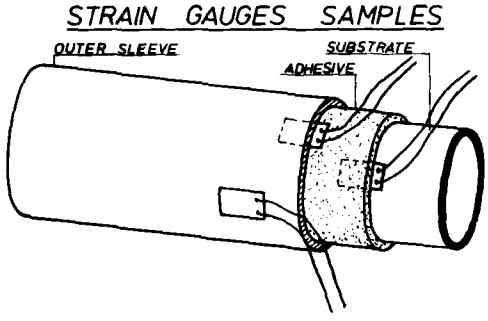



Fig. 5 : Comparison of constant stress and fatigue data



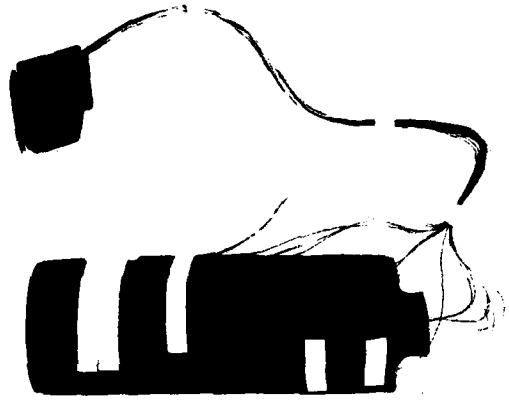



Fig. 6 : Test sample construction for thermal stress analysis

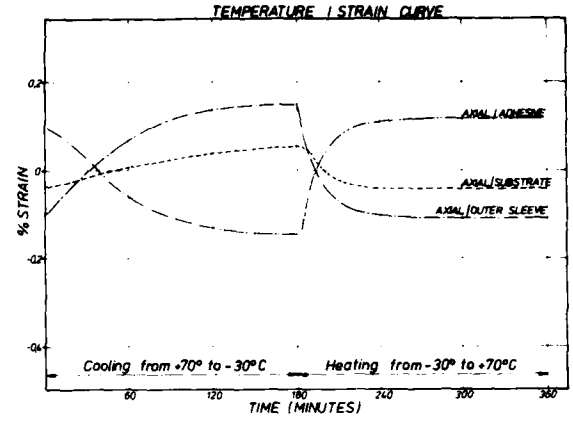



Fig. 7 : Magnitude of axial strain in outer sleeve, adhesive and substrate during temperature cycling

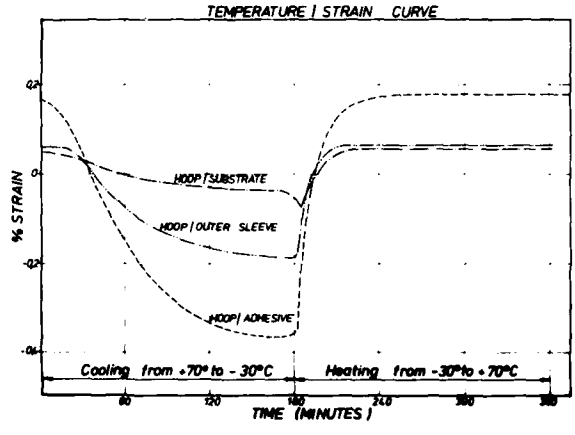



Fig. 8 : Magnitude of hoop strain in outer sleeve, adhesive and substrate during temperature cycling

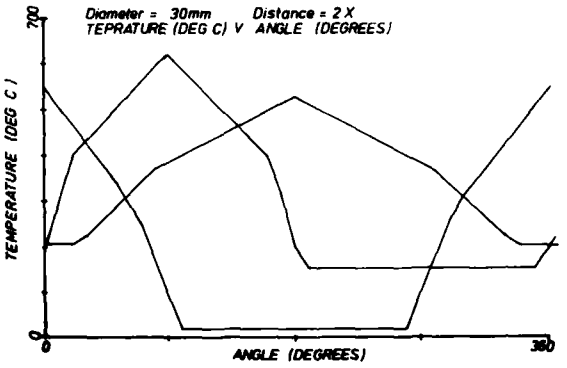



Fig. 9 : Air temperatures around a sample with a diameter of 30 mm. The propane torch being held in different positions around the test sample



Fig. 11 : Heatshrinkable wraparound splice closure

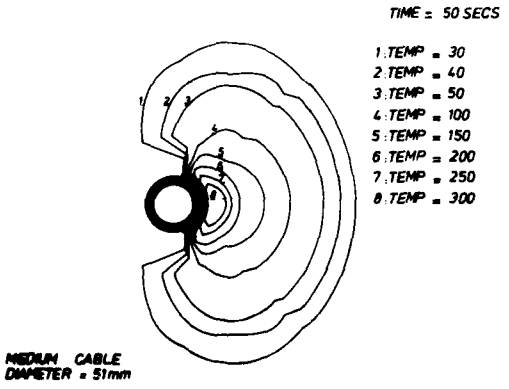



Fig. 10 : Air temperatures around a cable/ adhesive/outer sleeve combination. The propane torch being held under an angle of 90° perpendicular to the axis of the sample

# NON-COATED BONDABLE POLYIMIDE/FLUOROCARBON TAPE INSULATION FOR LIGHTWEIGHT ELECTRICAL WIRE

ALVIN T. SHEPPARD

MARTIN MARIETTA AEROSPACE
MICHOUD OPERATIONS

## SUMMARY

This report covers the detail studies leading to the selection and configuration of insulating materials for the electrical wire and cable to be used on the outside surfaces of the Space Shuttle External Tanks. Environmental capability as well as electrical characteristics and weight were used to establish criteria for material selection with flexibility, abrasion resistance and adhesive bondability being determining factors for configuration. The resulting configuration consists of two crosswrapped (with 50% minimum overlap) polyimide/fluorocarbon (fluorinated ethylene propylene) tapes applied such that the outside tape exposes an uncoated layer of polyimide film as the insulation surface.

## INTRODUCTION

Studies conducted on wire and cable fabrication for the weight savings phase of the Space Shuttle External Tanks Program have resulted in a redesign of the insulation configuration for electrical conductors to be used on the External Tank surfaces. The new design offers greater reliability in mechanical properties and sealing and adhesive bonding capabilities with little or no change in electrical characteristics, conductor diameters and weight while decreasing processing time and high temperature exposure during fabrication.

## DISCUSSION

The insulation configuration previously used for the External Tank electrical wiring consisted of double cross-wrapped polyimide-fluorocarbon film tapes with an outside coating of aromatic polyimide resin as specified in MIL-W-83181/8 and /10 (Wire, Electric, Polyimide-Insulated, Copper or Copper Alloy). The films for this construction were composed of polyimide film coated on both sides with Fluorinated Ethylene Propylene (FEP). The FEP was used to provide a heat-sealable structure for fabrication purposes, but with the FEP on the outer surface of the insulation, that surface must be treated to provide a bondable substrate for the addition of the polyimide finish coating.[3] During processing of the finished coating, the film-wrapped conductor may be subjected to five or six exposures at temperatures as high as +900°F to provide proper cure and thickness.

## HISTORY

The aromatic polyimide adhesive coating is found by laboratory evaluations to be inherently weaker than a polyimide film surface for adhesive bonding, potting and sealing applications. Comparisons of FEP/Polyimide film insulated conductors with FEP/Polyimide adhesive coated conductors for overall characteristics revealed other disadvantages of the polyimide coating during early studies of the light weight wire insulations (see Table I). Typical early constructions (see Table II) did not incorporate the polyimide coating, but rather utilized a fluorocarbon dispersion coating for added protection.[1] The more recent configurations of the MIL-W-81381 added the polyimide over the thinner polyimide-fluorocarbon films to provide radiation protection, abrasion resistance and adhesive bondability which was not sensitive to environmental exposure. The addition of the adhesive coat resulted in the need for rigorously controlled processes for surface treatment, coating application and cure, as well as adding new tests for coating thickness, uniformity, adherence and cure.

TABLE I

THIN-WALL CANDIDATES

| WIRE TYPE | FEP-H-FILM* | FEP-POLYIMIDE PYRE ML COATING* |
|---|---|---|
| Insulation Thickness, inch (nom.) | 0.006 | 0.007 |
| O.D. of No. 24 AWG wire, inch | 0.036 | 0.038 |
| Mandrel Wrap (1 x diam.) | Wrinkles, minor delamination | Slight coating wrinkling on inside |
| Soldering minimum heating | No insulation damage | No insulation damage |
| Soldering excessive heating | " | " " " |
| Solder Iron Contact (5 sec.) Insulation Cold Flow, room temp., .015 inch radius edge, grams withstand 24 hours | No damage Exceeds 15,000 | No damage 2400 |
| Insulation Cold Flow, 160°F .015 inch radius edge, gram withstand 24 hours | Exceeds 10,000 | 1700 |
| Low temp. bend (-68°F) | Satisfactory | Satisfactory |
| Flexing Cycles to first 2 failures | 14108 21618 | 2260 3344 |
| Mandrel heat aging 225°F, 1/8 in. diam., 1 lb. weight | Satisfactory | Satisfactory |
| Thermal strippability (Rheostat setting) | Conductor strands fray when insulation removed (high heat 9, 10) | Satisfactory (medium to high 5, 6, 7, 8) |
| Marking, Kingsley | Satisfactory | Satisfactory |
| Bondability Average pull in lbs., 5 samples | 18.6 | 8.6 |

Exerpt from "Polyimides Plastics: A State-of-the-Art Report" by John T. Milek, Hughes Aircraft Company, dated October 1, 1965.[1]

*Kapton "H", "F" and PYRE ML are registered trademarks of materials offered by Dupont.

TABLE II

MIL-W-81381 INSULATION CONSTRUCTIONS

| SPEC. NO. MIL-W-81381/ | TAPE CODES (1) | (2) | (3) | OUTSIDE COATING | INSULATION THICKNESS |
|---|---|---|---|---|---|
| 1, 2, 5 & 6 | 0/1/.5 | .5/1/.5 | | FEP Dispersion | 7.5 Mils |
| 3, 4 | 0/2/1 | .5/2/.5 | | FEP Dispersion | 12.5 Mils |
| | 0/1/1 | .5/2/.5 | .5/2/.5 | TFE Tape | 20.0 Mils |
| 7, 8, 9, 10, 21 | .1/1/.1 | .1/1/.1 | | Polyimide | 5.8 Mils |
| 11, 12, 13, 14 | 0/2/.5 | .1/1/.1 | | Polyimide | 8.4 Mils |
| | 9/2/.5 | .5/1/.5 | .1/1/.1 | TFE Tape | 15.4 Mils |
| 15, 16 | | | | CANCELLED | ---- ---- |
| 17, 18, 19, 20 | .1/1/.1 | | | Polyimide | 4.6 Mils |
| 22 | 0/2/.5 | .1/1/.1 | | Polyimide | 8.4 Mils |
| | 0/2/.5 | .5/1/.5 | | Polyamide Braid with Clear Finisher Coat. | 15.4 Mils |

MIL-W-81381/1 through 16 are inactive for new design, and MIL-W-81381/15 and /16 are cancelled. All tape layers are 50% overlap minimum, except for MIL-W-81381/17 through /20 which requires a 67% minimum overlap for the single tape. Polytetrafluoroethylene (TFE) tape is a wrapped construction over the primary film insulation which requires sintering for adherence.

When two or more tapes are used in the construction, the tape layers are cross-wrapped to provide better sealing, abrasion protection and flexibility. See Table III for Kapton "F" film designations as specified in MIL-W-81381.

TABLE III

KAPTON "F" FILM CONSTRUCTIONS[2]

| FILM CODE | NOM. TH. MILS | TEFLON FEP | KAPTON TYPE H | TEFLON FEP | STD. WIDTH W X L, IN. | AREA FACT. $Ft^2/lb$ |
|---|---|---|---|---|---|---|
| 616A | 1.2 | 0.1 | 1.0 | 0.1* | 3/16 X 18 | 103 |
| 616 | 1.2 | 0.1 | 1.0 | 0.1 | 3/16 X 18 | 103 |
| 019 | 1.5 | 0 | 1.0 | 0.5 | 3/16 X 18 | 77 |
| 919 | 2.0 | 0.5 | 1.0 | 0.5 | 3/16 X 18 | 54 |
| 011 | 2.0 | 0 | 1.0 | 1.0 | 3/16 X 18 | 54 |
| 929 | 3.0 | 0.5 | 2.0 | 0.5 | 3/16 X 18 | 39 |
| 021 | 3.0 | 0 | 2.0 | 1.0 | 3/16 X 18 | 39 |
| 022 | 4.0 | 0 | 2.0 | 2.0 | 3/16 X 18 | 27 |
| 031 | 4.0 | 0 | 3.0 | 1.0 | 3/16 X 18 | 30 |
| 131 | 5.0 | 1.0 | 3.0 | 1.0 | 3/16 X 18 | 23 |
| 051 | 6.0 | 0 | 5.0 | 1.0 | 1/2 X 18 | 21 |

*Controlled tolerance (a) to prevent FEP from entering the wire strands during the heat sealing of the insulation tape(s). This is useful for conductor sizes less than 22 AWG.

## PROCESSING

Processing of the tape surface for the coating and for the application and cure of that coating is critical in that:

1. The surface must be uniformly treated for adhesive bondability.
2. The materials introduced for treating and the resultant residues must be removed.
3. The polyimide coating must be evenly applied to provide a smooth unbroken cover over the surface.
4. The coating must be properly cured and adhere well to the surface in order to provide good mechanical, adhesive and electrical properties.

Improper processing during any one of these four applications will result in poor surface adherence and eventual coating failure. When this occurs, the conductor insulation will lose the capability to be adhesively sealed or bonded and the adhesive coating will particulate or flake off of the conductor surface resulting in contamination of surrounding areas.

## SOLUTION

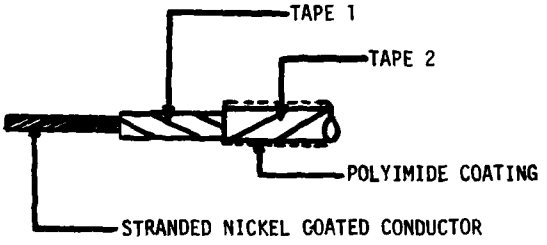
The optimum tape wrap construction has been established for MIL-W-81381 utilizing two tapes, each have a 50% overlap and applied in reverse cross-wrap to the other (see Figure 1). Besides being one of the simplest lay-ups to fabricate, the configuration provides the cross-wrap for maximum flexibility and a four layer thickness for abrasion protection. By substituting a Kapton "F" 019 film tape for the outside tape, Kapton "H" polyimide film will be exposed on the outside layer of the insulation and no additional treatment or coating is required for surface bondability (see Figure 2). Mechanical and operational characteristics are essentially unchanged while:

1. Wet processing (etching or other surface treatment) is no longer required.
2. Cleaning, adhesive applications and curing steps are unnecessary.
3. Abrasion protection and adhesive bonding capabilities are improved.
4. Contamination problems with adhesive coatings are eliminated.

## TESTING AND FEASIBILITY

Adhesive Bondability: Individual conductors as well as cables were used in adhesive bonding tests to evaluate adhesive types for bonding wire and cable to the External Tanks' surfaces. The bonded assemblies were subjected to tensile, shear and peel forces over a temperature range of -253°C to +200°C. The types of conductor and cable insulations included etched Teflon (FEP), polyimide coated Kapton "F" film with Kapton "H" outside surface. Of all the types tested, the conductors and cables having the exposed Kapton "H" surface provided higher bond strengths with bond factors of a minimum 3 to 1 for polyurethane adhesives to as high as 15 to 1 for epoxies. The normal modes of failure were: adhesive for etched and coated conductors, cohesive for the Kapton "H" surfaces.[4]

Physical and Operational: The new insulation configuration is the same as that presently used for MIL-C-27500 cables requiring overall jackets designated by jacket symbol 12. Cables of this configuration have met the environmental and operational requirements established for the External Tanks.




CONDUCTOR: AWG 22 and smaller are constructed of nickel coated high strength copper alloy.

AWG 20 and larger are constructed of nickel coated copper.

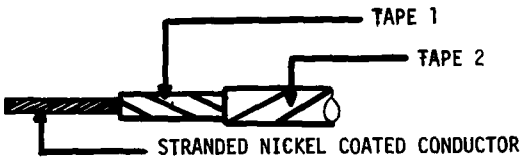
TAPE 1 & 2: 616 Kapton "F" film, 50% minimum overlap. Reverse cross-wrap construction. 616 is 0.1 mil FEP/1 mil Kapton/0.1 mil FEP.

COATING: Polyimide Resin, 0.0005 inch thickness.

SPECIFIC GRAVITIES: Film, 1.55; Resin, 1.42.

INSULATION THICKNESS: Minimum 0.0045 inch; Maximum 0.0071 inch.

FIGURE 1 - PREVIOUS CONFIGURATION




CONDUCTOR: AWG 22 and smaller are constructed of nickel coated high strength copper alloy 135.

AWG 20 and larger are constructed of nickel coated copper, ASTM B355.

TAPE 1: 616 Kapton "F" film, 50% minimum overlap. 616 is 0.1 mil FEP/1 mil Kapton/ 0.5 mil FEP.

TAPE 2: 019 Kapton "F" film, 50% minimum overlap, reverse cross-wrapped over Tape 1 with FEP side of film facing to Tape 1 to leave uncoated Kapton on outside surface.
019 is 1 mil Kapton/0.5 mil FEP.

COATING: None.

SPECIFIC GRAVITIES: 616 Tape, 1.55: 019 Tape, 1.67.

INSULATION THICKNESS: Minimum 0.0045 inch; Maximum 0.0063 inch.

FIGURE 2 - NEW CONFIGURATION

COMPARISON

Using maximum allowable dimensions for wire size, films and coating, the old and new configurations for AWG 22 through 12 compare as follows:

| COND. AWG | COND. DIA. INCHES | INSUL. DIA. OLD | INSUL. DIA. NEW | DIMENSIONAL DIFFERENCE |
|---|---|---|---|---|
| 22 | 0.033 | 0.047 | 0.045 | 0.002 |
| 20 | 0.042 | 0.056 | 0.054 | 0.002 |
| 18 | 0.052 | 0.066 | 0.064 | 0.002 |
| 16 | 0.058 | 0.072 | 0.070 | 0.002 |
| 14 | 0.073 | 0.087 | 0.085 | 0.002 |
| 12 | 0.091 | 0.105 | 0.103 | 0.002 |

| COND. | WT. LBS/MFT | WT. LBS/MFT | WEIGHT DIFFERENCE |
|---|---|---|---|
| 22 | 0.589 | 0.547 | 0.042 |
| 20 | 0.721 | 0.672 | 0.049 |
| 18 | 0.869 | 0.810 | 0.059 |
| 16 | 0.957 | 0.894 | 0.063 |
| 14 | 1.178 | 1.102 | 0.076 |
| 12 | 1.443 | 1.351 | 0.092 |

Specification MIL-W-81381 Requirements

All requirements are the same for both constructions, except, the new configuration does not require:

1. Insulation coating or tape jacket defects inspection.
2. Polyimide cure test.
3. Coating Durability test.
4. Coating Thickness measurements.
5. Wet processing to prepare surfaces for adhesive bonding.

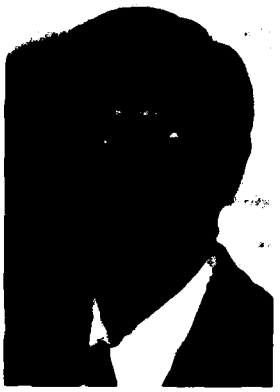
## BIBLIOGRAPHY

[1]AIR FORCE MATERIALS LABORATORY. Polyimide Plastics: A State-of-the-Art Report. Contract AF33(615)-2460, Project 7381: Task 738103, dated October 1, 1965.

[2]E. I. DUPONT DE NEMOURS & CO. (INC.) FILM DEPARTMENT. "Kapton" Polyimide Film-Type F Summary of Properties. Bulletin F-1C.

[3]TENSOLITE COMPANY DIVISION OF CARLISLE CORPORATION. Aircraft, Missile and Space Vehicle Wiring. Bulletin 115.

[4]Crockett, R. R. and G. Voida. Bonding Strength of Encapsulating Materials to Hookup Wire. INSULATION/CIRCUITS, April, 1970.



ALVIN T. SHEPPARD
Senior Materials Engineer
Department 3516
Martin Marietta Corp.
P. O. Box 29304
New Orleans, LA 70189

Mr. Sheppard is presently the responsible electrical materials and process engineer for the Space Shuttle External Tanks. His experience includes engineering support for electrical materials and process specifications in such programs as Titan, Skylab and Viking at Martin Marietta, as well as design, research, development and implementation of test instrumentation for Cryogenic, Exotic and Solid propellant fuel systems used during the Gemini, Saturn and Apollo programs at Rocketdyne.

# TELECOMMUNICATION CABLE SPLICING METHOD USING A NEW HEAT SHRINKABLE SLEEVE

K. Yokoyama*, N. Sato**, S. Goto**, M. Makiyo** and S. Mase**

* The Tokyo Electric Power, Co., Inc. Tokyo Japan
** The Fujikura Cable Works, Ltd. Tokyo Japan

## SUMMARY

Heat shrinkable sleeves are widely used for polyethylene sheath splicing, but the long term reliability is not sufficient because they use hot melt adhesive.

In the present paper, the new remarkable splicing method used for thermo-welding type heat shrinkable sleeve and its properties are described. The new sleeve consists of two layers, the inner layer is non-crosslinked polyethylene and the outer layer is crosslinked and stretched polyethylene. So that this sleeve is welded together with polyethylene sheath completely and such properties as airtightness, watertightness and mechanical strength are excellent.

This method can be accomplished surely even by the unskilled operator with heating apparatus such as torch lamp or exclusive electric heater.

## 1 INTRODUCTION

Various kinds of splicing method for polyethylene sheathed telephone cable have been developed and used in practice. However, it is considered that satisfactory splicing method which satisfies long term reliability and workability, has not been established yet at present.

Recently we have developed the new splicing method using the very remarkable heat shrinkable sleeve. Heat shrinkable sleeve has been utilized widely at present, because of easiness of splicing work, shorter working time, and less splicing materials. However, it is considered that reliability of splicing methods using these heat shrinkable sleeves is not always satisfactory, particulary at the high temperature, because adhesive strength is incomplete due to the hot melt adhesive coated inside of the heat shrinkable sleeve. In the present paper, the new splicing method is described using the remarkable heat shrinkable sleeve which can be welded with cable sheath without using any hot melt adhesive.

## 2 FEATURES OF NEW HEAT SHRINKABLE SLEEVE AND SPLICING METHOD

Conventional heat shrinkable sleeve is bonded to a cable sheath with hot melt adhesive. But it is difficult to bond polyethylene surely with adhesive because of its chemical property, therefore reliability of the cable splice is not sufficient. To guarantee the long term reliability of the cable splice, welding is the best way. However, the shrinkable sleeve is difficult to be directly welded to the cable. So all efforts were made to solve this problem, and as a result the heat shrinkable sleeve which can be welded to cable sheath has been developed. This sleeve consists of two layers, namely, outer layer is crosslinked and stretched polyethylene and inner layer is a little high melt flow polyethylene comparing to that of cable sheath, both layers are completely welded together in manufacturing of the shrinkable sleeve.

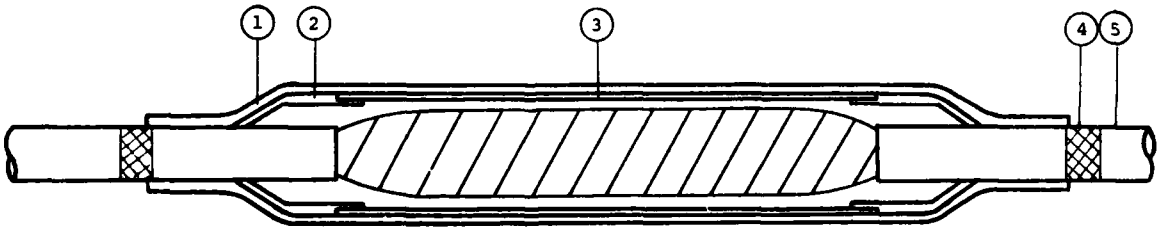



Figure 1

Longitudinal Section View of the Cable Splice

1. Heat Shrinkable Sleeve
2. Reducer
3. Aluminum Sleeve
4. Adhesive Glass Tape
5. Polyethylene Sheathed Cable

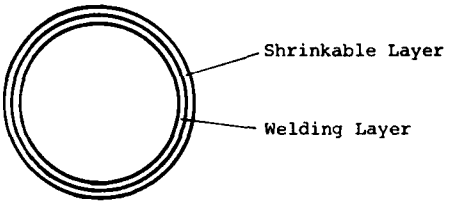



Figure 2

Cross section View
of the New Heat Shrinkable Sleeve

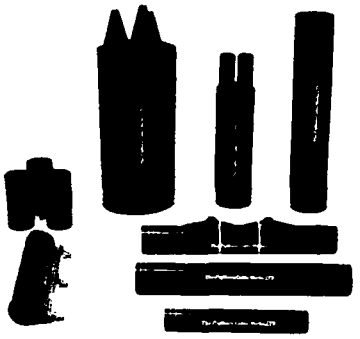


Photo. 1

Various Types of New Heat
Shrinksble Sleeve

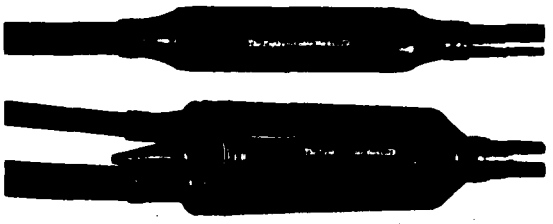


Photo. 2

Cable Splice

## 3 REQUIREMENTS FOR WELDING POLYETHYLENE SHEATH AND HEAT SHRINKABLE SLEEVE

### 3.1 PRESSURE REQUIREMENT FOR WELDING

Pressure between polyethylene sheath and heat shrinkable sleeve is due to radius direction stress by the shrink of heat shrinkable sleeve. If the stress is too large, it causes a constriction on the sheath, so the value of the stress must be designed less than about 300 g/cm$^2$. The inner layer material of the sleeve is very important, because the welding between the sheath and the sleeve must be achieved under limited pressure. An experiment was made to estimate the value of pressure required for welding sheath grade polyethylene mutually. Two sheets of sheath grade polyethylene, with 1 mm thickness, surface brushed, are put one upon another, and are set to an apparatus preheated to 140 °C as shown in Figure 3 . Then, this unit is placed into an 210 °C air oven. When the temperature of polyethylene sheets interface has reached 140 °C, a load which gives 10~100 g/cm$^2$ pressure to the sheets is put on. After 5 minutes, the unit is taken out,put off the load, and is cooled at room temperature, peeling test is done for this sample, with 10 mm width and 100 mm/min. peeling speed.

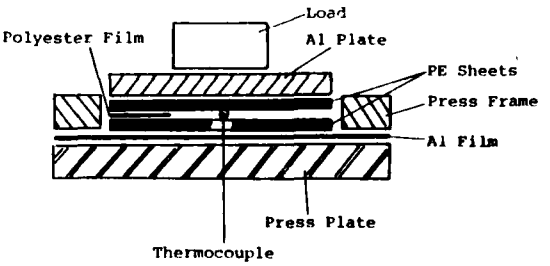



Figure 3

Apparatus to Estimate the Value of
Pressure for PE Sheets to Weld

The results are shown in Figure 4 . At this experimental condition, it occures an interface failure even with 100 g/cm$^2$ pressure, and cohesive failure (breaking of sample), which may be obtained in case of fully welding, is not achieved. So, several EVA copolymers was selected which had slightly lower melting point than sheath grade polyethylene, and tested the welding easiness with sheath grade polyethylene by the same method above mentioned. The lower the melting point of polyethylene goes down, the easier the welding is achieved, but heat resistance also falls. Welding property of the copolymer, which has been selected from several EVA copolymers considering the balance of welding easiness and heat resistance to sheath grade polyethylene is also shown in Figure 4 . In this case peeling strength is stable even at 10 g/cm$^2$ pressure and sample breaking occures more than 30 g/cm$^2$ pressure. So, by using this copolymer, welding can be achidved with pressure more than this value.

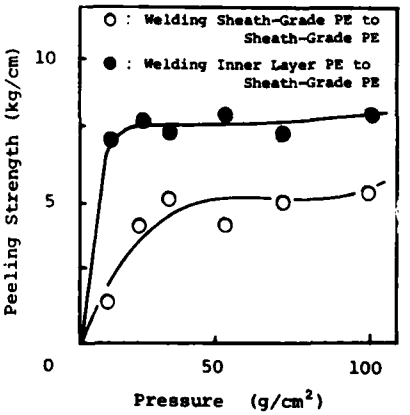



Figure 4 Pressure Dependence of Peeling Strength

### 3.2 SHRINK STRESS AND SHRINK RATE

Shrink stress of heat shrinkable sleeve varies widely with the quality of shrinkable layer's polyethylene and it's degree of irradiation (degree of crosslinking). And it also varies with shrink rate of sleeve. The relation between shrink rate and shrink stress for the materials of various shrinkable layer is shown in Figure 5 . The shrink rate is defined as follows;

$$S = \frac{D_o - D}{D} \times 100 \ (\%)$$

where

S : Shrink Rate

$D_o$: Inner Diameter of Sleeve Before Heating

D : Inner Diameter of Sleeve After Heating (When Used)

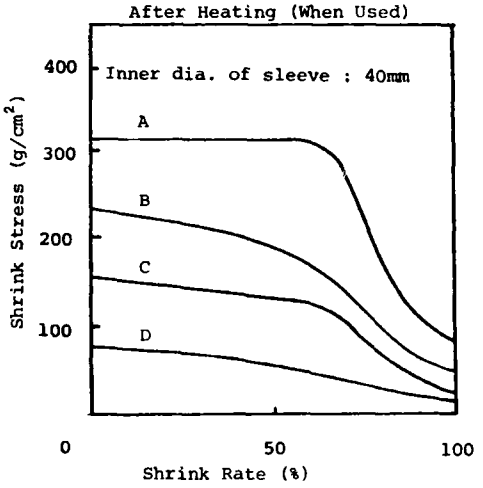



Figure 5

Shrink rate- Shrink stress Curves of Heat Shrinkable Sleeve with Various Shrinkable Layer

In this case, practical shrink rate comes up to 100 % by the thickness effect of inner layer's polyethylene, though the shrink rate of outer layer (shrinkable layer)is 75 % . The case C in Figure 5 is of our product, and it may be seen that a shrink stress for welding (30 g/cm$^2$ at 140 °C) is always available within the application limits of shrink rate 70 % . It is possible to design a sleeve with an adequate shrink stress by choosing suitable shrinkable layer's material and shrink rate in case of other sizes.

### 3.3 CRACK RESISTANCE OF HEAT SHRINKABLE SLEEVE DURING HEATING

Generally, a sleeve with large shrink stress and large shrink rate is desirable. But the question about crack resistance during heating must be considered also.

Notch stability test is carried out for the estimation of crack resistance. A sleeve, cut 1 mm deep notch on a sleeve edge by a razor blade,is put on a steel pipe having an outer diameter of testing shrink rate. Then, the sleeve is shrunken by putting into a 150 °C silicone oil bath for 20 minutes and the proceeding of notch is measured. (Figure 6) The data on our sleeve (Table 1 ) shows that it's crack resistance is good enough even for an application of lower shrink rate.

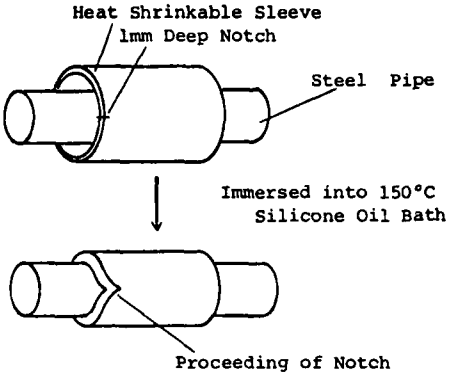



Figure 6

Illustration of Notch Stability Test

Table 1

Notch Stability of Heat Shrinkable Sleeve

| Shrink Rate (%) | Length of Notch* Proceeded (mm) |
|---|---|
| 10 | 6 |
| 20 | 2 |
| 30 | 1 |
| 50 | 0 |
| 70 | 0 |

* Measured after immersing sleeve into 150°C silicone oil bath for 20 minutes.

### 3.4 WELDING STRENGTH

A heat shrinkable sleeve with some kind of hot melt adhesive (e.g. polyamide) as an inner layer is generally used for a cable splicing. Temperature dependence of peeling strength between cable sheath and shrinkable sleeve is shown in Figure 7 comparing polyamide adhesive type with weld type. In this case, the sleeve was shrunken by the electric heater as described below. Peeling strength of polyamide adhesive type goes down to nearly zoro at 50 °C , while that of weld type is practically enough even at 60 °C.

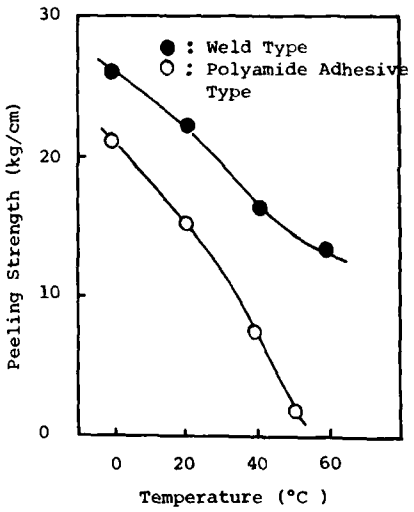



Figure 7

Temperature Dependence of Peeling Strength between Cable Sheath and Sleeve

### 4 TEMPERATURE CONDITION OF WELDING

In order to comfirm the temperature condition for getting a stable welding between the cable sheath and the shrinkable sleeve, the relationship of welding interface temperature and welding strength was investigated. In this investigation, the electric heater as described below was used and the method for peeling strength test is shown in Figure 8 9 10 .

This result shows that the cable sheath and shrinkable sleeve are welded surely and stably at a temperature above 130 °C as shown in Figure 10 .

### 5 TEMPERATURE INDICATOR

In order to confirm easily and surely in a field operation whether the temperature of welding surface is above 130 °C or not, temperature indicator is inserted in the external surface of shrinkable sleeve. Indication temperature must satisfy the following conditions;

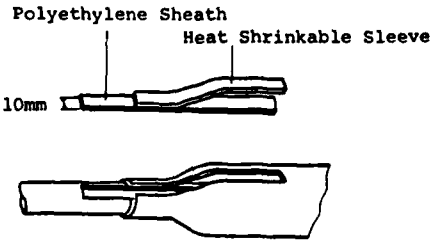



Figure 8

Removal of Peeling Strength Test Sample

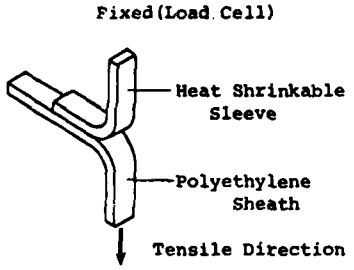



Figure 9

Peeling Strength Test

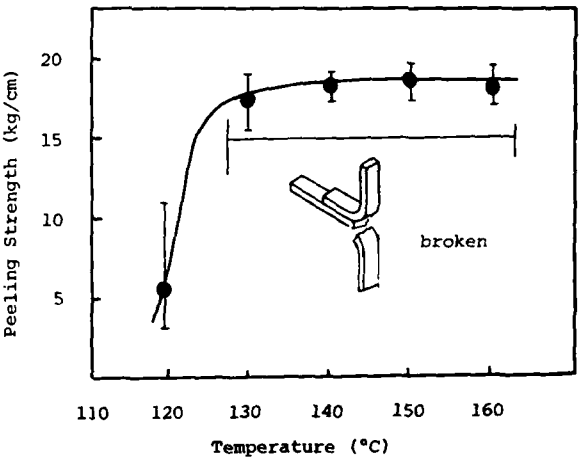



Figure 10

Relation Between Peeling Strength and Interface Temperature

1. Temperature of welding interface is above 130 °C
2. Temperature of insulated wire is below 80 °C

Figure 11 shows the result of the temperature in each portion (insulated wire, welding interface, surface of shrinkable sleeve) against the heating time.

As above mentioned, cable sheath and shrinkable sleeve are welded stably at a temperature above 130 °C. But in practice, shrinkable sleeve is additionally heated up to 160 °C to consider sure and

stable welding condition. At this time surface temperature of shrinkable sleeve is 230 °C and so temperature indicator which disappear at 230 °C is inserted in the shrinkable sleeve. Indicator has aromatic amide for its main ingredients. And then maximum temperature of insulated wire is 70 °C therefore characteristics of insulated wire is independent of temperature.

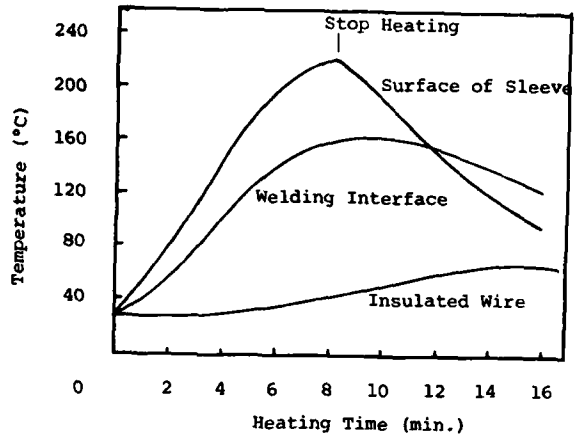



Figure 11

Temperature Incrase of Welding Portion

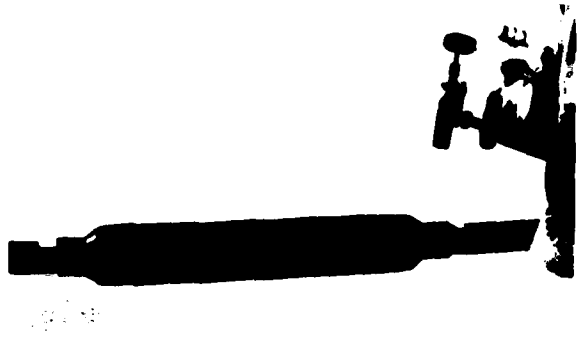


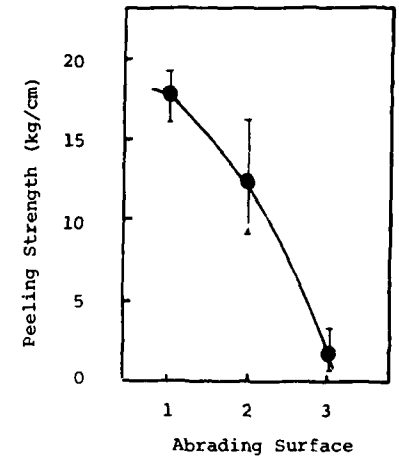
Photo. 3

Heating Operatin (generally torch lamp is used)

## 6 ABRADING EFFECT OF CABLE SURFACE

It is necessary to clean out surface of welding portion, because surface of cable sheath has been soided and oxidized during transporting and installation.

In general, it has been recognized that welding strength of polyethylene is promoted by cleaning and abrading surface of cable. However it is difficult to understand this effect quantitatively, wellding strength is compared incase of abrading cable surface with emery paper, wire brush and not abraded. Peeling strength and degree of cable abrading is shown in Figure 12 and Photo. 4




Fegure 12

Effect of Abrading Surface

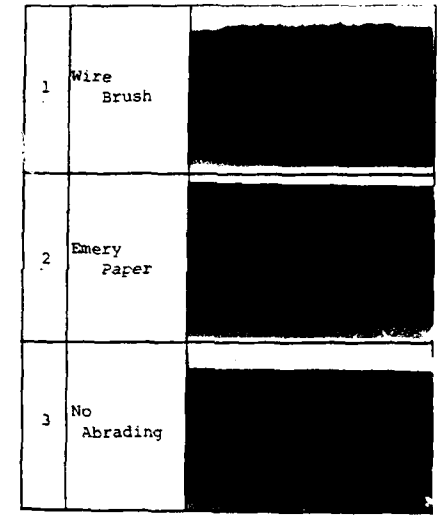



Photo 4

Abrading Surface

From this result it was found that abrading with wire brush brought firm welding. The reason of this effect is considered that the oxide film of the cable surface is eliminated enough and inner layer polyethylene of shrinkable sleeve encroaches on uneven surface of the cable.

## 7 RELIABILITY TEST

The reliability tests of the cable sheath splice were performed. Testing items are shown in Table 2 . From results of these tests, it was found that this splicing method satisfied long term reliability.

Table 2 Testing Items

| Test Item | Test Condition |
|---|---|
| Water tightness test | Water pressure : 0.3 kg/cm$^2$ (Under pressurized water)<br>Period : 3 months<br>Measurement : Insulation resistance |
| Air tightness test | Sealed air pressure : 1 kg/cm$^2$ (at 20°C)<br>Period : 1 day<br>Measurement : Air pressure decrease |
| Temperature cycle test | Temperature : -20°C→+20°C→+60°C 2 cycles a day<br>Number of cycles : 100 cycles<br>Sealed air pressure : 0.65 kg/cm$^2$ (at 20°C)<br>Measurement : Air pressure decrease |
| Tensile strength test | Sealed air pressure : 0.65 kg/cm$^2$ (at room temperature)<br>Tensile speed : 100 mm/min.<br>Measurement : Tensile strength Air pressure decrease |
| Vibration test | Sealed air pressure : 0.65 kg/cm$^2$ (at room temperature)<br>Amplitude : ±10 mm<br>Frequency : 10 Hz<br>Number of cycles : 1 x 106 cycles<br>Measurement : Air pressure decrease |
| Bending test | Sealed air pressure : 0.65 kg/cm$^2$ (at room temperature)<br>Bending radious : Cable dia. x 6<br>Number of bendings : 6 times<br>Measurement : Air pressure decrease |
| Static load test | Sealed air pressure : 0.65 kg/cm$^2$ (at room temperature)<br>Load<br>Cable dia. 18 mm : 10 kg<br>30 mm : 20 kg<br>Period : 5 months<br>Measurement : Air pressure decrease |
| Low temperature test | Sealed air pressure : 0.65 kg/cm$^2$<br>Temperature : -30°C<br>Period : 30 days<br>Measurement : Air pressure decrease |
| High temperature test | Sealed air pressure : 0.65 kg/cm$^2$<br>Temperature : -60°C<br>Period : 30 days<br>Measurement : Air pressure decrease |

## 8 EXCLUSIVE ELECTRIC HEATER

The exclusive electric heater has been developed to use when flames such as a torch lamp must be avoided, and this electric heater (Photo 6) is supported with exclusive instrument. By using this electric heater, even unskilled operator can splice cable sheaths stably and surely.

General specification of electric heater

| | |
|---|---|
| Heater element | Electric Heater |
| AC voltage | 100 V |
| Power consumption | 600 W |
| Temperature controll | Thermostat |
| Applicable cable diameter | 14 mm 65 mm |
| Weight | 2 kg |



Photo. 6
Exclusive
Electric Heater

## 9 CONCLUSION

Investigating the construction and the materials of the heat shrinkable sleeve, the new heat shrinkable sleeve is developed. This heat shrinkable sleeve is constructed with two layers, outer layer is crosslinked and stretched polyethylene, and inner layer is a little high melt flow polyethylene. This heat shrinkable sleeve can be welded to polyethylene sheath (not be adhered). Welding sleeve and cable sheath is accelerated by abrading cable surface. And reliability of the cable splice is confirmed to be superior. This splicing method is planned to be adopted next year (1981) in the Tokyo Electric Power, Co., Inc.

## 10 ACKNOWLEDHMENT

The authors wish to express their gratitude to the coleagues of the Tokyo Electric Power, Co., Inc. and the Fujikura Cable Works, Ltd. for their many enlightening discussion.



Kiyoshi Yokoyama

Senior Engineer,
Electronics and Telecommunication Div.
Power System Operation Dept.
The Tokyo Electric Power, Co., Inc.
3-1-1, Uchisaiwai-cho,
Chiyodaku, Tokyo, Japan

Mr. Yokoyama graduated in Telecommunication Engineering from Oita Technical High Shcool. He jointed The Tokyo Electric Power, Co., Inc. in 1960 and has been engaged in designing and managing of telecommunication system.



Nobuyasu Sato

Chief,
Telecommunication Cable Reserch and Development Dept.
The Fujikura Cable Works, Ltd.
Sakura-shi, Chiba-ken,
Japan

Mr. Sato received B.E. degree in Telecommunication Engineering from Tohoku University in 1966 and has been engaged in development of telecommunication cables. He is a member of the Institute of Electronics and Communications Engineers of Japan.



Shigenori Goto

Engineer,
Telecommunication Cable Reserch and Development Dept.
The Fujikura Cable Works, Ltd.
Sakura-shi, Chiba-ken,
Japan

Mr. Goto received B.E. degree in Metallurgical Engineering from Iwate University in 1974 and has been engaged in development of telecommunication cables. He is a member of the Institute of Electronics and Communications Engineers of Japan.



M. Makiyo

Engineer,
Materials Engineering
Reserch and Development
Dept.
The Fujikura Cable Works,
Ltd.
Sakura-shi, Chiba-ken,
Japan

Mr. Makiyo gruaduated in Chemical Engineering from Gunma Technical College in 1972 and has been engaged in reserch and development of plastic materials for telecommunication cables. He is a member of the Society of Polymer Science of Japan.



Saburo Mase

Engineer
Telecommunication Cable
Engineering Dept.
The Fujikura Cable Works,
Ltd.
1-5-1, Kiba, Koto-ku,
Tokyo, Japan

Mr. Mase received B.E. degree in Mechanical Engineering from Keio University in 1971 and has been engaged in engineering of cable accessaries. He is a member of the Society of Mechanical Engineers of Japan.

# LOW PRESSURE MOLDING FOR ENCAPSULATION OF CABLE SPLICES

L.J. Charlebois F.A. Huszarik

Bell-Northern Research
Box 3511, Station C
Ottawa, Ontario, Canada

## ABSTRACT

Laboratory research on pre-encapsulated cable splices using the Low Pressure Molding process has shown this to be a reliable, cost-effective splice closure.

This method is adaptable to pre-terminated splices. With such splices, service entrance wires of specific lengths and numbers are terminated at pre-determined intervals on distribution cables. The splices and closures are made under controlled factory conditions. These splices are used in new housing developments, where lot sizes and trenching access can be planned in advance.

The process relies on the injection of molten plastic into a mold, or cavity, under low pressure. The molding pressure is controlled by using overflow ports in the mold.

## INTRODUCTION

Bell Canada adopted the technique of pre-encapsulating cable splices in a factory environment in 1973. The encapsulation system at that time was a two-part polyurethane mix which was poured into a plastic enclosure surrounding the spliced assembly.

Although the performance of this system was better than similar encapsulations installed in the field, there were several drawbacks: the materials were moisture-sensitive, expensive and had a short shelf life.

Two years later, another system was adopted, using heat-shrinkable sleeves as the mechanical closure for the splice. This system uses sealing tapes to seal the spliced pairs. The splice is then enclosed with a heat-shrinkable sleeve. The closed assembly is placed in an oven and heated for 12 to 17 minutes to shrink the sleeve over the tapes. Approximately 30 minutes is then required for cooling the assembly.

Heat shrink sleeves are presently used with excellent results. In terms of long-term reliability, pre-encapsulated heat shrink closures perform much better than any field installed buried closure. However, the process is costly and time consuming.

## Low Pressure Molding: What Is It?

Low pressure molding (LPM) is the process of filling a mold cavity with molten plastic. The low pressure is maintained by using overflow passages in the design of the mold. At present, the LPM process is being evaluated specifically for the pre-fabrication of splices in a factory environment.

## How Does It Work on Cable Splices?

Service wires are spliced to pairs selected from the main distribution cable. The spliced pairs are imbedded in ethylene propylene rubber tape. The spliced and taped assembly is placed in a mold and encapsulated with molten plastic (Fig. 1).

The plastic is injected into the mold with a 38 mm (1 1/2") extruder. As molten plastic fills the mold cavity around the taped assembly, the tapes are softened and begin to flow. When the plastic cools it shrinks, forcing the softened tapes into and around the connectors to create a moisture-proof seal (Fig. 2).

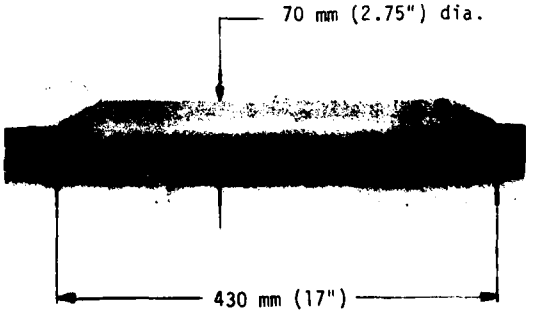



Fig. 1

ENCAPSULATED CABLE SPLICE



Fig. 2

ENCAPSULATION CROSS SECTION



Fig. 3

EXTRUDER

Due to the size of the equipment involved in the process, low pressure molding is especially suited for factory application where assembly line splicing operations are performed.

## PROBLEMS ENCOUNTERED DURING EXPERIMENTAL DEVELOPMENT

### Extruder

One of the major considerations in the fabrication of large plastic parts is the cost of the machinery required. The LPM cable splice requires two or three pounds of molten plastic injected into the mold. Normally an injection molding machine costing about $100K is required to inject this much plastic at one time.

An alternative solution is to use a small extruder (cost approx. $20K, Fig. 3) and specially designed molds that eliminate any pressure build-up in the mold. It is important to eliminate this pressure build-up to prevent crushing of the spliced cables during the plastic injection process.

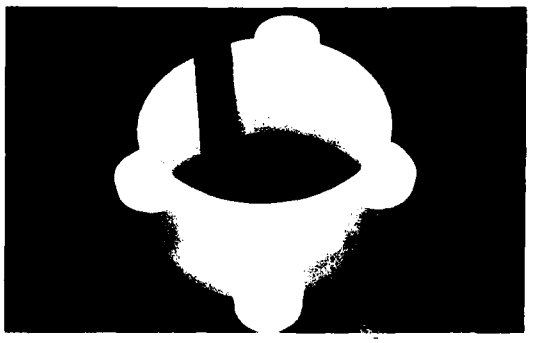


Fig. 4

CABLE CENTERING RING

### Cable Centering

One problem encountered during molding of the spliced assembly was the movement of the cable to one side of the mold causing an incomplete encapsulation. This was overcome with the use of a cable centering ring (Fig. 4). This ring is split so that it may be installed over the assembly before encapsulation (Fig. 5). The centering ring was designed so that it is self-centering when the mold is closed.



Fig. 5

CABLE CENTERING RING INSTALLED

Too Many Molds

Six different cable sizes are used in the pre-encapsulation process. The use of separate molds for each cable size would be time consuming and expensive.

The process has been designed so that the use of one mold with two inserts is all that is required (Fig. 6). The inserts have rubber spacers at both ends to adapt to the cable and service wire sizes. These spacers also protect the service wires and cable from damage during mold closing.

The aluminum inserts are easily interchanged by loosening two screws and lifting them out of the main mold cavity.

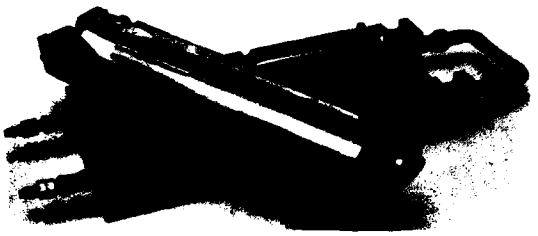


Fig. 6

MOLD AND MOLD INSERT

Mold Cooling

Initial experiments were performed using plexiglass molds. Flow patterns of the molten plastic were established. The optimum location and size for the inlet and exit ports for the molten plastic were defined. Furthermore, the clear molds identified any air entrapment problems. Although these molds were helpful during early experiments, irregular shrinkage of the molded closure occurred due to the poor cooling properties of plexiglass.

Water-cooled aluminum molds eliminated the shrinkage problems experienced with the plexiglass molds. With the aluminum molds the cooling time on the largest encapsulations is approximately ten minutes.

Material Selection for the Low Pressure Molding Concept

The materials tested for the process included low-density polyethylene acrylic acid, ethylene methacrylic acid and ethylene vinyl acetate. Initial tests indicated that low-density polyethylene and ethylene acrylic acid were best suited for the LPM process. The final choice was low-density polyethylene because of its desirable material properties.

LABORATORY TESTING

Several laboratory tests were performed which were representative of the conditions that the closures would be subjected to during their in-service life.

Environmental

Thermal investigations established the temperatures within and around the splice during the molding process. A time-related temperature profile of the molding process is shown in Figure 7.

Thermocouples were placed in the cable core, splice area and the area of contact between the molten plastic and the cable sheath. The highest temperature measured in the cable core was 70°C (158°F). The highest temperature in the splice area was 95°C (203°F). The temperature on the cable surface and plastic interface reached 150°C (302°F) for an instant, then dropped to 100°C (212°F) within three minutes.

These temperatures did not present problems in terms of insulation resistance of the conductors or the general quality of the splice.

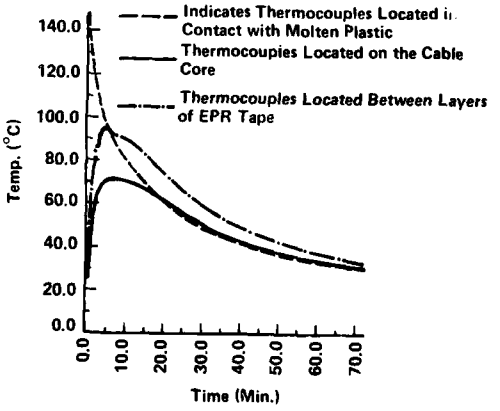



Fig. 7

ENCAPSULATION TEMPERATURE PROFILE

Temperature Cycling in Water

Sample splices with moisture sensors located near the splicing connectors were immersed in one meter of water and cycled from +40°C (104°F) to 1°C (34°F) for 50 cycles. Insulation resistance readings were taken between the connected pairs during the first few cycles and every five cycles thereafter.

Results showed that the insulation resistance between pairs was $10^9$ ohms or greater on samples encapsulated with polyethylene before, during and after temperature cycling. No moisture was detected by the moisture sensors.

Temperature Cycling (Freeze/Thaw)

Sample splices with moisture sensors located near the splicing connectors were immersed in 100 mm of water and temperature cycled from -40°C (-40°F) to +60°C (140°F) for 50 cycles.

Again the results showed that samples encapsulated with polyethylene maintained insulation resistance between pairs greater than $10^9$ ohms before, during and after cycling. No moisture was detected by the moisture sensors.

Mechanical

Static load, impact resistance, axial pull and vibration tests were performed on the encapsulated splices. Samples encapsulated with ethylene acrylic acid and polyethylene withstood all these tests.

Electrical

High current and insulation resistance tests were performed on samples at several points during the test program. All samples passed the tests.

Summary of Test Results

Based on the results of the laboratory testing, low-density polyethylene was chosen as the best material for the molding process. The polyethylene selected has a melt index of 28 to allow ease of material flow into the mold. Further, polyethylene was the least costly material tested.

## BENEFITS OF USING LPM FOR ENCAPSULATION OF CABLE SPLICES

Some of the advantages of adapting low pressure molding to pre-encapsulation centres include:

- 80% material saving over the heat shrink method
- 65% faster process time
- material readily available from many suppliers
- reduced craftsman sensitivity resulting in consistently good closures.

A preliminary economic evaluation indicates a substantial cost saving to Bell Canada over their present method.

## OTHER APPLICATIONS

Low pressure molding has several potential applications to the telecommunications industry. Some of these are:

Field Application of LPM for Encapsulation of Cable Splices

For this application an extruder and associated molds would be trucked to job sites for encapsulating the splices. This method will provide a reliable, consistent splice closing system.

Cable Pulling Eyes

Preliminary tests on the application of pulling eyes for fibre optic cable (Fig. 8) have shown favourable results. A patent is pending on pulling eyes produced with the LPM process.

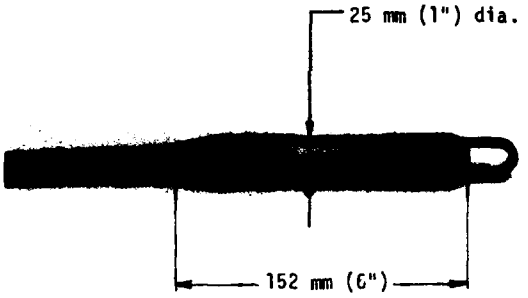



Fig. 8

CABLE PULLING EYE

Pre-bonded Cable

Rural aerial cables require bonding between the cable sheath and the support strand every 275 m (1000 ft.) or less. With the LPM process these cables can be pre-bonded at the factory. This approach could significantly increase field productivity. A patent has been granted on this type of system.

Cable Capping

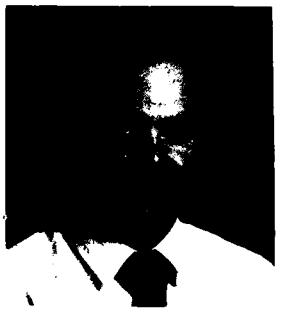
Using the LPM process, caps can be easily molded over the ends of cables to provide water and air tight seals.

## Cable Plugging

LPM can be adapted to cable plugging using a high melt index and low melting temperature polymer.

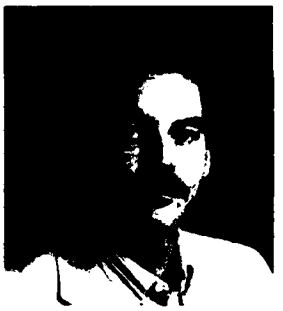
## SUMMING UP

LPM will be field trialed in a Bell Canada pre-encapsulation centre early in 1981. Further evaluation will be directed by Bell-Northern Research towards the use of LPM on the other applications described above.



Len Charlebois joined Bell-Northern Research in 1964 as a member of technological staff. Since then, he has been involved in many areas such as injection mold design and consultation, mechanical packaging, MDF design, CO cable vault studies and cable closure evaluations.

He is presently responsible for the design and evaluation of the Low Pressure Molding project. Len has been granted two patents and has five more pending.



Fred Huszarik received his B.Sc. in Civil Engineering in 1972 and his M.Sc. in Geotechnical Engineering in 1974. Since joining Bell-Northern Research in 1973, Fred has been responsible for research on various aspects of telephone outside plant construction methods, tools and materials.

Fred holds memberships in the Canadian Society for Civil Engineering, Canadian Geotechnical Society, American Underground Association and the International Society for Soil Mechanics and Foundation Engineering. Since 1976, Fred has been chairman of the IEEE Task Force on Cable Installation Methods.

# APPLICATIONS FOR MODULAR AND DISCRETE WIRE CABLE SPLICING

Robert Young
Product Manager
and
George Foster
Development Engineering Manager

AMP Incorporated
Telecom Division

## ABSTRACT

The available products and techniques for splicing telephone cables can be divided into two basic categories, each with unique characteristics suited for use in specific applications. Because many splicing situations are heavily influenced by local conditions or work practices, there are no hard and fast rules to guide in the selection of the most applicable method.

The two splicing methods discussed in this paper are discrete wire splicing connectors and modular connectors. Discrete wire splicing offers easy access to any individual pair, yields the most compact splice bundle and is convenient for maintenance and rework. Modular connectors have the advantage of preconnectorization and are well suited to in-process testing. These and other general characteristics are covered in detail for each method. Also, by describing applications that take maximum advantage of each approach, this paper identifies those characteristics that provide unique capabilities or special limitations.

## DISCRETE WIRE SPLICING

Suitable for use on any size and type telephone cable presently used in the telecommunications industry, discrete wire splicing can be tailored from small cables of 6 or 12 pair to much larger 3600 and 4200 pair cables. This method enables easy access to individual pairs and permits the craftsperson to situate and organize individual pairs or groups within the splice. Generally, discrete wire splicing results in a smaller splice than is obtainable with modular connectors.

Although maintenance and rework are easily accommodated with discrete wiring methods, there are limitations. For example, discrete wire splicing is not conducive to locating and identifying pairs within a cable. Furthermore, most discrete wire systems do not lend themselves to in-process testing and none are suitable for pre-connectorization.

A variety of applicator tools specifically designed for crowded or cramped work areas is available in both simple hand tool and high production versions.

There are several proven types of discrete wire splices that share these general characteristics. Rather than attempt to completely describe all available types, this paper will concentrate on the discrete wire splice method that comes closest to the application rates possible with modular connectors.

### An Example

The connector design and applicator tooling discussed in this paper is unique in that it eliminates the need to prestrip or cut wire to length prior to splicing, thus reducing installation time. The final termination results in a gas-tight, compact splice.

In describing this Discrete Wire Splicing Connector, emphasis is placed on versatility of application. The connector is an extremely versatile discrete wire connector which has been accepted by major telephone companies worldwide. Applications of this connector are used as examples in the following discussion.

The compact connector is manufactured from tin-plated, copper alloy with bonded insulation. The termination is based on the insulation displacement concept, and any solid core wire (AWG #19 through #28) with pulp, paper or plastic insulation can be accommodated. For use on jelly-filled cables, all types are available filled with sealant. Additionally, the compact in-line connector design typically provides a smaller splice than can be obtained by other methods.

The connector line originated with the standard product and hand tool. However, the introduction of new connector configurations and applicator tools to the line has resulted in several uniquely different applications. For example, weather resistant connectors give added protection against environmental exposure; load coil connectors simplify installation of load coil stub cables by providing two separate terminations in one connector; breakaway load coil connectors accomplish physical separation of the connector halves during crimping. Additionally, the tooling line has been expanded to include a hand tool holder which allows the craftsperson free utilization of both hands for tool operation, and reel-fed equipment specifically designed for high-count cable applications. All these features will be discussed in further detail.

## APPLICATIONS

An obvious advantage of this Discrete Wire Splicing is its ability to splice, tap, bridge, rework or otherwise access individual pairs without disrupting other pairs in the same cable. It is even possible to tap onto a working line without cutting and interrupting service. Pair loading and cutting in slack can also be achieved.

The introduction of the standard and breakaway load coil (dual) connectors offered additional unique capabilities.

The standard load coil connector design provides a dual butt splice in one connector. This allows simultaneous termination of the "in" and "out" leads to the line, with complete electrical isolation. This application previously required two connectors.

The breakaway load coil connector incorporates the same features except that perforations between the connector halves enable physical separation of the two segments during crimping. In addition to loading, this connector is extensively used to cut slack for pole moves or pedestal installations.

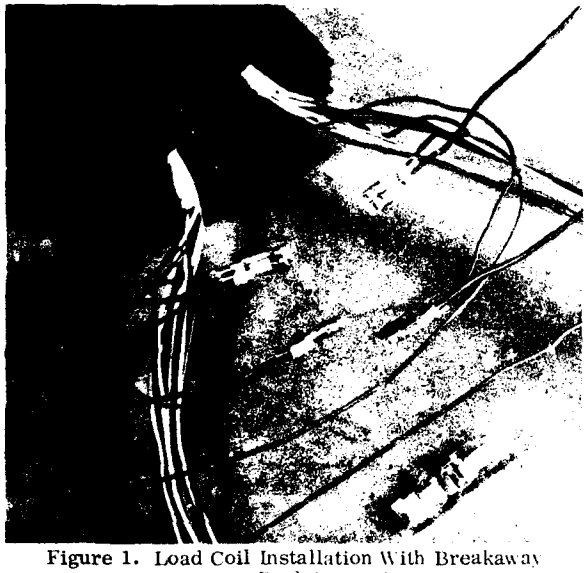


Figure 1. Load Coil Installation With Breakaway Dual Connector

Both connectors are available with weather resistant features for maximum protection against environmental exposure. They can also be utilized with the hand tool or applicator, depending on specific application needs.

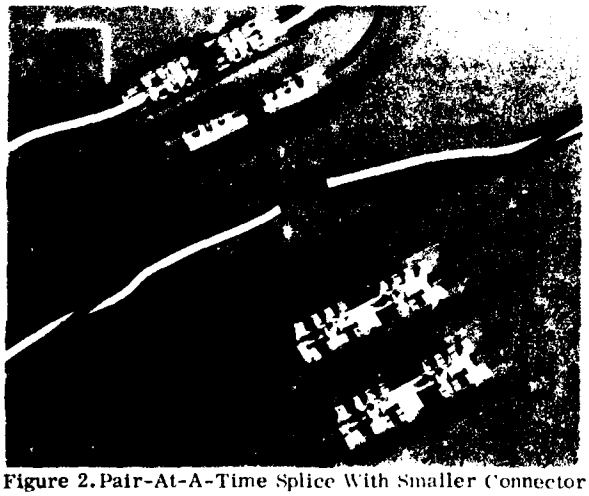


Figure 2. Pair-At-A-Time Splice With Smaller Connector

The smaller version of this connector line has the same basic features as the regular connectors and are designed for straight splicing only. For crowded situations where the most compact splice bundle is necessary, this connector can yield a finished bundle that is up to 33 percent smaller than that achieved by other methods.

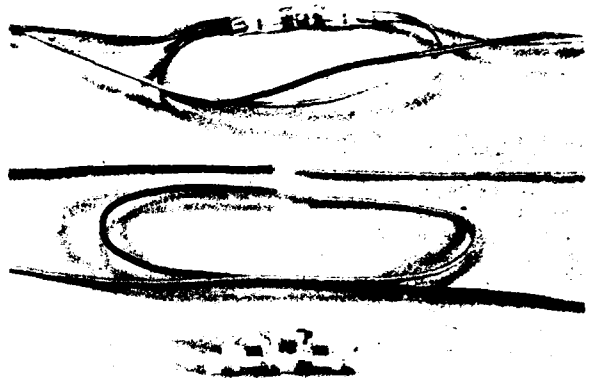


Figure 3. Pair-At-A-Time Splice With Dual Connector

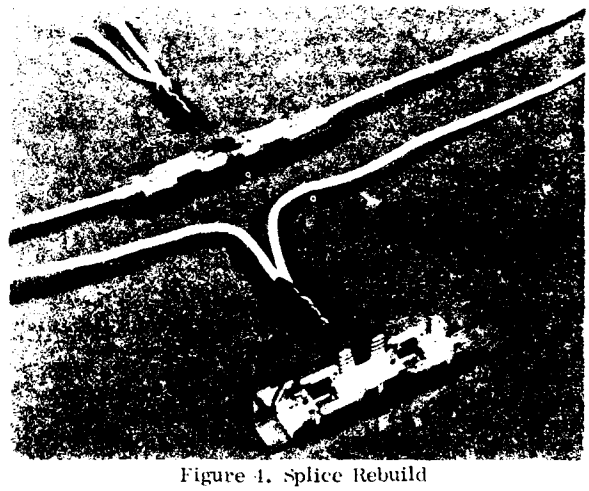


Figure 4. Splice Rebuild

According to Telco craftspersons, versatility is the domain of discrete wire splicing. To dramatize this, all the applications discussed, plus other special applications, can be accommodated with this Discrete Wire Splicing Connector.

## APPLICATOR TOOLING

A variety of applicator tooling and accessories are available to meet splicing needs in any splicing situation.

The hand tool features a ratchet for positive crimping action. A hand tool holder has also been designed which provides insulation between the mounting surface and the tool. Suitable for aerial, buried and underground applications, the hand tool can be utilized with all loose-piece connectors in the product line, with the exception of the smaller version of this connector.

The applicator tool provides high speed, strip-fed capability in a compact size that can be used for all splicing applications. It allows tapping at high production speeds without any service interruption. As with all these connectors and associated applicator tooling, minimal training of craftspersons is required.

Additionally, an applicator has been designed to terminate the smaller connector at high production rates in a pair-at-a-time straight splicing mode. This tool is also available with a test adapter for use with a test set.

## MODULAR SPLICING

With rising labor costs and a shortage of skilled craft personnel, modular splicing is becoming increasingly important. All modular splicing systems take advantage of mass termination to minimize wire handling time during installation. Because each module handles 25 pairs, binder group organization is simplified and modules can be labeled to aid in identification. The application speed of mass termination coupled with the efficient 25-pair organization result in field splicing rates that are equal to or greater than, all but the fastest discrete wire splicing methods.

The most dramatic advantages of modular splicing are realized through pre-connectorization. Factory terminated and tested cable minimize the time required for field installation, allowing better manpower utilization through more efficient scheduling. Such installations are especially suited to applications where on-site time must be held to a minimum. Some users report that field splicing time is reduced by up to 75 percent through pre-connectorization. The larger the cable being installed, the greater the labor saving advantages to the operating Telco.

The maximum benefit of pre-connectorization is realized when modules are applied to both ends of the cable in the factory. With both ends of a cable pre-connectorized, cable placement must be precise to allow proper mating. This requires more than normal pre-engineering of the overall job and is suitable only in buried or aerial applications. For underground applications, the necessity to place the cable in ducts limits pre-termination to one of the cables only. Modular splicing produces a splice that is larger than one made with discrete wire splicing methods. As a result, a larger, more expensive splice closure may be required.

Another disadvantage of modular splicing is that access to individual pairs is limited, random bridging and tapping are not feasible. Rearrangements are relatively difficult and with most module maintenance and repair is likely to result in a hybrid splice having a mixture of modules and discrete wire splices.

### An Example

With versatility being one of the strong cases for discrete wire splicing, we have chosen to describe the most versatile of the currently available pluggable modular connectors. As opposed to other modular connectors, this connector is a truly pluggable device made possible by a unique contact design. For the first time, true connector capability has been brought to the telephone outside plant marketplace.

In the system discussed, wire termination is accomplished with slotted plate insulation displacement contacts designed to accommodate 26 through 72 AWG solid conductors (maximum O. D. .056"). Two types of contacts are used; one a simple slotted blade (starter); and the other, (main body) a double ended contact with tuning fork and slotted blades at opposite ends. During mating a slotted blade is plugged into a tuning fork. The contacts can be mated or unmated without disturbing the terminated wires.

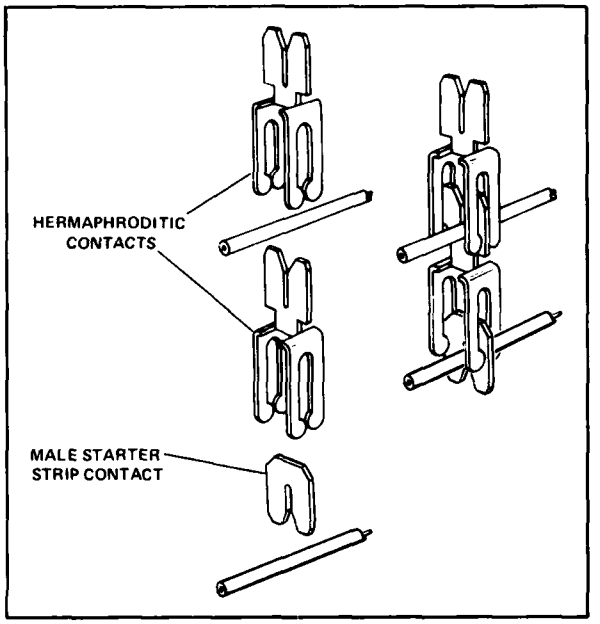



Figure 5.

This pluggable modular connector is composed of three basic units; the starter strip, the main body and the cap. These units can be combined to provide either a polarized (male-female) arrangement or a unique hermaphroditic configuration. The basic polarized splice is made by terminating wire from one cable to the starter strip and wires from the mating cable into the main body. The splice is completed by the addition of a protective cap to the main body.

In the hermaphroditic arrangement, wires from both cables are terminated to main bodies. The two bodies can be mated together in either direction. The splice is then completed with a blank starter and a protective cap. A hermaphroditic splice is particularly suitable to high activity areas since additions and rearrangements can be more easily accommodated. This type

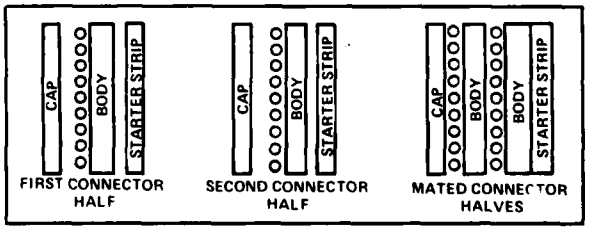



Figure 6.

of splice also facilitates pre-connectorization because orientation of cable ends are not necessary.

By extension of the basic pluggability concept, bridging, tapping, section throws and loading are accomplished by addition of main bodies to the basic splice. Many of these applications are possible without service interruption. In the case of half tapping, a special main body and cap allows termination of through wires without cutting.

## APPLICATOR TOOLING

The applicator tool for the connector is well suited in both field and factory applications. It is a compact all mechanical tool, capable of cutting and inserting 25 pairs at a time. Conductors can be visually inspected to assure proper placement prior to termination. Using a special test adapter and industry standard test sets, each splice can be tested in the applicator tool.

## SUMMARY

Because they deal with individual connectors, discrete wire splices are suitable for a wide variety of applications. They yield the smallest possible overall splice for a given size cable and are well suited for cramped locations. Toc'ing has been developed to apply discrete wire splices at high rates that rival field-installed modular splicing connectors for small and medium size cables.

High count, factory tested pre-connectorized cable makes possible shorter field installation times and more effective use of available personnel. The introduction of pluggability to modular connectors facilitates initial installation. In addition, subsequent splice rearrangements are easily achieved with no degradation of the original termination.

Because of the overlapping capabilities and limitations of discrete wire splices and modular splicing connectors, the user should determine those features most suitable for his application. It is hoped that the information presented in this paper will help in that determination.

# MODULAR HARDWIRE BLOCK WITH SWITCHING CAPABILITY

Gary B. Matthews

3M

St. Paul, Minnesota

## ABSTRACT

A hardwire binding post connecting block is described, wherein each binding post is a single pole - double throw switch. The block was originally developed to meet the requirements of the Bell System RAND concept; providing feeder pairs which are common to two interfaces and available at either interface but not at both interfaces at the same time. Additional design criteria included simplicity of operation, and dimensional interchangeability with other components of the 3M Modular Hardwire System. Design difficulties encountered in satisfying all of the above requirements are reviewed. Electrical test data and field trial results are presented which demonstrate the craft advantages and technical merit of this hardwire design for the RAND application. In addition, further applications for the block's outside plant, individual pair switch capability which have been defined and implemented by telephone operating companies since its introduction are reviewed. These include a more cost effective central office cut-over and use at interface points.

## INTRODUCTION

The ever-increasing costs of labor and materials have combined to cause a rapid escalation of the in-place costs of telephone cable plant. This fact has caused increasing emphasis to be placed on the engineering of outside plant facilities which has, in turn, resulted in the generation of a multiplicity of network design concepts over the past several years.

The designer of outside plant facilities in rural areas is faced with a unique combination of challenges and constraints. The service provided will be inherently expensive even if the cable plant were to be sized based on current customers in the rural area, due to the low density and large distances involved. Compounding these costs is the practical necessity of planning for the inevitable future growth in the area and selecting appropriate cable plant sizes for those projected growth areas. The amount and rate of growth, its location, and pattern within the rural area are all too frequently out of consonance with the best projections of only a year or two prior, and additional network upgrading is required.

In an attempt to provide increased flexibility in rural networks, the Bell System developed the Rural Area Network Design (RAND) concept. The RAND concept is intended for use in low density rural areas where satisfactory projections of the ultimate growth and development patterns cannot be made.

It is particularly good for areas where growth is anticipated but the exact location of the growth within the area cannot be defined. RAND is designed to be used where customer density is less than 300 main stations per square mile or 50 main stations per route mile during the planning period. Rural farmland with existing or projected zoning for residential development and population densities located long distances from urban centers (such as trailer parks or seasonal facilities) are typical examples of areas suitable for implementation of RAND facilities.

The subject Modular Hardwire Block with switching capability was developed to provide the hardware capability to implement the RAND design concept.

## RAND DESIGN CONCEPTS

In order to develop a fuller appreciation for the advantages provided by the RAND design concept, it may be helpful to describe service provided to a rural area by other commonly used design and administration practices. Having determined appropriate locations for two cross connect points or interfaces, the following design approaches might be used, with the potential consequences noted.

### 1. NON-MULTIPLED FEEDER

In this design, administration and assignment is very simple since feeder pairs are not multipled between the two interfaces. An installer need visit only one interface to provide service. The limitation of this design approach however, is that it provides very little flexibility in feeder utilization. If the growth at interface number one occurs more rapidly than projected, the cable splice at this interface would have to be opened to transfer feeder pairs from interface number two. This design will almost certainly be costly in rural areas due to the growth uncertainty and subsequent requirements for rearrangements.

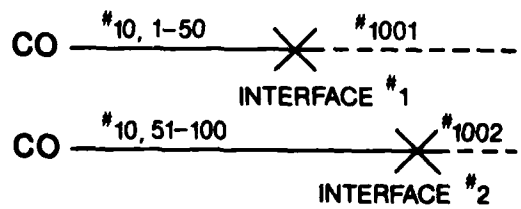



Figure 1. Non-Multipled Feeder

2. MULTIPLED FEEDER

In this design, all feeder pairs appear in both interfaces. Any imbalance of growth between the two interface locations can be readily accommodated. The true cost for the feeder flexibility provided by this design is high, however, since it is extremely difficult to ensure accurate record keeping. The installer must visit both interfaces to run cross connection jumpers to provide service from the second interface. Since the Central Office identity of the pair changes at each intermediate interface, trouble repair can be very difficult whenever cross connections have not been made in accordance with assignment records.

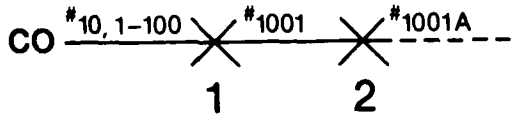



Figure 2. Multipled Feeder

3. RAND DESIGN

The basic RAND design concept provides for two Rural Area Interfaces (RAI's) which have feeder pairs that are common to both interfaces. These feeder pairs are available for use at either of the two interfaces but cannot be used at both interfaces at the same time. Further, maintenance of the Central Office pair identity through the intermediate (A) interface is ensured by the design of special hardware developed for RAND which prevents random cross connection of "FEEDER IN" and "FEEDER OUT" pairs. Thus, the RAND concept provides full feeder flexibility between the two interfaces to accommodate growth imbalance, while ensuring simplified administration and assignment. The installer need visit only one interface to provide service.

The RAND design concept combines the advantage of multipled and non-multipled feeder designs while eliminating the disadvantages of each through special hardware design for the intermediate (A) interface.

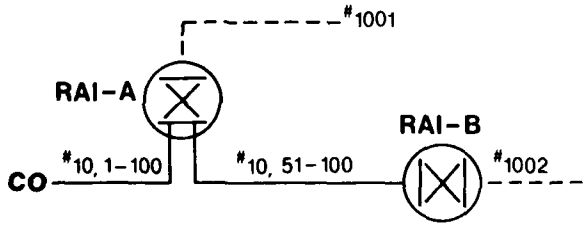



Figure 3. Rural Area Network Design

HARDWARE DESIGN FOR THE RAND APPLICATION

The two fundamental hardware design requirements for the RAND application are:

1. To provide access to common feeder pairs at either of two interfaces but not at both interfaces at the same time.
2. To maintain the Central Office pair identity through each intermediate interface.

The following additional requirements were considered desirable in order to provide hardware which would minimize the probability of craftsperson error in using the RAND concept:

3. No loose parts.
4. No special tool.
5. Simple operation.

After reviewing each of the above requirements, it was decided that the optimum product design could best be achieved by designing a Modular Hardwire Block with a switch capability for use in the intermediate (A) interface. The remainder of the hardware requirements were readily satisfied by the standard 3M binding post blocks, cabinets, and other components of the 3M Modular Hardwire System. Thus the "Controlled Feeder Block" was designed to meet all of the above requirements and to be dimensionally interchangeable with the other system components in order to afford maximum route design flexibility using this overall hardware system.

The Controlled Feeder Block is depicted in Figure 4. When in use, the block is placed in the intermediate rural area interface (RAI-A) (see Figure 5a). Feeder pairs which are common to both interfaces (RAI-A and RAI-B) are terminated in the MS² modules which are preterminated to the block. The Central Office side of the cable is terminated in the "FEED IN" module and the RAI-B side of the same pair count is terminated in the "FEED OUT" module. The "FEEDER IN" pair is connected internally to the "FEEDER OUT" pair when the associated binding posts are pulled out. In this position, the "FEEDER" pairs are expressed through RAI-A to RAI-B and do not appear on the front face of the block.

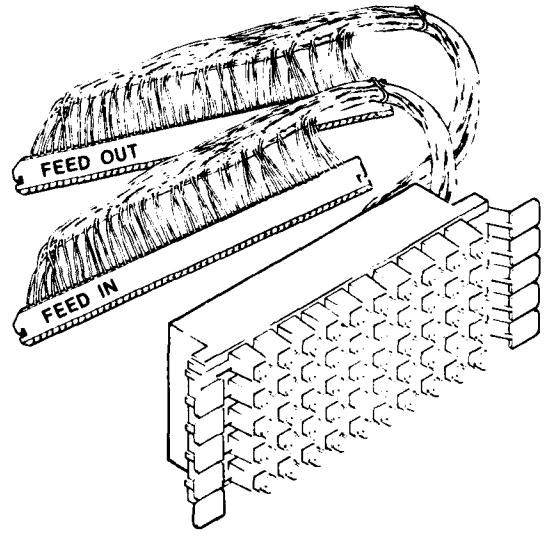



Figure 4. Modular Hardwire Block with Switching Capability (Controlled Feeder Block)

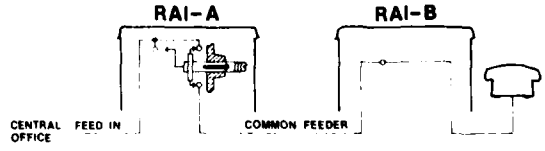



Figure 5a. Binding Post Out, Feed Thru

When it is desired to utilize the subject pair count at RAI-A, the tip and ring binding posts are simply pushed in. The "through" connection is broken, making the pair electrically "dead" at RAI-B. The binding post screw at RAI-A is now connected to the subject Central Office pair count and a jumper is cross connected to the appropriate distribution pair to provide service from RAI-A. (See Figure 5b). Other system components are shown in Figures 6 and 7.

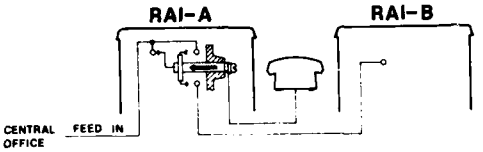



Figure 5b. Binding Post In, Feed Terminated

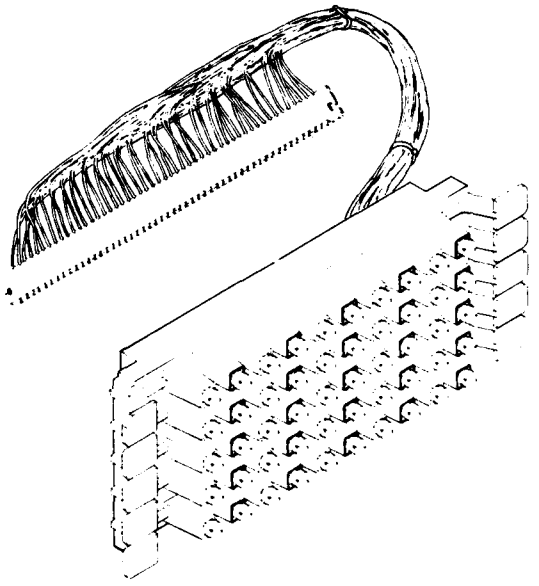


Figure 6. Modular Hardwire Block (Non Switching)

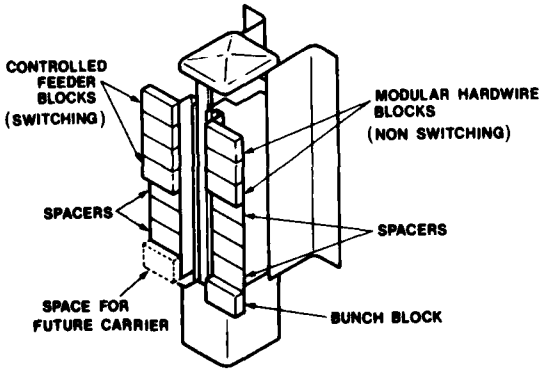



Figure 7. Typical Layout of Blocks in an RAI

## DESIGN OF THE "CONTROLLED FEEDER BLOCK" HARDWIRE BINDING POST WITH SWITCHING CAPABILITY

The Controlled Feeder Block is comprised of a thermoplastic polyester insulative block which houses fifty (25 pair) sliding terminal post switch assemblies on a 2½" x 5" face area. A cut-away view of the block is shown in Figure 8. Each of the switch assemblies is made up of the components shown in Figure 9. These switch assemblies are placed in the block and the internal switch area is filled with a moisture sealant. An isolator plate is then permanently attached to the rear of the block. Color coded pre-connectorized tails are then factory terminated in the u-contact end of both the "feed-in" and the "feed-out" contacts. These u-contact connections are then sealed in a hard encapsulant material to provide both moisture protection and strain relief. The switch shown in Figure 9a is in the "up" or "expressed through" configuration. The feed through contact is carried in an insulator base which is attached to the sliding terminal post. In the "up" configuration the "feed through contact" engages the fork contact portion of the "feed in" and "feed out" contacts, completing the "in" to "out" connection. The binding post and screw head are electrically dead in this position.

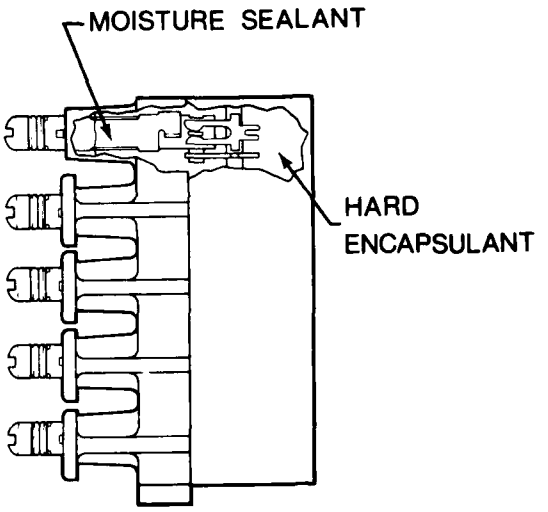



Figure 8. Block Cut-A-Way View

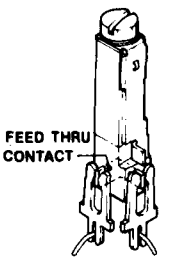



Figure 9a. Switch Assembly (Post Up)

When the sliding terminal post is pushed to the "in" position depicted in Figure 9b the jumper contact blade engages the fork contact portion of the "feed in" contact and the binding post and screw are electrically connected to the Central Office "feed in" count. The "feed through contact" is simultaneously moved to a position in the open portion of the fork contact and is thus electrically isolated.

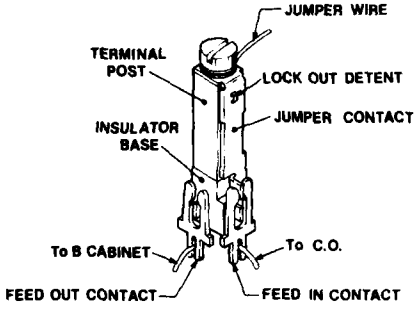



Figure 9b. Switch Assembly (Post Down)

The lock out detent formed on the jumper contact acts in combination with the plastic block to prevent movement of the sliding terminal post from one position to the other until a force of approximately nine pounds is applied.

Thus, the subject block design provides the capability of switching the Central Office pair count terminated on the "in" contact to either the other "out" contact (field terminated to RAI-B) or to the binding post (for jumpering in RAI-A). The installer can perform this operation with a simple push of the sliding binding post and the use of a screwdriver for the jumper wire termination.

After the block is terminated by the splicer (Figure 4.), Central Office pair count identity is assured at both interfaces and a given pair is accessible at only one interface at a time, depending on the switch position.

The block design described above evolved from a multitude of design requirements. Part of the requirements have been previously mentioned and several others will be reviewed at this time.

A. The amount of space available to accomplish the factory pre-termination of the tails with MS² modules was very limited due to the following three requirements:

1. Design the block to have the same face dimension as the standard 3M Modular Hardwire Block (2½" x 5").
2. Maintain the deep, wide channels between binding posts to ensure high insulation resistance performance and ample wire space to ensure good housekeeping.
3. Minimum torque requirements dictated the use of the #8-32 screw with brass post and also dictated the minimum allowable plastic thickness in the post area.

The space was so limited that a wire-wrap connection was evaluated as a potential solution. However, electrical performance of the wire-wrap elements was inferior to the u-contact elements. The problem was resolved by shifting the post matrix within the mounting dimension of the block and re-designing the manufacturing tooling for wire insertion. This was done following prototype evaluation work.

The validity of maintaining these design requirements is borne out by electrical test data and by customer feedback concerning the unique "interchangeability" of system components as requirements change.

B. The mold construction and operation were complicated by the following requirements:

1. Material - PBT thermoplastic polyester for solvent and moisture resistance properties.
2. The overall block height (face to rear) was dictated by the following:
   a) The required minimum screw length which determined minimum binding post length
   b) The required minimum switch travel to provide electrical isolation of the two circuits
   c) The minimum required hard encapsulant depth to provide coverage and strain relief
   d) The minimum required post height (plastic) for good insulation resistance performance
   e) The provision of detents and stops within the plastic

Electrical and field trial performance data demonstrate the beneficial results of maintaining these requirements.

C. Market and product use requirements dictated that the electrical contacts within the block could not be gold-plated. As a result a variety of contact element configuration and platings were evaluated to yield the best electrical performance in a non-noble metal sliding contact system.

Although the present design is complete and thoroughly functional, additional designs have been developed for possible implementation at the appropriate manufacturing scale-up point.

## ELECTRICAL PERFORMANCE OF THE BLOCK

The Controlled Feeder Block or Modular Hardwire Block with switching capability combines u-contact connections, sliding contact connections and a screw terminal connection in providing the switching capability between the two interfaces.

During the initial product design stages, each of these connections was isolated during electrical performance testing under accelerated aging conditions to determine the relative performance of each. The performance of the factory terminated and hard encapsulated 24 AWG PIC wire in the u-contact by itself was found to be superior to that of the sliding contact. This is to be expected since the sliding contact design, which allows multiple insertions and withdrawals to be made during its life span, does not generally provide an electrical contact of the quality of a permanent contact. Bright tin plating (Tinglo Culmo) was used on the fork contacts in early prototype test samples. While the u-contact portion performed very well with this plating, the sliding contact performance was not satisfactory in accelerated aging tests. Improvement in performance resulted from the addition of pre-platings to the phosphor bronze base metal prior to bright tin plating. The best results were obtained by changing to a 60/40 tin lead plating.

In testing, measurements of connection resistance and connection resistance change (ΔR) are accomplished by mounting the test samples on special printed circuit boards which interface a temperature stabilized electrical measuring device, allowing automated measurements to be made. The apparatus allows resistance changes to within .01 milliohms to be determined.

All testing reported below was done using standard production blocks, pre-wired with 24 AWG plastic insulated conductors with 22 AWG PIC jumper wires used in the screw terminals. For uniformity, all test sample screw terminals were torqued to 12 inch-pounds. The ΔR values presented represent the total resistance change for all three types of connections in each "switch". For example; with the terminal in the "up" position the following electrical connections are involved:

1. U-connection to the "Feed In" conductor.
2. Wiping contact to the "Feed In" element.
3. Wiping contact to the "Feed Out" element.
4. U-connection to the "Feed Out" conductor.

With the terminal in the "down" position the following electrical connections are involved:

1. U-connection to the "Feed In" conductor.
2. Wiping contact between terminal post element and "Feed In" element.
3. Terminal post screw contact.

In the data summary which follows, the electrical stability of all these various contacts is considered, with each ΔR value reported representing the accumulated changes in all of these. Following a brief description of each test, a "Typical Value" will be reported. This typical value should be considered representative of the overall performance of the Control Feeder Block under the given test conditions. In the reporting of ΔR values, only absolute values will be given, indicating the typical overall magnitude of the change from the initial value.

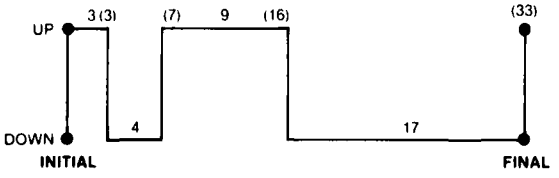
## TEST DESCRIPTION AND RESULTS

1. Stress Relaxation

The samples were maintained at 244°F (118°C) for 33 days. Initial readings were made in both UP and DOWN positions. The block terminals were cycled between the UP and DOWN positions as indicated in Table 1. Final readings were made at the test completion. The numbers in parenthesis indicate the accumulative days on test.

### TABLE 1

### Stress Relaxation Test




Terminal Positions During Test

NOTE: Dots indicate data readings.
Numbers indicate days on test, for the indicated terminal position.

Typical Results:

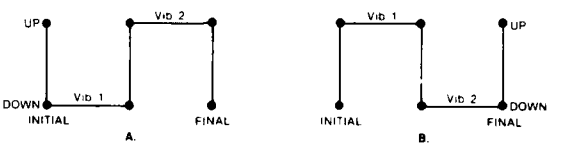
| Position | ΔR at Test Completion (milliohms) |
|---|---|
| UP | .5 |
| DOWN | .3 |

2. Vibration

The samples were mounted on a fixture allowing vibration for 20 minutes in each of three mutually perpendicular planes. The vibration rate was changed from 10 to 55 Hz and back at a uniform rate allowing one-minute cycles. The maximum vibration amplitude was .06" (1.5mm). The apparatus is capable of detecting opens of 10 microseconds duration. The control feeder blocks were tested in one of two configurations as indicated in Table 2. Note that each sample experienced two complete vibration tests.

### TABLE 2

### Vibration Test




Test Configurations

NOTE: Dots indicate data readings.

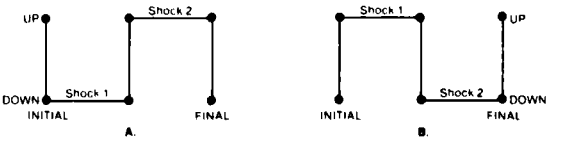
| Test Configuration | Screw Terminal Position | ΔR At Test Completion (milliohms) Vibration 1 | Vibration 2 |
|---|---|---|---|
| A | UP | .10 | .05 |
| A | DOWN | .05 | .08 |
| B | UP | .06 | .04 |
| B | DOWN | .08 | .10 |

3. Thermal Shock

The samples were subjected to five temperature cycles, each cycle as follows: One hour at —67°F (—55°C); 5 minutes at 77°F (25°F; one hour at 185°F (85°C); 5 minutes at 77°F (25°C). The control feeder blocks were tested in one of two configurations as indicated in Table 3. Note that each sample experienced two complete Thermal Shock tests.

### TABLE 3

### Thermal Shock Test




Test Configurations

NOTE: Dots indicate data readings.

Typical Results:

| Test Configuration | Screw Terminal Position | ΔR At Test Completion (milliohms) Shock 1 | Shock 2 |
|---|---|---|---|
| A | UP | .20 | .20 |
| A | DOWN | .18 | .20 |
| B | UP | .20 | .15 |
| B | DOWN | .18 | .20 |

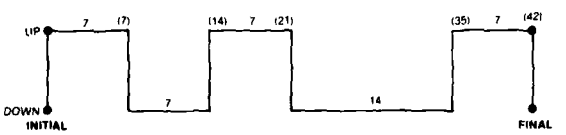
4. Salt Spray Aging

The test samples were placed in a salt spray chamber operated per ASTM B 117. The chamber temperature was maintained at 95°F (35°C) with the salt solution consisting of 5 parts (by weight) salt in distilled water.

The test was run continuously for 1,000 hours (42 days) with the terminals being switched from one position to another as indicated in Table 4. The numbers in parenthesis indicate the cumulative days of salt spray aging.

TABLE 4

Salt Spray Aging Test




Typical Results:

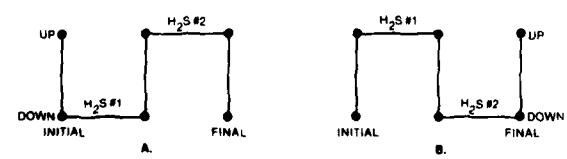
| Terminal Position | ΔR At Test Completion (milliohms) |
|---|---|
| UP | .18 |
| DOWN | .17 |

5. Hydrogen Sulfide Exposure

The test samples were exposed to a highly corrosive $H_2S$ atmosphere at 176°F (80°C) for one hour followed by exposure to a normal atmosphere at —67°F (—55°C) for one hour. The control feeder blocks were tested in one of two configurations as indicated in Table 5. Note that each sample experienced two complete hydrogen sulfide exposure tests.

TABLE 5

Hydrogen Sulfide Test




Test Configurations

**NOTE: Dots indicate data readings.**

Typical Results:

| Test Configuration | Screw Terminal Position | ΔR at Test Completion (milliohms) $H_2S$ #1 | $H_2S$ #2 |
|---|---|---|---|
| A | UP | .3 | .4 |
| A | DOWN | .3 | .6 |
| B | UP | .1 | .6 |
| B | DOWN | .2 | .2 |

6. Room Temperature Terminal Cycling

The Control Feeder Block terminals were cycled from the "IN" to the "OUT" position and back for the number of cycles indicated in Table 6. The change in connection resistance (from the initial value) was determined after the number of terminal cycles indicated. All tests were conducted at room temperature and in a normal room temperature atmosphere.

TABLE 6

Room Temperature Terminal Cycling

Typical Results:

| Screw Terminal Position | No. Cycles | ΔR at Test Completion (milliohms) |
|---|---|---|
| UP | 25 | .15 |
| DOWN | 25 | .15 |
| UP | 50 | .17 |
| DOWN | 50 | .17 |
| UP | 100 | .19 |
| DOWN | 100 | .25 |
| UP | 200 | .30 |
| DOWN | 200 | .40 |

7. High Humidity Insulation Resistance

The test samples were set-up with a constant 48 volts D.C. maintained between tip and ring throughout the test. The samples experienced twelve-hour temperature cycles from 40°F to 140°F (4°C to 60°C) for 75 days. Throughout the test the relative humidity was maintained at 95 ± 5% with 4¾ hour temperature stabilization at the temp. cycle end points.

Prior to testing, the terminals were cycled from the "UP" to "DOWN" positions as indicated in Table 7 with the insulation resistance measured using a D.C. potential of 250 volts. Insulation resistance readings were made as indicated in Table 7.

TABLE 7

High Humidity Insulation Resistance Test

Typical Results:

| No. Cycles | Final Terminal Position | Insulation Resistance (ohms) Feed In-Feed Out | Screw-Feed Out |
|---|---|---|---|
| 0 | UP | — | 100G |
| 0 | DOWN | 100G | — |
| 5 | UP | — | 100G |
| 5 | DOWN | 140G | — |
| 20 | UP | — | 100G |
| 20 | DOWN | 130G | — |

NOTE: G = 10⁹; 1 G in the table above represents 1,000 megohms

8. Dielectric Strength (Voltage Breakdown)

The test samples were maintained at room temperature and normal relative humidity. The electric potential between the appropriate terminals was increased at the approximate rate of 500 volts per second until voltage breakdown occurred. The data is presented in Table 8.

TABLE 8

Dielectric Strength

Typical Results:

| Terminal Position | Reading | Breakdown Voltage (kv r.m.s.) |
|---|---|---|
| UP | Tip-Ring | 11 |
| DOWN | Tip-Ring | 8 |
| UP | Tip-Tip | 12 |
| DOWN | Tip-Tip | 9 |
| UP | Ring-Ring | 10 |
| DOWN | Ring-Ring | 8 |

NOTE: The above voltage breakdowns occurred external to the block with arcing taking place between the screw terminals. Subsequent testing indicates that the typical dielectric strength between switch components within the block are 10 kv in the "DOWN" position, 13 kv in the "UP" position.

## APPLICATIONS

The development of the RAND design concept was a Bell System effort with input from the various operating company personnel. Thus, it is not surprising that there are several variations on the basic concept practiced by various operating companies today.

One basic requirement of the standard RAND design is that there should be only one "switch" between the subscriber and the Central Office. Common Feeder Pairs can be expressed through only one A-type interface to feed only one B-type interface. Adherence to this rule provides the simplest administration and assignment control of the common feeder pair counts. Common feeder is assigned in the A interface from the lowest pair counting forward and from the highest pair counting in a reverse sequence in the B interface, with buffer zones defined.

In special situations requiring increased flexibility, the standard RAND design allows for providing common feeder pairs between more than two interfaces, but the one "switch" limitation between Central Office and subscriber is still maintained. In these cases preferred counts must be established for each interface.

One of the variations on the standard RAND design is called extended RAND or ERAND. ERAND was developed for those portions of the feeder routes where feeder cable sizes are 100 pairs or less. The most significant difference between standard and extended RAND is that more than one "switch" is allowed between Central Office and subscriber in the ERAND design. Thus common feeder pairs generally appear in more than two interfaces and are expressed through more than one interface. Feeder pairs still maintain their Central Office identity through all interfaces. The engineer must assign each rural area interface a separate feeder preferred count.

## ERAND INSTALLATION

Rural service was designed using ERAND and the subject block and related hardware of the 3M Modular Hardwire System in a Northwestern Bell field trial in Waverly, Iowa. The hardware was installed and put in service in May, 1979. A schematic of the cable network design is shown in Figure 10. A total of 25 Controlled Feeder Blocks and 53 Modular Hardwire Blocks were used in the six rural area interfaces shown. Figure 11 shows typical jumpering from the CFB to the MHB for distribution in this cabinet. In this installation, 75 pairs are expressed through to the cabinets further from the Central Office.

As of the date of preparation of this manuscript, final field trial evaluation is not completed and Northwestern Bell has neither approved nor disapproved the block for use in the RAND application. However, discussions with engineering and craft personnel indicated that no problems were encountered during installation or have been encountered in normal route activity since that time. Although the time interval since installation has been too short to realize the true benefits of this flexible design, the facilities assignment supervisor for this area reported that record keeping and assignment for this route were error-free thus far.

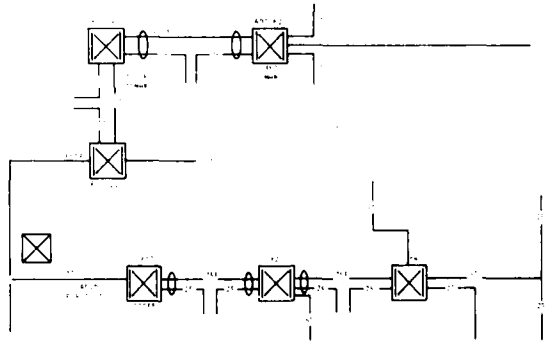
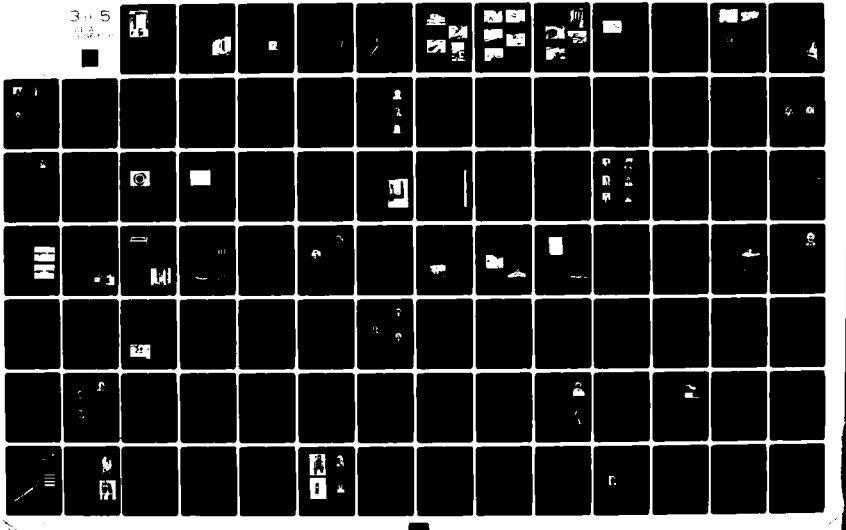


Figure 10. ERAND Schematic

AD-A096 308 ARMY COMMUNICATIONS RESEARCH AND DEVELOPMENT COMMAND --ETC F/G 9/1
PROCEEDINGS OF THE INTERNATIONAL WIRE AND CABLE SYMPOSIUM (29TH--ETC(U)
NOV 80 E F GODWIN

UNCLASSIFIED NL



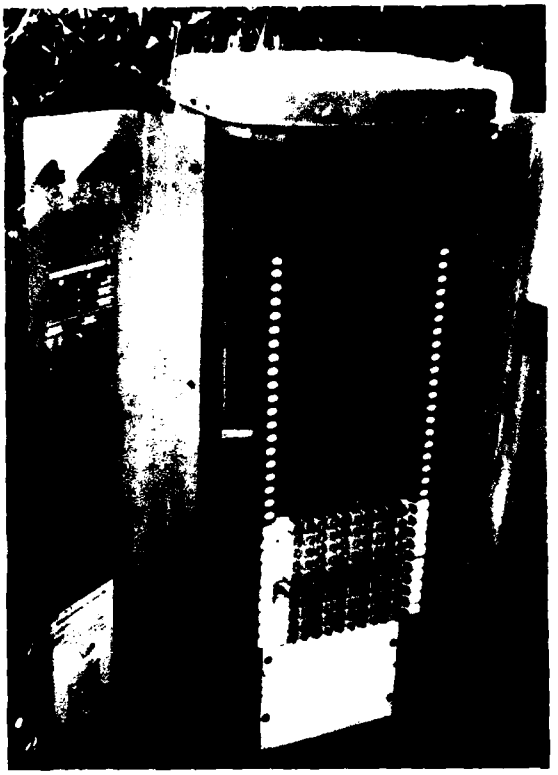


Figure 11. Typical jumpering from CFB to the MHB

The CFB has been used in additional RAND installations in nine operating companies.

## CENTRAL OFFICE CUT-OVERS

Another product use which has been defined for the Controlled Feeder Block since its introduction is in transferring service between Central Offices. The replacement of existing step-by-step Central Offices by new Electronic Central Offices has been a common, and major, occurrence for telephone operating companies in recent years. Extensive and thorough planning and testing are required prior to the actual time of the Central Office cut-over. Testing of each individual subscriber line from the new Central Office must be completed and all problems resolved prior to the cut-over date.

Since the cable plant construction and testing frequently require many months to complete, it is normally necessary to isolate the connection to the new Central Office to prevent excessive bridge loading on the existing circuits prior to cut-over. Similarly, when testing the new Central Office circuit it is necessary to eliminate the bridge tap created by the old Central Office connection.

The Modular Hardwire Block with switching capability provides the capability of selectively switching an individual subscriber line between the two Central Offices and eliminates the bridge tap problem. When the block is wired as shown in Figure 12, a new Central Office to subscriber circuit is tested by simply pushing in the appropriate tip and ring binding posts. Upon completion of testing, the subscriber is returned to control through the old Central Office by pulling the posts back out, and the craftsman moves on to test the next pair. At the time of the actual Central Office cut-over all the posts are pushed in.

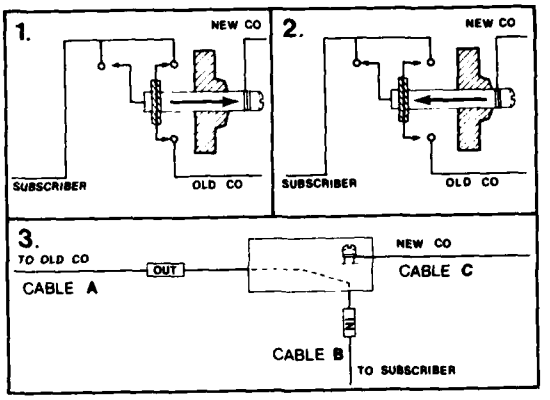



Figure 12. Block Wiring Schematic for Central Office Cut-over

Although the block was not originally designed for this purpose, several operating companies have found that it provides a time and cost-saving advantage over alternate methods which they have previously used for Central Office cut-overs. Most of the alternate methods have involved devices designed for inside plant, controlled environment applications and have resulted in reliability problems and the necessity of construction of large temporary structures to house them. In this respect, the pair density of the block is greater than most alternate devices and since the blocks are standard outside plant hardware, pedestal cabinets are readily available.

Other available outside plant devices are very expensive and not designed for inclusion as a part of the new Central Office cable plant. As a result, the block has been used in operating companies' designs where the cut-over pedestals became cross connect points in the new Central Office cable plant and in designs where they were semi-permanent; to be cut out as needed for further cut-overs or for RAND applications.

General Telephone of the Southwest used the CFB for transferring service from step-by-step Central Office to a new Electronic Switching Central Office in a suburb of Dallas, Texas.[1] Construction of the new Central Office began in late 1977 and approximately 3000 working lines were cut-over in July, 1979. Each of these lines were tested at least three times in a dial-through program to verify the functionality of the new Central Office circuit. Since the distance between Central Offices was approximately four miles, excessive bridge loading would have been a problem for the majority of the subscriber circuits if conventional cut-over techniques had been used.

In the GTSW cut-over design, both the Modular Hardwire Block and the Controlled Feeder Block were used.

The wiring method is shown in Figure 13. The new Central Office cable was terminated in the MS² module on the back of the Modular Hardwire Block and then jumpers were run to the binding posts of the CFB. This was done because some of the cut-over points were planned as permanent cross connect points in the new Central Office cable plant.

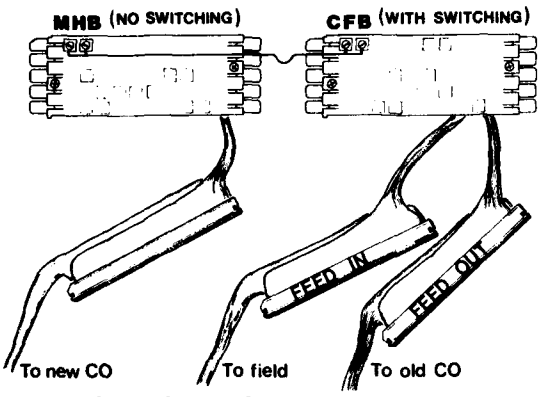


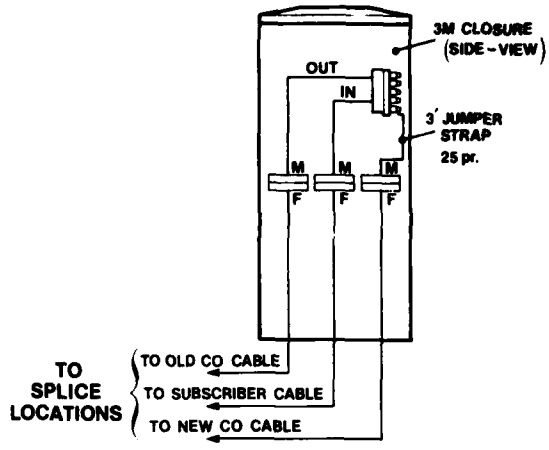

Figure 13. GTSW Central Office Cut-over Wiring Method

Once the modules had been spliced to the respective cables and jumpers from each subscriber had been connected to the assigned new Central Office pairs, the testing program began. The testing was done using two out-dial people at the new Central Office and a person located at one of the cross connect pedestal locations. The talk block pair at the pedestal was used for coordination. The customer was called on the old line first. Then the CFB posts for the customer were pushed in at the pedestal location and the operator called on the new Central Office number. A return call from the subscriber on the new circuit completed the verification procedure, and the CFB posts were pulled out to return control to the old Central Office. Each test caller completed about 300 test calls per day.

GTSW personnel indicated that both the preparation time for the cut-over and the cost of cut-over related equipment and labor were reduced to about one-half of what would have been required using their previous methods. In addition, they had the added benefit of nine completed cross connect points in their new cable plant.

The Modular Hardwire Switching Block was also used in a Central Office cut-over in the General Telephone Company of the Northwest. This 8000 line cut-over in North Richland, Washington was be[illegible] 1979 and completed in June 1980. Th[illegible] consolidated three old step-by-step offices into or[illegible] new Electronic Central Office and involved twenty-six [illegible]eparate locations. Since these offices were up to four m[illegible]les apart, excessive bridge loading was once again a consideration in the cut-over design. Inside plant cut-over devices had been used in previous cuts, but the high incidence of trouble in these devices (many had not been removed after two years), the extensive time required to wire-wrap the connections, and the problems with providing temporary structures convinced GTNW personnel that they were not suitable for further consideration. An alternate outside plant cut-over device was considered but eliminated in favor of the CFB due to both cost and size (one 2700 pair cabinet is located in a cable vault).

Due to limited craft availability, it was decided to pre-stub the cabinets to minimize the field installation time. Accordingly, the subscriber and old Central Office stubs were pre-connectorized with female ends for splicing to the MS² tails on the block. In addition, a three foot jumper strap with one end terminated in a male MS² module and the other ends pre-stripped for connection to the binding post screws on the block were pre-assembled. Thus, the pre-stubbed cabinets, as shown in Figure 14a and 14b, were delivered to the field for splicing to the respective cables.



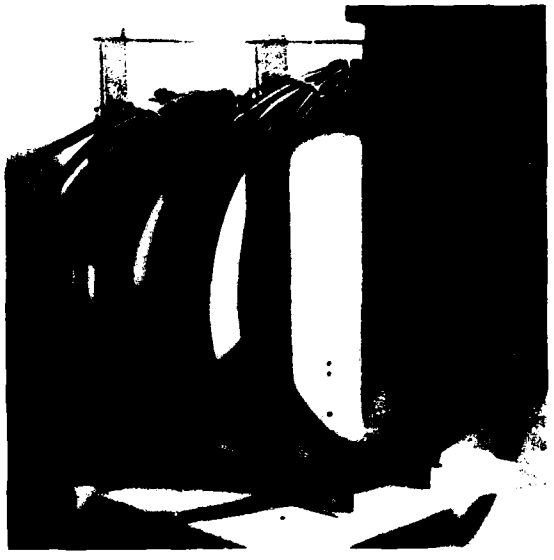



Figure 14a and 14b. Pre-stubbed GTNW Central Office Cut-over Cabinets

Since the GTNW cut-over design called for all of the cut-over cabinets to be removed following cut-over, the use of the three foot jumper strap for connection to the new Central Office cable provided cost advantages over the GTSW design.

## OTHER USES

Several other uses for the Modular Hardwire Switching Block have been defined including:

1. Test Points (Figure 15)
   Cable pairs can be isolated for testing without allowing access to the wire.

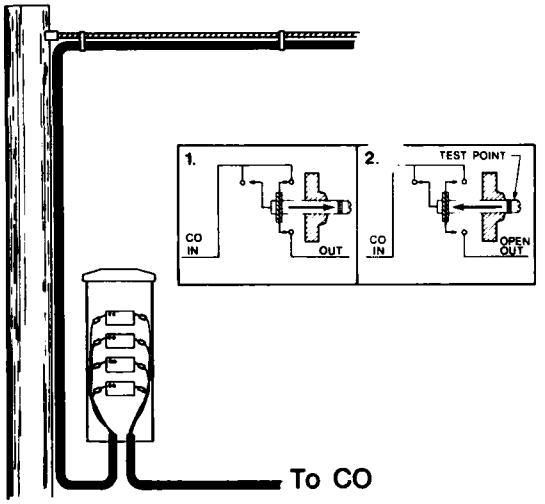



Figure 15. Block Used for Test Point

2. Boundary line test point (Figure 16)
   Use of the block at this interface allows connection between two telephone companies without jumper wires and without front face appearance of the pair. Access to either Central Office is available by simply pushing in the binding posts.

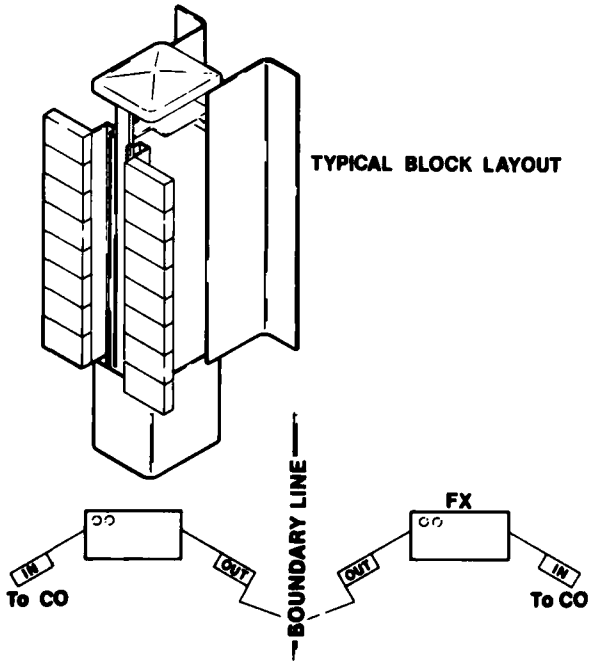



**Figure 16. Block Used for Boundary Line Test Point**

## SUMMARY:

The Modular Hardwire Block with switching capability (CFB) was designed to meet the basic requirements of the Bell RAND concept. The design approach used, however, also strongly emphasized human engineering, reliability, and compatibility with other components of the 3M Modular Hardwire System. Michigan Bell and the General Telephone System have standardized this product for RAND applications as a result of field trial performance.

In addition, many operating companies have found that this block, as a component of the total hardwire system, provides a cheaper, more reliable, and more compact solution to several other outside plant "switching" requirements.

## ACKNOWLEDGEMENTS:

The author wishes to express his gratitude to the Northwestern Bell, General Telephone of the Northwest and General Telephone of the Southwest personnel who provided candid and invaluable product performance information in their respective applications. The many contributions of colleagues at 3M TelComm Products Division are also gratefully acknowledged.

## REFERENCES:

[1] "Cross-connecting to simplify cutover" Telephone Engineer and Management, September 1, 1979

---



**Gary B. Matthews**
**TelComm Products Division/3M**
260-3A1 3M Center
St. Paul, Minnesota 55144

Gary B. Matthews is a Product Development Specialist in the TelComm Products Division of 3M. He received his MS degree in Mechanical Engineering in 1970 from Clarkson College of Technology. Prior to joining TelComm Products in 1976, he worked in the 3M Central Research Laboratory.

# AUTOMATIC CONNECTORIZATION OF 25 PAIR CABLE

Roger. G. Ebrey
Herbert A. Sckerl

Western Electric Co., Inc.
Norcross, Ga.

Gary G. Seaman

Western Electric Co., Inc.
Denver, Co.

## Summary

A new process is described for automatically terminating telephone connector cable to solderless connectors. Discussed in depth is a machine capable of automatically connectorizing one end of a length of 25 pair cable say 400 feet long after the other end has been connectorized manually. The automatic operations performed by the machine result in the wires being collated and inserted into a connector. An alternate design approach to the machine will be described in wnich relatively short single-ended connectorized cable can be produced on a continuous basis by paying off from a reel of connector cable which has been pre-connectorized on the inside end. Of particular interest in the report is the manner in which wires are individually identified and manipulated at high speeds.

## Introduction

Connector cables are used extensively throughout the Bell System to interconnect equipment and apparatus. Millions of these cables are manufactured annually at Western Electric, and the demand for their usage is expected to remain high. Typically, connector cables are 25 pair, 24 or 26 gauge, sheathed and connectorized at one or both ends with solderless connectors. Lengths vary from about two feet to more than four hundred feet. Through the years, the assembly techniques for these cables have become nearly standardized and consist of the following basic steps: (1) Dereel cable from cable reel and cut cable to length; (2) remove a specified length of sheath from one end of the cable to expose wire leads; (3) select individual leads in accordance with insulation color coding and place leads in proper sequence into a manual or semi-automatic wiring fixture; (4) using the wiring fixture, cut leads to length and insert them into a solderless connector; (5) repeat the connectorizing operations on the opposite end of the cable if required. With the exceptions of mechanized cable dereeling and an automatic wire cutting and insertion capability, all operations are performed manually.

Because of the high labor intensity associated with connectorized cable, the idea of complete automatic assembly has long appeared attractive. Until recently, however, the inability to rapidly identify and sort large numbers of wire has been a major factor preventing the success of such a project. Now, with the development of two new devices, a wire identification mechanism and a wire collating mechanism, automatic assembly of connectorized cable has become feasible.

Figure 1 and Figure 2 depict the basic concepts associated with these mechanisms.

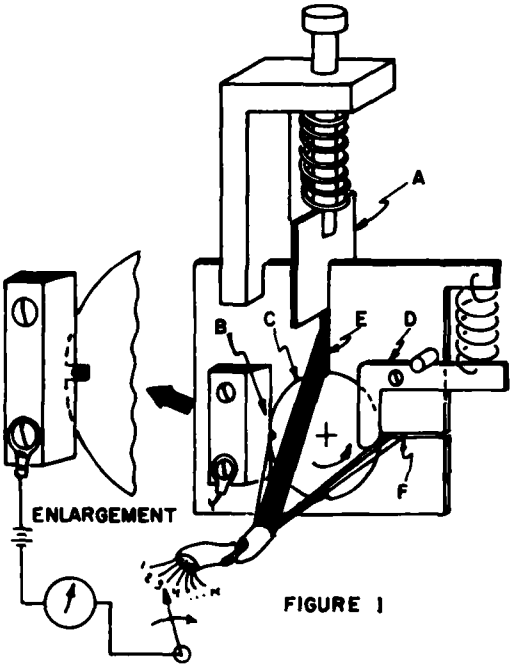



FIGURE 1

In Figure 1, a cable consisting of 50 wires is desheathed for a short distance and the wires are stacked into slot (E) as shown. A spring-loaded blade (A) is lowered into the slot producing a compressive force on the wires. An indexing disk (C) with four equally-spaced notches rotates counterclockwise in 90 degree increments. The notches are sized to allow entry of only a single wire. Upon the first index, a wire drops from slot (E) into a notch in the disk. On the next index, the wire is carried to position (B). Here, as shown by the enlarged view, a knife blade has been so positioned that it cuts through the wire insulation and makes electrical contact with the copper conductor. If

the opposite end of the wire has been previously connected to a known terminal, such as Number 3, the identity of the wire at the knife blade can be easily established as the Number 3 wire, since the Number 3 terminal is the only terminal providing continuity.

By the use of high speed electronic decoding techniques, the identity of any given wire in a 50-wire cable can be determined in a matter of a few mili-seconds. Finally, disk (C) is indexed to the next position where the identified wire is transferred into the exit slot (F). By repeated indexing of the disk, the process is continued until all the wires in slot (E) have been identified and transfered into slot (F). With the use of an electronic memory, the identity and order of the wires in slot (F) can be retained until subsequent wire collating operations can be performed.

By adding a second exit slot and a special controllable escapement to the mechanism shown in Figure 1, it is possible to separate the identified wires into two groups, one group for all wires numbered from 1 to 25 and the other group for all wires numbered from 26 to 50. In an early experiment, using a mechanism of the type just described, it was demonstrated that a column of 50 randomly distributed wires could be identified and separated into two groups in 3.7 seconds or less.

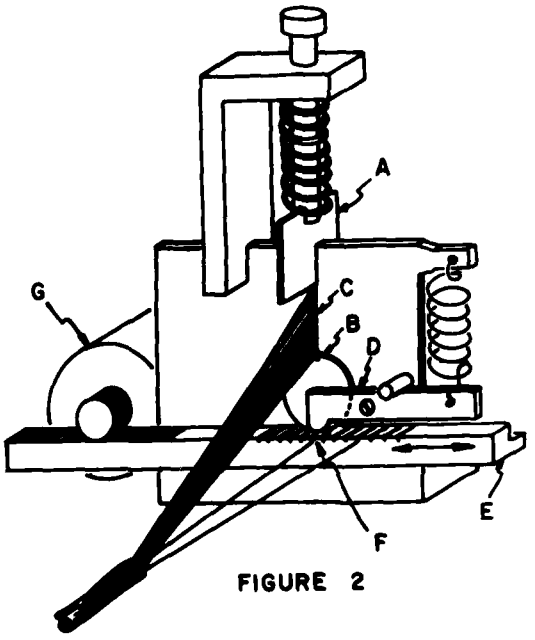



FIGURE 2

Figure 2 represents a wire collating mechanism. Wires are stacked into slot (C) as shown, but in this case the identity and order of the wires are already known-typical of the condition of wires that have been processed through the wire identification mechanism. Again, a spring-loaded blade (A) is lowered into the slot to produce a compressive force on the wires. An indexing disk (B) with two equally spaced notches rotates counterclockwise in 180 degree increments. As before, the notches in the disk are sized to allow the entry of only a single wire. As the disk rotates, the first wire from the column of wires is picked off and is carried toward a transfer position (F). S'ightly in advance of the rotation of disk (B), a pre-selected notch on rack (E) is indexed by means of a stepping motor (G) to the transfer position (F). When the wire in the rotating disk (B) arrives at position (F), a spring-loaded escapement lever (D) transfers the wire into the pre-selected notch on the rack. Disk (B) indexes again and the second wire from the column of wires is picked off and carried towards position (F). Once again, a pre-selected notch on rack (E) is moved to position (F) to await the transfer of the wire from the rotating disk. The process is repeated until each wire in slot (C) has been transferred into a selected notch on rack (E).

Any desired order of wires in rack (E) can be established by pre-selecting which notch in the rack is at position (F) at the time of wire transfer. With the use of a computerized controller operating from stored information as to the order of the wires in slot (C), the rearrangement of wires to any new order in rack (E) is readily accomplished. A mechanism like the one shown in Figure 2, has repeatedly demonstrated that 25 randomly ordered wires can be collated into a sequential numerical order in less than 3.5 seconds.

In an effort to maintain lower production costs in the connector cable market, Western Electric has developed and built an automatic connectorizing machine utilizing the wire identification and collating concepts just described. This machine is referred to as Autoconn.

## Autoconn Machine

Autoconn (Figure 3) is a fully automatic machine capable of attaching a 25 pair solid wire cable to a variety of commercially furnished connectors. It is a pneumatically operated, electronically controlled machine and, with the exception of an externally located vacuum system, is totally self-contained. This seven station indexing machine is 12'0" long, 4'0" wide and approximately 5'0" high. The working level is about 3'6" from the floor making it a stand-up operation.

It is supplied with a length of 25 pair connector cable say 400' long with one end connectorized as a reference in the identifying process.

Electrically, the machine is divided into four micro-processor controlled sections. All of the electronics are contained within the structure of the machine with an interface provision for de-bugging, reprogramming and maintenance purposes.

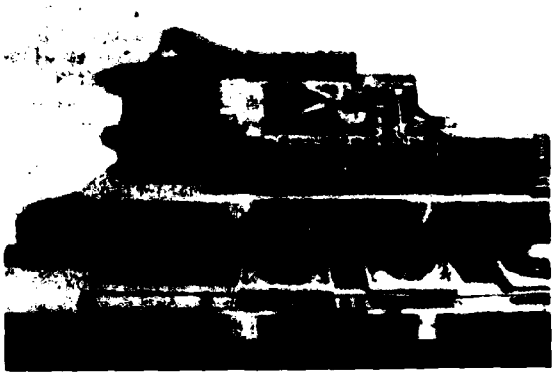


FIGURE 3

Mechanically, the machine has seven major stations plus an indexing conveyor, a vibratory feed system for orienting and supplying connectors to the load station and a reference connector unit. Also, part of but not attached to the Autoconn is a 14 foot long conveyor (Figure 4) which is positioned in front of the machine slightly below the reference connector unit. This conveyor has an escapement mechanism which controls the rate of feed of the supply containers as they pass through the Autoconn operations. The escapement is controlled and synchronized by the machine program.

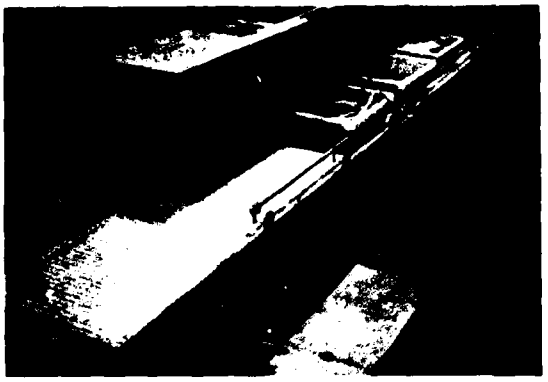


FIGURE 4

The seven major stations on the machine are:

1. Desheath (Figure 5)-which removes required length of sheath.
2. Comb (Figure 6)-which removes twist from pairs.
3. Transfer - which holds wires in a flat plane.
4. Identify and Collate (Figure 7)-which identifies individual wires via pre-connectorized end and places them in a like sequence for insertion into the connector.
5. Transfer and Space (Figure 8)-which transfers and spaces the wires at the proper intervals required for insertion into the connector.
6. Connectorization (Figure 9)-which locates and secures the wires in the correct position adjacent to the connector and then cuts and inserts the wires into the connector sequentially 5 pairs at a time.
7. Connector Load (Figure 10)-which positions the correctly oriented connector in the connectorizing station.



FIGURE 5



FIGURE 6

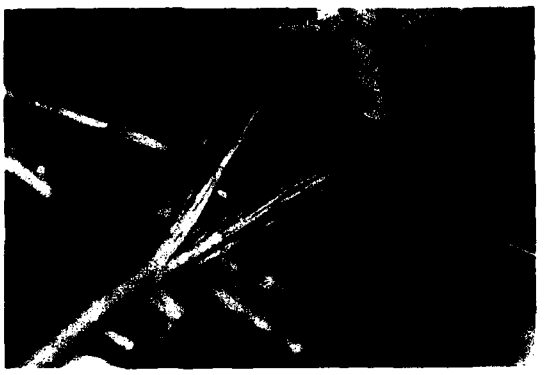


FIGURE 7



FIGURE 8



FIGURE 9

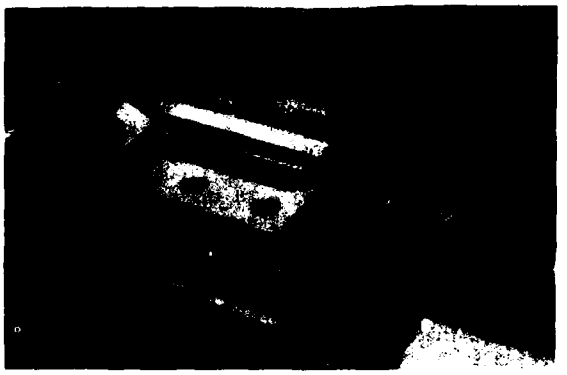


FIGURE 10

The indexing conveyor (Figure 11) consists of a number of re-circulating cable-holding units which clamp and transport the individual cables through the various work stations. Each unit returns to a beginning point after completion of its cable.

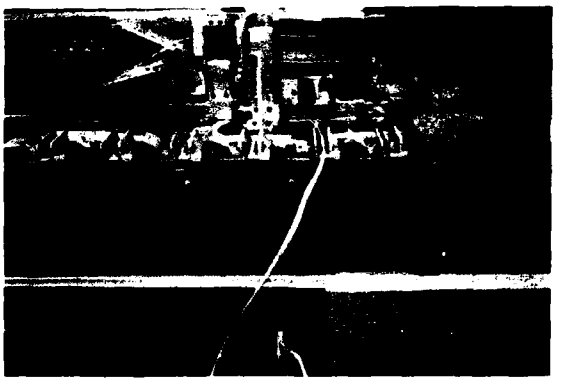


FIGURE 11

The vibratory feed system (Figure 12) feeds connectors to an orientation device after which they are delivered to a loading mechanism for insertion into the load station.

The reference connector unit (Figure 13) has a number of connectors which are wired to a microprocessor unit. Prior to insertion of the blank cable end into the machine the pre-connectorized end of the cable is plugged into the reference connector unit. This is required to allow the "Identify and Collate" station to function correctly. After all wires have been identified and collated, the reference unit automatically ejects the pre-inserted cable allowing the loose end to fall into the container which transported the cable to the machine.

The operator's control panel (Figure 14), located on the extreme right-hand side of the machine table, consists of several control buttons and a 'Christmas Tree' light display showing at a glance the functional condition of the machine at any given time through the use of green, 'Go', and red, 'Don't Go', indicators. There is a red and green indicator for each major machine function. Operating in conjunction with the operator's 'Christmas Tree' is an alpha-numeric display unit (Figure 15) centrally located above the machine casing. This will display malfunction descriptions at the locations indicated on the operator's display panel. This display will also instruct the operator during the start-up routine, asking such questions as "Correct plug or receptacle being used?", "Multiple or single mode of operation?" and other conditional questions which have to be resolved before the machine can be put into full operation.



FIGURE 14

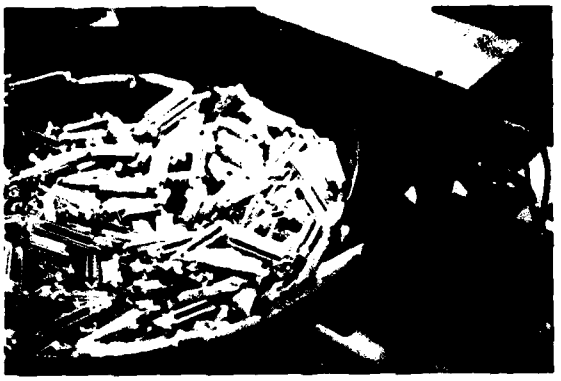


FIGURE 12

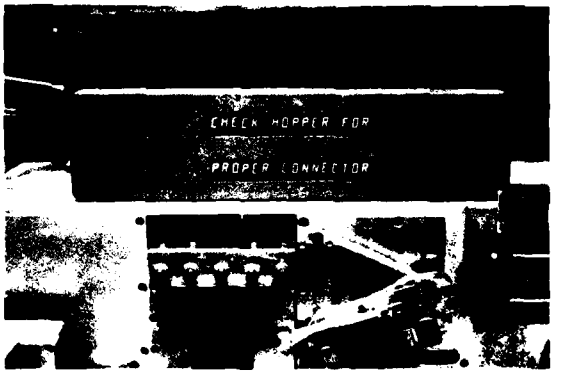



FIGURE 15

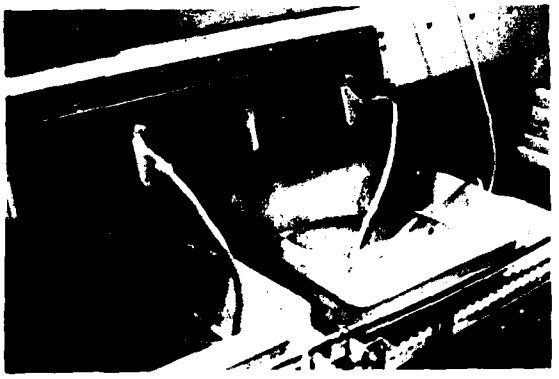


FIGURE 13

In addition to the previous start-up routine, the operator's major function is to feed connector cable to the machine and to remove connectorized cables from the machine upon completion. Secondary functions include loading the connector feed hopper with connectors as required, removal of de-sheathed ends of cable jacket as accumulation occurs in the container, also, periodic disposal of cut wire ends, resulting from the connectorizing operation, which are transported by the vacuum system (Figure 16) into a reusable container.

The fully automatic operation results in a double ended connectorized cable, one end of which has been pre-assembled by other means, the second end being automatically attached by the Autoconn. At this point, the assembled cable can be tested for 'Opens', 'Shorts', or crosses using a standard test set. If this was a 400'0" cable, it would now be practical to produce say forty 10' double ended cables by repeatedly recycling the cable

through the machine and cutting off a 10' length after each pass. The 10' length of cable could be connectorized on the opposite end by using the newly attached connector as a reference. Thus, of a total of 80 connectorized ends, 79 could be attached by Autoconn.



FIGURE 16

The cycle time of the Autoconn at this time is around 30 seconds which is three to four times faster than existing assembly methods. The machine is not, however, limited to this speed since the addition of dampers to certain stepper motors in the collate mechanism will enable the cycle time to be decreased to approximately 15 seconds.

The machine is controlled by three 8080 microprocessors. To allow simultaneous and independent operation of the seven sections of the machine, their control is partitioned as follows:

Microprocessor 1 - Desheath Station
- Comb Station

Microprocessor 2 - Transfer Station
- Identify and Collate Station

Microprocessor 3 - Transfer and Space Station
- Connectorize Station
- Connector Load Station

This arrangement greatly simplifies the programming, debugging and maintenance of the machine. Each microprocessor inputs the status of various switches to confirm correct machine operation. This feedback is converted to error codes which are output to the master microprocessor.

A fourth 8080 microprocessor acts as a master controller. It communicates with the three slave microprocessors through input/output ports using handshaking techniques. Its sequence of functions is:

1. Output status to slave processors.
2. Output start signal for each cycle.
3. Index both conveyors.
4. Input end-of-cycle signal from slaves.
5. Input error status from slaves.
6. Output error information and operator instructions to alpha-numeric displays.
7. Operate front panel lights and read selector switches.

The master microprocessor could easily be programmed for data collection and maintenance routines.

## Autoconn-Sequence of Operations

A container, holding a coil of cable having a connector on the inside end, is loaded onto the machine conveyor. The operator inserts the connectorized end into a plug or receptacle on the reference connector panel (Figure 13). The outside end of the cable is examined for any obvious defects after which it is then inserted into the de-sheathing station (Figure 5). The cable is then clamped into a carrier (Figure 11). The loading of this end into the de-sheath mechanism automatically initiates the total machine operation.

The machine sequences are as follows:

1. De-sheath (Figure 5)
   a) Insert free end of cable into the de-sheath head and clamp cable into carrier.
   b) A heating process softens the sheath to a point where it may be separated from the cable.
   c) The head retracts removing the required length of sheath which is deposited into a container for later removal.
   d) Machine indexes.
2. Comb Station (Figure 6)
   a) The released conductors are fed between two comb jaws which advance and retract a number of times. At each stroke the upper jaw raises and lowers as the heads move longitudinally over the conductors. The action unwinds the the twisted pairs and at the completion of the operation,

the conductors are all lying flat in a plane within the two jaws. The gap between the jaws is sufficient to give a slight clearance over the wire diameters enabling the wires to feed from the station in a flat array.

b) Machine Indexes.

3. Transfer Station

a) This is a holding position at which no machine activity occurs.

b) Machine Indexes.

4. Identify and Collate Station (Figure 7)

a) The flat array of conductors is fed through a slotted plate to a pick-off wheel. Conductors are removed one at a time by this pick-off wheel and rotated approximately 25 degrees where they engage a steel disc having a sharp edge. This disc is electrically isolated from the machine frame and carries a small electrical voltage. The edges of the disc nicks the wire insulation just enough to make electric contact with the copper conductor. Because the opposite end has been plugged into a reference unit, we have now created a 'ring-out' condition in which we can electrically establish the location of each wire in the connector. The conductor having been identified, it now becomes a simple matter to transfer it to an upper or lower gate where it is transferred to a lateral moving rack. This rack is positioned by a stepping motor which has received information from the identifying disc, via the electronic controls, telling it which slot to position at the gate. The conductor now unloads through the gate into the pre-positioned slot. This process is repeated for the remaining 49 conductors until each one has been correctly collated into upper and lower racks. This is the longest operation on the machine and is variable depending upon the sequence of conductors as they are received by the stations.

b) Machine Indexes.

5. Transfer and Space Station (Figure 8)

a) The two collate racks from the previous station have unloaded the upper and lower wire arrays into slotted ramps where they maintain their collated condition. These arrays are subsequently transferred at index to a connector rack which spaces the wires at the correct center distances for insertion into the connector.

b) Machine Indexes.

6. Connectorize Station (Figure 9)

a) As the machine indexes the loaded connectorizing rack moves between the connectorizing heads. At the same time, a mandrel, which has previously been loaded with a connector, is also advanced between the connectorizing heads from the opposite direction. The heads now advance in two movements. The first movement brings spacers in between the wires in the rack and aligns them with the connector elements. The second movement cuts and inserts five wires at a time, top and bottom, until full insertion is completed. (Since the amount of pressure required to cut and insert one conductor is approximately 35 pounds, it was felt from a design standpoint that inserting five wires at a time represented the optimum condition without unduly overloading any components.) Both heads then retract to their open position. The connectorizing rack, which now has small wire ends in it, returns to the previous station. Located between these two stations are an upper and lower vacuum nozzle. It is during this return stroke that the wire ends are removed by the vacuum system.

Meanwhile, the assembled connector remains at the station until manually removed by the operator. This station has electrical interlocks which prohibit the machine from any further movement until the completed cable is removed.

Upon removal of the cable, the machine is now under the influence of the de-sheath station which reinitiates the machine cycles.

The machine is capable of being run in either a single or multiple mode. In single mode, a cable is processed through the machine on its own with no further cables being inserted. In multiple mode, each cable carrier is loaded as it reaches the de-sheath position thus ensuring a continuous production capability.

## Single-Ended Cable Connectorizing Machine

A second machine (Figure 17), employing many of the principles used on the Autoconn machine, has been developed for manufacturing relatively short, single-ended connectorized cables. By feeding cables from two separate reels, each containing a mile or more of cable, the machine is capable of continuous high-speed operation. A unique feature of this facility is that hundreds of short connectorized single-ended cables can be produced with only one connectorizing set-up per reel.

The basic machine consists of a commercial straight line chassis approximately nine feet in length. Mounted on the chassis are six work stations and a wire shuttle mechanism. Cable carriers, mounted

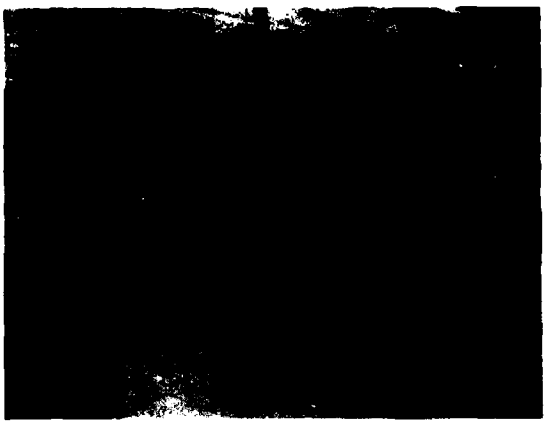


FIGURE 17



FIGURE 19

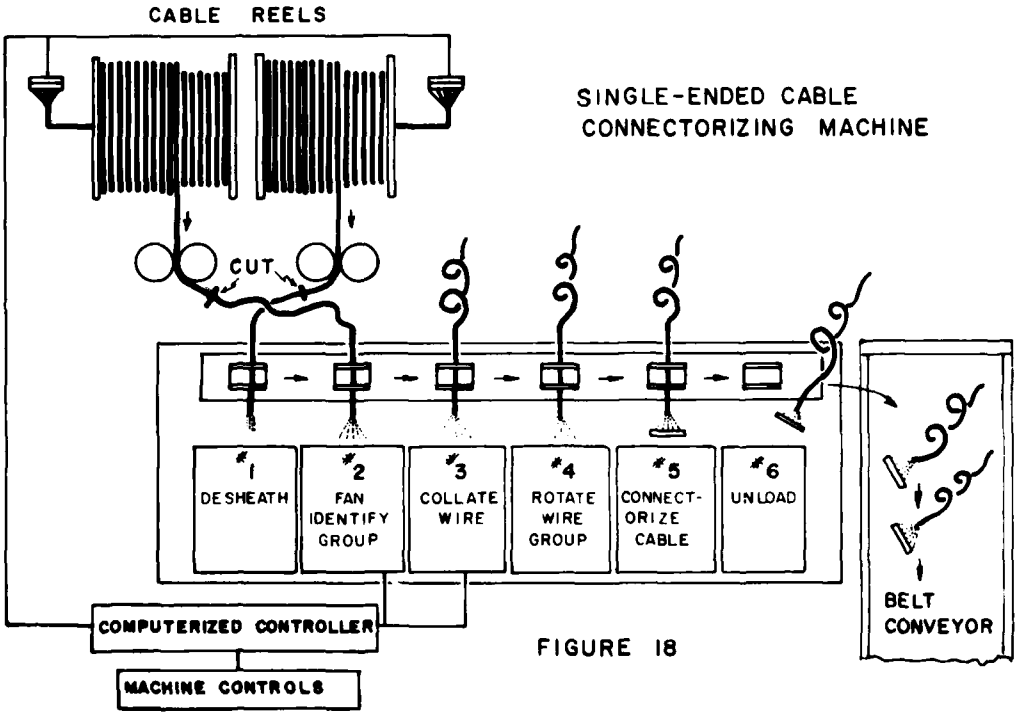



FIGURE 18

to an over and under style indexing conveyor, advance cables from one work station to the next. Located out board from the machine chassis are two reels of cable with their associated dereeling mechanisms. All machine functions are fully automatic and are controlled by a miniature computer. Machine cycle time is 12 seconds.

The procedure for setting up the machine requires that an operator manually connect wires from the inside coil of a reel of cable to a terminal field which, in turn, is connected to the machine's computerized controller (Figure 18). All wires must be connected to the terminal field in accordance with a pre-selected wire color code. Any wiring error in this operation will result in a duplicate error on the finished cable assemblies. The manual wire connectorizing operation is performed once per cable reel.

In operation, cable is fed directly from the first cable reel through its dereeling system into the first work station. The dereeling mechanism (Figure 19) is designed on a spinning reel concept and eliminates the need for electrical slip rings. At the first work station, a 5-inch section of sheathing is removed from the end of the cable. The machine is indexed and the de-sheathed end of the cable is advanced to the second work station. Here, the exposed wire leads are fanned to a single layer and then electrically identified and placed into two wire groups as previously described. The wire identity information is fed back to the computer and temporarily stored in its memory.

During the time the de-sheathing and wire identification operations are taking place, a section of cable is fed from the reel and measured to length. As soon as the wire identification process is complete, the cable is cut. Immediately, the loose end of the cable still attached to the cable reel is directed, through a series of guides, back to the first work station in preparation to repeat the process. On alternate machine index cycles, the cable from the second reel is fed into the first work station and processed in the same manner as the first cable. By utilizing two reels of cable, the production output of the machine is effectively doubled since the first work station is supplied with a new charge of cable after each index of the machine. As the machine is currently designed, the maximum length of cable that can be conveniently processed is about 8 feet, longer lengths become cumbersome and difficult to handle. With the development of an automatic coiler, long lengths of cable can be accommodated.

To continue the process, the cable at the second work station is indexed to the third work station. A wire shuttle mechanism prevents the original order of the wires from being altered during index. At the third station, a pair of servo-driven wire collating mechanisms, operating from the stored information in the computer, rearranges the wires in each wire group into proper sequential order. After collating, the cable is indexed to the fourth work station. Again, a wire shuttle mechanism prevents the order of the wires from being altered during the index. At the fourth work station, the two wire groups are rotated 180 degrees to alleviate a wire twist problem. With a second generation machine, the twist problem will be corrected and the need for the station eliminated. On the next index of the machine, the cable is advanced to the fifth work station. Here the cable wires are individually inserted into a solderless connector in the same sequential order as established at the collating station. Finally, the connectorized cable assembly is indexed to the end of the machine where it is unloaded by the operation of the sixth work station. Under continuous operating conditions, the machine is capable of producing completely connectorized, single-ended, 25 pair cable of a designated length, every 12 seconds.

## Conclusion

Two automatic connectorizing machines have been developed, each satisfying a specific production need. By using the concepts presented here, it is conceived that other machines, capable of performing similar tasks, can also be developed. Care needs to be exercised, however, for mechanical manipulation of wires is beset with difficulties; and as the number of wires being processed is increased, the difficulties are significantly increased. Nevertheless, many projects now lend themselves to automatic connectorization; and with skilled and dedicated effort, successful results can be achieved (Figure 20).

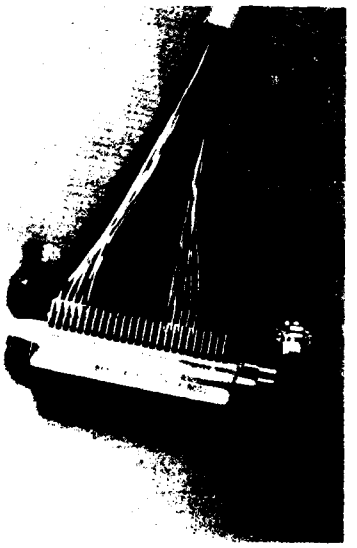


FIGURE 20



Roger G. Ebrey
Western Electric Co., Inc.
2000 N.E. Expressway
Norcross, GA 30071

Roger G. Ebrey is a Senior Development Engineer at the Western Electric Atlanta Works in Norcross, Georgia where he has been actively involved in the automatic connectorization of solderless connectors since 1976.

Mr. Ebrey was born in Birmingham England where he received both his formal and technical education. He emigrated to the United States in 1967 and has been employed by Western Electric since 1970. He has had several articles published in the Western Electric "Technical Digest" associated with connectorization.



Gary G. Seaman
Western Electric Co., Inc.
1200 W. 120th Avenue
Denver, CO 80234

Gary G. Seaman is a Senior Engineer at the Western Electric Works in Denver, Colorado. He received a B. S. Degree in Mechanical Engineering from Iowa State University in 1956 and a M. S. degree in Engineering Mechanics from the University of Nebraska in 1968. Since joining Western Electric in 1956, Mr. Seaman has been engaged primarily in the design and development of automatic assembly and processing machines. Eleven patents have been granted to Mr. Seaman for his work in the field of mechanization.



Herbert A. Sckerl
Western Electric Co., Inc.
2000 N.E. Expressway
Norcross, GA 30071

Herbert A. Sckerl is a Senior Engineer at the Western Electric Atlanta Works. He received his Bachelor of Electrical Engineering from the Georgia Institute of Technology in 1964.

Since joining Western Electric in 1966, he has worked primarily on machine and process control systems.

# CONNECTOR PERFORMANCE MONITORING IN THE OUTDOOR CROSS CONNECT ENVIRONMENT

I.E. Martin A.N. Satar C.D. Gupta

Bell-Northern Research
Ottawa, Canada

Bell Canada
Toronto, Canada

## ABSTRACT

Bell Canada, like other telephone operating companies, has a considerable investment in outdoor cross connect cabinets and connector hardware in the local distribution network. A serious problem associated with these outdoor connectors is intermittent line noise generated by fluctuating insulation resistance or contact resistance. In view of the maintenance costs involved, it was decided to conduct a thorough investigation into the causes of these failures and determine what factors can influence them.

A long term study was undertaken by BNR in 1978 to monitor the environment and the behaviour of connectors in a cross connect cabinet. This provided detailed knowledge of the mechanisms causing connector degradation and failure. It provided correlation of laboratory testing to actual field conditions, thus allowing more reliable, accurate and representative laboratory testing.

## INTRODUCTION

The majority of telephone companies use some form of outdoor connector cabinets for interfacing feeder cables with subscriber distribution cables. Bell Canada finds, as do many operating companies, that certain kinds of connectors eventually become unreliable, depending on their external environment and location. Because of the considerable investment in these devices, retrofitting or replacing them can be very costly.

In 1978 BNR undertook an investigation to determine the actual field performance of various connectors and outdoor cross connect cabinets. There were two main objectives: to determine the factors and mechanisms leading to connection failure, and to find a correlation between actual field service and accelerated-environment testing in the laboratory.

Daily temperature and relative humidity are being monitored, both inside cabinets and in the outdoor environment. It is known that temperature cycling and moisture are major contributors to connection failures. Electronic equipment continuously monitors and records changes in insulation resistance on connectors and terminals. Contact resistance is also measured on a periodic basis. An understanding of the factors controlling these two parameters can aid the telephone operating company in selecting and installing outdoor cabinets and connectors for optimum service life.

## FAILURE MODES

For telephone users, failure of a connection occurs when electrical noise is generated. In terms of interconnection hardware, there are two modes of failure: below-normal insulation resistance and above-normal contact resistance.

The nominal level of insulation resistance (IR) between the tip and ring wires in a pair is $10^8$ ohms or better. In this range, good telephone transmission is assured. When the IR drops to $10^6$ ohms, some noise is noticed by the user. At $10^5$ ohms or less, the line is very noisy or even unserviceable. Figure 1 illustrates the relationship between IR and noise level. In the outdoor connector cabinet this type of failure occurs when water condenses on the connectors. This film of water contains dissolved impurities from the surroundings and therefore forms a conductive bridge over the insulation between terminals (See Figure 2). The formation of this water film is directly influenced by the temperature and relative humidity inside the cabinet. The conductivity of the film depends, to some extent, on the types of impurities present in the atmosphere.

Contact resistance, between a wire and a connector, is acceptable at 1 to 2 milliohms. Resistance changes above this range are probable sources of noise and are frequently a first step towards complete connection failure. A number of different connector types are in use, but all depend

on a high compression force to maintain a gas-tight joint between metal surfaces. Unfortunately, whether the wire is clamped under a screw head or between parallel spring beams or by some other means, repeated wide temperature excursions may lead to ultimate breakdown of the gas-tight joint.

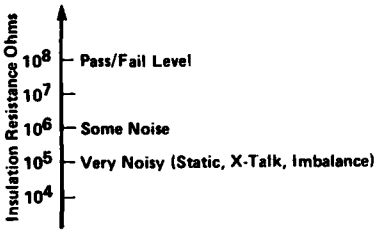



Fig. 1 Noise Levels

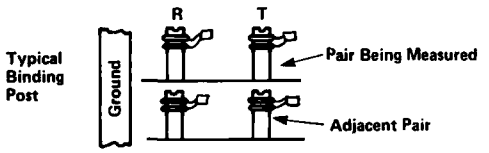



Fig. 2 Insulation Resistance is Typically in the Order of Mega Ohms. Dirt and Moisture Between the Ring and Tip, Adjacent Pairs or Ground are Typical Causes for a Reduction in I.R.

In the cabinet environment, as will be seen later, there is a wide variation in the daily temperature. As a consequence, the wire and connector expand and contract regularly, but at slightly different rates as they are made of different metals. Eventually this cycling will lead to failure of the gas-tight seal between contacting surfaces. As soon as air enters the interface, an insulating film forms, and failure of the connection is under way.

## FIELD MONITORING APPROACH

The first step in the program to monitor field performance of connectors was to select four sites within Bell Canada territory. Two urban sites were chosen, in Montreal and Hamilton, representing cities near large bodies of water and having an industrial environment. The other two sites are near Ottawa and Simcoe, representing more rural environments. Each of the sites is close to a government weather monitoring station.

Identical cabinets were installed at all four locations and fitted with six different types of connecting devices. Each connector was completely terminated with wires of a type and size specified for that connector.

The internal environment of each cabinet is measured by a single instrument which produces a 31-day continuous chart of temperature and relative humidity (hygrothermograph). The outdoor temperature and relative humidity statistics are obtained from the government weather office.

Since contact resistance does not change rapidly, it is measured in the cabinets at 6-month intervals. A precise resistance measurement method is used. This can be compared with the accelerated laboratory test in which a connector is subjected to temperature cycles from -40 to 55°C at a rate of 6 cycles per day. The correlation between the two methods is discussed later.

Changes in insulation resistance tend to occur rapidly. Our main interest is in the frequency and duration of fades below $10^8$ ohms. Although noise starts occurring at $10^6$ ohms, this study used $10^8$ ohms as its criterion because of the relatively small connector sample size. This is a basic measure of telephone line quality. As a result of the irregular behaviour of insulation resistance, it was realized that a method was needed to continuously monitor a number of connections and record the occurrence and duration of each fade.

To meet this requirement BNR designed and built a recording monitor which is small enough to fit into a cross-connect cabinet. The monitor is a solid-state device which counts the number of IR fades below $10^8$ ohms and measures the duration of the fades. The recording capacity of the monitor is sufficient to store data for a full month of operation. A maximum of 96 pairs can be monitored at each cabinet. To ensure that the monitors are functioning properly, some control samples are also being continuously monitored. The monitor shown in block diagram form (Figure 3) consists of four basic circuits: $10^8$ ohm threshold detector, clock, time recorder and event counter. The event counter comprises a 40 volt regulator, powered by a 48 volt central office pair, a 500 K ohm resistor and an amplifier.

Current leakage through the observed pair of terminals produces a voltage drop across the 500 K resistor. This forms one input to the amplifier, while a fixed.2-volt source is applied to the other input. As long as the resistor voltage drop is lower than.2 volts, (i.e., IR is $10^8$ ohms or more), there is

no output from the comparator. When the resistor voltage drop exceeds.2 volts, (i.e., IR is below $10^8$ ohms) the amplifier produces an output.

The clock feeds a continuous stream of pulses into a gate. When the detector circuit opens the gate, these pulses activate a series of counters which, in effect, record the duration of the fade. When the fade ends, the gate closes and no further pulses are counted. The event counter is advanced one count each time the detector circuit produces an output.

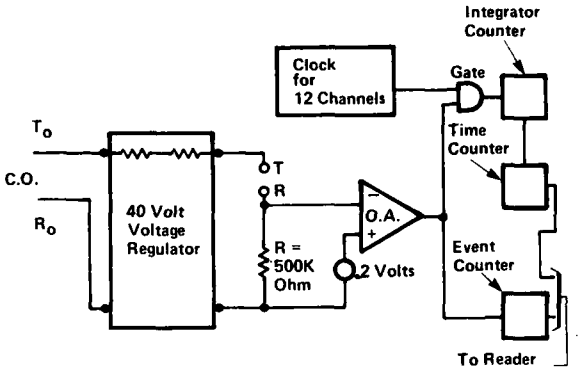



Fig. 3 Memory Circuit for the Insulation Resistance Monitoring

The stored data is unloaded at monthly intervals. To do this the monitor is manually connected to a special reader which reads out the contents of the memories and resets the counters to zero.

All the terminals and splicing connectors which are being monitored were placed in identical cabinets. However, in order to determine the effect of cabinet design on the internal environment, four different cabinets were installed at a field test site in Ottawa. No connectors were installed, but each cabinet was fitted with a temperature and relative humidity recorder (Hygrothermograph).

## OBSERVATIONS

After 2 years of field monitoring the following observations were made.

1. Temperature

Table 1 shows the temperature behaviour of identical cabinets at three locations through the summer months. This shows the important effect of sun loading, since the internal temperature fluctuation during a 24 hour period is considerably greater than the outside temperature change.

Table 2 compares the temperature behaviour of four different types of cabinets in the same location. It becomes apparent that differences in design features have a considerable effect on the internal temperature.

**Table 1 Temperature Change Within Cabinets at Remote Test Sites**

| | Maximum One Day Change During Month °C | | | Average Change During Month °C | | |
|---|---|---|---|---|---|---|
| | Ham. | Ott. | Simcoe | Ham. | Ott. | Simcoe |
| May 1979 | 23 | 21 | 24 | 15 | 13 | 15 |
| June | 26 | 27 | 25 | 17 | 16 | 15 |
| July | 26 | 24 | 26 | 16 | 17 | 18 |
| August | 23 | 24 | 21 | 14 | 15 | 12 |
| September | 22 | 22 | 23 | 17 | 13 | 14 |

**Table 2 Comparison of Internal Temperature on Different Cabinet Types**

| Type of Cabinet | For Month of July 1979 | |
|---|---|---|
| | Average Temp. °C | Maximum Temp. °C |
| Type 1 | 29 | 47 |
| Type 2 | 23 | 41 |
| Type 3 | 25 | 42 |
| Type 4 | 30 | 50 |

* *Maximum Outdoor Temp. 32°C*

Since daily temperature excursions in a cabinet can commonly be 27°C or more, it is important that the operating companies look at ways to reduce this. Selection of cabinets should include consideration for adequate ventilation and heat-reflecting colours and finishes.

2. Humidity

Figure 4 displays the variation of relative humidity over a four-day period during the winter months. This shows clearly that the daily variation of relative humidity is much greater inside the cabinet than outside. The low points correspond to midday when the internal temperature is highest. It is important to note that the relative humidity inside rises well above the outside level on every cycle. Therefore the daily occurrence of condensation within the cabinet is a

common event. It can be observed during the winter months when the condensation is visible as hoar-frost. Sun loading during the day melts the frost, causing bridging of the contacts. This condensation is one of the main causes of low IR and accelerated corrosion.

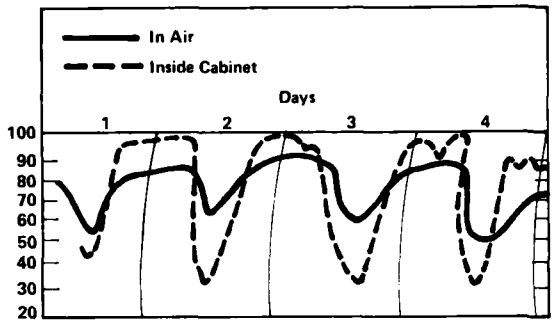



Fig. 4 Relative Humidity – Simcoe Site Feb 28/78 – Mar 3/78

Table 3 is a summary of the relative humidity conditions of identical cabinets at four different locations. The relative humidity inside the cabinet approaches the saturation level between 2 to 4 times as often as does the outside relative humidity. Table 4 compares the humidity behaviour of four different cabinets at the same location. The same trend to higher inside relative humidity is apparent, but differences in construction do have an effect. Cabinets are constructed from steel, aluminum and plastic. One type has an enclosed metal box separating the connection chamber from the ground. Each cabinet type also has a different venting system. Significant design features affecting internal humidity are: ventilation, drainage, insulation, mounting method, colour and location. Unplugged cable ducts and poor installation practices are sometimes overlooked as a source of moisture.

3. Insulation Resistance

Figure 5 shows the typical incubation cycle for IR generated noise. A new installation will often exhibit very little noise for a considerable time. The occurance of noisy pairs suddenly begins to rise rapidly. This can occur as early as 16 months in a severe environment or as late as 30 months in a mild environment.

Table 3 Humidity Inside & Outside Cabinets

| | Period December '78 to April '79 | |
|---|---|---|
| | Number of Days RH ≥ 95% | |
| | Inside Cabinet | Outside Cabinet |
| Montreal | 78 | 18 |
| Hamilton | 114 | 29 |
| Ottawa | 87 | 39 |
| Simcoe | 110 | 63 |

Table 4 Comparison of Relative Humidity Inside Different Cabinet Types

| Type of Cabinet | Period Nov. & Dec. 1979 | | | |
|---|---|---|---|---|
| | No. of Days RH ≥ 90% | | | |
| | *Inside Cabinet* | | *Outside Cabinet* | |
| | Nov. | Dec. | Nov. | Dec. |
| Type 1 | 20 | 21 | 13 | 11 |
| Type 2 | 28 | 30 | ↓ | ↓ |
| Type 3 | 28 | 22 | | |
| Type 4 | 24 | 18 | | |

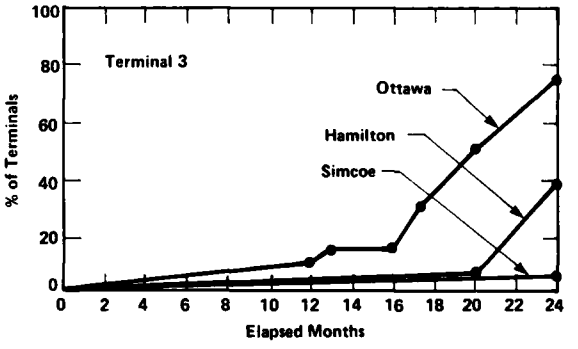



Fig. 5 Percentage of Pairs Which Have Been Noisy at Least Once During 24 Month Period

Table 5 shows the monthly behaviour of different terminals and connectors over a period of 13 months. Terminal #1 is an old binding post design, mounted in a phenolic board with a minimum barrier between the posts. There is considerable field experience with this design and it is being monitored for reference purposes. Again the period is apparent during which the incidence of noisy pairs is low. There is evidence that some terminal types behave better than others.

4. Contact Resistance

Table 6 shows the contact resistance change after 2 years, for three terminal types and three connector types, in identical cabinets at the four locations. There are considerable differences between connectors. For example, connector 2 is a potential source of noise and is regarded as unacceptable. Terminal #2 is also questionable and is undergoing further tests. In general, the differences attributable to location are minimal.

The graph in Figure 6 establishes a very important correlation between time in an actual field location and the accelerated-life laboratory tests. By measuring the times required to produce similar contact resistance changes, it is found that one year of outdoor service is roughly equivalent to ten thermal cycles in the laboratory.

**Table 5 Percentage of Terminals Noisy (I.R. $\leq 10^8\Omega$) for More Than 15 Mins. Location – Ottawa**

| Type of Connector | Sample Size (Pairs) | Sept. 1978 | Oct. | Nov. | Dec. | Jan. | Feb. | Mar. | Apr. | May | Jun. | Jul. | Aug. | Sept. 1979 |
|---|---|---|---|---|---|---|---|---|---|---|---|---|---|---|
| Terminal 1 | 24 | 33 | 0 | 80 | 70 | 30 | 36 | 12 | 4 | 12 | 64 | 4 | 12 | 8 |
| Terminal 2 | 25 | 0 | 0 | 0 | 0 | 0 | 0 | 0 | 0 | 68 | 84 | 0 | 64 | 0 |
| Terminal 3 | 24 | 4 | 0 | 0 | 14 | 0 | 0 | 0 | 0 | 29 | 50 | 0 | 12 | 0 |

**Table 6 Contact Resistance Change After 24 Months of Field Exposure**

| Type of Connector | Sample Size | Maximum Change in Contact Resistance milliohms | | | | No. of Connectors With Greater Than 1 milliohm Change | | | |
|---|---|---|---|---|---|---|---|---|---|
| | | Mont. | Ham. | Ott. | Simcoe | Mont. | Ham. | Ott. | Simcoe |
| Terminal 1 | 30 | 0.2 | 0.2 | 0.8 | 0 | 0 | 0 | 0 | 0 |
| Terminal 2 | 10 | 0.1 | 1.2 | 3.1 | 0 | 0 | 1 | 4 | 0 |
| Terminal 3 | 30 | 0.1 | 0.4 | 0.2 | 0.1 | 0 | 0 | 0 | 0 |
| Connector 1 | 20 | 0.6 | 0.1 | 0.8 | 0 | 0 | 0 | 0 | 0 |
| Connector 2 | 30 | 5.8 | 4.7 | 3.2 | 12.8 | 4 | 2 | 9 | 7 |
| Connector 3 | 10 | 0 | 0.7 | 0.1 | 0.4 | 0 | 0 | 0 | 0 |

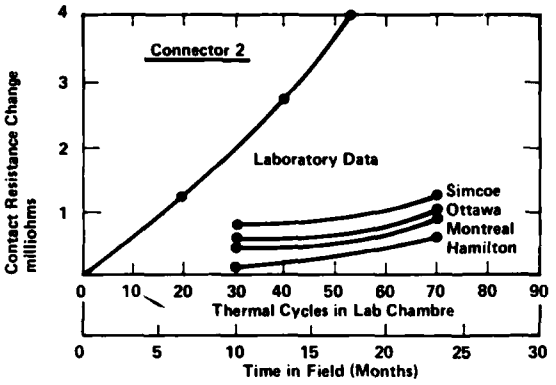



**Fig. 6 Correlation of Laboratory and Field Contact Resistance Data**

## CONCLUSIONS

Some of the basic conclusions reached so far in this monitoring program are:

### Cabinets

- Temperature cycles greater than 25°C per day inside cabinets are common.
- Relative humidity exceeds 90%, two to four time more often inside than outside the cabinets.

### Insulation Resistance

- All splicing connectors and terminals exhibit low insulation resistance during wet months.
- Fifty hours of noisy circuit conditions, on 25 pairs in a five month interval, is common.
- A 15 to 30 month incubation period, before the onset of noisy circuits, is typical.

### Contact Resistance

- Lab to field correlations indicate that approximately 10 thermal cycles (-40°C to 55°C) are equal to one year in the field.

The data obtained so far in this program has proven valuable in understanding the failure process. It provides some insight into the cabinet's internal environment and its effect on connection performance. It also provides some data which allows for a correlation of lab test and field conditions.

It is anticipated that this correlation will provide a means of more reliable and accurate laboratory testing of connectors. It has also aided in determining the parameters necessary to design better O.P. Systems and specify O.P. Components.



Ivan E. Martin graduated from Michigan Technological University with a BSME, in 1970. He spent several years as an Outside Plant Engineer with British Columbia Telephone before joining Bell-Northern Research. Currently he is Manager of a Metallic and Plastics Materials Engineering Group.



Christopher D. Gupta graduated in 1974 from the University of Waterloo with a Bachelor of Applied Science Degree in Electrical Engineering. He joined Bell Canada at that time. His career at Bell Canada has been in Technology Developments in the Transmission Systems Division. Currently he is Supervising Engineer in Outside Plant for Wire Connecting, Apparatus & Closures.



Neddy Satar graduated with a Diploma in Metallurgy from Ryerson Polytechnical College in 1974. He joined Bell-Northern Research in 1977 and has since been involved with the evaluation and testing of connectors.

# FIBER OPTIC CABLE COIL PACKS FOR AIR DEPLOYMENT

R. E. Thompson, X. G. Glavas, V. E. Kalomiris*
ITT Electro-Optical Products Division
7635 Plantation Road, N.W.
Roanoke, Virginia 24019

H. Wichansky
U.S. Army CORADCOM
ATTN: DRDCO-COM-RM-I
Fort Monmouth, New Jersey 07703

## Abstract

The paper discusses the design and packaging of fiber optic cables for deployment from helicopters at high speed, up to 75 m/s. Successful deployment and subsequent survival on the ground in a tactical field environment dictate many design constraints for the cable and coil pack including cable size and weight, tensile strength and modulus, surface friction, minimum pullout force, and allowable rigidity of the cable. These design constraints and design considerations are discussed as well as results of prototype fabrication and testing. The cable dynamics at the peel point is of particular importance in high speed payout from a coil pack. This problem has been analyzed and the results will be reported.

## Introduction

The incentive for using fiber optics in a broad range of applications in Army communications is its ability to functionally replace metallic cable with fiber optic cable of greatly reduced weight and bulk. Development efforts are underway to replace twin coaxial cable in long haul systems[1] and multiconductor cable in local distribution[2] systems. These fiber optic cable systems would be greatly enhanced with the development of a fiber optic cable and dispensing techniques that would permit rapid deployment of cable from a helicopter, ground vehicle, or backpack.

This paper will discuss efforts to develop a fiber optic cable that can be deployed from a helicopter at high speed - the most stringent of deployment conditions. The concept of a helicopter deploying a high performance, lightweight fiber optic cable in addition to greatly reducing communication setup time provides a much needed capability in air assault operations. Radio communications are relied on heavily for this air lift operation since metallic wire is not mobile enough. The radio links present an unavoidable signature that permit detection of unit positions. The air layable cable will provide for the implementation of the long haul and local distribution fiber optic systems within the air assault environment.

By employing optical fibers, a cable capable of data carrying capacity in excess of twin coaxial cable is possible in a cable slightly larger than one of the wires of twisted-pair metallic field wire. The main characteristics of fiber optic cable and field wire are listed below.

| | Fiber Optic Cable | Metallic Field Wire |
|---|---|---|
| Diameter (mm) | 2.54 | 1.78 each wire |
| Weight (N/km) | 55.31 | 111.41 |
| Breaking strength (N) | 666.88 | 931.67 |
| Cable length per package | 2 km | 0.8 km |
| Data rate | 20 Mb/s | 20 kb/s |

The objectives are to provide a fiber cable that is lightweight (10 kg/km), low cost in production quantities ($0.60/m), and can be deployed from a helicopter at high speeds (70 m/s).

The engineering effort includes the development of high strength fiber optic cable with matched dispenser of 8 km without repeaters. The cable length will be made by connecting a number of sections of optical cable in tandem for coaxial or parallel axis serial deployment; each

*V. E. Kalomiris is now affiliated with U.S. Army CORADCOM.

dispenser will deploy a 2 km long section. The fiber optic cable is designed to operate in the 0.8 μm to 1.30 μm wavelength region at data rates up to 20 Mb/s.

The cable contains a single optical fiber which will permit full duplex communication when used in conjunction with a bidirectional coupler.[3]

## Cable Design Considerations

A viable cable design must incorporate the necessary characteristics for successful deployment and ground survival. However, the cable cannot be "over" designed since this will add excessive cost and increase weight and volume of the cable. Under normal conditions the stresses imparted to the cable will be more severe during payout than after deployment; therefore, the cable which will survive payout will survive on the ground under normal conditions. The exceptions to this are the presence of unusually extreme conditions of very long span lengths and small sag with high winds and heavy icing. Designing for these rare conditions would reduce the expendable nature of the cable and greatly increase the bulk of the cable. For these reasons the parameters associated with deployment are considered as primary in designing the cable. Those concerning survival under all conditions after deployment are secondary. Figure 1 shows the resulting cable cross section and its main characteristics. The optical cable contains no metallic components. Its tensile strength is supplied by nine 380d Kevlar® 49 yarns.

The most important considerations for the cable are the following:

a. Ability to be deployed
   (1) External surface of cable
   (2) Low lineal density
   (3) High strength
   (4) Sharp bending
b. Ability to operate after deployment
   (1) Impact resistance
   (2) Abrasion resistance
   (3) Cable tensile strength
   (4) Fiber proof test level
   (5) Low excessive optical loss due to deployment and service

### External Surface of Cable

The external surface of the cable is extremely important because it contributes heavily to the tension and bending developed at the peel point due to friction and/or adherence of any adhesive or binding agent. The ideal outer surface would be one with zero friction which would allow only enough bonding between it and the adhesive to stabilize the coil.

### Low Lineal Density

It is important to keep the lineal density or weight per unit length of the cable as low as possible to minimize the internal forces due to decelerating it from the coil pack. The component of tension due to this deceleration is proportional to the lineal density of the cable. The lineal density is also important for minimizing the magnitude of any shock load which is induced on the cable due to decelerating a clump mass such as a connector. The peak load induced on the cable due to deceleration of a clump mass is proportional to the square root of the cable's lineal density.

### High Strength

The cable must be strong enough to withstand payout tensions and limit fiber strain to less than about 0.5% for 1% proof tested fiber. The tensile load required to generate 1% elongation in the cable is 275 N and its breaking strength is 650 N. The main contributor to the cable's strength is the presence of the nine 380d Kevlar® 49 yarns applied helically around the 0.5 mm optical fiber with a lay length of 5.0 cm.

### Sharp Bends

During deployment the cable will be pulled out of the coil pack; it will be bent sharply in making the 90° turn to exit the canister. The cable must recover from this bending without serious degradation of its mechanical and optical properties.

### Impact Resistance

Impact resistance of the cable is of special importance in tactical field environments. One of the important techniques for making a cable impact resistant is to use a resilient jacketing material such as polyurethane which will absorb some of the energy of an impact load.

### Optical Fiber

The light transmitting element of the cable is the graded index optical fiber shown in Figure 2. It consists of a doped silica glass core and optical cladding surrounded by a silica glass substrate. To preserve the mechanical strength of the glass fiber, it is dip-coated with silicone RTV and extruded to 0.5 mm with a thermoplastic elastomer. The graded index optical fiber meets the following requirements:

| | | |
|---|---|---|
| a. | Attenuation: | <5 dB/km |
| | Dispersion: | <2 ns/km |
| b. | Core diameter: | 50 μm ±5 μm |
| | Bare fiber diameter: | 125 μm ±5 μm |
| c. | Silicone RTV primary buffer: | 300 μm ±50 μm |
| | Hytrel® outer jacket, secondary buffer: | 500 μm ±50 μm |
| d. | Numerical aperture (90% power): | NA >0.14 |
| | Fiber tensile strength: | 0.0690 GPa ($1 \times 10^5$ psi) |

The optical cable should perform satisfactorily in the temperature range -57°C to +85°C.

## Cable Packaging

Winding cable into a coil for subsequent payout at high speeds is far more complex than it may initially appear. Through experience it has been found that many parameters affect the successful deployment of a fiber optic cable from a coil pack. These parameters have been identified first in coil fabrication and second in deployment schemes. The major advantage of packaging a cable into a coil pack is to allow deployment without rotational motion of the cable matrix. This type of technique eliminates the need for a complicated rotational drive system to spin the mass of the cable pack.

The orthonormal coil pack design is used in coil winding because it provides the following advantages:

a. Produces minimum impact on the optical properties of the fiber optic cable
b. The coil can be fabricated with essentially no deformation beyond that required to bend it into a radius equal to the inside radius of the coil
c. Offers maximum volumetric efficiency approaching a perfect close center packing efficiency of 0.907; 0.88 is typical
d. The coil can be fabricated on standard wire coiling equipment

Conventional cable coiling methods are adequate for low speed payout. Winding methods such as universal figure eight winding are prone to kinking at high speed deployment.

To avoid complications that can arise during payout, sufficient attention must be given to the following aspects of the coil design and fabrication:

a. Mandrel design
b. Precision of winding
c. Cable diameter control
d. Nature of turnaround points
e. Stability of coil pack
f. Degree of back twist wound into the cable
g. Winding tension

### Mandrel Design

The design of the mandrel necessary to produce a precision orthonormal wound cable coil is extremely important. The mandrel shown in Figure 3 is used to define the geometry of the first layer and the turnaround points and is the foundation upon which the coil is built. The first coil layer must be wound perfectly since any imperfection will propagate and be amplified in each successive layer until the uniformity and stability of the coil pack are lost. In addition, the mandrel must be designed so that it can be separated from the adhesive and collapsed from the coil pack.

### Precision of Winding

The degree of precision in winding a cable coil pack must be very high for the same reasons that require careful mandrel design. Loss of precision of the wind in one layer will be propagated and amplified in successive layers.

### Cable Diameter Control

Cable diameter control is critical because it determines an absolute limit on the degree to which precision winding can be accomplished. By monitoring the Kevlar® tensions periodically during cabling and precision control of the jacket extrusion, the cable diameter tolerances can be held to ±1%.

### Nature of Turnaround Points

It was observed that the nature in which the winding direction is reversed requires careful attention to prevent disturbing the precision wind and/or causing excessively small bend radii for the cable. Layer transition must occur within a predefined region along the mandrel endplates. Transitioning to the next layer too soon leaves a void region that will be filled by the next layer as it migrates downward. This causes a loss in precision wind.

### Stability of the Coil Pack

The stability of the coil pack is of paramount importance and depends on the selection of the proper adhesive and cable jacketing material. A stable coil pack

allows for vibration and shock absorption during transportation and deployment.

## Degree of Back Twist Wound into the Cable

The amount of back twist wound into the cable must be controlled. Too much back twist will result in excessive torsion on the cable and retention of excess twist upon payout. Not enough back twist will result in payout with induced twist. The degree of pretwist applied at the coil winding payoff station is one twist for every wrap of cable wound on the take-up mandrel. This neutralizing or back twist allows the cable to be installed on the ground at zero tension without developing kinks or twists.

## Winding Tension

During coil winding experiments, it was noticed that the applied tension must be held nearly constant. A winding tension which is too high will result in creep and/or cold flow in the jacket due to tension induced pressure, causing the coil to relax and become less stable with time. A winding tension which is too high or too low will result in loss of precision wind. A winding tension which varies too much can result in uneven application of the adhesive and an unstable layer upon which subsequent layers must be coiled causing loss of precision wind and uneven payout. Tensions of 15 N and 30 N are currently used.

## Packing Efficiency

The length of a cable that can be stored on a given spool or coil is dependent on the dimensions of the coil (traverse, inside diameter, and outside diameter), the diameter of the cable, and the packing factor. The equation which relates these parameter is

$$L = \frac{PF(T)}{d^2} (D^2_o - D^2_i)\ 10^{-3} \qquad (1)$$

where

- $L$ = length of stored cable (km)
- $T$ = coil traverse (cm)
- $D_o$ = coil outside diameter (cm)
- $D_i$ = coil inside diameter (cm)
- $d$ = cable cross-sectional diameter (mm)
- $PF$ = packing factor

The packing factor is the volumetric efficiency by which a cable is wound. For any given cable the minimum size coil can only be achieved when it is precision wound. The packing factor, PF, is the volume of the cable contained in a coil divided by the volume of the coil. The packing factor is dependent on the shape of the cable and the way in which it is wound. Inevitably, there are interstices between the turns, and these represent wasted space so that PF is less than unity even in an ideal coil. The theoretical packing factor for a close center packing geometry is 0.907. The packing factors of the prepared coils were calculated and are given in Table 1.

## Prototype Cable Fabrication and Evaluation

Severe constraints imposed on an optical system and performance in the temperature range of -57°C to +85°C require a compatibility study to be performed on the cabling and coiling materials used in various configurations.

Experimental samples were fabricated using 0.94 mm and 0.5 mm optical fibers wrapped with 9, 14, 16, and 18 380d Kevlar® 49 yarns with a 5.0 cm lay length and jacketed with the most promising jacketing materials - high density polyethylene and polyurethane.

From this study of performance of the cable at -57°C, it was concluded that 0.5 mm optical fiber wrapped with nine 380d Kevlar® and jacketed with polyurethane would be the ideal candidate.

Prototype cable made using 0.5 mm optical fiber, nine 380d Kevlar®, and a polyurethane ED-65 jacket was evaluated versus temperature; the results are depicted in the table below.

| Attenuation (dB/km at 0.85 μm) | | Temperature (°C) |
|---|---|---|
| Before cabling | 2.81 | +20 |
| After cabling | 2.75 | +20 |
| After cabling | 3.37 | -20 |
| After cabling | 4.43 | -40 |
| After cabling | 6.97 | -57 |
| After cabling | 3.07 | +20 |

Polyurethane is a thermoplastic elastomer with a Young's modulus which behaves significantly differently at low temperatures than does high density polyethylene. The Young's modulus of the high density polyethylene rapidly increases as the temperature decreases while the Young's modulus of the polyurethane increases at a much slower rate. This difference in tensile modulus behavior drastically reduces the linear compression forces generated by the contracting jacket. This results in considerably lower microbending losses at the critical temperature of -57°C which was verified by the cable's performance at that critical temperature. Laboratory payout tests were performed successfully simulating a payout

deployment speed of 96 km/h. This payout speed is laboratory equipment limited. The tension applied on the cable during laboratory payout tests was measured to be between 2.5 and 20 N. Higher payout speeds will be performed using a helicopter as the deploying vehicle.

## Cable Deployment Dynamics

In order to design a cable to meet the dynamic constraints present during deployment, analytical work was performed by Dr. G. Nowak[4] of ITT and Dr. Y. H. Pao and Dr. F. C. Moon[5] of Cornell University. Dr. Nowak's task involved modeling the cable behavior beyond the peel point while Dr. Pao's and Dr. Moon's work entailed defining the equations of curvature of fiber optic cable at the peel point during axial payout from a precision-wound coil canister package using internal peel. Due to the nature of the payout technique, very high bending stresses are generated at the cable peel point. Figure 4 shows unwinding of a cable package.

In the analysis the cable behaves first like a thin rod and second like a thread or string. When the cable is payed out at a constant axial speed, the payed out cable length is divided into two regions: (a) the inner region near the peeloff point, and (b) the outer region away from it. Within the inner region the cable is modeled by a thin rod; in the outer region, it is modeled by a thread. The inner and outer regions are separated by a transition zone or boundary. In so doing, the dynamic effects of centrifugal force, Coriolis force, and air resistance on the ballooning cable in the outer region are accounted for. The study performed by Pao and Moon neglects these forces because their effect is minimal at peel point. The Nowak study which addresses cable behavior after peel point accounts for these forces.

The inner region was considered to be of highest importance for analysis because optical fiber survivability is a function of the radius of curvature during peel. If the radius is too small, excessive bending stresses are induced in the fiber which would result in fiber failure during deployment. The radius of curvature is found to be independent of length and is given by:

$$K = \frac{1}{\rho} = 1.415 \left(\frac{T}{EI}\right)^{1/2} \qquad (2)$$

where

E = Young's modulus of the cable
I = moment of inertia
T = vertical force on the cable

using experimental values of

EI = 0.00071745 N·m$^2$
T = 0.587165 N (sufficient to produce vertical slope at the ends of the cable in order to simulate an infinite cable)
$\rho$ = 0.0247 m

The maximum tensile stress in the fiber resulting from bending and tension is given by:

$$\sigma = E \frac{b}{2R} + 4 \frac{T}{\pi b^2} \qquad (3)$$

where

E = modulus of elasticity
b = fiber diameter
R = radius of curvature of the cable axis
T = tension

## Conclusion

It has been shown that an expendable fiber optic cable without metallic components can be fabricated, can perform reasonably well over the temperature range of -57°C to +85°C, and can survive laboratory payout tests at 96 km/h. Cable deployment tests from a helicopter at a speed up to 185 km/h are scheduled later this year.

## Acknowledgment

The work described in this paper is partially supported by the U.S. Army Communication Research and Development Command (CORADCOM) contract entitled "Air Layable, Expendable Fiber Optic Cable Assembly Package," (contract DAAK80-79-C-0803).

## References

[1] E. Howe, A. Mondrick, and J. Wright, "Army Fiber Optic Initiatives in Tactical Communications for the 1980's," FOC '80 (September 1980).

[2] L. A. Coryell, R. W. Taylor, V. Mordowitz, and D. Rice, "Intershelter Fiber Optic Cable System," FOC '78 (September 1980).

[3] A. Nelson, G. Gasparian, and G. Bickel, "Bidirectional Coupler for Full Duplex Transmission on a Single Fiber," CORADCOM-77-1798-F (August 1979).

[4] G. Nowak, "Theory on Dynamics of an Unwinding Cable from a Bobbin in Fast Translatory Motion," (December 1979, unpublished).

[5]Y. H. Pao and F. C. Moon, "Dynamics of Fiber Optic Cable Payout," published as Appendix A in "Air Layable, Expendable Fiber Optic Cable Assembly Package" by X. Glavas, and V. Kalomiris, R&D Technical Report, CORADCOM-79-0803-1 (July 1980).

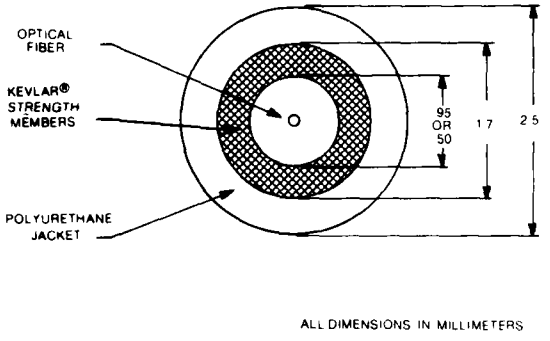



Figure 1. Cable Cross Section.

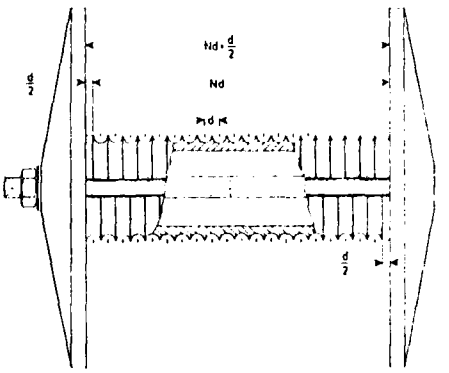


Figure 3. Mandrel Design.

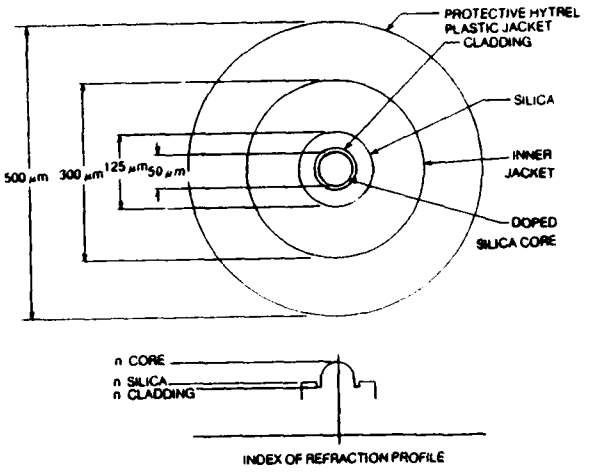



Figure 2. Graded Index Optical Fiber.



Figure 4. Unwinding of a Cable Package.

Table 1. Experimental Precision Coil Winding Parameters.

| Coil No | Cable Dia (mm) | Cable Jacket | Cable Length (m) | Packing Factor | Winding Tension (N) | Adhesive |
|---|---|---|---|---|---|---|
| 1 | 2.54 | HDPE* | 388 | 0.86 | 17.65 | GE Silicone RTV®-664 |
| 2 | 2.54 | HDPE | 727 | 0.87 | 17.65 | Dow Corning Sylgard® 184 |
| 3 | 2.54 | HDPE | 689 | 0.85 | 31.38 | GE Silicone RTV®-670 |
| 4 | 2.54 | PU**E-9 | 1746 | 0.88 | 31.38 | Dow Corning Sylgard® 184 |
| 5 | 3.00 | PU ED-65 | 1150 | 0.88 | 13.73 | Dow Corning Sylgard® 184 |
| 6 | 3.00 | PU ED-65 | 234 | 0.90 | 13.73 | PRC PR-1564 |
| 7 | 3.00 | PU ED-65 | 981 | 0.87 | 13.73 | Isochem Transflex Gel |
| 8 | 3.00 | PU ED-65 | 699 | 0.85 | 13.73 | NL Chemicals Polycin 989 |
| 9 | 3.00 | PU ED-65 | 259 | 0.84 | 13.73 | GE Silicone RTV®-664 |

*High density polyethylene.
**Polyurethane.




Robert E. Thompson - Fiber and Cable R&D

BS, Electrical Engineering, Worcester Polytechnic Institute


6 years experience in optical fiber systems design and project engineering management. As manager of fiber/cable/measurements R&D, Electro-Optical Products Division, his responsibilities include the development and fabrication of all optical fibers, cables, and measurement equipment.




Xenophon G. Glavas - Fiber and Cable Engineering

MSME, Mechanical Engineering, San Diego State University
BSME, Mechanical Engineering, San Diego State University


9 years experience in mechanical design principally in optical systems. As senior project engineer in the Fiber Optics Laboratory, Electro-Optical Products Division, his duties include mechanical design of components for undersea systems, design and development of a high strength fiber optical cable for missile control, and development of payout schemes for fiber optical cable deployment from moving craft. He has developed special equipment and tooling used to manufacture precision wound coils for rapid deployment for helicopters.

Vasilios E. Kalomiris - Cable Engineering

MSEE, Electrical Engineering, New York University
BSEE, Electrical Engineering, New York University
BA, Mathematics, New York University

6 years experience in electrical and mechanical investigation, design, evaluation, and manufacture of fiber optic cables. As senior cable engineer in the Fiber Optics Laboratory, Electro-Optical Products Division, his responsibilities included design and evaluation of fiber optic cable incorporating armoring for rodent protection, and evaluating filling compounds used in cable waterproofing.



Howard Wichansky - U.S. Army CORADCOM

BS, Ceramics, Rutgers - The State University
Ph.D, Ceramics, Rutgers - The State University

Dr. Wichansky has been associated with the U.S. Army since 1967 and involved with fiber optics since 1974. His thesis work and early experience with the U.S. Army Electronics Command involved the study of ferroelectric materials as electronic tuning elements. His knowledge of ferroelectric and piezoelectric materials led to responsibilities for development of substrates and thin films for a variety of surface wave devices. This background was applied to the investigation of optical switching techniques for fiber optics. In 1977 he joined the fiber optics team within CORADCOM where he was involved with devising fiber optic measurement facilities and participating in the fiber optic cable and connector programs. More recently he has been project engineer on a series of programs to develop the communication link for a fiber optic guided weapon system and an air deployed fiber optic cable assembly.

# AN OPTICAL FIBRE LINK IN A MOUNTAINOUS ENVIRONMENT

J.R. Osterfield
J.R. Norman

D.N. McIntosh
A.J. Rogers

R. Castelli
M. Tamburello

Pirelli General Cables Works Ltd.
Eastleigh Hants U.K.

CERL
Leatherhead Surrey U.K.

Telettra SpA
Milan Italy

## 1. Abstract

Coatings for optical fibres to meet a wide range of temperatures expected in mountainous terrain are discussed. A cable construction is described to enable cable up to 1500 m to be installed. Results for v-groove splices and the improvement for fusion splices when monitored by a backscatter method are given.

The optical link is required to pass video information by a PPM system which is described together with a digital system for remote control of the camera.

To test the suitability of the link to carry telephone channels fibre has been looped to a 34 Mb/s line terminal, described in the paper. Finally implications of future operation at longer wavelengths are discussed.

## 2. Introduction

The British Central Electricity Generating Board (CEGB) operates an integrated system for the generation and transmission of bulk electricity supplies in England and Wales. It has, therefore, a very large requirement for telecommunications systems of all sorts, much of which have to be installed and perform satisfactorily under extremes of physical and electrical environment. The potential advantages to the CEGB in using optical-fibre systems include immunity to electrical interference and rises of earth potential, electrical isolation, reduced insulation problems, and high information capacity. As one of several projects aimed at developing, evaluating and promoting optical-fibre techniques, the Central Electricity Research Laboratories (CERL) decided on an experimental installation on the site of the 1800 MW Dinorwic pumped-storage power station in the mountains of North Wales. An important reason for the choice is the rock and slate composition of the terrain, the high electrical resistivity of which causes large rises of earth potential especially under electrical fault conditions. It would also provide a good test of the ruggedness of a suitable optical-fibre cable during installation and operation in a severe environment.

For experimental and demonstration purposes, it was decided to transmit video information from a television camera, to provide remote control of the camera and to operate some high bit-rate digital equipment appropriate to the fibre characteristics.

## 3. Route

The 5.3 km route runs from the top of the machine hall's ventilation shaft, through a disused slate quarry in a tortuous manner and up to the head-works at the upper reservoir. It climbs 300 m in the first 2 km. Except for 500 m of troughing a single cable is contained in 100 mm diameter PVC duct which is buried under discarded slate fragments. As the quarry is south facing, temperatures can rise to 30°C in strong sunlight. The rest of the route follows more gentle contours climbing a further 200 m to the head-works as it follows a mountain road. As the head-works are at 700m above sea level very cold temperatures to -15°C can be experienced.

## 4. Optical Fibres

Low-loss germania phosphosilicate glass multimode fibres were produced at Southampton University using an automatic deposition system[1] for an inside chemical vapour deposition technique. To buffer the core of the preform against diffusion of hydroxyl ions present in the silica tube substrate, layers of borosilicate glass were deposited before depositing the core materials. The preforms were pulled into fibres of 4 to 5 km length which were coated with silicone rubber to protect their surfaces and to minimise micro-cracking. The design specification for the fibres is as follows:

| | | |
|---|---|---|
| Core diameter | 63 | microns |
| Borosilicate barrier thickness | 4 | microns |
| Cladding diameter | 125 ±1 | microns |
| Diameter over silicone rubber | 250 | microns |
| Effective numerical aperture | 0.2 | |
| Attenuation at 850 nm | < 5 | dB/km |
| Intermodal dispersion at 850 nm | < 3 | ns/km |

## 5. Fibre Characteristics

A typical cross-section of fibre is shown in Figure 1. This fibre was manufactured in a length exceeding 5 km and was used for one channel over most of the route. As can be seen, achieving fibre circularity presented no difficulties and the specified core diameter was obtained. Core diameters varied from 58 to 68 microns but it was possible to group fibres for particular channels to minimise jointing losses.

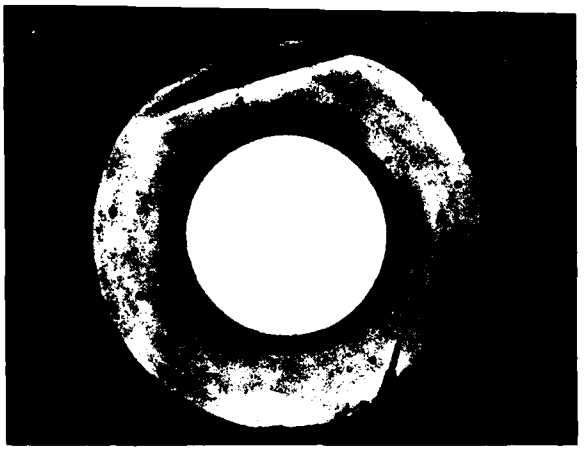


Fig 1 Cross-section of multimode fibre

Since fibres were drawn to a constant 125 ±1 microns diameter, variations in core diameter occurred largely because of cross-sectional area fluctuations in the substrate tube. Another cause of variations was the variability in the amount of silica volatilised during collapse of the preform. The spectral attenuation is given in Figure 2 for the envelope of results.

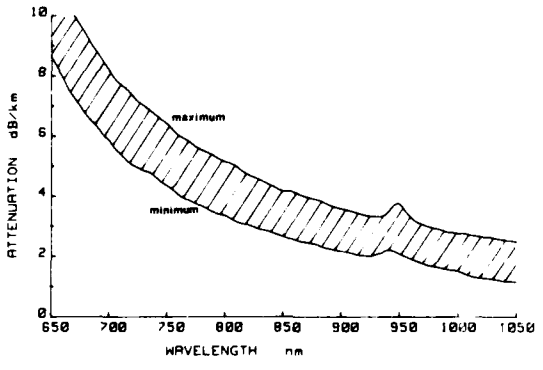



Fig 2 Envelope of spectral attenuation

The attenuation is 3.4 ± 0.8 dB/km at 850 nm. Subsequent work has shown the importance of holding the cladding diameter constant during the pulling operation. Two fibres were pulled, one with 2 microns random deviations in diameter and the other with less than 1 micron deviation in diameter. An improvement in attenuation by 0.8 dB/km at 850nm was obtained in the latter case, as shown in Figure 3.

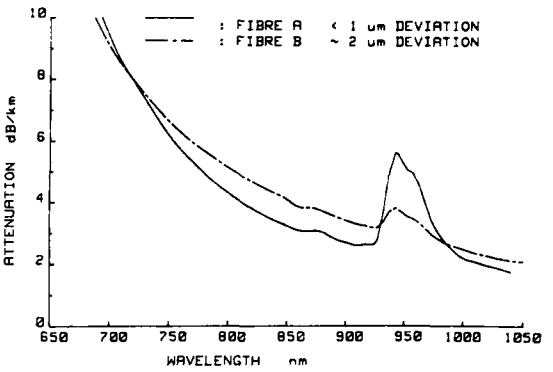



Fig 3 Effect of diameter noise variations on spectral attenuation

The refractive index profile of the fibres was measured by the near-field scanning technique and a typical profile is given in Figure 4. The dotted line shows the near-field intensity distribution, whilst the solid line shows the refractive index profile calculated by applying correction factors for the leaky modes normally present. The individual layers of the deposition can be clearly seen in the central core region. The out-diffusion of dopant from the core during collapse of the preform is compensated by a dopant enriched gas within the closure zone.

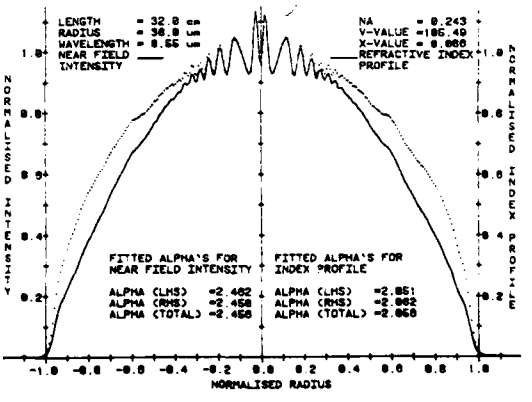



Fig 4 Refractive index profile

An example of the pulse broadening in a fibre when excited by a GaAlAs laser operating at 850 nm and having a 2 nm linewidth is shown in Figure **5.** Pulses of 0.7 ns full-width, half-weight (fwhm) duration were launched into a 3 km length of fibre at a 10 kHz repetition rate, and the input and output pulses were detected using matched Si avalanche diodes. Deconvolving the input pulse from the 1.6 ns fwhm output pulse gives the amount of pulse broadening as 1.44 ns which is equivalent to a bandwidth in excess of 800 MHz.km.

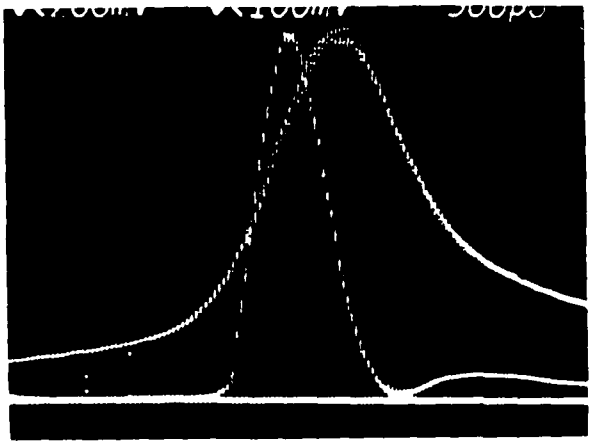


Fig 5 Pulse broadening over a 3 km length

## 6. Coating of Fibres

Losses associated with the coating of fibres have been described by Grasso et al[2]. Notwithstanding the problems arising with tight secondary coatings it was decided to follow this way to take advantage of the easy application of silicone rubber as a primary coating.

In order to determine the effect of the secondary coating thickness on losses, primary coated fibres were jacketed with natural nylon 12 to diameters of 1000 and 500 microns, the latter being chosen to provide the minimum of protection necessary to safeguard the fibre during the operations of cable manufacture. Lengths of secondary coated fibre, 2 to 3 km long, were lightly wound on polystyrene drums and their attenuation measured from $+20^{0}$C to $-20^{0}$C. Measurements were made at 1000 nm wavelength (because of lower fibre attenuation) and the results are given in Figure 6. It was decided to adopt the 125 microns coating thickness to minimise shrinkage and the resulting losses from microbends. Increases in attenuation caused by lateral pressure were not considered to be a problem as a loose sheath construction (described in section 7) was planned for the Dinorwic installation.

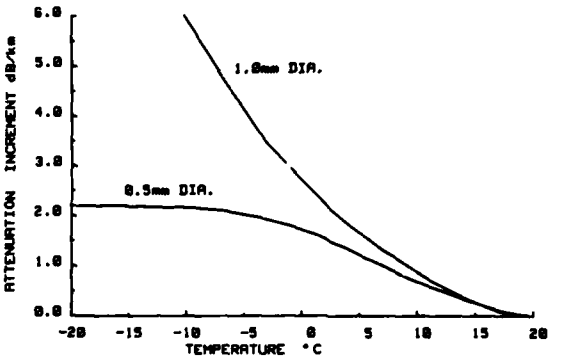



Fig 6 Effect of secondary coating thickness on losses

A number of secondary coating materials were evaluated and measurements of attenuation changes with temperature were plotted as shown in Figure 7. Nylon 6 was considered the most promising material.

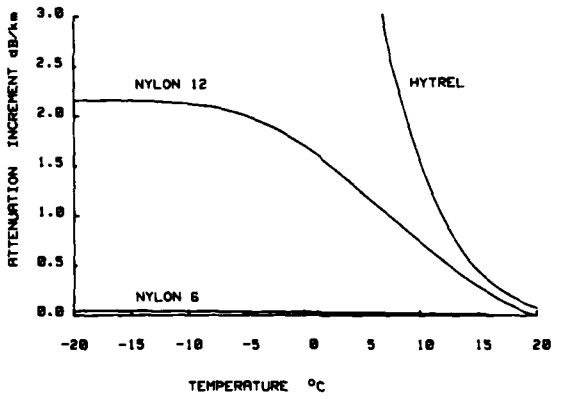



Fig 7 Effect of various material secondary coatings on losses

Normally the extrusion coating of nylon 6 is cooled sufficiently slowly to minimise the difference between the degree of crystallinity on the surface and inner layers of the secondary coating[3]. The addition of pigment increases the overall degree of crystallinity and unless the surface is cooled more slowly larger stresses are built up in the coating due to an unbalance of crystallinity and greater microbending losses result. This effect is shown in Figure 8 for a fibre coated with fully pigmented material.

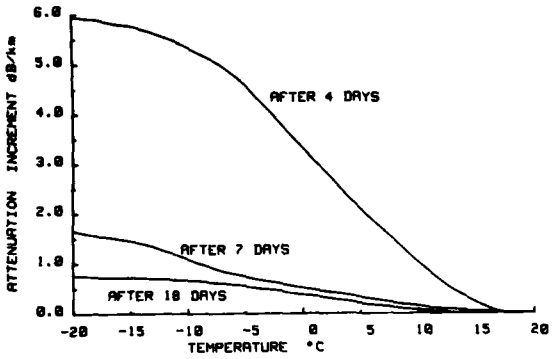



Fig 8 Effect of moisture absorption by fully pigmented coatings on losses

Exposure of nylon 6 to water in the atmosphere increases the crystallinity of the outer surface due to increased molecular mobility and secondary re-crystallization. Better crystallinity equilibrium is achieved across the coating layer and so stresses and the resultant microbending losses decrease with ageing.

To overcome the problem of losses associated with fully pigmented material, experiments were carried out with diluted mixes such that the colours remained readily identifiable. In this way variations of less than 0.1 dB/km were achieved over the temperature range -40 to +60°C. A typical result, for example a weak red mixture of nylon 6, is shown in Figure 9.

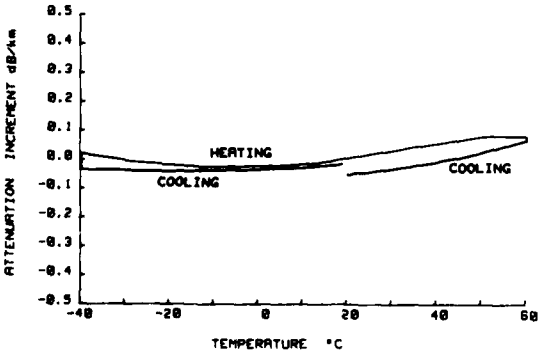



Fig 9 Losses associated with weakly pigmented nylon secondary coatings

## 7. Cable Construction

To choose a cable construction the following points were taken into consideration:

- Minimum stress on tight coated fibres
- Metallic element to minimise sheath retraction
- Low elongation to strength ratio (0.3% for 1000 N)
- Sufficiently flexible to flake during installation
- Light weight.

It was decided to provide a loose sheath to allow the fibres to lie slack within it. A central tensile member was not therefore possible and the sheath construction had to balance tensile strength against stiffness. A number of designs were tried including longitudinal welded tape and wires embedded in the sheath. In the case of the former, tape thicknesses to provide adequate strength were discarded as being too stiff for drawing into duct especially when it is necessary to pull half the length in from the mid-point and flake off the remainder from the drum to pull it in.

The difficulty with high tensile steel or glass wires applied longitudinally arose when the sheath was bent to put them in compression. When they were applied in a strand the problem was overcome but the initial elongation to strength ratio suffered.

An elegant solution materialised with the use of tin plate steel 150 microns thick which is polymer coated on both sides. A 25 mm width tape can be formed into a 7 mm diameter tube with longitudinal overlap which can be bonded during the extrusion of an oversheath in polyethylene. Sufficient metal is present to provide a pulling strength of ~1000 N (100 kg) for 0.3% extension and a hoop strength in excess of ~2500 N (250 kg) per 100 mm of cable.

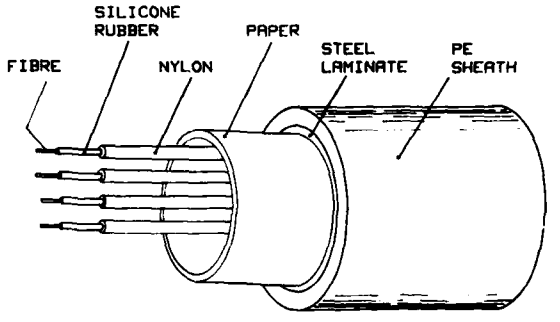



Fig 10 Diagram of cable sample

Within the sheath there is adequate room to apply a longitudinal paper and four secondary coated fibres each 0.5 mm in diameter required for the Dinorwic project; see Figure 10.

To achieve an even greater degree of strain relief within the cable a novel fibre feeding technique was employed to drive an excess length of fibre into the cable. By driving the fibres 0.6% faster than the application of the steel tape it was possible to provide an excess fibre length in the cable of 0.4 to 0.5%; the loss in excess length being caused by stretch in the steel tape at the tape forming head. Excess fibre length after cabling was checked by the measurement of the propagation delay through the fibre using a sub-nanosecond pulse. For example on 1540 m length the propagation time in a fibre was 7637 ns. The delay for unit length of the uncabled fibre was measured to be 4.932 ns/m thereby giving an excess length of cabled fibre of 8 m. The spectral attenuations of a fibre at its various stages of manufacture and installation are shown in Figure 11, indicating the negligible increase in attenuation for the cable construction.

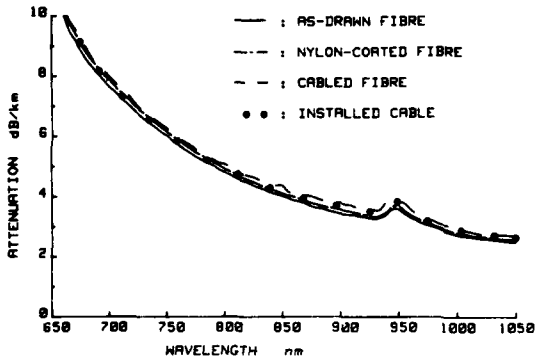



Fig 11 Spectral attenuation for various stages of fibre manufacture and installation

Trials have shown that at least eight fibres can be accommodated within the sheath. A smaller size of tube was not used because the reduced amount of steel would reduce the maximum allowable pulling tension. It was also found that 7 mm diameter appears to be close to the limit for forming 150 microns thickness steel using a tube forming shute.

## 8. Metallic Elements in the Sheath

The inclusion of metallic elements in the sheath would at first sight appear to negate the advantages of optical fibres in areas of strong inducing fields, differential earth potentials, etc. However, if low-loss performance of fibres is required because of the length of the route the introduction of metallic strength members can greatly simplify the situation. Metallic elements oppose sheath retraction which is often a cause of increased pressures on cabled fibres, particularly tight secondary coated fibres, leading to increased losses.

Metallic elements provide a high strength to weight ratio permitting installation of cable in longer lengths and thereby reducing the number of joints. Also better protection is given to fibres during installation because the metallic elements give an immediate strength resistance to elongation.

To overcome the problems of induced voltage in the metallic elements caused by earth fault conditions, etc., the metallic elements are sectionalised at the fibre jointing positions and isolated from earth. For the Dinorwic cable the steel tape was subjected to a 10 kV d.c. voltage withstand test for 1 minute. The ends of the cable were then potted into the base of a ready access joint, to allow safe handling of the optical fibre joints on subsequent openings. In fact, if particularly strong field strengths are anticipated the sheath can be further sectionalised to limit the induced voltage.

## 9. Installation

The cable had to be installed in duct except for 500 m of troughing over a section rising at 30° to the horizontal. Jointing chambers were placed at every 250 m along-side those for power cables in adjacent duct. During installation of the first two lengths, each of 1 km, the pulling tensions were monitored and did not exceed 600 N. In fact, most of the tension appeared to be generated by the friction of the pulling ropes in the ducts.

As the remainder of the route was known to be less demanding it was decided to increase the lengths of cable in steps of 250 m until 1500 m was attained, the maximum length of the steel tapes. 1250 m and 1500 m lengths were successfully installed and a maximum pulling tension of 800 N was recorded.

Joints were made initially using a precision V-groove technique[4]. Alignment of the fibre ends was optimised by observing the scatter from visible helium-neon laser light. This proved unsatisfactory due to exceptionally dusty conditions and mechanical fatigue caused by persistent heavy vehicle movements along the mountain road. The joints were remade using a fusion splicing method which was monitored by a backscatter technique. The resulting improvements are given in Figure 12 which shows the backscatter plots of a single fibre channel over the first three cable lengths.

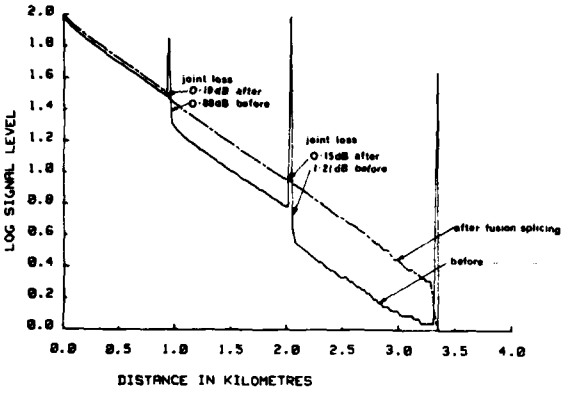



Fig 12 Backscatter over three cable lengths before and after fusion splicing

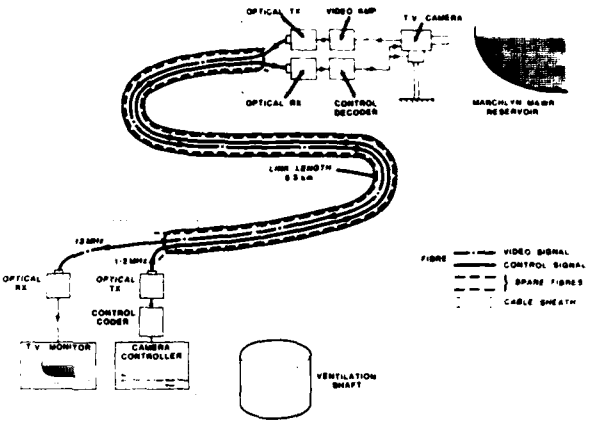



Fig 13 Schematic diagram of video and tele-control equipment

## 10. Video and Tele-control Systems

For the transmission of video signals from a monochrome television camera, it was proposed to use commercially available analogue/optical transmitter and optical/analogue receiver modules designed for the purpose. A 50 Hz to 5.5 MHz analogue bandwidth is provided by the analogue modulation of a 13.3 MHz carrier pulse position, that is, pulse position modulation (p.p.m.). The transmitter uses a pulsed laser at 850 nm and the receiver an avalanche photodiode (APD); in both cases a demountable coupling to a single multimode optical-fibre is provided by the jewelled ferrule technique.

Attenuation and dispersion requirements were imposed on the optical fibre link. For a 35 dB signal/noise ratio the insertion loss of the link could be up to 50 dB. However, owing to the proposed use of 63 microns diameter and 0.2 numerical aperture optical fibre, compared with 85 and 0.48 respectively for the laser tail, a loss of about 10 dB would occur at the transmitter coupling, thereby reducing the permissible link loss to about 40 dB. The qualitative effect of pulse dispersion on the p.p.m. system is that the slower rise times of the received pulses lead to uncertainty of timing which results in noise and which is significant at the lower signal levels. The dispersion along the link could be in the order of 5 ns before a significant trade-off against permissible attenuation would be necessary. This implies a minimum desirable bandwidth requirement of about 100 MHz.

For the remote control of camera functions (on/off, focus, zoom, pan, tilt, wash and wipe), a conventional 15-function tele-control unit, normally used with wired connections, has been employed but with suitable interfaces to optical modules. The normal repeater train of fifteen 0.5 ms pulses from the two-wire control unit, each corresponding to one of the functions, is encoded to provide an

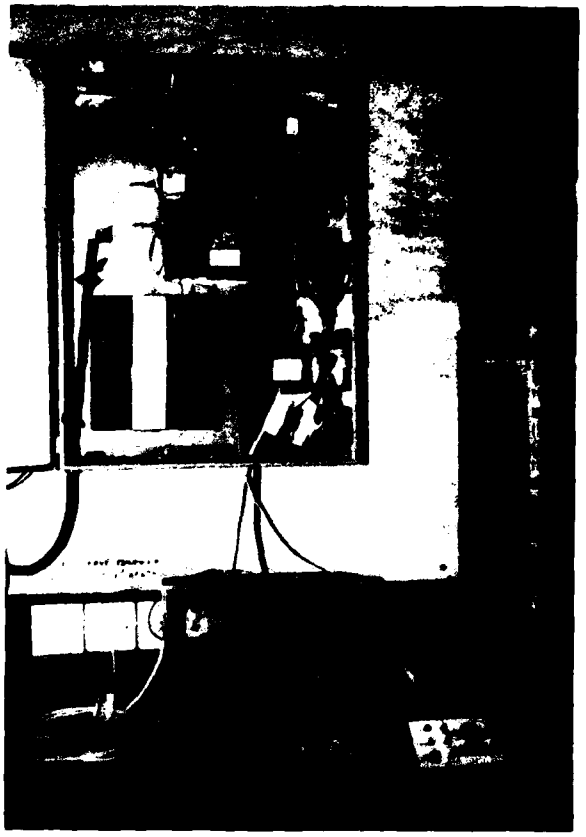


Fig 14 Video and tele-control equipment

appropriate 1.0 ms pulse for each function. The high and low pulse levels are converted to corresponding 1 MHz and 2 MHz pulse streams and applied to the optical transmitter. At the far end the reverse process takes place and the tele-control decoder switches the appropriate control function. Suitable digital transmitter and receiver modules incorporating respectively a pulsed laser and avalanche photodiode were selected which in fact were less demanding of the optical characteristics of the link than the video channel. A schematic diagram of the video and tele-control equipment is shown in Figure 13.

The terminal equipment at the video transmitting end of the link is now housed in the telecommunications room of the permanent head-works building adjacent to the top reservoir. The terminal equipment at the video receiving end and the 34 Mb/s equipment, described in Section 12, are housed in a 2.6 m x 3.6 m cabin adjacent to the top of the ventilation shaft. The video and tele-control equipment in the cabin is shown in Figure 14.

## 11. Operation of the Video and Tele-control Systems on the Link

Very good performance of both systems has been provided during preliminary trials. From the subjective viewpoint, a steady noise-free video display is received and the tele-control operates with precision. Measurement of the respective transmitter output powers at 850 nm and the corresponding received powers on the link channels 3 and 4 gives fibre attenuations of 23 dB and 25 dB respectively. The pulse dispersion was measured to be 5.0 ns and 5.3 ns for each channel respectively.

Although, as yet, neither system has been thoroughly evaluated it is evident from the attenuation and dispersion figures for the link, that in both cases there is ample margin in hand. In the case of the video system, yet to be optimised, it was demonstrated that 34 dB fibre loss could be tolerated without significant loss of picture quality.

Some difficulty has been experienced with the fibre terminations using jewelled ferrules. It seems to be absolutely essential to remove every trace of the silicone rubber primary coating and to epoxy into the ferrule a good length (15 mm) of the bared fibre in order to prevent the problem of fibre 'grow-out' from the jewel.

## 12. 34 Mb/s Line Terminal

As a more searching test of the optical fibre link it was decided to evaluate its performance with a single 34 Mb/s line terminal[5]. The equipment was installed in the cabin at the lower end of the link and connected to a convenient length of optical fibre by looping at one of the cable joint positions. The length was made 6.6 km by looping at the third cable joint position to suit the transmitter which is an LED operating at 900 nm.

The line terminal is designed to work with any 34 Mb/s source meeting the recommendations of CCITT, Rec G703, that is, to provide 480 telephone channels. The HDB3 34 Mb/s ternary signal is first converted into a binary signal and scrambled to obtain a stream of bits which are statistically independent whatever the input stream may be. The bits are coded into a 5B/6B signal having a bit rate of 41.242 Mb/s. The 5B/6B signal is then converted into a stream of binary optical pulses of the same rate. The transmitter is equipped with an LED instead of a laser diode because of the greater reliability of the LED.

In the receive direction a signal is detected using an APD and regenerated with a self-synchronizing regenerator. A simple equalising network which is part of the receive amplifier shapes the transmission channel. An automatic level control adjusts the APD gain to compensate for temperature variations of the transmitter and the receiver so that the signal level at the decision section is kept constant. Changes of the link attenuation are compensated partly by the AGC and partly by presetting the amplifier gain. Finally the regenerated 5B/6B signal is decoded, descrambled and then reconverted into HDB3 code.

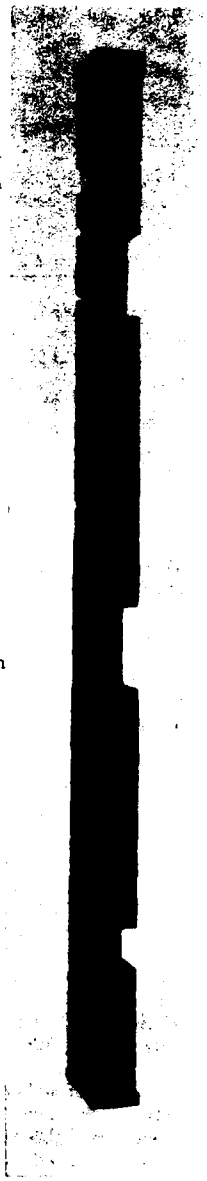


Fig 15 34 Mb/s Line Terminal

Particular care has been taken with the line code in order to achieve the following advantages:

- low spectral density at low frequencies
- low sensitivity to equalisation errors
- easy extraction of clock pulse
- a line error can be recognised

The use of a 5B/6B code, in preference to other codes using binary blocks, is justified by the small increase in line bit-rate which is important when using an LED and by the reduced circuit complexity.

The equipment is provided with monitoring and alarm facilities. These are based upon the control of the correct operation of each unit by means of fault detectors which initiate alarm lamps.

The line terminal, shown in Figure 19, is mounted on a slim line rack normally 600 mm high to house two systems but up to 1000 mm for interconnection in the cabin and beyond. Only one system was required. The line terminal is composed of three main subracks, as shown in the block diagram in Figure 20. The rack also contains a service subrack and a duplicated power supply subrack to improve equipment availability. Two 8-core and two 12-core screened cables are used to connect the optical fibre link to the equipment.

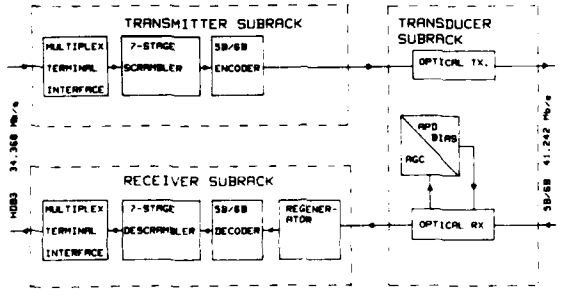



Fig 20 34 Mb/s line terminal block diagram

The main characteristics of the line terminal and the fibre link are given in the following tables.

| | |
|---|---|
| Information rate | 34.368 Mb/s |
| Interface code at 34 Mb/s | HDB3 |
| Line code | 5B/6B |
| Transmitted symbol rate | 41.242 Mb/s |
| Type of light emitter | LED at 900 nm |
| Type of light detector | APD |
| Measured transmitted power into fibre line | -9.1 dBm |
| Measured received power from fibre line (6.6 km) | -42.7 dBm |
| Line loss | 3.4 dB/km |
| Line intermodal dispersion | 5.6 ns |
| Line material dispersion | 14.6 ns |
| Minimum received power (BER=$10^{-9}$) | -45.7 dBm |
| System margin | 3.0 dB |

During the first four days after commissioning of the terminal an error rate of better than $1 \times 10^{-10}$ was obtained except for two bursts of errors related to transients caused by switching on test equipment in the cabin. This is probably associated with the provision of remote power supplies and unsatisfactory earthing and is currently being investigated. Subsequent checks have, in fact, shown that the accumulated errors over one month have been maintained at a rate of $10^{-10}$.

## 14. Operation of 34 Mb/s Line Terminal at Longer Wavelengths

In order to achieve longer distances between line terminals without the use of intermediate repeaters the LEDs can be replaced by laser diodes or longer wavelength devices. In the former case the line length could be increased to about 11 km. In the latter case the maximum line length, as limited by the attenuation, could be 16 km because the fibre attenuation drops from an average value of 3.4 dB/km to 1.1 dB/km at 1300 nm. In either case the LEDs can be replaced by changing cards in the transmitter subrack.

The use of LEDs emitting at 1300 nm is particularly attractive due to the reduction of material dispersion. In fact, the performance of the 34 Mb/s system with graded index fibre of good attenuation and bandwidth characteristics is limited by material dispersion when using LEDs operating in the first window. When operating at the longer wavelength the material dispersion reaches a near-zero value and the problem disappears. The limiting factor becomes the attenuation of the fibre assuming that the modal dispersion is small enough. Since the refractive index profile of the fibre for Dinorwic was designed for optimal bandwidth at 850 nm there is a fall-off in bandwidth towards 1300 nm similar to that described by Eve et al[9] e.g. 500 MHz. km dropping to 200 MHz. km. This situation can be improved by either designing the optical fibre to have an optimum bandwidth at 1300 nm or optimising half-way between 850 nm and 1300 nm to provide reasonable bandwidth at both wavelengths.

If the Dinorwic fibre is typical, it would suggest that unless the profile of fibres is designed for longer wavelength operation, bandwidth will be the limitation to maximum span lengths for systems at 34 Mb/s.

## 9. Conclusions

The experimental optical fibre link of about 6 km length, recently installed in mountainous terrain,

has shown the feasibility of pulling-in optical fibre cable in lengths up to 1500 m. This has been achieved by using a cable construction with low weight and high tensile strength, and the use of fibre length within the limits of strain applied during pulling operations.

Assembly of the cable in a dirty environment and subsequent splicing of fibres in a pulling box in the open air, monitoring the splices during splicing by a backscattered signal, have proved reliable.

The equipment for transmitting digital signals at 8 Mb/s and 34 Mb/s and the protection switching system have achieved with an error rate of $10^{-9}$. Commercially available opto-electronic components using laser diodes operating at 850 nm wavelength, employing analogue pulse position modulation and digital techniques, respectively.

A 34 Mb/s line terminal, using an LED at 900 nm, has been shown to work satisfactorily over a 6.6 km link. Evaluation of the system suggests that the maximum distance between terminals will be limited on bandwidth should the equipment be re-equipped with second window (1300 nm) devices.

The experimental optical fibre link will continue to be monitored to evaluate the performance of both cable and equipment encorporating current and future technologies.

## 10. Acknowledgements

The authors would like to express their deep appreciation for much valuable help and advice to the following:

Staff of the CSELT's Innovation Development and Optoelectronics Division, especially Mr. A.M. Bilo, the Project Plant Manager, and Mr. Pierluigi Di Vita, Engineer Dr.

Mr. Mario Bertolotti

Mr. Ivo Montanari and his staff at Telettra Milano.

Mr. Robert Lewis of Pirelli General Cable Works Ltd.

Mr. Alberto Scotti of Telettra pA.

This paper is published by permission of the British Telecommunications Engineering Board, Telettra SpA and Pirelli General Cable Works Ltd.

## 11. References

1. M.A. Tumbling et al : Optical fibres based on germanosilicate glass fibres. IEE Vol 15, pp 570 - 576.

2. G. Grasso et al : High quality optical fibre cables for telecommunications. 27th IWCS. pp 143 - 149.

3. L.L. Buccelli and J.P.M. Bonnaure : Structure and properties of injection-moulded nylon 6. J. of Material Sci. pp 1167 - 1177.

4. J. Bensoussan et al : Some aging optical fibres. Electronics Letters Vol 15 pp 155 - 156.

5. M. Pacelli et al : Design, manufacturing and performance of a 34 Mb/s optical fibre transmission system. 26th IWCS (Asbury Park 1977) pp 1-8.

6. M. Pacelli et al : Development aspects of high performance optical fibre links. 27th IWCS (1978) pp 65 - 69.



J. Richard Osterfield born in 1931 has a general science degree and a master's degree in mathematics achieved at London University. He is a member of I.E.E. He joined GEC Research Laboratories in 1955 to work on telecommunication cable problems and transferred to Pirelli General in 1960. He is Assistant Chief Engineer (Telecommunications) and is responsible for telecommunications research and development.



Alan J. Rogers graduated at Cambridge with first class honours degree in Part I and II of the Natural Sciences Tripos. He obtained a PhD in space physics at London University and was engaged in lecturing and research at the University from 1964-69. In 1969 he joined Central Electricity Research Laboratories. He is leader of the Photon Physics Group which pursues activities in optics over a wide range of applications.



Stephen R. Norman born in 1950 graduated at Southampton University with an honours degree in mechanical engineering. He joined Pirelli General in 1972 and has been working in the field of optical fibres since 1974. He is engaged in work for his doctorate at Southampton University in optical fibre technology and is currently head of the optics laboratory at Pirelli General.



Roberto Castelli born in 1947 has a masters degree in electronics engineering at Bologna University. He joined Telettra in 1972 and is now leader of a group working on equipment for optical fibre communications.



D. Neil McIntosh graduated at London University with honours degrees in physics and mathematics. He joined CERL in 1957 and is a member of a physics group investigating optical techniques for measurement and communications. He holds the posts of radiological and laser safety officer at CERL. He previously worked on nuclear radiation measurement and non-destructive testing.



Mario Tamburello born in 1952 has a masters degree in electronic engineering at Palermo University. He spent one year on optical fibre measurement at Bologna University and joined Telettra in 1977. He is working on optical fibre systems.

# OUTSIDE PLANT HARDWARE FOR USE IN FT3 LIGHTWAVE SYSTEMS

N. E. Hardwick III and J. L. Baden

Bell Laboratories
Norcross, Georgia

## ABSTRACT

Outside plant hardware has been developed for Bell System lightwave applications such as the FT3 Lightwave Digital Transmission System. Together with the ribbon-based lightguide cable, the splicing, closure, and cable terminating hardware form the outside plant transmission media system. Central office terminations, splice manhole interconnections, and repeater station terminations are provided for the optical fibers. Grounding, bonding, and pressurization methods are also provided.

Up to 144 optical fibers can be efficiently spliced within one splice closure using ribbon-array splicing technology. FT3 repeater spans of over four miles are permitted. In addition, all hardware is designed for Telco outside plant craft personnel use. To date, over 50 route miles involving approximately 3200 km of fiber and 600 ribbon-array splices have been successfully installed by Telco craft.

## INTRODUCTION

Installation began in March 1980 at Atlanta, Georgia, on the first standard Bell System FT3 Lightwave Digital Transmission System. This 6.5 mile-long (400 fiber-km) application was followed by the Pittsburgh-Greensburg FT3 Installation which is 40.2 miles long (2800 fiber-km) and for which installation began June 1980. Bell Laboratories developed the hardware for these standard FT3 systems. All hardware components are compatible with the crossply lightguide cable[1] and have been designed for installation by Telco craft personnel.

## OVERVIEW OF OUTSIDE PLANT HARDWARE

Initially, the principle application for FT3 lightwave systems is interoffice trunking. Up to 144 fibers are contained in one cable and each fiber carries 672 one-way voice circuits at the FT3 rate of 44.732 Mb/s.

As shown in the system block diagram in Figure 1, standard digital transmission signals are fed into the Line Terminating and Multiplexing Assembly (LTMA) from a digital cross-connect (DSX). In the LTMA equipment a small semiconductor laser couples the light into each glass fiber for outgoing transmission and the incoming light pulses are received by an avalanche photo diode. The Lightguide Cable Interconnection Equipment (LCIE) forms the interface between the outside plant and central office hardware. The outside plant cables and the central office cables are interconnected here. The LCIE also provides a means for cable rearrangements and single fiber-to-multifiber cable interconnections.[2]

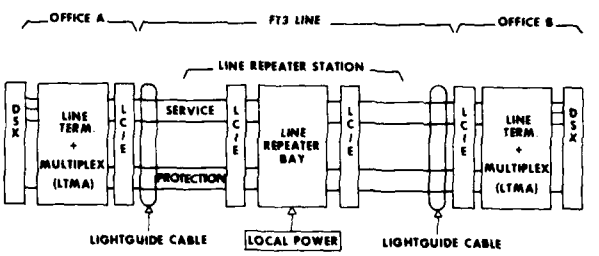



FIGURE 1. FT3 LIGHTWAVE DIGITAL TRANSMISSION SYSTEM

A schematic drawing of the outside plant hardware in an FT3 repeater span is shown in Figure 2. Although several additional manhole splices usually will be present on each side of the midpoint splice manhole in a repeater span, this figure shows the positions of all the major outside plant hardware components in the FT3 lightwave systems. Each of these components will be discussed in detail in this paper.

## FACTOPY TERMINATED CABLE SECTIONS

Lightguide cables for FT3 systems are shipped from the factory with both ends terminated. The cross-ply lightguide cable design[1] (see Figure 3) is used; it has a ribbon structure[3-5] with twelve

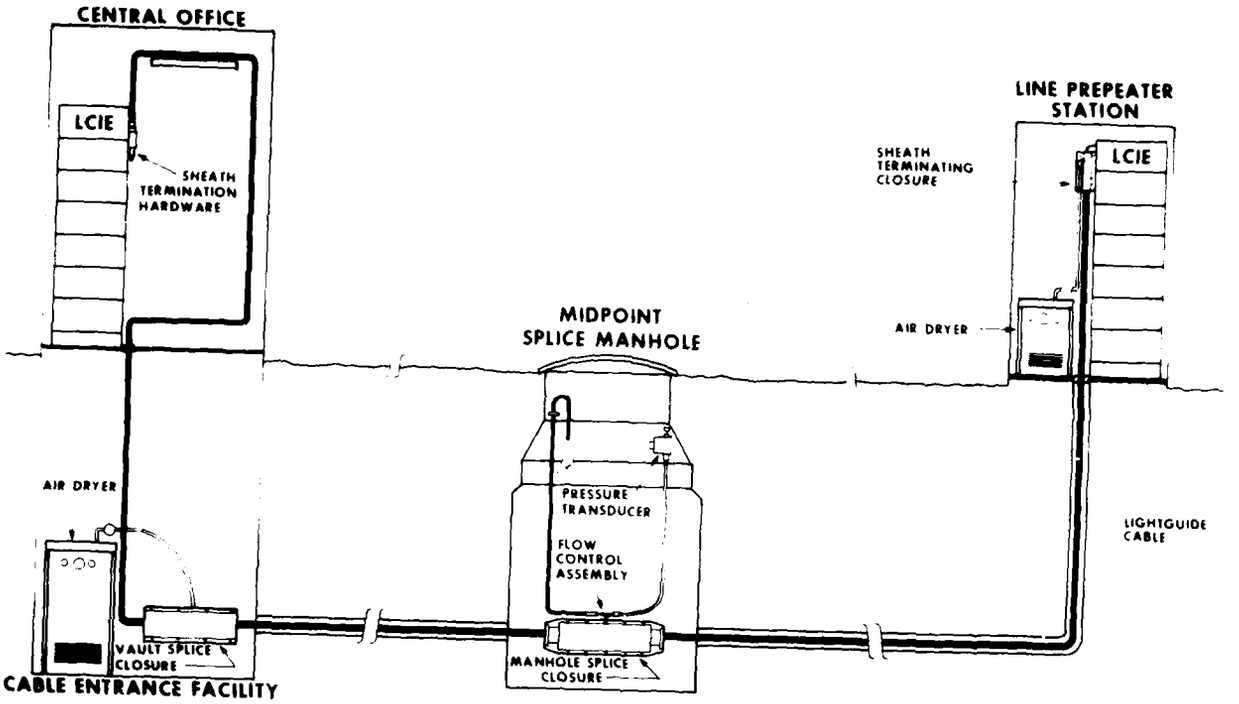



**FIGURE 2. SCHEMATIC REPRESENTATION OF FT3 LIGHTWAVE OUTSIDE PLANT WITH ALL TERMINATIONS AND CLOSURES.**

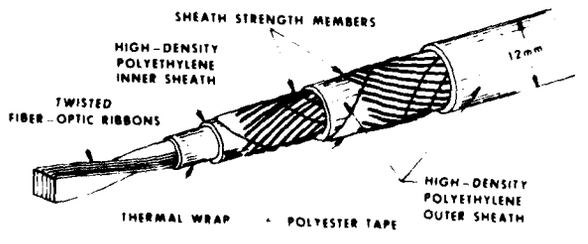



**FIGURE 3. CROSSPLY LIGHTGUIDE CABLE**

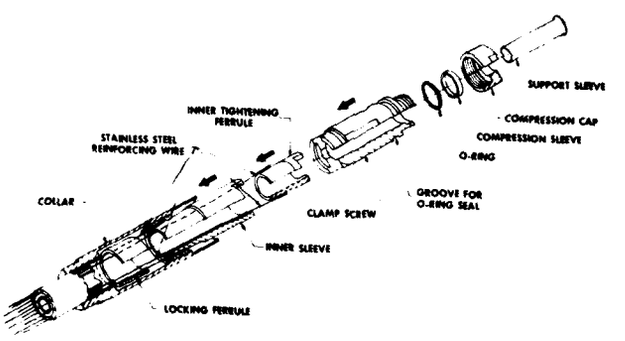



**FIGURE 4. SHEATH TERMINATION HARDWARE**

fibers in each ribbon. Early work[6] revealed that the fibers may be more efficiently spliced ribbon-to-ribbon as compared to individual fiber splicing. Therefore the end of each ribbon is terminated with an array connector[6,7] using etched silicon chips. Cable pulling loads are limited to 600 pounds to ensure adequate protection against long term static fatigue.

## Sheath Termination Hardware

All mechanical junctions to the lightguide cable sheath are made through the Sheath Termination Hardware (STH) shown in Figure 4. The Sheath Termination Hardware is designed to interface with either the LCIE or one of the closures in the outside plant system. However, the STH's most important function is to provide a secure means of gripping directly onto the 28 stainless steel reinforcing wires in the cable so installation loads can be transmitted to the sheath and in situ cable forces transmitted across splices. The STH has a self-tightening feature that allows it to support tensile loads up to 1700 pounds. (This value is more than 85% of the intrinsic strength of the reinforcing wires and more than twice the allowable installation load.)

## Ribbon Array Connectors

The manufacturing plant prepares each end of a lightguide cable with connectorized ribbon leads for splicing as shown in Figure 5. The ribbon leads, which are about 2 feet long, exit the cable through the Sheath Termination Hardware. The fiber ends appear on the polished face of the ribbon array connector as shown in Figure 6. The glass fibers are held in place by precise grooves in the two silicon chips[7] which are bonded together with epoxy. These grooves are etched in the chips using photolithographic techniques common to the integrated circuit industry.[8] The inner chip grooves are also precisely positioned relative to the outside array grooves so they can be used to align two ribbon arrays for cable joining (splicing).

## Flexible Pulling Eye

The ribbon leads must be protected from mechanical damage and from water during cable shipment, storage and installation. Therefore, a strong protective housing is required that is air tight to maintain cable pressure and prevent water entry. This housing acts as a pulling eye for the long leads during installation, so it must also withstand pulling loads without excessive deformation but remain flexible enough to be pulled through curved ducts. The Flexible Pulling Eye (shown in Figure 7) meets all the above requirements as well as being weather resistant, reusable, and easy to install or remove. The key to this design is the stainless steel corrugated-tube housing that is prestressed so that it can withstand the allowable installation forces while undergoing a small elastic strain.

The pressure valve in the Flexible Pulling Eye (FPE) valve port provides a means for pressurizing the cable after the FPE is in place. As shown in Figure 8, the pulling eye cap protects the pressure valve and can be removed at any time to check the pressure.

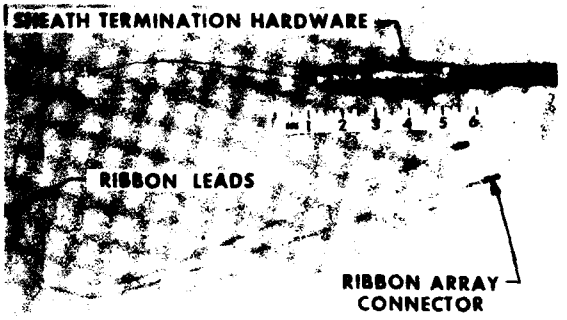



FIGURE 5. END OF LIGHTGUIDE CABLE WITH TWO FACTORY CONNECTORIZED RIBBON LEADS

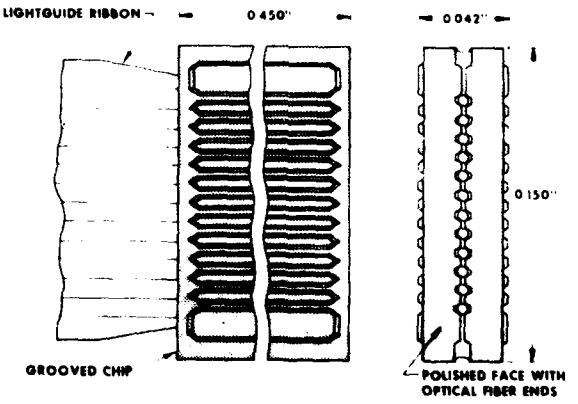



FIGURE 6. DETAILED VIEW OF CONNECTORIZED ENDS

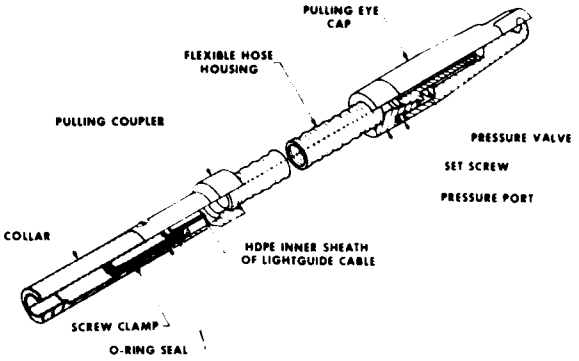



FIGURE 7. FLEXIBLE PULLING EYE ATTACHED TO SHEATH TERMINATION HARDWARE (SHADED PORTION)



FIGURE 8. FLEXIBLE PULLING EYE WITH PULLING EYE CAP REMOVED TO ACCESS F VALVE STEM FOR CHARGING OR PRESSURE CHECK

## JOINING OF CABLE SECTIONS

The lightguide cables are installed and racked in the manhole with the cable ends slightly overlapping. The flexible pulling eyes are removed by the splicers for cable joining.

### Sheath Joining

In all FT3 installations, sheath joining is accomplished using the sheath termination hardware. The cable sheaths at a manhole or vault splice are joined by locking the STH to the splice organizer inside the splice closure. The back of the splice organizer is shown in Figure 9. The STH of each of the two cables to be joined is secured in a cable clamp so cable forces cannot be transmitted to the ribbon splices. The cable clamp compresses a metallic bonding ribbon against the STH. The bonding ribbons then exit the closure through slits in the closure sealing grommets. (The STH has contact with the reinforcing wires so cable bonding is accomplished by bonding the STH).

The front of the splice organizer is shown in Figure 10. The large splice organizer is needed in order to store the ribbon pigtails without violating the 1.5" minimum ribbon bend radius. The ribbons are looped in an oval fashion to allow full flexibility in interconnecting ribbons from the cables, and to provide additional ribbon length should a repair have to be made on a ribbon lead.

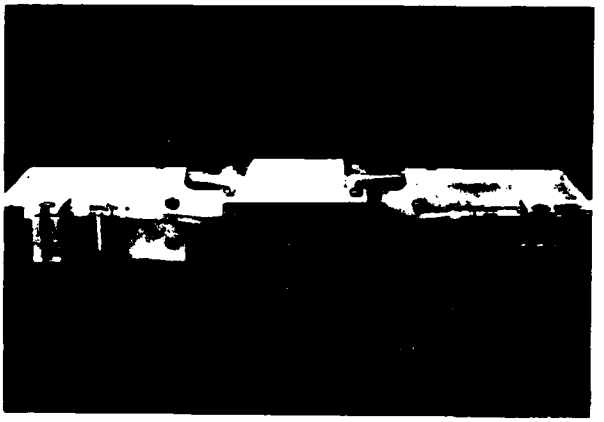


FIGURE 9. REAR VIEW OF SPLICE ORGANIZER

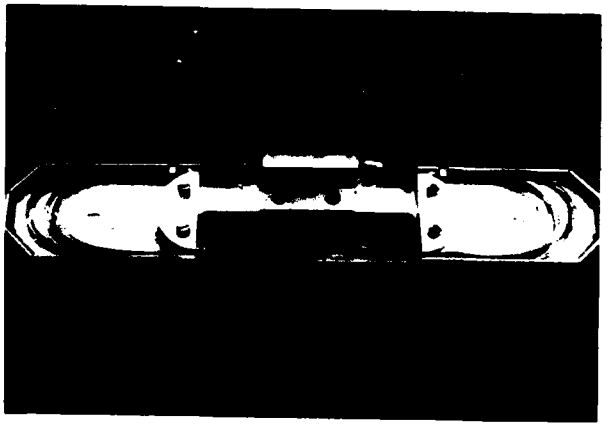


FIGURE 10. FRONT VIEW OF SPLICE ORGANIZER

### Ribbon Joining

The simple steps in the ribbon splicing operation will now be outlined. The Exploded View in Figure 11 shows the two factory-installed ribbon arrays to be joined in which positive chips with

precise grooves on the top and bottom hold the optical fibers in precise locations. Also shown are two oppositely-grooved, bridging chips (referred to as negative chips) and two spring clips. The first step in forming a field splice is to clamp one array connector between the two negative chips as shown in Step 1. Then the other connector to be joined is slid along the negative chips' grooves to butt up against the first connector. Next the two metal clips are positioned to mechanically hold the splice together (see Step 2). The final step is to insert an index matching material between the array faces to reduce splice loss by preventing index of refraction mismatches. The ribbon connections (or splices) are protected inside the platform located at the top of the splice organizer. (See Figure 12 showing 7 of 12 ribbon splices completed.)

Each pair of fibers has the capacity of 672 digital voice channels (two-way) when operating at the 44.7 megabit per second FT3 rate. Therefore, this ribbon splice, which can be formed in less than 15 minutes, can carry up to 4032 two-way voice channels.

## LIGHTGUIDE SPLICE CLOSURES

There are two types of splice closures in the FT3 system outside plant: (1) the vault splice closure, and (2) the manhole splice closure. A vault splice closure, located in the Cable Entrance Facility (CEF), is recommended for all central office (CO) cable terminations because of the flexibility it gives and because it greatly facilitates bonding, grounding, pressurizing and plugging the cable. A manhole splice closure is required for splicing every cable section between line repeater stations; it is structurally similar to the vault splice (see closures locations in Figure 2).

### Vault Splice Closure

The heart of the vault splice closure is the splice organizer which fits inside a Bell System plastic closure (Type 2B3). The vault splice closure with the splice organizer enclosed and in position is shown in Figure 13. Since the fiber ribbons do not conduct electricity, insulating joints can be formed by placing plastic spacers behind the metallic cable clamps. These spacers electrically isolate the two STHs from each other (and, in turn, the joining cables). Also, the riser cable to the CO interconnection equipment can be plugged by inserting epoxy into the cable core at the STH. Therefore, with a vault splice, there is no need to cut the cable sheath for either bonding, pressurizing, forming insulation joints, or gas blocking.

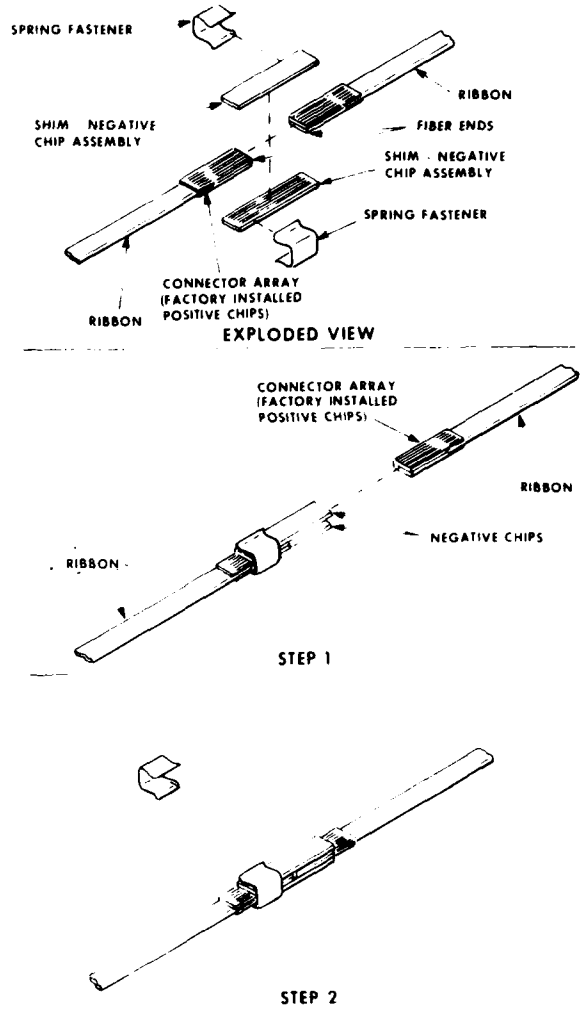



FIGURE 11. RIBBON SPLICING OPERATIONS

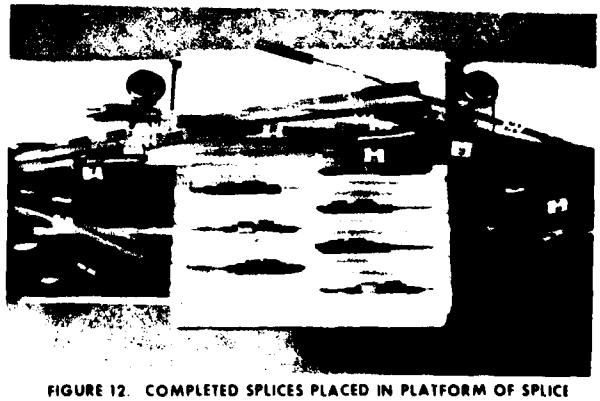


FIGURE 12. COMPLETED SPLICES PLACED IN PLATFORM OF SPLICE ORGANIZER

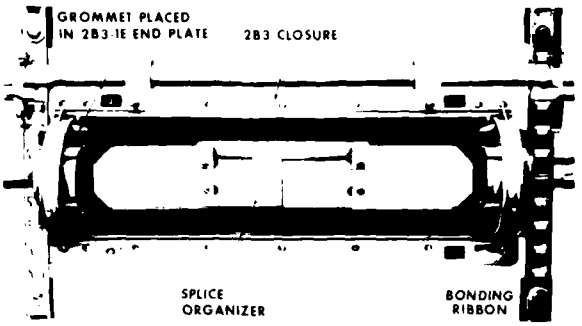



**FIGURE 13. VAULT SPLICE CLOSURE WITH SPLICE ORGANIZER**

## Manhole Splice Closure

A drawing of the manhole splice closure is given in Figure 14 to show how it is secured to the manhole rack and the bonding arrangement. The splice organizer inside the manhole splice closure is identical to that used at the vault splice. The primary difference between the vault and manhole closures is that the latter is a 50D3 type, since manhole closures usually aren't required to be flame retardant. Also, the air path is continuous through this closure rather than plugged as in the vault splice closure.

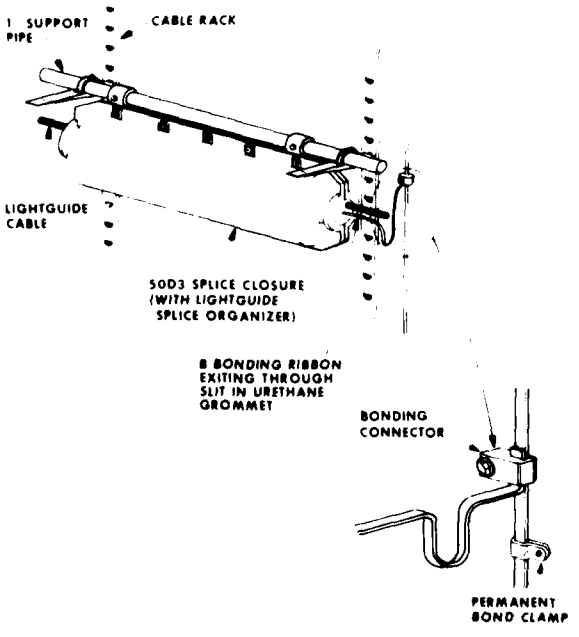



**FIGURE 14 LIGHTGUIDE CABLE BONDING CONNECTIONS IN SPLICE MANHOLE**

## CABLE SPAN TERMINATION POINTS

Cable spans are generally terminated at central offices or line repeater stations. Figure 15 illustrates the facilities used to interconnect or terminate lightguide cable in the central office. The STH on the end of the riser cable (from the vault splice) is merely clamped to the LCIE as shown in Figure 16. Inside the LCIE the riser cable ribbon leads are either spliced to a fanout array or another riser cable. The other side of this fanout (shown in Figure 17) is in the form of single fiber cables which connect to the single-fiber connectors[9] on the LCIE patch panel. Single fiber jumpers from this patch panel connect the LCIE to either the Line Terminating and Multiplexing Equipment or a Line Repeater Frame.[2]

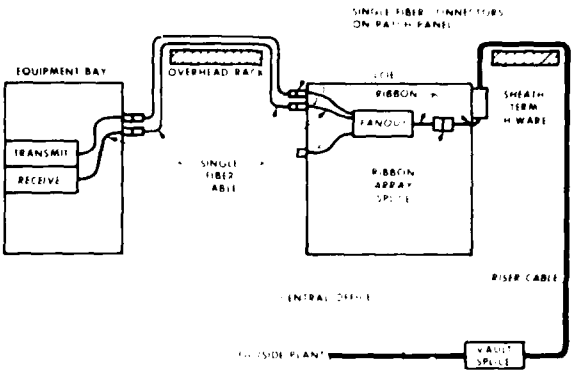



**FIGURE 15 TERMINATION OF A CABLE SPAN AT THE CENTRAL OFFICE EQUIPMENT BAY**

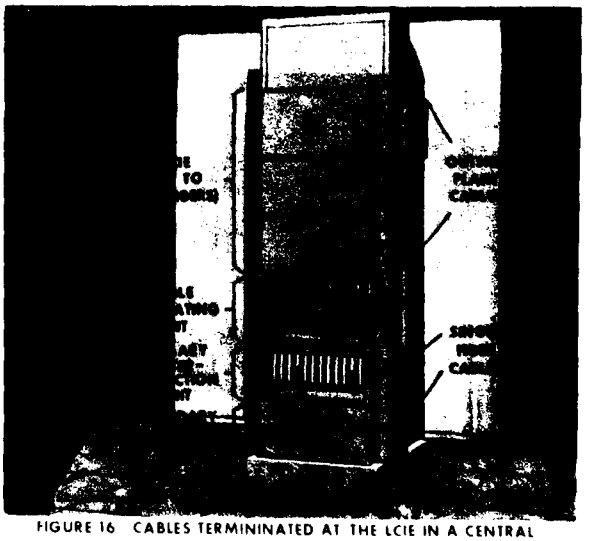


**FIGURE 16 CABLES TERMININATED AT THE LCIE IN A CENTRAL OFFICE**

At the other end of a repeater span is another LCIE that is the same internally as those located in COs. The repeater station LCIEs can accommodate up to 12 cables; however, there is insufficient room in most repeater huts to accommodate even two 50D3 splice closures. Therefore, the miniature Sheath Terminating Closure (STC) was designed to accomplish all the bonding, pressurizing, and plugging tasks done at the vault splice. Instead of the cable STH being clamped to the side of the LCIE (as is done in central offices), Sheath Terminating Closures are mounted in their places on repeater station LCIEs as shown in Figure 18. As its name implies, the STC terminates the lightguide cable sheath (i.e., a cable sheath enters and only the ribbon leads exit).

The interior of the STC shown in Figure 19 illustrates how the functional requirements are satisfied. (The dotted portion is the STH which always remains on the cable.) The locking disc is fastened to the STH and positioned in a slot to prevent cable loads from being transmitted to the ribbons.

The key to the STC design is the use of polyurethane grommets to form air-tight seals around the lightguide cable and ribbons without damaging the fibers. Therefore cutting into the cable to form a plug is again avoided.

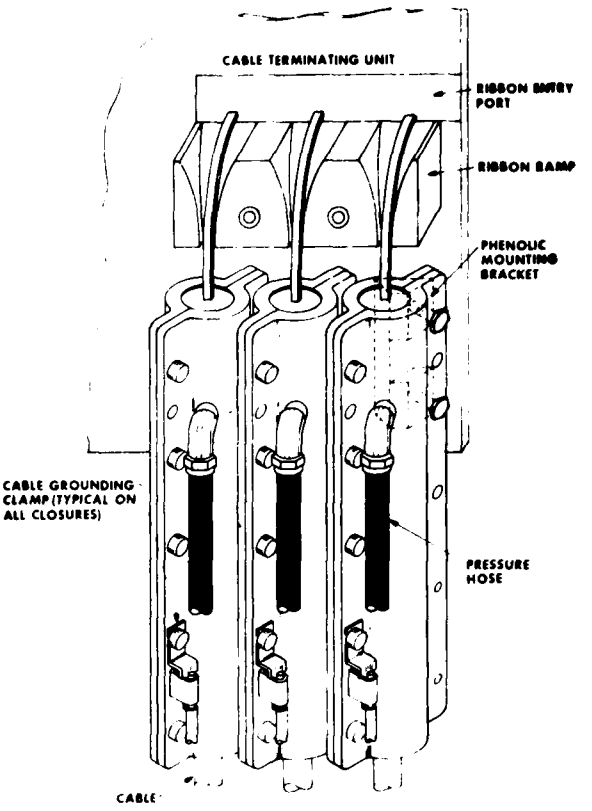



FIGURE 18 SHEATH TERMINATING CLOSURES MOUNTED ON LCIE FRAME FOR LINE REPEATER STATION

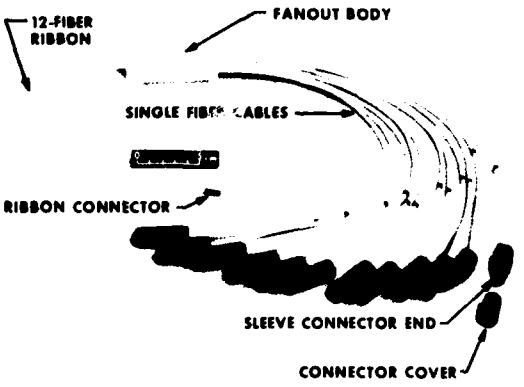



**FIGURE 17. RIBBON-TO-SINGLE FIBER CABLE FANOUT LOCATED INSIDE LCIE**

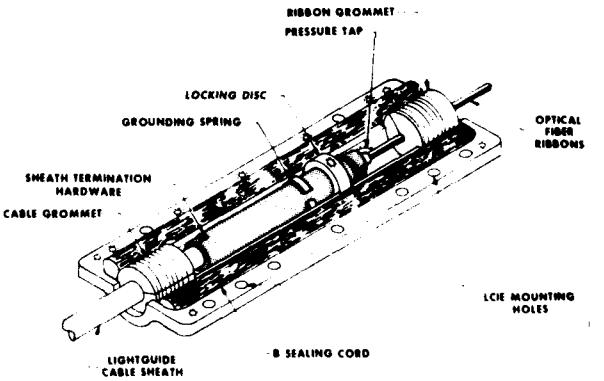



FIGURE 19 INTERIOR OF SHEATH TERMINATING CLOSURE

## CONTROLLED FLOW PRESSURIZATION SYSTEM

All the outside plant components have now been described other than those included in the pressurization system. For FT3 the controlled flow pressurization system performs two functions. Like standard pressurization systems, a specific pressure level is maintained in a cable span to prevent liquid water entry through inadvertent leaks in the cable and/or closures seals. In addition, a small controlled-flow bleed is used to continuously bleed off moisture permeating through the cable sheath to produce a low relative humidity environment. This environment provides an extra margin of safety against static fatigue effects.

As can be seen in the schematic in Figure 20, the controlled-flow pressurization system is simple and requires essentially no engineering. The amount of flow required to purge the moisture is small enough that air dryers are only needed at COs and repeater stations regardless of the number of ribbons in the cable. As shown in Figure 20, the pressure monitoring devices needed to reveal any detrimental pressure drop are only required at the 1/4, 1/2 and 3/4 pneumatic resistance points. A simple, fixed orifice flow control valve provides the desired moisture bleed level when pneumatically connected to the midpoint splice closure. It requires no adjustment and automatically closes if the pressure drops below 5 psi.

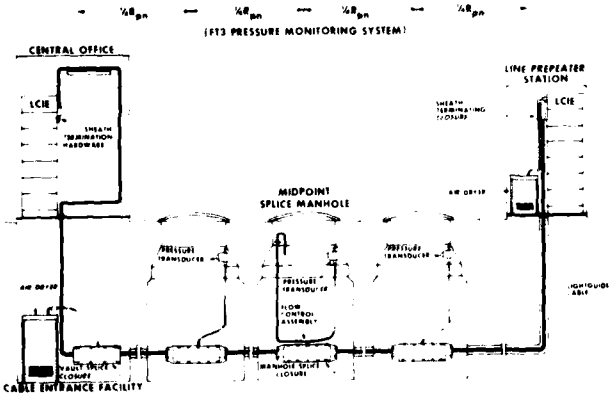



**FIGURE 20. FT3 CONTROLLED FLOW PRESSURIZATION AND PRESSURE MONITORING SYSTEM**

## CONCLUSION

Underground outside plant hardware has been developed for the Bell System FT3 Lightwave Digital Transmission System. The designs of the cable, splicing, closure and terminating hardware as well as methods for bonding, insulating, and pressurization are integrated to form the overall outside plant system. Because this system concept was applied in the hardware development, normal installations can be accomplished without craft personnel cutting the lightguide cable sheath or touching optical fibers. This hardware system has been successfully used in Atlanta, Georgia and between Pittsburgh and Greensburg, Pennsylvania. By early 1981, approximately 90 miles of FT3 lightguide cable will have been installed.

## ACKNOWLEDGEMENT

The authors wish to acknowledge T. C. Cannon, Jr. for his suggestions concerning the hardware designs.

## REFERENCES

1. P. F. Gagen and M. R. Santana, "Design and Performance of a Crossply Lightguide Cable Sheath," 28th International Wire and Cable Symposium, Cherry Hill, New Jersey, November 1979

2. M. R. Gotthardt, "Lightguide Cable Interconnection Equipment (LCIE)," Third International Fiber Optics and Comm. Expo., San Francisco, California, September 1980.

3. R. D. Standley, "Fiber Ribbon Optical Transmission Lines," B.S.T.J., Vol. 53, No. 6 (July-August 1974), pp. 1183-1185.

4. M. J. Saunders and W. L. Parham, "Adhesive Sandwich Optical Fiber Ribbons," B.S.T.J., Vol. 56, No. 6 (July-August 1977), pp. 1013-1014.

5. M. J. Buckler, M. R. Santana, and M. J. Saunders, "Lightguide Cable Manufacture and Performance," B.S.T.J., Vol. 57, No. 6 (July-August 1978), pp. 1745-1757.

6. M. I. Schwartz, "Optical Fiber Cabling and Splicing," Technical Digest of Papers of the Topical Meeting on Optical Fiber Transmission I, Williamsburg, Virginia, January 1975, p. WA2.

7. C. M. Miller, "Fiber Optic Array Splicing with Etched Silicon Chips," B.S.T.J., Vol. 57, No. 1 (January 1978), pp. 75-90.

8. C. M. Schroeder, "Accurate Silicon Spacer Chips for an Optical-Fiber Cable Connector," B.S.T.J., Vol. 57, No. 1 (January 1978), pp. 91-97.

9. P. K. Runge and S. S. Cheng, "Demountable Single-Fiber Optic Connectors and Their Measurement on Location," B.S.T.J., Vol. 57, No. 6 (July-August 1977), pp. 1771-1790.



BIOGRAPHY

Nathan E. Hardwick, III, has received B.S. and M.S. Degrees in Mechanical Engineering from the University of South Carolina and a Ph.D. in Mechanical Engineering from Lehigh University. After joining Bell Laboratories in 1965, he initially designed and thermally characterized ceramic integrated circuit packages. Later work included formulating analyses for natural convection cooling of multichip IC substrates, air pressurization source and transducer locations in toll and trunk cables, vaporation drying of wet PIC cable, allowable cable installation loads, and trouble comparisons using filled, pressurized and nonpressurized cable in buried plant. One year was spent as a Bell Laboratories Visiting Processor at N.C. A&T State University.

Currently, Nate is a member of the Lightguide Joining Group where he is responsible for UG outside plant hardware and pressurization systems for FT3 lightguide cable. He also coordinated the cable splicing and terminating phases of the first two lightwave installations including the training programs for Telco craft.



John L. Baden is a Member of Technical Staff at Bell Laboratories in Norcross, Georgia. At present he is responsible for splicing operations of lightguide cable. Since joining Bell Labs in 1961, he has been involved with the design and development of multi-paired cable, coaxial cable, CATV cable installations and in splicing studies. Mr. Baden received a BS Degree in Physics from American University.

# Splicing Techniques for Tactical Fiber Optic Systems

Scott F. Large

The MITRE Corporation

Bedford, Massachusetts

## Abstract

Tactical Fiber Optic Communications will require quick, efficient maintenance to support system operation. An evaluation was made to determine if military fiber optic systems can be repaired in the field. Areas of investigation include cable handling, outdoor splicing and the effects of field conditions, splice protection and user skill level requirements. Conclusions are made as to appropriate maintenance levels, as well as specific system design considerations.

## Introduction

In the design and construction of any communications system consideration must be given to system maintenance requirements. The design of a system which is difficult to repair or maintain would obviously be of limited use. When considering Fiber Optics for use in a tactical communication system the problem of link maintainability cannot be overlooked.

The repair of a tactical system's fiber optic cable plant presents the greatest stumbling block in the development of an overall system maintenance concept. Since this component represents the major technological change in the system's design, it creates special problems in terms of maintenance. Care must be exercised when choosing a repair method appropriate to the environment in which the link is to be used.

Presented herein are the observations from an evaluation of several cable splice techniques which might lend themselves to use in a tactical environment. A comparative analysis of these methods is discussed as well as a report on the results of actual field splicing. A discussion on splice protection and design constraints is also presented.

## Splice Techniques

Numerous splicing techniques have been proven feasible for many applications. Each method has inherent advantages and disadvantages. These methods include the V-Groove, Loose Tube, Precision Sleeve, 3-Rod, Grooved Chips, Arc Fusion, Flame Fusion and Laser Fusion splices. Not all of these methods are suitable for use in a tactical environment, and some are used only in a laboratory setting.

Since consideration was being given to optical cable repair in the field, only three techniques were evaluated; the fusion splice, for its low loss; the loose tube splice, as a feasibility model of a simple method; and a commercially available V-Groove splice. Each method was examined with the following parameters being considered most important.

1. Splice Loss - The loss of a splice is very important with regard to link degradation. The splice loss must fall within the value allotted to it in the link budget power margin.

2. Repeatability - Not only must the splice loss be low but this loss should be consistent with each splice.

3. Time - The time necessary to perform a splice must be within reasonable limits. These limits would depend on type of splice and the environmental conditions.

4. Splice Strength - An unprotected splice should be able to withstand moderate tensile stress. This is important when the cable may undergo rough handling during installation or may encounter extreme environmental variations.

5. Splice Size - The size of the finished splice must allow it to be housed in a splice boot (protective cover) with other splices.

6. Aging - A change in splice characteristics with time is important, particularly when considering epoxied splices.

7. Post Splice Handling - Once the splice is completed it must be rugged enough to allow removal from any tools or jigs.

8. Instructability - The splice technique itself must not be so complicated so as to require a great deal of training to master it.

9. Skill Level - The skill level required to make the splice must not be inconsistent with current maintenance skill levels.

In addition to these parameters the splices were also analyzed for effects from wide environmental variations. These techniques were also evaluated in outdoor splicing exercises.

As with the splice technique itself, the methods used for cable and fiber preparations are very important. These methods must be compatible with cable and fiber design, repair time constraints and user skill level. Cable preparation and fiber breakout are, of course, dependent upon cable design. At this time there are two basic cable designs in use, a close packed or tightly bound cable and a loose tube or loosely bound cable.

The manufacture of the tightly bound cable involves the extrusion of a protective sheathing directly over the helically wound buffered fibers and KEVLAR strength members. This construction offers small size, very high crush resistance and remarkable flexibility. See Figure 1. The loosely bound cable construction has the buffered fiber floating loosely in larger tubes which are grouped together with strength members and then covered by a protective sheathing. The tubing can be filled with viscous silicone to form a moisture barrier. Although slightly larger, this design provides good fiber cushioning and allows for cable expansion and contraction due to temperature variations. Another advantage of this design is that when used in conduits, the fibers float freely in the tube and are able to recede back into the cable if it is stretched during the pulling operation. Both types are being considered for use in military systems.



Figure 1 - Four Fiber Cables Tied In A Knot Around Stake

The major difference in the construction of these cables can be seen when considering access to the individual fibers. In the tightly packed design the extrusion of an inner jacket directly over the fibers and strength members presents the worst problem. The fibers tend to become surrounded by the sheathing material and when an attempt is made to separate the fiber from the jacket they often stick and sometimes break. Of greater importance is the fact that opening the inner jacket with a knife or other sharp tool is extremely hazardous to the fibers. Extreme care must be taken so as not to penetrate too deeply into the inner jacket and nick any of the fibers. A tape wrapped around the fiber might prevent such damage.

Once the fibers have been broken out of the cable the next step is to strip the buffering from the glass fiber. The method used will depend on the material used to buffer the fiber. Presently some buffers require immersion in a chemical reagent or thermal stripping with a high temperature source while others may be stripped using wire strippers. The fiber used in this evaluation had a HYTREL buffering which was stripped with 0.010 inch Clauss "NO-NIK" wire strippers.

Preparation of the fiber ends is an important step in the splice process. Early in the development of fiber optics a great deal of attention was given to the best method by which to obtain a flat,mirror-like fiber end. However, as time went on it was found that simpler hand methods were sufficient for nearly all splicing work. The technique which was used during this evaluation was quite simple and could be easily mastered. The "scribe and pull" technique, as it is called, involved securing the end of the stripped fiber, either with a clamp or tool, then applying a very light tension to the fiber. A scribing tool, usually a diamond or tungsten carbide blade, was then brushed very lightly across the fiber perpendicular to its length. The tension on the fiber was then increased until the fiber broke. This whole process took about 15-20 seconds. Hand held cleaving tools have also been developed for use in the field however they seem to be susceptible to dirt and misalignment after heavy use.

When considering a tactical environment for repair of a field cable it may be necessary to accept low quality ends for "quick fix" repairs. Even shattered fiber ends were prepared and tested using diagonal cutting pliers.

After the fibers have been cleaved they may need cleaning to remove dirt, grease and debris. This can be achieved by dipping them in alcohol or any other non-hazardous solvent. An effective method for cleaning the face of the fiber is to take a piece of SCOTCH Magic Tape and lightly tap the end of the glass. This removes all loose debris and does not leave any adhesive residue as some other tapes do. The use of tape is a simple technique to assure clean ends and offers a good alternative in the field.

Outdoor Splicing Analysis

Testing was done in an outdoor environment to emulate conditions which might be found during actual field repair. An attempt was made to

splice one fiber of a five fiber ITT tight packed design cable using a loose tube splice.

A large loop of the cable was laid out on a hillside for this test. The weather conditions were: clear with scattered clouds; temperature, -2°C, winds N-NW 15 MPH gusting to 23 MPH; wind chill factor -15°C to -21°C. Timing of the splice operation began when the cable was cut. Leather gloves (not mittens) were worn by the operator during the entire exercise. The tight packed cable construction presented a problem in fiber breakout. This problem seemed to be augumented by the surroundings. No work surface was provided as might be the case in a tactical environment and the operator sat on the ground. The breakout of one fiber of sufficient length was terribly difficult at best. Figure 2 shows that the other fibers in the cable were severely damaged in the exposure process. In all, it took a total of approximately 80 minutes to break out roughly four inches of the desired fiber on each cable end. It should be noted that the cable used was an older ITT cable design. Newer cables appear to require somewhat less breakout time as shown at Fort Gordon. This was due to a larger buffer diameter.



Figure 2 - Fiber Damage During Outdoor Breakout

Once the fibers were broken out they were stripped and cleaved. The epoxy used in the splice was mixed and the fibers were dipped in it since the lower temperature increased the epoxy's viscosity making capillary action impossible. No problems were encountered when inserting the fibers into the tube, however, once in the tube it was very difficult to manipulate the cables to secure them without either pulling the fibers out of the tube or, as in the majority of the cases, breaking the fibers at the tube end. Several attempts were made to complete the splice but after a total time of 90 minutes the exercise was abandoned.

Although no complete splices were made outdoors, a great deal of information was obtained concerning a field, "in the mud," splice. Even though the working conditions were not ideal they could certainly have been much worse. Rain or blowing sand and dust would make the entire operation uncomfortable at best for the operator. (It should be noted that a 36C MOS cable installer troop was able to complete an outdoor loose tube splice on an updated tight construction 3 fiber cable. This took place at Ft. Gordon, GA under fair weather conditions. The splicing of one fiber took approximately 25-30 minutes.) It was determined that the driving factors in a true field splice are: a) cable design and b) conditions under which the repairer must work. The field splice technique itself is of only secondary importance since the method will tend to be as simple as possible.

It cannot be stressed enough as to the importance of cable design. A tactical field splice is undoubtedly one which would require a minimal amount of time - on the order of 15-20 minutes. If the cable design is such that fiber access is extremely time consuming then a practical "in the mud" splice cannot be expected. This puts a burden on the cable designer to develop an accessible cable while maintaining the specified cable ruggedness. Testing has shown that in an indoor environment a loose tube splice on one fiber of a five fiber cable, made while wearing gloves, requires 45 minutes, 35 of which were breaking out the fibers. Again it must be emphasized that fiber access would mean breakout of all fibers with no damage. Consideration should also be given to a cable design allowing the repair of a single fiber in a multi-fiber cable without having to break the good fiber(s). Figure 3 shows shrapnel damage in which only two out of four fibers were broken.



Figure 3 - Shrapnel Damage To Four Fiber Cable

Another major factor in the development of a field splice is the conditions under which the repairer may be required to work. In many situations the repairer will have to work on the ground without the amenities that might be found in a field shelter. Figure 4 shows damage done to buried cables by a 500 pound aeriel bomb. Some

form of work surface is necessary to support the cable while working with the exposed fiber. Weather conditions will greatly effect the performance of the repairer.

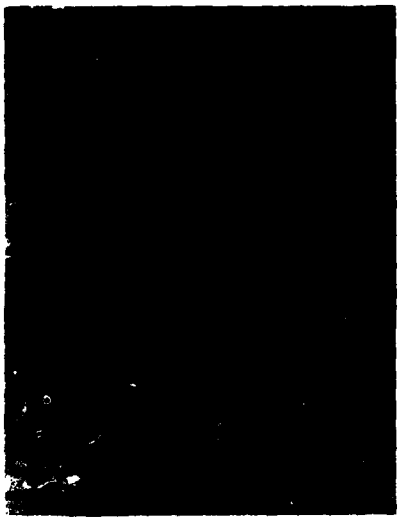


Figure 4 - Cable Damage From 500 lb. Aerial Bomb

Finally, one aspect of the field repair which cannot be overlooked is the psychological effect of open field repair. A situation under which a cable assembly cannot be retrieved is one in which the cable is near or in a forward battle area and is critical to tactical operations. This would mean quick repair, i.e., a field splice, to restore the link as soon as possible. The psychological pressure this situation would create on the repairer would have a definite influence on the repair time and splice quality. The mobile, tactical nature of the system would present the possibility of the repairer finding himself in a active free fire zone which would add to the pressure. As long as the above points are taken into account, field repair is a viable maintenance procedure.

Field Environment Splice Protection

When considering a mobile tactical system, protection of repair points in a cable assembly becomes imperative. The rough handling and wide variation in environmental conditions dictates comprehensive protection.

Except for a fusion splice, most methods offer some basic safeguard from damage. However, this is not sufficient to allow the splice to be permanently exposed. The Japanese have done a great deal of work in analyzing the strength and protection of arc fusion splices.[1] It has been found that the arc fusion process creates stresses within the fiber itself due to rapid cooling from a high temperature. This weakens the fiber resulting in the need for good fiber protection. Definitive results were obtained which indicate that splice reliability is dependent upon the particular sleeve which surrounds the splice. It was shown that metallic sleeves which are filled with epoxy failed repeatedly during temperature excursions. This was due the thermal expansion of both the sleeve and the epoxy. After evaluating several protection schemes it was found that the use of a V-type protector made of polybutylene terephthalate and RTV silicone adhesive provided excellent support and thermal protection.

Other splice techniques are sensitive to environmental conditions due to the very nature of their construction. The metallic V-Groove with epoxy is very susceptible to environmental changes. It is believed that any splice method which uses a resin epoxy and some form of metallic sleeve or groove which covers and comes into intimate contact with the bare glass will experience a higher probability of splice failure due to thermal variations.

After the point to be repaired is found the cable will have to be cut if it is not already severed. Once the cable is cut its designed tensile strength will not be fully recovered. Regaining tensile strength and relieving the tension on the spliced fibers is very important. The splice housing or "boot" must provide this relief by securely clamping the strength members that are within the cable itself. The abuse that a splice boot would have to endure would be greater than that of a connector, since it experiences higher tensile forces during the deployment and retrieval activities. The boot will have to be able to withstand severe mechanical shock without causing splice failure within. (In July of 1980 a test was made at Fort Knox, Kentucky to determine the vulnerability of an ITT tactical splice boot containing two fusion splices and two Thomas & Betts splices. The boot and cable were buried in a trench three meters from a 500 pound aerial bomb. The blast created ground stresses of 1350 psi. Figure 5 shows the resulting failure of the cable). It must, of course, be

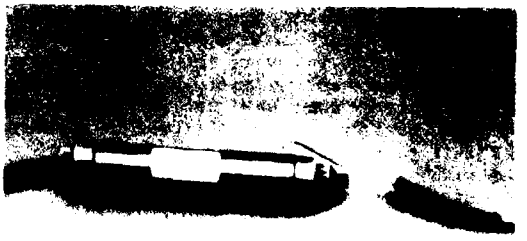


Figure 5 - Stress Damage To ITT Splice Boot

waterproof and have an exterior form which will not snag underbrush and other obstructions while being deployed or retrieved. In addition, the size of the splice boot must be such that it does not interfere with the reeling operation. Ideally the boot should be semiflexible yet should withstand 100 percent of the original cable tensile strength.

Design Impact

The design of the fiber optic transmission system and the development of effective repair procedures for that system must go hand in hand. When considering fiber optics for use under operational conditions, the maintenance of the system under these same conditions must be evaluated.

In the event of component failure the design of the system must allow for quick, efficient repair. A tactical system's cable assembly, as well as the optical repeater, will undoubtedly receive the harshest treatment under normal use. With this in mind, the manufacturer should make provisions for easy cable repair at both direct (in the field) an nondirect (depot or general support) levels. The cable design itself can greatly influence operational maintenance. The construction of a cable which can be spliced in the shortest possible time may result in an assembly not compatible with the rough environment as well as military equipment. At Fort Gordon, GA it was demonstrated that 1 km of the AN/GAC-1 fiber optic cable overfills the existing CX-11230 reels. If any changes were to be made to the cable so it would fit the reel, e.g., a smaller diameter, there could be a direct impact on cable ruggedness and, of equal importance, the ability to quickly splice the cable. Not only does the cable design play an important role, the splice technique itself will drive the system design. The link power budget must take into account splice losses. The system design can be adversely impacted if the total loss of multiple splices can not meet power budget requirements. If ultra-low loss splices are required for all repair situations then repair time and skill level may be influenced.

Conclusions and Recommendations

The preceeding sections have described the consideration which must be given to maintenance procedures when using fiber optics in a tactical environment. As was shown, many parameters must be taken into account when repair to a cable assembly is a requirement of the system's overall design.

Several problem areas were identified with regard to cable handling and preparation. It is felt, however, that these areas can be dealt with effectively. The design of extremely ruggedized, tightly bound cables has attained an outstanding degree of reliability as shown in recent field tests. However, care must be taken to make sure that the cable design itself does not preclude access to the fibers. Loose tube design cables are becoming more and more ruggedized and may offer one or two possible advantages over the tight design. At this time, though, it does not appear that this cable type can meet the ruggedness requirements of a tactical system.

In addition to accessible cable design, specialized yet simple tools must be developed to speed cable preparation. Some hand tools are currently available, however not in a form which can withstand the hostile environments of tactical operations.

It is felt that more work is needed to develop cleaving tools which do not dull after many uses and maintain their alignment. This tool should be expected to be used in both direct and general support environments. Cleaning the fiber after the cleave can be easily accomplished in the general support maintenance shelter using "canned air" or an aerosol solvent and tape. In the field a piece of tape will suffice.

The evaluation of the three splice techniques provided an excellent insight into the applicability of each method to tactical use. The arc fusion splice was found to have the lowest loss and highest repeatability of the three methods compared. This splice uses no other components other than the fibers themselves. Of course splice protection is required. The time to complete one splice was not exceedingly long. For a non-field splice it would be quite acceptable. The most time consuming part of the repair will be cable preparation and post splice protection and packaging. The size of this splice will be determined solely by the type of splice protection used. At this time there appears to be no aging problem. An important point which should be noted about this splice is that reasonably good splices can be made regardless of the condition of the fiber ends. The collection of cumulative distribution functions in Figure 6 shows that a respectable confidence level can be maintained regardless of the prefusion level or the quality of the cleave. This data would indicate that any skill level presently identified in the Army could perform this type of splice, as evidenced at Ft. Gordon. Presently, more work is needed to determine the effects that large temperature excursions have on fusion splices.

The loose tube splice was a good feasibility model used to illustrate a quick, field installable splice. It proved to be simple, with medium loss characteristics and somewhat forgiving with regard to cleave quality. This particular splice demonstrated good temperature stability. After being frozen in ice the splice exhibited its lowest strength. The presence of water around the epoxy at varying temperatures is suspected to cause this effect.

In evaluating the V-Groove it became apparent that there may be some problems when using this splice with non "loose-tube" design cables. None of the splices met the manufacturer's loss figure of 0.25 dB. Many splices failed completely when the outer protective heat shrink sleeve was used. The splices did survive without the sleeve, however this would remove the protection from environmental influences, particularly moisture. As was

IB-59,080

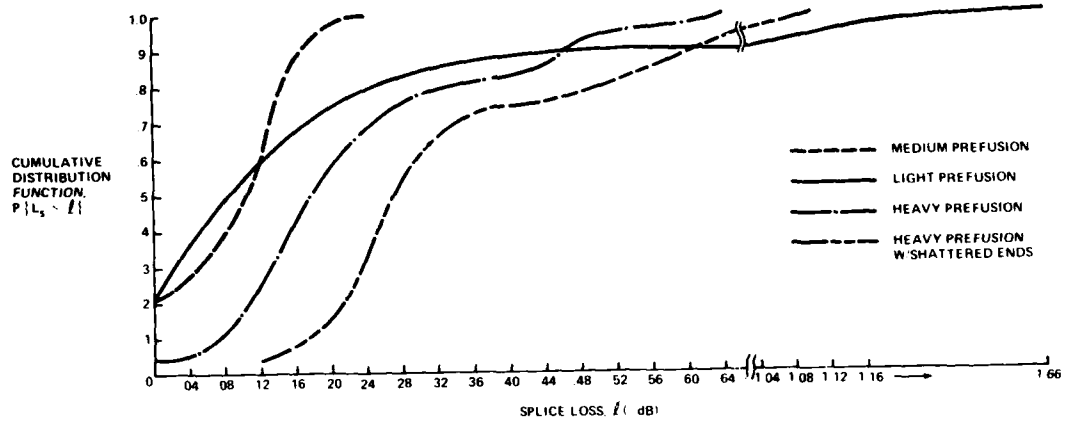



Figure 6 COMPARISON OF ARC FUSION SPLICE CONFIDENCE LEVELS AS A FUNCTION OF FIBER END PREPARATION

seen with the loose tube splice, water may have a deleterious effect on the epoxy. Completion of the splice takes approximately as long as a fusion splice, 10-11 minutes. This splice, proved to be the strongest of the three tested. The splice was relatively small, however, it may have problems fitting properly into a splice boot small enough to fit on a cable reel. The skill level required for this splice is appropriate for use by unskilled personnel, as shown at Ft. Monmouth. All the splices which were subjected to wide temperature variations failed at low temperatures (-35°C).

From the outdoor splicing analysis, though not successful in some aspects, it has been shown that it is possible to repair optical cable in the field. Two factors are identified in this evaluation which impact outdoor repair. They are cable design and working conditions. The cable design will have to allow access to the fibers. The splice itself is not as important as long as it can withstand the environmental conditions. Field conditions will have a great effect on the time to repair as well as the quality of the work. In addition, a psychological factor must be considered when such close-in and delicate work may have to be done under a great deal of pressure.

The effects that environmental conditions will have on a splice will vary with the splice technique used. With the exception of the V-Groove splice, there was no permanent damage to the splices. It should be noted, however, that these tests did not examine splice strength at various temperatures.

The design of a practical splice protection housing must take into account several points. First, if the splice method does not provide any protection of the glass (fusion splice) the housing will have to do so or a separate splice cover will have to be provided. If so, close attention must be paid to the choice of materials. The boot will have to provide positive strain relief allowing for no slippage. Resistance to shock and water intrusion must also be provided. Also, the size and shape must allow for easy deployment and retrieval.

Given the above insight into the requirements for the repair of tactical optical cable plants, the following recommendations are made. Due to the unavailability of an ultra-low loss splice which is extremely simple, rugged and quick, two levels of repair are considered most appropriate. The first is a permanent repair in which a fusion splice is used to provide a low loss splice. Loss figures for this type of repair should be below -0.5 dB. This repair should be conducted in a shelter or some other form of cover. Assuming the use of a two fiber cable, the repair time, including fiber breakout and protection of the bare splice, should be less than fifty minutes. Packaging the completed splice in a ruggedized splice boot, including complete strain relief, should take no more than another 25 minutes. A second level of repair is one in which the cable must be repaired "in the mud." This repair should be specified as a temporary or field expedient splice. It should be temporary in nature providing a loss figure of less than -1.0 dB. A small splice kit should be provided containing all necessary tools, a large number of splices and sufficient materials to afford the splice some environmental protection until such time that cable can be retrieved and a permanent repair made (~72 hours). The repair time should total less than 20 minutes. This time may be doubled if a section of cable is to be spliced into the cable as a patch. Figures 7 and 8 show the type of tensile stress damage which might necessitate a cable patch. The actual splice technique itself cannot be identified since a number of mechanical splices will meet these requirements. Obviously, the simpler the splice the better.



Figure 7 - Results of Cable Jacket Bursting Under High Tensile Stress



Figure 8 - Effects of High Tensile Stress on Buffered Fibers

All future cables to be used in tactical operations must be designed to allow rapid access to the fibers. Special hand tools should be developed for particular use in a hostile field environment. Taking into account all the points presented above the repair of fiber optic cable in a tactical environment is entirely possible and has been demonstrated.

Acknowledgements

The work reported above was done under the sponsorship of the U.S. Army, Communications Research and Development Command, Fort Monmouth, New Jersey.

References

1. Arai, T., et. al., "Protection and Reliability of Optical Fiber Arc Fusion Splicing," Proceedings of the 28th International Wire and Cable Symposium, pp. 344-51, November 13-15, 1979.



Scott F. Large
Member of the Technical Staff
The MITRE Corporation
M/S E190
P.O. Box 208
Bedford, Massachusetts 01730

Mr. Large received his Bachelor of Science in Engineering in Electrical Engineering in 1979 from the University of Central Florida, Orlando, Florida. As an undergraduate he spent two years working for NASA in fiber optic implementation at Kennedy Space Center, FL. He is currently responsible for the maintenance concept development for the U.S. Army's Long Haul Fiber Optic System.

# A MILITARY SIX FIBER HERMAPHRODITIC CONNECTOR

John G. Woods, Malcolm H. Hodge and James F. Ryley, Jr.

TRW Research & Development Laboratories, Philadelphia, Pa.

## SUMMARY

A six channel hermaphroditic connector which will function with 125μ to 150μ diameter optical fiber has been designed, constructed and tested. Discussions will touch upon the principal aspects of basic design, including the incorporation of the TRW Cinch Optalign fiber alignment "Double Elbow" guide concept. The rapid and simple connector assembly procedures are described, along with a unique fiber scribe-and-break tool which was designed specifically for use with this connector. Means for connecting either Siecor or ITT six fiber cable were developed. The results of mating durability, vibration and thermal shock tests are discussed in the context of the <1 dB insertion loss target. Optical connection problems generated by a "military" environment are also discussed. Both the problems which are overcome by the TRW design and those seen as requiring further development will be addressed.

## INTRODUCTION

The U.S. Army requires connectors for multiple optical fiber cables for use in communications between tactical units in the field. To assure interchangeability and minimum logistical problems with parts, it is desirable that the connectors be hermaphroditic.

A contract was made with TRW entitled "Optical Fiber Communications Cable Connector", number DAAK80-79-C-0772. The work was perfomed under the auspices of the U.S. Army Communications Research and Development Command (CORADCOM), Fort Monmouth, New Jersey.

The primary requirements for the connector are:

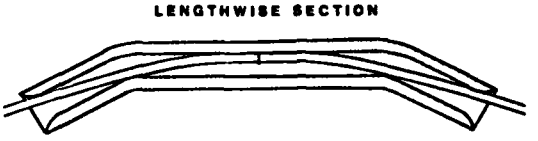
1. Ease of assembly.
2. Hermaphrodicity
3. Less than 1.0 dB insertion loss.
4. Vibration, MIL-STD-202E, Method 204C, Condition A (.06 in. amplitude, 10 to 500 Hz).
5. Thermal shock, MIL-STD-202E, Method 107D, Condition A (-55°C, 25°C, 85°C, 25°C).
6. Mating durability: 1000 cycles. Free running coupling nut torque, <12 in. oz.

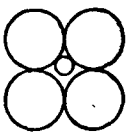
The test data reported in this paper were obtained in tests of the first prototype connector for Siecor six fiber cable[1]. Additional sample connectors are being built for the same tests, and delivery to the Army, using ITT six fiber cable. Table 1 shows the specifications for the

TABLE 1

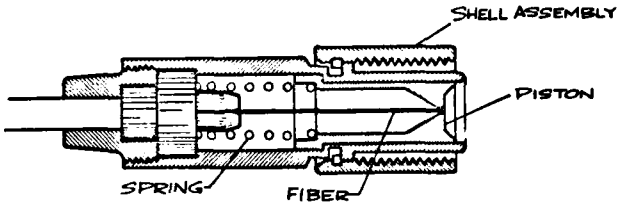
OPTICAL FIBER SPECIFICATIONS

| | Siecor | ITT |
|---|---|---|
| Core diameter (μm) | 63 | 50 |
| Glass outer diameter (μm) | 125 | 125 |
| Numerical Aperture (N.A.) | 0.21 | 0.23-0.28 |

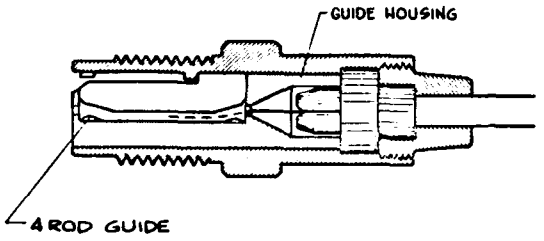



FIBER ALIGNMENT GUIDE
FIGURE 1




PLUG ASSEMBLY




RECEPTACLE ASSEMBLY

FIGURE 2

fibers used in the Siecor and ITT cables.

The basic principle of the connector is to obtain fiber alignment with the TRW patented glass fiber optic connector guide. This approach is currently used in a four rod, double elbow, glass guide for the TRW/Cinch Optalign (R) single fiber connector. The scheme for the six fiber connector is to use six sets of the internal parts of the Optalign connector in a circular array. To provide hermaphrodicity, there are three plugs and three receptacles in each connector half.

## THE ALIGNMENT GUIDE

The four rod glass alignment guide can be described as a ferrule/v-groove device, which provides a loose fitting channel to guide the fibers into an alignment v-groove. Figure 1 is a schematic diagram showing the principle of the fiber alignment guide. The two fibers are fed into the ends of the guide, and forced toward the top cusp by the double elbow configuration. The geometry of the guide is such that normal tolerances of molded or machined parts achieve sufficient location accuracy of the fiber ends to prevent angular or gap losses in the fiber connection. A mathematical description of the dimensional factors of the alignment guide was presented in a previous paper[2].

## THE SINGLE FIBER CONNECTOR

A single fiber connector incorporating the four rod alignment guide is manufactured by TRW/Cinch Connectors Division. A sectional view of this Optalign (R) connector is shown in Figure 2. The guide is enclosed in an injection molded plastic housing which is retained in the aluminum receptacle shell by the molded fiber clamp and aluminum retaining nut. The plug assembly contains a plastic piston, which slides in the aluminum shell, and is spring loaded to protect the fiber end until the guide housing pushes it back as the connector is mated. Upon mating of the connector, the fiber in the plug enters the end of the four rod guide. As the coupling nut is rotated to pull the two shell halves together, the fiber moves through the guide channel and is forced along the same v-groove, or cusp, in which the receptacle fiber end lies. The two fiber ends meet near the center of the four rod guide. To assure physical contact of the fiber ends, an overtravel of .001 to .020 in. is allowed. The overtravel range is minimized by proper dimensioning and holding the tolerances to locating shoulders in each of the shells to control the distance between the faces of the fiber clamps. The fibers are also pre-cut to dimensions measured from the fiber clamp faces, assuring minimal tolerance build-up.

The Optalign (R) connector provides a simple connection system utilizing an easy scribe/break fiber preparation process. The readily assembled connector gives repeatable results through the use of the four rod fiber guide. These factors led us to design the six fiber connector using the internal parts of the Optalign connector.

## DESCRIPTION OF THE SIX FIBER CONNECTOR

The design for the six fiber connector prototype is shown in cutaway view in Figure 3. Each connector half contains three guide housings, or slugs, and three spring loaded pistons. The slugs are located in one half of a circular array, and the pistons in the other half.

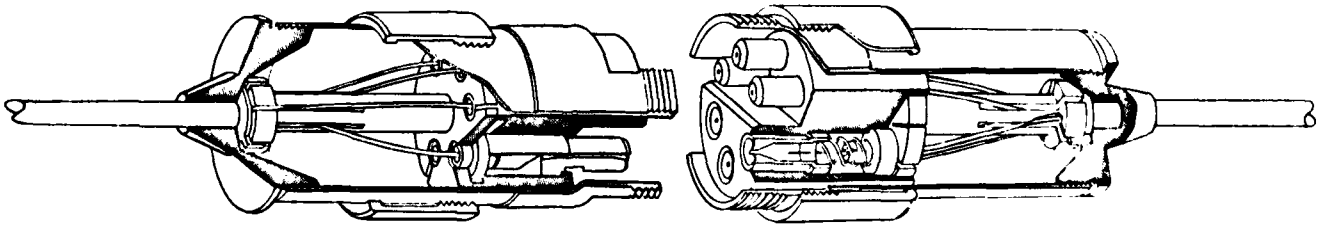


FIGURE 3

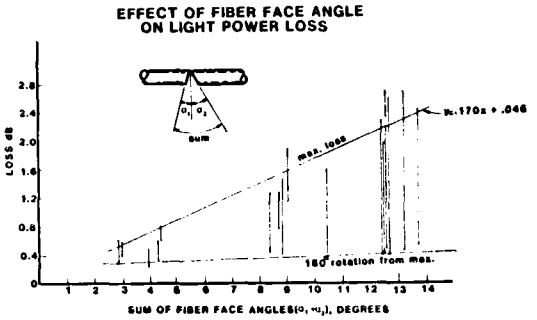



FIGURE 4

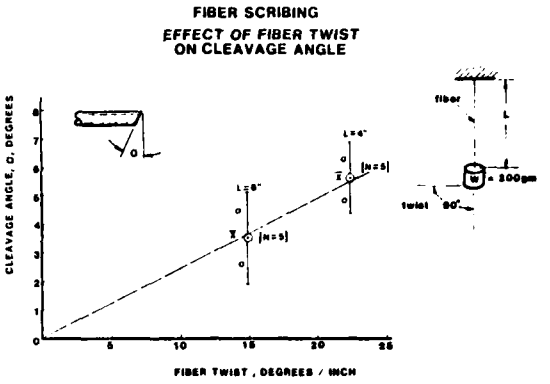


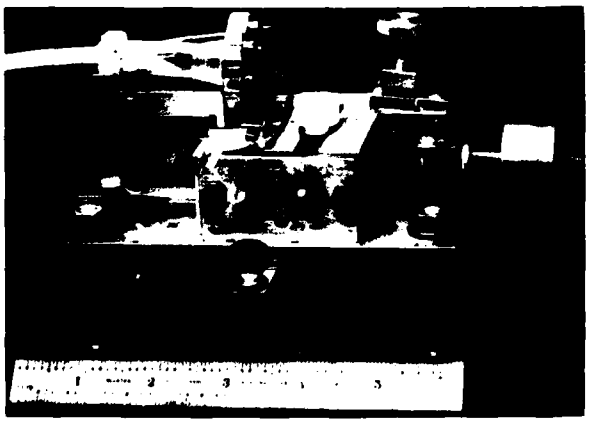

FIGURE 5

Both connector halves are identical in design. Each shell has a coupling nut to engage the three interdigitated threaded segments of the mating shell. The block holding the pistons and slugs is stepped to key with the identical block in the mating connector half.

In this prototype, the cable is retained by an internally threaded plastic nut, which is twisted on to the outer cable jacket. The six stripped optical fibers are fed through the fiber clamps spaced around a plastic clamp holder. The clamp holder and assembled clamps provide the means for retaining the individual fibers for accurately scribing and breaking each fiber prior to insertion into the separate fiber guides and pistons. After cleaving the fibers, the clamp holder is snapped into the slug/piston block. The entire internal assembly, from the rear cover and cable clamp to the slug/piston/block assembly, is then inserted in the shell/coupling ring assembly and the rear cover is screwed into the shell.

## FIBER SCRIBING AND CLEAVING

The alignment guide provides nearly perfect axial alignment of the fiber ends. Loss levels will depend on how closely the fiber ends can be made to the ideal of optically flat surfaces, perpendicular to the axis of the fibers. We have been able to obtain low losses with a scribe and break procedure, by controlling the tension and torsion forces while the fiber cleavage occurs.



SCRIBING MACHINE
Figure 6

Figure 4 shows experimental data obtained with 125μ silica fibers. Loss, in dB, is plotted against the sum of the fiber face angles. Two readings were taken with each pair of fibers; one fiber being rotated until maximum loss was obtained, and then turned 180°, and the loss calculated again. A straight line approximation for the maximum loss was found by the linear regression method:

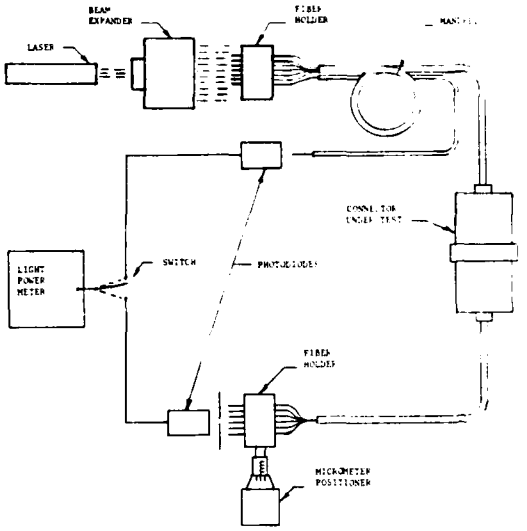
$$\text{dB loss} = .170\ (\alpha_1 + \alpha_2) + .045$$

The coefficient of determination is 0.9, indicating a reasonably good fit of the above equation to the experimental data.

It can be seen from Figure 4 that the sum of the fiber face angles should be less than 4°, to be sure that dB loss will be less than 1.0. Variable results were obtained with our initial scribing attempts. During our investigations, we found that small torsion angles applied to the fiber during scribing caused angular cleavage of the fiber.

An experiment was performed to measure the effect of fiber twist on cleavage angle. A 200 gm weight was suspended by a fiber of 4 inch or 6 inch length. A twist angle of 90° was imparted to the fiber. The fiber was scribed with a tungsten carbide knife edge. The results of fiber face cleavage angle vs. twist angle, in degrees per inch are plotted in Figure 5. The average cleavage angle of 3.5° for a 15°/in. twist is in close agreement with some of the data reported by Saunders[3].

A machine built for scribing the six fibers, after assembly to the fiber clamp holder, was modified to reduce the twist angle during cleavage to near zero. A photograph of the modified prototype scribing machine is shown in Figure 6.




INSERTION LOSS TEST SET-UP
FIGURE 7

Control of the fiber twist angle, and an applied tension force of 185 gm to the fiber, caused average cleavage angles of $0.5^{o}$ to $0.6^{o}$. As a result, losses generally less than 1.0 dB are consistently obtained with fibers connected in the six fiber connector.

## CONNECTOR PERFORMANCE

### INSERTION LOSS MEASUREMENTS

The connector prototype has been tested for insertion loss, using the test setup in Figure 7. A helium-neon laser ($\lambda$=632.8 nm) was used as the light source. The scribed and cleaved fiber ends of the six fiber cable were rigidly retained in a holder within the expanded laser beam. A seventh fiber was also located in the beam to furnish the means for monitoring variations in laser output.

Both the six fiber and the single fiber monitoring cable were wound around a 1 inch diameter mandrel to provide mode mixing, and removal of the light traveling in the fiber cladding. The six fiber cable was joined in the test connector beyond the mode mixer. Following the connector the six prepared fiber ends were positioned in a holder mounted on a precision micrometer-adjusted stage. The stage can be positioned to locate each fiber end, in turn, in front of a slit, behind which is a photodiode. The monitoring fiber was positioned in front of a similar diode. The outputs of the two diodes can be compared on the same light power meter, by switching from one diode to the other.

The insertion loss is the light power loss due to introduction of the connector in the cable. In our tests, we measured the power transmitted by the cable, then cut it in the middle, and assembled it with the connector, as described above. The light output was again measured.

TABLE 2

INSERTION LOSS EXCURSION, dB - VIBRATION TEST

FIBER NO.

| FIBER NO. | $F_1$ | $F_2$ | $F_3$ | $F_4$ | $F_5$ | $F_6$ | $\bar{X}$ | $\sigma$ |
|---|---|---|---|---|---|---|---|---|
| X axis | .37 | .31 | .20 | .19 | .16 | .11 | .22 | .10 |
| Y axis | .30 | .18 | .19 | .07 | .07 | .05 | .14 | .10 |
| Z axis | .08 | .14 | .23 | .12 | .09 | .05 | .12 | .06 |
| | | | | All Readings | | | .16 | .09 |

Insertion loss is expressed in decibels, calculated as follows:

$$\text{dB loss} = 10 \log_{10} \frac{\text{light power without connector}}{\text{light power with connector}}$$

When meter readings are made of light power through the six fiber cable, a correction is made, based upon the reading obtained with the laser monitoring fiber.

It was found that the initial readings taken through the cable, without the connector, varied with time up to the equivalent of $\pm$0.5 dB, compared with the laser monitoring fiber. Because of this, some readings indicated that negative losses occurred, due to the low loss levels, and the cyclic variations in cable: monitor ratio. The variations could be caused, at least in part, by mode shifts in the expanded laser beam. After the connector was introduced into the cable, six sets of output readings were made on each of the six fibers, to

TABLE 3

INSERTION LOSS (dB) BEFORE AND AFTER VIBRATION

36 CYCLES, 10 Hz - 500 Hz

| Fiber No. | Initial 6 Readings Each Fiber | | Final |
|---|---|---|---|
| | $\bar{X}$ | $\sigma$ | |
| 1. | 1.02 | 0.17 | 1.13 |
| 2. | 0.05 | 0.26 | 0.40 |
| 3. | 0.33 | 0.36 | 0.74 |
| 4. | 0.76 | 0.15 | 0.80 |
| 5. | 0.93 | 0.13 | 0.83 |
| 6. | 0.20 | 0.05 | 0.26 |
| $\bar{X}$ | .55 | | .67 |
| $\sigma$ | .41 | | .28 |

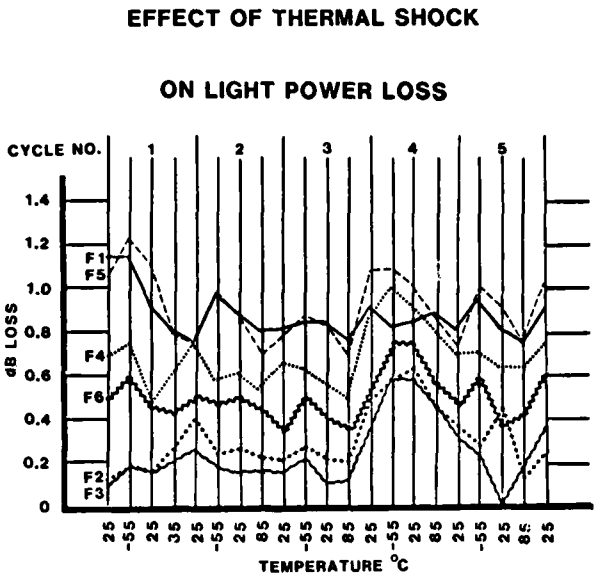



FIGURE 8

obtain averages and to minimize the effects of variations in power output ratio with time. The calculated mean values of six readings on each of the six fibers ranged from 0.05 to 1.02 dB insertion loss. The 36 measurements, taken together have mean ($\bar{X}$) and standard deviation ($\sigma$) values as follows:

| | No Readings | $\bar{X}$ | $\sigma$ |
|---|---|---|---|
| Fibers #1 through #6 | 36 | 0.55 | 0.41 |

This loss level, of 0.55 dB, is considered to be excellent for connection of dry, scribed and cleaved fibers.

VIBRATION TEST

The MIL-STD-202E, method 204C, Condition A test specifies that the component under test be subjected to 12 complete cycles of 10 Hz to 500 Hz in each of three mutually perpendicular planes. Calculations indicated that the fiber alignment guide configuration prevents the fiber ends from moving away from the cusp. Also, no fiber resonance occurs within the 10 Hz to 500 Hz frequency range.

An actual test of the connector prototype was conducted to the MIL specification. Each

TABLE 4

INSERTION LOSS EXCURSION, dB

REPEATED MATINGS, 1000 CYCLES

| $F_1$ | $F_2$ | $F_3$ | $F_4$ | $F_5$ | $F_6$ | $\bar{X}$ | $\sigma$ |
|---|---|---|---|---|---|---|---|
| 0.69 | 0.45 | 0.54 | 0.22 | 0.63 | 0.35 | 0.48 | 0.18 |

TABLE 5

INSERTION LOSS (dB) BEFORE AND AFTER

1000 MATING CYCLES

| FIBER NO. | INITIAL | 10 CYCLES | 600 CYCLES | 1000 CYCLES |
|---|---|---|---|---|
| 1. | 0.64 | 0.58 | 0.12 | 0.53 |
| 2. | -0.06 | -0.35 | -0.43 | -0.29 |
| 3. | -0.15 | -0.28 | -0.06 | 0.18 |
| 4. | 0.62 | 0.57 | 0.64 | 0.79 |
| 5. | 0.86 | 0.83 | 1.31 | 1.33 |
| 6. | -0.05 | -0.33 | -0.16 | -0.01 |
| $\bar{X}$ | 0.31 | 0.17 | 0.23 | 0.42 |
| $\sigma$ | 0.44 | 0.55 | 0.64 | 0.59 |

fiber was monitored for one complete cycle in each of the three directions. No significant losses of light transmission were observed. During the monitored vibration cycles, the maximum excursion (max. minus min.) of insertion loss averaged 0.16 dB for all six fibers (Table 2). The initial and final insertion loss measurements are shown in Table 3. The apparent changes in insertion losses during vibration are similar in magnitude to predicted variations in a stable environment, based on the deviations observed in the initial measurements.

It is concluded that the vibration test has no adverse effects on the light conduction and caused no damage to the mechanical integrity of the connector.

THERMAL SHOCK

The thermal shock test of MIL-STD-202E, Method 107D, Test Condition A was conducted on the connector. Five temperature cycles of -55°C (one hour), 25°C (five minutes, maximum ), 85°C (one hour), and 25°C (five minutes, maximum) were performed.

There was no mechanical damage to the connector. The insertion loss was monitored throughout the test, six readings taken for each channel during the one hour dwell at each of the extreme temperatures. The average losses at each temperature level for each fiber, through five cycles, are shown in Figure 8. The maximum levels barely exceeded 1.0 dB at any time. Apparent variations in dB loss are small and are probably related to the laser beam mode shifts, rather than temperature.

There were no discontinuities or other adverse effects noted during the thermal shock test; any differential expansion problems are overcome by the axial force applied to the connected fiber ends, through the overtravel-created fiber spring.

CONNECTOR MATING DURABILITY

The connector was subjected to 1000 matings to test the effects of repeated insertions and contact of the fibers in the guides. Light measurements were made, and insertion losses calculated, after

each cycle for the first 10 cycles, at 25, 50 and 100 cycles, and after each 100 cycles up to 1000. The maximum excursions of insertion losses for each of the six channels are shown in Table 4. Calculated insertion losses before and after the 1000 cycles are shown in Table 5.

The data show that repeated making and breaking of contact between the fiber faces causes no appreciable degradation of the insertion losses.

The effects of 1000 matings of the coupling rings were determined by complete mating, and unmating, of the assembled connector for 1000 cycles. Damage to the threads was minimal and free-running torque of the coupling rings was less than 1.0 inch-ounce before and after the test, well below the required 12 in.-oz. maximum.

## CONNECTOR DESIGN IMPROVEMENTS

After assembly and test of the first prototype, the design of the six fiber connector was re-evaluated considering the following factors:

- Ease of fiber preparation and connector assembly.
- Test results.
- Adaptability to ITT cable.
- Military environmental considerations.

Our analyses indicated that the basic design concepts were sound. The preparation of Siecor fiber, using the scribing and cleaving concepts as described, were fast and provided low loss connections. The use of the four rod glass alignment guides, as well as the slugs and pistons of the Optalign single fiber connector, affords a system which is easy to assemble and performs admirably in the required tests.

It was felt that the connector system should be adaptable to more than one type of cable. The procedures and parts design worked well with Siecor cable, which has a lacquer coat and a plastic protective jacket over each fiber. Another cable designed for military applications is the ITT version, which has a silicone RTV layer with a plastic outer jacket over each fiber. A modification to the original contract provides for the development of procedures to strip both the silicone and plastic jackets, and immediately apply an optical lacquer to prevent degradation of fiber strength. It is necessary to remove only 0.3" of the silicone from the cleaved fiber end, in order that the fiber will enter the alignment guide. These procedures are currently under development and the new connector design has been modified, dimensionally, to accept ITT cable.

Further consideration of the military field environment has indicated areas for improvement in connector design. Even though the tests of the first prototype divulged no deficiencies, it is felt that the mated connector should have protection to prevent entry of water, especially into the alignment guides. Subsequent freezing of moisture in the guides could, conceivably, cause signal degradation. The next generation of samples, now being constructed, has neoprene rubber seals at all points where moisture could enter the coupled connector.

Another environmental factor not simulated in the original tests involves the physical effects of dragging the cable and connector through underbrush, around obstructions, etc. Provisions have been made in the new connectors to retain the cable's Kevlar strength members with a threaded aluminum nut. Additional strength and bending strain relief is provided by a mesh cable grip slipped over the cable, and extending through the opening in the rear cover. The rear cover is chamfered to help prevent snagging of the connector on obstructions when dragged over the ground. Preliminary tests show that connector pull strength will exceed 80 lb, using the improved retention design.

The design improvements will provide connectors with improved moisture and dirt resistance of the mated connector, as well as greater strength. It is recognized that the effects of the field environment on unmated connector halves have not been addressed. We are currently developing methods to seal uncoupled connectors, and we expect to report on this work in the near future.

## CONCLUSIONS

A six channel hermaphroditic connector has been designed, constructed and tested successfully to meet the basic requirements for a first generation military connector. Design improvements incorporated in the final version for delivery to the Army include improved sealing of the mated connector, as well as greater pull strength and compatibility with at least two commonly used cables.

Future work will include development of methods for excluding dirt and moisture from unmated connector halves.

## ACKNOWLEDGEMENTS

The authors wish to thank the U.S. Army CORADCOM for funding this contract, as well as for their coordination and encouragement of the work on the six fiber connector.

We also wish to acknowledge the connector design work which was done by Edwin Rowlands, Mark Margolin, Robert Lumpp and Lynn Michal of TRW/Cinch Connectors Division.

## REFERENCES

1. Woods, John G., Hodge, Malcolm H., Ryley, James F., Jr., "A Military Six Fiber Hermaphroditic Connector", Fiber Optic Conference, 1980.

REFERENCES (Continued)

2. Hodge, Malcolm H., "A Low Loss Single Fiber Connector Alignment Guide", Fiber Optic Conference, 1978, Proceedings, pp. 111-115.

3. Saunders, M.J., "Torsion Effects on Fractured Fiber Ends", Applied Optics, Vol. 18, No. 10, 15 May 1979.



Malcolm H. Hodge joined TRW at the Eastern Research Laboratories in 1973. He is Manager, Electro-Optics Department of the R&D Labs. He has been engaged in thick film resistor materials and connector research and, most recently directs R&D activities for fiber optic components. Prior to joining TRW, Dr. Hodge worked at the Advanced Reactor Division of Westinghouse Electric Corp. at Westinghouse, he was involved in government funded activities in the fabrication and evaluation of (U,Pu)C and (U,Pu)$O_2$ breeder reactor fuel. Dr. Hodge has fourteen patents and patent applications and has published numerous technical papers.

Education:

B.S. in Ceramic Science, University of Leeds. Ph.D. in Ceramic Science, Penna. State University.



John G. Woods has contributed to TRW/IRC product development activities since 1954. He is currently a Senior Project Engineer. Mr. Woods has been involved with the development of resistor products, potentiometers and small electric motors. Most recently, he has managed government contract activity concerned with fiber optic connectors and optical sensors. Prior to joining IRC, Mr. Woods was a Sr. Engineer with Philco Corporation, and was a Test Engineer with the Babcock and Wilcox Co., R&D Division. He holds six patents and has written several papers and articles. Professional activities include holding several offices at Chapter, State and National levels of NSPE. Mr. Woods is also a member of ASME, IEEE, ISHM, Electronic Connector Study Group, American Society of Inventors, The Franklin Institute and the Cornell Society of Engineers. He is a Registered Professional Engineer in Pennsylvania.

Education:

Bachelor of Mechanical Engineering - Cornell University. MS in Mechanical Engineering - Drexel University.



James F. Ryley, Jr. has worked at TRW, Eastern Research Laboratories since 1978. He is currently a Senior Research Scientist. Mr. Ryley has been involved in research on switched mode power supply systems, and for nearly two years in research on fiber optic components. Before joining TRW, he was employed by Teledyne Energy Systems where his research included systems analysis and modelling of radioisotope thermoelectric generators for space vehicles and oxygen generators for nuclear submarines. Mr. Ryley has one patent and has published several technical papers. He is a member of AIP-IEEE.

Education:

B.S. in Physics, John Carroll University. MS in Physics, The Johns Hopkins University.

The authors' address is:
TRW Research and Development Labs.
401 N. Broad Street
Philadelphia, Penna. 19108

# INDEXING METHOD FOR CABLE CLASSIFICATION USING THE FM LABORATORY-SCALE COMBUSTIBILITY APPARATUS

J. L. Lee, A. Tewarson, R. F. Pion

Factory Mutual Research Corporation
Norwood, Massachusetts 02062

## ABSTRACT

Fire hazards from electrical cables have been of great concern for many years. An economical and realistic test method is needed for cable classification. At Factory Mutual, a laboratory-scale combustibility apparatus has been developed, in which a range of full-scale fire conditions can be simulated. Moreover, the measurements taken can be expressed in terms of the following indices: ignition/flame spread index ($I_1$); material consumption rate index ($I_m$); heat release rate index ($I_q$); product generation rate index ($I_p$); and light-obscuration index ($I_o$). These indices are determined in such a way that they tend to become independent of external parameters such as external heat flux, ventilation rate (in the overventilated environment), and cable size. The method is a useful tool to classify cable combustibility characteristics in a generalized and realistic fashion. These indices can be used as a base for predicting full-scale fire behavior and for the determination of the fire detection and fire protection requirements.

## I INTRODUCTION

Electric cables play an important role in human society. In facilities such as industrial plants, power generating stations, and transportation subway stations, where electricity is the primary source of power for maintaining equipment operation, cables are used extensively. The cables are mostly insulated with synthetic polymers such as polyethylene, polyvinyl chloride, ethylene-propylene rubber, and silicone. Within these polymers are added various chemical compounds such as fire retardants, plasticizers, antioxidants, colorants, vulcanizers, and smoke suppressants.[1] In fires, cables with and without additives under certain conditions may present a hazard in terms of the release of heat, generation of toxic compounds, optical obscuration, suffocation by oxygen depletion, corrosion, and electrical integrity failure. Some losses from cable fires have been reported in the literature.[2]

In order to optimize the cable selection process for a facility and to improve the design of fire detection and protection systems, the fire behavior of the cables should be examined and identified realistically, preferably by tests which are repeatable and for which data are quantified.

Recognizing that the full-scale fire tests are expensive to operate and results cannot be readily extrapolated to conditions other than those tested, it is desirable to develop a simplified laboratory-scale technique that can assess and predict the fire behaviors of electric cables under real world situations in a cost-effective manner.

## II APPARATUS

In fire research, it has been well recognized that full-scale fires are dominated by the radiation heat transfer process. At Factory Mutual Research Corporation (FMRC) a Laboratory-Scale Combustibility Apparatus[3,4] has been developed for the evaluation of the fire properties of materials by taking into account realistic fire conditions including flame radiation. The fire properties evaluated include fuel consumption rate, product generation rates ($CO_2$, CO, total hydrocarbons as $CH_4$, $NO_x$, HCl, HCN and Smoke), oxygen depletion rate, and optical transmission through products. All these properties are measured from within the same apparatus simultaneously. With minor modifications, the electrical integrity failure of cables can also be assessed. Figure 1 is a diagram of the apparatus with its various components.

In the apparatus, a cable specimen is placed on the sample platform located above a load cell assembly which monitors the weight loss of the sample continuously. Air is supplied from the bottom of the apparatus. Just above and around the sample are four coaxially arranged radiant heaters providing the sample with external radiant heat flux of up to 70 kW/m$^2$. The heaters are used to simulate the radiation from external fire sources. Between the heaters and the sample is a quartz tube confining to an upward direction the gaseous products generated in the test, yet allowing the heat flux to reach the sample. A small pilot flame (~.01 m long) is provided at about 0.01 m above the sample surface. The products are captured with ambient air in the sampling duct and measurements are made of the mass and volumetric flow rates; gas temperature; optical transmission through products; and concentration of CO, $CO_2$, $O_2$, HCl, HCN, $NO_x$, total gaseous hydrocarbons such as $CH_4$, and smoke. All the instrumentation is put on line to a minicomputer for data acquisition and analysis.

## III INDEXING METHOD

At Factory Mutual Research Corporation (FMRC), an indexing method[5] has been developed for the classification of electric cables based on their combustibility behavior. These indices are expected to be useful in 1) evaluation of the relative fire hazard of cable materials, 2) analysis and extrapolation of full-scale test data, and 3) providing input data for the design of protection and detection systems.

### 3.1 INDICES DEVELOPED FOR THE CABLES

3.1.1 Ignition And Flame Spread Index ($I_f$) - In the Laboratory-Scale Combustibility Apparatus, the time to ignition of cable samples is measured as a function of various known values of external heat flux. From the relationship of the time to ignition with external heat flux, $I_f$ is derived, and is defined as the total energy required for the sustained ignition of a material vapor/air mixture. $I_f$ is equal to the product of time to ignition and net heat flux absorbed by the material, i.e., the anount of energy absorbed for ignition per unit surface area of the material. The lower the $I_f$ value, the faster is the ignition and flame spread expected in the cable under a given fire environment.

3.1.2 Material Consumption Rate Index ($I_m$) - The rate of material consumed determines the generation rate of heat, products and smoke and is itself dependent on the heat of gasification property of the material. The material consumption rate index, $I_m$, is derived by measuring the mass loss rate of the cable sample under various known values of external heat flux in a 100% nitrogen environment. This index is defined as the amount of material consumed per unit amount of energy absorbed by the material. The higher the $I_m$, the easier it is for the material to vaporize.

3.1.3 Heat Release Rate Index ($I_h$) - The heat release rate index is a nondimensional parameter and is defined as the ratio of heat produced in a fire to heat absorbed by the cable material. It is obtained by measuring the heat release rate under various external heat flux environments. Under the same fire exposure, the cable with a higher $I_h$ has a greater potential in releasing heat than one which has a lower $I_h$.

3.1.4 Product Generation Rate Index ($I_p$) - This index defines the tendency of a cable in generating the individual gaseous species such as $CO_2$, CO, $NO_x$, HCl and HCN. It is defined as the amount of the product produced per unit amount of energy absorbed by the material and is derived by measuring the actual generation rates of the various species under various external heat flux environments. The larger the value of $I_p$, the greater is the potential for the generation of the particular species.

3.1.5 Light Obscuration Index ($I_o$) - The generation of smoke from a cable under flaming and nonflaming fires is characterized by the light obscuration index ($I_o$). This index is defined as the light obscuration per unit mass of material vaporized per unit volume of the product-air mixture, where light obscuration is the conventional definition used in the fire protection field, i.e., optical density of "smoke" per unit path length. $I_o$ can also be defined as the area of light obscuration by "smoke" produced from a unit mass of the vapors of materials.

## IV EXPERIMENTAL RESULTS

Table I shows a comparison of the various material indices computed from the measured data for four different generic type cables. These four cables may not be representative of their particular generic group because of variations in construction type, size and number of conductors, thickness of insulation, and amount of additives such as retardants, plasticizers, etc. Therefore, the results presented in the table are not to be taken as an absolute measure of the combustibility behavior of the individual generic type of insulation material. The cables shown in Table I were tested in the Laboratory-Scale Combustibility Apparatus in flaming fire conditions under various known values of external heat flux exposure and an overventilated environment.

From these results one can see the hazard potential among the four cables in terms of ignition/flame spread, fuel consumption rate, heat release rate, product generation rate (products of incomplete combustion) and light obscuration by-products. Moreover, the table also indicates that a cable having the highest index in one aspect of combustibility behavior does not necessarily imply the same rating in other aspects. The PE/PVC cable having the greatest potential for ignition/flame spread has a low index in fuel consumption rate and product generation rate. The reverse situation is true for the EPR/hypalon cable. Hence, one can realize that it is difficult to assign a single number to classify the cables according to their overall performance; rather, each individual combustibility behavior needs to be considered independently for the cable selection depending on the individual situation. In addition, if it is possible to estimate, a priori, the heat flux exposure that a cable system may be expected to receive, one could use these indices to predict the potential fire hazard posed by the cables. For example, if the strength of the source fire upon the cable in a facility in terms of heat flux is known, the time to the ignition of cables can be predicted by dividing the ignition and flame spread index ($I_f$) by the available heat flux. Also, by multiplying the heat release rate index ($I_h$) by the available heat input, the heat release rate of the cables can be calculated, which is useful for the design of fire detection and protection systems.

## V CONCLUSION

In conclusion, it is believed that the indexing method using the FM Laboratory-Scale Combustibility Apparatus (LSCA) is a reliable technique. It establishes a relative basis for comparing the

combustibility of various cables, and provides data for the prediction of full-scale fire behavior if the environmental conditions are known. However, this method does not suggest the possibility of eliminating full-scale fire testing of cables; rather, it implies that, after a priori selection of cables based on the material indices obtained in a laboratory-scale apparatus, full-scale fire tests should be conducted to verify the predicted behavior of the cables. With this application, full-scale fire test results will become much more meaningful. Moreover, it should be emphasized that the indices presented in this paper are based on an overventilated fire environment. In the case of underventilated environment, the cable fire behavior is much more complicated. Nevertheless, the assumption of overventilation is believed to be applicable to most of the scenarios of interest, at least for the beginning fire stages. It is expected that this indexing method will prove to be useful in providing a means to the cable manufacturers and polymer researchers for the optimization of the fire safety design of cables.


## ACKNOWLEDGMENT

The authors are grateful to the EPRI Project Manager, Mr. R. E. Swanson for releasing the information for the publishing of this work. The results of this paper are based on the work performed under an EPRI contract NP-1200 Research Project 1165-1.


## REFERENCES


1. A. Tewarson, J.L. Lee and R.F. Pion, "Categorization of Cable Flammability Part I: Laboratory Evaluation of Cable Flammability Parameters," EPRI Project RP1165-1, Report EPRI NP-1200, Part I, prepared by Factory Mutual Research Corporation, Norwood, Mass., October 1979.
2. B.M. Halpin, E.P. Bedford, R. Fisher and Y. Ceplan, "A Fire Fatality Study," Fire Journal 69, 11, 1975.
3. A. Tewarson and F. Tamanini, "Research and Development for a Laboratory-Scale Flammability Test Method for Cellular Plastics," Factory Mutual Research Corporation, Norwood, Mass., Technical Report RC76-T-64, September 1976.
4. A. Tewarson and F.F. Pion, "A Laboratory-Scale Test Method for the Measurement of Flammability Parameters," Factory Mutual Research Corporation, Norwood, Mass., Technical Report 22524, October 1977.
5. A. Tewarson, "The Factory Mutual Combustibility Apparatus for Reliable Fire Testing of Materials on a Small Scale," Modern Plastics, in press.

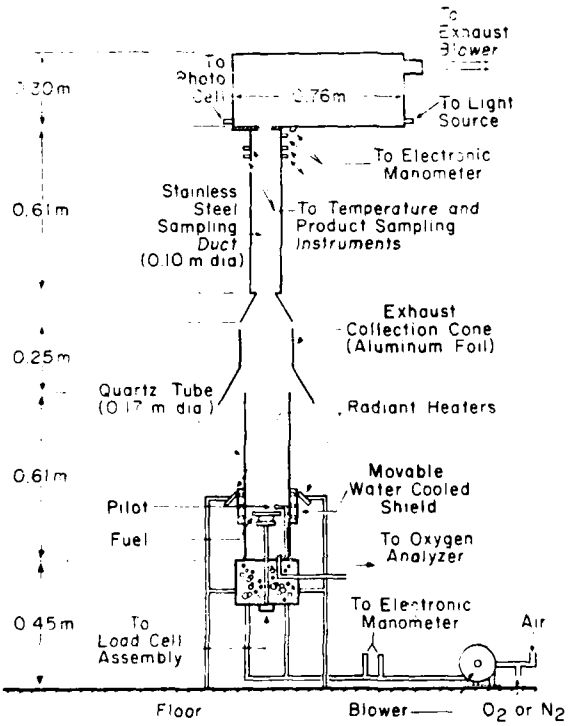




FIGURE 1 FACTORY MUTUAL COMBUSTIBILITY APPARATUS

TABLE I

MATERIAL INDICES OF FOUR DIFFERENT GENERIC TYPE CABLES

| Index[b] | Insulation/Jacket[a] PE/PVC | XPE/neoprene | EPR/hypalon | Silicone/asbestos |
|---|---|---|---|---|
| $I_f$ | 728 | 826 | 1105 | 778 |
| $I_m(x10^{-2})$ | 22 | 38 | 47 | 10 |
| $I_h(x10^{-1})$ | 55 | 40 | 65 | 23 |
| $I_{p,co}(x10^{-4})$ | 110 | 304 | 564 | 30 |
| $I_{p,HC}(x10^{-4})$ | 22 | 38 | 94 | ~0 |
| $I_o(x10^{-4})$ | 104 | 69 | 63 | 104 |

[a] PE/PVC - polyethylene insulation with polyvinyl chloride jacket cable
XPE/neoprene - cross-linked polyethylene insulation with neoprene jacket cable
EPR/hypalon - ethylene propylene rubber insulation with chlorosulfonated polyethylene jacket cable
Silicone/asbestos - silicone rubber insulation with asbestos jacket cable

[b] $I_f$ - ignition and flame spread index ($m^2/kJ$)
$I_m$ - material consumption rate index (g/kJ)
$I_h$ - heat release rate index (nondimensional)
$I_{p,co}$ - product generation rate index for carbon monoxide (g/kJ)
$I_{p,HC}$ - product generation rate index for total hydrocarbon as $CH_4$ (g/kJ)
$I_o$ - light obscuration index ($m^2/g$)

James L. Lee
Research Scientist
Factory Mutual Research Corporation
Norwood, Mass. 02062

James L. Lee, joined the Flammability Section of the Applied Research Department at Factory Mutual in 1978 after receiving his M.S. degree in Fluid Mechanics from Brown University, Providence. R.I. He has been conducting experimental research on the combustibility behavior of materials such as plastics, wood and flammable liquids.

Archibald Tewarson
Research Specialist
Factory Mutual Research Corporation
Norwood, Mass. 02062

Archibald Tewarson joined the Flammability Section of the Applied Research Department at Factory Mutual in 1968. He received his Ph.D. degree in Fuel Science from Pennsylvania State University, University Park, Pennsylvania. Dr. Tewarson has been involved extensively in research on the physico-chemical aspects of fires including flammability of materials, smoke and toxic compounds generated in fires.

Russell F. Pion
Associate Research Scientist
Factory Mutual Research Corporation
Norwood, Mass. 02062

Russell F. Pion joined the Flammability Section of the applied Research Department at Factory Mutual in 1970. He received his B.S. degree in Industrial Technology from Roger Williams College in Bristol, R.I. He has been involved extensively in carrying out experiments on the flammability of materials such as plastics, wood, polyurethane foam, and flammable liquids.

# FLAME RESISTANT COMMUNICATION CABLE WITH LEAD SCREEN TAPE COATED WITH POLYMER

K. Yoshioka, Y. Amano and G. Morikawa

Sumitomo Electric Industries, Ltd.

Yokohama, Japan

## Abstruct

The development of flame resistant communication cable with metallic screen have been long awaited. However, it was very difficult to produce such a cable, since metallic screen combined with existing flame resistant cables reduce the flame resistant characteristics.

The authors, after a carefull study of various cable structures, were successful in developing cables which meet current demands. These cables employ a lead tape coated with polymer as the screen on the cable core. The newly developed lead tape adheres to inside of polymeric sheath preventing penetration of moisture and giving good electrostatic shielding effect. In addition, it doesn't reduce the flame resistant characteristics because of its low melting point.

## 1. Introduction

Along with the introduction of disaster-prevention systems into tall buildings and large-scale plants (such as petro-chemical complexes, power plant facilities, etc.), various other measures have also been taken — especially for fire prevention, detection of fire in its early stages, and limitation of damage caused by fire. Cables that are superior in flame resistance and flame retardation are extensively employed in the power supply circuits of these facilities. In addition, the Fire Services Act requires that flame resistant cables which pass flame resistance examinations be used for emergency power supply circuits of these facilities such as fire hydrants, fire alarms, emergency broadcasting facilities, emergency guide lamps, etc.

Investigations have recently been made into various centralized watching and controlling systems which, in case of fire, automatically monitor the state and range of the fire and give pertinent instructions from the watching and controlling center, while effecting automatic control of various facilities so as to keep the damage to a minimum.

In the disaster-prevention system described above, it has become necessary to employ a new type of communication cable for use in fire alarms, signal circuits of various sensors, emergency link circuits, whole broadcasting circuits, control circuits for electical and mechanical facilities, ITV systems, etc. The development of a new type of communication cable has been strongly demanded. Such a cable must simultaneously satisfy the following conditions:

(1) Under normal use conditions, it must display minimal degradation caused by penetration of moisture from outside. Also, it must be sufficiently high in reliability against electrical noises.
(2) Even in the case where a cable which is exposed to a fire is burnt, it must be capable of normal signal transmission, at least for a predetermined period of time.

In order to present particular constructions which satisfy all these conditions at the same time, the authors have been working on the development of a flame resistant communication cable which has a metallic screen over the cable core to resist moisture. We have succeeded in achieving our objective (as reported herein) by constructing a communication cable core using the insulation barrier structure of the existing flame resistance cable for power circuits with respect to the conductor, and applying lead tape coated with polymer on the core as a metallic screen.

## 2. Review of Cable Construction

Although various structures were considered for conductor construction, we concluded that it was most suitable to employ the construction generally employed in the present power circuit flame resistant cable. In this case, mica tapes are wrapped over copper to form a flame resistant layer, since mica tapes show high stability and little reduction of dielectric strength in high temperature, and PE insulation is also provided.

In terms of sheath construction, metallic screen is necessary to enhance reliability against moisture and electrical noises. In general alpeth sheath, stalpeth sheath, corrugated steel tube armour, bonded aluminum PE sheath, lead sheath, etc. have been put into actual use for communication cables.

The characteristics obtained when these sheaths are applied to flame resistant cables which use mica tape for a flame resistant layer have been assessed as follows. Generally, degradation in flame resistant characteristics in cases where cables are subjected to high temperatures is considered to be attributable to the fact that organic materials constituting the cable core (such as PE insulation) decompose. Therefore, if conductive decomposites (such as

carbon, etc.) which enter the flame resistant layer are incapable of being discharged from the cable core, the result is degradation of the insulation resistance.

Therefore, for quick evaporation of the conductive decomposites from the cable, it is desirable that the metal(s) constituting the metallic screen have a low melting point and be rapidly melted under high temperatures. In the metals used for the sheath constructions which are put into actual applications as described above, lead has the lowest melting point (327°C), and the melting point is lowered further if formed into lead alloys. Thus, it may be said that the lead sheath is the most suitable from the viewpoint of flame resistant characteristics. However, in ordinary lead sheaths, lead alloys of 2 - 3mm in thickness are extruded by a lead sheath machine for covering; thus, such lead sheaths may have some problems as cables for disaster-prevention systems in terms of cable weight and handling ease.

In Table 1, comparisons of flame resistant characteristics, reliability against moisture, and cable weight are shown according to the differences of sheath construction. As can be seen in Table 1, it has been extremely difficult to achieve cables superior in every aspect.

| Sheath Construction | Melting Point of Metallic Screen (°C) | Flame Resistance | Against Moisture | Cable Weight |
|---|---|---|---|---|
| Alpeth Sheath | Al 660 | unfavorable | unfavorable | favorable |
| Stalpeth Sheath | Al 660<br>Fe 1535 | unfavorable | favorable | favorable |
| Corrugated Steel Tube Armoured | Fe 1535 | unfavorable | favorable | unfavorable |
| Bonded Aluminum PE Sheath | Al 660 | unfavorable | faborable | favorable |
| Lead Sheath | Pb 327 | favorable | favorable | unfavorable |

Table 1. Characteristic Comparison of Various Sheathes

As a result of repeated investigations carried out on the basis of the above studies, we have reached a conclusion that the bonded lead PE sheath employing newly developed lead tape coated with polymer is best suited to the sheath construction of the flame resistant communication cable. This bonded lead PE sheath is constructed by longitudinally applying tape formed by coating a special plastic layer on one side of the lead onto the cable core, and also applying a PE sheath onto it, thus providing an integral structure of the lead tape and PE sheath by means of heat at the PE sheath extrusion.

Fig. 1 show the construction of the newly developed flame resistant communication cable. The conductors are stranded after quad twisting or pair twisting and they are so arranged that the tracer quads (or pairs) are identified by the colors of the PE insulation.

## 3. Confirmation of flame resistant characteristics

### 3-1 Samples for the flame resistant characteristics examination

For confirmation of the difference in flame resistant characteristics resulting from the differences in sheath construction, samples were prepared in which the sheaths were applied onto the same flame resistant cable core (as shown in Figs. 2, 3 & 4).

In Fig. 2, the sheath is limited only to PE for confirmation of the flame resistant characteristics of the cable core, since PE sheath affects little on its characteristics, while those in Figs. 3 & 4 are intended to confirm the topics discussed in item 2 above.

### 3-2 Examination method

A furnace with construction specifications in accordance with JIS A1305 was employed (Fig. 5). The temperature in the furnace was controlled according to the normal temperature transition in the fire (JIS A1304 heating temperature curve) (Fig. 6) to set the testing temperature. The measurements were taken for 30 minutes, and the conductor of the sample was alternately divided into two portions, with one portion being grounded together with the metallic wire for supporting the sample, while DC 500V was applied between them to measure the insulation resistance.

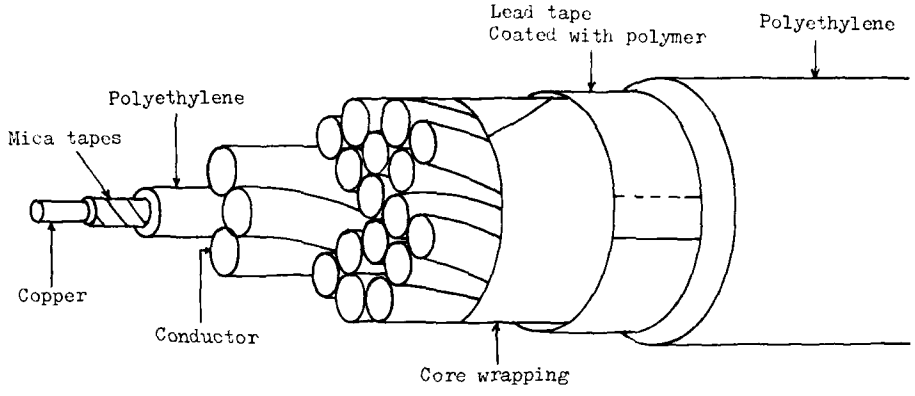



Fig. 1 Construction of Flame Resistant Communication Cable

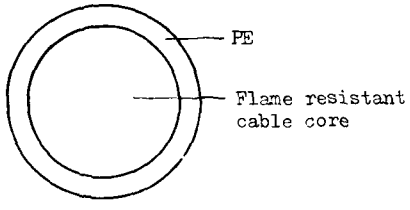



Fig. 2 PE Sheath

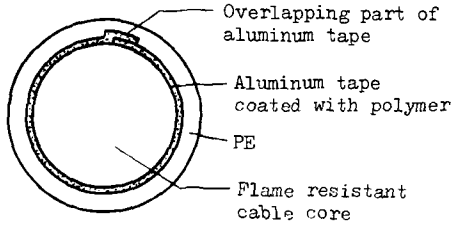



Fig. 3 Bonded Aluminum PE Sheath

Aluminum tape and PE sheath are adhered to each other. Overlapping part of aluminum tape is also adhered.

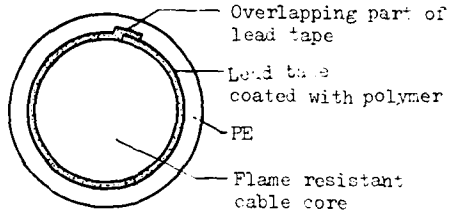



Fig. 4 Bonded Lead PE Sheath

Lead tape and PE sheath are adhered to each other. Overlapping part of lead tape is also adhered.

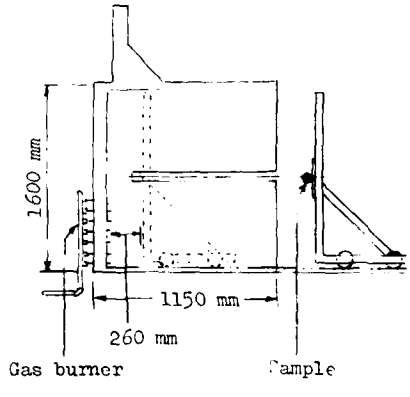



Fig. 5 Furnance and Fixed Sample

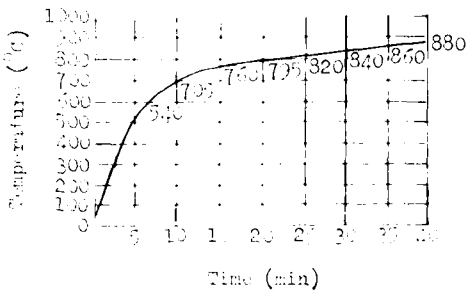



Fig. 6 JIS A 1304 Heating Temperature Curve.

### 3-3 Examination results

The test results are shown in Fig. 7. The PE sheath and bonded lead PE sheath constructions are maintained at an insulation resistance higher than $10^4\Omega$, displaying favorable flame resistant characteristics. On the other hand, in the bonded aluminum PE sheath, the insulation resistance started to fall rapidly about 12 minutes after heating, thus reaching a state approximately close to short-circuiting after about 15 minutes. This indicates that even if the flame resistant characteristics of the flame resistant cable core are favorable, differences in the flame resistant characteristics take place due to the differences in sheath construction. In other words, it has been confirmed that, in the case where the melting point of the metallic screen is low for quick melting under high temperatures (as in the bonded lead PE sheath), the conductive decomposites of the organic materials constituting the cable core are rapidly evaporated to the outside, without giving rise to degradation of the flame resistant characteristics. However, when the melting point of the metallic screen is high (as in the bonded aluminum PE sheath), the flame resistant characteristics are adversely affected.

The bonded lead PE sheath is superior in the following points:

(1) The construction of the metallic barrier against moisture prevents degradation due to penetration of moisture, and is also superior in electostatic shielding characteristics.

(2) In case of fire, since the shielding layer rapidly melts, the flame resistant characteristics of the cable are not deteriorated.

Employment of the above sheath construction has made possible the realization of a cable which satisfies the characteristics that are indispensable for flame resistant communication cables (as stated in the introduction earlier herein).

## 4. Conclusion

In this paper, we have discussed the construction of the newly developed flame resistant communication cable and its characteristics. Although demands for the flame resistant cable have been steadily increasing year by year—despite its comparatively short history—there have been relatively few examples of actual applications of a flame resistant communication cable in which degradation caused by moisture and electrostatic

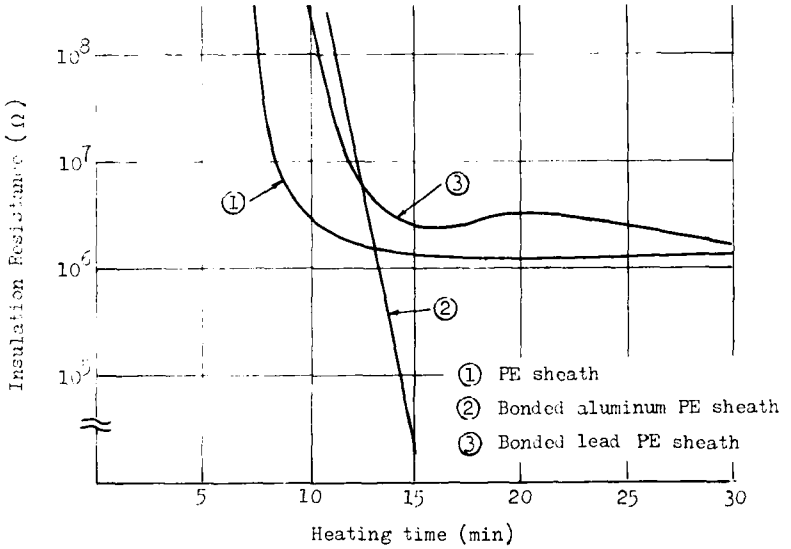



**Fig. 7 Comparative Data of Insulation Resistance During Examination of Various Flame Resistant Communication Cables which Differ in Sheath Construction.**

shielding construction has been taken into consideration. It is considered that flame resistant communication cable with lead screen tape as stated herein is best suited to high grade disaster-prevention systems. These systems will be put into actual use to a greater extent in the future, and highly dependable system engineering will be facilitated through employment of this cable.



Keiji Yoshioka

Sumitomo Electric
Industries, Ltd.
1, Taya-cho,
Totsuka-ku, Yokohama,
Japan

Mr. Yoshioka graduated from Osaka University in 1964 with a B.E. degree in electrical communication engineering. Then, he joined The Sumitomo Electric Industries, Ltd. and has been engaged in development and designing of telecommunication cables.
He is now manager of 1st Communication Cable Engineering Section of Communications Division.



Yoshikazu Amano

Sumitomo Electric
Industries, Ltd.
1, Taya-cho,
Totsuka-ku, Yokohama,
Japan

Mr. Amano graduated from Osaka University in 1968 with a B.E. degree in electrical engineering. Then, he joined The Sumitomo Electric Industries, Ltd. and has been engaged in development and designing of telecommunication cables.
He is now Senior Engineer of 2nd Communication Cable Engineering Section of Communications Division.



Gen Morikawa

Sumitomo Electric
Industries, Ltd.
1, Taya-cho,
Totsuka-ku, Yokohama,
Japan

Mr. Morikawa graduated from Kyoto University in 1977 with a M.E. degree in electrical engineering. Then, he joined The Sumitomo Electric Industries, Ltd. and has been engaged in development and designing of telecommunication cables.
He is now a member of 1st Communication Cable Engineering Section of Communications Division.

# DEVELOPMENT OF A FLAME RESISTANT NONCONTAMINATING PVC JACKET FOR COAXIAL CABLE

J. T. Loadholt and S. Kaufman

Bell Laboratories
Norcross, Georgia

## ABSTRACT

The migration of plasticizer from a PVC jacket into the polyethylene core of a coaxial cable can significantly alter high frequency transmission characteristics. Evaluation of a series of PVC compounds confirmed a correlation of the degradation of transmission characteristics with plasticizer volatility. Linear trimellitate plasticizers give stable electrical performance with optimized fire resistance, low cost, and excellent processing characteristics.

## I. INTRODUCTION

A transmission line design is usually constrained by a combination of electrical, mechanical, environmental and economic requirements. Careful consideration must be given to the choice of materials to assure that all constraints are met without conflict.

Fire resistance is of prime importance for cables used inside buildings and greatly influences the choice of plastic materials for insulation and jacket. The coaxial cable is often used where a transmission line of precise electrical performance is needed, especially at high frequency. Central office coaxials usually have a solid core and the electrical requirements limit the selection of dielectric materials to a few choices, principally polyethylene and fluoropolymers. Although the fluoropolymers have excellent fire resistance, high cost limits the scope of their application.

The problem addressed here is the first step in improving the fire resistance of coaxial cables, viz., the development of a noncontaminating, fire resistant PVC jacket for high frequency coaxial cables. Plasticizer can migrate from the PVC jacket and contaminate the polyethylene core, causing an increase in dissipation factor which is especially pronounced at frequencies above 10 MHz.[1]

In this paper we investigate the contamination phenomenon by monitoring loss in a series of PVC jacketed coaxial cables. The relationship between excess attenuation and plasticizer volatility is determined, and the development of a trimellitate plasticized jacket is described.

## II. COAXIAL TRANSMISSION

The motivation for this development is improvement in fire resistance but the primary concern is maintaining stable electrical characteristics. Contamination of the polyethylene core will appear as an increase in dielectric loss. This part of loss is usually small compared to conductor loss until the frequency of operation reaches the 100 MHz range. With contamination, however, the effects may be significant as low as 10 MHz. A system designer who must equalize for the coaxial cable loss needs to know both the absolute level and the slope (or shape) of the loss versus frequency curve. A typical loss curve, Figure 1, shows that high frequency loss varies almost directly with the square root of frequency.[2] Two factors affect the

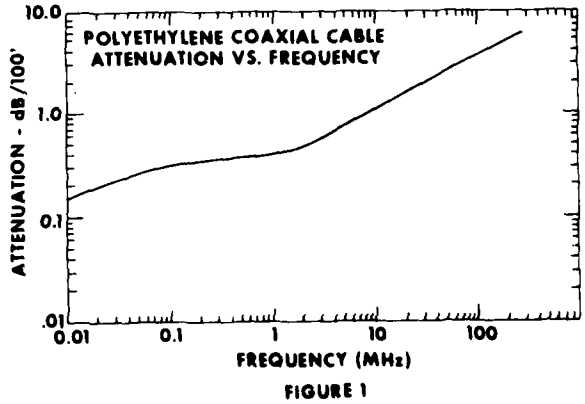



FIGURE 1

frequency dependency. There is a small but predictable nonlinearity in the conductor loss that causes a deviation from a pure square root frequency behavior. Dielectric loss causes all additional deviation. As shown below, plasticizer contamination alters this behavior by increasing dielectric loss and a system designed for square root behavior could encounter difficulties with time.

The insertion of a length of cable between a source (generator) and load (detector) causes two effects. Neglecting mismatch losses at the source and load, the signal traveling the length of cable will require, on a unit basis, a finite amount of time ($\tau$) and will undergo a certain loss ($\alpha$) and phase shift ($\beta$). The loss is separated into the two components, conductor loss ($\alpha_c$) and dielectric loss ($\alpha_d$). The total loss is then

$$\alpha = \alpha_c + \alpha_d \qquad (1)$$

With reference to the quantities defined in Appendix I, we often model the transmission line by a distributed circuit model and find that Equation (1) can be written

$$\alpha = \frac{R}{2Z_o} + \frac{G}{2Y_o} \qquad (2)$$

The first term on the right relates conductor loss to the conductor resistance and the second term relates dielectric loss to the dissipation factor of the dielectric.

Woodard has shown that $\alpha$ per Equation (2) can be normalized by $\tau\sqrt{f}$ to give

$$\frac{\alpha}{\tau\sqrt{f}} = A + \frac{B}{\sqrt{f}} + \pi \tan\delta \sqrt{f} \qquad (3)$$

where A and B are constants depending on the geometry, tan$\delta$ is the dissipation factor and f is the frequency.[3] These constants are defined in Appendix II. In practice $B/\sqrt{f}$ is only a few parts per thousand compared to A at 1 MHz and is negligible above 10 MHz. Therefore, at high frequencies

$$\alpha/\tau\sqrt{f}\Big|_{h.f.} = A + \pi \tan\delta \sqrt{f} \qquad (4)$$

The quantities $\alpha$ and $\beta$ may be measured per Appendix III. The normalized quantity of Equation (4) is then easily computed since

$$\tau = \frac{\beta}{\omega} \qquad (5)$$

where $\omega = 2\pi f$.

Any slope in the normalized attenuation data above 10 MHz is a direct measure of tan$\delta$ for the cable dielectric. When plasticizer contaminates the core, tan$\delta$ changes and this affects the shape of the $\alpha$ versus frequency curve so monitoring the change in slope of this normalized data gives a direct measure of the degree and rate of contamination.

Consider the data of Figure 1. Taking the accompanying data for $\beta$ and $\tau^2$ and normalizing, the result is shown in Figure 2. Close examination of the curve between 10 MHz and 100 MHz shows that the curve has nearly constant slope, which means tan$\delta$ is essentially constant over that range. The upturn below 1 MHz is due to the $B/\sqrt{f}$ part in Equation (2) that becomes significant at low frequencies. By simply taking points from the curve of Figure 2, tan$\delta$ is in fact estimated to be .0002. This is in excellent agreement with the expected value from material data on low density polyethylene.

Each cable tested in the program will be seen to have an initial characterization similar to Figure 2. Acceptable jacket formulations will cause minimal change in tan$\delta$ after the exposure to elevated temperature over a period of time and little effect on normalized attenuation. On the other hand, the occurrence of contamination will alter the shape of this curve significantly.

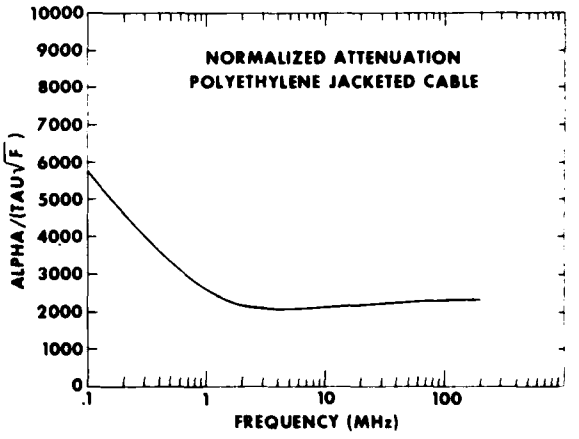


FIGURE 2

## III. MATERIALS

A PVC jacket compound must be formulated to meet physical, chemical and mechanical requirements. Plasticizer is an important constituent of the compound, imparting flexibility and low temperature impact resistance to an otherwise glassy polymer. A fundamental problem with plasticizers is

that they are readily combustible and compromise the fire resistance of PVC, an inherently fire resistant polymer. Thus, in order to meet fire resistance requirements, the amount of plasticizer in a jacket compound must be kept at the minimum level consistent with mechanical requirements.

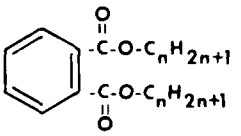
Maintaining minimal plasticizer level leads the compound designer to choose an efficient plasticizer. However, efficiency in most cases is contrary to the requirement of minimal migration into the polyethylene dielectric. Polymeric plasticizers, which are relatively inefficient, are generally used in applications requiring migration resistance. Instead of using polymeric plasticizers we chose to investigate two moderately efficient monomeric plasticizers with low volatility, pentaerythritol ester and trimellitate.

TABLE I

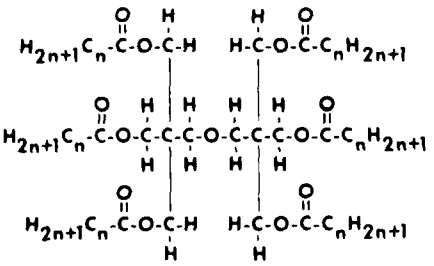
## Plasticizers Used in Cable Jacket

| | |
|---|---|
| Di (2-ethylhexyl) Phthalate | DOP |
| 7-9-11 Mixed Alkyl Phthalate | 711P |
| 8-10 Mixed Alkyl Phthalate | 810P |
| Diundecyl Phthalate | DUP |
| Ditridecyl Phthalate | DTDP |
| Polyester | S429 |
| Pentaerythritol Ester | H707 |
| 7-9 Mixed Alkyl Trimellitate | 79TM |
| Triisononyl Trimellitate | TINTM |

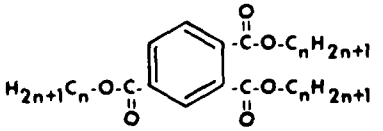
Phthalate Plasticizer



Pentaerythritol Plasticizer



Trimellitate Plasticizer



The development of the flame retardant jacket compound used has already been reported.[4] In order to study the expected relationship between plasticizer volatility and contamination of the polyethylene core, coaxial cables were manufactured with the flame retardant jacket compound prepared with each of a series of plasticizers. The series included highly volatile di(2-ethylhexyl) phthalate (DOP), other less volatile higher molecular weight phthalates, a polyester polymeric, linear and branched alkyl trimellitates and a pentaerythritol ester. Additionally, a widely used commercial PVC consisting of a blend of PVC and nitrile rubber was used as a control. Other controls were a flame retardant polyethylene and standard polyethylene. A list of the plasticizers used, in ascending order of volatility, is shown in Table I. Volatility was measured by suspending .075" thick discs of each compound in a 130°C circulating air oven. Weight loss versus time curves, Figure 3, show that the trimellitates and the pentaerythritol ester are leading candidates for use in a noncontaminating jacket.

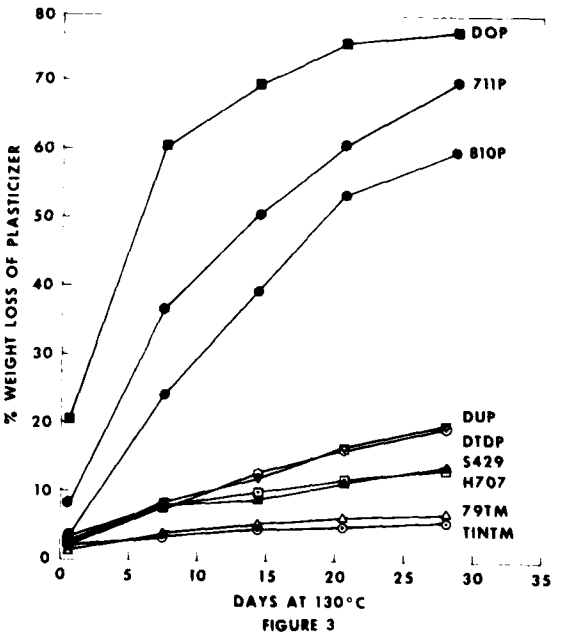


FIGURE 3

## IV. TEST PROCEDURE AND RESULTS

The test procedure was to monitor change in loss versus time under accelerated conditions to determine the relationship between plasticizer volatility and contamination. The test arrangement is shown in Figure 4. All samples were of identical length and placed in similar loose coils within a large environmental chamber. The cable ends were connectorized to a plug-in access panel at a porthole of the chamber. Aging and measurements were done at 85°C with air circulating around the samples.

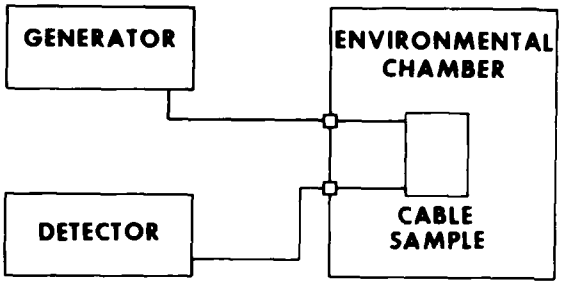



**FIGURE 4**

The test temperature was chosen to give maximum acceleration of the volatilization while avoiding initiation of secondary effects such as degradation of the polyethylene.

Loss was measured on each sample at room temperature before the aging procedure began. The measurements were then repeated after 24 hours at 85°C to establish a level for comparison at elevated temperatures. Subsequent measurements were taken at 85°C on a log-time basis for 100 days. The final characteristics were then measured after the samples had stabilized back to room temperature.

Each set of data was normalized per Equation (4) giving a family of curves showing the progressive degradation in dissipation factor. The results for DOP are shown in Figure 5. The DOP, in agreement with its ranking as the most volatile plasticizer in the series, produced the greatest change in dissipation factor. The second most volatile plasticizer used was the 711 phthalate whose results are shown in Figure 6. The 711 phthalate follows the same pattern as DOP but at a somewhat slower rate. The trend continues down the list of plasticizers. The DUP results shown in Figure 7 represent a moderately volatile plasticizer lagging substantially behind the DOP in rate of contamination.

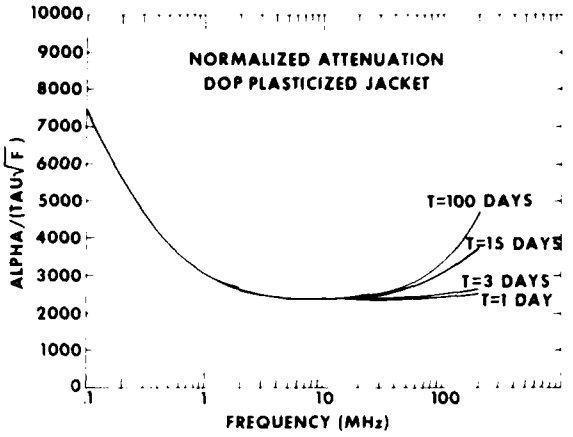



**FIGURE 5**

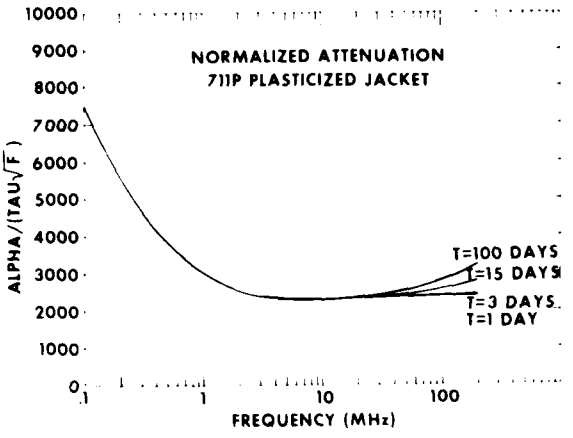



**FIGURE 6**

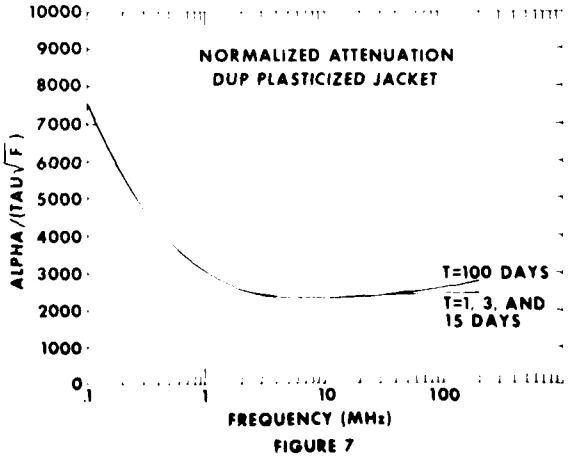



**FIGURE 7**

Figure 8 shows the results for the 7,9 trimellitate. No change in tan δ was evident at least to the resolution of the graphical plot. Similar results were obtained for pentaerythritol ester, triisononyl trimellitate and for the controls.

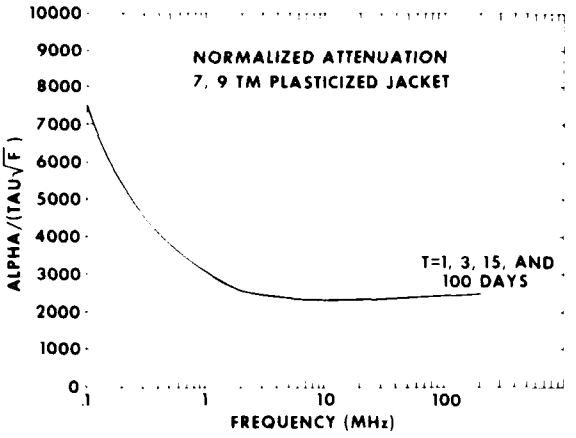


FIGURE 8

A close examination of the loss data indicates that all samples increased in loss somewhat, including the polyethylene control. Table II gives the percent changes in total attenuation at 100 MHz after 100 days. Table II is a comparison of the room temperature attenuation after 100 days aging to the initial room temperature attenuation. It should be noted that the percent changes will be less at lower frequencies and greater at higher frequencies. Several of the materials exceed the performance of the polyethylene control. Of particular interest are the pentaerythritol ester and the 7,9 trimellitate.

A likely cause of the increase in attenuation among the controls is cross-contamination. All samples were in the same chamber with minimal venting. The volatiles likely remained and migrated to the other samples. Position relative to the highly volatile samples probably caused some difference in the degradation of similar low volatility samples. For example, the polyethylene shows slightly more change than the flame retarded polyethylene and the triisononyl trimellitate is slightly higher than the 7,9 trimellitate. Only careful segregated measurements can confirm the cause of the differences but such an experiment would likely introduce other variations in the aging environment. Actually, the overwhelming presence of PVC in a telephone central office probably supports the argument that the test arrangement used for this evaluation is a good model.

It is informative to examine the true loss data for the DOP cable at room temperature. Figure 9 shows the initial and final loss curves. A user expecting to have a system equalize this cable over an extended period of time could discover system problems with time.

TABLE II

## Change in Attenuation After 100 Days at 85°C

| Compound | Excess Attenuation, % |
|---|---|
| H707 | 2.9 |
| PVC/nitrite rubber | 3.2 |
| 79TM | 3.2 |
| Flame Retardant PE | 3.8 |
| S429 | 5.1 |
| Polyethylene (PE) | 5.3 |
| TINTM | 6.3 |
| DUP | 10.6 |
| DTDP | 21.0 |
| 810P | 26.7 |
| 711P | 39.0 |
| DOP | 62.5 |

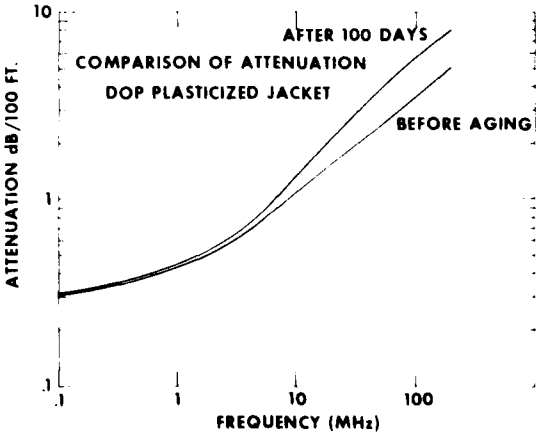


FIGURE 9

## V. CONCLUSIONS

The loss data support the correlation between rate of contamination and plasticizer volatility. If we assume the standard polyethylene an acceptable design, then we can use known activation energies to predict the maximum ambient temperature each plasticizer can experience while providing the desired service life. Central office telephone equipment is usually designed for forty year life. The cables in question are used primarily for interbay cabling and therefore see only central office ambient temperature. Conservatively, we can assume no further degradation of the polyethylene control is allowable and take a very reasonable maximum of five percent increase in loss as a goal for the PVC jacket. The 7,9 trimellitate, which experienced 3.2 percent degradation in 100 days at 85°C, would then be expected to reach the five percent level of attenuation in forty years only if ambient continuously exceeded 35°C. In fact, all of the plasticizers above polyethylene in Table II give comfortable service life predictions when used in coaxial cable jacket.

Plasticizer efficiency indicates that pentaerythritol ester and 7,9 trimellitate are the first choices as the fire resistance cable plasticizer. Cost, however, singles out the 7,9 trimellitate. Though not a crucial central office requirement, the 7,9 trimellitate gives somewhat better resistance to low temperature impact as well.

To complete the program, a 7,9 trimellitate plasticized jacket was used in a factory trial on a product normally jacketed with polyethylene. The formulation processed quite easily and actually gave a final product more supple in handling than the original design.

Samples of the cable were subjected to the various small scale fire tests relevant to such cable applications. The PVC jacket is sufficiently fire resistant to allow the complete cable to pass the flammability requirements of U.L. 83.


## ACKNOWLEDGEMENTS

We gratefully acknowledge M. M. Yocum for sample preparation and weight loss studies, T. T. Noble for assistance in making electrical measurements, C. J. Arroyo for flammability tests and P. R. Cammons for preparing cable samples.

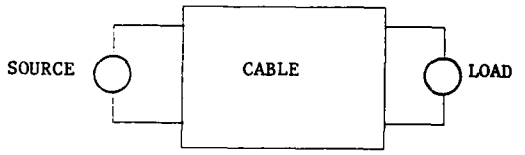

## REFERENCES


1. H. M. Hutson, Bell Laboratories internal memorandum.
2. H. M. Hutson, Bell Laboratories internal memorandum.
3. D. P. Woodard, Bell Laboratories, internal memorandum.
4. S. Kaufman, C. A. Landreth, "Development of Improved Flame Resistant Interior Wiring Cables," Proceedings of the 24th International Wire and Cable Symposium, November 1975, p. 9.
5. S. Ramo, et al, "Fields and Waves in Communications Electronics," John Wiley & Sons, Inc., New York, 1967.
6. D. Paris, F. Hurd, Basic Electromagnetic Theory, McGraw-Hill Book Company, 1969.


## APPENDIX I

### Transmission Line Models

The transmission line may be viewed as a two-port network.

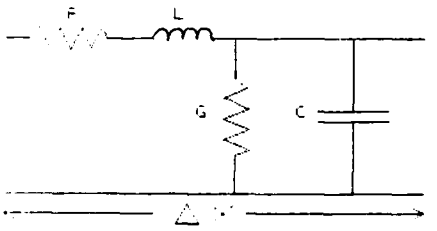



A signal leaving the source will undergo a loss and a phase shift before reaching the load. The voltage at the load is given by an expression of the form

$$V(\text{load}) = V(\text{source})\, e^{-\alpha \ell} e^{-j\beta\ell}$$

where $\alpha$ is the attenuation factor per length and $\beta$ the phase shift per unit length. The length of the line is $\ell$. Both $\alpha$ and $\beta$ are functions of frequency.

The transmission line may be modeled as a distributed circuit.




$\Delta x$ = incremental length of line
R = resistance per unit length
L = inductance per unit length
G = conductance per unit length
C = capacitance per unit length

The circuit analysis relates the distributed R, L, G, and C values to $\alpha$ and $\beta$ by,

$$\alpha + j\beta = \sqrt{(R+j\omega L)(G+j\omega C)}$$

where $\alpha + j\beta$ is a complex number and $j = \sqrt{-1}$.

It is also necessary to have the characteristic impedance

$$Z_o = \sqrt{\frac{R+j\omega L}{G+j\omega C}} = \frac{1}{Y_o}$$

and propagation delay

$$\tau = \frac{\beta}{\omega}$$

with

$$\omega = 2\pi f \ .$$

These relationships are standard in most basic texts on electromagnetics.[5,6]

The parameter of particular interest in this work is the conductance G. This quantity models the dielectric loss and is directly proportional to the dissipation factor of the coaxial dielectric. Per References (3) and (5) it is straightforward to show the direct relationship between G and the quantity $\pi \tan\delta$ of Equation 4 and Appendix II.

## APPENDIX II

### Attenuation Analysis of the Coaxial Cable

The loss of a coaxial cable is given by[3]

$$\alpha = \alpha_c + \alpha_d$$

$$\alpha_c = \frac{R}{2}\sqrt{\frac{C}{L_t}}$$

$$\alpha_d = \frac{G}{2}\sqrt{\frac{L_t}{C}}$$

where

$$R = \sqrt{\frac{\mu f}{\pi\sigma}}\left(\frac{1}{d}+\frac{1}{D}\right) + \frac{1}{G}\left(\frac{1}{d^2}-\frac{1}{D^2}\right)$$

$$L_t = L_s\left[1 + \frac{1}{2L_s}\frac{1}{\sqrt{f}}\sqrt{\frac{\mu}{\pi\sigma}}\left(\frac{1}{d}+\frac{1}{D}\right)\right]$$

$$L_s = \frac{\mu}{2\pi}\ln\frac{D}{d}$$

$$C = \frac{2\pi\varepsilon}{\ln D/d}$$

$$G = \frac{2\pi\varepsilon\tan\delta}{\ln D/d}$$

D = diameter over dielectric

d = inner conductor diameter

$\mu = 4\pi\times10^{-4}$ H/m (permeability of core and conductors)

$\varepsilon = \varepsilon_r\varepsilon_o$ (permittivity of core)

$\varepsilon_r$ = dielectric constant of core

$\varepsilon_o = 8.85\times10^{-12}$ F/m (permittivity of free space)

$\sigma = 5.83\times10^{7}$ S/m (conductivity of core)

The quantity R is resistance, $L_t$ is total inductance, $L_s$ is space inductance, C is the capacitance and G is the conductance as defined in Appendix I. If these quantities are in Ohms/m, H/m, F/m, S/m, respectively, then the units of $\alpha$ are Np/m. Multiplying by the factor 8.686 converts Np to dB which is the usual unit for measuring and presenting $\alpha$.

The quantity $\tau$ is $\sqrt{L_tC}$ with $L_t$ and C defined above. If we divide $\alpha_c$ by $\tau\sqrt{f}$ we obtain

$$\frac{\alpha_c}{\tau\sqrt{f}} = \frac{1}{2L_s}\sqrt{\frac{\mu}{\pi\sigma}}\left(\frac{1}{d}+\frac{1}{D}\right)\left[1 - \frac{1}{2\pi L_s\sqrt{f}}\sqrt{\frac{\mu}{\pi\sigma}}\left(\frac{1}{d}+\frac{1}{D}\right)\right]$$

or

$$\frac{\alpha_c}{\tau\sqrt{f}} \approx A + B/\sqrt{f} \ .$$

Similarly,

$$\frac{\alpha_d}{\tau\sqrt{f}} = \pi\sqrt{f}\tan\delta = \pi\tan\delta\sqrt{f} \ ,$$

where $\tan\delta$ is the dissipation factor of the dielectric core. Usually the quantity $B/\sqrt{f}$ is negligible compared to A above a few megahertz, therefore, $\alpha_c/\tau\sqrt{f}$ is essen-

tially constant at high frequencies. The slope of the $\alpha/\tau\sqrt{f}$ is then due to $\alpha_d$ and is a direct measure of tanδ. The contamination by plasticizer enhances the dissipation factor of the polyethylene and the slope gives direct measurement of that quantity and the level of contamination.

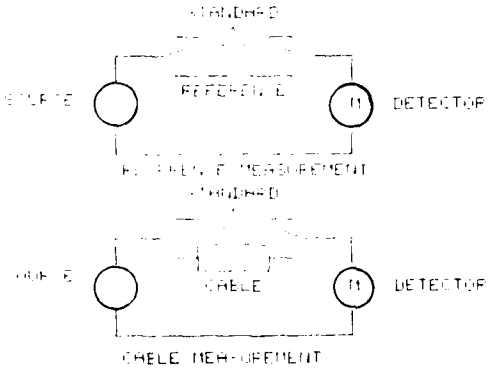
## APPENDIX III

### Transmission Line Measurements

The characteristics of transmission lines may be measured in a number of ways. The insertion loss scheme was used for this work. A generator excites two independent paths. One contains, in successive runs, a direct connection to the load and then the unknown (cable sample). The other contains a series of decade impedances. The loss and phase shift of the cable is compared to the loss and phase through the known reference path (the direct connection) and the difference is called the insertion loss and phase.



J. T. Loadholt is a Member of Technical Staff at Bell Telephone Laboratories, Norcross, Georgia. He received a B.E.E. Degree from Georgia Institute of Technology in 1970 and an M.S. in Electrical Engineering from the University of Illinois in 1971. He joined Bell Laboratories in 1970 and is a member of the Wire Media Group.




In the setup shown above, the decades are adjusted until the signal at the detector is identical to that through the reference line then the reference line plus the unknown. This loss and phase shift introduced by the unknown is a direct measurement of α and β. The measured values are affected by mismatches at source and load and this is usually corrected in software analysis of the data. In this case, 75 ohm coaxials were used and the source and load were 75 ohms. There is very little mismatch so insertion loss and phase were assumed to equal attenuation and phase shift.



Stanley Kaufman is the Supervisor of the Metallurgy and Fire-Resistant Plastics Group at Bell Telephone Laboratories in Norcross, Georgia. He received a B.S. in Physics from the City College of the City University of the City of New York, and a Ph.D. in Chemistry from Brown University. Before joining Bell Laboratories in 1970, he was a research scientist at the Uniroyal Research Center.

# NEW GENERATION OF NONHALOGENATED, FLAME RETARDANT COMPOUNDS AND CABLES

H.A. Mayer G. Hög

AEG-Telefunken Kabelwerke Aktiengesellschaft Rheydt
Duisburg Mönchengladbach 2

## Summary

New, nonhalogenated, flame retardant, low smoke compounds and cables have been developed, using such materials for jackets and insulations.
Their oxygen index is high, they pass flame tests like IEEE-383 or VDE 0472, Part 804, Type C. No corrosive chlorhydric acid is released in case of fire.
Different properties can be achieved as: Higher tensile strength, resistance to oil, resistance to sea-water, etc.
Examples of typical cable constructions, applications and measurement data are presented concerning mechanical and electrical data, including circuit integrity.
In case of fire, corrosion can be avoided and smoke formation considerably reduced.

## Introduction

For cables and insulated conductors with core insulation and sheaths made of plastics or elastomers, the required flame retarding properties are usually obtained by using base materials or additives containing halogen compounds.
For this purpose polymers or copolymers are used with monomeric compounds of halogens such as chlorine or fluorine, polymerized into their macromolecular structure.
The following are some examples of chlorine containing polymers which have proved their value in technology:
Polyvinyl Chloride (PVC), Polychloroprene Rubber (CR), Chlorosulfonated Polyethylene (CSPE/CSM) Chlorinated Polyethylene (CPE/CM). Polymers based on fluorinated hydrocarbons such as PTFE, FEP, E-CTFE, PVDF including other copolymers, may be mentioned as examples of fluorine containing polymeric compounds.

Polymers can also be made flame retardant by means of halogen compound additives, for example chloroparaffins, usually with auxiliaries such as antimony trioxide; or bromine compounds. The above-named flame protection systems have proved their value particularly in preventive fire protection, thus preventing actual fire outbreaks in the case of potential fire hazard.
However, in the case of actual fire, these materials liberate halogen compounds, in particular corrosive hydrogen halides.
In the course of time, cases have been documented, in particular where fires with PVC were involved, in which the secondary damages due to hydrogen chloride corrosion on machinery switching equipment, electronic devices and structural building components in telephone exchanges and industrial plant, were greater than the actual primary fire consequences [1].

In order to reduce these effects, for example Leuchs has attempted to bind hydrogen chloride with finely distributed fillers such as calcium carbonate of low particle size [2].
These measures certainly reduced the extent of HCl liberation within particular temperature ranges, but did not prevent it entirely. Thus the corrosion produced by HCL (hydrogen chloride) was not prevented too.

## Task formulation

In view of these considerations, we have attempted to develop mixtures and cables for certain fields of application in telecommunications and electric power engineering which do not liberate any halogen compounds in the case of fire, and which at the same time have flame retardant properties at least as good as those of plasticized PVC. Depending on the particular application, various conditions must be fulfilled with regard to flame retardancy, emergency running characteristics (circuit integrity), mechanical strength and other properties. Various different mixture types had to be developed, because at the present time it does not appear possible to meet all requirements with one mixture.

The cables and insulated conductors must pass not only the most commonly used flame tests with single test sample and Bunsen burners, such as VDE 0472 Part 804 Test Type A or IEC 332, but also flame tests with several parallel arranged test samples, for instance in the following order of increasing difficulty: IEEE 383, SEN-F4, VDE 0472 Part 804 Test Type C (draft). The last-mentioned test of more recent date according to VDE 0472 Part 804 C, is briefly presented in Annex hereto. In addition to passing these flame tests, the cables should also have emergency operation capabilities, i.e. retention of functional capability for a certain time. Customary tests have been defined too for maintenance of functional capability in the case of fire. These tests are described, for example, in IEC 331 and VDE 0472 Part 814. Furthermore, in our experiments, the emergency operation performance was proved also during the test according to VDE 0472 Part 804, Test Type C.
In order to maintain satisfactory emergency operation performance, it may be advisable to employ inorganic mineral materials such as mica or glass silk tapes.
Silicone rubbers may also be used.
But for reasons of price economics, such additional measures should be used only where this is really necessary.

The requirements imposed on the compounds and the cables made therefrom, can be summarized as follows:

a) Freedom from Halogens:

The compounds, including all cable components, must be free from halogen compounds. This can be confirmed by standard analytical methods. The absence of halogen compounds is a condition for low corrosive effect (see Annex, VDE 0472, Part 813) [5]

b) Flame Retardation/Flame Resistance

Practical technology calls for cables with various kinds of flame resistance, for example as mentioned above. Such tests are performed on the final product, so that for compounds it is customary to determine the oxygen index.
The oxygen index should show a value of at least 26 to 28, as for plasticized PVC, and, as far as possible, it should be greater than 30 for cable sheaths.

c) Low Smoke Generation

Confirmed in test furnace according to VDE 0472 Part 804, Test Type C (see Annex). [3]

Smoke formation as shown in figure 1 during flame test with PVC-cables is undesirable.



Figure 1: Top of test oven with smoke formation during flame test on PVC cable.

d) Processability

of the compounds in mixing equipments and extruders.

e) Mechanical Properties

such as tensile strength and other such charateristics, as far as possible based on existing standards.
It must be possible to manufacture cables and insulated conductors with good flexibility from these compounds.

f) Resistance to Oil

e.g. in ASTM Oil No. 2 or Diesel Oil, may be necessary for certain fields of application.

g) Resistance to Sea-Water

is particularly important for ship cables.

h) Electrical Characteristics

such as dielectric strength, insulation resistance and mutual capacitance, should be as for PVC-insulated conductors or better.

i) Resistance to Radiation

may be necessary for certain applications and testing conditions.

## Overview of some of the developed or used compounds

In the course of time we have developed a range of special polymer compounds, which fulfil the requirements set forth above, as such and on the cable. Some cables have already been proved over a considerable period of time.

In order to solve the posed problem, among other choices materials have been used which contain water of crystallization or chemically bound water, for example hydroxides of metals. In the case of fire, these materials liberate the bound water. A part of the thermal energy produced by the fire process is consumed in the process of splitting off and vaporizing this water. The resulting water vapour forms a kind of flame retarding protective layer. Other compounds which set free inert gases in the case of fire, can also be used, since they too have a flame retarding effect.
In view of the high demands imposed in the case of fire in the higher classes, for example when VDE 0472 Part 804 Test Type C is called for, unusually large proportions of such substances had to be employed in some instances. Special measures were then needed in order to achieve a still processable, extrudable, flexible and in some cases highly rupture-resistant product.

These endeavours have produced a whole set of such compounds and cables with which various fields of application can be served. In order to preserve synoptical clarity, only some of the mixture types and cables will be presented in the following discussion explaining their fields of utilization.

## Mixture Types

Table 1 shows some typical mixtures which have been developed and are in use in particular for cable sheaths.

There is very little smoke formation during flame tests on cables with such materials. No smoke can be seen at the top of the test oven; as compared to smoke formation, e.g. in the case of PVC (Fig. 1).

No corrosive gases like HCl are released in case of flame tests.
Most of the developed jacketing compounds are highly flame retardant and flame resistent.

Table 1: Jacketing Compounds

| Compound Type / Properties | A | B | C |
|---|---|---|---|
| Oxygen Index % | ≥30 | ~40 | 40-50 |
| Halogen % | 0 | 0 | 0 |
| pH of Pyrolysis Products, Conductivity µS/cm VDE 0472 Part 813 | ≥4 <40 | ≥4 <40 | ≥4 <40 |
| Tensile Strength N/mm² | 12.7-17.5 | 8.0-10.0 | 8.0-9.0 |
| Elongation %, min. | ≥150 | 150-200 | ≥150 |
| Immersion in Oil ASTM Nr. II 100°C 24 h % 90°C 168 h % % Retention of Tensile Strength and Elongation | ≥85 ≥70 | ≥80 | |
| Immersion in Sea-water 90°C, 7 d Retention of Mechanical Properties % | ≥80 | ≥80 | ≥70 |
| Hot Set Test 200°C | passed | passed | +) |
| Heat Distortion on 2 mm Plaques ≥50% at | | | 110°C |

+) Hot Set Test passed, when crosslinked

Comments with regard to the Compounds in Table 1

Type A: High tensile strength, high oil resistance, sea-water resistance, flame retarding

Field of utilization in particular for ships and drilling platforms. Also for cables which must fulfil high tensional stress requirements, such as encountered in mining.

Type B: Very high flame retardation.

Field of utilization in particular for cables which must pass very severe flame tests.
Very small smoke generation. Oil-resistant.

Type C: Particularly high flame retardation, not crosslinked and non-dripping in the case of fire

Non-crosslinked polymers, for example thermoplastic mixtures, usually drip more or less severely in the case of fire. This new compound is a non-dripping one, so that cables sheathed therewith will pass very severe fire tests.
Furthermore, such non-crosslinked compounds normally have inadequate tensile strength values. But this compound type C achieves a good tensile strength.
This mixture can be processed with techniques, specially developed for them.

Field of utilization: Conventional balanced pair and coaxial cables with high-quality transmission performance, which are the first cables made flame retardant and halogen-free with such a sheath.
Further uses: Non-crosslinked halogen-free and flame retardant electric power cables and insulated conductors.

Table 2 shows some possible typical mixtures which can be used for core insulations.

Table 2: Compounds for Insulation

| Compound Type / Properties | D | E | F | G |
|---|---|---|---|---|
| Oxygen Index % | ≥ 28 | ≥ 35 | ~28 | - |
| Halogen % | 0 | 0 | 0 | 0 |
| pH of Pyrolysis Products min. | ≥ 4 | ≥ 4 | ≥ 4 | ≥ 4 |
| Conductivity µS/cm VDE 0472 Part 813 | < 40 | < 40 | < 40 | < 40 |
| Tensile Strength N/mm² | ≥ 8.0 | 8.0-10.0 | ≥ 6.0 | ≥ 10.0 |
| Elongation % min. | ≥ 200 | ≥ 150 | ≥ 150 | ≥ 200 |
| Hot Set Test 200°C | passed | +) | passed | |

+) In case of non-crosslinked material heat-distortion on 2 mm plaques is measured: ≤ 50% at 70°C
When crosslinked, Hot Set Test is passed.

Comments on Table 2

The compounds type D and E are adjusted to be flame retardant in several stages, on the basis of water-liberating materials. Their electrical performance is roughly similar to the level achieved by PVC.

Type F is a commercial polymer mixture which offers improved circuit integrity performance, in comparison to the previously mentioned types. But the tensile strength is lower.

Type G has a higher tensile strength, is not flame retardant but offers improved circuit integrity compared with Types D and E, in conjunction with special constructions.
Flame retardation must be provided by specially flameproof sheaths.

The mixtures A, B, C, D and E produce only very little smoke in the fire test. No smoke can be seen at top of test oven (contrary to Fig. 1 for PVC).
The electrical performances may be seen in connection with the cable construction.

## Cable Constructions

Some examples of cable constructions with halogen-free flame retarding material for core insulation and sheath will now be presented and their fields of application and uses will be described. Only a few examples out of the numerous possibilities and conceivable constructions can actually be taken, graded according to fields of utilization.

The cable configurations can be classified as follows:

1) Core flame retardant and sheath flame retardant

2) Core not flame retardant, sheath flame retardant

The use of the new-type flame retardant insulation materials according to 1) leads to generally well-tolerable electrical performances. The characteristics obtained are roughly similar to PVC or better.

With cables insulated according to 2) the high electrical requirements, standard for telecommunication cables, such as line attenuation, characteristic impedance, capacitance, are fulfilled.

When the utilized core insulation is not flame retardant, protection barriers may be required, such as mica films, glass silk taping or

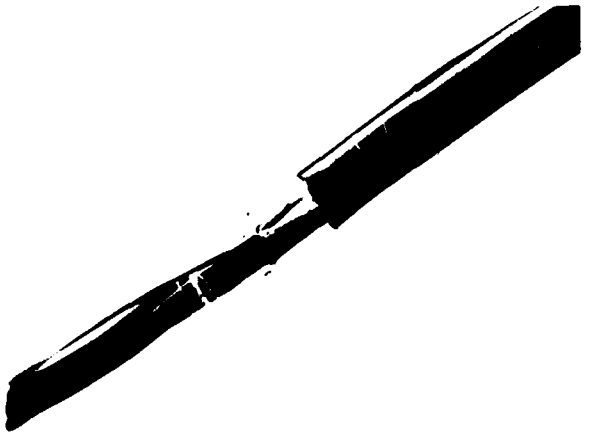
highly flameproof halogen-free inner sheaths from our own development. Metallic shields can also contribute towards improvement of the fire resisting charachteristics. These additional constructional measures also have a positive effect on the emergency operation (circuit integrity) performance of these conductors.

Tables 3 and 4 present some typical cables

Table 3: Overview for halogen-free telecommunication cables

| Running No. | 1 | 2 | 3 | 4 | 5 |
|---|---|---|---|---|---|
| Cable Type | installation cable | | | distribution cable | shipboard cable |
| Copper conductor diam. mm | 0.8 | 0.8 | 0.8 | 0.5 | 0.5 |
| Core insulation wall thickness mm | 0.45 | 0.3 | 0.25 | 0.33 | 0.4 |
| No. of pairs | 16<br>100 | 4 | 16 | 120 | 8 |
| Core insulation type | F | E | F | PE | G |
| Sheath type | B | E | C | C | A |

Figures 2, 3 and 4 show some examples of cables which are described in Table 3.



Installation cable Type 2



Fig. 3: Distribution cable type 4

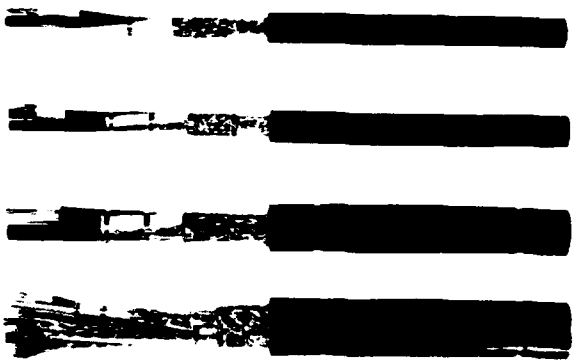


Fig. 4: Various shipboard cables type 5

Table 4: Some examples of low voltage cables

| Running-No. | 6 | 7 |
|---|---|---|
| Cable type | control cable 4-core | low voltage cable 4-core |
| Conductor cross-section $mm^2$ | 1.5 | 35 |
| Insulation wall thickness mm | 1.0 | 1,0 |
| Core insulation type | D | G |
| Sheath type | C | B |

Table 5 presents some results of fire tests and emergency operation tests for the constructions specified in Tables 3 and 4.

Table 5: Fire tests passed by various cable types

| Cable type from tables 3 and 4, running no. | Passed Tests | |
|---|---|---|
| | Fire Tests | Emergency operation (circuit integrity) |
| 1 | IEEE 383<br>VDE 0472/804 C | IEC 331, longer than 30 min.<br>VDE 0472/814 |
| 2 | IEEE 383<br>VDE 0472/804/C | - |
| 3 | IEEE 383<br>VDE 0472/804/C | IEC 331<br>VDE 0472/814 |
| 4 | IEEE 383 | - |
| 5 | IEC 332<br>VDE 0472/804/A | IEC 331<br>longer than 30 min. |
| 6 | IEEE 383<br>VDE 0472/804/C | +) VDE 0472/804/C<br>longer than 20 min. |
| 7 | IEEE 383<br>VDE 0472/804/C | +) VDE 0472/804/C<br>longer than 20 min. |

VDE 0472/Part 804, Test Type A with vertical single test sample and Bunsen burner inclined at 45°, all cables passed this test.

Test Type C: Cable test with several parallel vertical test samples (similar to IEEE 383), but additionally placed in a furnace (see Annex). 3

+) for the electric power cables 6 and 7, the circuit integrity performance was determined in the course of the fire test according to VDE 0472/Part 804 Test Type C.

After having described the construction and the association of the passed fire tests with the various cable constructions, we will now comment on the electrical transmission characteristics of halogen-free cables (according to Table 3). Thereby distinction will be made between installation cables, marine cables and cables for operation at higher frequencies.

Figures 5 and 6 show details of nonhalogenated flame retardant and flame resistent low voltage cables after the flame test.

The ladder is 3.60 m and the oven is 4 m high.



Fig. 5: Lower part of test oven with cable after VDE 0472/804/C-Test, with ribbon burner.
The cable resisted the test. The upper part of the cable jacket is intact until to the top of the oven.

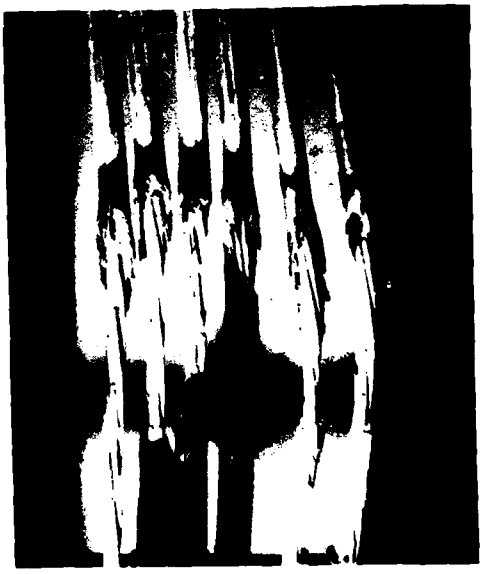


Fig. 6: Enlarged part between 2 lower rungs of the ladder showing another cable after VDE 0472/804/C-flame-test. Above the part (1 ft ) which has been in contact with the flame of the ribbon burner, the cable is intact.

Table 6 compares the electrical requirements for PVC-insulated installation cables with the values measured for two experimental cable types.

Table 6: Comparison of PVC-insulated installation cables with cables according to Table 3 (0,8 mm copper conductors)

| Property | Nominal Values according to VDE for PVC | Actual Values measured for halogen-free cable types Type 1 | Type 3 |
|---|---|---|---|
| Insulation Resistance (MOhm·km) | ≥ 100 | ≥100 | ≥ 100 |
| Mutual Capacitance (nF/km) | ≤ 120 or ≤ 100 +) | 80 | 87 |
| Capacitive Coupling (pF/100 m) | ≤ 300 or ≤ 200 +) | ≤ 50 | ≤ 100 |
| Test Voltage at 50 Hz (V) | 800 or 2000 +) | 2000 | 800 |

+) The first number applies for layer stranding, the second number for unit stranding.

Table 6 shows that the cable types 1 and 3 fulfil the performance requirements demanded for PVC-insulated conductors. Furthermore, considerably improved behaviour in the case of fire is to be expected, than is obtained with conventional cables.

The fields of application for these novel halogen-free cables would be telephone exchanges, skyscrapers, power stations,etc.

Nonhalogenated and flame retarding cables are also coming into use on shipboards,as control cables and as telecommunications cables for regulating and controlling highly sensitive electronic equipments, and they have already proved their value and good performance in these fields. Higher demands are placed on the performance of these cables than is the case for installation cables according to Table 5. Therefore, Table 7 summarizes some electrical characteristics for an 8-pair cable for utilization on shipboards (No. 5 in Table 3).

Table 7: Example of a nonhalogenated flame retarding telecommunication cable for use on ships (construction 8x2x0.75 $mm^2$) *Type 5 Table 3*

| | |
|---|---|
| Insulation Resistance (MOhm · km) | ≥ 200 |
| Mutual Capacitance (nF/km) | 68 |
| Capacitive Coupling (pF/100 m) | ≤ 20 |
| Test Voltage at 50 Hz (V) | 2000 |

So far the performance characteristics of halogen-free cables and conductors for the low frequency operating range have been considered. The electrical transmission performance of nonhalogenated flame retardant cables for coil loading of cable runs and at higher frequencies (like carrier frequency service or pulse code modulated systems) will now be examined.

The Figures 7 and 8 show the line attenuation and the characteristic impedance of some cables with special flame retarding cores according to Table 3, as a function of the operating frequency. For comparison, the curves for a (non flame retardant) local cable A-2Y(L)2Y ... 0.8mm with solid PE insulation are shown.

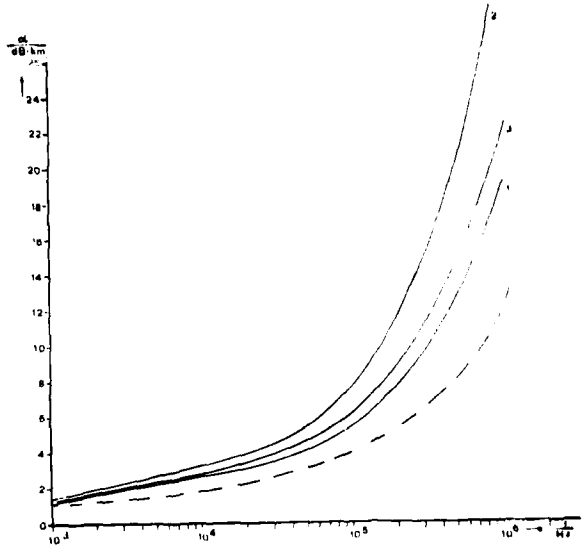


Fig. 7: Line attenuation of flame retardant, halogen-free telecommunication cables (Type 1, 2 and 3) in comparison with local cable (- - - -) with 0.8 mm conductor diameter.

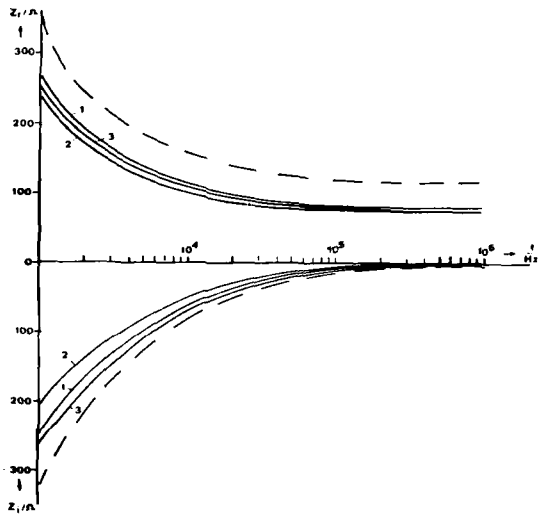


Fig 8: Characteristic impedance of halogen-free flame retardant cables (Type 1, 2, 3 of Table 3) in comparison with local cable (----) with 0.8 mm conductor diameter.

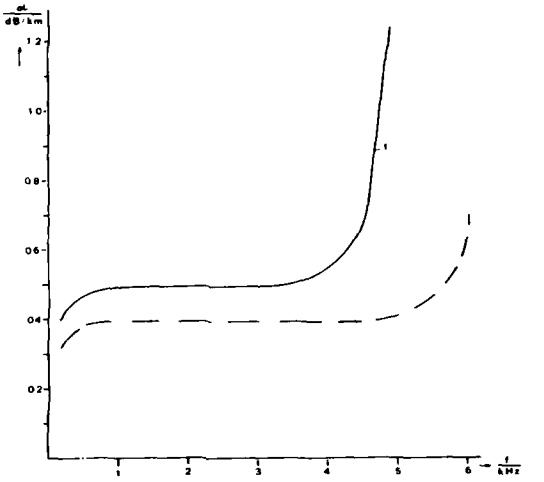


Fig. 9: Line attenuation of a flame retardant cable (Type 1 of Table 3) in comparison with a local cable (- - - -) with 0.8 mm conductor diameter.

It is found that the line attenuation is greater than for conventional local cables, on account of the relatively large mutual capacitance.
As *an example (cable 1), a determination* is to be made whether a bandwidth of 300 to 3400 Hz can be transmitted by coil-loaded halogen-free cables. A side circuit loading of 40 mH and a loading section of 1.275 km is thereby taken as basis.

Figures 9 and 10 show the line attenuation and the characteristic impedance of a coil-loaded cable run compared with a local cable. The cut-off frequency is found to be 4850 Hz for cable 1. This cable could be used along underground railway runs, in tunnels and for telephony links in regions subject to particularly high fire hazard, since it is seen that bandwidths according to CCITT can be transmitted with acceptable values for the coil and field lengths.

Furthermore, with digitalization of telephone networks in mind, the behaviour of halogenfree, flame retardant cables must be considered at higher frequencies up to 1MHz. Since these cables would be installed only on short distance runs as distribution cables in telephone exchanges, the relatively high line attenuation (Fig. 7) does not have any practical implication.

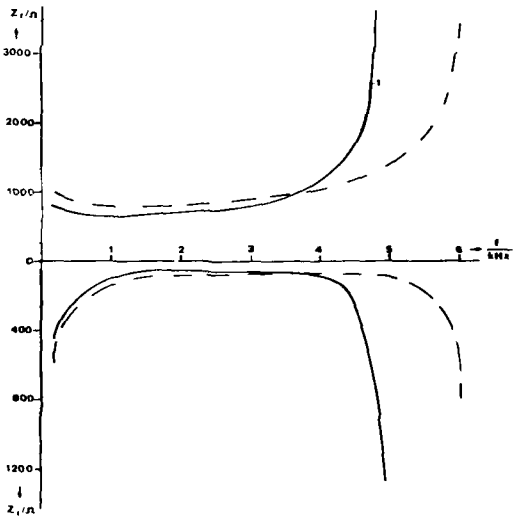


Fig. 10: Characteristic impedance of a flame retardant cable (Type 1 of Table 3) in comparison with a local cable ( - - - -) with 0.8 mm conductor diameter.

The electrical discontinuities due to differing characteristic impedances, leading to signal reflections, can be tolerated too, as experiments have shown.

With suitable chosen pitches, for example the following crosstalk attenuations have been achieved for cable 5:

| | 108 kHz | 252 kHz | 1 MHz |
|---|---|---|---|
| $\bar{a}_n$/dB | 75 | 69 | 65 |
| $\bar{a}_f$-a/dB | 78 | 74 | 63 |

$\bar{a}_n$ = near end crosstalk (NEX)

$\bar{a}_f$ = far end crosstalk (FEX)

The length of this experimental cable was about 500 m. The results show that high crosstalk attenuation is achieved, in spite of only simple shielding - copper braiding around the pairs and the mineral-filled insulation (type G) employed for other reasons.

In cases in which it is desired to achieve local cable quality or still higher electrical performance, then at present the core insulation is made in conventional PE or cellular PE quality. The cable sheath must then be particularly effectively flame retardant, in order to fulfil the requirements of the fire tests. Cable 4 from Table 3 can be cited as an example. This is a distribution cable with PE core insulation, aluminium shield (0.2 mm thick) and a type C flame retardant sheath. The advantage of this cable, compared with the previously discussed cables, is the lower line attenuation.

Any discussion of a larger number of electric power cable types (of which only two types, No. 6 and No. 7, are mentioned in table 4), would be outside the scope of this paper with regard to available time and selected contents. Therefore a detailed report on these cables will be given at some other suitable occasions.

## Conclusions

Special compounds have been developed for cables and insulated conductors which give at least equally good flame retardation as obtained with conventional PVC or polychloroprene rubber coated cables in case of fire, when used in properly designed cables, with the advantage that in case of fire, no corrosive substances such as hydrogen chloride are set free by these cables. Furthermore, emergency operation capability in the case of fire (30 minutes and longer) can be achieved where necessary. The electrical and mechanical characteristics are adapted to suit the particular application in any given case. Most of the cables are flame resistent.

Thus a range of halogen-free flame retarding cables is available for diversified applications. Some of these have already been proven in practical utilization, but of course further development must still be carried out even on these types.

Examples of possible fields of utilization are skyscrapers, power stations, telephone exchanges, pits, mining, tunnels, transport installations such as underground railways and ships. Also regions in which human beings and equipment would be endangered in case of fire outbreak. The advantages of flame retardation, very small smoke generation - important for escapeways - and the absence of set free corrosive pyrolysis products, are important aspects.

## Acknowledgements

The authors wish to express their thanks and to acknowledge the contribution of Mr. H. Briem, Mr. B. Ivanfy, Mr. W. Krestel, and Mr. W. Muno in the development of nonhalogenated compounds, and of Mr. D. Kaubisch in testing the cables.

## Appendix

Flame retardation according to VDE 0472 Part 804 Test Type C

The test method essentially consists of a test set-up with conductors fixed on a ladder and a propane gas burner as specified in IEEE 383 in a vertical test furnace, similar to a furnace according to SEN, in which the test samples are mounted mutually parallel.
Controlled throughput and temperature of air access is used.
The test duration is 20 minutes. The test is considered to have been passed, as long as the test samples do not burn out right up to the end of the conductor. Additionally we have determined the emergency operation behaviour in this test set-up.

### Corrosive Properties of Pyrolysis Fumes according to VDE 0472, Part 813

This is an indirect determination of the corrosive properties of the fire fumes and pyrolytically released gases (at 800°C) from cable sheathings, by measuring the pH-value and the electrical conductivity of their aqueous solutions.
The test is considered to have been passed if the pH-value is at least 4 and the specific electrical conductivity is $<100\ \mu S/cm$.

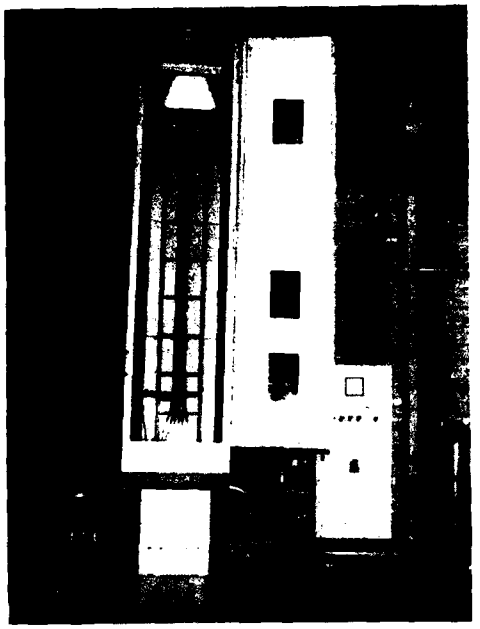


Fig. 11: Fire Test Furnace, opened



Fig. 12: Fire Test Furnace, closed



Hans A. Mayer
(Speaker)

AEG-TELEFUNKEN KABELWERKE AKTIENGESELLSCHAFT
270-276 Wanheimer Str., 4100 Duisburg 1
W. Germany

1951-1956 he studied industrial chemistry and obtained his degree as a Dipl.-Ing. He was 5 years in the plastics&rubber and 3 years in the organic chemical industry as Head of quality control and central laboratories.

In 1965 he joined AEG-TELEFUNKEN KABELWERKE He is an Oberingenieur and Head of the Departments of Materials&Process Development



Georg Hög

AEG-TELEFUNKEN KABELWERKE AKTIENGESELLSCHAFT
2-14 Bonnenbroicher Str.
4050 Moenchengladbach 2
W. Germany

As a Dipl.-Ing. of the Technische Hochschule Aachen, he joined AEG-TELEFUNKEN KABELWERKE in 1977 as an engineer in the Department of Symmetrical Cables.

## LITERATURE

1) Wire and Cable Considerations in Fires Tutorial- 24. IWCS -Cherry Hill 1975

2) O. Leuchs - New Flame Self-Extinguishing Chlorine Binding PVC Jacketing Compound for Cables, 19. IWCS, Atlantic City 1970

3) VDE-Specifications 0472, Parts 804,813,814.

# NEW FLAME RETARDANT HALOGEN-FREE CABLES FOR NUCLEAR POWER PLANTS

Hans Harbort

Standard Elektrik Lorenz AG

Stuttgart, Germany

## Abstract

Special halogen-free cables for installation in nuclear power plants have been developed, manufactured and installed. These cables are characterized by special flame retardant versions of crosslinked polyethylene for insulation, crosslinked EPDM/EVA for sheathing and mineral type flame barriers. Control and power cables provide specified and/or customer demanded performance in all aspects relevant to installation in nuclear power plants as for example flame retardance, freedom from corrosive combustion products, high radiation resistance, functional endurance and LOCA test.

## Introduction

15 years ago the general opinion was, that PVC was the most suitable material for in door cable insulation and sheathing; this was the true situation in comparison to the materials that were used before. During the last 10 years the concern for safety aspects in cable installations has increased. This can also be seen in the increasing number of contributions to this symposium dealing with safety problems. Besides a series of fire hazards in different installations (for example telephone switching office, power station, factory, hospital) has accelerated safety considerations in cable design and installations.[3]
The main emphasis so far has been on reducing flame propagation along cables, and in reducing damage to expensive equipment caused by corrosive combustion products. The development started from PVC compounds with reduced chlorine generation in case of fire compared with flame retardant PVC versions,[1,2] via reduced chlorine containing polymers to halogen-free but flame retardant materials which is the present stage of development. From the side of the cable users we see a very strong trend towards halogen-free cables and we find increasing interest in additional safety properties such as low smoke generation and functional endurance in case of fire.

## Special cable properties for nuclear power plants

Installations for power generation are becoming more complex and powerful and the dependence of society on these installations, together with the necessary reliability, is continually increasing. Nuclear power stations are even more complex and powerful and have to meet extremely high safety requirements caused not only by nuclear technology but also by the growing public interest. In comparison to the general safety properties of cables as described below additional requirements for nuclear power plants are:

Table 1:

| SAFETY PROPERTIES | |
|---|---|
| General Requirements | • Flame retardance<br>• No corrosive residues<br>• No toxic residues<br>• Low smoke generation<br>• Low calorific value |
| Additional Requirements For Nuclear Power Stations | • Radiation resistance<br>• LOCA-Test<br>• Functional endurance<br>• Operating temperature 90°C |

So far very few standards exist to describe appropriate test procedures and limiting values, but standardizing activity is starting in many countries, for example in W-Germany.

• LOCA means: Loss of Coolant Accident, which is the most severe event in a nuclear power plant.

Typical test requirements are in analogy to IEEE 383/74 and IEEE 323/74:

7 days thermal aging at 15o°C
+
5o Mrad γ- radiation
} for simulation of the normal cable life

and

5 hours 17o°C
2 days 16o°C
2 days 12o°C
} steam + boric acid

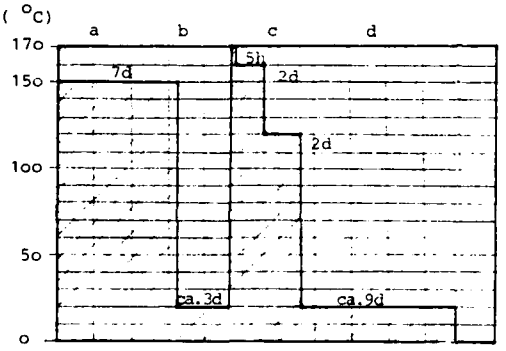
+

15o Mrad γ- radiation

} for simulation of the LOCA event

which means that cable materials have to withstand temperature and steam up to 17o°C and γ-radiation up to 2oo Mrad.

Figure 1:




LOCA Test

a) thermal aging

b) radiation 5o Mrad

c) temperature, steam, boric acid

d) radiation 15o Mrad

- Functional endurance over a certain time is extremely important to allow controlled switch-off in case of fire. While it is relatively easy to achieve a functional endurance of 2o minutes with thick wall insulated power cables, it is difficult to achieve such values with thin wall insulated control cables. So far, very few test specifications exist in the world and specification values are only under discussion with cable users. There is evidence however, that future specifications will at least demand 8oo°C endurance for 2o minutes. Functional endurance demands crosslinked materials, at least for insulation, because thermoplastic materials melt before they burn and cause early short circuits. As all carbon containing materials (for example PE, PVC, EPDM) tend to form carbon bridges in the residues of the burned insulation, long functional endurance can only be achieved with a carbon-free wire coating (for example silicone or mica tape).

- High operational temperature (9o°C) is required for cables inside the reactor. This requires tinned conductors in case of PE based insulation.

Summing up, we find the following minimum requirements for cables for nuclear power plants:

- Flame retardancy
- Freedom from corrosive material components
- Functional endurance 8oo°C > 2o minutes
- Radiation resistance >2oo Mrad
- Operation temperature >9o°C
- Pass LOCA-Test
- Normal service properties
- Normal installation properties (for example termi point)

## Materials

The properties listed above limit the range of materials and design parameters, which can be employed.
As indicated below there are very few materials meeting all the requirements:

- PVC fails because of poor radiation resistance, thermal overload, chlorine content and functional endurance.

- PE and PP are not sufficiently flame resistant, are not radiation resistant, and do not provide functional endurance.

- TPUR is highly radiation resistant, but not flame resistant.

- The fluoro polymers are normally not acceptable because of their fluorine content, but in addition:

  - ETFE (Tefzel) fails on functional endurance.

  - Teflon FEP and PFA are not radiation resistant.

- If we consider crosslinked (elastomeric) materials we find that:
  - normal crosslinked PE fails because it is not sufficiently flame retardant (LOI ~22)
  - Silicone rubber is extremely expensive and not sufficiently radiation resistant
  - normal EPDM and EVA are not flame retardant (LOI 22 only).

Table 2:

Material Rating
General Requirements

| | Material | LOI | Flame retardance IEEE 383 | Corrosive products |
|---|---|---|---|---|
| Thermoplastics | PVC spec. | 35 | yes | yes |
| | PE | <22 | no | no |
| | PP | <22 | no | no |
| | TPUR | 2o - 24 | no | conditional |
| High temperature polymers | ETFE | 3o - 35 | yes | yes |
| | FEP | >95 | yes | yes |
| | PFA | >95 | yes | yes |
| | PI (Polyimide) | >36 | yes | conditional |
| Cross-linked materials | CR | 3o - 35 | yes | yes |
| | CSM | 3o - 35 | yes | yes |
| | XLPE | <22 | no | no |
| | XLPE spec. | 25 - 3o | yes | no |
| | EPDM | <22 | no | no |
| | EVA | <22 | no | no |
| | EPDM spec. | 26 - 35 | yes | no |
| | SIR | 3o - 35 | yes | no |

Table 3:

Material Rating
Requirements For Nuclear Power Stations

| Material | Functional endurance 2o minutes | Radiation resistance 2oo Mrad | Thermal overload 17o°C | LOCA Test passed | Operating temperature 9o°C |
|---|---|---|---|---|---|
| PI(Polyimide) | no | yes | yes | yes | yes |
| XLPE spec. | limited } app. | yes | yes | yes | yes |
| EPDM spec. | limited } 8min | yes | yes | yes | yes |
| Silicon rubber | yes | no | yes | no | yes |
| XLPE spec. (sandwich) | yes | yes | yes | yes | yes |

Materials remaining are: Polyimide (PI) which is doubtful on functional endurance and which is extremely expensive and only available in the form of film suitable for wire insulation but not for sheathing, and special versions of crosslinked PE and elastomers (EPDM).
These are highly filled materials, with improved flame retardance, and in the case of XLPE also improved radiation resistance. The electrical and mechanical properties of the insulation and sheathing materials are of course not as good as in the case of pure polymers, because of the high filler content, but still within relevant specification requirements (for example VDE).

## Cables

After an initial basic materials evaluation , special flame and radiation resistant compounds based on

highly filled crosslinked PE
and
highly filled elastomers (EPDM based)

have been developed and tested with the following results.

| | Insulation | Sheathing |
|---|---|---|
| - LOI | 28 | 3o |
| - Operating temp., 4o years | 9o°C | 9o°C |
| - Radiation resistance | 2ooMrad | 2ooMrad |
| - Calorific value | 2o MJ/kg | 2o MJ/kg |
| - Electrical and mechanical properties | within relevant standard specifications | |

These final compounds have been used to produce control and power cables with the following general constructional elements:

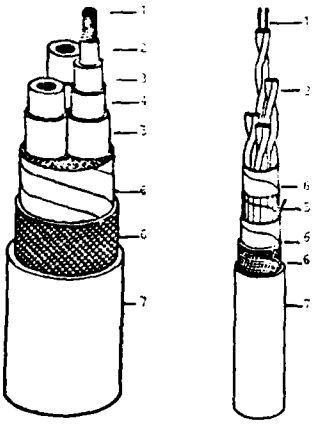
a) Control cables

- tinned copper conductors (stranded)
- flame/radiation resistant special XLPE insulation (wall thickness o,33 mm). For longer functional endurance mica tape + XLPE or silicone + XLPE sandwich type insulation is used
- pairs, triples, quads, or screened quads constructions
- helically or unit stranding
- flame retardant mineral (for example woven glass) tapes as a flame barrier
- flame/radiation resistant special EPDM outer sheath.

b) Power cables

- tinned stranded conductors 1,5 to 2ooo $mm^2$
- flame/radiation resistant special XLPE insulation (wall thickness > o,5 mm)
- 3 to 7 conductors stranded together
- flame retardant mineral (for example woven glass) tapes as a flame barrier
- flame/radiation resistant special EPDM outer sheath.

Figure 2:



Power and Control Cable for Nuclear Power Station

1. Tinned conductor
2. Semi-conducting layer
3. Special XLPE insulation
4. Semi-conducting layer
5. Screen
6. Flame barrier
7. Outer sheath

The most important properties of the finished cables are:

| | | control ($\leq$2,5 $mm^2$) | power ($\geq$2,5 $mm^2$) |
|---|---|---|---|
| Mutual Capacitance | nF/km | app 1oo | - |
| Crosstalk attenuation 1/6o kHz | dB/km | 11o/9o | - |
| Insulation resistance (2o°C) | MΩ · km | 2oo | 2oo |
| Operational temperature, 4o years | °C | 9o | 9o |
| LOI | | >28 | >28 |
| Functional endurance IEE 331 VDE o472 §814 draft | minutes | 5 to 15 | >15 |
| Flame retardance IEEE 383 EDF-oven VDE 472 §8o4 draft | | pass | pass |
| Radiation resistance | Mrad | >2oo | >2oo |
| Thermal overload 17o°C, 5 hours | | pass | pass |
| Low smoke (qualitative only) | | pass | pass |
| LOCA in analogy to IEEE 383/74 IEEE 323/74 | | pass | pass |

These cables have been approved by two German approval authorities (TÜV), and have been installed inside and outside the reactors of two nuclear power stations (Mülheim Kärlich in Germany and Doel III in Belgium).

## Outlook

While so far most existing nuclear power plants have beeen equipped with cables using "conventional" materials and designs, future installations will, for safety reasons, use special cables with specifications as described, but possibly more stringent on one or more properties. There is for example evidence that the functional endurance will be increased to ≥2o minutes at 8oo°C. This could lead to a different insulation system for the small diameter control cable conductors.

## References


1. A New Self-Estinguishing Hydrogen Cloride Binding PVC-Jacketing for Cables
   O. Leuchs 19. JWCS 197o

2. Flame Retardant PVC for Insulation and Cable Sheathing
   K. Grill, H. Geisler, H. Harbort
   Electrical Communication Vol. 5o No. 3 1975

3. Der Brand der Telefonzentrale Zürich Hottingen
   H. Werder, M. Wütherich
   PTT-Techn. Mitteilungen 197o, page 522 - 533 and 536 - 547

4. IEEE Standard 383/74

5. IEEE Standard 323/74





Hans Harbort
Standard Elektrik Lorenz AG
Hellmuth-Hith-Str. 42
7ooo Stuttgart 4o, Germany


H. Harbort received his Dipl.-Ing. degree in electrical communication and high frequency engineering from the Technical University of Hannover. He joined Standard Elektrik Lorenz AG in 1961 and is now manager of research and development of SEL's cable division.

# A NEW NON-HALOGENATED FLAME RETARDANT WIRE INSULATION BASED ON POLYPHENYLENE OXIDE

H. de Munck — General Electric Plastics, Bergen op Zoom, Holland.

J.R. Bury, W.E. Simpson — Standard Telecommunication Laboratories, Harlow, Essex, England.

J.A. Devoldere — Bell Telephone Manufacturing Co., Ghent, Belgium.

## SUMMARY

An increasing need for low aggressivity flame retardant polymeric materials for use on insulated wires, cables and associated electrical equipment has led to the development of a non-halogenated wire insulation based on a modified polyphenylene oxide. The basic materials development has involved the formulation of a compound having the required melt rheology and thermal and oxidative stability for processing as thin-wall wire insulation at high extrusion speeds. The product of this development, now coded NORYL FX 1700, is characterised by a high degree of flame retardance, low evolution of aggressive fumes on burning, and good mechanical and electrical properties over a broad temperature range. Applications are envisaged as a replacement for PVC and other halogenated polymers in switchboard cables, back panel wiring of electronic exchanges, equipment wiring, miniwires, and industrial cables.

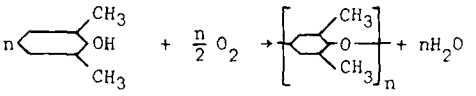
## INTRODUCTION

During the past few years a need for improvements in flame retardant polymers has become increasingly apparent in many application areas, particularly that of wires, cables and associated electrical equipment. Earlier work in this field was primarily directed towards a reduction in material flammability characteristics, especially those controlling the resistance to ignition and subsequent fire propagation. Progress in this area was mostly achieved through the use of halogenated polymers or by the incorporation of halogenated flame retardant additives. More recently there has been increasing concern regarding the corrosive nature of gases evolved from these halogenated materials when subjected to high temperatures in the vicinity of a fire or actually involved in a fire. This problem has been particularly highlighted in a number of instances of fires in telephone exchanges where serious damage to exchange equipment has resulted from the corrosive action of hydrochloric acid produced by the decomposition and combustion of PVC wire insulation. This type of experience has led to intensified activity during the past few years on the development of improved flame retardant polymers, with special emphasis on the elimination of halogens and consequent reduction in the evolution of corrosive or aggressive fumes, should the materials be involved in a fire. This trend is reflected in the introduction into several specifications, e.g. French CNET, ASTM and IEC, of tests designed to measure the corrosivity or aggressivity of the fumes evolved from polymeric materials when undergoing heating and combustion under controlled test conditions.

With the requirement of low aggressivity principally in mind a collaborative project has been undertaken by ITT and General Electric Plastics to develop a non-halogenated flame retardant wire insulation based on modified polyphenylene oxide.

## DEVELOPMENT OF WIRE INSULATION COMPOUND

Modified polyphenylene oxide under the trade name of NORYL was introduced about 15 years ago by General Electric and is now commercially available in a range of flame retardant injection moulding and extrusion grades. Many of its desirable properties are derived from the basic polyphenylene oxide structure. The polymer is obtained by the oxidative coupling of 2,6 - dimethylphenol in the presence of a suitable catalyst such as a cuprous salt and tertiary amine.



The basic polymer is however rather difficult to process by normal methods, and NORYL technology is essentially based on intimately blending the polymer with elastomeric deformation modifiers, flame retardants, stabilisers etc. The development of a suitable composition for application as wire insulation in cables has involved a number of significant changes in the design of the compound in order to satisfy the following requirements:

(1) Flame retardant with a Limiting Oxygen Index not less than 30.

(2) Polymer and additives to contain no halogens.

(3) Flame retardance to be achieved without the addition of fillers.

(4) Low aggressivity when tested by currently used test methods, e.g. French CNET test UTE C 204 53.

(5) Extrudable as thin-wall insulation on small diameter conductors at high line speeds, e.g. up to 2000 m/min, using standard extrusion equipment.

(6) Extruded insulation to have adequate mechanical and electrical properties to meet relevant insulated wire specifications, e.g. for jumper wire, equipment wire, etc.

(7) Satisfactory level of mechanical and electrical properties to be retained over a useful service temperature range, e.g. -20°C to + 100°C.

(8) Compound to have adequate thermal and oxidative stability to withstand processing and subsequent service conditions.

The attainment of all these objectives in a single compound has presented a considerable challenge to the polymer chemists, and has involved a development programme extending over about three years. During this period a series of compounds has been prepared, characterised, and evaluated for processing behaviour as thin-wall wire insulation and for product quality when processed in this form. The programme has involved systematic and continuing improvement to various properties of the compound and has culminated in the introduction of a material which substantially meets all the requirements listed above. This product, now coded NORYL PX 1700, has now satisfactorily progressed from pilot scale to full production scale manufacture.

NORYL PX 1700 is essentially an intimate blend of polyphenylene oxide with elastomeric deformation modifiers, processing aids, stabilisers and flame retardants based on phosphate esters. The more important characteristics of the material are discussed in the next section.

## COMPOUND CHARACTERISATION

### Rheological Properties

Capillary rheometry has been used to study the melt flow properties of PX 1700 and their significance in relation to high speed wire coating. The dependence of melt viscosity on temperature and shear rate has been measured, and the results related to extrudate quality. Figure 1 shows typical melt viscosity/temperature plots at two shear rates and indicates the temperature regions in which smooth extrudates are obtained. The considerable dependence of melt viscosity on shear rate is confirmed by the data shown in Figure 2, and in this respect it should be noted that shear rates encountered in high speed thin wall wire insulation processes may well be in excess of $10^5$ $s^{-1}$.

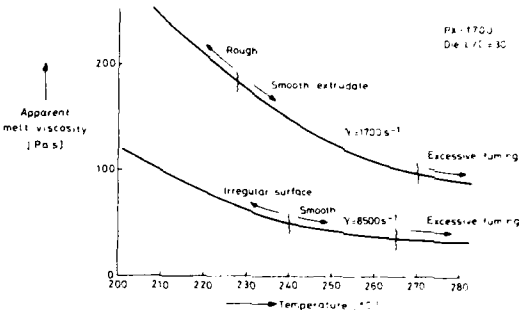



Fig 1 Melt viscosity / temperature dependence

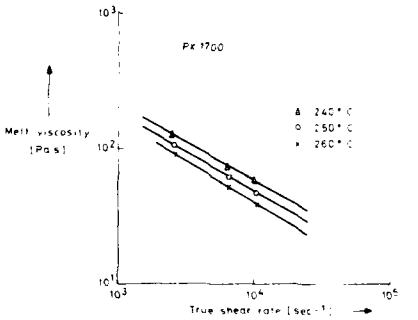



Fig 2 Melt viscosity/ shear rate dependence

In Fig. 3 a comparison is made with a typical high speed PVC insulation compound; it is seen that PX 1700 requires a 65-70°C higher temperature than the PVC compound in order to reach a comparable melt viscosity. The rate of change of viscosity with temperature, and hence the operating temperature range within which an acceptable product would be expected, is approximately the same for the two materials.

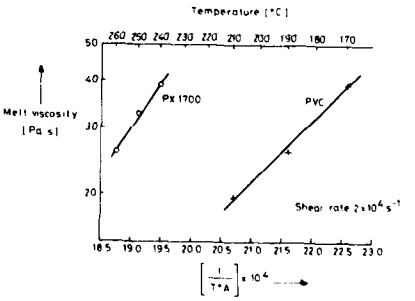



Fig 3 Melt viscosity / temperature dependence for PX1700 and PVC

## Oxidative and Thermal Stability

Ageing tests on the early experimental insulation grades indicated a possible deficiency in oxidative stability. This was taken into account in the later development and refinement of the compound. In particular a marked improvement in oxidative stability resulted from the replacement of unsaturated by saturated deformation modifiers and through the use of improved stabilisers. This is readily apparent from Figure 4 in which oxygen uptake at 124°C is shown as a function of time for earlier experimental compounds in comparison with the final PX 1700 material.

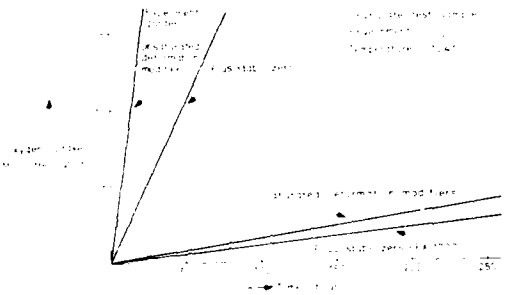


Fig 4 Oxidative stability of NORYL insulation compounds

The ageing behaviour of PX 1700 insulated wire samples at 80°C is discussed in a later section of the paper. The temperature rating according to Underwriters' Laboratories procedures (extrapolation to 100,000 hours) of similar saturated products to PX 1700 is estimated to be in the range 95-100°C.

## Mechanical Properties

Formulation of a polyphenylene oxide type compound for use as a wire insulation has required the incorporation of two types of deformation modifiers in order to achieve the required balance of mechanical and physical properties. In the first case an intimate dispersion of an elastomeric modifier in the polymer matrix is used to provide good resistance to crazing and stress cracking by a mechanism of multiple initiation and craze arrest. A second modifier which is considered to act synergistically provides improved bulk flow or shear deformation properties, resulting in a satisfactorily high elongation of up to 150% in the compound.

The dependence of the mechanical properties of the compound on temperature was determined using a Du Pont 980 Dynamic Mechanical Analyser. Young's Modulus and mechanical damping are plotted in Figure 5 as a function of temperature over a range of about -100°C to +120°C, and a comparison is made with a typical commercial grade of hard PVC insulation.

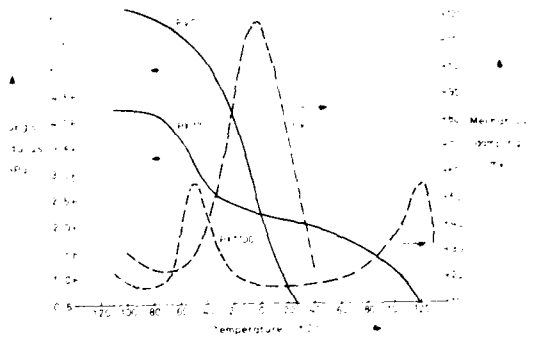


Fig 5 Temperature dependence of mechanical properties

It is seen from Figure 5 that the tensile modulus of PX 1700 remains at a reasonably high level up to about 100°C and shows no drastic change with temperature down to about -40°C, the 100°C modulus being approximately 50% of that at -40°C. The peaks in the damping curve at -50°C and 121°C correspond to the glass transition temperature ($T_g$) of the elastomeric modifier and resin matrix respectively. In contrast the marked temperature dependence of the modulus of the PVC compound having a $T_g$ of -3°C is readily apparent.

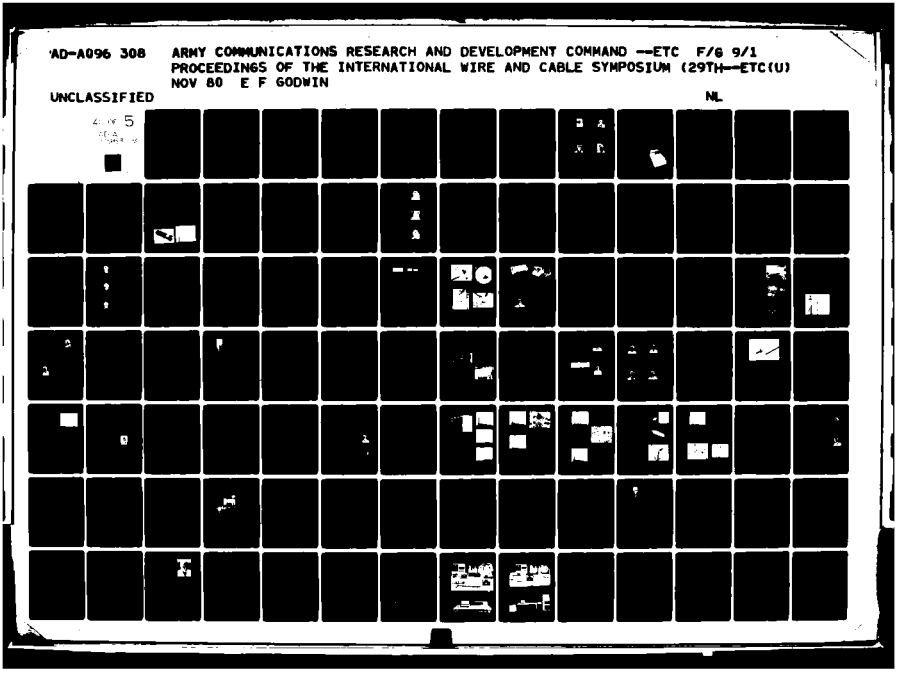
In connection with $T_g$ values it is of interest to note that the polyphenylene oxide chain structure is characterised by stiff molecular segments of aromatic rings joined by ether linkages and sterically hindered by the attached methyl groups. This results in a low chain segment mobility which is reflected in a high $T_g$ of about 190°C for the unmodified polymer. Addition of processing aids in PX 1700 reduces this to about 120°C for the polymer matrix.

## Electrical Properties

Since the polyphenylene oxide structure has no polar groups and is built up from stiff symmetrical molecular segments, its permittivity and dielectric loss are relatively low over a broad frequency and temperature range. The frequency dependence of these parameters is shown in Figures 6 and 7 where a comparison is made with a typical hard PVC insulation grade and with TEFZEL ethylene/tetrafluoroethylene copolymer as used for high performance wire insulation. It is seen that the dielectric properties of PX 1700 are much superior to those of PVC and close to those of TEFZEL.

AD-A096 308 ARMY COMMUNICATIONS RESEARCH AND DEVELOPMENT COMMAND --ETC F/G 9/1
PROCEEDINGS OF THE INTERNATIONAL WIRE AND CABLE SYMPOSIUM (29TH--ETC(U)
NOV 80 E F GODWIN

UNCLASSIFIED NL



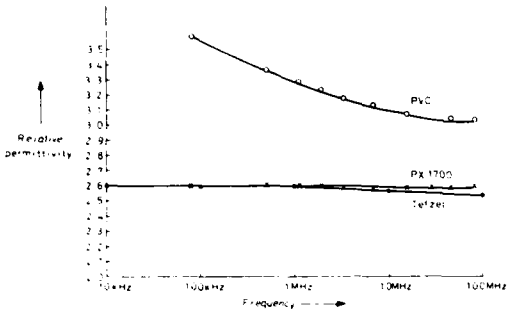



Fig 6 Frequency dependence of permittivity

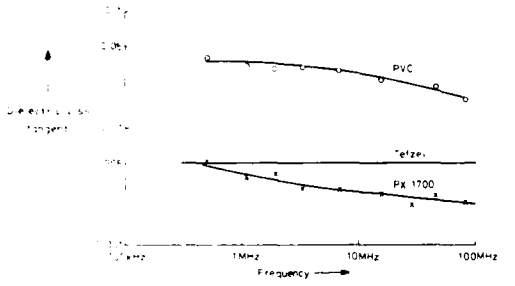



Fig 7 Frequency dependence of dielectric loss tangent

## Flammability

Due to the relatively low hydrogen to carbon ratio in the polyphenylene oxide structure the Limiting Oxygen Index is fairly high at 28-29. Furthermore the low content of hydrogen, which has a high heat of combustion, contributes to a lower flame temperature on burning. Addition of deformation modifiers and processing aids reduces the Limiting Oxygen Index, and this has necessitated the incorporation of additional non-halogenated flame retardants to achieve a value of 31-32 in the final compound. Attempts to determine the Temperature Index of the material, i.e. the temperature at which the Oxygen Index falls to 21, have indicated a value in excess of 300°C (Oxygen Index at 300°C still about 29).

When subjected to the Underwriters' Laboratories burning test as described in UL 94, the material is classified as 94V-1 when tested at 1.6 mm thickness and 94V-0 at 3.2 mm thickness. The compound tends to form a char without dripping when burned; this is beneficial in reducing flame propagation.

A particular advantage of NORYL PX 1700 is the virtual absence of corrosive gases in the products released during combustion. The French CNET has developed a test procedure, detailed in UTE C204 53, in which the so-called aggressivity rating of a material is measured by the effect of the products of combustion on the electrical resistance of a fine copper wire spiral, a maximum change of 20% being allowed. Under these test conditions PX 1700 shows a resistance change of 1.5% indicating an extremely low aggressivity rating. When tested for smoke evolution using the NBS Smoke Chamber, the following figures have been obtained for $D_m$, the Maximum Specific Optical Density.

Smouldering Conditions: $D_m$ = 210 at 28 minutes

Flaming Conditions: $D_m$ = 550 at 4 minutes

## Chemical Resistance

Because of its polyether type structure, polyphenylene oxide shows good resistance to aqueous bases and acids and to many organic solvents. PX 1700 insulated wire samples show no visual evidence of chemical attack after immersion in the following chemicals for one hour at ambient temperature.

Concentrated sulphuric acid
Nitric acid, S.G. 1.2 (approx. 32%)
10N sodium hydroxide solution
10N potassium hydroxide solution

Immersion as above in the following solvents showed no evidence of cracking of the insulated wire samples:

Methyl alcohol
Gasoline
Lubricating oil
Freon
Isopropyl alcohol
Perchloroethylene
Butyl acetate
Acetone

Due to its low polarity, the water absorption of polyphenylene oxide is very low, the equilibrium value for the unmodified polymer being 0.08% at room temperature. A similar value is obtained for PX 1700. This low moisture uptake is reflected in good retention of electrical properties when exposed to aqueous environments.

## PROCESSING AS THIN WALL WIRE INSULATION

### Extrusion Equipment

Extruder As indicated earlier in the paper an important requirement is that the material can be processed on standard thermoplastic extrusion equipment as designed for wire coating. Also that the polymer is non-corrosive in the hot molten state, thereby avoiding the need for using special and expensive materials in the construction of the barrel and screw.

PX 1700 has been satisfactorily processed on a range of extruders varying in size from 25 mm to 63 mm, and with $\frac{L}{D}$ ratios from 20:1 to 24:1.

Screw design There is no evidence at present that screw design is critical. Gradual transition type screws have been successfully employed with compression ratios varying from 1.75:1 as used for plasticised PVC to 3.5:1 as used for polyethylene.

Diehead design Pressure extrusion has been mainly used, and successful results obtained with several different diehead designs. As with most high speed wire insulation it is necessary to ensure that the diehead and tooling design promotes streamline flow of the polymer melt. A die land length of about five times the diameter is preferred.

Insulation of very small diameter conductors, e.g. 0.3 mm and below, is normally carried out using a tubing-on technique with a draw-down ratio of up to 10:1.

Instrumentation The use of modern thyristor controlled heat/cool systems for close temperature control on the barrel and diehead is necessary for high line speed operation. The provision of melt temperature and pressure monitoring equipment is advantageous. Control of insulation diameter requires sensitive indicating and control equipment in order to maintain product quality under high line speed conditions.

## Extrusion Conditions

Predrying Although the necessity for predrying the granular feedstock is not conclusively proven, the best results to date have been obtained using predried material. A drying cycle of 2-4 hours at 70°C with or without vacuum appears to be adequate.

Conductor preheat This is normally necessary in order to achieve a satisfactory combination of insulation elongation and adhesion to the conductor. Depending somewhat on conductor size, a preheat temperature of around 100°C is recommended.

Melt temperature Confirming the conclusions from the rheological investigations, a melt temperature of 240-250°C as measured at the extruder diehead has been found to give satisfactory extrudates. A typical barrel temperature profile increases from 150-160°C at the hopper to around 300°C at the diehead.

Melt pressure Using relatively small dieheads as normally designed for the insulation of telephone singles a typical value of melt pressure as measured at the diehead is around 35 $N/mm^2$ (5000 $lb/in^2$) when running at high line speeds.

Line speed Speeds of up to 2000 m/min have been successfully employed for the thin wall insulation of 0.5 mm and 0.4 mm conductors using a pressure extrusion technique. The insulation of smaller size conductors, i.e. 0.3 mm and below will normally necessitate the use of a tubing-on technique; under these conditions line speeds of up to 800 m/min have been employed.

Extrudate cooling As is normal when insulating small size conductors the main extrudate cooling consideration is the need to avoid excessive drag and resulting tension build-up during passage through the water cooling trough. Equipment specifically designed for this purpose is now available.

Fume extraction During extrusion some fuming occurs immediately the extrudate emerges from the diehead, and for production scale operation the provision of adequate extraction in this region is necessary. Analytical examination of the gases evolved when NORYL type compounds are subjected to normal processing temperatures has however shown that these fumes do not present a toxicity hazard.

Pigmentation Colourant masterbatches are not at present available for NORYL but pigmentation of wire insulation has been satisfactorily achieved using commercially available colour concentrates in the form of flakes or bars. These are added to the feedstock at a controlled rate using suitable dispensing equipment. The colour concentrates, containing a major proportion of powdered pigment and a minor proportion of polymeric binder, have been shown to have good compatibility with PX 1700 and have provided the necessary range of colours for most cable types.

Summarising this discussion of processing parameters, typical extrusion conditions employed for the insulation of 0.5 mm plain copper conductor with 0.2 mm radial thickness of PX 1700 are listed below. They refer to the use of a 63 mm extruder having a barrel $\frac{L}{D}$ of 24:1 and fitted with a screw of compression ratio 3.5:1

| | |
|---|---|
| Die diameter: | 0.90 mm |
| Point diameter: | 0.53 mm |
| Extruder set temperatures: | |
| Zone 1 | 160°C |
| Zone 2 | 190°C |
| Zone 3 | 220°C |
| Zone 4 | 250°C |
| Zone 5 | 280°C |
| Diehead | 300°C |
| Melt temperature: | 250°C |
| Melt pressure: | 35 $N/mm^2$ |
| Screw speed: | 30 rpm |
| Motor current: | 65 A |
| Conductor preheat: | 100°C |
| On-line conductor elongation | 1.0% |
| Line speed: | 1000 m/min |

## PROPERTIES OF INSULATED WIRE

A range of insulated wire samples has been produced and evaluated for product quality. These have included 0.25/0.60 mm, 0.4/0.74 mm, 0.4/0.90 mm, 0.5/0.9 mm and 0.5/1.0 mm, which are typical of wire sizes used in Europe for telephone exchange and equipment wiring. Evaluation has

been mainly carried out in accordance with BS 6746, a Specification for PVC Insulation and Sheath of Electric Cables, and with particular reference to the test requirements for Type 2 hard insulation compound together with those relating to Type TI1 insulation as specified in CENELEC Harmonisation Document HD21. It is relevant to note that the British Post Office Specification CW(M) 132M for jumper wire requires a grade of PVC insulation complying with Type 2 of BS 6746.

Table 1 summarises typical test results obtained on 0.5/0.9 mm PX 1700 insulated copper wire and provides a comparison with current specification requirements.

The special features of PX 1700 insulation, as indicated in Table 1, can be summarised as:

(1) High tensile strength which is retained after at least 10 weeks ageing at 80°C.

(2) Adequate elongation which, although lower than typical values for PVC insulation, has shown to advantage when the wire is used in automatic wire wrap guns.

(3) The decrease in elongation observed on ageing at 80°C occurs during the first 24 hour period. No further significant change was observed during subsequent 80°C ageing for up to at least 10 weeks.

(4) Excellent low temperature properties.

(5) Good resistance to heat shock and hot deformation.

(6) Good resistance to cut-through.

(7) Good retention of insulation resistance after immersion in water.

(8) Satisfactory resistance to flame propagation.

## CABLE MANUFACTURE AND TESTING

Switchboard cables for use in high speed digital switching systems require good high frequency performance. Evaluation of cable electrical performance can essentially be carried out using two different approaches:

(1) Using the normal analogue measurement techniques, for example at 1 MHz.

(2) Using exclusively digital techniques.

In order to fully evaluate and understand the difference in behaviour of similar cables made with different insulation materials, a more basic approach involving measurement of the cable secondary parameters (capacitance, conductance, resistance and inductance) via the $Z_{open}/Z_{closed}$ measuring technique and computing the cable primary parameters (impedance, attenuation and phase angle) is considered to give a better basic insight into cable performance.

### *Cable Construction*

In the present work, trial lengths of 9-pair cables were produced using 0.25 mm, 0.4 mm and 0.5 mm tinned copper conductors, and incorporating an aluminium foil shield. NORYL PX 1700 insulation was employed in one set of cables and a high quality PVC as the insulation in the other set.

The cable construction was basically identical for the 0.4 mm and 0.5 mm conductors, and utilised a layered arrangement with two pairs in the centre and seven pairs stranded in an opposite direction in the outer layer. The lay length of the twisted pairs ranged from 12 mm to 18.5 mm and the stranding lay length from 100 mm to 200 mm. A unit type construction was used for the 0.25 mm conductor cable. Two bundles of four pairs were stranded together with the ninth pair to form the cable core. The twisted pair lay length varied from 12 mm to 21.5 mm, and each four-pair bundle was assembled with a lay length of 80 mm. The final cable core was stranded with a lay length of approximately 200 mm.

### Test Results

All the measurements were made on 170 metre long cable samples. Tables 2 and 3 summarise respectively the analogue and digital test results. Table 4 gives the primary and secondary cable parameters obtained by means of the $Z_{open}/Z_{closed}$ measurement technique and computation.

From this comprehensive set of measurements the following conclusions, which indicate significant advantages of NORYL PX 1700 insulation over PVC, can be drawn:

1) The calculated values of insulated wire diameter for a characteristic impedance of 110 ohms, as given in Table 2, indicate a useful size reduction in favour of PX 1700.

2) The attenuation data in Table 2 show that the PX 1700 insulated 0.4 mm copper cable has a lower attenuation at 1 MHz than the PVC cable with 0.5 mm copper.

3) An important consequence of 1) and 2) above is that the use of PX 1700 insulation rather than PVC enables reductions of 55% and 35% respectively in the weight of insulation and copper to be achieved. A similar situation holds with respect to attenuation at audio frequencies.

4) The average relative permittivity calculated for pair-type cables is 3.10 for PVC and 2.60 for PX 1700.

5) The typical velocity ratio at 1 MHz is 0.57 for the PVC insulated cables and 0.61 for the PX 1700 cables.

6) Pulse delay is typically 5.1 ns/m for the PX 1700 cables compared with 5.4 ns/m for the PVC insulated cables.

7) When tested with 1 μs pulses (20 ns rise time) the PX 1700 insulated cables are superior with respect to rise time, fall time and edge skew.

## CONCLUSIONS

In summary this development programme has resulted in the introduction of a new flame retardant wire insulation material, NORYL PX 1700, which in cost and general performance bridges the gap between flame retardant materials such as PVC and those based on fluorinated polymers, while at the same time having the considerable advantage of low aggressivity due to the absence of halogen. In addition to flame retardance and low aggressivity, other outstanding characteristics include good mechanical properties over a broad temperature range, excellent electrical properties particularly when exposed to humid conditions, and processability as thin wall insulation on conventional thermoplastic extrusion equipment at high line speeds.

Trial cables incorporating PX 1700 insulation and a range of conductor sizes have been successfully produced and a comprehensive evaluation of their electrical parameters has confirmed the superiority of this type of insulation over PVC. It is expected to find applications as a replacement for PVC and other halogenated polymers in switchboard cables, back panel wiring of electronic exchanges, equipment wiring, miniwires, and industrial cables.

## ACKNOWLEDGEMENTS

We thank the directors of our respective companies for encouragement and permission to present this paper, and colleagues who have contributed to the progress of the work.

TABLE 1: TYPICAL PROPERTIES OF PX 1700 WIRE INSULATION

| Test | Specification | Specification Limit | PX 1700 Value |
|---|---|---|---|
| Density ($g/cm^3$) | | - | 1.06 |
| Ultimate Tensile Strength (MPa) | BS 6746, Type 2 | 18.5 | 35 |
| Elongation at Break (%) | BS 6746, Type 2 | 125 | 140 |
| Ageing 7 days at 80°C | | | |
| - Weight loss ($mg/cm^2$) | BS 6746, Type 2 & TI1 | 2.0 | 0.1 |
| - Tensile strength (MPa) | BS 6746, Type TI1 | 12.5 | 35 |
| - Elongation at break (%) | BS 6746, Type TI1 | 125 | 90 |
| Cold Bend | BS 6746, Type T2 & TI1 | -15°C | No cracks at -50°C |
| Cold Impact | BS 6746, Type TI1 | -15°C | No damage at -30°C |
| Heat Shock | BS 6746, Type 2 & TI1 | 150°C | No cracking |
| Hot pressure test at 80°C | BS 6746, Type TI1 | 50% max. deformation | No measured deformation |
| Insulation resistance | | | |
| - 24h water immersion at 23°C | BS 6746, Type 2 | K value* of 350 MΩkm | 40,000 MΩkm |
| - 4h water immersion at 70°C | BS 6746, Type TI1 | K value* of 0.037 MΩkm | 4,000 MΩkm |
| Piano wire cut-through (4 kg weight, 5 kV) | CNET L800 | 1 min. withstand | Pass |
| Scrape abrasion (100 gram weight) | BS G 212 | - | 175 cycles to failure |
| Resistance to flame propagation | P.O Spec. CW/M 132M | Extinction within 30 seconds | Pass |

$$^{*}K = \frac{IR}{1000 \log_{10} \frac{D}{d}} \quad M\Omega \text{ km}$$

where R is the insulation resistance in MΩ of an immersed length I metres of core of insulation diameter D mm and conductor diameter d mm.

TABLE 2: ANALOGUE TEST RESULTS

| | 0.5 mm tinned Cu | | 0.4 mm tinned Cu | | 0.25 mm tinned Cu | |
|---|---|---|---|---|---|---|
| | PVC | NORYL | PVC | NORYL | PVC | NORYL |
| Average insulation diameter (mm) | 0.95 | 0.94 | 0.84 | 0.85 | 0.54 | 0.54 |
| Mutual Capacitance (nF/km) | 68.3 | 56.4 | 63.2 | 50.8 | 60.5 | 46.8 |
| Characteristic Impedance (Ω) | | | | | | |
| At 1 kHz | 650 | 730 | 855 | 920 | 1400 | 1550 |
| At 1 MHz | 98 | 105 | 106 | 111 | 111 | 120 |
| Calculated insulation O.D.for impedance = 110Ω at 1 MHz (mm) | 1.12 | 1.00 | 0.89 | 0.84 | 0.53 | 0.48 |
| Attenuation (dB/km) | | | | | | |
| At 1 kHz | 2.7 | 1.7 | 3.2 | 2.6 | 4.4 | 3.8 |
| At 1 MHz | 29 | 24 | 32 | 27 | 42 | 36 |
| Calculated Permittivity | | | | | | |
| At 1 MHz | 3.13 | 2.56 | 3.12 | 2.53 | 3.05 | 2.36 |
| Near-end Crosstalk (dB/170 m) | | | | | | |
| At 1 kHz | >120 | >120 | >120 | >120 | 94 | 96 |
| At 1 MHz | 80 | 80 | 85 | 85 | 82 | 82 |

TABLE 3: DIGITAL TEST RESULTS

| | 0.5 mm tinned Cu | | 0.4 mm tinned Cu | | 0.25 mm tinned Cu | |
|---|---|---|---|---|---|---|
| | PVC | NORYL | PVC | NORYL | PVC | NORYL |
| Rise Time (ns) (10-90%) 1 μs pulse, 20 ns rise time, 170 m | 210 | 170 | 210 | 180 | 210 | 194 |
| Fall Time (ns) (90-10%) 1 μs pulse, 20 ns rise time, 170 m | 400 | 385 | 412 | 330 | 424 | 300 |
| Pulse delay (ns/km) 0% of leading edge | 5430 | 5163 | 5440 | 5185 | 5467 | 5133 |
| Leading Edge Skew (ns) | 158.8 | 117.7 | 164.7 | 105.8 | 76.5 | 64.7 |

TABLE 4: $Z_{(OPEN)}/Z_{(CLOSED)}$ MEASUREMENTS

| | F (kHz) | R (Ohm/km) | L (mH/km) | C (nF/km) | G (mS/km) | Z Modulus(Ohm) | Angle | A (dB/km) | B (Rad/km) |
|---|---|---|---|---|---|---|---|---|---|
| PVC | 10 | 182.76 | 0.653 | 65.3 | 0.1271 | 212.6 | -37.80 | 4.87 | 0.6789 |
| 0.5 mm tinned | 50 | 189.93 | 0.648 | 64.8 | 0.5406 | 117.6 | -20.70 | 7.79 | 2.1906 |
| copper | 100 | 209.45 | 0.543 | 64.3 | 1.0222 | 106.9 | -12.90 | 9.21 | 4.1215 |
| | 900 | 448.00 | 0.560 | 60.0 | 9.3000 | 97.7 | -3.55 | 23.55 | 32.8420 |
| NORYL | 10 | 181.47 | 0.654 | 57.0 | 0.0141 | 228.72 | -36.48 | 4.42 | 0.6346 |
| 0.5 mm tinned | 50 | 188.40 | 0.650 | 56.0 | 0.0522 | 125.18 | -25.58 | 7.05 | 2.0660 |
| copper | 100 | 207.44 | 0.645 | 56.0 | 0.1333 | 113.45 | -16.66 | 8.23 | 3.9008 |
| | 950 | 487.00 | 0.570 | 52.0 | 2.0106 | 105.30 | -12.31 | 20.06 | 32.6947 |
| PVC | 10 | 276.83 | 1.188 | 59.0 | 0.1183 | 278.79 | -37.72 | 5.54 | 0.8063 |
| 0.4 mm tinned | 50 | 283.37 | 0.683 | 57.0 | 0.4956 | 140.97 | -20.77 | 10.02 | 2.2427 |
| copper | 100 | 299.22 | 0.682 | 56.0 | 0.9727 | 121.39 | -13.09 | 11.71 | 4.0875 |
| | 900 | 611.30 | 0.590 | 55.0 | 6.6700 | 104.10 | - 3.62 | 29.36 | 32.2824 |
| NORYL | 10 | 271.76 | 1.170 | 52.0 | 0.0139 | 294.62 | -36.49 | 5.05 | 0.7575 |
| 0.4 mm tinned | 50 | 277.27 | 0.677 | 51.5 | 0.0723 | 146.97 | -26.13 | 9.17 | 2.1300 |
| copper | 100 | 291.72 | 0.676 | 51.0 | 0.1890 | 126.18 | -17.07 | 10.60 | 3.8974 |
| | 950 | 745.00 | 0.534 | 47.0 | 3.0039 | 101.10 | -2.94 | 22.15 | 32.2561 |
| PVC | 10 | 708.60 | 0.677 | 56.3 | 0.1189 | 447.83 | -42.30 | 9.60 | 1.1361 |
| 0.25 mm tinned | 50 | 712.82 | 0.700 | 54.3 | 0.4760 | 208.88 | -35.63 | 18.75 | 2.8446 |
| copper | 100 | 720.11 | 0.696 | 54.0 | 0.8200 | 157.85 | -28.65 | 23.22 | 4.6204 |
| | 900 | 978.00 | 0.630 | 53.0 | 3.0400 | 110.10 | -7.71 | 42.00 | 32.9558 |
| NORYL | 10 | 700.83 | 0.681 | 46.0 | 0.0122 | 494.41 | -43.15 | 8.47 | 1.0320 |
| 0.25 mm tinned | 50 | 710.88 | 0.699 | 45.5 | 0.0523 | 228.08 | -36.31 | 16.86 | 2.6216 |
| copper | 100 | 718.56 | 0.692 | 45.0 | 0.0695 | 171.24 | -29.32 | 20.98 | 4.2000 |
| | 950 | 1364.40 | 0.670 | 39.0 | 1.0520 | 128.10 | -6.79 | 35.44 | 30.7029 |

F = Frequency R = Resistance L = Inductance C = Capacitance G = Conductance Z = Impedance
A = Attenuation B = Phase Angle



Hans de Munck was born in 1946 in the Netherlands. He obtained a Chemical Engineering degree from the Higher Technical School in Breda in 1969.

After working on special glass development for the electrical industry with Philips Eindhoven, he joined General Electric Plastics B.V. in 1970. Here, he has been concerned with product development of Lexan and Noryl, plastics based on PC and PPO. He has worked on various aspects of the application of these materials for injection moulding and profile extrusion, and more recently on Noryl applications in the wire and cable industry



J.R. Bury joined Standard Telecommunication Laboratories in 1967 and is at present working on the development of new materials and techniques for wire and cable applications. He is a member of the Royal Society of Chemistry and the Plastics and Rubber Institute.



Eric Simpson received a first-class honours BSc degree in Chemistry from London University in 1940.

After working on plastics materials development, first with Fairey Aviation Company and then with Micanite and Insulators, he joined Standard Telecommunication Laboratories in 1949. Here he is now Head of the Polymer Laboratory which is principally concerned with new developments in the applications of polymers in electrical cables and components.

He is a Member of the Royal Society of Chemistry and a Fellow of the Plastics and Rubber Institute.



Johan A. Devoldere is in charge of product development and industrial engineering at Bell Telephone Manufacturing Co. (subsidiary of ITT) in Ghent, Belgium.

# OPTICAL ATTENUATION TESTING IN FIELD AND FACTORY

J.E.G. CHAPMAN
BICC TELECOMMUNICATION CABLES LIMITED, Prescot, England.

D. CHENG
BICCOTEST LIMITED Cheshunt, England.

D.R. CRONIN
BICC TELECOMMUNICATION CABLES LIMITED, Prescot, England.

## ABSTRACT

Simple and repeatable means of measuring attenuation is essential both in the factory and in the field. The attenuation meter discussed was developed to meet the needs of production testing in factories and to provide field operators with a convenient instrument for use when installing and commissioning systems. The instrument represents a compromise between ease of use and the establishment of equilibrium excitation of the fibre and gives a digital indication of attenuation on a decibel scale. The dynamic range is 60 dB, and the standard deviation of measurement repeatability is 0.1 dB throughout this range. A simple but effective fibre preparation tool for use with the instrument is also mentioned.

## INTRODUCTION

A prime need in exploiting any transmission medium for telecommunications is an ability to predict the attenuation and frequency or impulse response of the medium at the design stage. In metal pairs, this is, if not exactly a simple requirement, at least capable of being expressed in simple terms because of their single mode of propagation. Free space has its own special problems of variable, multipath propagation, and at the present time the multimode nature of the majority of optical fibres in practical service also presents a problem.

A multimode optical fibre can be likened to a cable comprising many hundred pairs of wires, each pair having its own characteristic attenuation and propagation velocity, and with appreciable crosstalk between pairs. The difference is that whereas a practical multipair cable may be intended to carry a different signal on each pair, the "crosstalk" between the different paths in an optical fibre cable compels the user to transmit the same signal over all of them. It is thus clear that the received signal at the end of such a composite assembly of parallel paths is likely to depend, at least to some extent on the way the energy is distributed among the various paths at the sending end.

Thus the establishment of a known modal distribution of energy at the sending end is an important factor in determining the value of attenuation that will be observed. Unlike the single mode, metal pair, there is no unique, easily defined attenuation for an optical fibre. It is however not enough to make reproducible measurements on single lengths of fibre. It is also necessary to study the way in which such measurements relate to the performance of complete working assemblies, formed by the tandem connection of many lengths of fibre, taking into account the effect of the splices between lengths.



*Figure 1. Portable optical attenuation test instrument.*

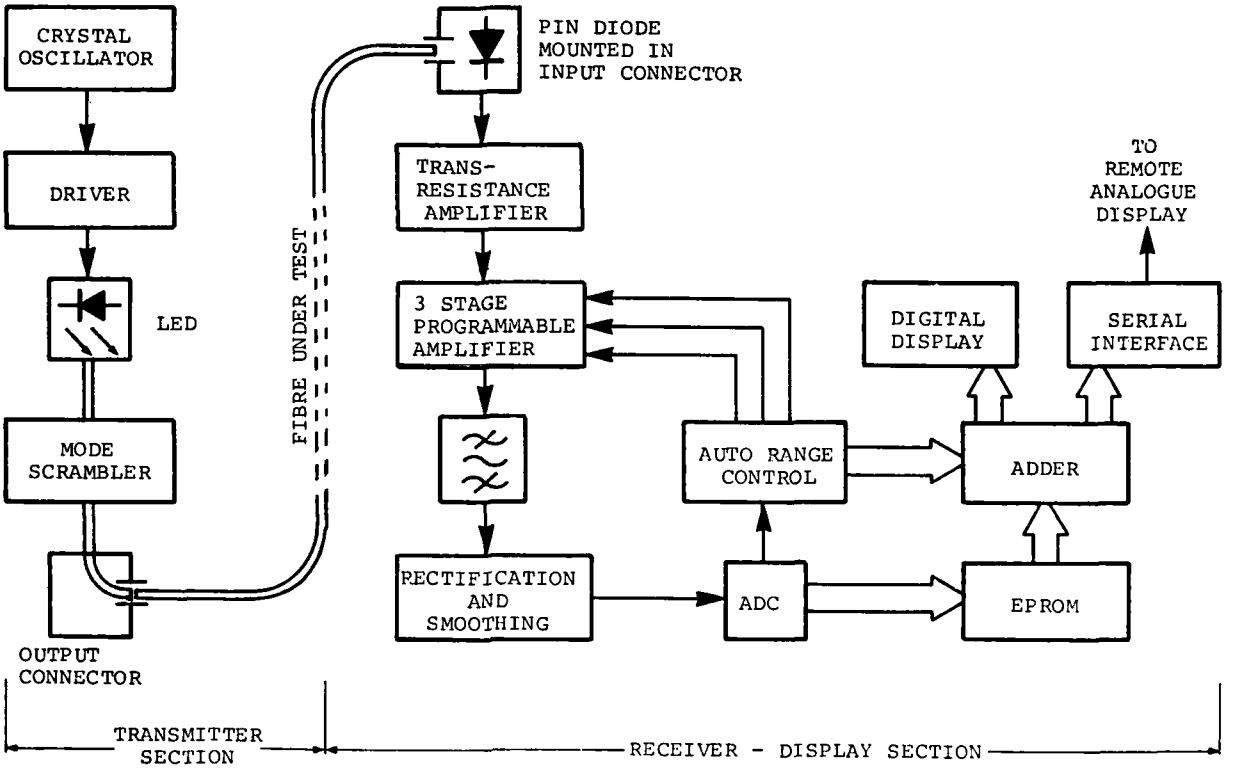



*Figure 2. Block schematic diagram of test instrument.*

This paper will be devoted to an account of the design of an attenuation test instrument, the considerations leading to the choice of operating principles, and experience with its use under practical conditions.

## DESCRIPTION OF THE INSTRUMENT

The instrument is illustrated in Figure 1 with a block schematic diagram in Figure 2, divided into two sections, one comprising the transmitter elements and the other the receiver and display. The modulated output of the source LED is launched into one end of the fibre under test, and the output from the opposite end is coupled to a PIN diode detector feeding a high-gain, narrowband amplifier. The output of the amplifying elements is rectified and smoothed before being applied to the input of an analogue to digital convertor which is used to address an EPROM "look-up table". The EPROM is used to translate the measurement of optical power incident on the PIN diode into a relative transmission reading in decibels which is then displayed on the liquid crystal read-out.

The instrument can equally well be used either for "cut-back" or for "reference" measurement methods. In the case of the cut-back method, the indicated result is characteristic of the fibre under excitation conditions determined by the instrument. The reference method yields a result in which the attenuation of the fibre is modified by its light acceptance capability relative to that of the reference fibre. Using the cut-back method, the transmission level $A_T$ of the total length of fibre is measured first, then the transmission level $A_R$ of a short length of the fibre, cut from the launch end without disturbing the launch conditions is obtained. The attenuation A of the fibre under test is then determined by subtraction

$$A = A_T - A_R \qquad (1)$$

This simple procedure avoids the problems of launching a pre-determined power into the fibre under test, and is especially suitable for use on unterminated lengths of fibre. However, it is essential that the fibre ends be correctly prepared to obtain good and stable coupling at each end. A good source to fibre coupling is required to maximize the launch efficiency, whilst the fibre to detector interface must be repeatable to ensure the validity of equation (1).

The couplers incorporated in the instrument are of simple construction, enabling efficient connections to be made quickly and easily, particularly if the fibre ends are prepared using a reliable cutter, such as the tool illustrated in Figure 10.

As a further aid to correct measurement technique, a matt black plate is provided on the instrument to facilitate the elimination of cladding mode transmission.

## CHOICE OF EXCITATION CONDITIONS

Referring once more to the conventional metallic transmission path such as a coaxial pair, it is recognized that, provided consecutive lengths are well matched to one another in terms of their characteristic impedance, the attenuation of a tandem connection of such lengths will be the sum of the attenuation of the individual lengths. This simple state of affairs arises from the single mode operation of coaxial cables, with the consequent unambiguity with which a signal can be launched.

It does not necessarily apply to optical fibres. In particular, it does not apply to multimode fibres, as mentioned in the Introduction. Only if the modal distribution of energy established when measuring the attenuation of individual lengths is matched by that applying in service, in each length, can the simple rule of addition be relied on to give an exact answer, hence the importance to be attached to the choice of excitation conditions.

Consequently, much attention has been given to this choice, with the object of defining attenuation measurement conditions yielding a directly additive result. The outcome, in general, of this work has been the conclusion that, in order to approach the required conditions, the excitation of the fibre under test must be restricted in two ways, in terms of both the area of core illuminated, and the range of illumination angles employed. Furthermore, gradual variations of intensity with angle or radius or both, can also be considered.

It is difficult to illustrate, in two dimensions, the range of variations possible but, recalling that for all but the shortest links, or for low bandwidth applications, the refractive index of the fibre core is designed to follow a graduated profile, the contour in Figure 4 can be taken as a boundary enclosing the principal propagating rays of such a graded index fibre. Rays outside the

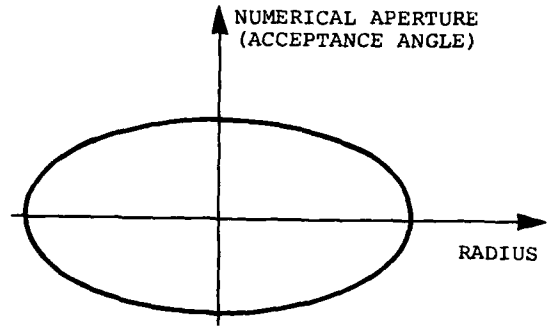



*Figure 4. Relationship of angle and radius of meridional rays in graded index fibre.*

contour escape more or less rapidly into the cladding. The contour shows the acceptance angle covering its widest range at the axis of the fibre and diminishing progressively towards greater radii, until, at the core periphery, only those rays incident parallel to the axis are accepted.

The corresponding diagram for a step index fibre is a rectangle, since the acceptance angle is constant over the whole diameter of the core. Thus, the launch conditions, when a step index fibre is used to illuminate a graded index fibre, can be illustrated by superimposing a rectangle on Figure 4, and the effects of lateral and angular misalignment between the two fibres can be studied by observing the effects of relative movement between the two contours. Also, the results of using step index launch fibres with different apertures and different core diameters can be illustrated. Figure 5 shows the illuminating conditions corresponding to:

a) angular and spatial overfill,

b) angular restriction but spatial over-fill,

c) both angular and spatial restriction, and

d) angular over-fill with spatial restriction.

Figure 5 shows the conditions at the end face of the test fibre, but the refractive index grading has a further effect, as represented in Figure 6. A ray incident on the core centre, but at an angle to the axis, becomes in a short distance parallel to the axis but displaced from it. The converse also applies. Thus the illuminating conditions represented by Figures 5 (b) and 5 (d) are not significantly different, provided they are established

exactly. The importance of this proviso will become clear shortly.

Assuming that the step index launch fibre itself is uniformly illuminated, the arrangement represented by Figure 5 (a) produces equal excitation of every mode, every ray path, in the receiving fibre. Figure 5 (b) shows that, at all distances from the axis, all ray paths are equally excited up to the maximum output angle of the step index fibre or the maximum acceptance angle of the graded index fibre whichever is less. In the extreme, using a step index fibre with very small aperture, Figure 5 (b) could imply that, although the whole area of the graded index fibre is illuminated, only rays parallel to the axis are launched. Figure 6 shows that a little way along the fibre, such rays come to a focus. Similarly if the conditions of Figure 5 (d) are taken to the extreme, only a small spot on the axis of the receiving fibre will be illuminated, by rays incident from all directions. Such rays become parallel a short distance away so that, on the face of it, conditions 5 (b) and 5 (d) are equivalent.

Consider now, however, the effect of misalignment between the test fibre and

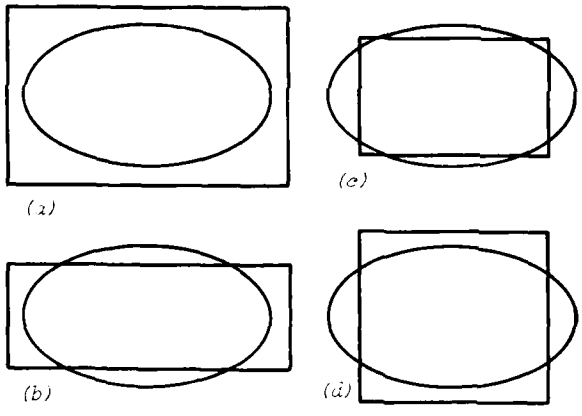



*Figure 5. Launch from step to graded index fibre;*

- *a) angular and spatial over-fill,*
- *b) angular restriction but spatial over-fill,*
- *c) both angular and spatial under - fill,*
- *d) angular over-fill with spatial restriction.*

the step index launch fibre. Misalignment can be represented by diagrams similar to Figure 5, but with the two contours displaced relatively to one another. If the axes of the two fibres are parallel

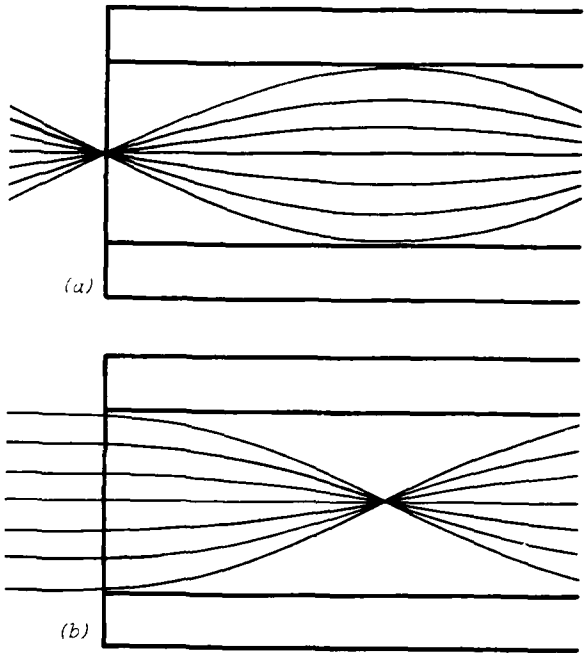



*Figure 6. Equivalence of different launch conditions:*

- *a) small diameter, high numerical aperture.*
- *b) large diameter, low numerical aperture.*

but not coincident, the effect is to move one of the contours along the radius axis. Similarly, if the fibre axes intersect at an angle to one another, the corresponding relative displacement of the contours is along the aperture or angle axis.

Figure 7 represents laterally and angularly misaligned cases of Figure 5 (b). In the case of lateral misalignment, conditions in the test fibre are unchanged, whereas angular misalignment results in the transfer of energy from some ray paths to others.

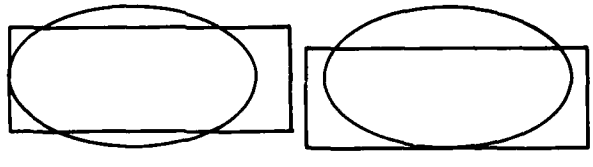
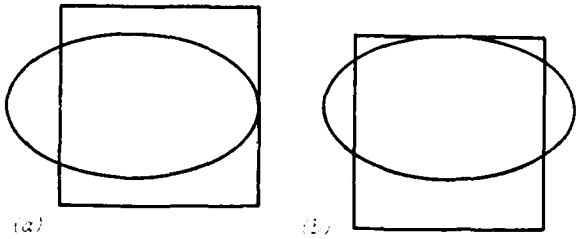



*Figure 7. Misaligned launch into graded index fibre from step index fibre with larger core diameter but lower numerical aperture:*

- *a) lateral misalignment*
- *b) angular misalignment*



(a) (b)

Figure 7. Misaligned launch into graded index fibre from step index fibre of smaller core diameter and lower numerical aperture

(a) Lateral misalignment
(b) Angular misalignment

**Compare this with Figure 8, which represents misaligned versions of Figure 5 (d). Now, it is angular misalignment that can be tolerated while lateral misalignment creates a problem.**

When both angular and spatial restrictions are imposed, as in Figure 5 (c), either form of misalignment results in a change in conditions.

## APPLICATION TO INSTRUMENT DESIGN

In making our choice of launch conditions, we considered the consequences of misalignment, as shown in these diagrams, and asked ourselves which would be least likely, under practical conditions, to result in measurement error. It appeared that if we restricted both aperture and area of launch, any misalignment could result in error. From the preceding discussion, we drew the conclusion that, as far as the resultant excitation conditions were concerned, we were free to choose either aperture or area restriction. We considered that in any simple form of alignment jig, it would be easier to minimize angular than lateral misalignment.

Before taking our final decision on the choice of launch conditions, we considered to what extent the concept of an equilibrium distribution could be considered valid under the practical conditions pertaining in an industrial environment, bearing in mind the launch conditions likely to apply in practice, the need for reasonably inexpensive equipment and ease of use, and finally the reason for making the measurement at all.

In the design of working systems, the primary source may be a laser or a light emitting diode. The former would tend to excite preponderantly low order modes and the latter a more uniform distribution. In either case, a connector would be inserted in the optical path at a fairly early stage, and this would tend to introduce some disturbance of the distribution. The relevant attenuation figure would differ slightly in the two cases, and that relevant to the LED would be on the safe side if used in relation to a laser. Since the purpose in making attenuation measurements is, in practical cases, to ensure that the system will work, it seemed a wise engineering precaution to use a possibly pessimistic rather than an optimistic technique. Furthermore, although there is, for any given type of fibre, some excitation condition which, once established would then persist indefinitely, any distribution is likely to be disturbed at splices. A final, albeit second order, consideration is that the equilibrium distribution applicable to one type of fibre may not be correct for some other type. It was therefore clear that some degree of compromise between the requirements of single length testing and testing on multiple length, spliced fibres, would be unavoidable, so that, although a restriction should be placed on the launch conditions in order to go some way towards establishing an equilibrium state, this aspect of the choice should not be allowed to over-rule the need for simplicity and immunity to misalignment.

The outcome of these considerations was the choice of a step index launch fibre having a core diameter larger than any fibre to be tested, but a lower numerical aperture.

## PHYSICAL REALIZATION

It will be seen from the block diagram (Figure 2) that a mode scrambler is interposed between the source LED and the fibre under test. Several forms of mode scrambler and mode filter have been



Figure 8. Far field pattern of launch fibre.

discussed in published literature [1] and [2] the purpose in each case being to secure some particularly desired mode distribution. In the present case, the object was to provide a uniform light output profile at the end of the launch fibre, and the scrambler was formed from a length of step index fibre, having a core diameter of 90 micrometres and a numerical aperture of approximately 0.16, representing in other words between 70% and 80% of the numerical aperture of acceptable test fibres. The far field pattern produced by this technique is shown in Figure 9, indicating that, although admittedly not uniform, an acceptable practical result has been achieved by a very simple device.

The output end of the fibre is mounted in a short piece of capillary tube closed by a glass cover slip and secured in a pre-set adjustable mount.

Accurately centred with this capillary tube is a second tube 150 micrometres in diameter, and approximately 32 mm long. The bore of this capillary being, at most, 30 micrometres greater than the diameter of the smallest fibre likely to be encountered, the lateral offset is limited to $\pm$ 15 micrometres. Thus a test fibre with a core diameter up to 60 micrometres and cladding diameter as small as 122 micrometres can be accepted while achieving the objective of approximately uniform spatial illumination. Angular misalignment is limited to a negligible value by the very high ratio of length to diameter of the capillary.

The source itself, in the instruments used by us so far, is a high radiance infra-red light emitting diode with a peak emission, using an integral lens, of 100 microwatts at a wavelength of 900 nm, and a spread of some 35 to 40 nm at half maximum. The construction is such as to enable the complete source-scrambler capsule to be removed and replaced, for example, by a 1300 nm unit.

## GENERAL DESIGN AND CIRCUIT DESCRIPTION

At the early design stage, two alternative instrument configurations were considered: either a combined instrument with both transmitter and receiver in the same housing, or the separation of these two functions into distinct units. For factory use, the choice was fairly obvious - a combined instrument would be convenient because both ends of the test fibre would always be available together in the same location. Overall, there would be cost savings by the use of common power supply facilities etc. Separate units were not ruled out, however.

For field use, the choice was less clear-cut. Once a cable is laid out, the transmitter and receiver must be separated and, on the face of it, separate units would have been of some advantage in terms of weight and cost. However, at the installation stage of a multiway cable, no decision is likely to have been taken as to which fibres are to be used for which direction of transmission. Indeed, the fibres may be intended to be used for duplex transmission. In any case, measurements are required in both directions, and the saving in travelling time, achieved by using a pair of combined instruments, was considered to outweigh the initial extra cost.

For descriptive purposes, it is convenient to consider the instrument as comprising two main sections, the transmitter and receiver, subdividing the latter into detector and display. The transmitter description has been largely covered in dealing with the source optics. It remains just to mention that the source is energized by a 2048 Hz square wave driver, the signal being derived from a crystal oscillator.

The detector is built round a PIN diode which is incorporated into a receiver coupler, formed from a capillary tube similar to that used in the transmitter. The diode output is fed to a trans-resistance amplifier compensated for dark current and ambient light to avoid saturation effects and to improve linearity. The signal then passes through a three stage programmable amplifier, the gain of which is controlled automatically by the display circuit before being applied to a narrow band laser-trimmed filter, after which it is rectified and smoothed.

In the display sub-section, the analogue to digital convertor takes the output of the detector circuit and, after conversion, uses it to address an EPROM "look-up table". The EPROM contains one decade of logarithmic data plus a 1.6 dB "hysteresis" band which is used to eliminate instability in the auto-ranging circuit when the signal lies close to the end of a decade. The auto-ranging control uses the under- and over-range signals from the ADC to increase or decrease the gain of the three stage amplifier by a factor of ten each time the signal goes out of range. The control circuit also provides a signal which is added to the output of the EPROM to change the display by 10 dB upwards or downwards each time the change of range

takes place.

The only feature not touched on so far is the serial interface, which provides an output for a remote analogue display. We have found it a very useful aid to confidence on the part of field splicing operatives to be able to supply them with a continuous indication of the success of their activities. The serial interface enables this facility to be provided over any low grade data circuit available between the remote ends of the cable and the joint at which the splicer is working. A pair of attenuation testers is used, one at each end of the cable. One operates as the transmitter, and the two least significant decimal digits displayed by the receiver are relayed via the serial interface and a separate digital transmitter to the splicer's display unit, where the digital bit stream is used to drive a simple analogue meter.

## PRACTICAL APPLICATION

As might be expected, the end preparation of the fibre to be tested is of paramount importance, if efficient and stable optical connections are to be achieved. Each end of the fibre is prepared by removing, mechanically or by solvent action as appropriate, the protective coatings over a length of approximately 25 cm. A special cutting tool, shown in Figure 10, is then used to cut the ends of the fibre to form suitable surfaces such as the one shown in Figure 11.

The prepared ends are inserted in the instrument couplers, adding a drop of index matching oil, and manipulated to obtain minimum indicated attenuation. To promote the stripping of cladding modes, the 25 cm ends of the fibre are laid down on the mode stripper plate, curving through a right angle, secured by plastic magnets and covered by glass slides entrapping a film of index matching oil.

Optimized positioning of the fibre is important in order to improve the repeatability of the measurement. When this has been achieved and the transmitter end of the fibre securely prevented from any possibility of accidental movement, the reading $A_T$ is noted. The receiver end is then removed, and all but about 1.5 metres of the transmitter end is cut away, taking care not to disturb its attachment to the transmitter any way. The free end of this is prepared as before, and inserted into the receiver coupler. The new displayed reading $A_R$ is noted. The attenuation of the test fibre is then given by Equation 1.

When operating under field conditions, it is necessary to use a pair of instruments which must first be aligned. This is done by connecting the two instruments together by short pieces of fibre, one between the transmitter of each instrument and the receiver of the other. Reference level controls at the back of each instrument are then adjusted until the two display readings are matched. The two instruments can then be taken to opposite ends of the circuit under test and the overall attenuation measured in the normal way, one instrument acting as transmitter and reference receiver, the other as measurement receiver. Reverse direction measurements can be made in the same session.

Our experience in the use of this instrument has confirmed our choice of operating principles, and has yielded a quantity of interesting data. In the

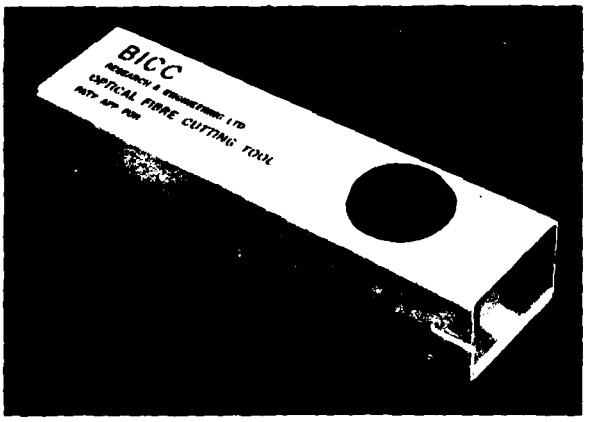



*Figure 10. Optical Fibre Cutting Tool.*

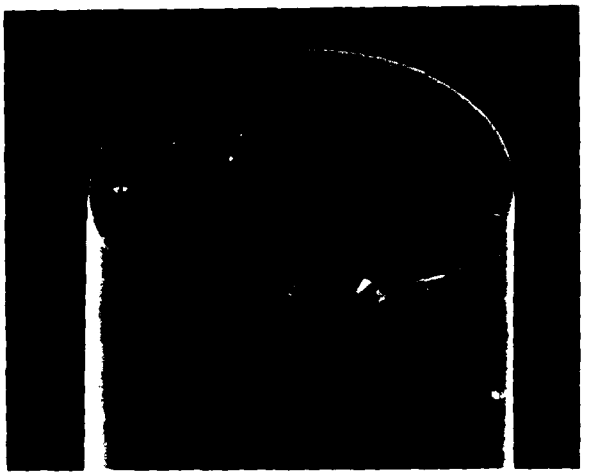


*Figure 11. Cleaved surface of Optical Fibre using Cutting Tool shown in Figure 10.*

| 1 | 2 | 3 | 4 | 5 |
|---|---|---|---|---|
| No.of Tandem Lengths | Set No. | Sum of Individuals (dB) | Direct Measurement (dB) | (Column 3) - (Column 4) (dB) |
| Two | 1 | 4.5 | 4.6 | -0.1 |
| | 2 | 5.1 | 4.9 | 0.2 |
| | 3 | 5.3 | 5.6 | -0.3 |
| | 4 | 4.7 | 4.3 | 0.4 |
| | 5 | 5.2 | 4.9 | 0.3 |
| | 6 | 5.7 | 5.5 | 0.2 |
| | 7 | 4.7 | 4.3 | 0.4 |
| | 8 | 4.5 | 5.1 | -0.6 |
| MEAN | | 4.96 | 4.90 | 0.06 |
| SIGMA | | 0.43 | 0.49 | 0.36 |
| Three | 1 | 6.6 | 6.1 | 0.5 |
| | 2 | 7.6 | 6.2 | 1.4 |
| | 3 | 7.4 | 7.2 | 0.2 |
| | 4 | 7.0 | 6.9 | 0.1 |
| | 5 | 7.1 | 6.8 | 0.3 |
| | 6 | 7.9 | 7.0 | 0.9 |
| | 7 | 6.7 | 5.0 | 1.7 |
| | 8 | 6.9 | 7.3 | -0.4 |
| MEAN | | 7.15 | 6.56 | 0.59 |
| SIGMA | | 0.45 | 0.76 | 0.7 |
| Four | 1 | 9.4 | 8.7 | 0.7 |
| | 2 | 9.8 | 8.9 | 0.9 |
| | 3 | 9.6 | 9.9 | -0.3 |
| | 4 | 10.2 | 11.4 | -1.2 |
| | 5 | 9.4 | 8.5 | 0.9 |
| | 6 | 10.4 | 9.7 | 0.7 |
| | 7 | 8.9 | 8.0 | 0.9 |
| | 8 | 9.5 | 8.9 | 0.6 |
| MEAN | | 9.65 | 9.24 | 0.40 |
| SIGMA | | 0.48 | 1.07 | 0.75 |
| Five | 1 | 11.4 | 10.2 | 1.2 |
| | 2 | 12.1 | 11.9 | 0.2 |
| | 3 | 11.9 | 12.6 | -0.7 |
| | 4 | 12.4 | 13.8 | -1.4 |
| | 5 | 12.0 | 11.0 | 1.0 |
| | 6 | 12.2 | 12.4 | -0.2 |
| | 7 | 10.9 | 10.6 | 0.3 |
| | 8 | 11.6 | 11.3 | 0.3 |
| MEAN | | 11.80 | 11.72 | 0.17 |
| SIGMA | | 0.48 | 1.19 | 0.85 |

| 1 | 2 | 3 | 4 | 5 |
|---|---|---|---|---|
| No.of Tandem Lengths | Set No | Sum of Individuals (dB) | Direct Measurement (dB) | (Column 3) - (Column 4) (dB) |
| Six | 1 | 13.6 | 12.0 | 1.6 |
| | 2 | 14.1 | 13.6 | 0.5 |
| | 3 | 14.4 | 15.4 | -0.1 |
| | 4 | 14.9 | 16.1 | -1.2 |
| | 5 | 14.3 | 12.8 | 1.5 |
| | 6 | 14.1 | 14.2 | -0.1 |
| | 7 | 13.4 | 12.6 | 0.8 |
| | 8 | 13.7 | 13.2 | 0.5 |
| MEAN | | 14.06 | 13.78 | 0.44 |
| SIGMA | | 0.49 | 1.41 | 0.92 |
| Seven | 1 | 16.7 | 14.2 | 2.5 |
| | 2 | 16.2 | 14.8 | 1.4 |
| | 3 | 17.0 | 16.4 | 0.6 |
| | 4 | 17.1 | 17.6 | -0.5 |
| | 5 | 17.2 | 14.5 | 2.7 |
| | 6 | 18.2 | 17.3 | 0.9 |
| | 7 | 16.7 | 14.0 | 2.7 |
| | 8 | 17.1 | 15.0 | 2.1 |
| MEAN | | 17.03 | 15.48 | 1.55 |
| SIGMA | | 0.58 | 1.42 | 1.16 |
| Eight | 1 | 20.0 | 16.1 | 3.9 |
| | 2 | 19.6 | 16.9 | 2.7 |
| | 3 | 19.5 | 19.0 | 0.5 |
| | 4 | 19.7 | 19.2 | 0.5 |
| | 5 | 19.5 | 16.3 | 3.2 |
| | 6 | 20.8 | 18.4 | 2.4 |
| | 7 | 18.9 | 16.8 | 2.1 |
| | 8 | 19.2 | 17.2 | 2.0 |
| MEAN | | 19.65 | 17.49 | 2.16 |
| SIGMA | | 0.57 | 1.21 | 1.20 |
| Nine | 1 | 22.4 | 18.7 | 3.7 |
| | 2 | 22.4 | 19.2 | 3.2 |
| | 3 | 21.8 | 23.1 | -1.3 |
| | 4 | 22.1 | 21.5 | 0.5 |
| | 5 | 22.2 | 19.6 | 2.6 |
| | 6 | 23.7 | 20.9 | 2.8 |
| | 7 | 21.8 | 19.3 | 2.5 |
| | 8 | 22.4 | 19.7 | 2.7 |
| MEAN | | 22.35 | 20.25 | 2.09 |
| SIGMA | | 0.60 | 1.48 | 1.65 |

Table 1. Attenuation measurements on spliced fibres.

cable factory, a single instrument has been in daily use since November, 1979, during which period rather more than 400 km of fibre have been converted into cable at the time of writing. Each length of fibre is tested initially and on completion of the cable, as well as passing sample checks at intermediate stages. It is always difficult, in applications of this kind where a manufacturing process is being monitored, to distinguish with certainty between the behaviour of the test instrument and the characteristics of the process. Small random changes of attenuation are to be expected as manufacture proceeds because of the varying state of relaxation of the fibre. Unfortunately, the demands of production have precluded a proper study of the repeatability of the measurement process itself on a large scale or in any systematic way, but when repeat measurements have been made on the same length of fibre, in an unchanged state, the results of the successive measurements have in every case been

within a span of 0.6 dB. Upon this we base the statement regarding repeatability made in the abstract, namely that the standard deviation of repeatability of the measurement is 0.1 dB, absolute deviations of 0.3 dB from mean being very rare.

In field use, where operating conditions are appreciably more harsh than in the factory, some minor problems have been experienced and overcome. Our early decisions remain largely undisturbed. However, we might consider, for example, replacing the capillary couplers by some form of V-groove alignment between the test fibre and the instrument optics, a possibility that was originally rejected largely on the basis of laboratory and very small scale field use.

The most interesting aspect of the field results is the light thrown on the question of whether the individual fibre attenuation measurements can be added in order to predict the attenuation of an assembly, previously discussed by Taylor, Stannard-Powell and Parr[3] and Keck[4]. Again, the picture is inevitably confused by the random contribution due to the splices, and to the fact that attention has been concentrated on the completion of working installations rather than on a controlled experiment to investigate the question in isolation.

Most sets of results indicate that the result obtained after splicing a number of lengths together, including the loss at the splices, tends to be less than the sum of the individual single length values. From this, one would conclude that the measurement is significantly pessimistic. Figure 12 is representative of this set of results, which are recorded fully in Table 1. Figure 13 however, suggests that the individual measurements are pessimistic only to an extent comparable with that of the splice loss. Whether this divergence of indications is due to the fact that Figure 13 represents fibres whose loss is, on average lower than those of Figure 12, or whether it is related to the fact that the latter all involve mechanically aligned splices, whereas Figure 13 represents arc welded splices, is at the present time, unresolved. If the second explanation were correct, the implication would be that these arc welded splices are not as efficient as their mechanically aligned counterparts.

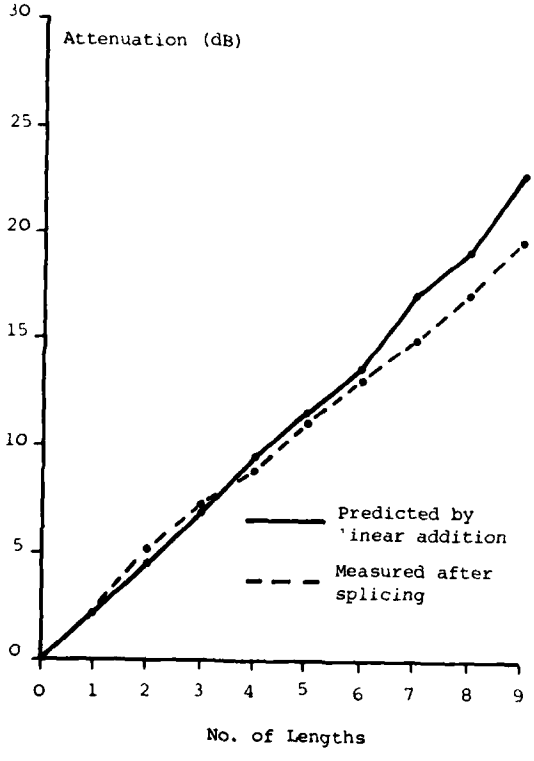



*Figure 12. Cumulative attenuation of fibre with mechanical splices*

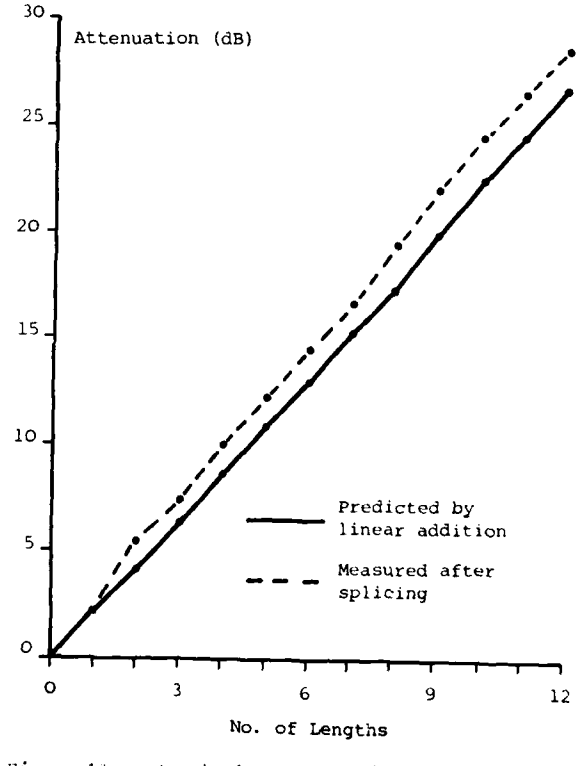



*Figure 13. Cumulative attenuation of fibre with arc welded splices.*

These observations tend, in our mind, to confirm at least our initial premise, namely that for practical everyday use, an easily reproduced launch condition is at least as advantageous as an arrangement designed to launch an equilibrium distribution, since in either case, allowances have to be made for a random spread of splice losses, so that a systematic correction to allow for instrumental bias represents no practical inconvenience.

## CONCLUSION

The instrument described has proved to be practical, robust and easy to use under both factory and field conditions, yielding results which, once an adequate body of practical evidence is accumulated will enable system requirements to be met with certainty and economy, and yielding measurements with a high standard of repeatability. From the data in Table 1, one might hazard a suggestion that the loss of a number of lengths of fibre in tandem might be evaluated from the following empirical formulae:

Probable attenuation of assembly = Sum of individual attenuations - $(N-1)^2/27$

Attenuation of assembly unlikely to exceed

Probable attenuation + 0.53 (N-1)

where N is the number of lengths of fibre, approximately 1 km each, in the assembly. Testing these formulae against the data in Table 1 shows that only in one case, and by a very small amount, does the observed attenuation exceed the predicted maximum. With a more sophisticated procedure, this could probably still be achieved while at the same time reducing the safety margin.

## REFERENCES


1. Love, W.F., "Novel mode scrambler for use in optical bandwidth measurements", Topical Meeting on Optical Fiber Communication, Washington 1979, p.118. Optical Society of America.

2. Stone, F.T., "Effects of different mode filters on optical-fiber measurements", Topical Meeting on Optical Fiber Communication, Washington 1979, p.122. Optical Society of America.

3. Taylor, S.E., Stannard-Powell, S.J., Parr, D.T., "Measurements on spliced cables manufactured for the Slough-Maidenhead field trial in the U.K.", Colloquium on Measurement Techniques for Optical Fibre Systems, London 1979, p.12/1. Institution of Electrical Engineers.

4. Keck, D.B., "Optical-fiber measurements", Topical Meeting on Optical Fiber Communication, Washington 1979, p.44. Optical Society of America.



ACKNOWLEDGEMENTS

The authors would like to thank the Directors of BICC Limited for permission to publish this paper and their colleagues for assistance with its preparation.

J.E.G. CHAPMAN B.Sc.(Eng.)

BICC Telecommunication Cables Limited,
P.O. Box 1,
Prescot, Merseyside, L34 3NA.



Born 3rd March, 1925 at Hornsea, England and educated at Kingston-upon-Hull. Took 2nd class honours degree in engineering at University of London, specializing in telecommunications. Joined BICC Limited in 1945 and became involved in rf connector design, multicore connectors, telephone cable splices and accessories. In 1960 joined section specializing in telecommunication systems engineering and became its manager in 1974. Currently engaged in technical and commercial aspects of optical fibre communications. Married, with three daughters, regards maintenance and restoration of Victorian home as main hobby. Enjoys "dabbling" in geology and listening to classical and renaissance music.

D.K.W. CHENG B.SC.

Biccotest Limited,
Delamere Road,
Cheshunt,
Hertforshire EN8 9TG.
England.



Born in Hong Kong where he attended the Salesian School before joining the Avionics section of Hong Kong Aircraft Engineering Co. Ltd., as an apprentice.

Came to England in 1972 and studied at Brighton Polytechnic receiving an honours degree in Electronic Engineering in 1975. After graduation employed as Project Leader at Pye Ether where he worked on industrial control and laboratory instrumentation. Joined Biccotest in 1978 and worked on optical attenuation meter and various cable fault location instruments.

DAVID R. CRONIN

BICC Telecommunication Cables Limited,
P.O. Box 1,
Prescot, Merseyside L34 3NA.



Born in Waterford, Republic of Ireland, on January 11th 1952. He received a B.Sc degree in Communication Engineering from Plymouth Polytechnic in 1977.

He joined BICC Telecommunication Cables in 1977 where he worked on a number of projects related to Communication Cables. Since 1979 he has been involved with installation of optical cables in the British public telecommunications network.

# WATERBLOCKING IN OPTICAL CABLES.

O.R. Bresser, A.J.H. Leenen, S.H.K. in 't Veld.

NKF Kabel B.V., Waddinxveen, The Netherlands.

## ABSTRACT.

The transmission characteristics of optical fibers, unlike those of copper pairs, are not directly influenced by changes in the dielectric constant of the surrounding medium. However, because of a number of chemical/mechanical effects, protection of the fibres from any potential degrading effect of water penetration resulting from sheath damage is of considerable concern. Special attention is paid to waterblocking in cable structures with loose packaged fibres in which the blocking medium should allow radial and tangential movements of the fibre as reaction to elongation and shrinkage of the cable. Requirements for a suitable waterblocking material are discussed. Based on these requirements a new waterstop material has been developed of which chemical and physical properties are presented. Design and development of compartimentilized optical fibre cables, filled with this material, are discussed.

## A. INTRODUCTION.

A major requirement for telecommunication links is a reliable operation during 20-40 years. In links with cables as a transmissionmedium the reliability of the system can greatly be influenced by water ingress in the cable. In cables with copper conductors main concern is the deterioration of transmission properties. Although in optical cables water could affect the light transmission properties of the fibre in the long run by diffusion of water through the cladding glass into the core region, main concern is the reduction in mechanical lifetime caused by moisture and water in combination with stress on the fibre. The latter being always present in practical cables. Measures should be taken to avoid the cable from being filled up with water.

The discussion will be limited to waterblocking by suitable filling compounds in the cable. A method like pressurization, which is also applicable for optical cables, is not discussed in this paper.

## B. EFFECT OF MOISTURE ON OPTICAL FIBRES.

### 1. Static and dynamic fatique.

The strength of glass fibres is governed by flaws which are present at the glass surface. According to Charles [1], these flaws can grow in time and weaken the fibre under influence of a stress- and temperature dependent chemical reaction which breaks up the Si-O-lattice in the presence of moisture.
Zero-stress aging of fused silica optical fibres in a humid or water environment has no effect on the mechanical properties and lifetime of these fibres [2,3]. To keep the static fatigue of fibres to a minimum, cable design should allow for the incorporation of optical fibres under minimum stress conditions. However, a cable construction which is also designed to minimize dynamic loading of the fibres during transport and storage, pulling and bending during installation, entails unavoidable an amount of static load on these fibres. (see paragraph D for a discussion about this subject.) Cable or sheath damage and subsequent water ingress in the cable combined with this stressing results in an accelerated weakening of the fibres. It should be noticed that a plastic coating of the fibres presents no effective moisture barrier, since all plastics are more or less waterpermeable.

### 2.Coating-fibre interface.

Since a plastic coating is waterpermeable a build-up of the waterconcentration at the polymer-fibre interface takes place in a moisture or water environment.
With a weak interfacial molecular bond this can lead to a break up of this bond.

## C. WATERBLOCKING.

To prevent optical cables from being filled up with water over long lengths the cable can be made watertight in two ways:

- Continuous filling

- Discontinuous filling, i.e. the cable is divided into a number of compartments by means of periodic waterblocks.

Advantages of blockfilling include:

- Lower interaction between fibre and blocking medium.

- Ease of splicing.

- Reduced cost and weight.

Some preliminary requirements for a waterblocking material include:

- Water ingress limited to at the most a few meters.

- Minimal influence on the transmission properties.

- No restrictions should be imposed on handling and environmental specification of the cable.

- No hindering of splicing procedures.

- Low cost.

## D. CABLE DESIGN.

One can classify optical cables roughly in two groups based upon the way the optical fibres are incorporated in the cable, loosely or tightly.

### 1. Structures with loose packaged fibres.

Two examples of this cabling principle are:

- Fibres in loose tubes stranded round a central member in a helical lay or with an alternating twist.

- Fibres in a slotted core. The slots are helical or sinusoidal.

Basic in this type of cable constructions is the freedom of movement of the fibre perpendicular to the cable axis, i.e. the fibre has the possibility to accomodate to variations in cable length during pulling or temperature changes. For example in a helical stranded loose tube cable, on reel at ambient temperature, the average position of the fibre is the centre of its tube (fig.1). The fibre can react upon variations in cable length by changing its average position along a radial path.
The most inner position of the fibre shows the cable in maximum elongation (pulling- and high temperature limit), whereas the outer position shows the cable in a maximum shrinkage situation (low temperature limit) [4,5].

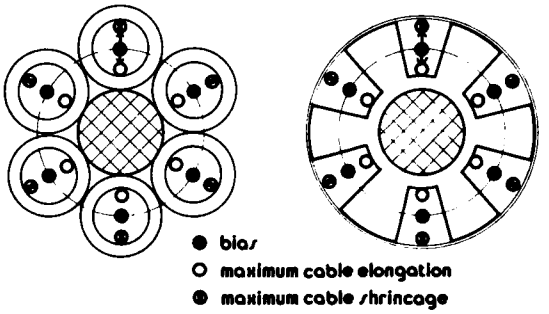



Fig. 1 Average fibre positions in loose tube resp. slotted core.

Depending on the design specification the position of the fibre immediately after production can be chosen inbetween these two limits. Quantitatively the freedom of the fibre is determined by the difference between the two ultimate helix diameters and the helical period.

Fig. 2 shows the freedom in dependence of the helical period for a given construction (pitch circle diameter D = 3 mm, buffer clearence w = 1 mm).

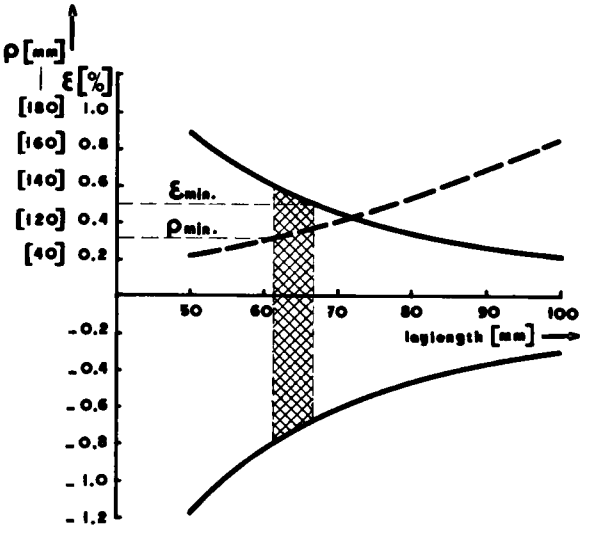



Fig. 2 Fibre freedom as a function of laylength.

For constructions with an alternating lay the mechanism is more complex. In fact the fibres lay in a folded sine. The momentane amplitude of this sine is determined by the environmental situation of the cable.

With respect to the lifetime of fibres in these loose cable structures there is a point of concern. The freedom of movement of the fibre is created at the cost of continuous bending of the fibre. In practical designs the maximum bending radius is about 100 mm which corresponds with a minimum stress level of 45 N/mm$^2$ for a 125 µm. fibre.
For example in fig. 2 the adopted allowable cable elongation of 0.5% requires a bending radius of 75 mm (60N/mm$^2$). The minimum tolerable bending radius depends upon the static fatigue properties of the fibre. In combination with moisture or water static fatique is accelerated, leading to a decrease in lifetime of the fibres. If one wishes to avoid the need for fibres with extreme initial strengths or unpractical and thus uneconomic cable designs with loose structures, there certainly is a need for waterblocking measures. From the described cable mechanism it follows that the undisturbed freedom of movement of the fibre is the major requirement for any blocking procedure. The most extreme situation in this respect will occur during installation when fast changes in cable length can be expected, requiring the fibre to respond quickly to the new situation in order to avoid excessive axial stresses.

## 2. Structures with tight packaged fibres.

In cables of this type the fibres, primary coated with mostly a soft material are embedded in a plastic. Each fibre has its individual cover (tight coating) or fibres are jointly protected (ribbons). In this way the fibres are reasonably insensitive to microbending and can readibly be incorporated in a cable.

Since in tight coated structures there is no way for the fibre to accomodate to changes in cable length, the fibres are stressed directly by cable elongation. During installation this leads to high stress levels on the fibres. For pratical cables strain levels up to 0.5% are realistic during installation, which gives a stress of ~ 350 N/mm$^2$ on fibres in tight coated structures. Once installed the stress levels for the fibres are determined directly by stress, bending and temperature changes of the cable.
In combination with moisture or water these unknown stresses lead to an unpredictable static fatigue rate. Since the fibres have a proper protection against external influences, waterblocking can occur with conventional filling compounds like petroleum jelly, silicone rubber, etc. It should be noticed that incorporation of special filling compounds like swelling powder could result in unacceptable microbending of the fibre.
From mechanical point of view loose packaged fibre configurations are advantageous compared with structures comprising tight coated fibres because in the former configuration dynamic stresses can be kept at a minimum during installation and once installed, static stresses are low and well defined.

## 3. Requirements for a waterblocking material in loose packaged structures.

As pointed out in section D.1 a major requirement for any waterblocking material is to allow for an undisturbed movement of the fibre due to changes in cable length. The most severe situation is expected during installation when length variations of the cable can occur almost instantaneous, requiring the fibre to respond quickly. The response time of the fibre is influenced by the waterblock material. A material with a high viscosity sets bonds to this response time. Extreme cases are a tight coated fibre. (i.e. the fibre has no freedom of movement) and a loose tube with no waterblocking at all, which allows for an undisturbed movement. The response of the fibre to instantaneous cable elongation is shown qualitatively in fig. 3.

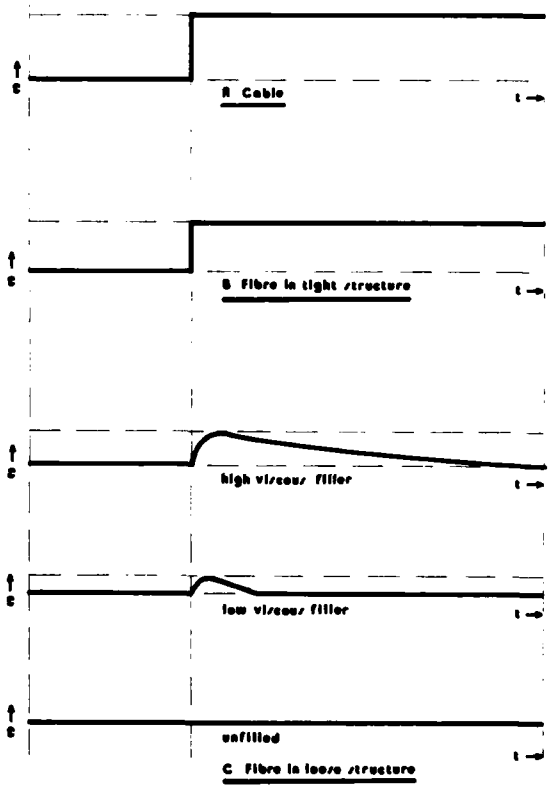



Fig. 3 Response of fibre elongation on a stepwise cable elongation.

In this respect a filling compound with a low viscosity is preferable, however such a material would drop out at the cable ends and in a slotted core configuration from the cable core during production. In a blockwise filling, blocks would smear out. A solution for this problem is found in a material with an apparent viscosity, which is almost infinite until the applied force reaches a critical value, the yield value, then it decreases abruptly. By an appropiate choice of the waterblock material movements of the fibre are almost undisturbed once the yield value is surpassed. This yield value can be kept as low as $10^{-3}$ N/mm$^2$ and therefore presents no serious threshold for fibre movement. This behavior is also advantageous for the application of the filling compound.

Once the yield value is reached, the material is easely injectable, while once injected the material stiffens and stays in place. Blockwise filling gives a reduction of the influence of the blocking material on the fibre movement. Dependent on block length and block distance, blockwise filling can approximate the ideal case of fig. 3. (unfilled loose tube). The above indicated rheological behaviour assures that fibres are not damaged at the blockends by allowing movements of the fibres. In combination with the preliminary requirements from paragraph C a suitable waterblocking material should come up to the following requirements:

- The waterblock material should allow for the displacements the fibre has to make in order to accomodate to temperature changes, bending, pulling, etc.
- The filling compound should be stable in a specified temperature range, i.e. no dripping out at higher temperatures resulting in loss of the waterblock properties and no hardening at lower temperatures resulting in microbending or damage of the fibre and not influence the optical or mechanical properties of the fibre.
- Chemical and physical stability, i.e. no sag out or conversion in time.
- Easy to apply, once applied the material should stay in place.

In addition to the above requirements discontinuous filling (i.e. blocks) requires that:

- The blocks are not smeared out by movements of the fibres within the blocks.
- Waterpressure should not lead to shifting of the blocks over considerable distance.
- No additional bending of the fibre should take place at the blockends.

Materials which can meet these requirements are for instance silicone- or PUR-gels. In our laboratory a new filling compound has been developed which consists of a dispersion of fumed silica in silicone oil. Compared with silicone- or PUR-gels this material possesses several advantages:

- No vulcanizing or heating is required.
- No reaction products are involved.
- Problems with potlife or limited storage times do not apply to this material.
- Low cost.

## E. PROPERTIES OF THE NEW WATERBLOCKING MATERIAL.

### 1. General.

The new waterblocking material consists of a dispersion of fumed silica in silicone oil. The desired gellike properties of this dispersion are obtained by mixing of a proper amount of fumed silica and silicone oil. Due to the presence of hydroxyl groups on the surface of the fumed silica a network is formed as schematically shown in fig. 4.

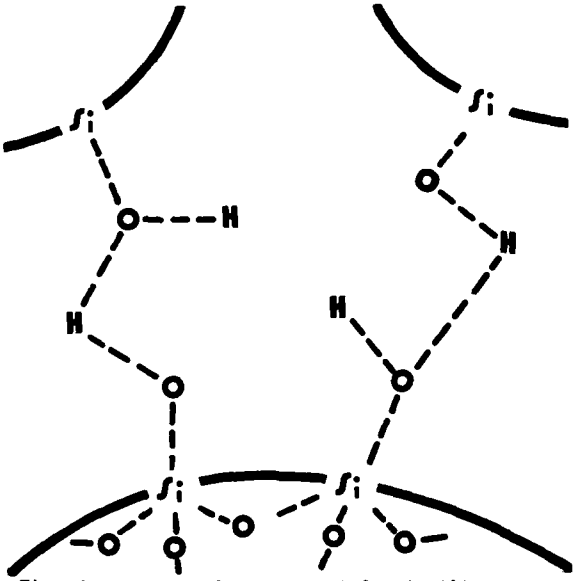


Fig. 4 Network formation of fumed silica in liquids by hydrogen bonding between surface hydroxyl groups.

This network is responsable for the gellike properties of the dispersion. In the presence of hydrogen bonding liquids like water, alcohols, etc., the establishing of such a network is prevented, as shown in fig. 5, resulting in a low efficiency of the fumed silica.

Network formation is promoted by a non- or low-hydrogen bonding medium such as silicone oil in which the fumed silica displays its greatest efficiency in networkformation. The choice of the appropriate type of fumed silica is determined by the value of its surface area. In general large surface areas lead to more efficiency in networkformation. However increasing surface areas are attended with an increase in moisture absorption capacity, leading to reduction in chain-formation as pointed out in fig. 5. So a balance has to be found in a fumed silica with an average value of the surface area. First handmixing experiments revealed that the fumed silica was not proper dispersed in the silicone oil, which resulted in sag out, low droppoint and a high penetration. Therefore mixing was performed with dispersion equipment. (Janke and Kunkel, Ultra Turrax T45).

It should be stressed that proper dispersion is a stringent condition for the application of this material.

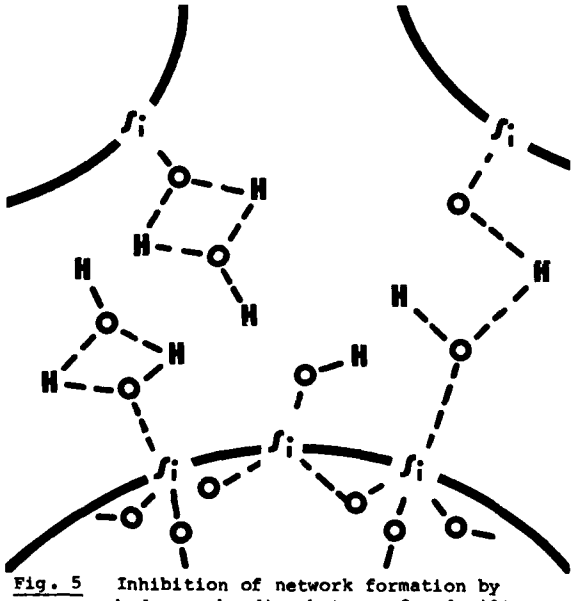


Fig. 5 Inhibition of network formation by hydrogen bonding between fumed silica and other polar substances.

## 2. Rheological properties.

Due to the networkformation a stress maximum is observed with increasing shear rate in stress shear curves. Better dispersion will result in a higher value of this stress maximum. Based on this phenomenon optimum mixing times were obtained by measuring the stress maximum as a function of mixing time. Stress shear curves were obtained with a coaxial cylinder viscometer (Contraves Rheomat 30) and mixing was conducted at about 12.000 rpm.(unloaded). Results are shown in fig. 6. For dispersions from 5% up to 8% fumed silica (based on silicone oil

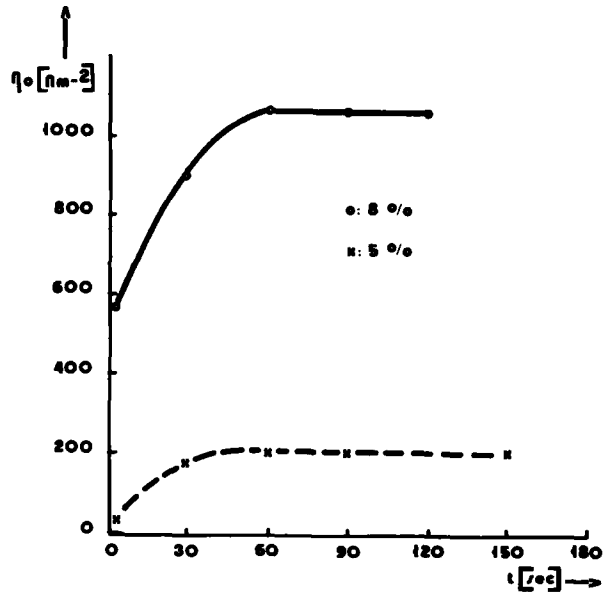



Fig. 6 Yield value vs. mixing time as a function of percentage fumed silica.

weight) the optimum mixing time is about 90 sec. Longer mixing times lead to breaking up of the network while shorter mixing times result in incomplete dispersion. The network formation of the fumed silica in the silicone oil results in a firm gel, which stays in place on sloping or vertical surfaces. When a proper shear force is applied the gel has a relatively low viscosity which facilitates injection. Once this shear force is removed the network is restored.

## 3. Stability.

Once a proper dispersion of fumed silica in silicone oil has been established the question arises whether this dispersion is stable in time. Therefore stability tests were performed in accordance with FTZ 52 TV 1. Also the influence of network formers on the stability was investigated. Results of these tests with polyethyleneglycol are shown in fig. 7.

It follows that a dispersion of 8% fumed silica (based on silicone oil weight) in silicone oil, without additives, mixing time 90 sec. at about 12.000 rpm (unloaded) meets the stability test.
A further 8 weeks at 80° C showed no separation of the silicone oil.
All further experiments were conducted with this material which we will call Aquagel.

## 4. Temperature behaviour.

The behaviour of Aquagel with respect to temperature was investigated.

| % fumed silica | % PEG | stability at 80° C |
|---|---|---|
| 5 | 0 | - |
| 6 | 0 | - |
| 6 | 0,10 | - |
| 6 | 0,25 | - |
| 6 | 0,50 | + |
| 6 | 1,00 | + |
| 7 | 0 | + |
| 7 | 0,10 | + |
| 7 | 0,25 | + |
| 7 | 0,50 | + |
| 7 | 1,00 | + |
| 8 | 0 | + |
| 8 | 0,10 | + |
| 8 | 0,25 | + |
| 8 | 0,50 | + |
| 8 | 1,00 | + |

- seperation
+ no seperation

Fig. 7. Results of stability tests on dispersions with different percentages fumed silica and polyethyleneglycol in accordance with FTZ 52 TV 1. Mixing time 90 sec. at 12.000 rpm

Penetration measurements in accordance with ASTM D 217 were performed at different temperatures. Results are shown in fig. 8. Also results of a typical petroleum jelly are shown in the same figure. In contrast with petroleum jelly Aquagel shows only a slight increase in penetration as a function of temperature indicating a stable product between -35° C and +80° C. The droppoint of Aquagel is >200°C, measured in accordance with IP 31, compared with a typical value of 70 - 100°C for petroleum jelly.

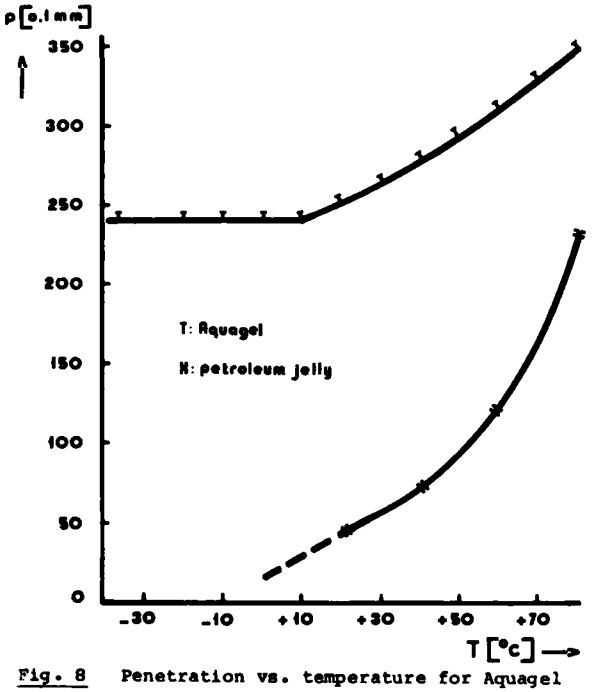



Fig. 8 Penetration vs. temperature for Aquagel and a typical petroleum jelly, measured according to ASTM D217.

The stability of Aquagel was once more tested by measuring the penetration in accordance with ASTM D217 at 25°C as a function of time. Results are shown in fig. 9.

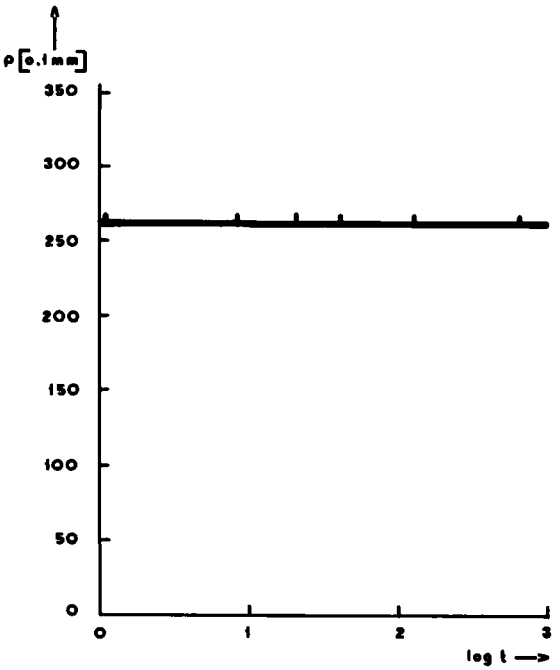



Fig. 9 Penetration vs. log time, measured according to ASTM D217 at 25°C.

## F. INJECTION EQUIPMENT.

Due to the rheological behavior of Aquagel i.e. low viscosity during injection and almost infinite viscosity once injected, injection is a straight forward process. We have developed injection equipment for loose tube as well as for slotted core structures.

### 1. Loose tube structures.

The waterblocking of loose tubes without damaging these tubes can only take place through the extruder die head. The complexity of the tube forming process, attended with a draw down of the melted jacketing material, followed by a shrinkage of this material during cooling forced the design of a special injection needle. This needle allows the waterblocking material to be shot in the cooling-area of the tube, by passing the draw down area. (fig.10). In this way

no scattering of the blocking material occurs and even a slight compression of the filling compound can be reached. Special attention was paid to the reduction of the required injection pressure by minimizing the flaw resistance of the injection channel in order to prevent the blowing up of the tube. An open air connection to the inside of the tube was formed around the needle by adapting the diehole. No vacuum or pressure build up in the draw down area can take place now. Both the injection of solid blocks and continuous filling can be performed without distortion of the tube or fibre lay. Since filling with Aquagel is only appropriate inside the tubes, waterblocking of the remaining part of the cable structure can be accomplished with standard filling techniques using petroleum jelly or silicone rubber.

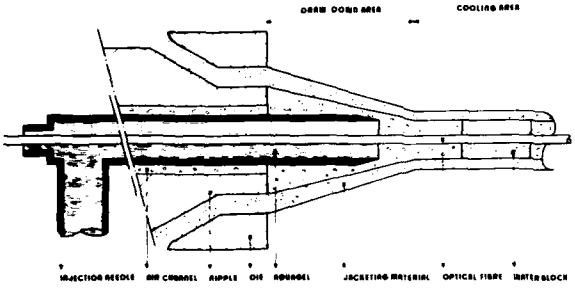


Fig. 10 Detail extruder die head.

## 2. Slotted core structures.

Slotted core structures are more suitable for waterblocking than loose tube structures, because in the former structure the blocking material can be applied from outside the cable, in line with a jacketing process. All slots are injected at the same time and at the same position with a nipple, having a low flow resistance, requiring only a low injection pressure.

This low pressure combined with the low viscosity of Aquagel during injection, cause a minimal distortion of the fibre lay. Best preliminary results are obtained with a running nipple. However, because of its reciprocating stroke only blocks can be applied in this way.

## G. TEST RESULTS ON LOOSE TUBE WATERBLOCKED BUNDLES.

Three lengths of 6 fibre bundle were produced in order to test waterblockproperties and temperature behaviour of filled loose tubes. Two lengths (each 1 km) were filled with 5 cm blocks Aquagel with a respective distance of 1 and 2 metres, the third length was an unfilled reference bundle. A bundle contained 6 tubes, stranded around a Kevlar® central strength member and wrapped with polyester tapes.

## 1. Temperature behaviour.

Bundles were cycled between -25° C and +75° C. All types show an excess attenuation of about 0,5 dB/km (5 dB/km fibre) at -25° C, the theoretical limit for the produced bundles. At 75°C no change in attenuation occured, the Kevlar® strength member limiting the elongation. This result clearly indicates that waterblocking with Aquagel has no effect on the temperature behaviour of loose tube structures.

## 2. Mechanical behaviour.

A bundle length of about 10 metres was clamped and given a cyclic elongation treatment in a set-up as schematically shown in fig. 11. The resulting elongation curve is also shown in fig. 11.

The fibres were looped through and attenuation was monitored in order to reveal possible influences of the elongation treatment. Within the design boundaries no change in attenuation has been observed during this cycling in any of the three bundles. Furthermore no fibre breaks were observed after 24 hours of cycling.
Obviously there is no influence of Aquagel on the fibre response during elongation/shrinkage of loose tube constructions.

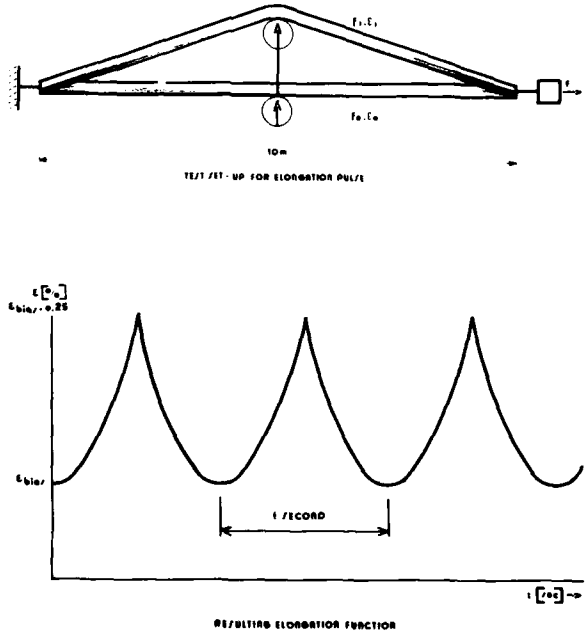


Fig. 11 Cyclic elongation test.

### 3. Wateringress.

Bundles were tested in a waterpenetration test, 1 m. watercolumn during 7 days, before and after the cyclic elongation test. Short tube lengths containing only one block of 5 cm Aquagel, lead to desintegration of this block during the waterpenetration test, both before and after a 24 hours cyclic elongation test. Tube lengths containing three blocks, blocklength 5 cm and blockdistance 1 or 2 metres, show the wateringress to be limited to about 25 % of the available space up to the first block, both before and after the cyclic elongation test. No movements of the waterblocks were observed during this waterpenetration test. From these experiments it follows that the waterblock properties of Aquagel are very good and are not influenced by movements of the fibre in its tube.

## CONCLUSION.

Based on a number of requirements (with respect to rheological properties, stability and temperature behaviour) resulting from the nature of optical cables with loose packaged fibres, a new waterblock material, Aquagel, which consists of a dispersion of fumed silica in silicone oil, has been developed and tested. Furthermore suitable injection techniques for Aquagel were developed both for loose tube and slotted core constructions. First tests on prototype waterblocked loose tube bundles show very promising results.


### Acknowledgements.

The authors gratefully acknowledge the assistence of Fred W. Aalbertsberg and Dick C. Huysman in the compilation of data for this paper.


### References.


1. a. Charles, R.J., Static fatigue of glass J.Appl. Phys. 29 ,p.1549 (1958).
   b. Charles, R.J., Static fatigue of glass J.Appl. Phys. 29 ,p.1554 (1958).

2. Wang, T.T., Zupko, H.M., Long-term mechanical behaviour of optical fibres coated with a UV-curable epoxy acrylate, J. Mater. Sci., 13, p.2241 (1978).

3. Kalish, D., Tariyal, B.K., Chandan, H.C., Effect of moisture on the strength of optical fibers, Proceedings of the 27th International Wire and Cable Symposium, Cherry Hill, p.331, November 1978.

4. Bresser, O.R., Metal-free optical fibre cables, Philips Telecommunication Review, 37, p.251 (1979).

5. Bark, P.R., Oestrich, U., Zeidler, G., Stress strain behaviour of optical fiber cables, Proceedings of the 28th International Wire and Cable Symposium, Cherry Hill, p. 385, November 1979.



Onno R. Bresser born 21th of november 1948 in Rotterdam received his degree in electrical engineering at the Delft University of Technology in 1975. After his studies he joined NKF Kabel BV member of the Philips Group of industries. End of 1977 he started the foundation of a Fibre Optics Development Group within NKF which he is currently managing.



Ton J.H. Leenen was born in 1953. He holds a degree in Chemical Technology from the Eindhoven University of Technology (The Netherlands). He joined NKF Kabel BV in 1978 where he is a development engineer in the Fibre Optics Development Group, working in the areas of mechanical properties of optical fibres and development of materials for lightguide cables.



Steven H.K. in 't Veld was born in 1949. He received a degree in mechanical engineering at the Delft University of Technology in 1976. He joined NKF Kabel BV in 1978 as a member of the fibre development group. His main concern is the development of production techniques for optical cables.

# INNOVATIVE METHODS FOR INSTALLING FIBER OPTIC CABLES

J. B. Masterson

General Cable Company
Research & Development Center
Edison, New Jersey 08817

## ABSTRACT

As applications for fiber optic cable expand, new methods have evolved for installing multi-kilometer lengths of fiber optic cable. Special cable handling and placing techniques were developed which are more appropriate for the size cable and physical characteristics of the cable involved. Specific points of interest include fusion splicing techniques, pulling equipment, tension control and methods to partition existing ducts. In addition, fiber organizers, cable accumulators and splice case sub-assemblies were developed to simplify splicing and to permit splicing into remote locations.

## INTRODUCTION

Previous papers described a wide variety of experience in the installation of fiber optic cables.[1-2-3] These experiences encouraged General Cable Company to undertake one of the most challenging urban installations - A 5.2 km repeaterless high quality system under the streets of New York City for Manhattan Cable Television Company.[4]

This installation encountered several difficult situations such as installation in occupied ducts, congested manholes, stringent safety requirements during splicing and restricted access at the jobsite. Methods were evaluated and implemented to permit installation which are discussed in this paper.

## A. OPTICAL CABLE CONSTRUCTION

The basic optical cable structure consists of a fiber core assembly incorporating a waterproof compound, an inner polyethylene jacket, Kevlar serving and an outer polyethylene jacket.

All fibers are tested under humidity and temperature conditions before the fibers are incorporated into a cable that simulate the conditions inside urban underground ducts or rural aerial installations. Fiber strength of short gage lengths is measured as received; after exposure to 100% humidity and after preload and static fatigue conditions. The data is analyzed using Weibull statistics and the maximum permissible load is computed for a designed life expectancy of 20 years. As a result of cable design this maximum load is never exceeded during cable fabrication or installation.

Attenuation and bandwidth were also evaluated as a function of temperature cycling, and under varying humidity environments to ascertain that the fibers will perform adequately after installation in varying operating conditions.

The requisite number of fibers are stranded around an appropriate size epoxy impregnated glass rod strength member. A controlled low fiber tension is used on a planetary strander. The core is filled with a water impervious filling compound which minimizes fiber exposure to moisture thereby reducing the effects of microcracking.

A first polyethylene sheath is extruded over the stranded core. Appropriate ends of Kevlar are wrapped over this jacket in two directions (right and left handed lay) with optimum payoff tension. A second jacket of polyethylene is extruded over the Kevlar servings so that they become an integral part of the sheath and reduce Kevlar slack. This jacket reinforced construction is the standard non-metallic cable structure.

All our other cable designs are built upon this basic construction, for example FPA* (Fused Polyethylene Aluminum), GP, aluminum tube, etc.

The FPA cable structure incorporates a moisture barrier of aluminum coated on both sides with polyethylene which is applied over the second jacket. A third and final jacket of polyethylene is extruded over the FPA aluminum tape.

If further strength is required in the cable structure, for example to resist undue compressional loads, a welded aluminum tube can be applied over the inner jacket followed by a final polyethylene jacket. For gopher protection, a conventional 6 mil corrugated steel sheathing with corrorsion protection can be applied, followed by a final polyethylene jacket. Typical cable construction is shown in Figure 1.

Tensile, compression and bend tests were performed on test samples of finished cable. During the test a light beam of wavelength 0.85 microns is focused on one end of a fiber in the cable. The output

* Registered Trademark

light from the other end of fiber is monitored continuously. Output light power at each cable test load and its value on release of load is determined. Data are plotted as shown in Figures 2, 3 and 4. From the figures the maximum applicable safe load for 100% power level recovery is noted and this value is used to determine the maximum permissible load for cable handling or installation.

## CABLE/CONDUIT PROBLEMS

### Handling Long Lengths of Cable:

The installation of long lengths of fiber optic cable presents several areas of concern for the outside plant engineer. There are immediate advantages in reducing the number of splices therby increasing system reliability. In addition, the reduced number of reels to be handled, pulling eyes to be attached, and lengths to be tested can improve overall efficiency of the installation.

The typical 1 kilometer (3280 ft.) length of cable has to be installed in a conventional duct plant where manhole spacing can vary typically from 300 to 1000 feet. The size of the duct is usually 3 to 4 inches, and depending on plant age, can be made of any number of materials from older concrete type to current plastic types. The typical fiber cable size range from 0.3 to 0.7 inches and takes up very little duct space. The efficient use of space usually means that several cables, or several sub-ducts, be pulled into an unoccupied duct and the fiber optic cable can be pulled through several manholes. Future new duct plants may include partioned ducts in which as many as seven sub-ducts can be placed in the space of the present 4 inch duct.

### Installing Fiber Optic Cables in Existing Ducts:

The logistics of installing long cable lengths through the existing duct plant requires several considerations. The existing plant was designed for installing larger conventional cables in much shorter lengths. The inherent frictional drag of these heavy cables constrained the length that could be installed without damage to the cable. Fiber optic cable being very light and small in size enables the installer to place the cable through multiple duct spans.

The size and availability of the duct throughout the plant must be established. The location of the assigned ducts must be checked for position in the duct bank and where not aligned, the amount of transition noted. A study must be made of the number of pull through manholes and their respective size; surface traffic conditions and working space; and possible locations for reel pay-off stand and pulling equipment In some instances it may be advantageous to make bi-directional pulls from a single location.

The expected pulling tension can be calculated from the number, radius and angle of bends, the spacing between manhole and the transitions due to non-aligned ducts. The use of appropriate pulling lubricant can be used to reduce frictional drag to a minimum.

The sub-duct concept requires installing a pull line through the sub-duct for pulling in the fiber optic cable. This pull line must incorporate a swivel, which will remain operatable under required tensile load. Conventional methods for blowing a pull line through conduit pneumatically can be employed.

It is usually necessary to mandrel the duct or the sub-duct system prior to placing the cable. The mandrel should be 1/4" larger than the cable or pulling eye assembly and in the order of ten to twenty feet long. Obstructions due to mud, dirt, foreign material, duct deterioration, collapsed, dropped or shifted ducts can be found during the mandrel operation.

A jacketed flexible conduit should be installed in pull through manholes where transitions are made due to non-aligned duct. This conduit must be secured on the manhole to support the cable, and act as a guide through the transition. The flexible conduit shall fully bridge across the entering and exiting ducts to prevent point loading and scuffing. It also provides protection to the cable in the manhole after the cable is dressed.

Adequate cable slack must carefully be pulled back into each pull through manhole with sufficient cable length at each end for either splicing or terminating.

### Development of Duct Rodding Equipment:

An experimental method for rodding occupied ducts was developed to make use of the space available between the cable and the duct. In many instances there can be sufficient space into which a sub-duct can be placed.

The method developed utilizes a special sub-duct, "mini-duct", which serves as a hollow rod which can be driven or pushed into the occupied duct without damage to the installed cable. This "mini-duct" was constructed with a pre-installed pull line, footage marker, and coated with pulling lubricant on the inside surface for subsequent installation of the cable. The design of the "mini-duct" was evaluated for column strength to withstand sufficient pushing forces without collapsing or buckling.

A pneumatic drive mechanism was developed to push the "mini-duct" into the occupied duct. The system utilizes a caterpillar capstan drive which is portable and can be set-up in a manhole. The pneumatic drive system utilizes an air motor with a required delivery range of two to 180 psi,(Figure 5). The "mini-duct" is rigidly supported by a guide tube between the capstan drive and the duct entrance. No special efforts should be used in occupied duct, as this might cause damage to the installed cable.

A simulated duct run was built using "Schedule 40", 4 inch PVC pipe. Six hundred feet of duct was constructed, 300 feet was occuped by a 3 inch OD Stalpeth cable. Several successful experiments were carried out in rodding both the occupied and unoccupied sections. This system is now ready for field trial.

## FIELD TENSION CONTROL EQUIPMENT

A running line tensiometer (RLT) was developed to measure the tension in the winch line used to pull in the fiber optic cable. The RLT is placed on the winch at the manhole which is next in line with the "head end" of the cable and indicated the winch line tension at that location. When the cable pulling eye arrived at the manhole the RLT was removed and moved to the next manhole. The tensiometer was constructed at any position in the system being pulled,(Figure 6). Measurements were made as close to the pulling eye as possible to ascertain the true tension being applied to the cable. Measurements at the winch end should recognize that higher pulling forces can be expected as a result of the drag of the winch line itself.

### Load Cell Tensiometer:

Another method which can be employed consists of strain gauges mounted in a load cell. This load cell is placed at the head end of the cable between the winch line and the swivel. The electrical output of the strain gauge is transmitted to the far end of the winch by means of electrical conductors incorporated into a specially designed GCC winch line. This tensiometer has been used to indicate an accurate indication of the actual forces applied at the pulling eye when installing a long length of cable. The strain at the pulling eye is indicated by a digital read out on the strain gauge monitor,(Figure 7).

## DEVELOPMENT OF INTEGRATED COMPONENT SPLICING SYSTEM

### A. A Splice Case and Fiber Organizer:

Fiber optic cables are quite often installed in 1 km lengths and joined or spliced to make up the required system length. Splicing is commonly carried out by butting the fiber ends and fusing them together. Unlike conventional copper wires, glass fibers cannot be bunched, tied, wrapped and shoved into a splice case. Nor can they be crimped or bent at small angles because fibers will break or their attenuation will increase beyond permissible limits. Accordingly, General Cable has developed an organizer* to satisfy the unique jointing requirements of optical fibers. The fiber organizer has individual channels to hold the fiber snugly and yet not add enough pressure to cause any excess attenuation,(Figure 8). The length and number of channels are designed to accommodate the number of fibers in the cable and the length of excess fiber to be stored within the splice case for any future use. The fiber organizer fits into a standard telephone splice case with access holes for cable entry and exit. Also the fiber organizer module is designed for retention in the fusion welder for ease of splicing operation. Major advantages of the above unit are:

(1) Reliable and secure arrangement of spliced fibers.

(2) Easy placement and storage of spare fiber length for future use.

(3) Ready identification of each fiber by placement in a separate marked channel; and

(4) Quicker fusion splicing because the fibers are systemmatically organized.

### B. Cable Accumulator, Splice Case Sub-Assembly:

There are many situations where it would be advantageous to do the fusion splicing operation away from the final splice location. We have designed a cable accumulator sub-assembly* to permit such remot splicing operations,(Figure 9). The cable accumulator stores 25 feet of cable from each end and thus allows splicing to take place at a distance of up to 25 feet from the case. Also the additional cable storage permits future flexibility with regard to repair and relocation of the splice. The fiber organizer is assembled piggy back on the cable accumulator but is also demountable and can be moved around to a distance of 25 feet.

### C. Modified Fusion Splicer:

A commercially available fusion splicing unit was modified to accommodate the features indicated above for field use. The large binocular microscope was replaced with a smaller side mounted removable monocular microscope. Side mounting of microscope permits mounting of a splice case on the back end of the splicing plate by two rotating semi-circular brackets. This minimizes the movement of the fibers from the splicing area into the support area of the splice case.

A heating station was added to the splicing plate of the fusion splicer to heat shrink an irradiated expanded polyolefin tube over the fused splice. This heat shrink tubing provides mechanical support and strain relief to the splice area. The splice case and the splicing unit have thus been combined into an inegrated splicing system for field use.

### D. Apparatus for Controlled Environment Splicing in Potentially Hazardous Areas:

On occasion it becomes necessary to do fiber fusion splicing in a potentially explosive or flooded environment. We have modified the splice unit for such usage by containing it in an air tight enclosure. The power cord hoses that carry power to the fusion unit are hollow through which air or nitrogen is fed to maintain a positive pressure inside the enclosure. A water level indicator switch and a pressure switch are interlocked to the fusion power supply so as to interrupt the current flow to the splice unit in case of air flow failure or flooding of the float switch unit.*,(Figure 10).

## OPTICAL FIELD TEST EQUIPMENT

Attenuation and bandwidth are the two most significant parameters used to specify the propagation characteristics of an optical fiber cable. Two

* Patent pending

*Patent pending

special units were developed at General Cable Research Center to measure attenuation and pulse dispersion of long lengths of optical fiber cables installed in the field.

Attenuation Measurements:

The light source selected is a CW laser with a single wavelength operating at 850 nm. The majority of cable installations are operating at or near this wavelength. The optical arrangement as well as the electronic schematic is shown in Figure 11. Two identical optical power meters are located at each cable end to determine the input and output power level respectively. In order to measure the cable loss at the equilibrium power distribution, the laser light must be launched through a reference fiber and then into the cable under test. The dynamic range and measuring accuracy are approximately 50 dB and 0.3 dB respectively.

The laser, power supply and reference fiber are contained in a case approximately a 12 inch cube. The unit is battery operated with a built-in charger and a working life of 12 hours between charges. Hand held optical power meters, also battery powered, are used as detectors.

Bandwidth Measurements:

The bandwidth measurement is related to the information carrying capacity of the fiber. At present, we use time domain approach to measure fiber response to a very short pulse. Figure 12 shows the electrical and optical arrangement of the optical transmitter and receiver. A compact injection laser diode is used as a light source. A common switching transistor, operated in its avalanche region, is the main element to drive the laser diode and to generate an optical pulse of 500 picoseconds FWHM (full wave half magnitude). The laser diode, as well as the APD detector, are attached to short fiber tails which are utilized as an optical coupling device to eliminate the conventional lens approach. To enhance the measurement dynamic range, cascade wideband amplifiers are inserted between the APD and the scope. An overall dynamic range of 40 dB with good signal reproducibility is achieved.

The field test unit is comprised of a pulsing unit, a detector and a scope. The pulsing unit and detector are mounted on a chassis approximately one foot by three feet. The unit requires a one gigahertz bandwidth scope to detect the pulse dispersion. The power requirements for the field test unit, including scope is 400 watts at 120 volts, 60 Hz.

## CONCLUSIONS

It is evident from the above discussions that fiber optic cables cannot be handled and installed with the same procedures, methods and equipment used on conventional cables. However, the same careful engineering considerations are necessary to ensure high reliability and optimum performance. This paper described the special devices and techniques that have evolved from such experience.


## ACKNOWLEDGMENT

The author gratefully acknowledges the contributions of Ken Korbelak in the design and development of several of the devices described.


## REFERENCES


1. J. B. Masterson and J. Peveler, "Up Date on the Optical Performance of Field Installed Fiber Optic Cables", 28th IWCS, Cherry Hill, N.J. November 1979.

2. G. Bahder and J. A. Olszewski, "Experience To-Date with Optical Fiber Cables", 26th IWCS, Cherry Hill, N.J., November 1977.

3. J. A. Olszewski, A. Sarkar, Y. Y. Huang, "Optical Fiber Cable for T1 Carrier System", 25th IWCS, Cherry Hill, N.J., November 1976.

4. Robert C. Tenten, John Kaye, Joe Masterson, "A 5.1 km Repeaterless Multi-Channel Fiber Optic Video Trunk", 3rd International Fiber Optics and Communications Exposition in U.S., San Francisco, California, September 1980.

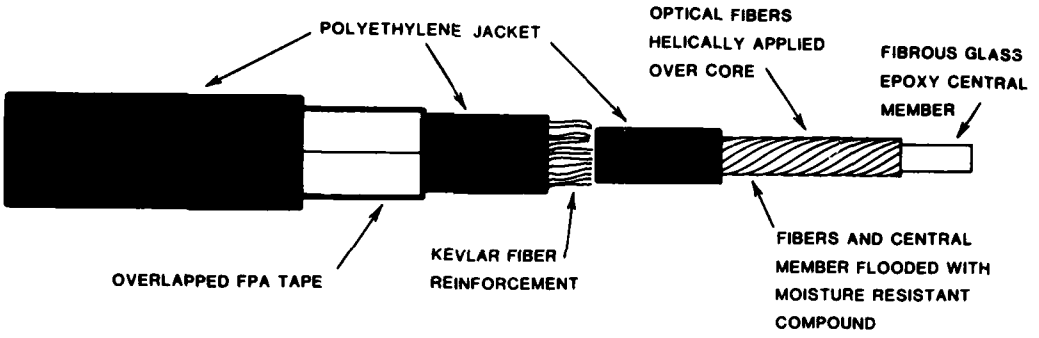



FIGURE 1: Cable Construction

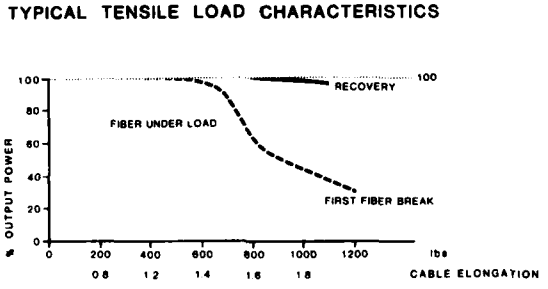



FIGURE 2
Tensile Load Characteristics

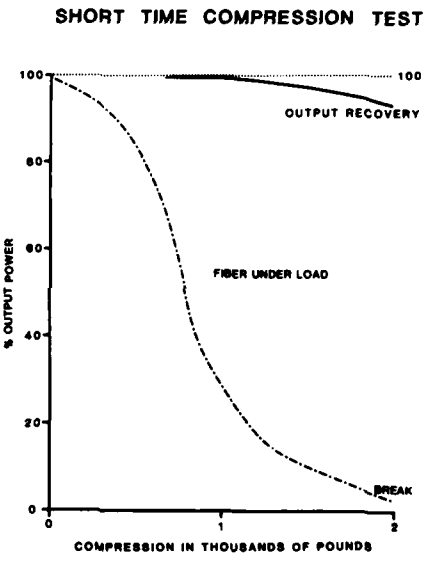



FIGURE 3
Compression Test

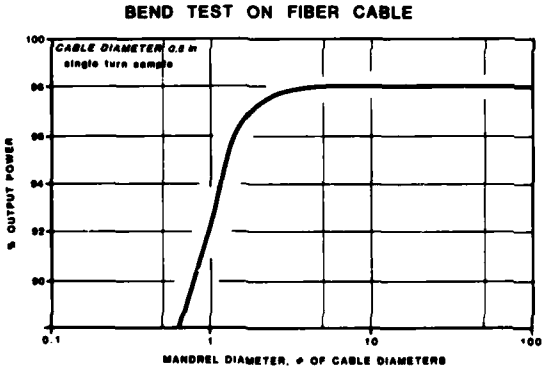



FIGURE 4
Bend Test

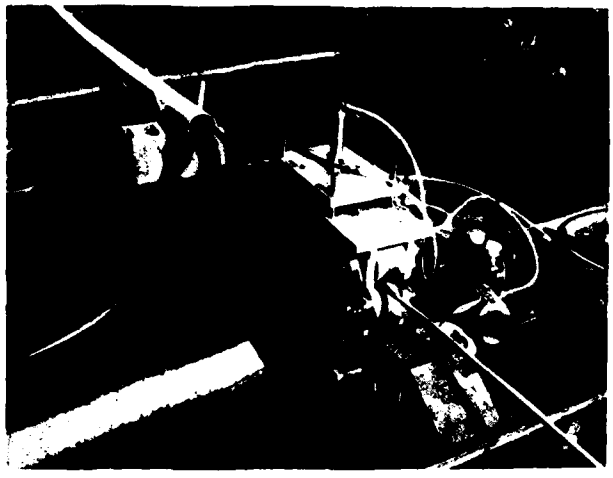


FIGURE 5
Duct Rodding Drive System

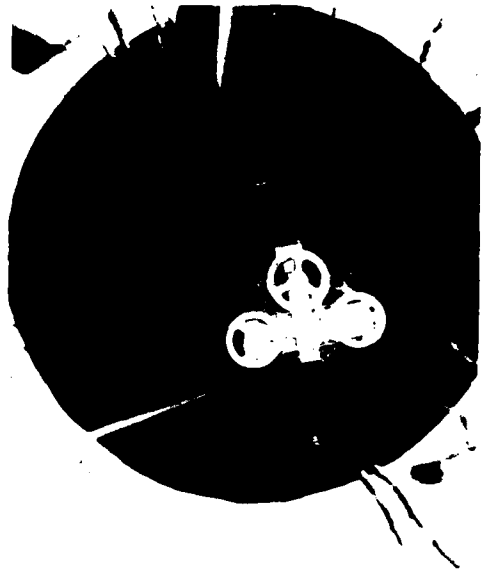


FIGURE 6
Running Line Tensiometer



FIGURE 7
Load Cell Tensiometer

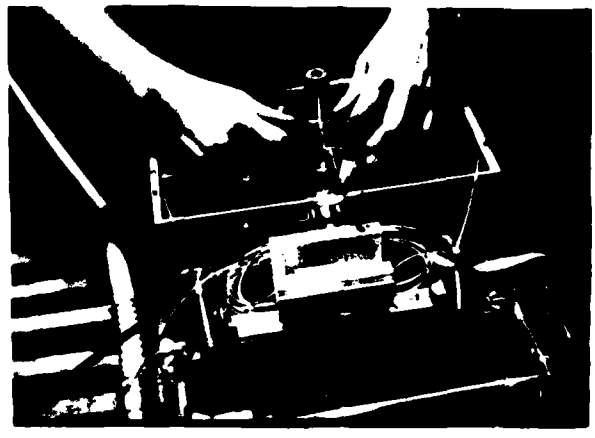


FIGURE 8
Splice Case Organizer



FIGURE 9
Cable Accumulator

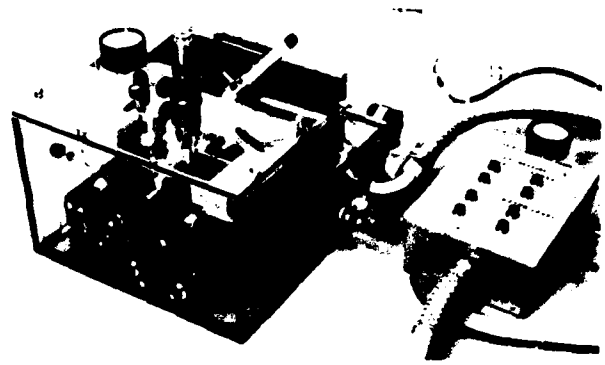
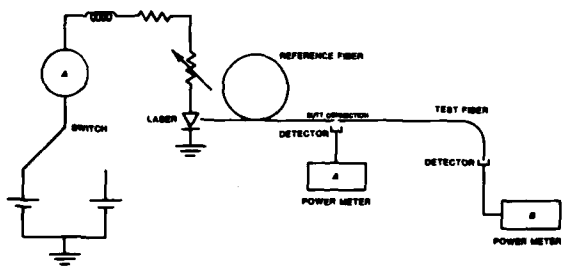
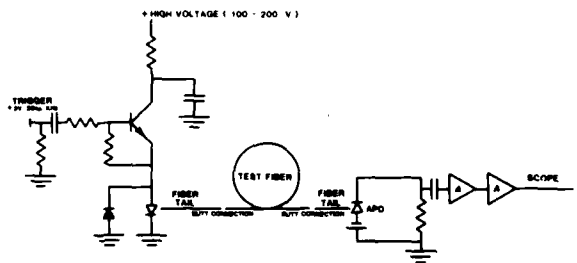


FIGURE 10
Controlled Environment Splice Unit




CIRCUIT SCHEMATIC AND OPTICAL ARRANGEMENT FOR MEASURING ATTENUATION

FIGURE 11
Attenuation Test Set




CIRCUIT FOR PULSING LASER DIODE AND OPTICAL ARRANGEMENT FOR MEASURING FIBER BANDWIDTH

FIGURE 12
Fiber Bandwidth Test Set



Joseph Masterson is Assistant Director of Research and Development, Fiber Optics, with General Cable Company Research Laboratory in Edison, New Jersey. He has been involved with the design and installation of fiber optic cables. He received his BSEE degree from Newark College of Engineering and an MS in Operations Research and Systems Analysis from Polytechnic Institute of Brooklyn.

# FABRICATION AND TEST OF OPTICAL FIBRE CABLES FOR MILITARY AND PTT APPLICATIONS

W. Schmidt and U. Zwick

Standard Elektrik Lorenz AG, Stuttgart, Germany

## Abstract

The construction, fabrication and test of various optical fibre cables are reported. For military purposes a thin field deployable cable consisting of two tight jacketed, high tensile strength fibres is described. The high performance of this cable with respect to mechanical and environmental behaviour is shown. A filled cable with 4 graded index fibres and 10 copper wires is demonstrated which has been designed for a 15 km route of the Deutsche Bundespost. For a PTT field trial in Berlin a 320-core cable with standard graded index fibres has been developed. It is based on a 16-core element, five of which are combined in an 80-core group and four groups then form the 320-core cable. In the final length of 905 m attenuation and dispersion values at 850 nm are $< 4$ dB/km and $< 2$ ns/km respectively.

## Introduction

The progress in the development of optical fibres with low attenuation and high bandwidth has forced their use as a transmission medium in communication systems. Besides their high information capacity over large repeater spacings their small size, light weight and immense flexibility are advantageous for many applications.

In practice fibre cables are used which often have to meet requirements of conventional cables, e.g. winding or laying performance. Various optical fibre cable designs have been proposed and cable constructions for several applications have been realized.[1-6]

In this paper we describe three types of optical cables designed and tested for use under different environmental conditions. First a new concept of a field deployable cable with a construction and performance which result from several experimental investigations. The second type is a filled cable where in a composite structure fibres are incorporated aside of copper wires serving for regenerator power feeding. Third a multifibre cable is described which is based on the unit type of a 16-core element.

## Field deployable cable

Conventional military copper cables designed for portable use in the field have outer diameters in the range 10 - 12 mm. On the standard military drum 400 m of that cable can be carried having a weight of 65 kg. The aim was to design and produce a cable using optical fibres in order to increase the possible length on the drum and therefore the transmission span length and to reduce the weight. This had to be achieved with similar mechanical behaviour as that of the conventional cable type which is a very important parameter for the field application.

## Cable construction

The cable construction is shown in fig. 1. Two optical fibres and one filler are stranded together with a short laylength and fixed with a thin Nylon tape. 16 Kevlar elements are then stranded around the cable core with a long laylength.

The theoretical breaking load is more than 3200 N. Practical experiments have shown that the cable withstand 1000 N under field conditions without change in the optical and mechanical performance. The low temperature grade PVC sheath gives the cable the needed flexibility down to - 55 °C. The final outer diameter is 5 mm. A length of 1600 m is now possible to wind on the standard drum compared with the 400 m in conjunction with an additional weight reduction of about 10 kg.

Graded index fibres are used with a silicone primary and a tight plastic secondary coating. Fibre structure parameters are given in table 1.

The fibres are proof-tested over their full length with 11 N tensile strength. A trial cable with a length of 1600 m has

been made where at 850 nm the attenuation in the two fibres was 3.9 and 4.4 dB/km. The loss increased to 4.4 and 5.2 dB/km after cabling, the dispersion was 1.0 ns/km in both fibres.

Table 1 Fibre structure parameters

| | |
|---|---|
| core diameter | 50 µm |
| cladding diameter | 125 µm |
| buffer diameter | 220 µm |
| jacket diameter | 0.95 mm |
| N.A. | 0.23 |

Mechanical tests

With a laboratory set-up the winding behaviour using small size mandrels has been tested. The results are shown in fig. 2 for mandrel diameters of 12 and 27 mm. In the case of the small mandrel diameter the excess loss is only 0.8 dB even when 10 windings are applied. Cycle tests with winding and rewinding the cable showed no hysteresis effect.

As examples two other tests with simulated and real conditions are described in the following: The 1600 m cable length was loosely layed across each other on the ground. Beginning and end of the cable were connected to an attenuation measuring device. The signal change was then recorded when a car was driven across the cable as seen in fig. 3. During load a signal reduction of only about 10 % was observed, but the effect was fully reproducible.

To demonstrate and test the feasibility the same cable was layed in the field under similar environmental conditions as applied for a conventional cable. It was for instance layed across roads and hanged from one tree to another in a distance of about 100 m. The rewinding of the cable onto the drum was carried out in a short time using a motor winch on a lorry. In the test the cable exhibited a good handling behaviour and no degradation of the optical and mechanical characteristics occured during and after the test.

Mobile system

In fig. 4 the mobile military system is shown. It includes the 1.6 km length of cable which is wound on a standard drum and connected to two field telephone units. Both ends have common field cable plugs, only modified in the inner part. In one side a LED is built in as a transmitter and in the other a PIN diode as a receiver, so that the optical part of the cable is an inherent unit and only the plugs have to close the electrical connections.

Compared with the conventional copper cable the advantages of the optical fibre cable are:

-longer transmission span length
-lower weight
-higher bandwidth
-electromagnetic pulse immunity
-electrical isolation between terminals
-metal free

Filled optical cable

For a Deutsche Bundespost project in the urban network of Stuttgart a composite cable containing optical fibres carrying real telephone traffic and copper wires for regenerator power feeding was developed. The route length of 15 km is devided in two sections with a repeater in the middle. According to the Bundespost requirements the cable has to be protected against water infiltration, e.g. by techniques like gas pressure control or Jelly filling. Because of the small cable diameter we decided to fill the cable with Petrol Jelly.

To check the fibre performance selected secondary coated lengths have been layed in Petrol Jelly at temperatures up to 70 °C for some months. No change in their transmission parameters could be observed and mechanical measurements after the test run showed no degradation effect[5] which is in agreement with Horima et al.[5]

Fig. 5 shows the cable construction. 4 graded index fibres with parameters as described in table 1 are used. They are each arranged between 5 copper wires and an additional glass filament cord for sheltering. This cable core is not a round figure but the aluminium tape corrects it. The final PE sheath leads to an outer diameter of about 15 mm, the weight is 220 kg/km and the strength is about 3000 N.

The 16 elements were stranded round an extruded Kevlar strength member using our optical cable stranding machine. The filling process took place at an extrusion line in the cable plant which is normally used for filling copper cables. It is an on-line filling process with APL tape forming and sealing, as well as the final PE sheathing. In table 2 cable losses of a 800 m long trial cable are shown for each production stage. Higher loss figures in column A or B compared to C or D may be due to the fact that the final cable contains only parts of the original fibre lengths.

Table 2 Loss in dB/km at 850 nm for each production stage

| | A | B | C | D |
|---|---|---|---|---|
| red | 4,1 | 4,4 | 3,7 | 3,7 |
| white | 3,1 | 4,7 | 4,4 | 3,7 |
| blue | 3,9 | 3,9 | 3,5 | 3,7 |
| natural | 3,5 | 4,6 | 4,7 | 4,2 |

A: fibre with primary coating
B: fibre with secondary coating
C: stranded cable
D: filled cable

## 320-Core optical fibre cable

In a joint program by the Deutsche Bundespost and the Ministry of Research and Technology a second field trial is carried out in Berlin where in one project the telephones of about 150 subscribers are connected via optical fibres to the local exchange office. To combine the necessary 300 fibres in one cable and to use only one duct, a multicore cable with 320 fibres has been developed.

### Cable construction and fabrication

The cross-sections of the 320-core optical fibre cable and of the 16-core elements are shown in fig. 6 and 7. For the basic structure (16-core element) Kevlar extruded with 4.2 mm Ø polyethylene is used as a central strength member. Graded index fibres are used with a silicone primary and a tight plastic secondary coating. Fibre parameters are given in table 1. Fibre attenuation and dispersion in the cable are specified to be less than 6 dB/km and 3 ns/km respectively at 850 nm. These parameters are measured off-line in the fibre, additional the attenuation value is checked at each cabling stage. All fibres are proof-tested over their full length with 11 N tensile strength.

The 16 fibres in the basic structure are stranded with a pitch of 120 mm and covered by two foamed polyester tapes resulting in an outer diameter of 6.9 mm. Five of these elements are stranded into an 80-core group sheathed with 20.8 mm Ø PVC. Four of these groups are then stranded together with soft fillers into the 320-core cable finally sheathed with PVC. The cable has an outer diameter of 58 mm and weights 2100 kg/km.

A final length of 905 m were fabricated where only 2 of the 6 cabling steps took place on machines designed for optical fibre and cable use. Starting with the stranding of the 80-core groups, all steps have been carried out on conventional machines used for stranding and sheathing large copper cables.

The construction of the cable allows to strip the outer sheath at a cross connection point and to pull the sheathed 80-core groups into different ducts. The 80-core groups are again divided into 16-core elements leading into the houses. A small 4-core cable with 2 fibres and 2 copper wires is installed to the subscriber. A photograph of these four cable structures shows fig. 9.

### Results

Fig. 8 shows a diagram of fibre attenuation at 850 nm wavelength, with the distribution of all 320 fibres before and after cabling. The mean value in the fibres before cabling was 2.8 dB/km which increased to 3.2 dB/km after cabling. The average dispersion is $< 1$ ns/km.

Loss measurements at 850 mm were performed in long fibre lengths using filled core and filled NA conditions (cut-back method). Sample tests at each cabling stage and final measurements a 1 km launching fibre was used (insertion loss, non-destructive method).

### Cable laying

The main cable with the 20 Kevlar strength members in the 16-core elements has a theoretical breaking load of 100 000 N which refers to an elongation of 2.5 %. For laying a conventional cable winch is used where the pulling force can be adjusted to a limit value. A special pulling head is fixed to one cable end as shown in fig. 10. In the cable end the strength members are sealed in one block together with a metal housing. Then the tube is shrinked onto the cable sheath resulting in a uniformly distributed load during pulling.

The cable has been pulled into a duct in Berlin end of July 1980. The starting force was 1.8 t reducing to 1.3 t at the end. The pulling-in speed raised up to 10 m/min, so that the pulling-in time of the 905 m long cable has been less than two hours. Further results will be presented at the conference.

## Conclusion

Optical cables for three different applications have been developed, fabricated and tested. The practical use of the field deployable cable has been proved under adverse conditions. Further improvements seem possible by reducing size and weight without decrease of the good mechanical performance of the cable. A water tight filled cable containing fibres and copper wires has been presented allowing high quality optical transmission and repeater power feeding.

The feasibility has been shown to fabricate a multifibre cable based on the unit type. 320 fibres with loss 4 dB/km (850 nm) and dispersion 1 ns/km have been accomplished in a cable with an outer diameter of 58 mm.

Acknowledgement

The authors thank their colleagues in the fibre and cable group for the assistance throughout the work.

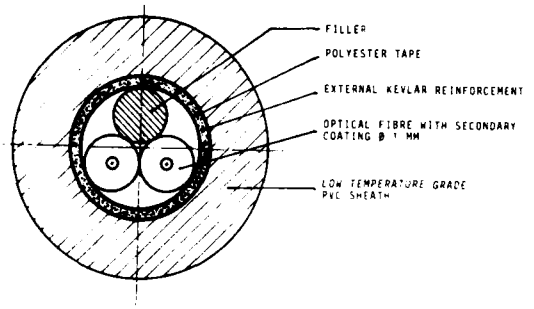



fig. 1 Cross-section of the field deployable optical cable

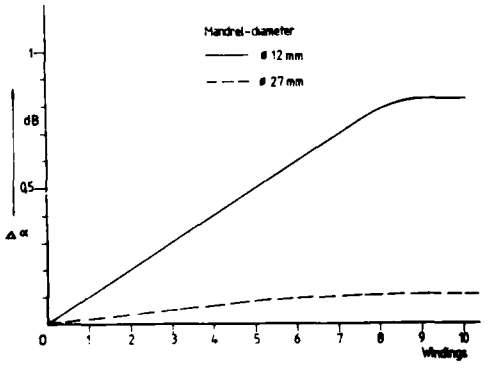



fig. 2 Winding performance of the field deployable cable for two mandrel diameters




fig. 3 Cable laying test



fig. 4 Mobile military system

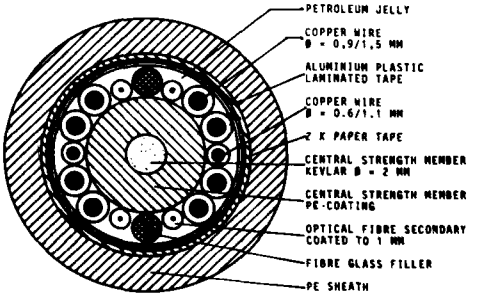



fig. 5 Cross-section of the filled optical cable

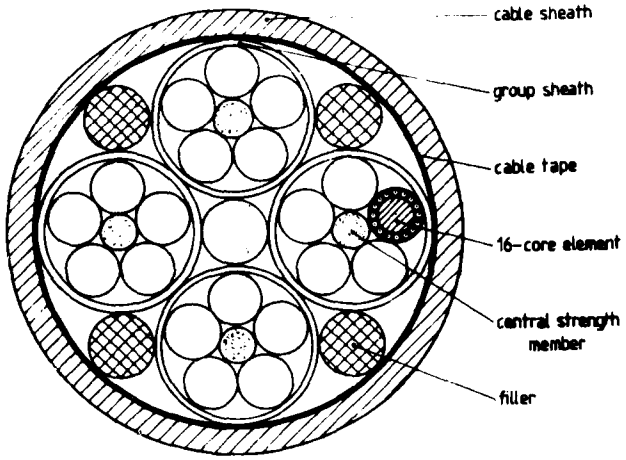



fig. 6 Structure of the 320-core cable

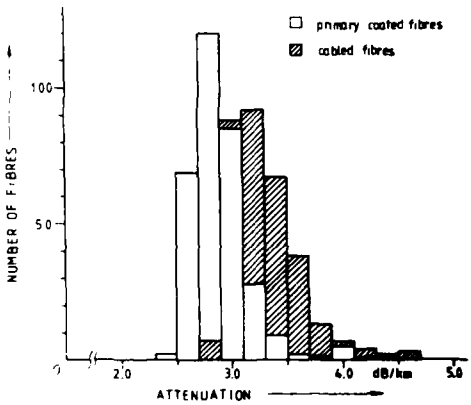



fig. 8 Histogram of fibre attenuation at 850 nm in the 320-core cable

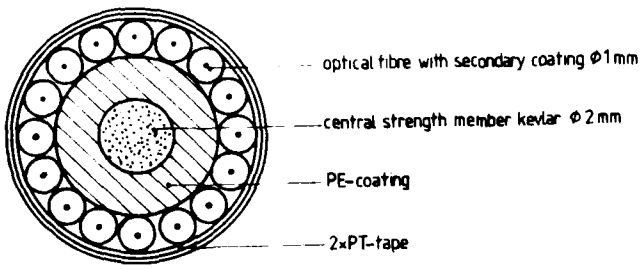



*fig. 7 Cross-section of the 16-core element*

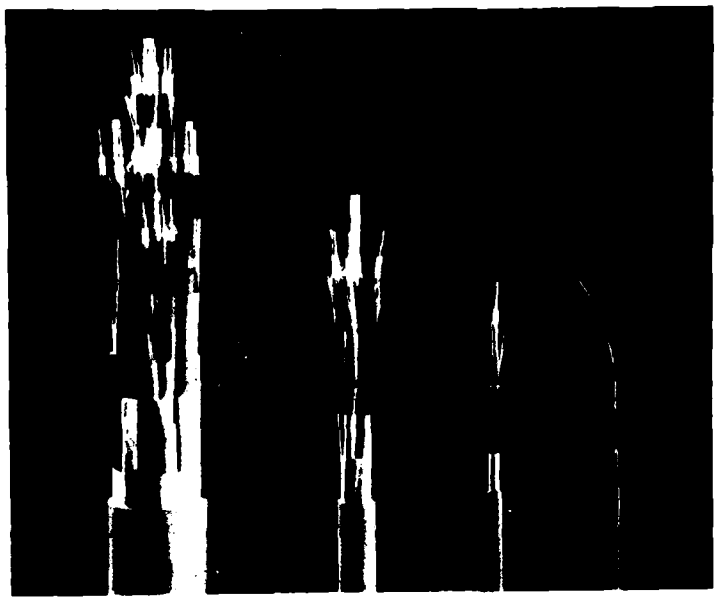


fig. 9 Photograph showing from left to right 320-core, 80-core, 16-core and two fibre/two copper wire cable

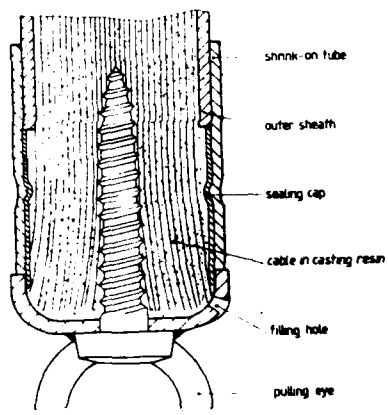



fig. 10 Pulling head

## References


1. S.G. Foord and J. Lees, "Principles of fibre-optical cable design", Proc. IEE, Vol. 123, No. 6, June 1976.

2. P.F. Gagen and M.R. Santana, "Design and Performance of a crossply lightguide cable sheath", 28th International Wire and Cable Symposium, Cherry Hill, N.J., Nov. 1979.

3. J.B. Masterson and J. Peveler, "Update on the optical performance of field installed fibre optic cables", 28th International Wire and Cable Symposium, Cherry Hill, N.J., Nov. 1979.

4. K. Inada, R. Yamauchi, Y. Sugawara, T. Kobayashi, H. Suzuki and K. Ishihara, "High density low-loss fibre unit and the cabling", Optical Communication Conference, Amsterdam, Sept. 1979.

5. H. Horima, S. Tanaka, T. Nakahara, H. Kumamaru and K. Ishihara, "Jeily filled optical fibre cables", Optical Communication Conference, Amsterdam, Sept. 1979.

6. E. Adler, H. Haupt and W. Zschunke, "A 34-Mbit/s optical field trial system" 4th European Conference on Optical Communication, Genova, Sept. 1978.




Wolfgang Schmidt was born in 1944. He studied physical engineering at the Ingenieurschule Wedel/Hamburg. After graduated in 1970 he started working at Farbwerke Hoechst, where he has been engaged in R&D-activities for plastics. In 1972 he joined Standard Elektrik Lorenz AG in Stuttgart, starting with R&D for plastic sheathing materials of wires and cables. Since 1975 he is engaged in the development, design and production of fibre optic cables.



Ulrich Zwick was born in 1947. He graduated in Physics at the university of Stuttgart in 1972 and received a Ph. D. at the Max-Planck-Institute for solid state research. In 1976 he joined Standard Elektrik Lorenz AG in Stuttgart to work on optical measurements. He is now responsible for development and production of optical fibres and cables.

# COMPOSITE FIBER-OPTIC OVERHEAD GROUND WIRE

M. IGARASHI
J. YOKOYAMA
H. IWAMURA

The Tokyo Electric Power Co., Inc. Japan

N. MORI
I. MATSUBARA
Y. SAITO

Sumitomo Electric Industries, Ltd. Japan

## SUMMARY

A "composite fiber-optic ground wire (OPGW)" which incorporates optical fiber into an overhead ground wire has been developed. Through the use of optical signals, this new wire provides additional communication capabilities in power transmission line networks. Its features are:

(1) performance characteristics and shape equivalent to those of conventional overhead ground wires, with minimum changes in design and minimal use of special parts required
(2) optical fiber with much improved heat resistance for more extensive applications
(3) a reinforced aluminum tube to house and mechanically protect the optical fiber
(4) a built-in aluminum tube structure located at the center of stranded conductors, providing rigid protection and high reliability

This paper describes the performance characteristics of our recently developed "composite fiber-optic ground wire, "together with its test results.

## 1. Introduction

As electric power systems in Japan continue to expand, and as more and more of the related equipment is being operated automatically, there have been significant increases in the amount of information gathered from electric power distribution networks for boosting power supply reliability. To ensure accurate collection and transfer of the pertinent data, measures have been taken to expand the microwave communication networks all over the country. Today, however, the demand is such that a much more drastic means to provide massive, error-free, long-distance data communication needs to be implemented very soon.

Meanwhile, improvement in the transmission characteristics of optical fiber has been prompting studies of how to put the much-hailed optical communication technique into practice. The prospect of introducing optical communication, which has been long anticipated, now appears quite encouraging.

Under these circumstances, a composite fiber-optic overhead ground wire combining the functions of an overhead ground wire and an optical communication line has been developed. The scheme is to set up an extensive data communication network by incorporating the new composite wire existing power transmission routes.

Reported here is a description of this composite-optic overhead ground wire which would enable quick and error-free collection of information on power distribution lines and their environments. The development is expected to help provide easier maintenance and higher public safety of power distribution system equipment.

## 2. Composite Fiber-Optic Ground Wire (OPGW)

### 2-1 Design

There are two ways to add an optical fiber to an overhead ground wire; incorporating it into the wire itself (build-in method), or placing it outside the wire (non-build-in method). The built-in method provides the following advantages:

(1) In application, there is no need to modify the design of supports because of the negligible difference in outside diameter, weight, and other physical properties from those of conventional overhead ground wires.
(2) Installation procedures are the same as for conventional overhead ground wires, and the existing tools and devices can be used.
(3) Since it is protected by strands, the optical fiber has high resistance to lightning.
(4) Thus it has long-term, high reliability.

On the other hand, there are some problems to be solved:

(1) Production becomes difficult because of the reduced outside diameter of the optical fiber unit.
(2) In case of breakage, it is difficult to isolate the optical fiber alone for repair.

On the other hand, the non built-in method may permit easier reinstallation in case of optical fiber breakage, but it involves another problems, i.e., the need for changes in support specifications in order to withstand the increased wind pressure against the OPGW with wider surface area. For example, some tests have revealed that when a 10-millimeter-across optical fiber unit is attached to a 21-millimeter-across GW, the wind presure is 1.6 to 1.9 times as high as otherwise. Also, the optical fiber unit is liable to develop fatigue-induced breakage and is susceptible to external damage. It is virtually impossible to protect it from lightning strikes. In addition, installation of the optical fiber unit requires a special set of procedures.

After evaluation the two methods mentioned above, we decided to use the built-in type with its numerous advantages taken into account. The problem of repairing was solved by constructing the OPGW so as to have higher reliability.

The use of overhead ground wires in various sizes depending on the power transmission voltage, transmission capacity, and line layout for each system was also considered, and two types of OPGW, have been developed: for heavy-load applications (type A), and for general-purpose applications (type B). Their typical specifications are given in Table 1.

As shown in Fig. 1, each type of OPGW contains one optical fiber unit (OP unit) at the center, consisting of 4 optical fibers housed within an aluminum tube having the same outer diameter as that of the individual wires that surround it. Figure 2 shows an outside view of the new OPGW.

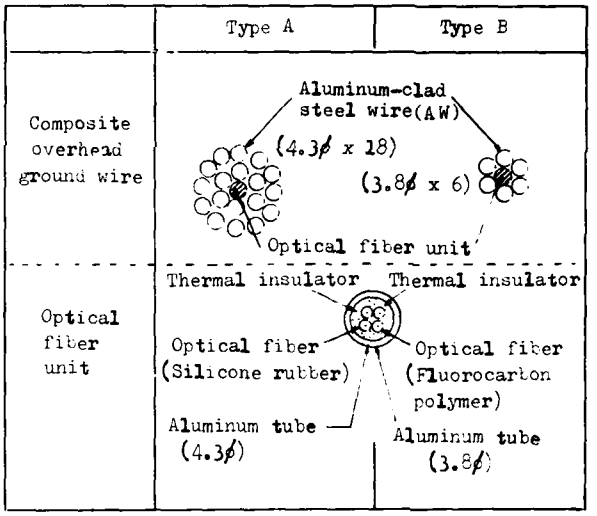



Fig. 1 Structure and Design of Composite Overhead Ground Wire

Table 1 Specification of Composite Overhead Ground Wire

| Description | | | Type of Cable A | Type of Cable B |
|---|---|---|---|---|
| Optical fiber | Core/cladding dia. (mm) | | 0.05/0.125 (Graded index type) | |
| | Number of fibers | | 4 | 3 |
| | Outer jacket | Material | Aluminum welded tube | |
| | | Outer dia. (mm) | 4.3 | 3.8 |
| | Attenuation (dB/km at $\lambda$ = 0.85 $\mu$m) | | 3.0 | |
| Ground wire | Wire of outer-layer | Material | Aluminum-clad steel wire (IACS 40%) | (IACS 23%) |
| | | Outer dia. (mm) | 4.3 | 3.8 |
| | Number of wires of outer-layer | | 18 | 6 |
| | Overall dia. (mm) | | 21.5 | 11.4 |
| | Sectional area ($mm^2$) | | 261.4 | 68.0 |
| | Modulus of elasticity ($kg/mm^2$) | | 10500 | 16500 |
| | D.C. Resistance ($\Omega$/km at 20°C) | | 0.167 | 1.11 |
| | Coefficient of thermal expansion (1/°C) | | $1.6 \times 10^{-5}$ | $1.3 \times 10^{-5}$ |
| | Calculated breaking load (kg) | | 16440 | 7940 |
| | Thermal short-time current (KA, 1S) | | 18.0 | 2.8 |
| | Operating temperature (°C) | | -30 ~ +150 | -30 ~ +100 |



Fig. 2 View of the new Type-A Composite Ground Wire

2-2 Heat-Proof Optical fiber

An optical fiber construction in which silica glass fiber is first coated with room-temperature-vulcanized silicone resin and then with Nylon-12 has been widely used in Japan. But Nylon-12 undergoes significant deterioration at high temperatures and thus cannot withstand the maximum operating temperature of 150°C required for the overhead ground wire.

After prolonged investigation, we decided to use heat-vulcanized rubber and easy-to-extrude fluorocarbon polymer instead of Nylon-12. Table 2 gives a comparison of the general characteristics of the above-mentioned resin-coated optical fibers and conventional Nylon-12-coated optical fibers.

The data in the table indicates that the new optical fibers have characteristics virtually equivalent to those of conventional optical fiber. The somewhat reduced resistance of the silicone-rubber-coated optical fiber to compression, attributable to the lower hardness of silicone rubber, can be compensated for by providing some improvements in the cable manufacturing process. In Fig. 3, the transmission loss variation is plotted against heat aging time for the silicone-rubber-coated optical fiber and the fluorocarbon-polymer-coated optical fiber, showing that they were stabilized at 160°C and 130°C, respectively. The latter shows an increase in transmission loss when heat-aged at 150°C. This may be attributed to the internal constriction caused by the crystallization and shrinkage of the fluorocarbon polymer.

Figure 4 shows by percentages of retention the decrease in elongation of coating materials coating materials under heat aging. Assume that 50% retention in elongation is the life of the resins. When their lives are estimated from the change in the characteristic at 80°C according to the law of 10°C octave, fluorocarbon polymer has a life to 22 years at 100°C, and silicone rubber, over 20 years at 150°C. The silicon-rubber-coated optical fiber is applicable to the type-A OPGW and the fluorocarbon-polymer-coated optical fiber to the type-B OPGW.

Table 2 Characteristics of the Optical Fibers

| Description \ Coating material | | Silicone rubber | Fluorocarbon polymer | Nylon-12 |
|---|---|---|---|---|
| Fiber | Core/cladding dia. | 50/125 μm | | |
| | Δn | 1.0% | | |
| Tensile strength (kg) | | 5.7 | 5.8 | 6.0 |
| Resistance to compression: 30kg ( Δα dB/0.5m) | | 3.5 | 0.1 or less | 0.1 or less |
| Resistance to water exposure: 24 hrs ( Δα dB/km) | | 0 | 0 | 0 |
| Splicing loss (dB/location) | | 0.098 | 0.072 | 0.083 |

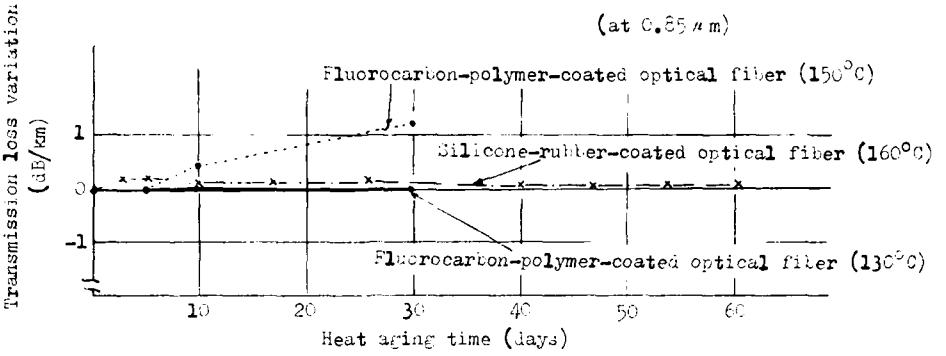



Fig. 3 Transmission Loss Variation vs. Heat Aging Time

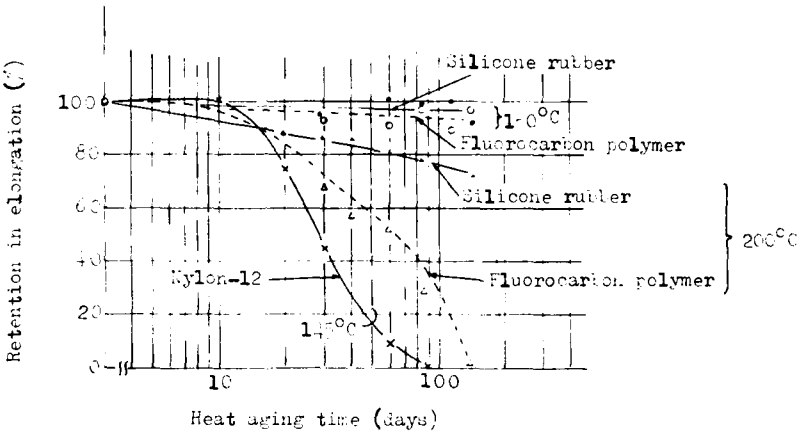



Fig. 4 Changes in Elongation of Coating Materials under Heat Aging

2-3 Optical Fiber Unit

The OP unit needs to withstand various kinds of stress applied during production and installation of the OPGW, as well as sever ambient conditions involving vibration and change in temperature after installation. The following tests were conducted to find the critical strength of the OP unit with respect to these external forces. To simulate the condition of being built-in in a long OPGW, the fluorocarbon polymer OP unit under test was fixed at both ends with resin in order that good bonding is achieved between the optical fiber and the aluminum tube. In another test, a silicone-rubber-coated optical fiber proved to have almost the same characteristics.

Figure 5 shows the measured change in transmission loss of the optical fiber versus bending diameter of the OP unit bent around a mandrel. Under test, the two OP units proved quite satisfactory in flexibility, with no increase in transmission loss occurring in the optical fiber of either OP unit in the range of bending diameters 100 mm above.

Figure 6 illustrates the measured elongation of the OP unit with tension applied thereto. It was found that the type-A and type-B OP units could endure tensile strain up to 300kg and 230kg, respectively, no damage was detected in the optical fiber. At the time of fracture, the elongation of the OP unit was approximately

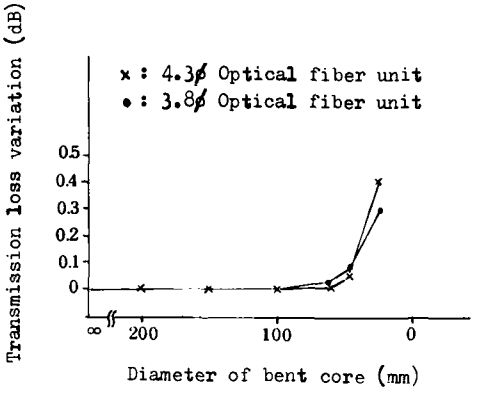



Fig. 5 Transmission Loss Variation with Bending (at 0.85 $\mu$m)

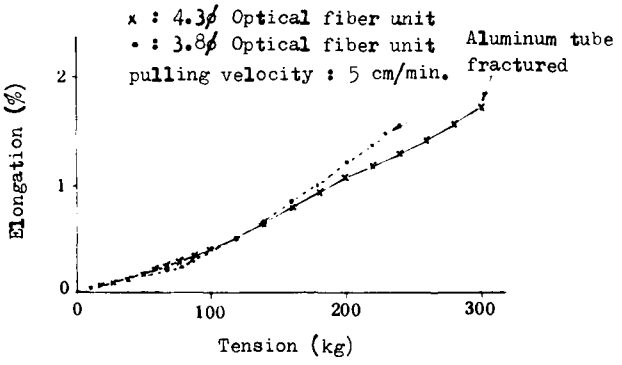
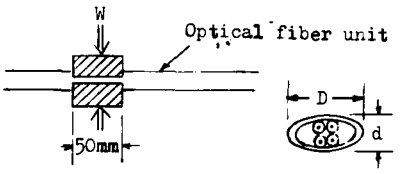



Fig. 6 Tensile Strength vs. Elongation

1.8%, about 0.1% larger than that of the optical fiber. The elongation of the optical fiber was measured by electrical length on a continuous basis. In any cases, a breaking extension of the OP unit of 1.8% would be suitable enough for any application (extension of Aw: 1.6-2.0%).

Figure 7 reveals how much the OP unit is flattened and how much an increase in transmission loss occurs in the optical fiber under a crushing load applied on a 5 cm-long section of the OP unit. The flatness of the OP unit is defined by the following expression:

$$K = (1 - \frac{d}{D}) \times 100 \ (\%)$$




$$K = (1 - \frac{d}{D}) \times 100$$

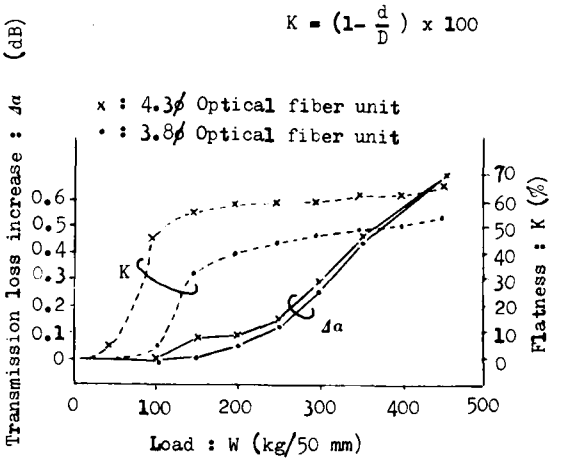



Fig. 7 Crushing Load Characteristics

where, K is the flatness of the OP unit, d the length of the minor axix of the crushed portion, and D the length of the major axis thereof. It was confirmed that transmission loss in the optical fiber did not change until the OP unit exceeded 30% in flatness, thus proving that crushing loads up to 100 kg/50 mm could be withstood.

Table 3 shows typical results of repetitive fatigue tests on the OP unit conducted with a rotation-bending fatigue testing machine. It was verified that no damage was inflicted to the optical fiber when a stress of about 7 kg/mm$^2$ was applied to the aluminum tube surface $10^7$ times, or even when the aluminum tube was fractured under 9 kg/mm$^2$ stress.

Table 3. Fatigue Characteristics

| Stress applied to the aluminum sheath | Rotation-bending cycles until aluminum sheath fractured | Damage to optical fiber |
|---|---|---|
| 7.0 kg/mm$^2$ | $\geqslant 1.09 \times 10^7$ | None |
| 7.5 kg/mm$^2$ | $\geqslant 1.04 \times 10^7$ | None |
| 9.0 kg/mm$^2$ | $1.69 \times 10^6$ | None |

2-4 Composite Fiber-Optic Ground Wire

The tests on the OP unit alone discussed so far were effective for evaluating its characteristics: the sample was easy to handle, the equipment necessary for testing even long samples was relatively small, and scattering of the samples' performance data was minimal. But the tests were not sufficient for evaluating the performance of OPGW as a whole. That is, the performance of the OP unit in combination with the AW (OPGW) had to be tested. A 300m sample of type-A and a 50m sample of type-B OPGW were manufactured and subjected to various performance tests.

2-4-1 Producibility

Changes in transmission loss of the optical fibers during stranding the aluminum-clad steel wires with the OP unit at the center were investigated. This test was performed on three of the four fibers in the type-A OPGW, which is intended for application under heavy load conditions. As shown in Table 4, the changes in transmission loss, which were at the same level as the accuracy of measurement ($\pm$0.2 dB/km), were negligibly small.

Table 4 Changes in Transmission Loss of Optical Fiber Before and After Stranding (dB/km at 0.85$\mu$m)

| Optical fiber | Before stranding | After stranding |
|---|---|---|
| 1 | 2.81 | 2.94 |
| 2 | 3.05 | 3.45 |
| 3 | 2.76 | 3.13 |

2-4-2 Mechanical Characteristics

The behavior of the optical fiber characteristics was tested by applying load to both types of OPGW until fracture occured. The OPGW proved to have satisfactory resistance to tention, as the results verified that:

(1) The strength against rupture was several percent higher than the design value (Table 1) for both types.
(2) No damage was observed on the OP unit even after some of the AW broke, and no increase in transmission loss of the optical fiber occurred.

2-4-3 Temperature Characteristics of OPGW

Because the OP unit and AW are known to be different in linear expansion coefficient, it is considered possible that the transmission loss of the optical fiber might increase. Tests of various temperature characteristics were made on the type-A OPGW. The results were satisfactory, as shown in Table 5.

3. Accessories

3-1 Dead-end Clamp

A compression-type dead-end clamp for use on both type-A and type-B OPGW has been developed. It has a special structure to protect the OP unit during compression. To achieve the required gripping force with a dead-end clamp, it usually is necessary to apply high compressive force to the wire. But our tests indicated that using an ordinary clamp to compress the wire would deform the OP unit and cause an increase in transmission loss too large for actual use. The new structure incorporates a protective tube for prevention of deformation of the OP unit. When inserted, the clamp allows the OP unit, together with the protective tube, to extend beyond the end of the clamp.

The resulting compression-type dead-end clamp is as practical as any of those with conventional structures. Figure 8 shows an outside view of the components of the new dead-end clamp.

Table 5 Temperature Characteristics of OPGW

| Test | Length of sample | Test condition | Result |
|---|---|---|---|
| Heat run test | 2.5 m | 150°C x 24 hrs | No damage on OP unit. Optical fiber not ruptured. |
| Cooling test | 10 m | -27°C x 24 hrs (dry) | same as above |
| Freezing test | 20 m | -27°C x 24 hrs (in water) | same as above |

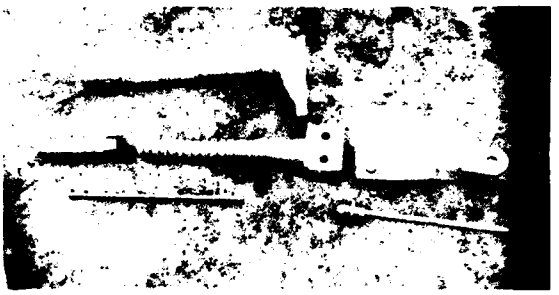


Fig. 8 View of the Components of the new Dead-end Clamp

Table 6 shows the result of a tensile test of this dead-end clamp. The gripping force of the clamp was found to clear the rated value with ample margin. Also confirmed was the fact that there was nothing unusual in transmission characteristics of the optical fiber even after partial rupture of the OPGW.

Table 6 Test Result of Dead-end Clamps

| Type | Measured value (kg) | Rated value (kg) |
|---|---|---|
| A | 16,800 | 15,620 |
| B | 9,300 | 7,540 |

3-2 Joint Box

Since the OPGW is to be installed in overhead lines up to several hundred kilometers long, it naturally requires a number of connections midway. Three types of optical fiber joints are needed: one for simple connection of the optical fiber, one for connecting the optical fiber to a regenerative repeater and one for connecting the optical fiber to an optical terminal for signal input/output. To accomplish these purposes, a compact, long-term weatherproof joint that can be used for any of the three functions has been developed. Figure 9 shows an inside view of the new joint box.

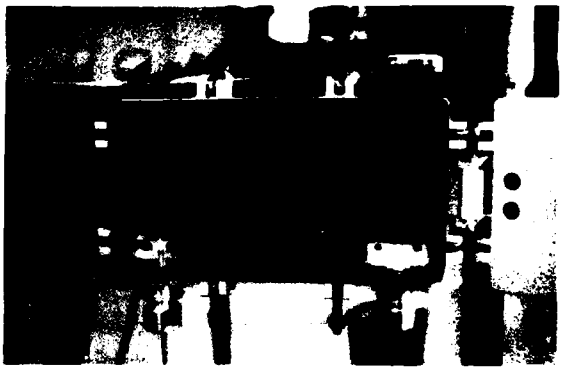


Fig. 9 View of the new Joint Box

4. Laboratory Test

As the OPGW is unwound from the drum during installation, it passes through a stringing sheaves with pulling tension being applied to the end. After covering the required distance, the OPGW is pulled taut under high tension with the dead-end clamps attached on both ends. Our test consisted of these procedures using the type-A

OPGW, with a view to checking experimentally if the OPGW would have performance equivalent to that of the ordinary GW. The results, obtained under the testing conditions shown in Table 7, were satisfactory : The initial elongation of the OPGW by stretching was 0.003%.

Table 7 Testing Conditions

| Item | Condition |
|---|---|
| Diameter of tensioner (m) | 1.5 |
| Diameter of stringing sheaves | 300 |
| Number of stringing sheaves | 3 |
| Tension during pay-out (kg) | 1,000 |
| Tension for sagging (kg) | 1,800 |
| Span length (m) | 300 |

During installation, the transmission loss of the optical fiber was continuously measured, but no change was detected. After installation, the OPGW has been placed under a longterm exposure test for continuous observation of creep, change in transmission loss, and anything else that may prove unusual.

Figure 10 shows the amount of creep measured in the OPGW after installation. The OPGW proved to have the same amount of creep as ordinary overhead ground wire. As indicated in Fig. 11, an increase in transmission loss was not detected even 5 months after installation. As of five months of exposure, nothing unusual that might be unfavoirable for actual use noted. Figure 12 shows how the long-terms reliability test is being conducted on the type-A OPGW after installation.

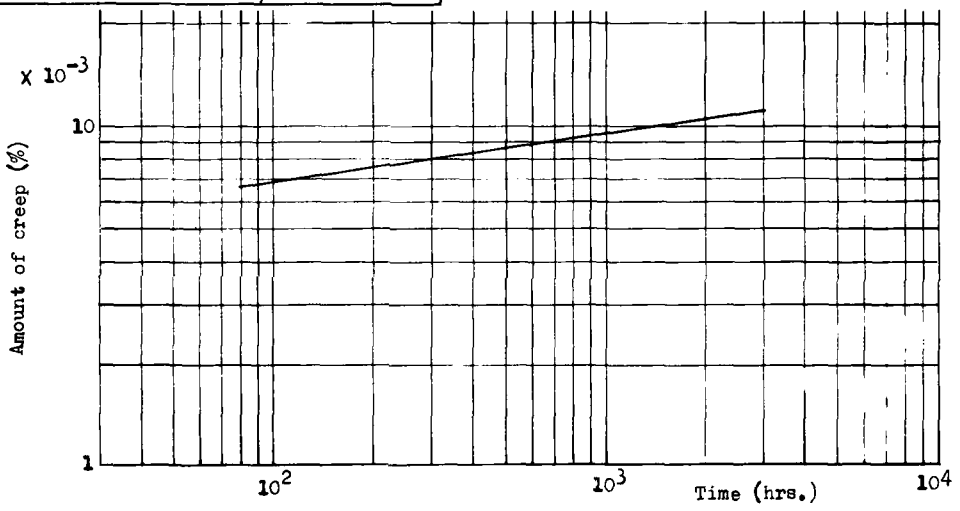



Fig. 10 Creep Characteristic of OPGW

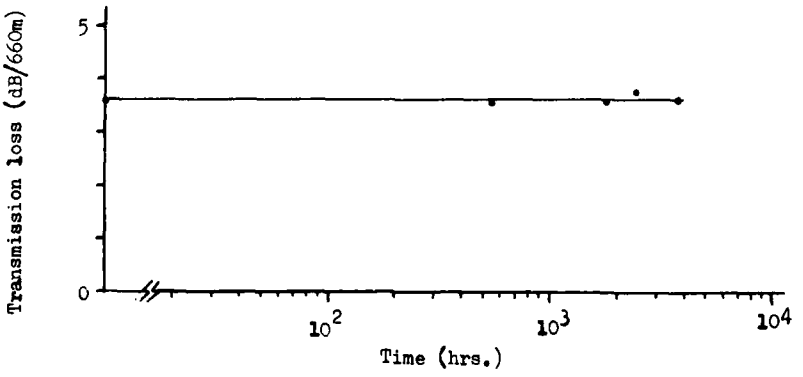



Fig. 11 Change in Transmission Loss (at 0.85 μm)

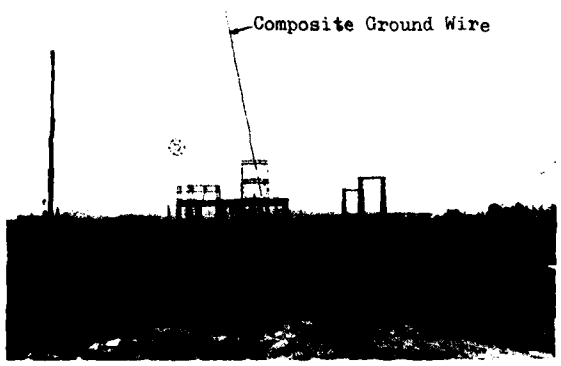



Fig. 12 OPGW Installed for Test

## 5. Conclusion

A new built-in type OPGW and its accessories were developed, and various unit tests as well as a long-term, long-span exposure test were conducted to check the performance of each component involved. The results confirmed the OPGW's suitability for application. We are now working on improving the new OPGW so it will have (1) higher resistance to heat, and (2) better mechanical strength. It will soon be installed overhead on actual power transmission line steel towers for final tests before commercial application.



Masahiro Igarashi
The Tokyo Electric Power Co., Inc.
1-3, 1-chome, Uchisaiwai-cho, Chiyoda-ku, Tokyo, Japan

Masahiro Igarashi was born on January 15, 1927. He joined the Tokyo Electric Power Co., Inc. in 1947, where he has been engaged in the section of overhead power transmission lines.
Mr. Igarashi is now a researcher of Power Engineering Division in the Engineering R & D Center.



Jyun Yokoyama
The Tokyo Electric Power Co., Inc.
1-3, 1-chome, Uchisaiwai-cho, Chiyoda-ku, Tokyo, Japan

Jyun Yokoyama was born on October 24, 1941. He joined the Tokyo Electric Power Co., Inc. in 1960, where he has been engaged in the section of electronic tele-communications.
Mr. Yokoyama is now a senior engineer of Electronic & Tele-Communication Division in Power System Operation Department.



Hisashi Iwamura
The Tokyo Electric
Power Co., Inc.
1-3, 1-chome,
Uchisaiwai-cho,
Chiyoda-ku, Tokyo,
Japan

Hisashi Iwamura was born on April 5, 1949. He joined the Tokyo Electric Power Co., Inc. in 1968, where he has been engaged in the section of overhead power transmission lines. Mr. Iwamura is now a member of Power Engineering Division in the Engineering R & D Center, and a member of the Institute of Electrical Engineers of Japan.



Ichiro Matsubara
Sumitomo Electric
Industries, Ltd.
1-3-12, Moto-Akasaka
Minato-ku, Tokyo
Japan

Ichiro Matsubara received the B.E. degree in electrical engineering from Kyoto University in 1966. He then joined Sumitomo Electric Industries and has been engaged in design research and development of various kinds of cables and overhead power transmission lines. Mr. Matsubara is now a manager of Overhead Power Transmission Line Engineering Section, and a member of the Institute of Electric Engineers of Japan.



Norihiro Mori
Sumitomo Electric
Industries, Ltd.
950, Oaza-Noda,
Kumatori-cho,
Sennan-gun, Osaka,
Japan

Norihiro Mori received the B.E. degree from Nagoya University in 1962, and in the same year he joined Sumitomo Electric Industries, Ltd. He has been engaged in design, research, and development of electric conductors and overhead transmission lines.
Mr. Mori is a chief research associate of the R & D group and a member of the Institute of Electrical Engineers of Japan.



Yasunori Saito
Sumitomo Electric
Industries, Ltd.
1, Taya-cho,
Totsuka-ku, Yokohama,
Japan

Yasunori Saito received his B.S. degree in electrical communication engineering from Tohoku University in 1969. He then joined Sumitomo Electric Industries and has been engaged in research and development of communication cables such as superconducting cable, leaky coaxial cable, phase stabilized coaxial cable and optical fiber cable.
Mr. Saito is a senior engineer of Communication R & D Group, and a member of the Institute of Electronics & Communication Engineers of Japan.

# DESIGN, MANUFACTURE, PEFORMANCE AND INSTALLATION OF A RUGGEDIZED FIBER-ELEMENT OPTICAL CABLE

by Phil Scadding

Times Fiber Communications
Wallingford, Conn 06492

## Abstract

This paper discusses improvements made to a ruggedized fiber cable design where individual fibers are manufactured into reinforced elements. This allows multi-fiber cables to be manufactured and installed using standard cable practices. Design considerations, manufacturing information and technical performance of the fiber cable product is described in detail. Installation experiences of a typical fiber optic system using this cable design are also discussed.

## Introduction

The concept of using individually ruggedized fiber elements in fiber optic cable designs is not new. Both metallic and non-metallic reinforcing members have been used to provide strength to individual fibers in multi-fiber cables.

This current paper involves further development to work that began early in the fiber optic cable industry.[1] The design involves using two high strength steel wires placed either side of a fiber, in the same plane, inside a polymer matrix. These wires give significant strength to the fiber during manufacture, installation and termination, and significantly improve the temperature performance of the fibers at temperature extremes. Earlier work[2] involved incorporating the fiber in a circular profile using a tight extrusion directly around the fiber. This product was successfully manufactured and installed in practical systems[2,3] however, the current work involves design changes that have significantly improved the performance of the ruggedized fiber element and the finished multi-fiber cable product. This new design is based on an oval reinforced element, where the fiber lays in a gel filled loose tube to minimize any forces on the fiber during manufacture, installation and service life.

## Ruggedized Cable Design

### Element Design

The basic component of this fiber optic cable product design is an oval or ellipsoidal thermoplastic extrusion in which a fiber and two high strength steel wires are embedded. (See Figures 1 and 2.)

The high strength steel wires are placed equidistant from the fiber and in the same plane. This minimizes any effect on the fiber that might occur due to tension or bending of the cable during manufacture and installation.

The high modulus of the steel also limits the expansion and contraction of the element during temperature variations. The plastic material, its cross sectional area and the steel wire size were chosen to yield a low coefficient of thermal expansion for the composite. The oval cross section was the result of this optimising process.

The other prime improvement in this product was the use of low modulus gels as filling compounds inside the loose tube that surrounds the fiber. This allows the fiber to effectively float freely inside the cable and minimizes any forces on the fiber during pulling and bending of the multifiber cables. The element also withstands large external impacts with little or no effect on the fiber itself.

Another obvious advantage of the filled oval reinforced element design is that ingress or migration of water is prohibited in the area of the fiber, due to the very low moisture absorption characteristics of the element filling gel. The gel maintains a low modulus down to below -50°C.

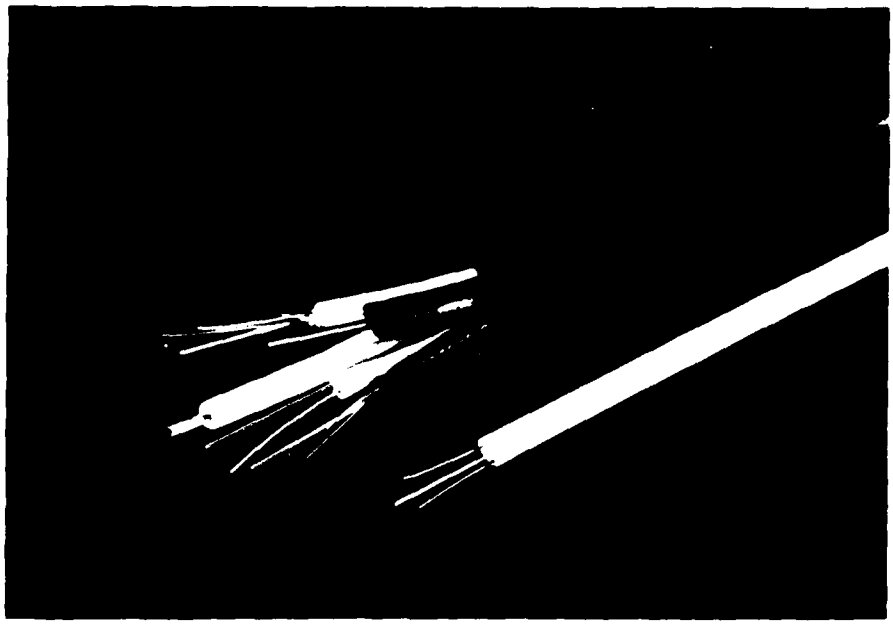


Figure 1. Photograph Showing Oval Reinforced Element and Four Element Completed Cable.

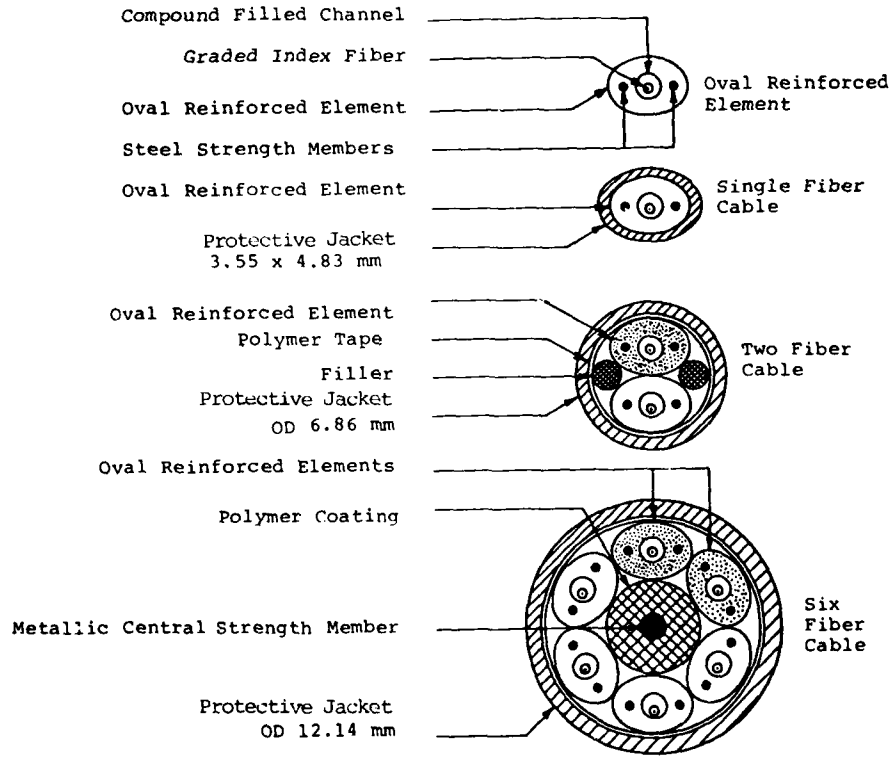



Figure 2. Cross Sectional Sketches of Oval Reinforced Element and of Representative Multi-Fiber Ruggedized Cables.

## Cable Design

Multi-fiber cables (see Figures 1 and 2) are made by stranding the reinforced elements around a polymer coated central strength member. In single and two-fiber cables, the oval reinforced elements are cabled without the central steel member. To allow for easy identification and orientation of the oval elements, they are normally color coded.

The oval reinforced element and multi-fiber cables are also very resistant to kinking because of the oval geometry and due to the planar placement of the two steel wires. This facilitates the pulling of cables through ducts or trays, and allows for easy coiling and uncoiling if required during installation. This is a definite advantage over aramid reinforced elements.

Due to the ruggedness of the oval reinforced elements virtually any jacketing or armoring techniques are possible.

The fact that each fiber is individually reinforced also facilitates field splicing and connectorization. The two steel wires can be terminated in the back sheel of the connector or splice case, and this yields a significant pull strength for the connection. Since the element is protecting the fiber right to the connector or splice, excellent temperature cycling results of field connections have been obtained, and no problems of fiber movement have been encountered.

## Temperature Performance

As discussed above, the temperature versus attenuation performance of fibers in this cable design is significantly improved over those of other designs. Even with fibers that are inherently sensitive to microbending losses, excellent attenuation stability with temperature is obtained.

In Figure 3, the attenuation change versus temperature is shown for a graded index fiber in both the reinforced element form (A) and in a standard 4-element cable (B). The multi-fiber cable shows improved attenuation stability with temperature due mainly to the extra reinforcement and rigidity of the central steel strength member. The maximum variation in attenuation of this fiber over the temperature range of -40°C to +60°C is 0.7 dB/km for the element alone and 0.4 dB/km in the multi-fiber cable. This represents ample stabiltiy for most commercial installations.

The position of the minimum of the attenuation curve can also be used to estimate the amount of excess fiber length present in loose tube cable designs.

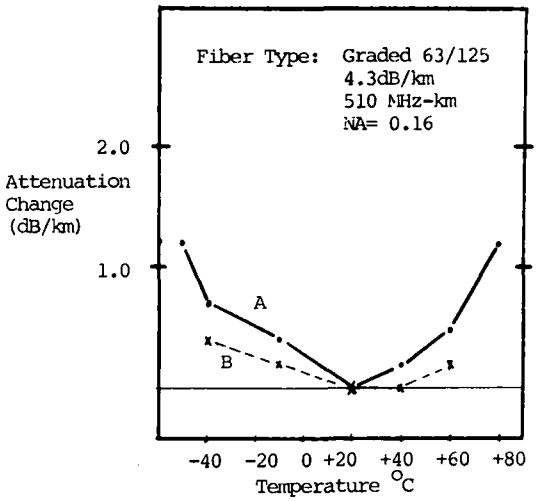



Figure 3. Attenuation Change Versus Ambient Temperature for a Single Reinforced Element (A) and a Multi-fiber Cable (B), After Temperature Stabilization at Each Temperature

## Manufacture of Ruggedized Cable

### Element Manufacture

The manufacture of the basic twin steel reinforced element is quite an interesting process. It involves a simultaneous tight extrusion around the two steel wires, and a tubing type of extrusion to form the loose channel in which the fiber lays. It also requires the simultaneous injection of the low modulus filling compound into this channel.

The filling compounds, of which silicone based materials are preferred, have been processed in a variety of ways and using a variety of tooling to inject them into the loose tube, depending on the filling compound properties. Screw and ram extrusion, positive displacement pumps and direct air pressure to move the materials are a few of the methods that can be used. Special materials that undergo temperature accelerated cures have been handled using special techniques.

The excess length of fiber in the loose tube is controlled by varying the following factors: loose tube and fiber size, fiber pay-off or feed method and fiber tension, steel wire tensions, and also the extrusion and quench conditions. This factor of having excess fiber length inside the element loose tube is important to the performance of the cable during and after the installation, and where wide temperature changes can occur. This phenomenon was well discussed in an earlier paper.[4]

Fibers can be manufactured into elements in continuous lengths and then cut to appropriate lengths for cable manufacture, where non-standard lengths are required.

## Cable Manufacture

Due to the bending and dimensional characteristics of the ruggedized elements, multi-fiber cables are manufactured using a rigid cabling motion. This has been accomplished successfully using a regular wire and cable rigid strander and a specially designed fiber optic cabler. Element back tensions used have ranged from 1 to 10 pounds and are not nearly so critical as compared to cabling unreinforced buffered fibers.

As can be seen in Table 1, the manufacturing process yields cables with little or no increase in optical attenuation. Fiber bandwidth also does not change significantly during cable manufacture. Many fiber types have been manufactured successfully using this cable design.

| Cable No. | Length | Fiber No. | Attenuations (dB/km) Fiber | Element | Cable | Jacket | |
|---|---|---|---|---|---|---|---|
| A | 1010m | 1 | 3.1 | 3.3 | 3.1 | 3.0 | -0.1 |
| | | 2 | 2.8 | 3.0 | 2.8 | 3.0 | +0.2 |
| B | 1086m | 1 | 3.2 | 3.4 | 3.2 | 3.3 | +0.1 |
| | | 2 | 2.8 | 3.1 | 2.9 | 2.7 | -0.1 |
| C | 1016m | 1 | 3.9 | 3.7 | 3.9 | 3.8 | -0.1 |
| | | 2 | 4.1 | 4.0 | 4.2 | 4.4 | +0.3 |
| | | 3 | 4.1 | 3.9 | 4.0 | 4.1 | 0.0 |
| | | 4 | 4.3 | 4.1 | 4.2 | 4.2 | -0.1 |

Table 1. Attenuation Performance of Manufactured Cables

(Note: Cables A and B used 63/125 fibers, .20 NA
Cable C used 63/125 micron finers, .16 NA)

The backscatter technique of using the OTDR (optical time-domain reflectometer) is used extensively in following the fiber and cable manufacturing processes. This allows measurement of attenuation and to follow any areas of stress that might be present in a fiber or cable. It is also a very useful tool in analysing and controlling field splicing and connectorization. This quick optical test method is carried out at all manufacturing steps in the production of fiber cables, and eliminates the great number of attenuation and bandwidth tests which can be very time consuming. Figure 4 shows a typical OTDR trace of a fiber in a completed cable. It quickly yields length, attenuation and any disturbance areas in the fiber or cable.

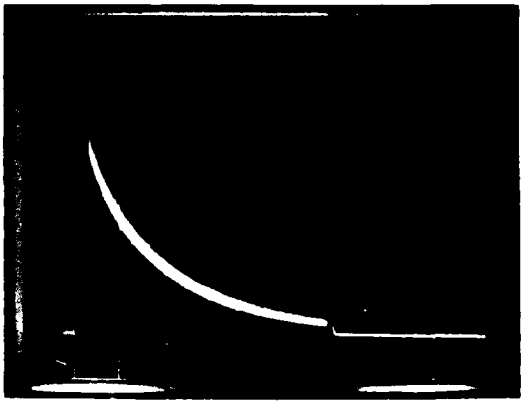


Figure 4. OTDR Trace of Fiber Cable
Length: 1135 meters
Attenuation: 5.2 dB/km

## Special Requirements

The cables described above were manufactured for standard overlash aerial and duct installations. The cables were stranded and then jacketed with a suitable thickness of black low density polyethylene for environmental protection.

However, a big advantage of this ruggedized fiber cable design is that it is easily manufactured in a modified form for special applications. These have included: the use of aramid, other non-metallic or steel external strength members for extra pulling strength; the use of flame retardant PVC for indoor cables; metallic armoring for direct burial and gopher resistant cables; and the use of a completely filled stranded core to eliminate ingress of moisture to the core or to gas block the cable.

Another design alternative involves the use of rigid non-metallic strength members in place of the two high strength steel wires, to yield an all dielectric cable. The ruggedized nature of the basic element allows easy handling of the fiber element in these varieties of modified designs and processing procedures.

## Cable/System Installations

A 2.4 km long, 3 fiber cable system, was installed in April 1980 for Vision Cable and is part of a system serving 20,000 cable-TV subscribers in 13 New Jersey communities. The three cables were overlashed to existing coaxial cables along the busy and heavily treed residential area. The importance of the cable installation was that a regular crew completely inexperienced in fiber optic cables, installed the cables with no problems in less than four days. A crew of two field technicians spliced the cables and had the system operating on-the-air within two days.

One fiber carries two TV signals from microwave receivers at the headend to the studio for signal processing and programming. A second fiber returns five CATV channels to the headend for distribution to other areas by microwave. A third fiber will be used to expand programming to a total capacity of 36 channels. The FM modulated system exceeded the contract performance specs with a measured 53-59 dB signal-to-noise level and with no visible picture distortion. The fiber cable and system have operated without interruption to this date.

Other systems currently being installed (September 1980) include: a 9.5 km four-fiber satellite down link for United Cable, Plainville Connecticut; a 4.5 km four-fiber system for antenna to headend distribution for Commonwealth Telephone Technology Corp in New Jersey; and a 10.0 km four-fiber teleconferencing link for Insilco Corp of Connecticut. All of these [5] cable systems have used the design described above. Installation and performance has proven very reliable.

## Conclusions

The modifications that have been made to this reinforced element design have improved the attenuation stability of the fiber during manufacture and wide temperature exposures. The basic cable design is adaptable to various installation needs and shows little or no optical change due to cable manufacture.

## References


1. N.S. Dean and R.J. Slaughter, "Development of a Robust Optical Fibre Cable and Experience to Date With Installation and Jointing", Proceedings 25th International Wire and Cable Symposium, Cherry Hill, NJ., November 1976.

2. Sol Yager, "A 12 Channel, 8.6 km Fiber Optic Super Trunk for Teleprompter of Lompoc, California", Communications-Engineering Digest, Volume 6, No. 2, pp28-35, February 1980.

3. P. Duyan, "An Optical Solution to Fiber Optic Interconnection", Communications-Engineering Digest, Volume 6, No. 2, pp37-47, February 1980.

4. P.R. Bark, U. Oestreich and G. Zeidler, "Stress-Strain Behavior of Optical Fiber Cables", Proceedings 28th International Wire and Cable Symposium, Cherry Hill, NJ., November 1979.

5. A.C. Deichmiller, "A Brief Look at Fiber Optic Communications for CATV", Presented to the Philadelphia Cable Club, June 1980.





Phil Scadding
Times Fiber Communications
358 Hall Avenue
Wallingford, Conn 06492
203-265-8500


Phil Scadding is currently Cable Development Manager, Fiber Optics, with Times Fiber Communications in Wallingford, Connecticut. He previously held positions in wire and cable product development, and had spent three years in fiber optic cable development and production.

He is an honors graduate in Applied Chenistry from the University of Waterloo, Ontario, Canada.

# COPPER INHIBITOR AND ANTIOXIDANT LEVELS IN HIGH DENSITY POLYETHYLENE: THEIR MEASUREMENT BY HIGH PERFORMANCE LIQUID CHROMATOGRAPHY AND RELATION TO INSULATION LIFE

John Fech
Ann De Witt

General Cable Company
Research Center
Edison, New Jersey

## ABSTRACT

Prior investigations established that insulations exposed in a pedestal environment must be properly stabilized with copper inhibitor and antioxidant in order to prevent copper catalyzed degradation.

The amount of each additive is significant. High performance liquid chromatography (HPLC), an instrumental analytical technique, is used to separate the additives and to measure the amount of active stabilizers without interference from their thermal transformation products. Spectrophotometric techniques do not provide separation and, therefore will yield high results due to interference from degradation products.

Conditions for the extraction, separation and quantitation of the commonly used copper inhibitors and antioxidants are given. The method described can be completed within an hour and it is suggested as a control test on incoming raw materials.

## INTRODUCTION

The useful life of polyethylene insulation, especially in the hostile environment of the pedestal which precludes the oxygen-limiting protection of a completed cable, has been shown to be dependent upon the presence of the proper level of antioxidant and, further, upon adequate protection against copper catalyzed degradation. The necessity for both antioxidant and metal deactivator has been recognized and reported.[1] Commercially available HDPE insulation compounds have incorporated such additives for almost a decade.

How to measure the levels of these vital additives has been a challenge to analytical chemists for an equal number of years. The techniques employed in the quantitative determination of stabilizer systems and the problems associated with them have been described in detail by Crompton.[2] Direct spectroscopic methods such as ultraviolet or infrared absorption have been reported, but are not specific for each active component. No distinction is made in spectrophotometric techniques between the degradation products and the active material. As concluded by Schabron and Fenska, a more desirable approach has been that of separation and determination of each additive in the polymer.[3]

High performance liquid chromatography (HPLC) lends itself to just such an analysis.[3,4] Like all types of chromatography, HPLC is a technique for the separation of a mixture into its components. The block diagram (Figure 1) illustrates the essential components of a typical HPLC system.

BASIC COMPONENTS OF HPLC SYSTEM

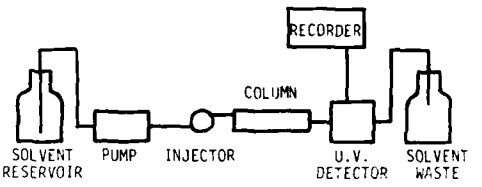



Figure 1

A mixture in solution is injected, carried by pumped solvent onto a column where separation occurs; each component as eluted from the column flows past a detector and its magnitude is recorded. Depending on the nature of the mixture to be separated, column packing may be polar ("normal phase") or non-polar ("reverse phase") material and, correspondingly, the solvent non-polar or polar. Differences in polarity and solubility produce separation. The components of the solvent system may be premixed and that concentration remain constant throughout the separation ("isocratic elution") or their ratios may be varied at a selected rate ("gradient elution").

In this paper we present the results of isocratic reverse phase HPLC separation and analysis of stabilizers and thermal transformation products found in three commercially available high density polyethylene insulation compounds.

## EXPERIMENTAL

### Instrumentation

The liquid chromatograph used was a Micromeritics Model 7000 equipped with a Model 725 Auto Injector, Schoeffel Spectroflow Monitor SF 770 variable wavelength detector set at 280 nm and a 10 mV Varian Model 20 strip chart recorder. The analytical column contained Whatman Partisil PXS 10/25 ODS-3 and preceded by a guard column of Whatman Co:Pell ODS.

## Reagents

Burdick and Jackson Distilled in Glass grade solvents - methanol, toluene, chloroform, acetic acid and water - were used. The chloroform was purchased without 1% ethanol preservative. The stabilizers were obtained from their respective manufacturers and were used without further purification. HDPE insulation compounds were obtained from three large suppliers to the telephone industry.

## Procedure

Approximately ten grams of HDPE were ground to 20 mesh size. One gram was weighed into a 250 ml Erlenmeyer flask, a magnetic stir bar added and 100 ml toluene pipetted into the flask. The stirred sample was dissolved by heating to reflux temperature under a nitrogen atmosphere. Refluxing was continued for about ten minutes. The solution was allowed to cool slightly while a dropping funnel containing 40 ml chloroform plus 60 ml methanol was placed atop the condenser. The chloroform-methanol solution was added dropwise to the rapidly stirred sample which precipitated the polymer. Stirring was continued until the solution cooled to room temperature. An aliquot of 100 ml was filtered, flash evaporated, the residue dissolved in 10 ml methanol and filtered into an Auto Injector vial. The Auto Injector was programmed for triplicate injections of 10 µl each followed by a methanol rinse before the next sample injection. Chromatographic conditions are listed in Table I.

TABLE I

CHROMATOGRAPHIC CONDITIONS

| | |
|---|---|
| Analytical Column: | Whatman Partisil - 10 ODS-3; 4.6 mm x 25 cm |
| Precolumn: | Whatman Co:Pell ODS |
| Column Temperature: | 30°C |
| Mobile Phase: | Methanol/Water/Acetic Acid (98/1/1) |
| Flow Rate: | 1 ml/min |
| Pressure: | 700 psi |
| Detection: | UV @ 280 nm, 0.1 Absorbance Range |

## Identification and Quantitation

Retention times of pure stabilizers dissolved in methanol were used for peak identification. Irganox 1010 and Irganox 1024 were injected and the eluted materials collected. These gave infrared spectra identical to Irganox 1010 and Irganox 1024. Calibration curves over the concentration range of interest were obtained relating peak height to concentration. A typical calibration curve for Irganox 1010 and Irganox 1024 is shown in Figure 2.

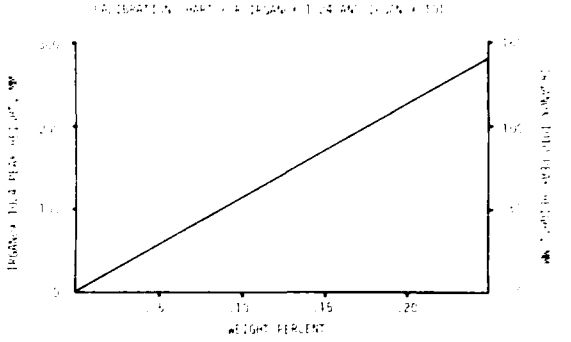



Figure 2

## RESULTS AND DISCUSSION

Initial attempts to extract commonly used stabilizers from high density polyethylene insulation compounds produced erratic results, even with prolonged extraction times. After modification of the British Standard method[5] of dissolution of the compound followed by the simultaneous addition of solvent for the additives and non-solvent to precipitate the polymer, recovery of additives improved dramatically. It seems probable that many of the recommended procedures involving prolonged heating actually speed up the rate of decomposition, resulting in low recoveries. Crompton[6] reported no oxidation of the antioxidant Nonox CI in HDPE following a 1-1/2 hour toluene extraction under reflux and a nitrogen atmosphere, although, under these conditions, 5% of the additive is not extracted from the polymer. As shown by the recovery results listed in Table II, our experience has been similar.

TABLE II

RECOVERY OF IRGANOX 1010 AND IRGANOX 1024 FROM HDPE*

| Concentration, Wt. % | | % Recovered | |
|---|---|---|---|
| 1010 | 1024 | 1010 | 1024 |
| 0.201 | 0.203 | 99 | 90 |
| 0.092 | 0.099 | 94 | 92 |
| 0.051 | 0.045 | 93 | 81 |

*Samples prepared by mixing HDPE with stabilizers in Brabender mixer at 160°C, 20 rpm, 20 min.

After quantitative extraction of additives was assured, separation by reverse phase HPLC proved straightforward. Characteristic of reverse phase chromatography, separation parameters can be readily optimized by simple manipulation of the ratio of water to methanol. Acetic acid was added to stabilize the column and to sharpen the peaks.

Shown in Figures 3 and 4 are two separations of commonly encountered combinations of antioxidants and copper inhibitors; chromatographic conditions for both are the same as listed in Table I.

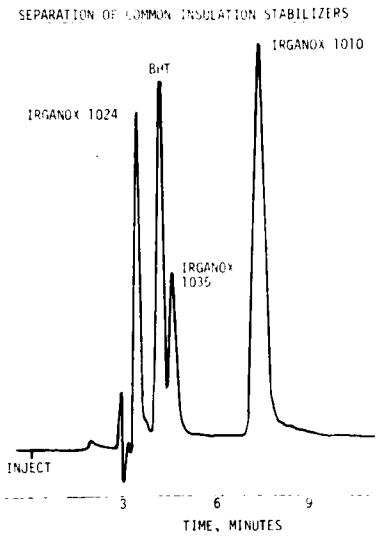



Figure 3

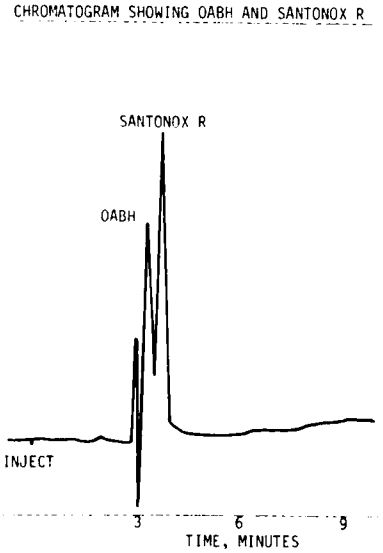



Figure 4

High density polyethylene insulation compounds as received from three suppliers to the telephone industry have been analyzed by the preceding method. All contained the same antioxidant and copper inhibitor but at markedly different levels, as listed in Table III.

TABLE III

RESULTS OF ANALYSES OF 3 HDPE INSULATION COMPOUNDS

| Sample | % Irganox 1010 | % Irganox 1024 |
|---|---|---|
| Supplier A | 0.13 | 0.15 |
| Supplier B | 0.23 | 0.13 |
| Supplier C | 0.04 | 0.05 |

The described method was also used to measure the levels of antioxidant and copper inhibitor remaining after thermal treatment. Lichtenthaler and Ranfelt[4] have studied the thermal and photochemical transformation products of several antioxidants and separated more than twenty from BHT, one of the most commonly used antioxidants. They employed gradient elution HPLC for the separation, changing the mobile phase from 2% dichloromethane in hexane to 100% dichloromethane in increments of 5%/min. The isocratic chromatographic conditions given in Table I, utilizing the same methanol-water-acetic acid system throughout the analysis, were sufficient to separate the active Irganox 1010 and Irganox 1024 from their thermal transformation products, as can be seen in Figures 5 and 6.

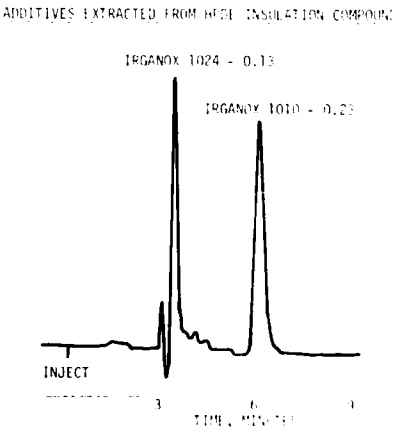



Figure 5

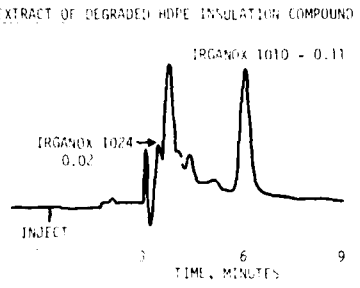



Figure 6: Treated at 230°C for 30 minutes

In the above instance, the concentration of copper inhibitor, Irganox 1024, had dropped from 0.13% to 0.02%; the Irganox 1010 went from 0.23% to 0.11%.

## CONCLUSION

The method described in this paper permits separation and quantitative measurement of the active stabilizers without interference from thermal transformation products. Results can be obtained within an hour. The method described cannot be used alone to predict the service life of insulations, since other factors contribute to insulation failure, such as crystalline embrittlement of the polymer and extraction of stabilizers by filling compounds.[7]

Since the long term stability of HDPE insulation can only be assured by the presence of adequate levels of active stabilizers, testing for these levels in incoming raw materials appears to be mandated. The increasing demand for HDPE has led to more efficient polymerization catalysts and advanced additive technology which requires close monitoring of the stabilizer system. Suppliers may certify to adding the specified amounts, but subsequent processing and additive procedures can reduce the amounts significantly. Ultimately, it is the cable manufacturer who bears the liability for the quality of his product. The assurance of the necessary amounts of active stabilizers coupled with the use of sophisticated cable making equipment will render insulations with the desired long service life.

## ACKNOWLEDGEMENT

We gratefully acknowledge the efforts and encouragement of our colleagues in the Material Science Department.

## REFERENCES

1. W. L. Hawkins, M. G. Chan and G. L. Link, Polym. Eng. Sci. 11, 377 (1971).

2. T. R. Crompton, Chemical Analysis of Additives in Plastics, Second Edition, Pergamon Press, 1977, Chapter 1.

3. J. F. Schabron and L. E. Fenska, Anal. Chem. 52, 1411 (1980)

4. R. G. Lichtenthaler and F. Ranfelt, J. Chromatogr. 149, 553 (1978).

5. British Standard 2782, Part 4, Method 405D (1965).

6. T. R. Crompton, J. Appl. Polymer Sci. 6, 538 (1962).

7. G. A. Schmidt, Proceedings of the 26th International Wire and Cable Symposium, 161 (1977).



John Fech, Senior Research Chemist, Material Science Department, General Cable Company Research Center is engaged in analytical and mechanism studies. He graduated from Alliance College, Pennsylvania.



Ann De Witt, Senior Research Chemist, Material Science Department, General Cable Company Research Center is a graduate of Rutgers University and Stevens Institute of Technology. Her special interest is the development of instrumental methods of analysis.

# IDENTIFICATION OF PARTICLES IN HIGH DENSITY POLYETHYLENE THAT CAUSE SPARK FAILURES DURING HIGH SPEED EXTRUSION

Gertraud A. Schmidt
Louis A. Bopp

General Cable Company
Research Center
Edison, New Jersey

## ABSTRACT

This paper is concerned with the determination of causes for excessive spark failures in high speed extrusion of HDPE insulation.

It has been found that residual catalyst particles and gels are the major causes for the existence of spark failures. The procedures employed in separating and identifying the particles are discussed and a method for preproduction analysis of HDPE for these impurities is included herein.

## INTRODUCTION

Pure polyethylene has outstanding dielectric strength and it can endure exceptionally high electrical stress. Commercial quantities of polyethylene unfortunately are not entirely free of contaminants. The power cable engineer is concerned about gels in low density based material. Gels are amber particles which are polyethylene in various stages of oxidation. In addition, there is concern about occasional small metal particles that may be present from the manufacturing process.

The communications cable engineer who uses high density polyethylene for insulation material is aware of gels and metal particles, but in addition, is also concerned with residual catalyst.

Described herein are various problems associated with off-standard catalyst, residual catalyst particles and gels, and possible means to detect these impurities before the polyethylene is transferred into storage silos at user plants.

The following problems were observed with respect to catalyst residue:

1. When most of the contaminants are larger than the openings in the extruder screens, the screens clog and rupture.
2. When most of the particles are smaller than the openings in the extruder screen, the fault rate is increased beyond an acceptable level.
3. When chemicals are added to high density polyethylene to modify the molecular weight range, to bind catalyst residue or to prevent discoloration of the polyethylene, plate out of these chemicals on extruder parts and extrusion tools may occur.

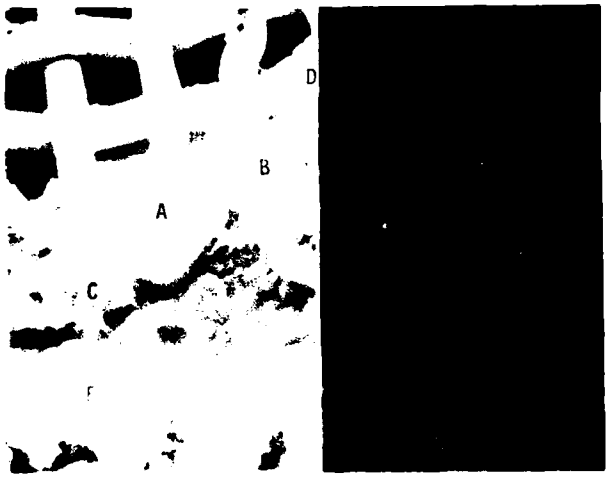
## LARGE PARTICLES CAUSING SCREEN RUPTURE

Frequent rupture of screens was experienced when a particular lot of HDPE was extruded on insulating lines at speeds up to 7000 ft/min. Prior to the screen rupture, the fault rate was within the acceptable range. It is standard procedure at this plant to utilize screen packs with a 120 mesh/inch screen as the finest screen. The openings in a 120 mesh/inch screen are 4.9 mils.

Prior to identifying the particles that caused the clogging of the screens, the polyethylene was removed from a screen with xylene in a reflux setup in accordance with the method inlcuded in the Appendix.

In examining the particles on the screen with a scanning electron microscope equipped with an energy dispersive X-ray system, it was found that most of the contaminants were large silica particles and large gels. It is suspected that the catalyst used for the polymerization process of this batch of HDPE was not quite up to standard. Some of the silica particles were not combined with chromium, they remained large since they did not fracture during the polymerization process.

Figure 1 below shows a section of a 120 mesh/inch screen after all polyethylene was removed. The silicon X-ray mapping of the same area is shown on the right.




75X Silicon X-Ray Mapping

Figure 1: Section of a 120 mesh/inch production screen that clogged due to large gels and large silica particles.

The identification of these particles is as follows:

TABLE I

IDENTIFICATION AND LENGTH DIMENSIONS OF PARTICLES IN FIGURE 1

| Particle Letter | Identification | Longest Dimension, mils | X-Ray Analysis Shown in Figure No. |
|---|---|---|---|
| A | Silica | 12 | 2 |
| B | Gel with small quantity of inorganic material | 7.8 | 3 |
| C | | 7.8 | 4 |
| D | Silica with traces of Titanium | * | 5 |
| E | Traces of catalyst residue are clinging to a large silica particle | 15.0 | 6 |

*Only section of particle visible in the picture.

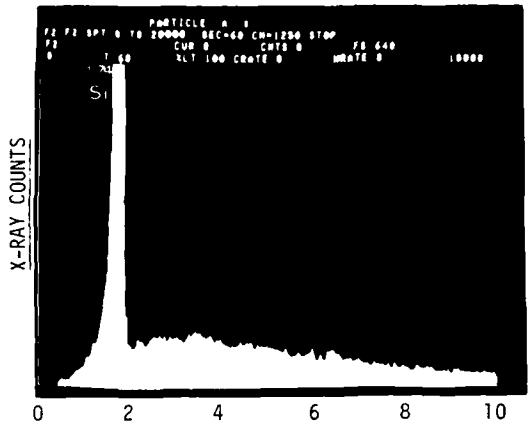



Figure 2: Energy in Electron Volts, $10^3$ (keV)

X-ray analysis of particle A identifies it as silica.

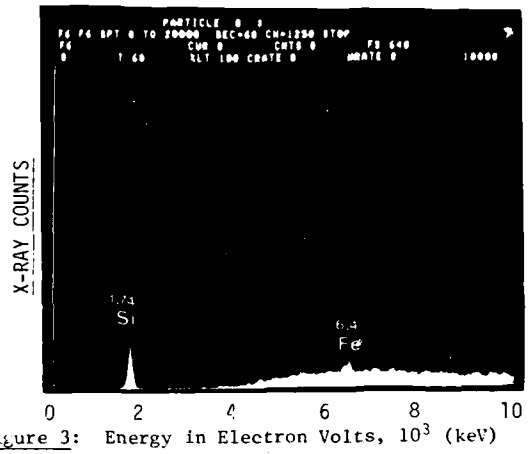



Figure 3: Energy in Electron Volts, $10^3$ (keV)

X-ray analysis of particle B, which is a large gel, reveals only traces of inorganic material.

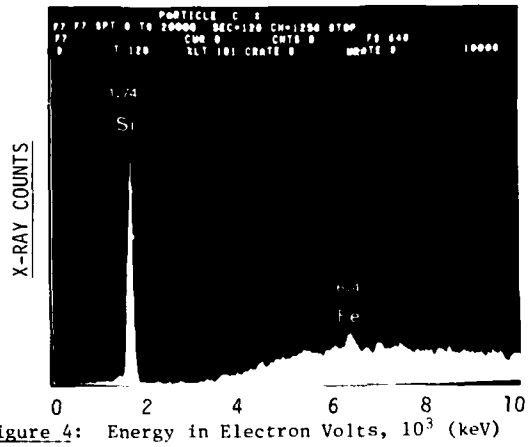



Figure 4: Energy in Electron Volts, $10^3$ (keV)

X-ray analysis of particle C is similar to that of particle B. Only a small amount of inorganic material is present.

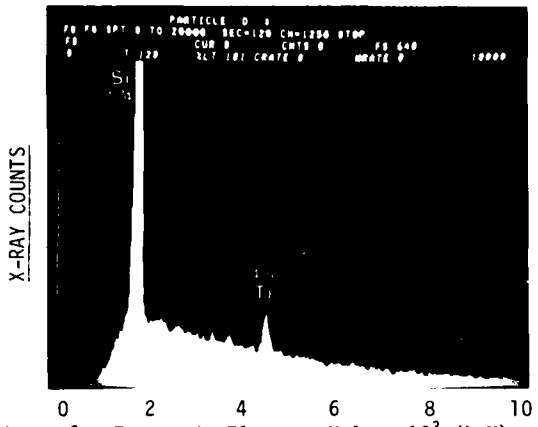



Figure 5: Energy in Electron Volts, $10^3$ (keV)

X-ray analysis of particle D identifies it as silica with traces of titanium.

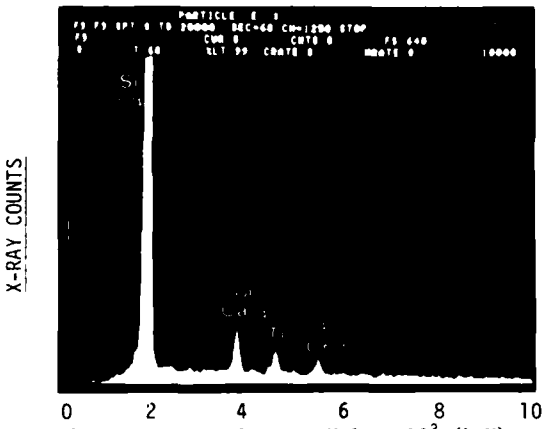



Figure 6: Energy in Electron Volts, $10^3$ (keV)

X-ray analysis of particle E. Traces of catalyst (Cr and Ti) are clinging to a silica particle.

A sample of the pellets of HDPE-A, as received, used for the extrusion discussed above, was tested in accordance with the method shown in the Appendix. The large silica particles and the large gels can be easily detected (Figure 7). 230 grams of HDPE pellets were extruded with a 3/4 inch machine through a screen pack with a 325 mesh/inch screen as the finest screen. The other screens are used behind it for support. Figure 7 shows a section of the 325 mesh/inch screen after all HDPE was removed by refluxing with xylene.

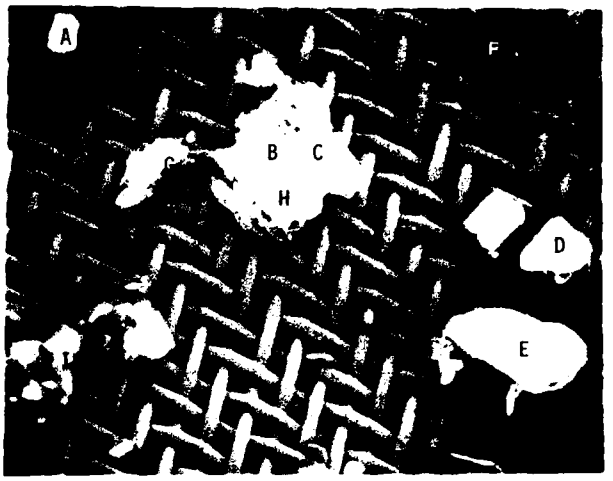



Figure 7: Magnification 75X

Section of a 325 mesh/inch screen with contaminants from a 230 gram sample of HDPE-A pellets.

The particles were identified by X-ray analysis. The X-ray analysis of particle F, the catalyst residue, is shown in Figure 8. The results and the longest dimension of the particles are listed in Table II.

TABLE II

IDENTIFICATION AND LENGTH DIMENSIONS OF PARTICLES IN FIGURE 7

| Particle Letter | Identification | Longest Dimension, mils |
|---|---|---|
| A | Silica | 4.0 |
| B | | 4.0 |
| C | | 3.3 |
| D | | 8.0 |
| E | | 14.6 |
| F | Catalyst residue | 2.6 |
| G | Gel | 12.0 |
| H | | 16.0 |
| I | Agglomeration of gel and silica | 17.3 |

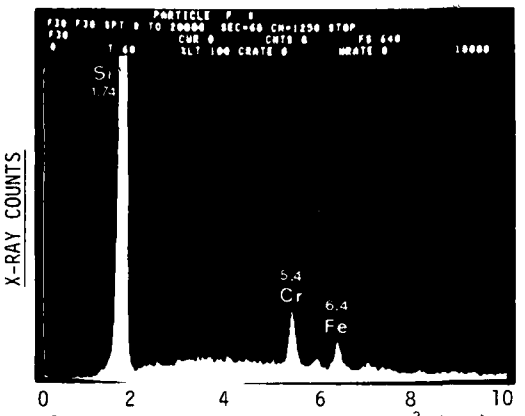



Figure 8: Energy in Electron Volts, $10^3$ (keV)

X-ray analysis of particle F, the catalyst residue. Silica is the catalyst carrier, while chromium is the active element.

In comparing the catalyst residue, particle F in Figure 7, with silica particles A, B, C, D and E, it can be seen that the silica particles charged during the application of the electron beam and this resulted in an overexposed appearance. In performing X-ray analysis, it is customary to make the surfaces conductive by vacuum deposition of a thin layer of carbon. Some contaminants that are lying loosely on the extruder screen will be lost if subjected to the vacuum deposition process.

## SMALLER PARTICLES CAUSING SPARK FAILURES

One cable plant experienced excessive spark failures when extruding HDPE-B insulations for filled cables and air core cables at speeds up to 7000 ft/min. The insulations of 6 to 20 mils in thickness were sparked at the appropriate voltage, ranging from 2 to 5 kV DC.

The particles that caused the failures in the insulations were analyzed and found to be mainly catalyst residue.

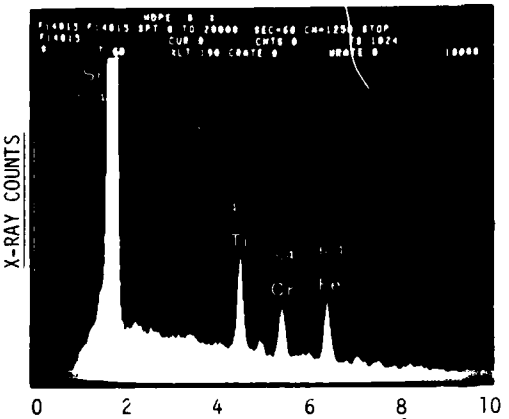


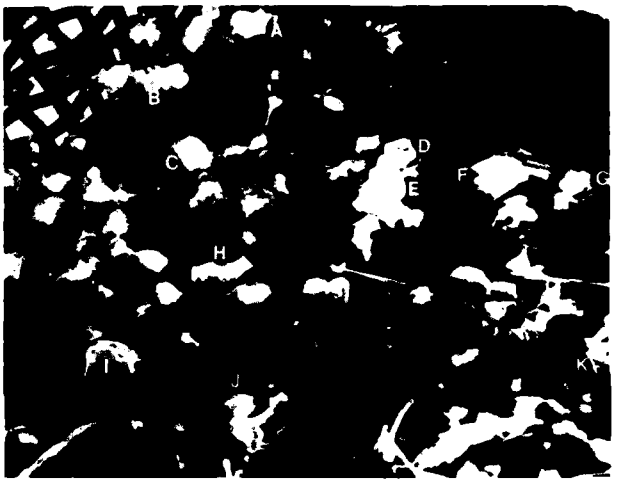

Figure 9: Energy in Electron Volts $10^3$ (keV)

X-ray analysis of catalyst residue in HDPE-B that caused spark failure. Silica is the carrier and titanium and chromium are the active elements.

The spark failures were reduced, but they were still too high after 80 mesh/inch screens and later 120 mesh/inch screens were substituted for the previously used 60 mesh/inch screens. For comparison, the openings in these screens are as follows:

| Screen, mesh/inch | Openings, mils |
|---|---|
| 60 | 9.8 |
| 80 | 7.0 |
| 120 | 4.9 |

By separating the contaminants from 230 grams of pellets of HDPE-B in accordance with the method shown in the appendix and measuring their size, it can be seen that 120 mesh/inch screens are not sufficient, since a considerable portion of the particles is smaller than 4.9 mils.




Magnification 75X

Figure 10: Section of a 325 mesh/inch screen with catalyst residue from 230 grams of HDPE-B.

The dimensions of several of the larger particles that are shown in Figure 10 were measured and the results are shown below. Four out of 11 of these particles (letters D, G, J, K) could have slipped through 120 mesh/inch screens.

| Figure 10 Particle No. | Longest Dimension, mils |
|---|---|
| A | 5.2 |
| B | 6.5 |
| C | 5.2 |
| D | 3.5 |
| E | 7.7 |
| F | 6.7 |
| G | 4.2 |
| H | 7.2 |
| I | 7.5 |
| J | 4.1 |
| K | 3.7 |

Many of the catalyst particles that are shown in Figure 10 are similar in size to these four particles.

It was of interest to determine the size of the particles that can be tolerated in thin wall insulation during high speed extrusion. For this purpose HDPE-B was screened by the polyethylene manufacturer through 200, 180 and 150 mesh/inch screens and repelletized. The three compounds were extruded on #24 AWG copper conductor in a wall thickness of 7.3 mils.

It was found, as indicated in Table III that particles smaller than 2.9 mils can be tolerated in a 7.3 mil insulation wall of HDPE-B when extruded at 6400 ft/min. It is important to note that this tolerance level is characteristic for this specific compound, HDPE-B, since it is a function of the melt strength of this polymer. Compounds with higher melt strength will have higher tolerance levels.

TABLE III

Conditions for Extrusion of #24 AWG Air Core Insulation:

| | | |
|---|---|---|
| Wall Thickness, mils | 7.3 of HDPE-B, prescreened as indicated | |
| Screens Used in High Speed Extruder mesh/inch: | One 60 | One 35 |
| Screen Openings, mils: | 9.8 | 19.7 |
| Line Speed, ft/min: | 6,400 | |
| Length in one bobbin, ft: | 125,500 | |
| Spark Voltage, kV DC: | 3 | |

| Screens Used to Prescreen HDPE-B Prior to Repelletizing | | Number of Bobbins Processed | Spark Failures per Bobbin |
|---|---|---|---|
| Mesh/Inch | Openings, mils | | |
| 200 | 2.9 | 7 | 7, 3, 5 7, 4, 5, 8 |
| 180 | 3.3 | 3 | 34, 19, & 27 |
| 150 | 3.9 | 1 | 266 |

ADDED CHEMICALS CAUSING PLATE OUT

Some polyethylene suppliers add chemicals during the manufacturing process of their HDPE to broaden, the molecular weight range, to bind catalyst residue or to prevent discoloration of the polyethylene.

In one specific case, it is suspected that dibasic magnesium phosphate was added which plated out on the extrusion tools as magnesium pyrophosphate, causing off center conditions of the insulations, spark failures, and severe problems in cleaning tips and dies. Figure 11 shows a die opening with severe plate out from HDPE-C and an X-ray mapping for phosphorus of this area. Figure 12 shows a tip die after the cleaning process in a fluidized bed bath. Some of the black magnesium pyrophosphate is still clinging to it.



Figure 11: 40X X-Ray Mapping for Phosphorus

Die opening showing severe plate out from HDPE-C.

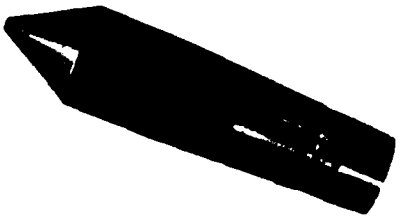


Figure 12 1.2X

Tip-die after removal from the fluidized bed cleaning bath.



Figure 13 50X

The plate out from the tip-die had the appearance of black rods. The X-ray analysis is shown in Figure 14.

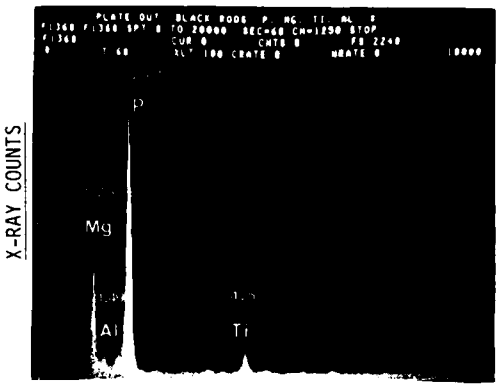



Figure 14: Energy in Electron Volts $10^3$ (keV)

X-ray analysis of plate out (black rods)

Based on the X-ray analysis, the plate out was identified as magnesium pyrophosphate, a transformation product of dibasic magnesium phosphate.

The impurities from 230 grams of HDPE-C were removed in accordance with the method described below. A few of these particles are shown in Figure 15 and their identification and length dimensions are listed in Table IV. Magnesium pyrophosphate was identified on the screen as well as catalyst residue, gels, clay and a large orange colored titanium particle. Several large severely oxidized black gels that cannot be seen in Figure 15, were present on the 325 mesh screen. One of them measured 16 mils by 13 mils.

TABLE IV

| Figure 15 Particle Letter | Figure 15 Identification of Particle | Elements Present per X-Ray Analysis | Largest Dimension, mils |
|---|---|---|---|
| N | Most likely magnesium pyrophosphate | Magnesium and phosphorus | 5.8 |
| C<br>F<br>G<br>J | Catalyst Residue (a) | Silicon, titanium, chromium, iron | 6.3<br>9.6<br>5.8<br>7.9 |
| L | Catalyst Residue (b) | Silicon, chromium, and iron | 5.2 |
| B<br>D<br>H<br>I<br>K | Gel | Organic material only | 7.9<br>9.0<br>6.3<br>7.5<br>7.1 |
| E | Orange colored titanium compound | Titanium | 12.5 |
| M | Clay | Aluminum and silicon | 4.6 |
| A | Unidentified | Zinc and iron | 8.3 |

All through the investigation, ash determinations were made on the various samples of HDPE. In the case of HDPE-C, the results appear significant.

HDPE-C that caused the severe plate out problem was found to have 0.05 ash, while a subsequent lot that caused lesser plate out had 0.03 ash. The amount of remaining chemicals in the high density polyethylene may be directly related to the amount of plate out that occurs during extrusion.




Figure 15: 75X

Section of 325 mesh/inch screen with a few particles from HDPE-C.

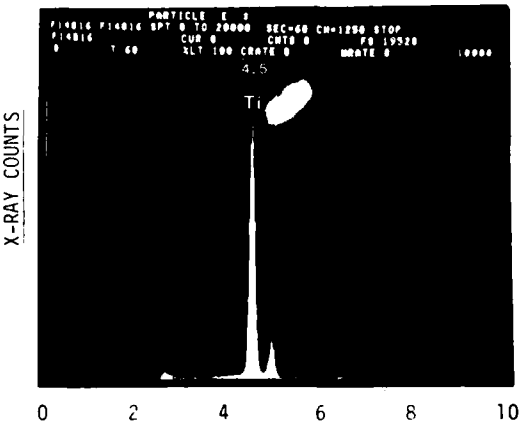



Figure 16: Energy in Electron Volts, $10^3$ (keV)

X-ray analysis of Particle E, a 12.5 mil long orange colored titanium particle. The two typical peaks for titanium can be seen.

## EFFECT OF CATALYST RESIDUE IN HDPE ON THE ACTIVE ANTIOXIDANT AND METAL INHIBITOR

It was of interest to demonstrate the effect of catalyst residue on the antioxidant and metal inhibitor in HDPE. For this purpose, the oxidation induction time of HDPE-A was first determined on the pellets as received, then again after it had been screened through a 325 mesh/inch screen and repelletized. Subsequently both materials were subjected to a processing degradation test and the oxidation induction times were determined again.

The data in Table V indicate that the screened material has a slightly longer oxidation induction time after the degradation test, although it had a shorter oxidation induction time due to the additional extrusion process, prior to the processing degradation test. Most of the catalyst residue was removed by the screening process and it could not, therefore, react with the metal deactivator Irganox 1024 and the antioxidant Irganox 1010.

TABLE V

OXIDATION INDUCTION TIME OF HDPE-A AS RECEIVED, AND AFTER A PROCESSING DEGRADATION TEST

| | HDPE-A | | | |
|---|---|---|---|---|
| | As Received | | After Extrusion Through a 325 mesh/inch Screen and Repelletized | |
| | Test 1 | Test 2 | Test 1 | Test 2 |
| Oxidation Induc-** tion Time, Minutes | 75.7 | 64.6 | 58.6 | 57.6 |
| Oxidation Induc-** tion Time, Minutes, After Processing Degradation Test* | 2.7 | 2.5 | 8.2 | 8.9 |

The results shown in Table VI demonstrate the need for sufficient stabilizer content in HDPE to protect the polymer after the stabilizer level has been reduced due to the extrusion process and reaction with catalyst residue.

High density polyethylene compounds A, B, and C were tested for active amounts of Irganox 1010 and Irganox 1024 in accordance with reference (1) before and after a processing degradation test. The oxidation induction time also was determined before and after the degradation test. HDPE-B contained sufficiently high quantities of stabilizers, therefore, the polymer is still protected after the processing degradation test. The quantities of stabilizers in HDPE-A are adequate and within GCC specification requirements, while the quantities of antioxidant and metal inhibitor in HDPE-C are inadequate and considerably below specification requirements.

TABLE VI

STABILIZER CONTENT AND OXIDATION INDUCTION DATA OF THREE HIGH DENSITY POLYETHYLENE COMPOUNDS, AS RECEIVED, AND AFTER A PROCESSING DEGRADATION TEST

| | | HDPE-A | HDPE-B | HDPE-C |
|---|---|---|---|---|
| Stabilizer Content, % | | | | |
| As received | | | | |
| Irganox 1010 | | 0.13 | 0.23 | 0.04 |
| Irganox 1024 | | 0.15 | 0.13 | 0.05 |
| After Processing Degradation Test* | | | | |
| Irganox 1010 | | 0 | 0.11 | 0 |
| Irganox 1024 | | 0.02 | 0.02 | 0 |
| Oxidation Induction Time, Minutes** | | | | |
| As received | Test 1 | 75.7 | 62.0 | 21.4 |
| | Test 2 | 64.6 | 65.5 | 33.4 |
| After Processing Degradation Test* | | | | |
| | Test 1 | 2.7 | 50.2 | 0 |
| | Test 2 | 2.5 | 53.4 | 0 |

*Conditions for Processing Degradation Test:

| | |
|---|---|
| Test Instrument: | Brabender Torque Rheometer |
| Mixing Chamber: | Type 5 Roller Head |
| Sensitivity: | 1:5 |
| Sample Charge: | 40 grams |
| Temperature of circulating oil, measured in head: | 230°C |
| Rotor Speed: | 62 RPM |
| Test Duration: | 30 Minutes |

**Test Procedure for Oxidation Induction Time:

| | |
|---|---|
| Sample: | Approximately 5 mg of HDPE compound |
| Calorimetric Sensitivity: | 0.5 mcal/sec/in. |
| Temperature Program: | Isothermal at 200°C ± 1°C |
| Zero Shift: | 0 in. |
| Time Base: | 5 min/in. |
| Inert Gas: | Nitrogen, purified grade |
| Reactive Gas: | Oxygen, purified grade |
| Gas Flow Rate: | 200 cc/min. |

a. The sample of HDPE compound is placed in an open (uncrimped) oxidized copper pan in the DSC cell at ambient temperatures. A nitrogen gas purge is supplied to the cell and the cell is sealed.

b. The temperature is increased to 200°C and the sample is equilibrated at that temperature.

c. The purge gas is switched from the inert nitrogen to the reactive oxygen and simultaneously the recorder time base is started.

d. The scan is continued until the sharp upward movement of the pen, that indicates the oxidation, has gone through the maximum and is sloping downward.

e. The elapsed time between zero and the extrapolated oxidation onset is the polymer induction time and it is recorded as a measure of oxidative stability. The oxidative exotherm is extrapolated to the base line by drawing a straight line (tangent) through the change in slope (position to negative) of that curve to the base line.

## SUMMARY

It has been demonstrated that spark failures in HDPE insulations are increased by catalyst residue, improperly prepared catalyst, large gels and added chemicals.

It was determined that one HDPE compound that only contained particles smaller than 2.9 mils could be extruded at high speed without excessive spark failures. The level for tolerating larger particles in the insulation wall without developing surface blemishes or spark failures increases with increasing melt strength of the HDPE compound.

It was found that chemicals that are added during the manufacturing process of HDPE plate out on tips and dies, causing eccentric wall thicknesses in the insulations, spark failures during high speed extrusion and additional work at the plant in their efforts to maintain clean extrusion tools.

It has been shown that HDPE compounds must contain sufficient quantities of active stabilizers so that they are properly protected after a portion of the stabilizers is used up by catalyst residue and the extrusion process.

A method has been developed that allows separation and identification of catalyst residue and other impurities from HDPE so that lots of HDPE that contain excessive contaminants can be detected before they are incorporated into the plant systems.

This study has resulted in a better understanding of the nature and the effects of contaminants in HDPE material and should lead to improved material selection.

## REFERENCE

1. Copper Inhibitor and Antioxidant Levels in High Density Polyethylene: Their Measurement by High Performance Liquid Chromatography and Relation to Insulation Life, J. Fech, A. De Witt, General Cable Company, Edison, NJ; 29th International Wire & Cable Symposium, 1980.

## ACKNOWLEDGEMENTS

The authors gratefully acknowledge the special efforts and contributions of their colleagues in the Material Science Department and from the Manufacturing Operation.



Gertraud A. Schmidt, Assistant Director of Research and Development, Material Science, General Cable Research Center, Division of GK Technologies, Inc., 160 Fieldcrest Ave., Edison, NJ 08817.

Ms. Schmidt is a graduate of the Ohm-Polytechnikum in Nürnberg, Germany. She is a member of ASTM, the American Chemical Society, the Society of Plastics Engineers, the Technical Association of the Pulp and Paper Industry and the Armed Forces Communications and Electronics Association. Ms. Schmidt is a Senior Member of IEEE.



Louis A. Bopp, Research Group Manager, Compound Development and Processing Laboratory, General Cable Research Center, Division of GK Technologies, 160 Fieldcrest Ave., Edison, NJ 08817.

Mr. Bopp is a graduate of High Point College with additional studies at New York and Wake Forest Universities. He is a member of ASTM, serving on the Committees for Electrical Insulating Materials, Rubber, and Aerospace Industry Methods.

## APPENDIX
## METHOD FOR SEPARATION AND IDENTIFICATION OF CONTAMINATION IN HIGH DENSITY POLYETHYLENE INSULATION COMPOUND


### Summary

The method described allows independent separation of contaminants from the surface and from the inside of HDPE pellets. The contaminants from the outside are washed off with a water-methanol solution which is filtered,while the contaminants from the inside of the pellets are collected on a 325 mesh/inch screen after an extrusion process. If it is only desired to obtain total contaminant level, the separation process may be bypassed and the 250 gram sample of pellets,as received, can be utilized for the extrusion through the 325 mesh/inch screen.

If only observation of the contamination is desired, the screen is observed while immersed in hot silicone oil.

If identification of particles is desired, the remaining HDPE is removed from the screen with hot xylene. Sections of the screen are photographed with a scanning electron microscope and the individual particles are identified with the SEM X-ray system.


### A. Removal of Contamination From the Surface of HDPE Pellets

The contamination is collected as follows: 250 grams of pellets are placed into a 1000 ml beaker with water-methanol solution (ratio 500:1). After the solution with the pellets has been stirred and is allowed to settle out for three minutes, filter the solution through No. 41 filter paper (diameter 5.5 cm) with vacuum. Cover the Buchner funnel that contains the filter paper with a watch glass and set it aside.

Lift the pellets carefully from the 1000 ml beaker with a slotted scoop and place them on an absolutely clean 10 mesh/inch brass sieve. Rinse the pellets with 2000 ml of the water-methanol solution and collect the rinse water in a clean beaker and cover the beaker.

Place the rinsed pellets in a 1000 ml beaker and dry them in a vacuum oven under maximum vacuum for 2 hours at 60°C.

Filter the rinse water through the above described No. 41 filter paper in the Buchner funnel. Place the filter paper in a covered Petri dish for observation and rating of the level of contamination. A record of the observation of the contamination is obtained by photographing the filter with an MP-4 Polaroid camera at 1X magnification. For identification of the particles, sections of the filter are placed into an SEM X-ray system under 75X magnification.

### B. Removal of Contamination in HDPE by Extrusion Through Fine Screens

The 250 grams of pellets that are (a) cleaned as shown under (A) above or (b) as received, if the separation from the contaminants from the surface of the pellets is not required, are extruded at 232°C (450°F) through a screen pack consisting of one screen each, 325, 120 and 60 mesh/inch. An absolutely clean 3/4 inch 15:1 L/D extruder with a breaker plate, but without a head, is used. A polyethylene type screw (compression ratio 1.5:1) is employed at 30 RPM.

Place the 250 gram sample into the hopper and let the screw turn for 10 revolutions, stop the movement of the screw and wait 5 minutes. This procedure allows the cold pellets that initially enter the stockscrew to become heated prior to their being forced through the screen pack and breaker plate. This avoids possible screen rupture at startup. The extruder is restarted and operated at 30 RPM. When the last pellet leaves the hopper, stop the screw, remove the flange and clean it immediately. Start screw again, the remaining compound pushes the breaker plate with the screen pack out of the barrel. Approximately 230 grams of HDPE are extruded through the fine screen, while approximately 15 grams remain in the extruder in order to push out the breaker plate with the screen pack. Five grams are lost due to the cleaning operations.

Using clean insulated gloves with a smooth leather surface, remove the breaker plate from the hot compound. Hold the breaker plate with one hand and cut off the excess polyethylene 1/8 inch away from the screens utilizing a new razor blade that has been wiped with Texwipe lint free cloth. Separate a small portion of the screens from the breaker plate with a small clean screw driver, insert clean pliers and remove the screen pack from the breaker plate. Place the screen pack into a Petri dish and identify it. While separating the screen pack, continue to operate the extruder screw which will push out the remaining compound. Remove the screw from the barrel and clean it thoroughly. The extruder barrel is cleaned with a brass brush, followed by cleaning with Texwipe lint free cloth.

The entire procedure of extrusion, screen separation and cleaning of the extruder requires approximately 1 hour per sample.

### C. Observation of Contaminants Without Identification

If only an observation of the relative degree of the contamination level is required, the screen pack is placed into silicone oil, DC-200-200, at 130°C. The silicone oil is in a 10 cm wide Petri dish that is resting on a hot plate under an MP-4 Polaroid camera. A picture may be taken at 2.4X magnification as soon as the HDPE on the screen reaches the temperature of the silicone oil and becomes transparent.

D. Observation and Identification of Particles on A 325 Mesh/Inch Screen

Place a section of 5 mil thick aluminum foil on a hot plate and place the screen pack on top of it. As soon as the HDPE on the screen becomes soft, remove the 325 mesh screen with tweezers. The 325 mesh screen is placed between two stainless steel rings, the assembly is clamped together and placed into a fluted filter that is inside of a Pyrex beaker. In order to hold the small 325 mesh screen, stainless steel rings with the following dimensions were found to be suitable: OD 1.12", ID 0.75", Width 0.44". Xylene is added to the beaker. The level of the xylene must be 0.5 inches below the screen. The beaker is placed on a hot plate in a hood and covered with a watch glass and xylene is gently refluxed until all of the polyethylene is removed.

After the screen is air dried in the hood, it can be inspected first with an optical microscope at approximately 45X magnification in order to obtain an initial impression of the relative amounts of gels and other particles present.

For identification of the individual particles, the screen is placed under the electron beam of a scanning electron microscope. A section of the screen is selected for a picture at 75X magnification, followed by X-ray analysis of the individual particles.

# A NEW TECHNIQUE TO EVALUATE THE TRANSMISSION CHARACTERISTICS OF COMMUNICATION CABLE PAIRS USING DEDICATED MINI-COMPUTER

S. Sammoun

Northern Telecom Canada Limited
Montreal, Quebec

*ABSTRACT*

Dedicated mini-computers are commonly used to perform high precision insertion loss and phase shift measurements on communication cables. This paper presents a technique to extend the capability of such equipment to measure the characteristic impedance ($Z_o$) on any manufactured length of cable. From these measured quantities, it is then shown how to compute $\alpha$, $\beta$, R, L, G and C and hence characterize the cable. Results of various measurements of $Z_o$ on different lengths of paired cables are presented. Comparison with results obtained using manual bridge methods shows the effectiveness of the new approach in achieving good accuracy and extending the measurement applications. A theoretical model is also developed to explain the small irregularities encountered in measuring the characteristic impedance for long lengths of cables at relatively high frequencies.

## *I. INTRODUCTION*

The traditional method of obtaining the transmission characteristics of communication cable pairs is performed by measuring the open-circuit and short-circuit impedances, using a manual balancing bridge concept. The primary parameters (R, L, G, C) and the secondary parameters ($\alpha$, $\beta$, $Z_o$) are then derived by performing the applicable calculations from transmission line theory. The impedance bridge method is usually restricted to short lengths of cables because of the inherent inaccuracies in the measurement approach for lengths exceeding $\lambda/8$. Therefore, this method is not adaptable for measuring shipping lengths of cable on a reel at relatively high frequencies. At carrier frequencies (up to 2 MHz), an extra length of 50 ft. is required for evaluation, which makes the method costly when cables of large pair sizes are to be characterized. Furthermore, this manual method is particularly time-consuming and impractical when characterization of cables is required on a rush basis.

An automated procedure for evaluating the primary and secondary parameters of communication cables has been previously presented[1]. It is based on insertion loss and phase shift measurements which can be accurately performed on long lengths of cable over a wide frequency range. These are combined with capacitance measurements at 1 kHz and an approximated value of the dissipation factor (tan $\delta$). The application of this method for some cable insulations (e.g. PVC, paper/pulp) is limited since the dielectric properties of the insulation system, as a function of frequency, are not known a priori.

The technique presented in this paper is aimed at eliminating these difficulties so that characterization of any type or length of communication cable pairs would be feasible in a very short time.

A description of the measurement procedure is presented in section II and is tailored to the mode of operation of the equipment installed in our laboratory[2]. The technique can be easily adapted to any other automated test set capable of measuring insertion loss and phase shift.

Results of various measurements of $Z_o$ on different lengths of paired cables are presented in section III for low and high frequencies. It was found that the measurement of $Z_o$ at relatively high frequencies deviates from the anticipated smooth behaviour of the characteristic impedance of an ideal transmission line. Non-uniformities in the physical dimensions of a real transmission pair are the cause of this phenomenon as shown in Appendix A.

In Appendix B, an algorithm, which can be implemented on the computer is presented to obtain the transmission line constants $\alpha$, $\beta$, R, L, G and C.

## *II. MEASUREMENT METHOD*

The measurement equipment shown in Fig. 1 consists of a set of instruments controlled by a mini-computer, designed to perform insertion loss and phase shift

measurements on communication cables. Its operating characteristics are;

(1) Frequency range: 1 kHz to 500 MHz
(2) Dynamic range : Loss/gain 0 - 145 dB
Loss/gain & phase 0 - 60 dB
Resolution 0.01° and 0.001 dB

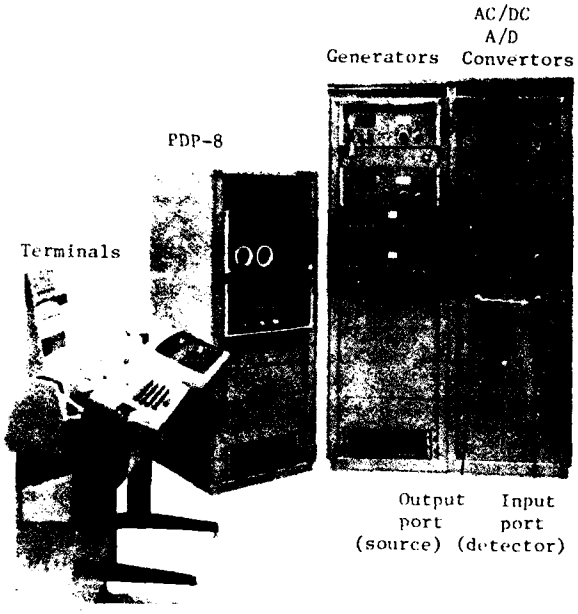



FIG. 1 TEST SET PICTURE

The measurement of insertion loss and phase shift is performed accordingly to the sequence of operations presented in Fig. 2.

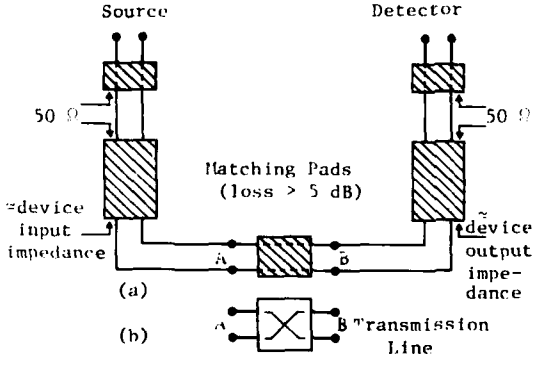



FIG. 2 I.L AND PHASE SHIFT MEASUREMENT CIRCUIT CONFIGURATION

First, the system is calibrated as shown in Fig. 2(a) over the suitable frequency band, and the values of insertion loss and phase shift at each desired frequency are stored in the computer memory. After the test set calibration, the transmission pair can be connected in series between points A & B and measured as shown in Fig. 2(b). The stored corrections from the calibration procedure are substracted at each point to obtain the final results which are stored for subsequent use.

*II.1 Development of Impedance Measurement Capability using the Test Set*

Assume the test set is calibrated through a "T" type connector then the pair is connected to the free end of the "T" and measured as shown in Figs. 3(a) and 3(b) respectively. The normal expectation is that the change in the transmission characteristics for this arrangement will reflect the input impedance of the transmission pair.

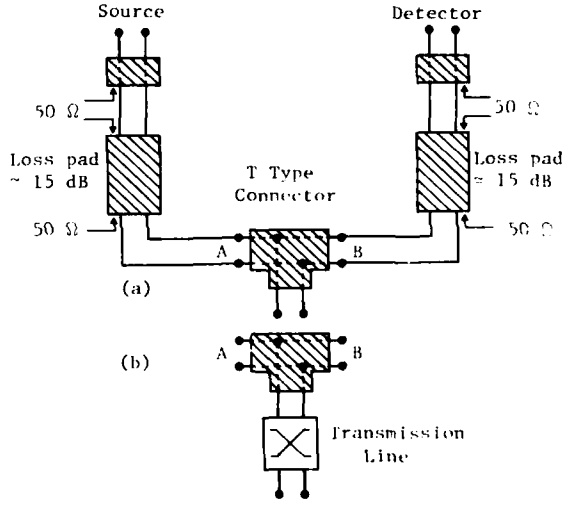



FIG. 3 IMPEDANCE MEASUREMENT CIRCUIT CONFIGURATION

In fact, based on the equivalent electrical circuits of Figs. 4(a) and 4(b), and assuming source impedance ($Z_S$) = load impedance ($Z_L$) = $Z_T$, it can be shown that the insertion loss and the phase shift measured can be related to the input impedance of the pair by:

$$Z = \frac{Z_T}{2(10^{(|I.L|/20)}\angle\theta - 1)} \qquad (1)$$

where $Z_T$ is usually a pure resistive component equal to the matching impedance

between the input/output ports of the test set and the "T" connector. I.L and θ are the insertion loss and the phase shift measured by the system.

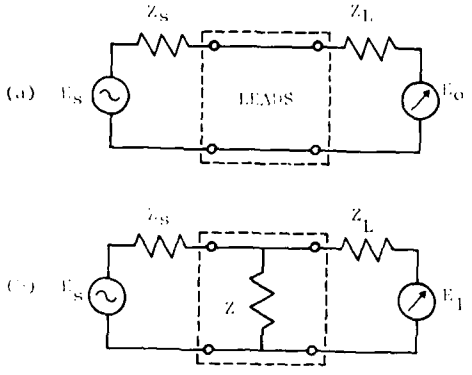



FIG. 4 EQUIVALENT ELECTRICAL CIRCUITS OF FIGS. 3(a) AND 3(b) RESPECTIVELY

Equation (1) can be used to evaluate the characteristic impedance $Z_O$ of any given transmission line by performing two measurements with an open and short circuit termination. It can be shown from transmission line theory that:

$$Z_O = \sqrt{Z_{OC} \cdot Z_{SC}} \qquad (2)$$

where $Z_{OC}$ and $Z_{SC}$ are the input impedances of the transmission line terminated with open and short circuits respectively.

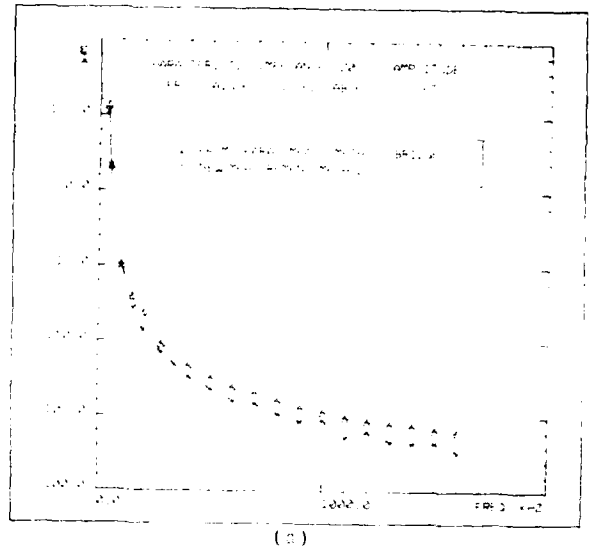
## III. COMPARISON OF THE BALANCED MEASUREMENT RESULTS

The technique presented so far has been implemented on the computer and measurements of $Z_O$ were performed on various types and lengths of communication cables. Some of these are presented in this paper and compared with results obtained using the traditional measurement method.

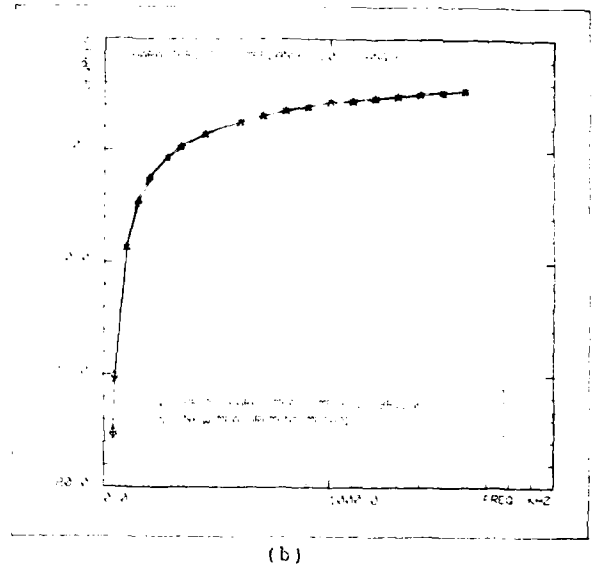
### III.1 Comparison of $Z_O$ Measurements

Figs. 5(a) and 5(b) show the characteristic impedance of a 52.5-foot length of a 25-pr./22 AWG filled PIC cable, measured with the automated test set and by the balanced impedance measurement method.

A direct comparison from the graphs shows the amplitudes are within 1.5 ohms while the angles are within 0.25° for this particular case.



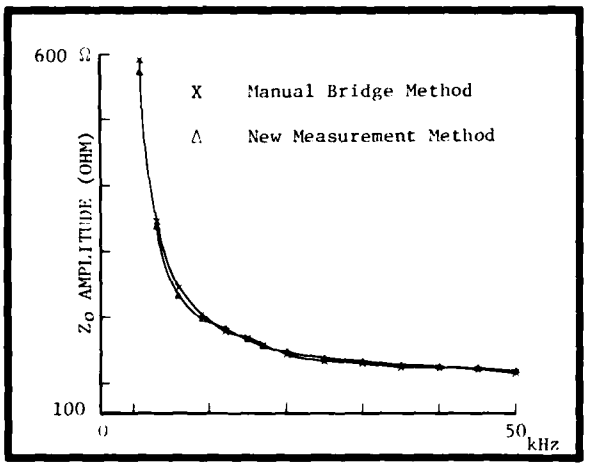
(a)



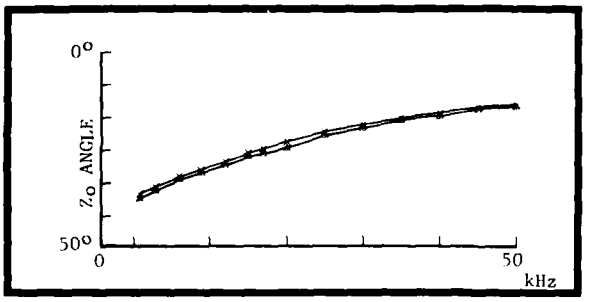
(b)

FIG. 5 COMPARISON OF $Z_O$ MEASUREMENTS FOR SHORT LENGTH OF CABLES

For long lengths of cable the comparison could only be done at low frequencies. This is shown in Figs. 6(a) and 6(b) for the amplitude and phase of $Z_o$ respectively.




(a)

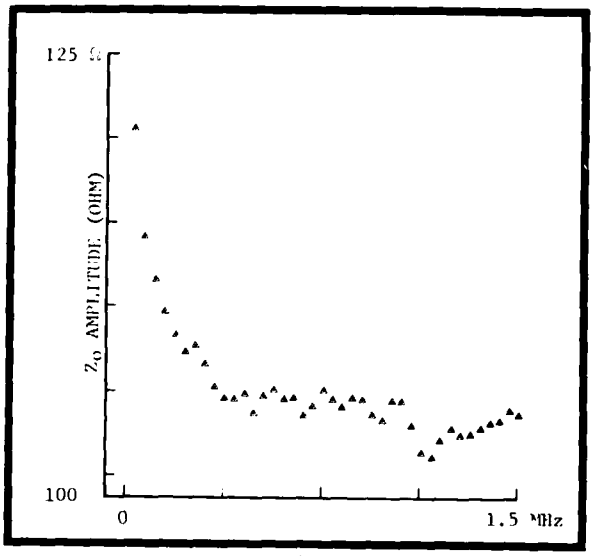



(b)

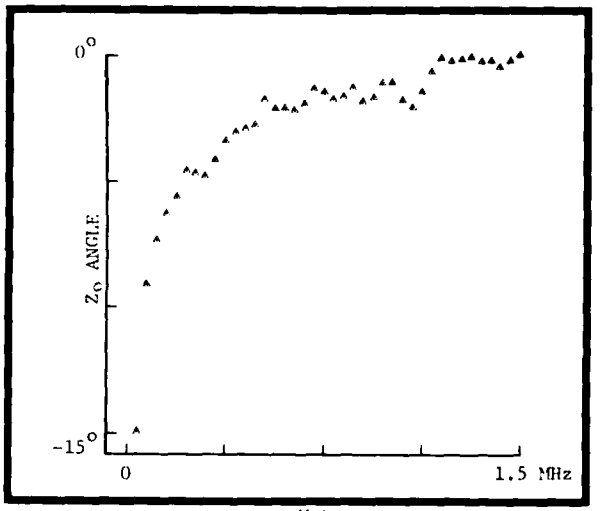
FIG. 6 COMPARISON OF $Z_o$ MEASUREMENTS FOR LONG LENGTHS OF CABLE AT LOW FREQUENCIES
(Typical pair, 1557 ft. of 25 pr./ 22 AWG Air Core PIC Cable)

### *III.2 Characteristic Impedance Behaviour of Communication Cable Pairs at High Frequency*

Ideally, the characteristic impedance of paired cables is represented as a smooth function of frequency which is asymptotic to fixed values (e.g. 100 Ω, 0°) at very high frequencies. In practice, for long cable lengths the characteristic impedance was found to vary from the idealized behaviour. This is shown in Figs. 7(a) and 7(b) where the amplitude and phase of $Z_o$ are plotted respectively for a typical pair as measured on a 5200-foot length of 25-pr./22 AWG filled PIC cable.




(a)



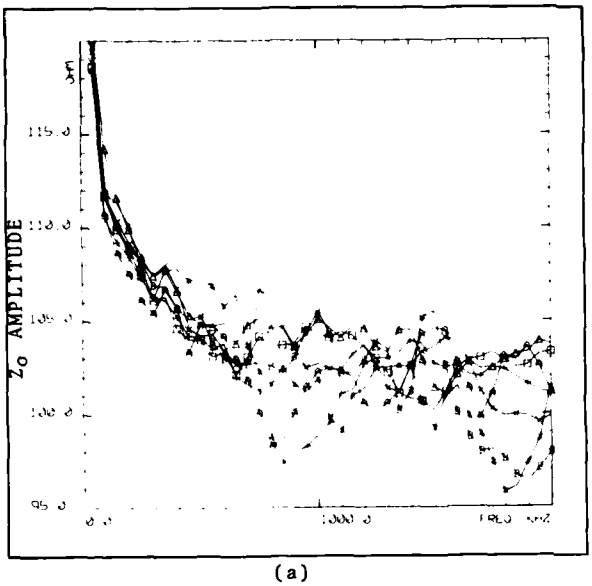

(b)

FIG. 7. CHARACTERISTIC IMPEDANCE OF LONG LENGTHS OF CABLE AT HIGH FREQUENCIES
(Typical pair, 5200 ft. of 25 pr./ 22 AWG filled PIC Cable)

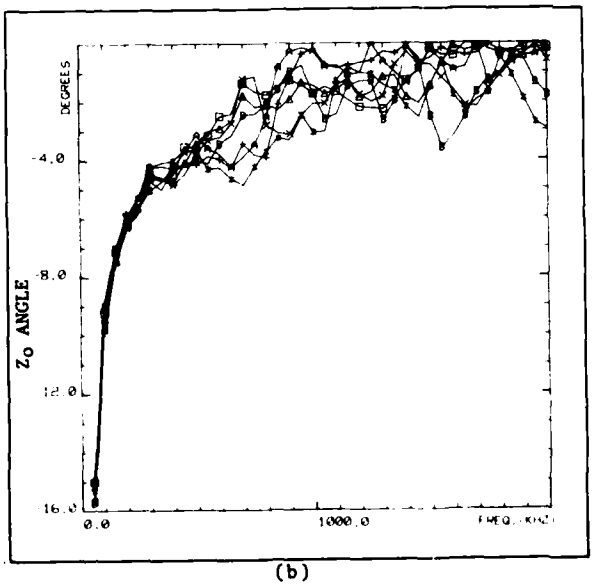
Measurements on all 25 pairs showed that the ripples behave randomly for each pair as shown in Figs. 8(a) and 8(b) where seven individual impedance traces have been superimposed on one graph.

After satisfying ourselves that the measured results were valid by using an independent measurement technique[3], it was hypothesized that multiple reflections caused by dimensional non-uniformities

along the length of cable resulted in the observed behaviour. To verify this, a mathematical model was developed and implemented on the computer. The theoretical development of this model, as well as the results of a computer simulation are presented in Appendix A. Although these deviations reflect actual cable behaviour, they cannot be used directly to represent the nominal or ideal characteristic. However, as it is shown in Figs. 9(a) and 9(b), by calculating the average behaviour of many pairs, the random distribution of physical imperfections would tend to cancel and converge toward the ideal solution for a uniform transmission line.

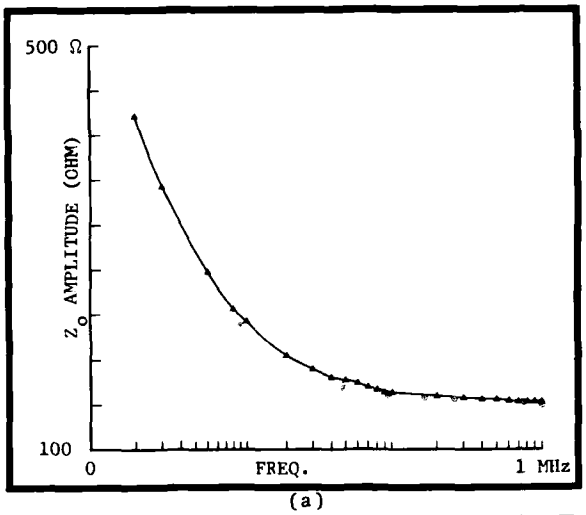



(a)

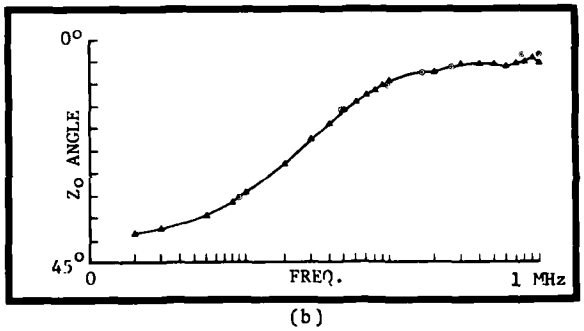



(b)

FIG. 8 CHARACTERISTIC IMPEDANCE OF LONG LENGTHS OF CABLE
(7 typical pairs, 5200 ft. of 25 pr./22 AWG Filled PIC Cable)




(a)




(b)

FIG. 9 COMPARISON OF AVERAGE $Z_o$ FOR LONG CABLE LENGTHS WITH NOMINAL $Z_o$

Δ = Average of 6-pr. characteristic impedances (1557 ft., 22 AWG Air Core PIC Cable) measured by the new technique at 68°F.

0 = Nominal Characteristic Impedances; (50 ft., 22 AWG Air Core PIC Cable)

The average characteristics presented in Figs. 9(a) and 9(b) can be approximated by measuring several pairs in parallel. It can be easily shown that for random distribution and assuming relatively small deviations around the nominal value, the mean input impedance $|Z| \angle\theta$ can be expressed in terms of the measured parallel impedance $|Z_p| \angle\theta_p$ as:

$$|Z| = n \cdot |Z_p|$$

and $v = v_p$

where n is the number of pairs.

Other methods can be used to obtain the idealized $Z_o$ characteristic which would involve curve fitting algorithm or smoothing algorithm[4]. Although these tools can be used efficiently, their accuracies are limited depending on the application.

At low frequencies, the calculation of R, L, G, C, $\alpha$ and $\beta$ is straightforward from open and short impedance measurements. At relatively high frequencies ($\ell > \lambda/8$), the calculation of the above parameters does involve non linear equations to be solved as it is presented in Appendix B. This calculation is based on the general equation of the insertion loss. An iterative algorithm is presented to converge on $\alpha$ by varying the propagation constant $\beta$. The initial value of $\beta$ is chosen accordingly to the length of cable with respect to the wave length. The computation of R, L, G and C is then performed using the transmission line theory.

## Appendix A

## Variation of the Characteristic Impedance of a Transmission Line due to Non-Uniform Physical Dimension

The transmission line is represented by subsections of different lengths $\ell_i$. The wire dimensions for each subsection are distributed randomly with a percent change (about 2%) around a fixed nominal value. Thus, the transmission line mathematical model could be represented by the cascaded two-dimension matrixes shown in Fig.A1;

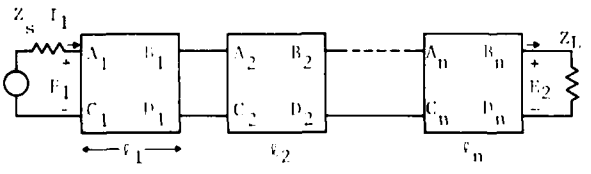



Fig. A1 MATHEMATICAL REPRESENTATION OF A TRANSMISSION LINE DIVIDED INTO n SECTIONS

where $A_i = \cosh(\gamma_i \ell_i)$

$B_i = Z_{oi} \sinh(\gamma_i \ell_i)$

$C_i = Y_{oi} \sinh(\gamma_i \ell_i)$

$D_i = \cosh(\gamma_i \ell_i)$

$$\gamma_i = \sqrt{(R_i + j\omega L_i)(G_i + j\omega C_i)}$$

and $$Z_{oi} = \sqrt{\frac{(R_i + j\omega L_i)}{(G_i + j\omega C_i)}}$$

The input/output equation system can be written as;

$$\begin{bmatrix} E_1 \\ I_1 \end{bmatrix} = \begin{bmatrix} A & B \\ C & D \end{bmatrix} \begin{bmatrix} E_2 \\ I_2 \end{bmatrix} \qquad (A1)$$

where $$\begin{bmatrix} A & B \\ C & D \end{bmatrix} = \prod_{i=1}^{n} \begin{bmatrix} A_i & B_i \\ C_i & D_i \end{bmatrix} \qquad (A2)$$

From (A1), the characteristic impedance $Z_o$ can be expressed as;

$$Z_o = \sqrt{\frac{A \cdot B}{C \cdot D}} \qquad (A3)$$

Equation (A3) has been simulated by a computer program and results of $Z_o$ behaviour were obtained for different combinations where the physical dimensions of the pair were varied at *random for each* subsection. An example is presented in Fig. A2 for 2% random variation of the in-

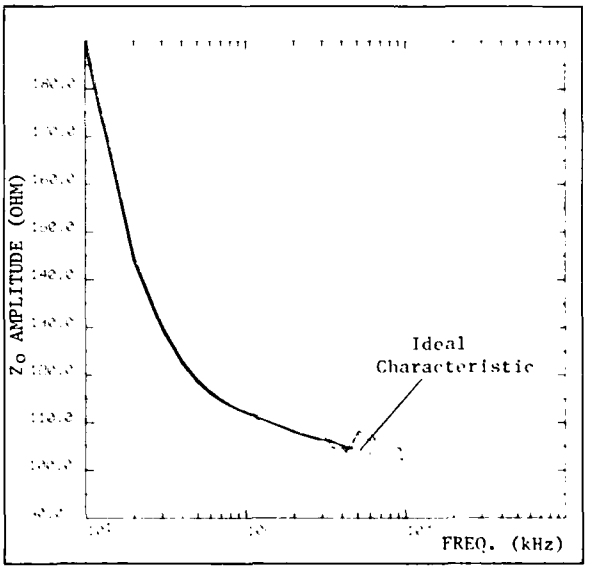



FIG. A2 SIMULATION OF '$Z_o$' BEHAVIOUR FOR A NON-UNIFORM TRANSMISSION LINE

sulated conductor dimensions for 10 subsections. The smoothed curve is the ideal case where all subsection dimensions are identical. The ripples become important as the frequency increases. The shape of the curve is dependent on the locations and magnitudes of the non-uniformities along the transmission line.

*Appendix B*

*Calculation of α, β, k, L, i & C from Measured Insertion Loss, Phase Shift and $Z_o$*

From transmission line theory, the insertion loss I.L equation expressed in term of $\gamma\ell$ and $Z_o$ is;

$$I.L = \cosh(\gamma\ell) + \frac{Z_s Z_L + Z_o^2}{Z_o(Z_s+Z_L)} \sinh(\gamma\ell) \qquad (B1)$$

where $I.L = |I.L| \angle\theta$, $\theta$ is the phase shift. $|I.L|$ is the insertion loss magnitude.

$Z_o = |Z_o| e^{j\theta_o}$ is the characteristic impedance.

$\gamma\ell = (\alpha+j\beta)\ell$ is the attenuation term.

$Z_s, Z_L$ are the source and detector impedances respectively of the test set.

Assuming $Z_s = Z_L$; $Z_3 = \frac{|Z_o^2| + Z_s^2}{2|Z_o|Z_s}$ and

$$Z_4 = \frac{|Z_o^2| - Z_s^2}{2|Z_o|Z_s}$$

Expression B1 can then be written as;

$$I.L = \cosh(\gamma\ell) + [Z_3 \cos(\theta_o) + jZ_4 \sin(\theta_o)] \sinh(\gamma\ell) \qquad (B2)$$

which can be broken down into real and imaginery parts in terms of α and β as;

$$R_e(I.L) = A\frac{e^{\alpha\ell}}{2} + B\frac{e^{-\alpha\ell}}{2} \qquad (B3)$$

where

$$A = \cos(\beta\ell) + Z_3 \cos(\theta_o)\cos(\beta\ell) - Z_4 \sin(\beta\ell)\sin(\theta_o)$$

$$B = \cos(\beta\ell) - Z_3 \cos(\theta_o)\cos(\beta\ell) - Z_4 \sin(\beta\ell)\sin(\theta_o)$$

and

$$I_m(I.L) = C\frac{e^{\alpha\ell}}{2} - D\frac{e^{-\alpha\ell}}{2} \qquad (B4)$$

where $C = \sin(\beta\ell) + Z_4 \cos(\beta\ell)\sin(\theta_o) + Z_3 \cos(\theta_o)\sin(\beta\ell)$

$D = \sin(\beta\ell) + Z_4 \cos(\beta\ell)\sin(\theta_o) - Z_3 \cos(\theta_o)\sin(\beta\ell)$

using B3 and B4 we can write after development;

$$e^{4\alpha\ell}(A^2 + C^2) + e^{2\alpha\ell}[2(AB-CD-2|I.L|^2)] + B^2 + D^2 = 0 \qquad (B5)$$

which is a quadratic equation in term of $e^{2\alpha\ell}$.

After some straightforward algebra, we get;

$$A^2 + C^2 = 1 + Z_3^2\cos^2(\theta_o) + Z_4^2\sin^2(\theta_o) + 2Z_3\cos(\theta_o)$$

$$B^2 + D^2 = 1 + Z_3^2\cos^2(\theta_o) + Z_4^2\sin^2(\theta_o) - 2Z_3\cos(\theta_o)$$

$$AB - CD = \cos(2\beta\ell)\{1 - Z_3^2\cos^2(\theta_o) - Z_4^2\sin^2(\theta_o)\} - 2Z_4\sin(\theta_o)\cdot\sin(2\beta\ell)$$

Note that (AB - CD) is a function of the unknown β.

At this point, equation (B5) can be easily solved for $e^{2\alpha\ell}$, provided we know $\beta\ell$. The solution is given as:

$$e^{2\alpha\ell} = \frac{-b \pm\sqrt{b^2 - 4ac}}{2a} = +R \qquad (B6)$$

where $a = A^2 + C^2$, $b = 2(AB-CD-2|I.L|^2)$, $c = B^2 + D^2$

N.B.: It can be shown that only the positive root +R is physically meaningful.

From (B6) we get:

$$\alpha\ell = \frac{1}{2}\ln(+R) \qquad (B7)$$

An appropriate iterative algorithm could be used to converge on α by varying

β. The simplest is to use the phase shift information as measured by the test set to find the combination of (α, β) which satisfies:

$$|I.L|^2 = |I.L_m|^2$$

and $R_e(I.L) = R_e(I.L_m) = |I.L_m| \cdot \sin(\theta_m)$

where

I.L is given by (B2)

$R_e(I.L)$ is given by (B3)

$|I.L_m|$ and $\theta_m$ are the insertion loss magnitude and the phase shift measured by the test set respectively according to section II.

Having determined the values α, β and $Z_o$ at each frequency, the calculation of R, L, G and C is determined from transmission line theory as follows;

Using

$$\gamma = \alpha + j\beta = \sqrt{(R + j\omega L)(G + j\omega c)}$$

$$Z_o = |Z_o| \angle\theta_o = \sqrt{\frac{R + j\omega L}{G + j\omega c}}$$

it can be shown that

$$R = R_e(\gamma . Z_o)$$

$$L = \frac{1}{\omega} I_m(\gamma . Z_o)$$

$$G = R_e\left(\frac{\gamma}{Z_o}\right)$$

$$C = \frac{1}{\omega} I_m\left(\frac{\gamma}{Z_o}\right)$$

Note: In the above, it was assumed a smoothed version of $Z_o$ corresponds to a uniform transmission line.

## CONCLUSION

A new automated technique was presented to obtain the primary parameters (R, L, G, C) and the secondary parameters (α, β, $Z_o$) of any type and length of paired communication cables. Based on insertion loss, phase shift and characteristic impedance measurements, it was shown how to derive α, β, R, L, G and C and hence characterize the cable.

Dedicated mini-computers offer high precision insertion loss and phase shift measurements on long length of cables. It has been demonstrated that measurement of $Z_o$ can be successfully implemented on this type of equipment. For long cable lengths at relatively high frequencies, the actual behaviour of ($Z_o$) is shown to vary from the ideal case of a uniform transmission line. It is shown that the deviations in ($Z_o$) behaviour are due to random non-uniformities along the cable length.

The new measurement technique offers certain advantages compared with the traditional method using a balancing bridge concept. Some of these are:

- Considerable reduction of the measurement time.
- Extension of the measurement application.
- Good measurement accuracy.
- Actual behaviour of $Z_o$ for long cable length at relatively high frequency.

## ACKNOWLEDGEMENTS

The author wishes to express his appreciation and gratefulness to Paul Kish, Yves Le Borgne and his colleagues at Northern Telecom for their valuable assistance and support.

## Reference

1. J. Krentzberg and T.D. Nantz, "Precision Insertion Loss Measurements and Data Analysis on Multipair Cable". 24th International Wire and Cable Symposium, Cherry Hill, N.J.

2. "Computer Control Transmission Test Set". L-5043.

3. Y. LeBorgne, "Characteristic Impedance Measurement on Long Length of Communication Cables". (TM-4090-80-12).

4. Y. LeBorgne, "Algorithm to Smooth Analogue Function with Superimposed Random Noise". (TR-4090-80-02).



Samir Sammoun is a Member of Research and Development Staff, Cable Division, Northern Telecom Canada Limited. He received a B.Ing. in 1977 and an M.Sc.A. in 1979 in electrical engineering, both from the Ecole Polytechnique, University of Montreal. He joined Northern Telecom in September 1978 and has worked on the design and development of new automated test methods. His present responsibilities concern the development of automated techniques for new product opportunity identification.

# COMPUTERIZED STATISTICAL QUALITY CONTROL OF TELEPHONE CABLES

LEO M. CHATTLER

DCM INTERNATIONAL CORPORATION
San Leandro, California

## ABSTRACT

Computerized Automatic Measuring & Management Systems (CAMMS) issued in a new era of controlling the quality of telephone cables. The ability to measure, monitor and process test data via computer, to rapidly and continuously accumulate a data base, to rapidly analyze the distribution and estimate the cumulative statistics with trend projections can insure that no reel of cable is rejected.

## SUMMARY

This paper discusses process control and final testing statistics for telephone cable including the establishment of a data base, the methods of accumulating data files and types of statistical distributions for each of the telephone cable parameters. In addition, an overall data management system is described for single plant and multiplant operation. Multiplant operation covers a distributed quality control network from a centralized data base utilizing the telephone network to transmit data. Specifications are controlled from the centralized location where the quality control expertise is located.

## HISTORICAL PERSPECTIVE OF STATISTICS

In dealing with statistics on the quality control of telephone cable, I would like to acquaint you with a brief history of probability statistics. The men of history we owe credit to for the beginning of probability and statistics starts with the famous Italian mathematician-astronomer, Galileo Galilei (1564-1642). In 1620 Galileo was asked by his patron, the Grand Duke of Tuscany, "If 3 dice are thrown at the same time what is the total score which will occur most frequently?" Galileo came forth with a 4-page essay which formed the basic laws of chance and began the field of probability and statistics. In 1713 a paper was published posthumously by Jakob Bernoulli (1654-1705), a Swiss mathematician, on the theory of probabilities and was called Bernoulli's theorem. Bernoulli's Theorem, now called the Binomial Formula, is applicable to any situation in which there are only two possible outcomes, such as tossing a coin (heads or tails). For example, if p is the probability of an event having a certain outcome (say heads), and q is the probability of the only alternative outcome (say tails), then the probabilities of various outcomes occurring in n trials are predictable.

Abraham de Moivre (1667-1754), a French mathematician, discovered in 1716 that many throws of the dice follows a continuous distribution which forms a bell shaped curve and published his findings in a paper entitled "The Doctrine of Chances". On the dividing line between the Eighteenth and Nineteenth centuries, a famous German mathematician-astronomer, Carl Frederick Gauss (1777-1855), in making many measurements on celestial bodies also discovered that these measurements followed a continuous distribution in the form of a bell shaped curve. He was the first to completely define the characteristics of the normal curve (Figure 1A).

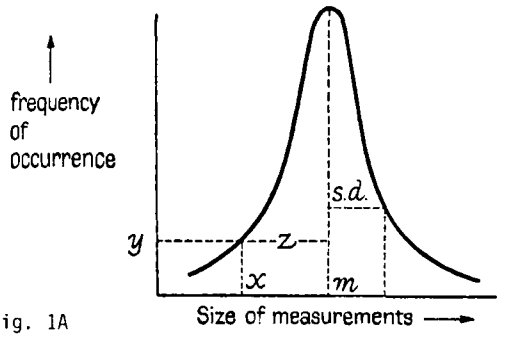



Fig. 1A

**The Normal Curve. The peak of the curve is directly over the arithmetic mean (*m*) of the measurements. The spread of the curve is specified by its standard deviation (*s.d.*); the greater the standard deviation, the broader the curve will be. The frequency of any particular measurement (*x*) is given by the height of the curve (*y*) at that point; its distance (*z*) from the mean, expressed in standard deviations, enables the probability of its chance occurrence to be calculated.**

This famous curve, now called the Gaussian distribution or the normal curve, is the backbone of modern statistical theory. The Gaussian distribution has seen exceptional growth in applications of physical and electrical measurements, physics, astronomy, biology, chemistry, quality control and all forms of science and nature.

One final contribution of the masters of old was in 1837 by a French mathematician named Simeon Denis Poisson (1781-1840). Poisson modified

Bernoulli's discrete Binomial Formula to suit the situation of isolated occurrences, such as found in dealing with insulation faults on telephone singles, pairs or quads. Modern statistics has many special versions of discrete and continuous distributions depending upon the application. In addition, many techniques are now available to determine the type of distribution the data exhibits.

## STATISTICS

The whole idea of using statistics in telephone cable production is to be able to reduce the amount of testing (and thereby the cost of the cable) by selecting a random sample from which the electrical characteristics of the production lot can be determined. In order to do this the sample must be representative of the lot and should follow some known defined distribution or a pattern from which a distribution can be determined by curve-fitting mathematical techniques. If the distribution does not fit a particular pattern, we must see if there is consistency of data such that a curve can be established. If there is no consistency we must test the complete lot to determine if all cables meet the customer specifications.

Keep in mind that statistics is the selection of a subset of a large collection of data, either existent or conceptual, in order to infer the characteristics of the complete set. The total body of data is called the population and the subset selected from it is a sample. In telephone cable our population is a complete order or lot of a particular type of cable and our sample is the selection of random units equivalent to some percentage of the order which will infer the characteristics of the total order or lot. The smaller the sample from which we can infer the characteristics of the total population the lower the cost of the cable. Thus the objective of statistics is to make an inference about a population based on information in a sample.

In telephone cable the characteristics we must infer from the sample are all defined by specifications for the total population. To characterize a set of measurements for a normal distribution we need to (1) locate the center of the distribution of the data, the mean ($\bar{x}$) and (2) the variance ($\sigma^2$) of a set of measurements which is a function of the deviation (or distances) of the measurements from their mean. Numerically they are:

$$(1)\quad \bar{x} = \frac{1}{n}\sum_{i=1}^{n} x_i \quad \text{or} \quad \bar{x} = \frac{x_1 + x_2 + x_3 \cdots x_n}{n}$$

$$(2)\quad \sigma^2 = \frac{1}{n-1}\sum_{i=1}^{n} (x_i - \bar{x})^2 \quad \text{or}$$

$$\sigma^2 = \frac{(x_1 - \bar{x}) + (x_2 - \bar{x}) \cdots (x_n - \bar{x})^2}{n-1}$$

where: $x$ = mean;

$\sigma^2$ = variance;

$n$ = total number of measurements

The larger the variances of a set of measurements, the greater will be the variations within the set. The variance is of great value when determining the dispersion of the data. This dispersion in terms of a normal distribution (Fig. 1B) has very definite characteristics which are measured in terms of the standard deviation. The standard deviation (Eq. 3) is the square root of the variance (Eq. 2).

$$(3)\quad \sigma = \sqrt{\sigma^2}$$

where: $\sigma$ = standard deviation

As an example, suppose we measure 10% of a production lot of cables and find that the average mutual capacitance (CM) of the samples has a normal distribution with a mean ($\bar{x}$) calculated from Eq. (1) of 52.47 nanofarads per kilometer (nF/km) and a standard deviation ($\sigma$) calculated from Eq. (2) and (3) of 0.65 nF/km. From Fig. 1B the abscissa would be CM in nF/km and the mean would be 52.47 nF/km in lieu of "0". If we now set the abscissa at $\pm 1\sigma$ and calculate $\bar{x} \pm \sigma = 52.47 \pm .65$ we get $+1\sigma = 53.12$, and $-1\sigma = 51.17$. If we repeat this for $\pm 2\sigma$ and $\pm 3\sigma$ we get $+2\sigma = 53.77$, $-2\sigma = 51.17$ and $+3\sigma = 54.42$, $-3\sigma = 50.52$. If we place these values on the abscissa (x axis) of Fig. 1B and refer to the C scale which is the cumulative distribution function, we can infer that 68% of all cables will have a CM between 51.82 and 53.12 nF/km ($1\sigma$). That 95% of all cables will have a CM between 51.17 and 53.77 nF/km ($2\sigma$) and that 99.7% of all cables will have a CM between 50.52 and 54.42 nF/km ($3\sigma$). Since the requirements of most specifications are 52±2 nF/km we can estimate that approximately .01% of the cables will fail which would be within acceptable limits considering the size and selection of the sample.

The reality of being able to infer the Mutual Capacitance of the whole cable as represented in the sample will depend on the random selection of units within the cable and how these units are representative of the manufacturing process. Once the proper sample is selected then we must determine the frequency distribution. If the distribution fits one of the known types which are well defined we can proceed in determining if the entire lot meets its specifications.

The process of producing multipair telephone cables involves six independent stages, any one of which can and does affect the final primary and secondary parameters and crosstalk characteristics of the cable (R, L, G, C, $\alpha$ & XT). These processes are annealing and drawing ($\alpha$, R & C) insulating ($\alpha$, R, C & G), twisting, pairs or star quads ($\alpha$, R, L, C & XT), stranding (L, C & XT), coring (L, C, & XT) and sheathing and jacketing (C & XT). In manufacturing the cable in-process quality control is essential to detect systematic errors

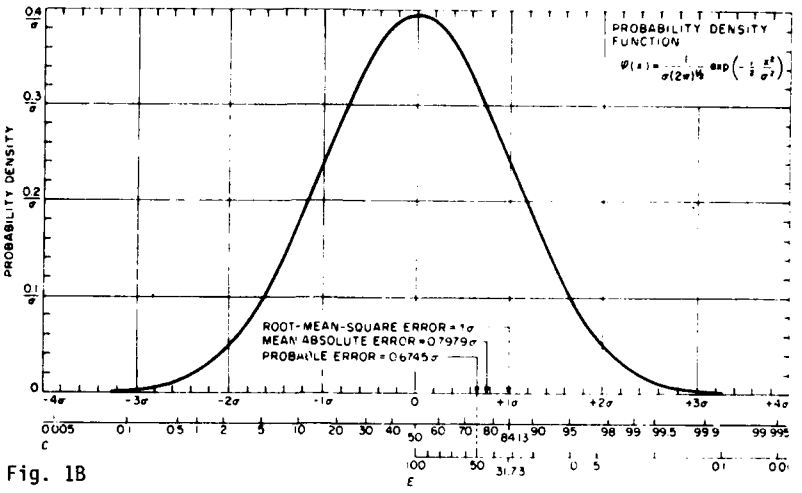



Fig. 1B

The normal distribution. $\sigma$ is the standard deviation. Scale $C$ is the cumulative distribution function in percent = 100 $\Phi(x)$. For example, the probability of finding $x$ between $-\sigma$ and $+2\sigma$ is 97 − 16 = 81 percent. Scale $E$ is the probability that the error (absolute deviation) exceeds the value read on the axis. For example, if the deviation is larger than $2\sigma$ in either direction, probability is 4.5 percent.

and out of control conditions. In final test of the product one controls the overall process and verifies the cable design.

## STATISTICAL PROCESS CONTROL

Computerized automatic measuring and management systems (CAMMS) of the type referred to in this paper utilize multipurpose disc computers. A multipurpose disc computer is capable of processing and storing many types of data simultaneously. Accordingly, along with the measurement, storage and processing of the primary parameters of finished telephone cable, one can provide quality control of the process.

### Drawing and Insulating

As an example, let us consider the process of producing insulated wire in continuous reels. The standard for this process allows one defect for each 40,000 feet of wire. The control of this process is best served by Poisson's discrete distribution.

$$(4) \quad e^{-\lambda} + \frac{\lambda}{1} e^{-\lambda} + \frac{\lambda^2}{2x1} e^{-\lambda} + \frac{\lambda^3}{3x2x1} e^{-\lambda}; \text{ etc.}$$

where: $\lambda$ = the Poisson mean or average, and

$e$ = base of Naperian Log

By determining the Poisson mean ($\lambda$) of past faults, the probability of 0, 1, 2, 3, etc. occurrences happening in the future can be predicted quite accurately by the successive terms of Eq. (4). The first term gives the probability of 0 occurrences, the second term the probability of one occurrence, the third term the probability of two occurrences, etc.

If we monitor the process on the insulating line and input to the computer the faults occurring, the computer will normalize the data in faults per 40,000 feet for each of the insulating lines. The computer can then calculate the mean ($\lambda$), process the data through Poisson distribution and predict the number of faults that will occur in the succeeding process. From this distribution one can also determine how many faults must be repaired per reel to meet the specification. In addition to insulation faults on the insulating lines one can monitor and control conductor diameter, diameter of the insulation over the conductor (DOD), coaxial capacitance of the insulated conductor, and eccentricity of the insulation over the conductor. For all these process factors, control limits can be established and monitored by CAMMS.

### Twisting, Stranding and Sheathing

As for the insulating process, upper and lower control limits can be established and process data can be monitored at each process station or fed directly to CAMMS for data analysis and control charting. Control factors which can be monitored for the twisting operation are insulation faults, twist eccentricity (wrap around), back tension on conductor, twist lay control, and resistance unbalance. Control factors for the stranding and sheathing operations may be insulation faults, pair drift, lay oscillation and core fill.

## STATISTICAL CONTROL OF FINAL PRODUCT

### Control Charts

Statistics can be used in many ways to control the process through final test data. We will briefly illustrate several methods. The use of time control charts as shown in Fig. 1C.1 and 1C.2 controls the individual and average capacitance unbalance pair to ground and pair to shield. A specification limit and an upper control limit is included. If any of the cable averages begin to exceed the control limit this triggers action to investigate the process for an out of control situation before the specification limit is exceeded. A least squares fit curve is computed for the average values in order to determine the trend of the running averages. This permits the quality control people to anticipate forthcoming problems and take corrective action in time to prevent any out of spec cables reaching final test.

Fig. 1C.3 illustrates another possible control chart where the capacitance unbalance per pair location within the unit is graphed. From this graph pair drift in the stranding operation can be detected, or how the location of the pair within the unit affects the unit design.

### Probability Distributions

Utilizing statistical techniques in manual testing of the final product is essential since the test methods employed are laborious, time consuming and expensive. In manual testing the sample is usually small and the determination of the probability density and the resulting statistical distribution is usually a learned estimation always in favor of proving the design and passing the specifications. The building of a data base is slow with only yearly comparisons to show improvement or decline of the manufacturing process.

With computerized automatic test systems, the core design can be verified before production begins by complete testing of the prototype cables. During production, large samples of test data can be obtained quickly and accurately thus providing the basis for economical statistical distribution analysis for each production run.

With a Computerized Measuring and Management System (CAMMS) test data will be continuously collected into a data base, from which probability distribution can rapidly be established and statistical analysis performed to determine the acceptance of the production run or lot. If the sample size is not sufficient to determine a probability distribution, more test data can rapidly be added to the sample base and another probability determination made.

It has been fairly well established by years of testing and published data that the various test parameters (Capacitance, Resistance, etc.) follow certain types of probability distributions dependent on the manufacturer (Table 1).

TABLE 1

PROBABILITY DISTRIBUTIONS

| PAIR | QUAD | DISTRIBUTION TYPE |
|---|---|---|
| CM | C1-C3 | Normal |
| CUPG | E1-E3 | One Sided Normal |
| CUPS | Ea1-Ea3 | Combination of Single-Sided Normal with differing variances |
| CUPP | K1-K12 | Combination of Single-Sided Normal with differing variances |
| CR | | Normal |
| RL | | Normal |
| RU | | One Sided Normal |
| GM | | One Sided Normal |
| AT (dB) | | Normal |
| EL FEXT (dB) | | Normal, Truncated Normal |
| I/O FEXT (dB) | | Normal, Truncated Normal, Variable Truncated Normal, Offset Gamma |
| NEXT (dB) | | Normal, Truncated Normal, Variable Truncated Normal, Gamma |

In reviewing these distributions we see, for example, that far-end crosstalk loss (EL FEXT) and near-end crosstalk loss (NEXT) list 5 different types of distributions as determined by different manufacturers. The authors [2-10] of these distributions have proposed various modified Gaussian distributions on the basis of their cable test data, which they say were more accurate models of the cable crosstalk loss and power sum loss.

Figures 2 and 3 illustrate some of these distributions. Figure 3c, Individual Within Unit NEXT Data, shows a poor fit for both the Gaussian and gamma distribution, although Fig. 3f, Power Sum of the same data, fits the gamma. Since the power sum is controlling for NEXT, the gamma distribution would be an acceptable model. Fig. 3d shows the attenuation curve as Gaussian. Note that when this curve is plotted on normal probability paper (Fig. 3a) the bell shaped curve is a straight line. Fig. 3a type curves are useful especially when the type of distribution is not clear.

Why is it important to have an accurate model of the crosstalk loss and power sum loss distributions? Here again, it is economics. Crosstalk is the main source of interference in paired communication cables. In the design of TDM/PCM (Time Division Multiplexed/Pulse Code Modulated) Systems, the crosstalk power coupled into a transmission line is a factor limiting the repeater span length and the number of pairs assigned to PCM. Thus, in obtaining an accurate statistical distribution model, the criterion on which to base acceptable crosstalk performance can be determined on a sample basis from which the production lot can be qualified.

In reviewing the literature [2-10] one point stands out: each authors' probability distribution was based on test data applicable to their company's manufactured cable. Since the characteristics of a cable is directly related to the plant that manufactures that cable, it is extremely difficult to establish a generalized probability distribution model that is applicable to all similar type cables made by different manufacturers or for that matter by different plants of the same manufacturer. One must consider that different manufacturers use different core designs, like twist lay, pair positions, unit position, binder groups, etc. Thus, one manufacturer may have a normal distribution, another manufacturer of the same type cable, a truncated normal or gamma.

Of course, as the authors [2-10] clearly illustrate, the important consideration is to have the proper type of distribution for the cable being manufactured so that sampling statistics can be used. Since the authors have each spent many months in testing to determine their distributions, it was important for them to try to generalize. However, with the availability of CAMMS' high speed testing and processing capability, it is no longer necessary to generalize; the proper distribution for each type of cable can quickly and accurately be determined. It is possible that all the models were satisfactory, but only for the cable produced in that author's particular plant.

## CAMMS DATA BASE

In establishing the data base, key files must be created so that data can be sorted, graphed and compiled in a useful manner. Table 2 lists the suggested keys for telephone cables. From these 15 keys we can select any one of the parameters in Key 1 and segregate data by any of the following 14 keys or combinations thereof. For example, CM by pair count and gauge or crosstalk by pair count, per group, per gauge, per cable type, etc. The data base will continue to grow as more cables are tested and the larger the sample size the more accurate probability distributions. If no meaningful distribution can be determined, then the cable lot can be completely tested for specification compliance. Comparisons can be made on a daily, weekly or monthly basis, or time charts (as shown in Fig. 1C) with control limits can be maintained. Keep in mind that the established probability distributions for a plant can be continuously monitored and if they begin to vary we can look for systematic errors, out of control process, or the establishment of more representative probability distributions from which more reliable trends can be estimated.

## CAMMS SYSTEM CONFIGURATIONS

Computerized Automatic Measurement and Management Systems may be arranged in three configurations: (1) Single Plant/Single Location as shown in Fig. 4 where all testing and measurement analysis is conducted at a single location. Management analysis is performed only at times when cable testing is completed. (2) Single Plant/Multiple Location where the cable testing is in one location and the management analysis in a remote location within the same plant. Management analysis can be performed at the same time cable testing and manufacturing process data is being stored in the data base. A "remote" management analysis system is shown in Fig. 5. (3) Multiple Plant Distributed System is for use where two or more manufacturing plants are being maintained. Each plant performs its own cable testing operations with a computerized automatic measuring system (Fig. 6) and sends data to a central quality assurance (QA) Computerized Management System data base (Fig. 7). This central QA management system may be located at one of the manufacturing plants or at a separate central quality control facility as shown in Fig. 8. This central location then controls all test specifications and may automatically input specification changes or add new specifications to the test system on a plant-by-plant basis. Analysis on a plant-by-plant basis is performed for each cable type tested; probability distributions are determined for each lot and thus the sampling procedure established for each manufacturing location. Cable types from different manufacturing locations may also be compared graphically. With the CAMMS Systems, systematic errors in the process in one plant can be quickly detected and corrective action taken to insure consistent quality cable.

## CONCLUSION

In the manufacture of telephone cables, the determination of the proper type of probability distribution permits the use of sampling techniques to qualify large production lots. These sampling techniques permit the cable manufacturer to produce higher quality cable at a lower cost. In addition, the accumulation, storage and processing of data can detect systematic errors and out of process control. Therefore in view of these advantages and since costs of labor rise faster than the cost of electronics, the Computerized Measurement and Management System is desirable for telephone cable production.

## REFERENCES


1. Mendenhall/Scheaffer "Mathematical Statistics with Applications", Duxbury Press, 1973.

2. S.H. Lin, "Statistical Behavior of Multipair Crosstalk", Bell System Technical Journal, p. 955, July-August 1980.

3. R. Hauschildt, "Crosstalk Considerations in Paired Communications Cables for PCM Use", Proceedings of the 26th International Wire and Cable Symposium, November 15-17, 1977, Cherry Hill, New Jersey, pp. 298-419.

4. B.R.N. Murthy, "Crosstalk Loss Requirements for PCM Transmission", IEEE Trans. on Commun., Vol. COM-23, No. 7, p. 722, July 1975.

5. S.D. Bradley, "Crosstalk Considerations for a 48 Channel PCM Repeatered Line", IEEE Trans. on Commun., Vol. COM-23, No. 7, p. 722, July 1975.

6. R.J. Oakley and R. Jaar, "A Study into Paired Cable Crosstalk", Proc. of Twenty-Second IWCS, p. 136, 1973.

7. B.B. Jacobsen, "Cable Crosstalk Limits on Low Capacity Pulse Code Modulation Systems", Elec. Communication, Vol. 48, No. 1 and 2, p. 98, 1973.

8. I. Nasell, "Some Properties of Power Sums of Truncated Normal Random Variables", Bell System Technical Journal, p. 2081, Nov. 1967.

9. N.A. Marlow, "A Normal Limit Theorem for Power Sums of Independent Random Variables", Bell System Technical Journal, p. 2081, Nov. 1967.

10. H. Cravis and T.V. Crater, "Engineering of T1 Carrier System Repeatered Lines", Bell System Technical Journal, p. 431, March 1963.



Leo Chattler received a B.S. degree in Aeronautical Engineering from the University of Illinois and a M.S. degree in Electrical Engineering from the University of Maryland. He was in Naval Aviation; aeronautical and electrical design with Chance-Vought Aircraft; Vice President and Division Manager with Northrop Aircraft; President of Advanced Technologies Corporation, a subsidiary of Beckman Instruments, and General Manager of the Electronic Instrument Division. He is currently President of DCM International Corporation and has been active in development of equipment for the telephone cable industry. He has four patents issued and three patents pending in connection with his work.

TABLE 2

DATA BASE KEY TABLE

| No. | KEY | | KEY VALUES |
|---|---|---|---|
| 1 | Test Type | Pairs | CR, RU, CM, CG, CS, GM, AT, EF, IF, IN, ON, & CP |
| | | Quads | CR, RU, RL, C1-C3, E1-E3, Ea1-Ea3, K1-K12, AT, EF, IF, IN, ON |
| 2 | Master Lot Number | | Up to 5 Master Lot Numbers |
| 3 | Date | | Month, Day, Year |
| 4 | Gauge Conductor Diameter | | SP, .3, .32, .4, .405, .5, .511, .6, .63, .644, .65, .7, .8, .9, .912, 1.0, 1.2, 1.27, 1.3, 1.4, 16, 19, 191C, 22, 24, 25, 26, & 28 |
| 5 | Cable Type | | Defines up to 50 entries. Each entry will be 1 to 40 characters. |
| 6 | Insulation Type | | SPECIAL, PULP, PULP/HF, PIC/S/A, PIC/S/F, PIC/F/A, PIC/F/F, PVC, PE/PVC, Paper |
| 7 | Pair Count/Cable | | 1 to 32,768 |
| 8 | Pair Count/Group | | 1 to 32,768 |
| 9 | Plant | | Defines up to 10 entries. Each entry will be 1 to 40 characters. |
| 10 | Construction Type | | 1 to 16. Defines Pair Location in Unit & Layer |
| 11 | Screen/No Screen | | SCREEN & NOSCRN |
| 12 | Frequency | | 1 to 12990 KHz |
| 13 | Group Color or ID | | Defines up to 10 entries. Each entry will be 1 to 40 characters. |
| 14 | Customer Defined | | Defines up to 10 entries. Each entry will be 1 to 40 characters. |
| 15 | Customer Defined | | Defines up to 10 entries. Each entry will be 1 to 40 characters. |

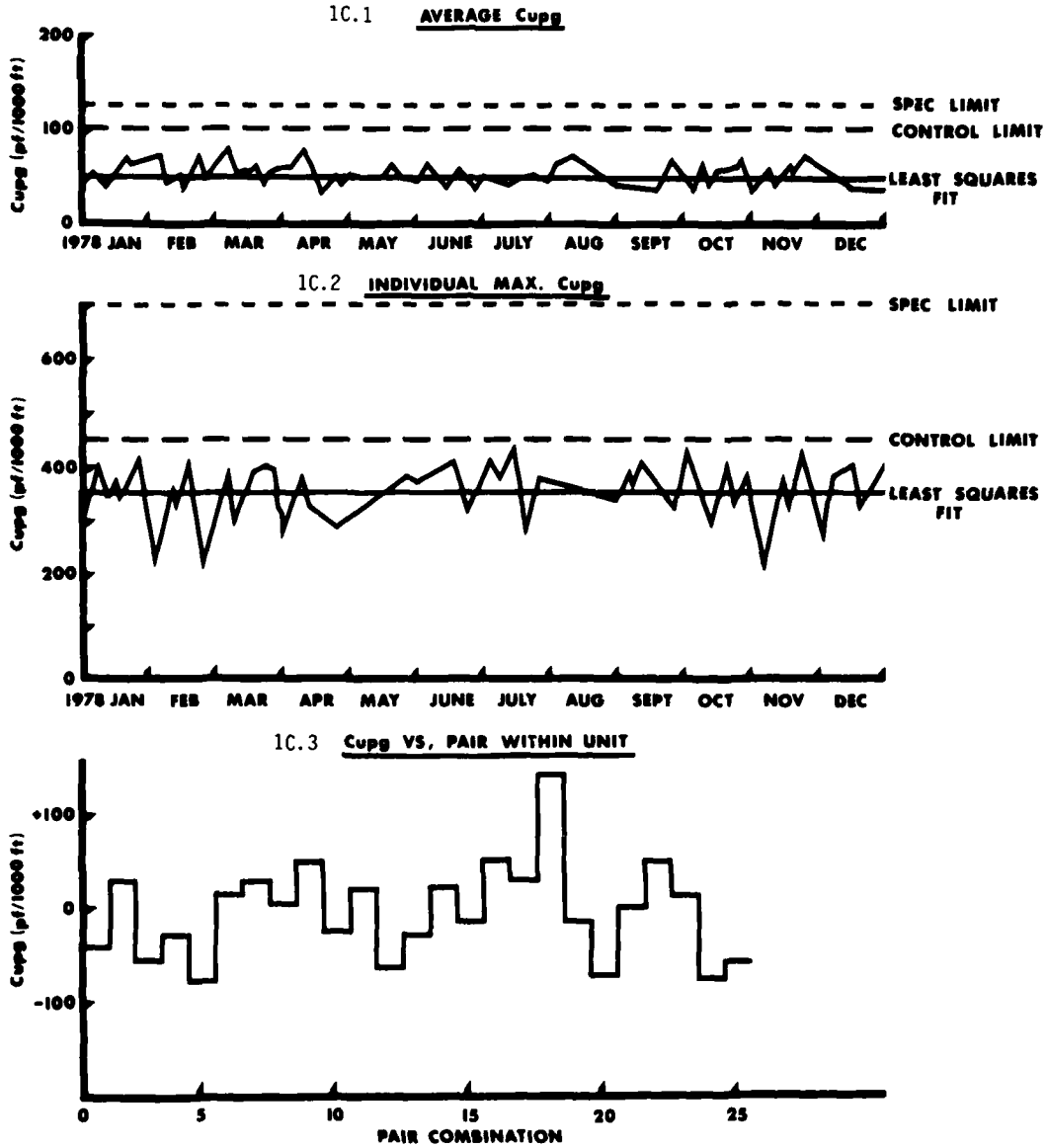



FIGURE 1C **CONTROL CHARTS**

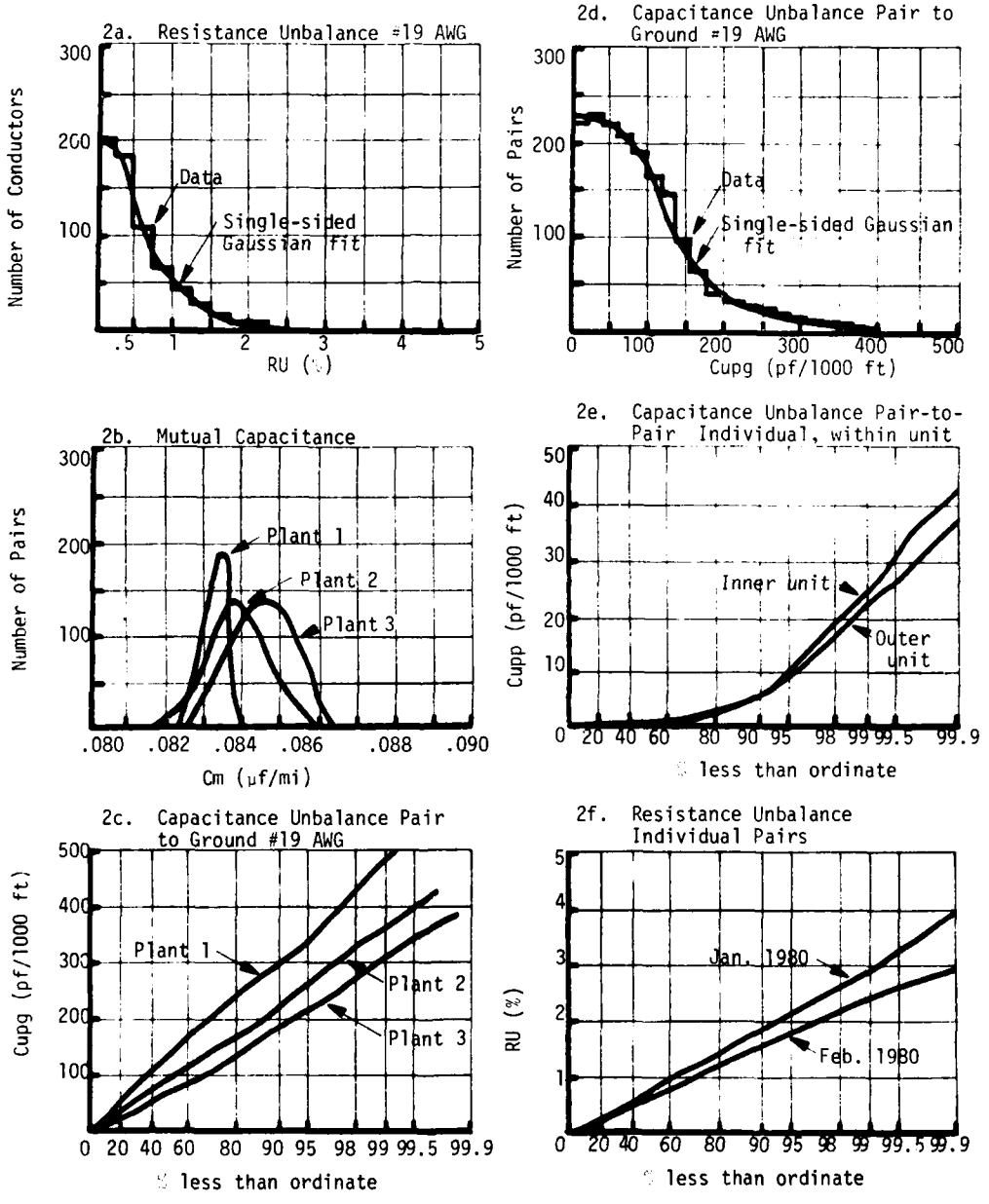



FIGURE 2

PROBABILITY DISTRIBUTIONS AND COMPARISONS

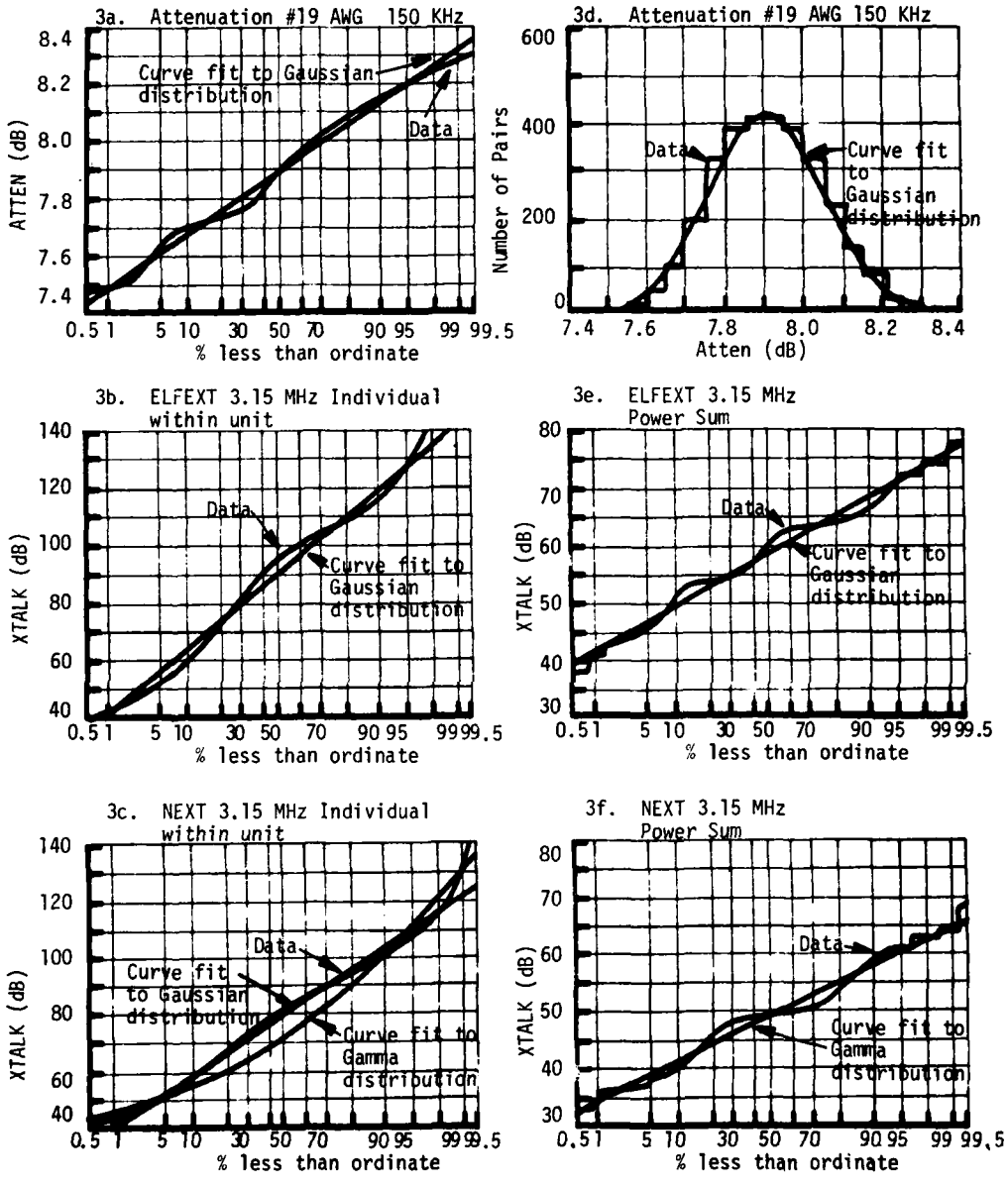



FIGURE 3
PROBABILITY DISTRIBUTIONS

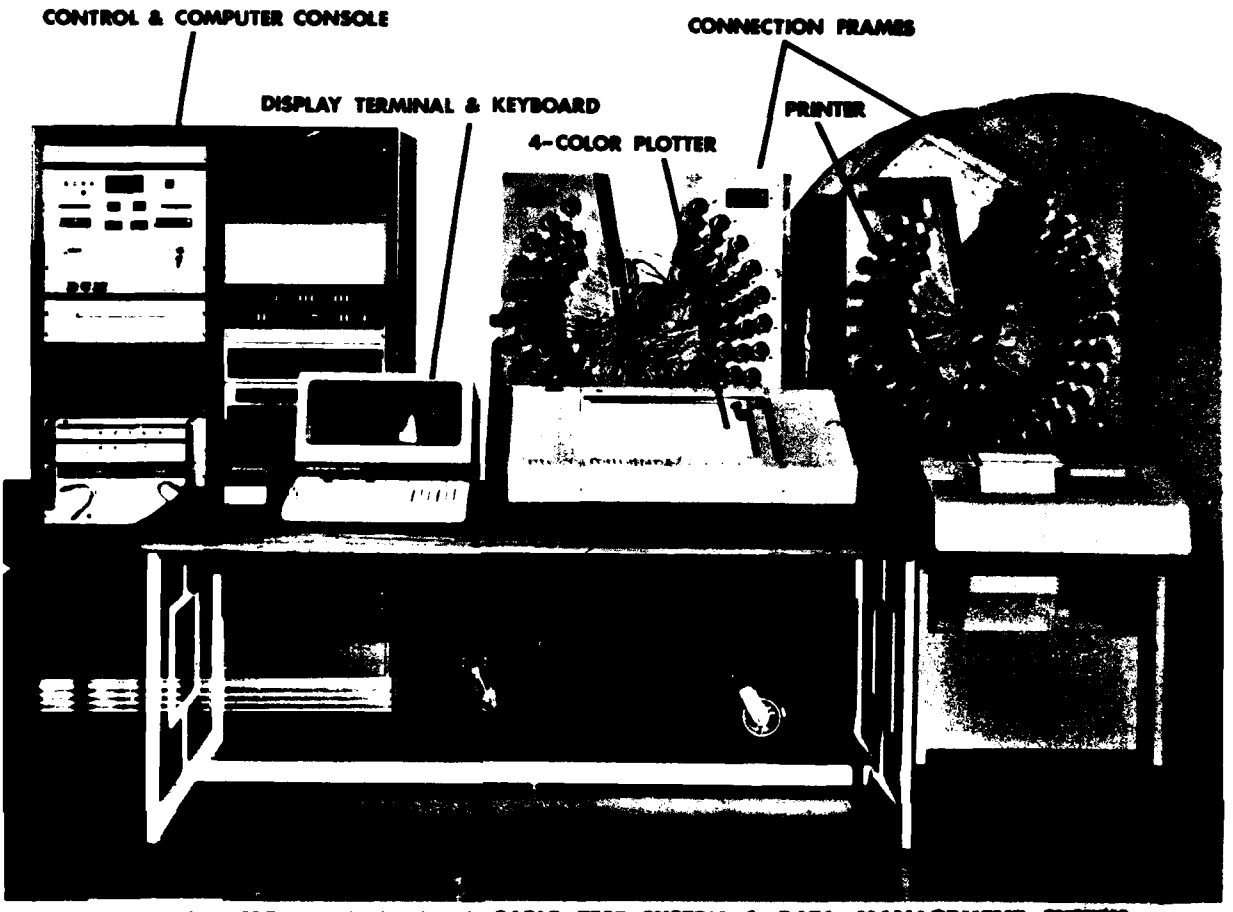



FIGURE 4 MODEL CMS-2/DMS CABLE TEST SYSTEM & DATA MANAGEMENT SYSTEM

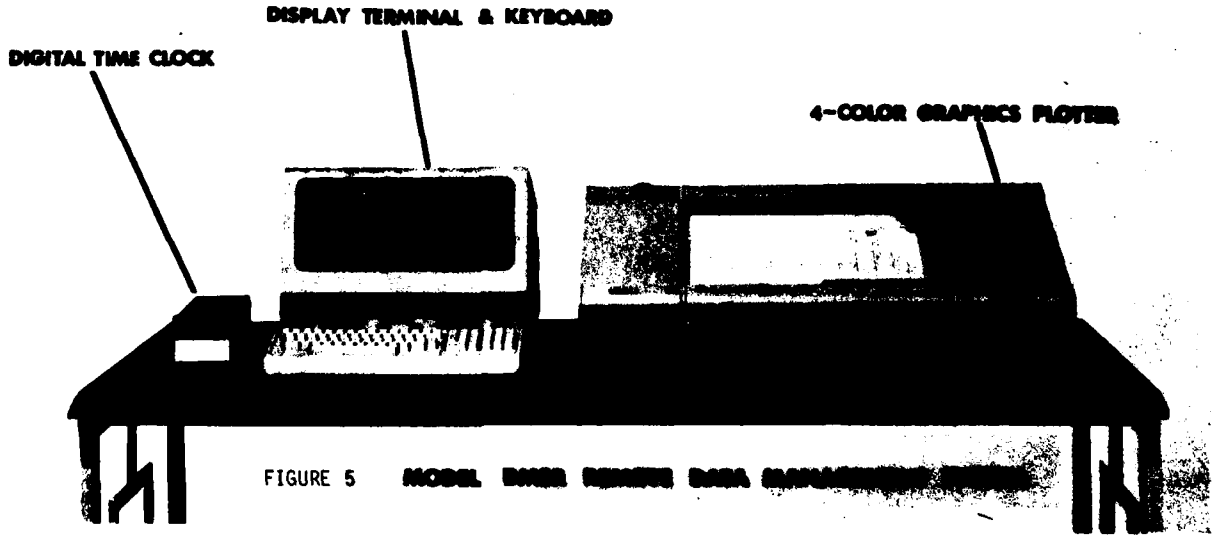



FIGURE 5 MODEL [illegible]

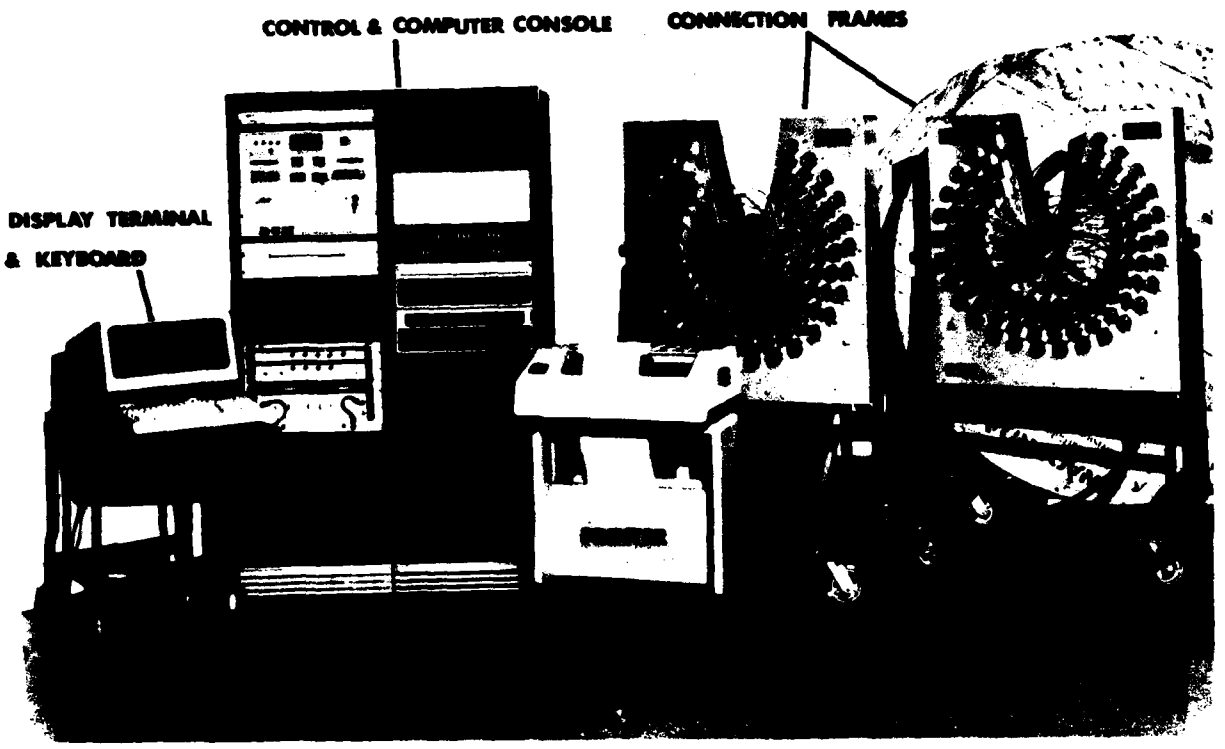



FIGURE 6 **MODEL CMS-2X CABLE TEST SYSTEM**

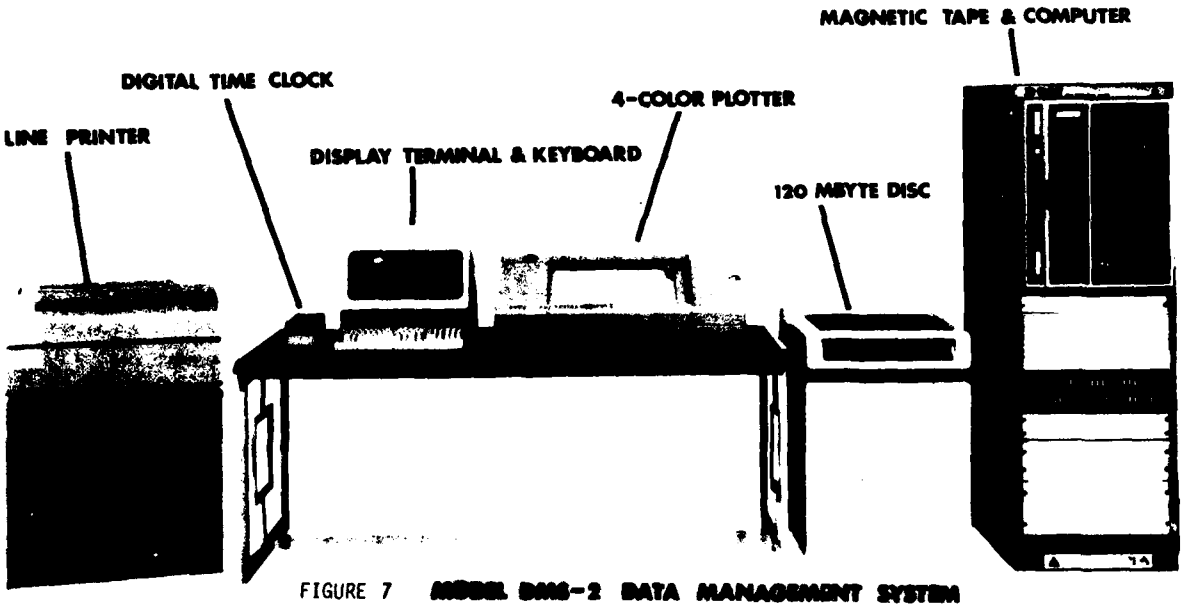
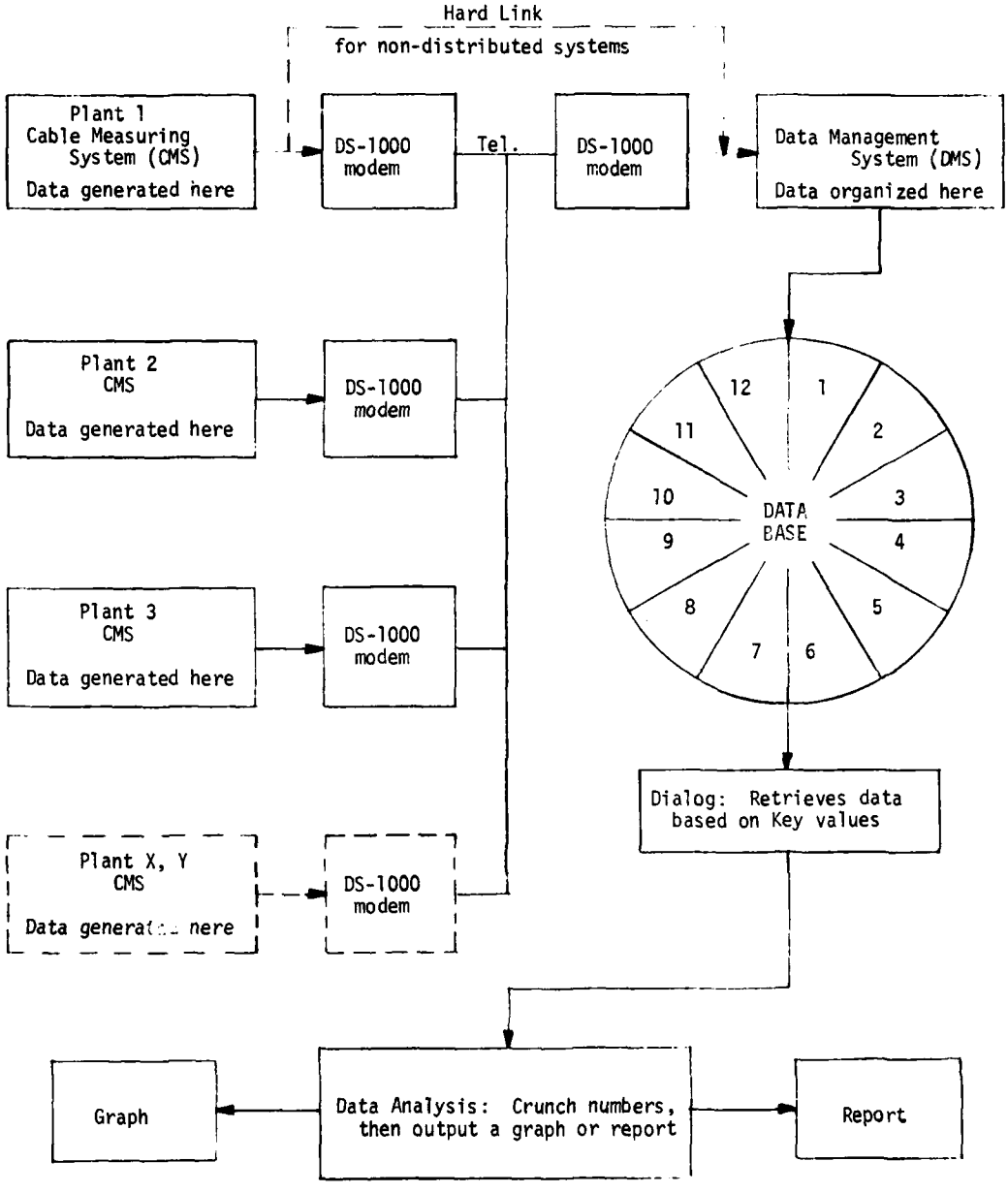



FIGURE 7 **MODEL DMS-2 DATA MANAGEMENT SYSTEM**




CAMMS Distributed System

FIGURE 8

# LIGHTNING SURGE WAVES INDUCED IN TRANSMISSION LINES

H. Koga, T. Motomitsu and M. Taguchi

Ibaraki Electrical Communication Laboratory, N.T.T.
Tokai, Ibaraki, Japan

## Abstract

This paper discusses lightning surge wave characteristics induced in transmission line theoretically and experimentally. Decision methods of test surge wave for the transmission equipment are also discussed considering lightning surge wave distribution and the transmission equipment trouble occurrence time. The optimum design for lightning surge proof equipment is also described.

## 1. Introduction

New transmission equipments differ from conventional electromechanical systems in their extensive use of electronic components. Especially, some mechanical switching equipments are replaced by the use of solid state devices. As these equipments have little ability to withstand overvoltages from induced lightning surge, there is a severe risk of equipments being damaged by overvoltage. So, they should have a protection which is designed correctly. To design a good protection against the lightning surge, the characteristics of lightning surge induced in transmission lines should be clarified. However, satisfactory actual data have not been obtained and the lightning surge inducing mechanism in transmission lines has not been clarified either.

This paper describes induced lightning surge characteristics theoretically and experimentally. As a result, lightning surge voltage distribution, front time distribution and time to half value distribution are made clear.

Test lightning surge waveforms for transmission equipment are obtained from the lightning surge wave distributions and the trouble occurrence time for various equipments. Optimum design methods for the equipment to withstand lightning surge voltage are described.

## 2. Analytical Method for Induced Lightning Surge in Overhead Lines

### 2.1 Lightning Surge Inducing Mechanism

To clarify the lightning surge wave characteristics induced in transmission lines, a lightning surge inducing mechanism should be made clear. Though the lightning surge inducing mechanism has been described before, when the ground is perfectly conducting, these results did not agree well with measurement data[1].

This paper describes lightning surge inducing mechanism when the ground has a finite conductivity, as shown in Fig. 1. At first, when lightning discharge occurs, electromagnetic fields appear in the atmosphere. As these electromagnetic fields are attracted by the condition of a finite ground conductivity, a vertical electric field and a horizontal electric field occur[2]. Lightning surge waves of the cable terminal are caused by both electric fields. Lightning surge induced in the transmission line is considered in the case of overhead line only, because the surge induced in an underground line is very small.

### 2.2 Assumptions for Analysis

In order to calculate induced lightning surges, assumptions for analysis are shown as follows.

(1) Lightning surges induced in a transmission line are induced by the return stroke. The return stroke current flows from the ground at time t = 0 into the sky.

(2) The return stroke current field is vertical to the ground and has a constant velocity.

(3) The return stroke current is assumed to have a triangular form, as shown in Fig. 2. A coordinate system for the return stroke and the return stroke waveform for analysis are also shown in Fig. 2.

### 2.3 Vertical Electric Field Calculation

The vertical electric field, associated with return stroke charge and current, is given by the following equation.

$$E_Z = -(\mathrm{grad}\ \phi)_Z - \frac{\partial A_Z}{\partial t} \tag{1}$$

where,

$\phi$ : Scalar potential caused by the return stroke charge
$A_Z$ : Vector potential along the z direction caused by the return stroke current

When the ground is perfectly conducting, the vertical electric field at point $(x_0, y_0, h)$ in Fig. 2 is given as follows, from Eq. (1), when the return stroke has a unit step current.

$$E_Z = 30\left\{ \frac{\frac{v_c - v_f}{v_f}}{\sqrt{T^2 + R^2}} - \frac{\frac{v_c}{v_f}}{\sqrt{h^2 + r_0^2}} \right\} \tag{2}$$

where,

$$r_0 = \sqrt{x_0^2 + y_0^2}, \quad T = \frac{\frac{v_f t - h}{v_f}}{1 + \frac{v_f}{v_c}}$$

$$R^2 = \frac{v_c - v_f}{v_c + v_f} r_0^2$$

$v_f$ : Return stroke velocity

$v_c$ : Light velocity

As the vertical electric field shown in Eq. (2) expresses the inditial response of the return stroke current, the surge wave of the vertical electric field is given by Duhamel's theorem, as follows, when the return stroke current has a triangular form, as shown in Fig. 2.

(1) $t < t_0$
$E_Z(t) = 0$

(2) $t_0 \leqq t < t_0 + t_f$
$E_Z(t) = E_1(t)$

(3) $t_0 + t_f \leqq t < t_0 + t_e$
$E_Z(t) = E_1(t) + E_2(t)$

(4) $t_0 + t_e \leqq t$
$E_Z(t) = E_1(t) + E_2(t) + E_3(t)$

where,

$$t_0 = \frac{\sqrt{h^2 + r_0^2}}{v_c}$$

$$E_n(t) = -60\, a_n \frac{v_c^2 - v_f^2}{v_c v_f^2} \log \frac{t_n + \sqrt{t_n^2 + \frac{v_c^2 - v_f^2}{v_c^2 v_f^2} r_0^2}}{\frac{r_0}{v_c} + \frac{r_0}{v_f}} + 60\, a_n \frac{v_c}{v_f} \left( \frac{t_n}{r_0} - \frac{1}{v_c} \right) \quad (3)$$

where,

- For $n = 1$
  $a_1 = I_0/t_f$
  $t_1 = t$

- For $n = 2$
  $a_2 = -I_0/t_f - I_0/(t_e - t_f)$
  $t_2 = (t - t_f)$

- For $n = 3$
  $a_3 = I_0/(t_e - t_f)$
  $t_3 = (t - t_e)$

## 2.4 Horizontal Electric Field Calculation

Zenneck has shown that the electromagnetic field inclines toward the advanced wave direction, when the ground has finite conductivity. The relation between vertical electric field and horizontal electric field is approximately given by the following equation.

$$\frac{E_H}{E_Z} = \frac{1}{\sqrt{\varepsilon_r + \frac{\sigma}{j\omega\varepsilon_0}}} \quad (4)$$

where,

$E_H$ : Horizontal electric field
$\varepsilon_r$ : Specific dielectric constant of ground
$\sigma$ : Ground conductivity
$\varepsilon_0$ : Free space dielectric constant

From Eq. (4), the inditial response $\mathcal{E}_H(t)$ (replacing $E_Z$ with a unit step function) of the horizontal electric field is given as follows, taking the inverse Laplace transform.

$$\mathcal{E}_H(t) = \sqrt{\frac{1}{\varepsilon_r}}\, e^{-ct} I_0(ct) \quad (5)$$

where,

$$c = \frac{\sigma}{2\varepsilon_0 \varepsilon_r}$$

$I_0$ : Modified Bessels function of zero order

The horizontal electric field surge wave can be computed by the application of Duhamel's theorem from Eq. (5), by using the surge wave of the vertical electric field. However, it is very difficult to calculate the convolution integral of the vertical electric field given by Eq. (3). As a vertical electric field given by Eq. (3) forms a surge wave like a return stroke current, a solution of the convolution integral can be obtained, by using the approximated triangular vertical electric field waveform. To obtain a more exact solution of the convolution integral we may approximate a vertical electric field by many short straight lines. The horizontal electric field is shown as follows.

(1) $t < t_0$
$E_H(t) = 0$

(2) $t_0 \leqq t < t_0 + t_f'$
$E_H(t) = E_{H1}(t)$

(3) $t_0 + t_f' \leqq t < t_0 + t_e'$
$E_H(t) = E_{H1}(t) + E_{H2}(t)$

(4) $t_0 + t_e' \leqq t$
$E_H(t) = E_{H1}(t) + E_{H2}(t) + E_{H3}(t)$

where,

$$E_{Hn}(t) = -\frac{K_n}{c} \sqrt{\frac{1}{\varepsilon_r}}\, e^{-ct_n} \cdot ct_n [I_0(ct_n) + I_1(ct_n)] \quad (6)$$

where,

- For $n = 1$
  $K_1 = E_{Z\max}/t_f'$
  $t_1 = t$

- For $n = 2$
  $K_2 = -E_{Z\max}/t_f' - E_{Z\max}/(t_e' - t_f')$
  $t_2 = t - t_f'$

- For $n = 3$
  $K_3 = E_{Z\max}/(t_e' - t_f')$
  $t_3 = t - t_e'$

where

$E_{Z\max}$ : Vertical electric field peak value
$t_f'$ : Time from vertical electric field commencement to its peak value
$t_e'$ : Time from vertical electric field commencement to the point in which time-axis and line connection peak value, with half of the peak value on its tail, intersect.
$I_1$ : Modified Bessels function of the first order

## 2.5 Calculation of Surge Wave in Transmission Line

The vertical electric field and the horizontal electric field caused by return stroke induced electromotive force in a transmission line, as shown by the equivalent circuit in Fig. 3. As the calculation of transient phenomena for telegraphic equations containing the electromotive force is difficult, differential equations are expressed by difference equations and the surge wave in the transmission lines is obtained from the difference equations by using a computer. The differential equations are given by the following equations.

$$-\frac{\partial V(x)}{\partial x} = \left\{ R\,I(x) + L\frac{\partial I(x)}{\partial t} \right\} + E_H(x)$$

$$-\frac{\partial I(x)}{\partial x} = C\frac{\partial}{\partial t}\{V(x) - h\,E_z(x)\} \qquad (7)$$

From Eq. (7), the difference equations are expressed as follows.

$$I_\nu(t+\Delta t) = -\frac{\Delta t}{L\Delta x}\{V_{\nu+1}(t) - V_\nu(t)\} - \left(\frac{R}{L}\Delta t - 1\right) I_\nu(t) - \frac{\Delta t}{L} E_{H\nu}(t)$$

$$V_\nu(t+\Delta t) = -\frac{\Delta t}{C\Delta x}\{I_\nu(t) - I_{\nu-1}(t)\} + V_\nu(t) + h\,E_{z\nu}(t+\Delta t) - h\,E_{z\nu}(t) \qquad (8)$$

## 3. Calculation Result

This section shows characteristics of lightning surge theoretically. Typical values shown in Table 1 are used for the calculation, if it has no reference[3].

### 3.1 Lightning Surge versus Strike Point

The relation between cable and strike point is shown in Fig. 4. Lightning surge waves in transmission lines are shown in Fig. 5, corresponding to the setup shown in Fig. 4. The lightning surge wave induced by return stroke, which occurs on the perpendicular bisector to the transmission line, becomes shaper than that which occurs on other points. The former is called "front return stroke". When the return stroke occurs on an extension of the transmission line (side return stroke), the lightning surge wave is larger and wider than other lightning surge waves, and the waveform is similar to the lightning surge waveforms caused by return strokes which occur on other ground points, except the point of the front return stroke. From the calculated values, it is clear that, in the case of the front return stroke, the lightning surge wave is mainly induced by the vertical electric field. In the case of the side return stroke, the lightning surge wave is mainly induced by the horizontal electric field. Therefore, the general lightning surge waveform shows an undulation shape that comes from the surge caused by the vertical electric field and by the horizontal electric field, as shown in Fig. 6. In Fig. 6, the sharp peak, which appeared on the front part of the surge, is induced by the vertical electric field, and the large dipole wave after the sharp peak is induced by the horizontal electric field.

### 3.2 Lightning Surge Dependency on Ground Conductivity

The horizontal electric field is a function of ground conductivity, as shown in Eq. (4). Peak value $V_p$ for the lightning surge caused by the side return stroke has approximately the following relation to ground conductivity.

$$V_p \propto 1/\sqrt{\sigma} \qquad (9)$$

The peak value of the lightning surge caused by the front return stroke is almost independent of ground conductivity, because its peak value is mostly induced by the vertical electric field, which is independent of ground conductivity.

### 3.3 Lightning Surge Dependency on Distance between Strike Point and Cable, and Lightning Surge Dependency on Cable Length

#### 3.3.1 Peak Lightning Surge Value

Figure 7 shows the relation between peak lightning surge value and cable length, when the distance between the strike point and the cable is fixed. The distance between the strike point and the cable means the distance between the strike point and the center of the cable, as shown in Fig. 4, except in the case of side return stroke. In case of the side return stroke, the distance is measured from the strike point to the terminal of the cable, as shown in Fig. 4, because the distance varies with the cable length, if the center of the cable is selected instead of the terminal of the cable.

Figure 7 shows the folloing properties.

(1) Lightning surge dependency on cable length for peak value caused by the side return stroke is larger than that caused by the front return stroke.

(2) As the distance between strike point and cable increases, lightning surge dependency on cable length decreases.

#### 3.3.2 From Time and Time to Half Value for Lightning Surge Induced in Transmission Lines

Front times and times to half value for induced lightning surges depend on cable length and the distance between strike point and cable. However, they mostly depend on $t_f$ and $t_e$ of the lightning current. Accordingly, they must be determined by lightning current waveform consideration. As 90% of $t_f \times t_e$ of the lightning currents exists in the range of $0.5 \times 40 \sim 5 \times 200\,(\mu s)$, calculated values for front time and time to half value of the induced lightning surge are shown in Fig. 8. Their values are given as follows.

(1) 90% of the front time exists in the $10 \sim 50\,\mu s$ range. The average is about $20\,\mu s$.

(2) 90% of the time to half value exists in the $25 \sim 110\,\mu s$ range. The average is about $55\,\mu s$.

As cable length increases, the front time and the time to half value are spread to the extent of about $10\,\mu s$/km, but they mostly exist in the range previously mentioned, because cable length variation is small.

### 3.4 Lightning Surge Dependency on Cable Terminal Earth Resistance

The relation between peak induced lightning surge value and cable terminal earth resistance is shown in Fig. 9. The variation in peak value caused by the side return stroke is in $20 \sim 30\%$ range, when earth resistance is in $70 \sim 1000\,\Omega$ range.

## 4. Measurement Method and Comparison with Measured Values

This section describes the relation between calculated values and measured values, and measurement method. If it is described to make the calculated values agree with the measured values, it will be necessary to determine the peak value and the waveform for the return stroke, as well as the strike point. However, it is very difficult to get these data, because it is not possible to accurately forecast the strike point. Therefore, fundamental factors about induced lightning surge obtained from calculation are compared with measured values.

### 4.1 Measurement Methods

This section describes instruments, items, locations and methods for measurement.

#### 4.1.1 Measurement Instruments and Measurement Items

The lightning surge counter and the lightning surge waveform recorder are used for the measurements. Specifications for instruments, measurement items and measurement methods are shown in Table 2.

#### 4.1.2 Measurement Location

Measurement locations are selected in three areas, namely, Kanto, Hokuriku and Kyushu. The characteristics for the three areas are shown in Table 3.

### 4.2 Comparison with Measurement Values and Calculated Values

The measurement surge waveform is very similar to the calculated surge waveform, as shown in Fig. 6. Though it is very difficult to get a perfect correspondence, some relations between measurement data and calculated values are described as follows.

#### 4.2.1 Relation between Lightning Surge Waveform and Horizontal Electric Field

Lightning surge waveforms, except one by front return stroke, mainly occur by horizontal electric fields, as mentioned in 3.1. The polarity of the lightning surge induced in the cable both terminals must be reversed, respectively. Measured lightning surges induced simultaneously in the cable at both terminals are shown in Fig. 10. These polarities are opposite from each other.

The relation between measured lightning surge induced in the cable terminal and the horizontal electric field, which is calculated from measured vertical electric field, using Eq. (4), is shown in Fig. 11. As a result, the lightning surge waveform depends on the horizontal electric field.

#### 4.2.2 Cable Length Dependency and Earth Resistance Dependency

Measured cable length dependency and measured earth resistance dependency are shown in Fig. 7 and Fig. 9, respectively. These measured values agree well with the calculated values. However, on cable length dependency, it is very difficult to get exact correspondence between them, because the exact strike point is often not found.

#### 4.2.3 Ground Conductivity Dependency

Measured lightning surge voltage, which occurred in different ground conductivity areas, as shown in Table 3, are shown in Fig. 12. Lightning surge voltage is nearly inversely proportional to the square root of ground conductivity.

#### 4.2.4 Lightning Surge Voltage in Summer and in Winter

Lightning surge voltages in summer and in winter at the three areas are shown in Fig. 13. The lightning surge voltages in summer are about two times larger than surges in winter. Therefore, the protection design requirements for lightning surge become more severe, in the case of summer lightning surges. Calculated values in summer or in winter cannot be determined, because the return stroke situation is unknown in Japanese summer and winter.

### 4.3 Lightning Surge Voltage Distribution, Front Time Distribution and Time to Half Value Distribution

#### 4.3.1 Lightning Surge Voltage Distribution

Induced lightning surge in an overhead line depends on cable length.

In Japan, the average overhead line length for telephone transmission is about 1 km[4]. Induced lighting surge voltages in the one kilometer cable length are calculated when ground conductivity has a constant value. Equivalent voltage loop-lines induced at an overhead line terminal are shown in Fig. 14.

The shape of the equivalent voltage loop-lines rounds out as ground conductivity increases. A peak voltage occurrence time that exceeds a certain induced voltage is obtained from the ratio of the area which exceeds a certain voltage loop-line to the area where the thunder storm is observed by a specific weather bureau.* The peak voltage occurrence time per thunderstorm day is obtained from the product of the peak voltage occurrence time, which exceeds a certain induced voltage, and the return stroke frequency per thunderstorm day, as shown in Fig. 15.

In Fig. 15, the solid line shows calculated value when ground conductivity is 0.01 (S/m). Symbol △ shows values which are measured by the lightning surge counter and symbol × shows values measured from discharge vestiges left on carbon arresters in Utsunomiya and its surrounding countryside (where ground conductivity is about 0.01 S/m). Calculated values agree well with measured values at the subscriber end, as shown in Fig. 15.

Peak value occurrence time at the office end cannot be obtained from the calculation, because lightning surge inducing mechanism is more complicated. So, only measured data are shown in Fig. 15. Peak voltage occurrence time, $N_s$, $N_o$, for both ends, are given as the following equations. Peak voltage induced in the subscriber end is about five times larger than one in the office end.

Subscriber end

$$N_s = 1.2 \times 10^5 \quad v^{-1.8} \tag{10}$$

Office end

$$N_o = 6.6 \times 10^3 \quad v^{-1.8} \tag{11}$$

Equations (10) and (11) describe the cumulated peak voltage occurrence time. Therefore, peak voltage density times are expressed as follows.

Subscriber end

$$n_s(v) = 2.16 \times 10^5 \cdot v^{-2.8} \tag{12}$$

Office end

$$n_o(v) = 0.12 \times 10^5 \cdot v^{-2.8} \tag{13}$$

#### 4.3.2 Front Time Distribution and Time to Half Value Distribution

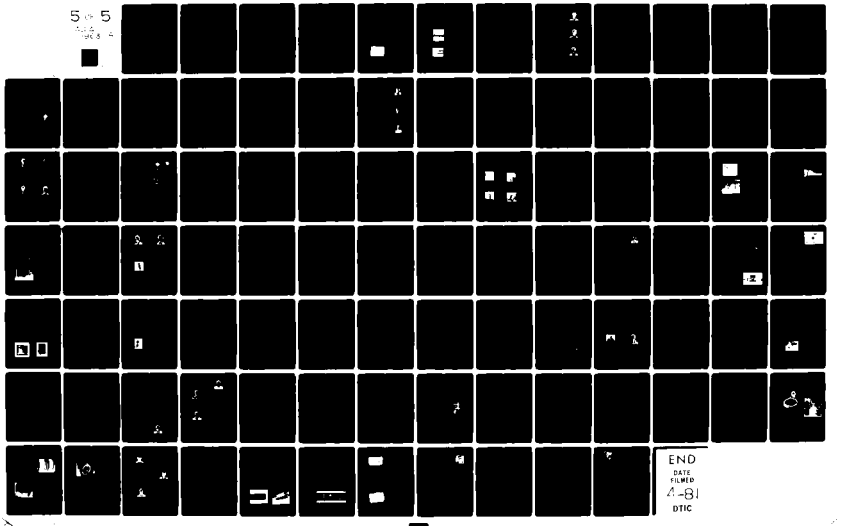
Front time and time to half value for the induced lightning surge were calculated, as shown in Fig. 8. When it is assumed that front time and time to half value probability distribution are log-normal probability distribution (though the authors cannot determine the probability distribution by calculation), the calculated values given by Fig. 8 are shown by solid lines in Fig. 16. Measured front time values and time to half values, induced on CCP-AP cable, are shown by circular symbols in

* In Japan, the area where thunder storms are observed by a specific weather bureau is 23 × 23 km².

AD-A096 308 ARMY COMMUNICATIONS RESEARCH AND DEVELOPMENT COMMAND --ETC F/G 9/1
PROCEEDINGS OF THE INTERNATIONAL WIRE AND CABLE SYMPOSIUM (29TH--ETC(U)
NOV 80 E F GODWIN

UNCLASSIFIED NL

5 of 5



END
DATE FILMED
4-81
DTIC

Figs. 16 and 17. They agree well with calculated values, in the case of the subscriber end. Average front time is about 20 $\mu$s and average time to half value is about 60 $\mu$s, in case of the subscriber end.

Calculated value for the office end cannot be given as mentioned in 4.3.1, but measured values are shown in Fig. 17. In this case, average front time is about 60 $\mu$s and average time to half value is about 250 $\mu$s. These data can be expressed by the following equations.

$$f(T) = \frac{1}{\sqrt{2\pi}\,\sigma} e^{-(\log_e T - m)^2 / 2\sigma^2} \qquad (14)$$

where,

- m : Mean value (Neper)
  $m = \log_e(t_m)$
- $\sigma$ : Standard deviation (Nep)
- T : Front time or time to half value or time to zero value* (Nep)

In case of subscriber end,

| | | |
|---|---|---|
| Front time | $t_m = 20\,\mu s$ | $\sigma = 0.56$ |
| Time to half value | $100\,\mu s$ | 0.56 |
| Time to zero value | $200\,\mu s$ | 0.56 |

(15)

In case of office end

| | | |
|---|---|---|
| Front time | $t_m = 60\,\mu s$ | $\sigma = 0.56$ |
| Time to half value | $250\,\mu s$ | 0.36 |
| Time to zero value | $500\,\mu s$ | 0.78 |

(16)

## 5. Test Surge Waveform Design Methods for Transmission Equipment

### 5.1 Philosophy of Test Surge Waveform Design Method for Transmission Equipment

The lightning surge induced in a transmission line feeds a longitudinal voltage between a balanced pair and ground to the transmission equipment, as shown in Fig. 18. The longitudinal voltage is discharged by the arresters, which are mounted in the equipment, but the real voltage between one line of a pair and the other line of a pair occurs by the difference between two arrester discharge voltages.

When earth resistance $R = 0\ (\Omega)$, longitudinal voltage and real voltage have the same value. So, the real voltage should be only considered to protect against the lightning surge. However, when earth resistance $R = R\ (\Omega)$, a large longitudinal voltage appears between ground and a balanced pair after the arrester has discharged. Therefore, test surge waveform for transmission equipment must consider both longitudinal voltage and real voltage. Two test surge waveforms will be obtained from the equipment trouble caused by a surge voltage which exceeds a certain threshold voltage or by a surge energy which exceeds a certain threshold energy.

This paper shows the two test surge waveform design methods for transmission equipment connected to a subscriber end, by using Eq. (10) and Eqs. (14) and (15). However, it will be possible to get test surge waveforms in case of the office end, if the same method is used.

* Time to zero value means the time length between the surge started time and the time, which becomes zero volts through the peak value.

### 5.2 Longitudinal Voltage Test Surge Waveform Design Method

The longitudinal voltage vs. earth resistance is shown in Fig. 18. As this voltage is very large, when the earth resistance is more than 50 ($\Omega$), arrester discharge characteristics can be neglected. The longitudinal voltage test surge waveform can be designed from Eq. (10) and Eqs. (14) and (15), according to the following method, which is shown in Fig. 19.

At first, the lightning surge peak voltage occurrence time and the lightning surge energy occurrence time must be known. If the permissible occurrence time of the equipment trouble is decided upon, peak voltage and surge energy which should be withstood are determined. The peak voltage is obtained directly from this condition. Front time and time to half values are obtained from the surge energy. Then, as the permissible occurrence time to withstand peak voltage and the permissible occurrence time to withstand surge energy have an equivalent value, the front time and the time to half value are determined.

As a result, the front time and the time to half value do not depend on the peak value. The lightning surge energy occurrence time N(E) is given by the following equation.

$$N(E) = \int_0^\infty n(v) \int_{\log_e \frac{E}{k_1 v^2}}^\infty f(T_0)\, dT_0 \cdot dv \qquad (17)$$

where,

$E = k_1 v^2 t_0$

- $f(T_0)$ : Probability distribution function of the time to zero value
- $k_1$ : Constant value
  If a surge wave is expressed as a triangular form,

$$k_1 = \frac{1}{3R}.$$

- R : Input impedance of the equipment

If Eq. (10) is made equal to Eq. (17), the next equation is given.

$$t_f = t_{fm}\, e^{0.45\left(1 + \frac{t_{fm}}{2t_{hm}}\right)\sigma^2}$$

$$t_h = t_{hm}\, e^{0.45\left(1 + \frac{t_{fm}}{2t_{hm}}\right)\sigma^2} \qquad (18)$$

For example, the longitudinal voltage test surge waveform is described as the following values, in the case of $N_s = N(E) = 10^{-3}$, by using Eqs. (10) and (18).

| | |
|---|---|
| Peak voltage : | 30 (kV) |
| Front time : | 20 ($\mu$s) |
| Time to half value : | 120 ($\mu$s) |

### 5.3 Real Voltage Test Surge Waveform Design Method

If two arresters in Fig. 18 work simultaneously, when a lightning surge comes in, real voltage cannot appear. Actually, as there is a distribution of arrester discharge voltage, a real voltage appears due to the distribution. So, equipment troubles are brought about by the real voltage. Arrester discharge voltage depends on the feeding lightning surge waveform. In the front time is very short, discharge voltage becomes high (by V-t curve). Especially, when one arrester has worked at 0 (V), the real voltage takes a maximum value.

In this condition, surge waves, as shown in the shaded portion in Fig. 20, are fed to the equipment. In Fig. 20, wave A has higher peak voltage than wave C, but wave C has larger energy than wave A has. Some equipments are damaged by wave A, but other equipments are damaged by wave C. Therefore,

equipment test surge waves need the wave like that in Fig. 21, because it contains many kinds of surge waves.

The test surge wave in Fig. 21 is composed of three parts, namely, rise part X, V-t curve part Y, cut-off part Z. These three parts must be determined according to the permissible equipment trouble occurrence time.

(1) Rise part X design method

Rise part X is determined by a lightning surge occurrence time which become steeper than steepness S. This occurrence time $N_a$ is given as follows.

$$N_a = \int_{V_a}^{\infty} n(v) \int_{-\infty}^{\log e \frac{V}{S}} f(T_f)\, dT_f\, dv \qquad (19)$$

$f(T_f)$ : Front time distribution function
$V_a$ : Mean arrester discharge voltage
S : Steepness (V/s)

(2) Design method for V-t curve part Y

If the arrester discharge voltage is constant value $V_c$, there is no lightning surge which exceeds voltage $V_c$. When the arrester discharge voltage is given by distribution function q (v), V-t curve part Y is determined by the lightning surge occurrence time which exceeds voltage $V_x$. This occurrence time $N_b$ is given as the next equation.

$$N_b = \int_{V_x}^{\infty} \left[ n(v) \left( 1 - \frac{\int_{V_x}^{\infty} n(v) \int_{-\infty}^{\log \frac{V}{S}} f(T_f)\, dT_f \cdot dv}{\int_{V_x}^{\infty} n(v)\, dv} \right) \cdot \int_{v}^{\infty} q(v)\, dv \right] dv \qquad (20)$$

(3) Cut-off part Z design method

Lightning surges, which are less than discharge voltage $V_x$ for the arrester, can pass through the arrester. As these lightning surges feed into transmission equipment, cut-off part Z is determined by the occurrence time of the surge energy which passed through the arrester. This occurrence time $N_c$ is given as follows.

$$N_c = \int_{0}^{V_x} n(v) \int_{E_0}^{\infty} P(E, v)\, dE\, dv \qquad (21)$$

P(E, v) : Surge energy occurrence density time (Eq. (17))

$$E_0 = k_2 V_x^2 t, \qquad k_2 = \frac{1}{R}$$

If the permissible equipment trouble occurrence time is determined as a certain value, three parts can be determined from Eqs. (19) ~ (21). For example, the real voltage test surge wave form is described as the following values, in the case of $N_a = N_b = N_c = 10^{-3}$.

Rise part : 2 (kV/s)
V-t curve part (the voltage V of flat Part) : 600 (V)
Cur-off part : 270 ($\mu$s)

## 6. Optimum Design for Lightning Surge Proof Equipment

This section shows the optimum design for lightning surge proof equipment, in case the equipment is damaged by the longitudinal voltage between the balanced pair and ground. The peak voltage occurrence time and the surge energy occurrence time were given by Eq. (10) and Eq. (17). However, it seems that the equipment trouble is distributed by the ununiformity of the production.

If the distribution of the equipment trouble is described by Weibull distribution, the equipment trouble occurrence time $Q_A$ caused by the peak voltage and the equipment trouble occurrence time $Q_B$ caused by the surge energy are given as the following equations, respectively.

$$Q_A = \int_{0}^{\infty} n(v_x) \int_{-\infty}^{v_x} P_v(v)\, dv\, dv_x \qquad (22)$$

$P_v(v)$ : Probability distribution function of equipment trouble caused by peak voltage

$$Q_B = \int_{0}^{\infty} n(v) \left[ \int_{-\infty}^{\infty} \left\{ f(T_0) \int_{-\infty}^{E} P_E(E)\, dE \right\} dT_0 \right] dv \qquad (23)$$

$f(T_0)$ : Probability distribution function of time to zero value
$P_E(E)$ : Probability distribution function of equipment trouble caused by surge energy

$P_v(v)$ and $P_E(E)$ are expressed as the following equation, if they are Weibull distribution.

$$P(x) = \frac{m(x-\gamma)^{m-1}}{x_0} e^{-\frac{(x-\gamma)^m}{x_0}} \qquad (24)$$

If the specific values, shown as Eq. (12) and Eq. (15), are substituted into Eq. (22) and (23), $Q_A$ and $Q_B$ are expressed approximately as the following equations.

$$Q_A = 4.44 \mu_0^{-4.25} \sigma_0^{2.44} + 0.478 \mu_0^{-1.8} \qquad \mu_0,\ \sigma_0 \ \text{(kV)} \qquad (25)$$

$$Q_B = 5.4 \times 10^{-2} \mu_0^{-3.23} \sigma_0^{2.34} + 0.0474 \mu_0^{-0.9} \qquad \mu_0,\ \sigma_0 \ \text{(kW·s)} \qquad (26)$$

where,

$\mu_0$ : Mean value of Eq. (24)

$$\mu_0 = x_0^{\frac{1}{m}} \Gamma\left(1 + \frac{1}{m}\right)$$

$\sigma_0$ : Standard deviation of Eq. (24)

$$\sigma_0^2 = x_0^{\frac{2}{m}} \left\{ \Gamma\left(1 + \frac{2}{m}\right) - \Gamma^2\left(1 + \frac{1}{m}\right) \right\}$$

If the permissible occurrence time of equipment trouble is $10^{-3}$, $Q_A$ and $Q_B$ must equal $10^{-3}$. When $10^{-3}$ is substituted into $Q_A$ and $Q_B$ (Eq. (25) and Eq. (26)), mean value $\mu_0$ and standard deviation $\sigma_0$ can have many values.

When $\gamma = 0$, Eqs. (25) and (26) become Eqs. (10) and (17), respectively (We write $\mu$ to replace $\mu_0$). The equipment cost will increase as the mean voltage $\mu_0$ increases, but will decrease as the standard deviation $\sigma_0$ increases. So, the equipment cost can be expressed as follows.

$$P = A\left(\frac{\mu_0}{\mu_{0c}}\right)^x + B\left(\frac{\sigma_0}{\sigma_{0c}}\right)^y \qquad (27)$$

where,

A, B : Proportional coefficient of each term
$\mu_{0c}$, $\sigma_{0c}$ : Normalized mean value and standard deviation
x, y : Cost increasing coefficient

Figure 22 shows the relation between the equipment trouble

occurrence time and the normalized mean voltage and standard deviation, with changing x, y, A and B. If the permissible equipment trouble occurrence time caused by the peak voltage is $10^{-3}$, the optimum value of the equipment should be the mean voltage $\mu_0 = 31$ (kV) and the standard deviation $\sigma_0 = 2.08$ (kV) (in case of $A = B = 0.5$, $\mu_{0c} = \sigma_{0c} = 1$, $x = 1$, $y = 1$). The optimum value of the equipment caused by the surge energy should be the mean surge energy $\mu_0 = 73$ (kW·s) and the standard deviation $\sigma_0 = 4.02$ (kW·s) in the same case.

## 7. Conclusions

This paper shows the induced lightning surge waveform in a transmission line theoretically, when ground conductivity is finite. Calculated values agree closely with measured values. The lightning surge voltage distribution, front time distribution and time to half value distribution are clarified. Test surge waveforms for the transmission equipment are determined by the permissible equipment trouble occurrence time, using the lightning surge voltage, front time and time to half value data. The optimum design for lightning surge proof equipment is described.


## Acknowledgement

The authors would like to thank Mr. H. Fukutomi, Director of the Outside Plant Development Division, Dr. Y. Kato, Deptuty Director of the Outside Plant Development Division, and Mr. R. Kaizu, Chief of the Cable Facility Section, for their contribution.


## References


1. Chowdhuri, P.: "Voltage surges induced on overhead lines by lightning strokes", P.I.E.E., 114, 12, p. 1899 (Dec. 1967).
2. Mushiake, Y. and Adachi, S.: "Fundamental theory of electromagnetic wave", Kyoritsu Publications (1970).
3. Uman, M. A.: "Lightning", McGraw Hill (1969).
4. Yokota, E., Horio, T. and Yagi, K.: "The actual state of telephone network subscriber loops", Shisetsu, 29, 11, p. 62 (1977).


Table 1 Representative calculation values.

| Items | | Representative Values |
|---|---|---|
| Return stroke | Peak current | 10 (kA) |
| | | 2 (μsec) |
| | | 80 (μsec) |
| | Velocity | $9 \times 10^7$ (m/sec) |
| Cable | Cable height above ground | 5 (m) |
| | Cable diameter | $2 \times 10^{-2}$ (m) |
| | Cable sheath material | Aluminum ($\sigma = 36.4 \times 10^6$ S/m) |
| | Cable sheath thickness | 0.2 (mm) |
| Ground | Conductivity | 0.1 ~ 0.001 (S/m) |
| | Specific dielectric constant | 10 |
| Cable terminal earth resistance | | 200 (Ω) |

Table 2 Measurement method.

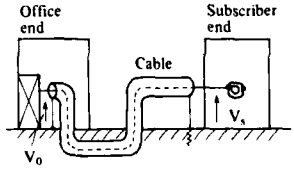
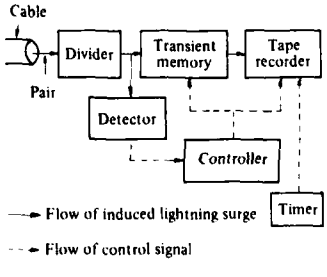
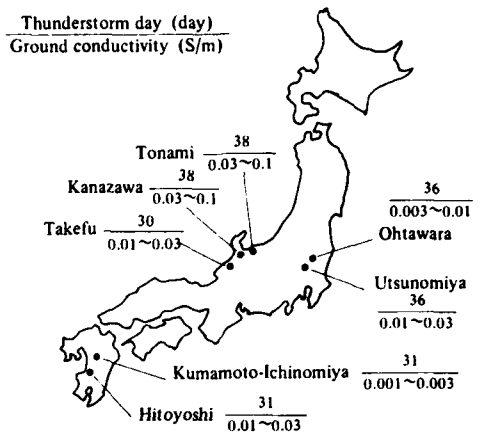
| Instrument | Specification | | Measured Method | Items | |
|---|---|---|---|---|---|
| Lightning Surge Counter | Terms | Characteristics |   | Voltage distribution | Subscriber end $V_s$ |
| | Input impedance | 300 kΩ | | | Office end $V_0$ |
| | Settled voltage level | 100, 200, 400, 600, 700, 800, 1000, 1500 (V) Errors ±10% | | Ground conductivity dependency | |
| | Polarity | Can work positive and negative | | Lightning surge difference between summer and winter | |
| Lightning Surge Waveform Recorder | Terms | Characteristics |   | Front time Time to half value | Subscriber end |
| | Input resistance | 1 MΩ | | | Office end |
| | Capacitance | 30 pF | | Basic characteristics of lightning surge | Cable length dependency |
| | Frequency band | D.C. ~ 10 MHz | | | Earth resistance dependency |
| | Voltage divided ratio | 1/200 ~ 1/2000 | | | Polarity |
| | | | | | Electric field |

Table 3 Measurement location.

| Area | | Instrument | Distinctive Feature | Map of Japan |
|---|---|---|---|---|
| Kanto | Utsunomiya | ·Lightning surge counter<br>·Lightning surge waveform recorder | As this area is near the laboratory, it is convenient for measuring | |
| | Ohtawara | | | |
| Hokuriku | Tonami | Lightning surge counter | There are many lightning strikes in winter | |
| | Kanazawa | | | |
| | Takefu | | | |
| Kyushu | Kumamoto-Ichinomiya | Lightning surge counter | Soil history is longer in Japan | |
| | Hitoyoshi | | | |



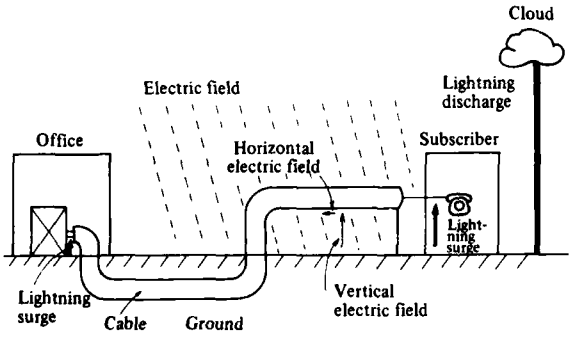




Fig. 1 Lightning surge inducing mechanism.

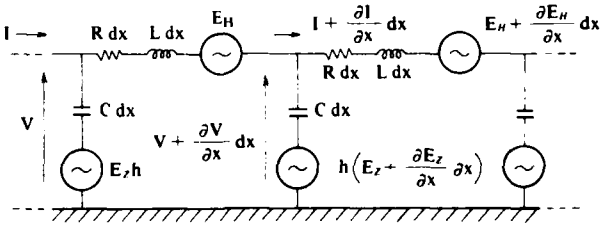



Fig. 3 Equivalent circuit for transmission line with inducing voltage.

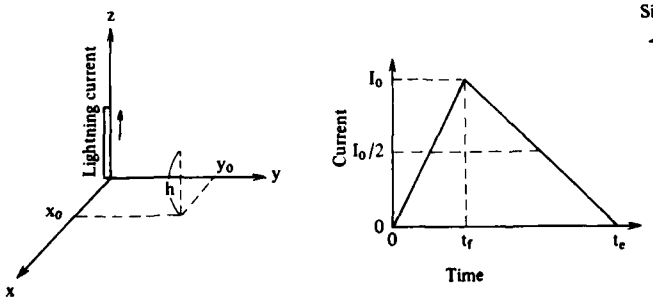



Fig. 2 Return stroke co-ordinate system and return stroke current analytical representation.

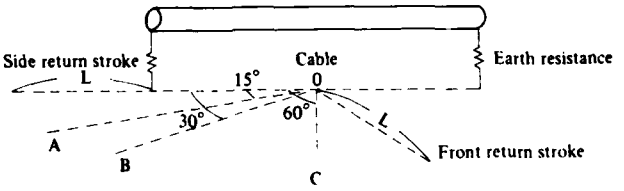



Fig. 4 Relation between strike point and cable.

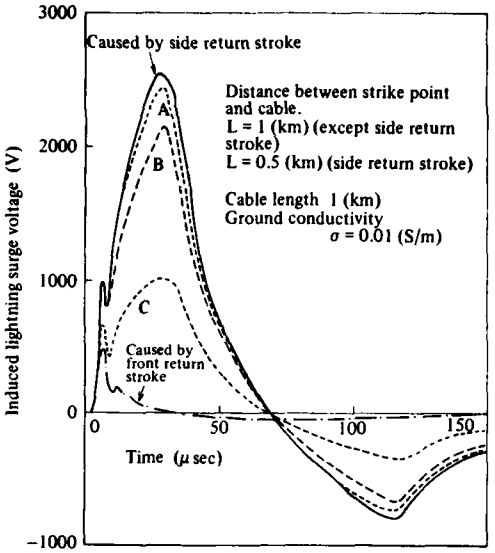
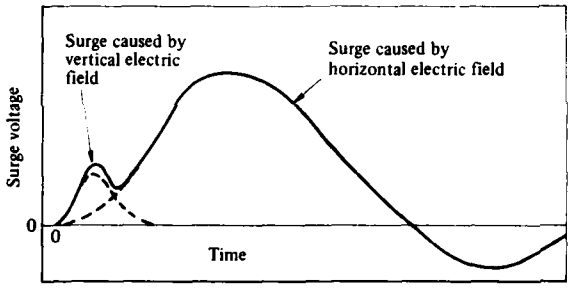



Fig. 5 Lightning surge waveform.



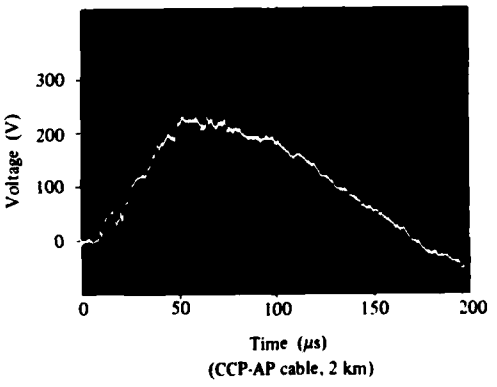




Fig. 6 Typical induced lightning surge wave.

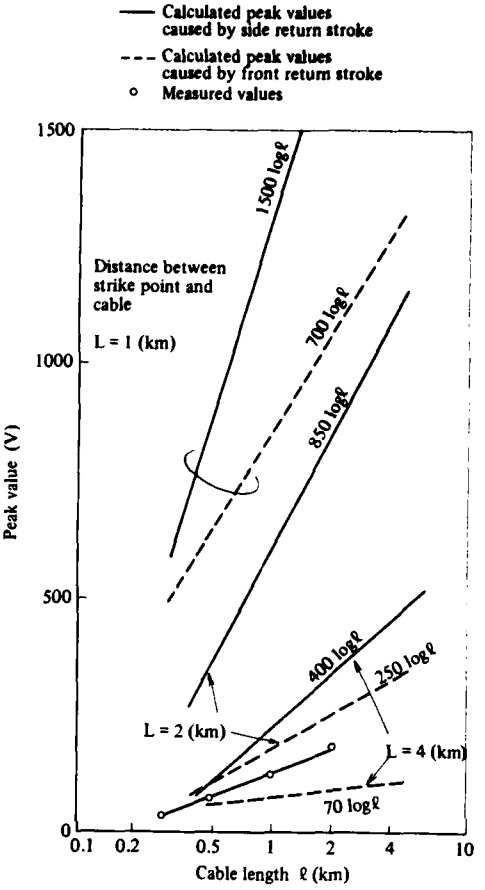



Fig. 7 Relation between cable length and peak induced lightning surge values (ground conductivity $\sigma = 0.01$ S/m).

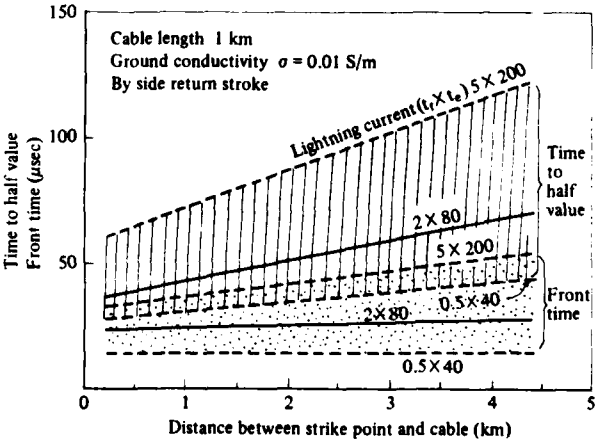



Fig. 8 Front time and time to half values vs. distance between strike point and cable for various lightning current waveforms.

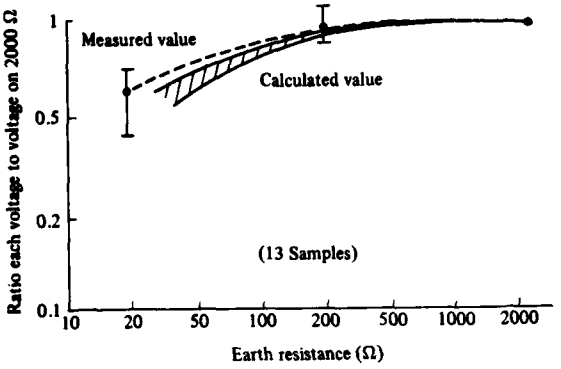



Fig. 9 Relation between peak induced lightning surge value and cable terminal earth resistance.

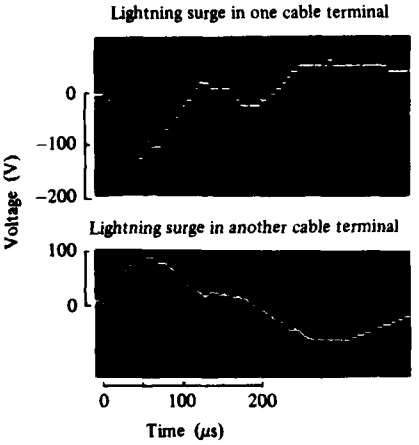



Fig. 10 Measured lightning surges in cable both terminals.

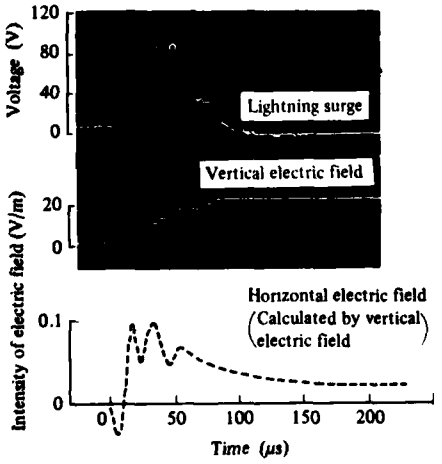



Fig. 11 Relation between lightning surge, horizontal electric field and vertical electric field.

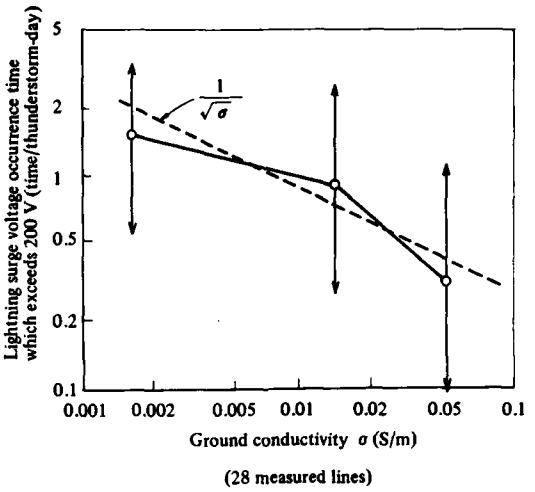



Fig. 12 Ground conductivity dependency.

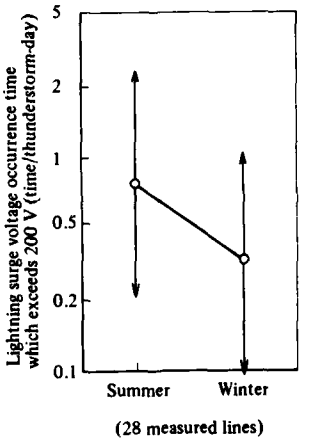



Fig. 13 Lightning surge voltage in summer and in winter.

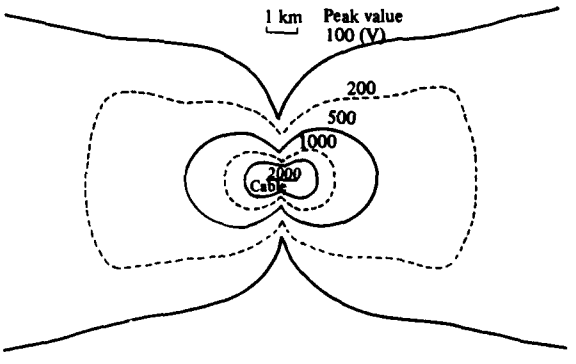



Fig. 14 Equi-voltage loop line for induced lightning surge on overhead line (ground conductivity $\sigma = 0.01$ S/m).

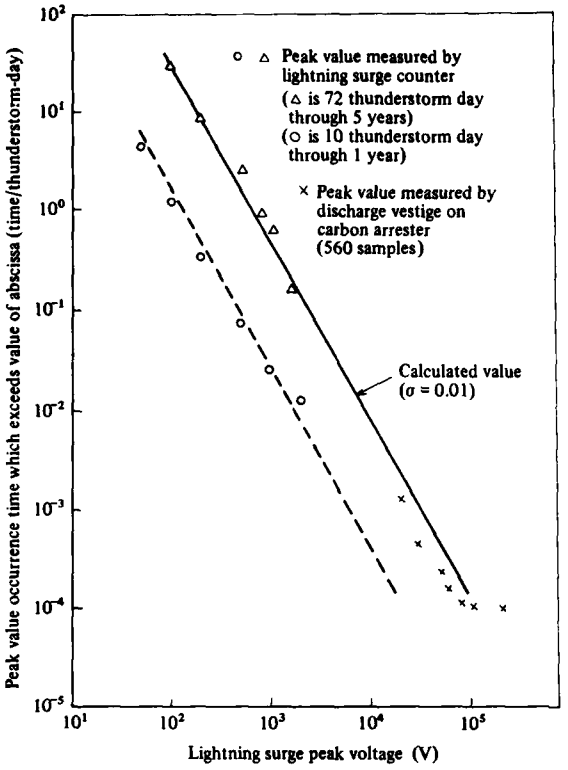



Fig. 15 Peak voltage distribution.

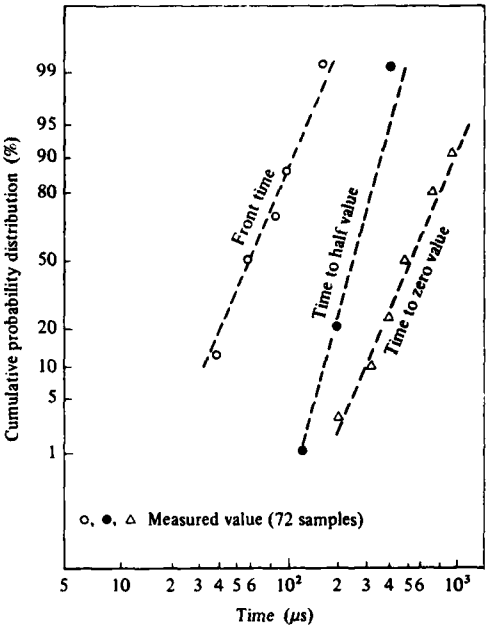



Fig. 17 Lightning surge waveform distribution (office end).

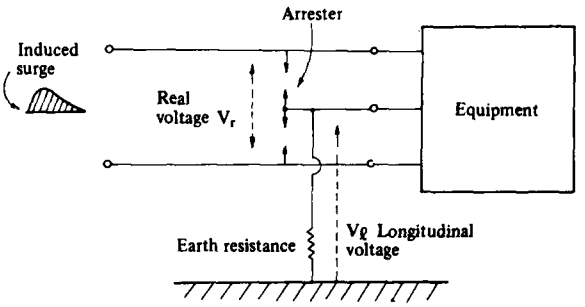



Fig. 18 Voltage fed to equipment.

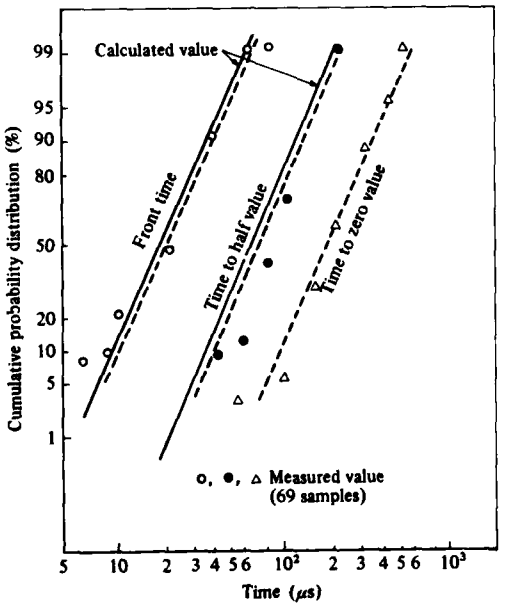



Fig. 16 Lightning surge waveform distribution (subscriber end).

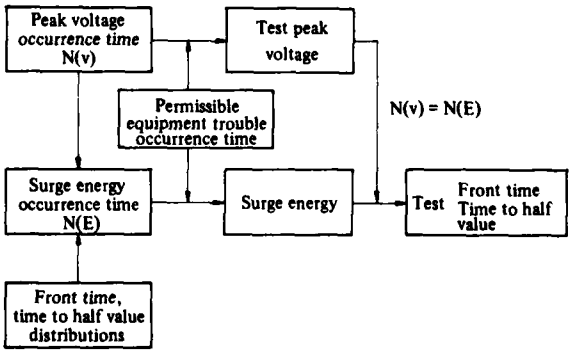



Fig. 19 Longitudinal test surge waveform design method.

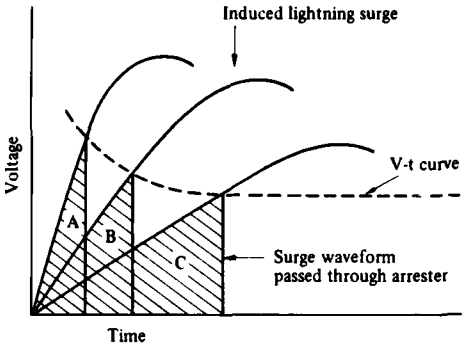



Fig. 20 Real voltage passed through arrester.

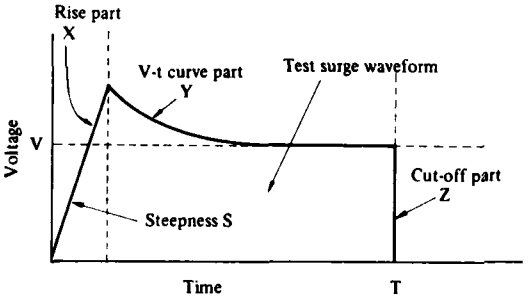



Fig. 21 Real voltage test surge waveform.

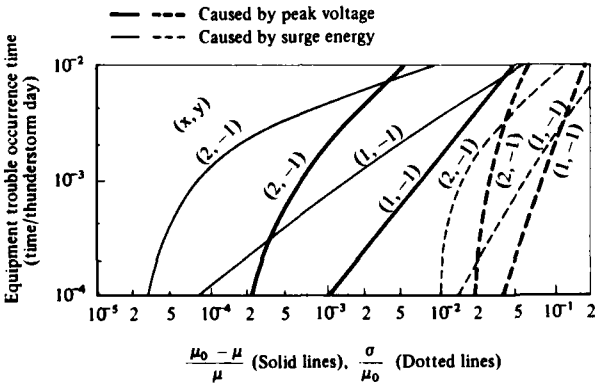



Fig. 22 Optimum mean value and standard deviation for equipment trouble.



H. Koga

Ibaraki Electrical Communication Laboratory, N.T.T. Tokai, Ibaraki, Japan

Mr. H. Koga received M.E. degree in electrical engineering from Kagoshima University in 1970 and then joined the Electrical Communication Laboratory, N.T.T. His early work dealt with the cable design for subscriber loop. He has been recently engaged in research on the protection against the lightnig surge.



T. Motomitsu

Ibaraki Electrical Communication Laboratory, N.T.T. Tokai, Ibaraki, Japan

Mr. T. Motomitsu joined the Electrical Communication Laboratory, N.T.T. after his graduation from Ube Technical College in 1967. He has been engaged in research of protection of telecommunication lines against lightning surges. He is the Engineer of Cable Facility Section.



M. Taguchi

Ibaraki Electrical Communication Laboratory, N.T.T. Tokai, Ibaraki, Japan

Mr. Taguchi graduated from Nagoya Institute of Technology in 1963 with the B.E. degree in electrical engineering. He joined the ECL in 1963, and his early work mainly dealt with design of high speed PCM transmission lines. He has been recently engaged in protection of telecommunication facilities against electric disturbances. He is presently Staff Engineer of the Outside Plant Development Division, Ibaraki ECL, and is a member of the Institute of Electronics and Communication Engineers of Japan.

# MEASURING TRANSMISSION LINE TRANSFER FUNCTIONS USING A FOURIER TECHNIQUE

N. H. Gholson

Naval Ocean Research and Development Activity
Ocean Technology Division
NSTL Station, Mississippi 39529

## Abstract

A Fourier transform approach has been applied to measuring transfer functions (phase and attenuation) of working ocean telemetry cables. The cable transfer function, $H(j\omega)$, is extremely important for designing telemetry systems, or parts of telemetry systems, such as equalizers. The major feature of the technique presented here is that transfer function measurements can be made with the transmission line in any mechanical configuration, i.e., only one cable end is necessary at the point of data acquisition. Typical measurement errors are less than $5^{o}$ and 0.5 dB for phase and attenuation, respectively.

## Introduction

Knowledge of the transmission line transfer function, $H(j\omega)$, is essential for effectively designing the overall telemetry system. Measuring the transfer function (attenuation and phase vs. frequency) is straightforward if both ends of the line are available at one location. Such measurements can be performed with very basic equipment, such as a synthesizer and dual trace oscilloscope, or with extremely accurate computer controlled analyzers, such as described in Reference 1.

The problem addressed in this paper is that of measuring the transfer functions of cables whose transfer functions cannot be realistically measured with both ends available. An example of such a transmission line is a single conductor (sea water return) used to transmit data from the ocean bottom to a small surface buoy (see Figure 1). The low frequency electrical skin depth of sea water is quite large. As an example, the electrical skin depth of sea water at 50 Hz is approximately 35 meters as opposed to 0.009 meters in copper (References 2 and 3). Altering large "natural" boundaries closer than approximately 3 skin depths (Reference 4) from the cable under test could cause substantial changes in the cable transfer function. A "natural" boundary is defined as one present during normal operation of the cable (ocean surface, bottom, etc.). For this reason, the transfer function of a transmission line such as shown in Figure 1 cannot be realistically measured unless the line is in a mechanical configuration very similar to that of its intended operation.

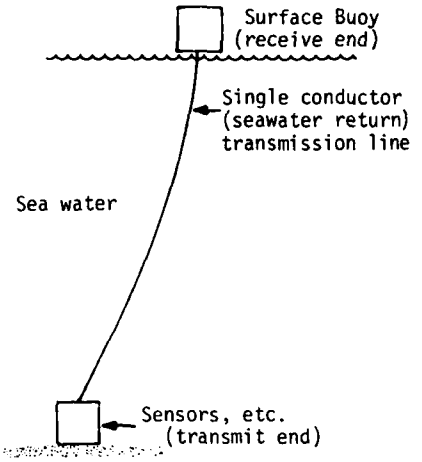



Figure 1

Single conductor (sea water return) transmission line

The technique described in this paper performs the desired in situ measurement of cable transfer function by exciting the transmit end with a wide band linear phase pulse and performing a Fourier analysis of the pulse arriving at the receive end. The cable transfer function, $H(j\omega)$, can then be determined from the ratio of the Fourier transform of the output (receive end) to the Fourier transform of the input (transmit end).

## Hardware Description

The basic hardware configuration for the transfer function measurement technique described in this paper is shown in Figure 2.

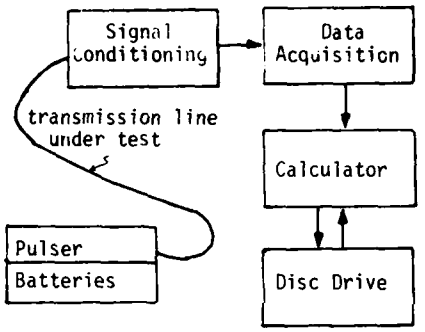



Figure 2

Basic Hardware Configuration

The battery-powered pulser produces a periodic rectangular pulse of approximately 2 volts amplitude, as shown in Figure 3.

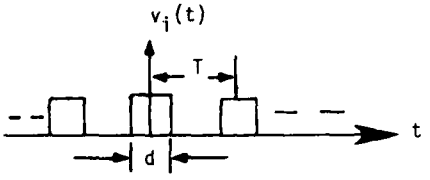



Figure 3

Pulser Output Waveform

Pulse duration, d, and pulse period, T, are adjusted to meet the particular cable test requirement. A rectangular pulse was chosen over perhaps a sine wave portion, to allow the pulse generating and line driving circuitry to be realized with nonlinear (binary) components. A control circuit allows the pulser to be commanded on and off from the far end (receive end) of the cable. The pulser, with lead-acid batteries for 10 hours of *continuous* operation, fits inside a pressure vessel approximately 18 inches long and 5 inches in diameter. The pressure vessel is designed to withstand a hydrostatic pressure of 10,000 psi.

The data acquisition unit is a Tektronix digital processing oscilloscope (DPO). The DPO performs a 10 bit analog-to-digital conversion in 10 microseconds allowing real time data acquisition for signals low pass limited to less than 50 KHz. Acquisition of *periodic* signals with higher frequency (greater than 50 KHz) is accomplished by sampling for more than one period of the periodic waveform.

A programmable calculator interfaces with the DPO via an IEEE 488 bus. The calculator performs the functions of recording and processing data. A single floppy disk has the capacity to store approximately 100 digitized pulses.

The signal conditioning shown in Figure 2 is sometimes necessary to equalize or "spectrally flatten" the received signal to avoid dynamic range problems in the data acquisition unit. A single active network was configured to realize 2 poles and 2 zeros for providing a bounded equalization with a maximum rate of 12 dB/octave.

## Theory of Operation

The measurement technique presented in this paper is based on the following property of a linear time invariant system (such as a transmission line).

$$V_o(j\omega) = H(j\omega)V_i(j\omega) \tag{1}$$

where $H(j\omega) \triangleq$ Fourier transform of the system impulse response,

$V_i(j\omega) \triangleq$ Fourier transform of the system input excitation, $v_i(t)$, and

$V_o(j\omega) \triangleq$ Fourier transform of the system output response, $v_o(t)$.

The complex valued function, $H(j\omega)$, is labeled the transfer function. The transfer function is extremely useful in that it allows the system output to be computed for any input. The magnitude and phase of $H(j\omega)$ represent the ratio of output-to-input magnitude and phase difference for a sinusoidal input of frequency $\omega$. The phase, $\phi$, of $H(j\omega)$, is defined by the following:

$$\phi(\omega) \triangleq \text{Tan}^{-1}\left[\frac{\text{Imag }(H(j\omega))}{\text{Real }(H(j\omega))}\right]$$

where "Imag" denotes imaginary part and "real" denotes real part of the complex function $H(j\omega)$. Rearranging equation (1) results in the following familiar expression (Reference 5) for determining $H(j\omega)$ from the input and output transforms.

$$H(j\omega) = \frac{V_o(j\omega)}{V_i(j\omega)} \tag{2}$$

The input transform, $V_i(j\omega)$, is simply the Fourier transform of the pulser waveform, i.e.,

$$V_i(j\omega) = \sum_{n=o}^{\infty} b_n \,\delta(\omega - n\omega_o) + \delta(\omega + n\omega_o) \tag{3}$$

where $\omega \triangleq$ angular frequency,

$\omega_o = 2\pi/T$,

$T$ = pulser period,

$b_n = 2A \sin(n\omega_0 d/2)/n$,

$A$ = pulse amplitude, and

$\delta \triangleq$ dirac delta function.

The output transform, $V_0(j\omega)$, is defined as the Fourier transform of the output response $v_0(t)$, i.e.,

$$V_0(j\omega) = \int_{-\infty}^{+\infty} v_0(t)\varepsilon^{-j\omega t}dt \qquad (4)$$

where $j \triangleq \sqrt{-1}$ .

The definition, equation (4), is not directly used to compute the output transform, but instead, the numerically more attractive fast Fourier transform (FFT) is used to compute the Fourier *series* coefficients. The transform can be quickly determined from these coefficients.

The pulser output $v_i(t)$ and transmission line output $v_0(t)$ being periodic allows $V_i(j\omega)$ and $V_0(j\omega)$ to be non-zero only at integer multiples of $\omega_0$ ($\omega_0 = 2\pi/T$). *Therefore, using a periodic input pulse allows $H(j\omega)$ to be theoretically determined only for discrete frequencies; specifically, only for integer multiples of the pulse repetition rate (1/T).*

The engineer may use his intuition, however, to estimate the cable transfer function for frequencies other than those just discussed. This is accomplished by observing the transmission line response to a periodic pulse and then *estimating* the response to a single (not periodic) pulse. In practice, this is easily accomplished since the pulse response of any transmission line of interest decays to very nearly zero in a short time. As an example, the response of a 16,000-ft coaxial cable (similar to RG8) to a 40 KHz pulse (.4 microsec. duration) was not measurably different from the true single pulse response. The continuous transfer function is then determined by equation (2) where the input transform, $V_i(j\omega)$, is given by:

$$V_i(j\omega) = 2A\,\frac{\text{Sin}\,(\omega d/2)}{\omega} \qquad (5)$$

and the output transform, $V_0(j\omega)$, is given by:

$$V_0(j\omega) = \int_{-\infty}^{+\infty} \hat{v}_0(t)\varepsilon^{-j\omega t}dt \qquad (6)$$

where $\hat{v}_0(t)$ is an estimate of the transmission line response to a single pulse.

As a final note, it should be mentioned that the technique presented in this paper can determine transfer function phase only to within an *unknown* linear phase component. In other words, the estimated transfer function, $\hat{H}$, is related to the true transfer function, H, by

$$\hat{H}(j\omega) = H(j\omega)\varepsilon^{-j\omega\Delta} \qquad (7)$$

where $\Delta$ is an unknown time delay that is *not* a function of frequency. In virtually all applications, however, this ambiguity in delay is of no importance.

## Errors Due to Noise

The analysis presented here attempts to quantify the effect of noise on the computed output transform $V_0(j\omega)$. For simplicity, the noise is assumed to be an additive zero mean white sequence of variance $\sigma_n^2$ corrupting the measured output signal $v_0(t)$. In other words, the measurement process is modeled by:

$$v_0(t) = \underset{\text{true}}{v_0(t)} + n(t) \qquad (8)$$

where $v_0(t)$ is the measured output and $n(t)$ is the measurement noise.

The computed magnitude of $V_0(j\omega)$, $\hat{M}(\omega)$, in dB is given by:

$$\underset{dB}{\hat{M}} = 10\ Log\left[(F_r(\omega) + E_r(\omega))^2 + (F_i(\omega) + E_i(\omega))^2\right] \qquad (9)$$

where $F_r(\omega)$ and $F_i(\omega)$ are the real and imaginary parts of $V_0(j\omega)$, and $E_r(\omega)$ and $E_i(\omega)$ are the errors (due to noise) in the computed real and imaginary parts. For large signal-to-noise ratios, a close approximation of equation (9) can be obtained by linearizing the dependence of $\hat{M}$ on $E_r$ and $E_i$ to obtain the following approximate expression describing the error $(\hat{M} - M)$.

$$\underset{dB}{\hat{M}} - \underset{dB}{M} \simeq \frac{\alpha}{(F_r^2 + F_i^2)}\left[F_r E_r + F_i E_i\right] \qquad (10)$$

where $\alpha = 20/Ln(10)$.

From equation (10), an approximation for the statistical variance of the magnitude error, $\sigma_{dB}^2$, can be derived to yield:

$$\sigma_{dB}^2 \simeq \left[\frac{\alpha}{F_r^2 + F_i^2}\right]^2 \cdot \left[F_r^2\sigma_{E_r}^2 + 2F_rF_i\sigma_x + F_i^2\sigma_{E_i}^2\right] \qquad (11)$$

where $\sigma_{E_r}^2$ and $\sigma_{E_i}^2$ are variances of the errors in computed real and imaginary parts of $V_0(j\omega)$. The

parameter $\sigma_x$ is the expected value of the product $E_r E_i$. It is easily shown that error variances of the computed Fourier series coefficients in the presence of additive white noise are given by:

$$\sigma^2_{E_r} = \sigma^2_{E_i} = \frac{2\Delta t}{T}\sigma_n^2 \quad \text{and} \qquad \sigma_n = 0 \tag{12}$$

where T is the pulse period, $\Delta t$ is the interval between data samples and $\sigma_n^2$ is noise variance. Substituting (12) into (11) and taking the square root results in the following expression for the standard deviation of magnitude error:

$$\sigma_{dB} \simeq \left[\frac{2\Delta t}{T\left[F_r^2(\omega) + F_i^2(\omega)\right]}\right]^{1/2} \alpha\,\sigma_n \tag{13}$$

where $\alpha = 20/\mathrm{Ln}(10) \simeq 8.69$.

Similarly, an approximate expression for standard deviation phase error (in radians) can be derived to yield:

$$\sigma_{\phi_{rad}} \simeq \left[\frac{2\Delta t}{T(F_r^2(\omega) + F_i^2(\omega))}\right]^{1/2} \sigma_n \tag{14}$$

Expressions (13) and (14) can be more conveniently stated by realizing that $\left[F_r^2(\omega) + F_i^2(\omega)\right]^{1/2}$ is simply the magnitude of the output component at frequency $\omega$, $|V_o(j\omega)|$. Also, $T/\Delta t$ is simply the number of data points, N, used to compute the output Fourier series coefficients; therefore, (13) and (14) can be expressed by:

$$\sigma_{dB} \simeq \alpha\left(\frac{2}{N}\right)^{1/2} \frac{\sigma_n}{|V_o(j\omega)|} \tag{15}$$

$$\sigma_{\phi_{rad}} \simeq \left(\frac{2}{N}\right)^{1/2} \frac{\sigma_n}{|V_o(j\omega)|} \tag{16}$$

Expressions (15) and (16) provide a convenient method of estimating performance of the measurement technique as a function of signal-to-noise ratio. Field experience, as well as computer simulations, have indicated the expressions to be not only useful, but quite accurate as well.

## Examples

The first test conducted using the Fourier technique addressed measuring the characteristics of a 16,000-ft long, 0.69-inch diameter spaced armor, torque balanced coaxial cable. Specifically, the test was designed to determine the effects of an ocean tow cable operating environment on the cable transfer function. Figure 4 displays the measured attenuation and phase as a function of frequency with the cable on a reel. The cable was then sea tested as a tow cable with the pulser mounted on the tow body. Results of the test showed *virtually no change* in the cable transfer function (to 1 MHz). The significance is that for this particular cable, a telemetry system can be "dry" tested with the cable conveniently on its reel.

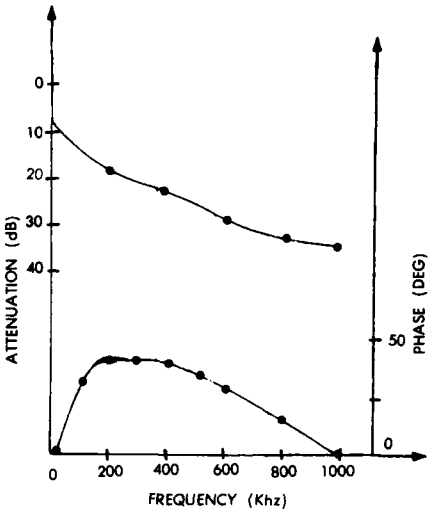



Figure 4

Characteristics of a Spaced Armor Coax Line

The second series of tests involves determining the characteristics of a 10,000-ft small diameter ($\simeq$ 0.1 inch) semi-shielded cable. The preliminary results presented here show the effect of cable payout length, where payout length is defined by Figure 5. The first configuration was the cable completely on the reel (zero payout length). The second configuration was 2000 ft payed out (8000 ft still on reel). Unfortunately, due to an interfering power line, the payout length could not be extended.

Figure 6 shows the measured attenuation and phase for the two different test configurations. The most noticeable result is the difference in attenuation ($\simeq$ 6 dB) at 20 KHz. Based on these data, one can only expect that very significant differences would be observed for longer payout lengths.

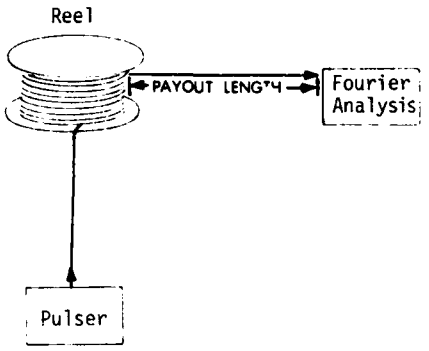



Figure 5

Test configured for small semi-shield cable

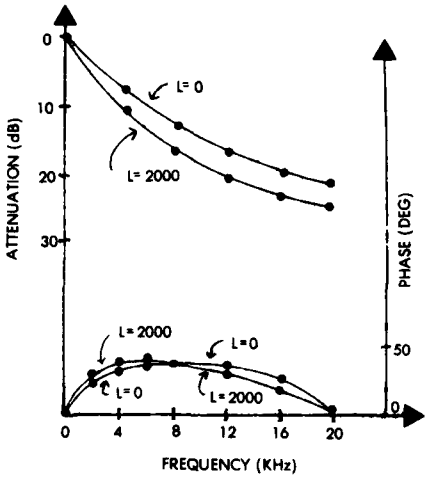



Figure 6

Transfer function for different payout lengths


## Summary

Hardware has been developed for realizing a Fourier transform technique of measuring transmission line transfer functions. The major feature of the technique is that it allows measurements to be conducted with only one cable end available at the point of data acquisition. Among other things, the technique permits measuring transmission line characteristics as a function of mechanical configuration. Examples are cited showing that mechanical configuration is sometimes important. An error analysis was conducted with respect to the effect of measurement noise. Results, both theoretical and empirical, show the errors to be acceptably small. Practical applications have resulted in measurements better than 0.5 dB and $5^{0}$ error for attenuation and phase, respectively.



## Acknowledgement

I would like to acknowledge the work of Mr. Frank Rakoczy and Mr. Terry Sullivan for their valuable assistance in obtaining experimental data and performing computer simulations.


## References


1. Nantz, T. D., "Transmission and Crosstalk Measurements on Installed Multipair Cable," 28th International Wire and Cable Symposium, November 1979.

2. Harrington, R. F., "Time-Harmonic Electromagnetic Fields," McGraw-Hill, 1961.

3. Durrani, S. H., "Air to Undersea Communication with Magnetic Dipoles," IEEE Trans. Antennas and Propagation, Vol. AP-12, July, 1964.

4. Conferences with John Preble, Sanders Associates.

5. Kuo, B. C., "Linear Networks and Systems," McGraw-Hill, 1967.




## Biography

Dr. Gholson is a design engineer for the Ocean Technology Division of the Naval Ocean Research and Development Activity (NORDA). He received a B.S. in electrical engineering from North Carolina State University in 1970, and a Ph.D. in electrical engineering from Virginia Polytech in 1977. His primary responsibility at NORDA is the design and development of optimal telemetry systems for ocean related experiments.

# EVALUATION OF TRANSMISSION LOSS IN OPTICAL FIBER CABLES BY MEANS OF THE BACKSCATTERING TECHNIQUE

M. Eriksrud, S. Lauritzen and N. Ryen

Electronics Research Laboratory
Norwegian Institute of Technology
7034 Trondheim, Norway

## Summary

The backscattering technique appears to be a very useful and simple non-destructive measuring method for loss evaluation in optical fiber cables. This paper discusses reliability of the backscattering method, and statistics of experimentally obtained loss data are reported.

Extensive loss measurements have been performed on nearly 50 km graded-index fibers, applying both the backscattering technique and the more conventional cut-back method. Good agreement was found between the loss values obtained by the two different methods.

Thorough investigations of loss characteristics of 12 km cabled fibers have also been made. The backscattering technique was employed to determine if there was any change in fiber attenuation due to the cable manufacturing process and during temperature exposure tests of the cables. Changes of 0.1 dB/km were easily revealed.

## Introduction

The backscattering technique[1,2] provides a powerful method for investigation of attenuation characteristics of optical fibers. The method, based on measurement of the optical power scattered backwards when an optical pulse is launched into the fiber, offers the advantage of requiring access to only one end of the fiber and does not require that the fiber be cut. In principle, there is however a certain ambiguity in the interpretation of the experimental results. This problem, in addition to a certain limitation of dynamic range ($\sim$ 40 dB total), seems so far to have restrained the use of the method. But more recently, experimental results have been reported which demonstrate a reasonable accuracy and repeatability[3-5].

Further experimental studies on practical fibers are needed in order to fully clarify the reliability of the backscattering technique as a reference method for attenuation measurements. This paper compares the backscattering technique with the more widely used cut-back (or two-point) technique using the data obtained on 48 km graded-index fibers. In addition, results of various excess loss measurements on cabled fibers are also reported in order to further illustrate the performance of the backscattering technique.

## Backscattered power

When an optical pulse is propagating through a fiber, some of its energy is scattered. A fraction of this scattered light is trapped by the fiber and returned in the backward direction. The backscattered signal is observed as a decaying pulse, and the rate of decay is determined by the fiber attenuation.

If the launched pulse has peak power $P_o$ and width $\tau$, the time dependence of the backscattered power, P(t), at the input end is given by[2,6]

$$P(t) = \frac{1}{2} P_o \tau \alpha_s S v \exp\left(-2 \int_0^{\frac{1}{2}vt} \alpha(\xi) d\xi\right) \quad (1)$$

where $\alpha_s$ is the scattering coefficient (mainly Rayleigh scattering), S the backscatter factor, i.e. the fraction of scattered light recaptured by the fiber in the backward direction, v the group velocity and $\alpha(\xi)$ the average value of the attenuation coefficients of the forward travelling and the backscattered wave along the fiber length.

Equation (1) can be interpreted in spatial terms by introducing the variable

$$z = \frac{1}{2} vt \quad (2)$$

representing the distance from the input end to the scattering point. The fiber attenuation can then be determined from the slope of the logarithmic plot of the backscattered power function P(z). The average attenuation coefficient over the section of fiber in the region $z_1 \leq z \leq z_2$ can in decibels be estimated as

$$\alpha(z_1, z_2) = \frac{1}{(z_2 - z_1)} 5 \log\left(P(z_1)/P(z_2)\right) \quad (3)$$

provided that the product $\alpha_s S$ in equation (1) is independent of z within the fiber section of interest.

However, imperfections or fluctuations in optical and geometrical parameters along the fiber will in general perturb the backscattering product $\alpha_s S$ and thus affect the backscattered signal. Such nonuniformities along the fiber may therefore have some influence on the absolute accuracy which can be obtained by using equation (3). But for fibers with significant nonuniformities a method has been proposed[7] for separating the actual power decay contribution from the imperfection effects by comparing the backscattered power functions measured at both ends of the fiber.

Another point is that the mode spectrum of the backscattered light will not equal that of the incident light, and since actual attenuation values may depend on the power distribution among the propagating modes, the attenuation coefficients of the backscattered light and the incident light may differ from each other. Equation (3) represents the average value of these two coefficients.

## Experimental measurement procedure

The experimental apparatus used for the backscattering measurements is schematically shown in figure 1. An optical pulse obtained from a single heterostructure semiconductor laser is launched into the fiber after passing through a beam splitter unit. The backscattered light is reflected from the beam splitter onto the detector. The spatial filter, placed in front of the detector, is a 120 μm pin-hole aperture, thus reducing the undesirable contribution of spurious scattered light from the beam splitter, the microscopic lenses and the fiber terminating unit.

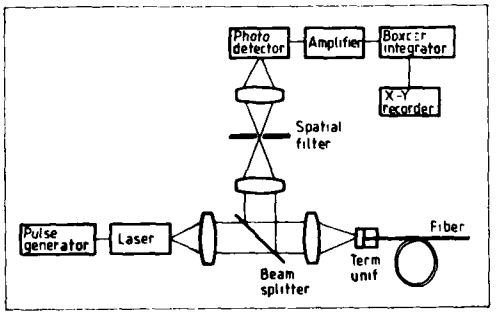



Figure 1. Schematic of experimental apparatus.

The fiber being tested is inserted, through a glass capillary tube, inside a cell filled with an index matching liquid for reducing the Fresnel reflection from the fiber endface. By using a 5 mm thick flat of fused quartz as front surface of the cell, the reflected light from the terminating unit focused back onto the detector is reduced to a tolerable level.

Temperature controlled lasers with different emission wavelengths (793, 840 and 900 nm) have been used. The pulse width was about 100 ns and the output peak power typically in the range of 1 - 5W. The emitting area of the laser was imaged by microscope objectives onto the fiber core with a magnification close to one.

The backscattered signal was detected by an avalanche photodetection system with a 60 MHz bandwidth, and waveform averaging was performed with a boxcar integrator operating in the scanning mode.

## Attenuation coefficient measurements

Backscattering measurements have been performed on 27 individual graded-index fibers of lengths varying from 1 km to 2.5 km. The fibers were made in-house by the modified chemical vapour deposition technique with a 50 μm core of $GeO_2$-$B_2O_3$-$SiO_2$ composition and a numerical aperture in the range 0.18 - 0.22. Outer diameter of the fiber was 125 μm and the primary coating was a 50 μm thick layer of silicon resin.

All fibers were also measured by conventional cut-back technique, where the fiber loss is determined from the ratio of total power levels at the far-end and broken off near-end (or reference) point, without changing the launching condition. To avoid a transient loss contribution[8] to the measured loss value a spatial and angular restricted launch beam was employed. A tungsten lamp with a monochromator was used as a light source for a launching numerical aperture of $\sim$ 0.1 and a launching spot size of $\sim$ 30 μm. The reference length was about 1 m. This cut-back measurement procedure was chosen as a reference method because this procedure has previously been shown to give values adequate for predicting the fiber loss of long concatenated lengths[8].

The results of the measurements are shown in table I. All the attenuation coefficients measured by the backscattering technique are compared to those obtained at the same wavelength with the cut-back technique. An excellent agreement was obtained, the maximum observed deviation being only 0.2 dB/km with an average value of the absolute difference of 0.05 dB/km.

The results, summarized in figure 2, clearly indicate that the backscattering technique can be confidently employed to determine the attenuation value of optical fibers.

| Wave-length | Fiber length (km) | Attenuation (dB/km) | | |
|---|---|---|---|---|
| | | Backs. techn. | Cut-back techn. | Differ-ence |
| 793 nm | 1.41 | 4.8 | 4.8 | 0.0 |
| | 1.93 | 4.7 | 4.9 | -0.2 |
| | 1.72 | 5.1 | 5.2 | -0.1 |
| | 2.27 | 4.3 | 4.3 | 0.0 |
| | 2.48 | 4.4 | 4.4 | 0.0 |
| | 2.55 | 4.4 | 4.4 | 0.0 |
| | 1.30 | 4.7 | 4.6 | 0.1 |
| | 2.21 | 4.3 | 4.3 | 0.0 |
| | 1.73 | 4.3 | 4.3 | 0.0 |
| | 2.24 | 4.2 | 4.3 | -0.1 |
| | 2.25 | 4.1 | 4.1 | 0.0 |
| 840 nm | 2.20 | 4.2 | 4.2 | 0.0 |
| | 1.24 | 3.5 | 3.4 | 0.1 |
| | 1.01 | 3.3 | 3.4 | -0.1 |
| | 1.76 | 3.5 | 3.5 | 0.0 |
| | 0.94 | 3.5 | 3.6 | 0.1 |
| | 2.07 | 3.6 | 3.6 | 0.0 |
| | 1.47 | 3.3 | 3.4 | -0.1 |
| | 1.25 | 3.8 | 3.8 | 0.0 |
| | 2.47 | 4.1 | 4.1 | 0.0 |
| 900 nm | 2.52 | 2.6 | 2.6 | 0.0 |
| | 1.94 | 2.8 | 2.9 | -0.1 |
| | 2.30 | 2.5 | 2.5 | 0.0 |
| | 1.23 | 2.8 | 3.0 | -0.2 |
| | 1.27 | 3.2 | 3.2 | 0.0 |
| | 1.09 | 3.3 | 3.1 | 0.2 |
| | 1.66 | 2.6 | 2.6 | 0.0 |

Table I.

To further investigate the accuracy and precision of the backscattering technique, a series of repeated measurements was made on the same fiber. Figure 3 shows a histogram of the attenuation coefficients obtained with repeated insertions and different breaks of the fiber terminating end. The standard deviation for 51 measurements was no greater than 0.03 dB/km.

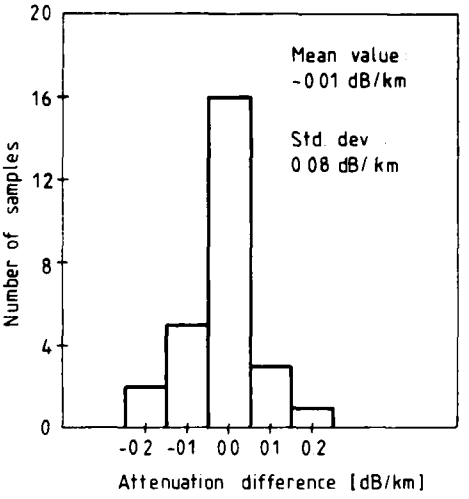



Figure 2. Difference in loss values obtained by the backscattering and cut-back technique (27 samples).

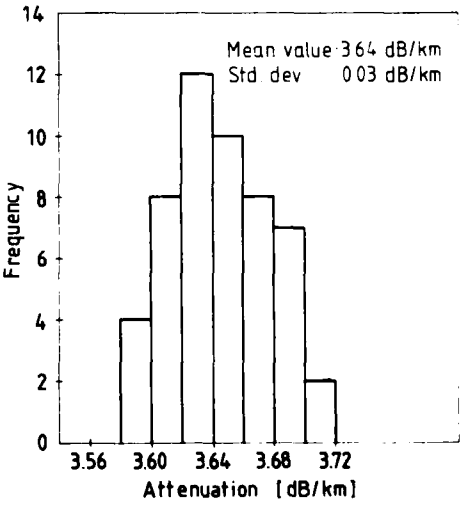



Figure 3. Statistics of loss values measured by the backscattering technique.

## Loss change measurements

With its high degree of repeatability the backscattering technique should be very suitable for detecting small loss changes in a fiber. The uncertainty in the interpretation of the backscattered waveform due to inherent inhomogeneities of the fiber structure itself, can be eliminated when one is only looking for changes in the loss value.

If $P_1(z)$ denotes the backscattered waveform measured when the fiber is in a state 1 and $P_2(z)$ the corresponding waveform in state 2, the slope of the function

$$\Delta I_{1,2}(z) = 5 \log \frac{P_2(z)}{P_1(z)} \qquad (4)$$

corresponds to the equivalent loss change along the length of the fiber, as long as the loss change mechanism does not introduce fluctuations in the backscattering product $\alpha_s S$ of equation (1).

To investigate the ability of the backscattering method to resolve loss changes in practice, extensive measurements have been made on two one-kilometer lengths of optical cable. The cables, manufactured by A/S Norsk Kabelfabrik, contained six loosely tubed fibers laid helically around a central steel strength member. Excess loss measurements were performed after the cable manufacturing process and during a subsequent long term temperature exposure test (-20°C to +30°C).

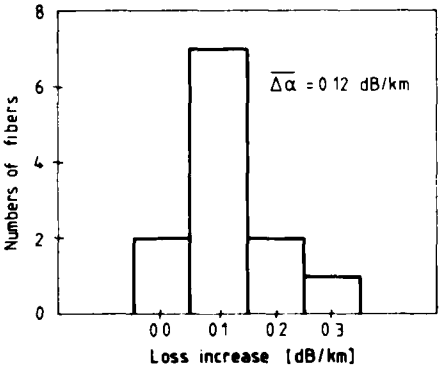



Figure 4. Increased losses due to cabling measured by the backscattering technique (12 samples).

The distribution of the measured loss increase during manufacturing is shown in figure 4, and some of the results from the temperature exposure test are illustrated in figure 5.

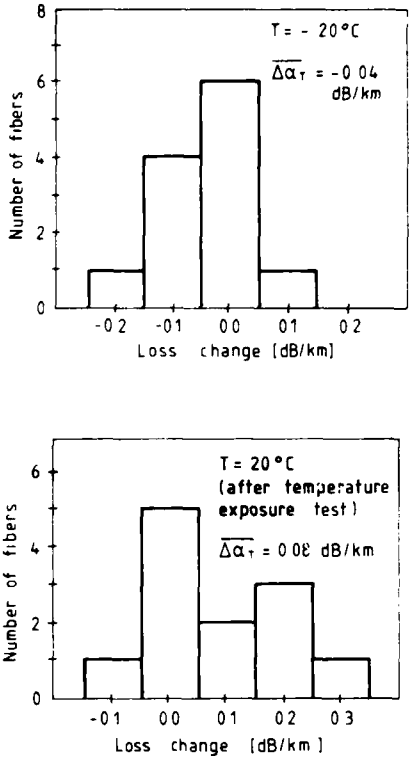



Figure 5. Loss changes (referred to the initial loss at 20°C) induced by temperature exposure measured by the backscattering technique (900 nm).

The average loss increase due to cabling was measured to 0.12 dB/km. A slight additional loss increase was likewise observed after the temperature exposure test was completed. However, some statistical fluctuations in fiber loss can be expected due to the relative movement between the primary coated fiber and the loose jacket during temperature changes. No significant loss increase was found at -20°C.

The backscattering technique proved in these measurements to be very effective in detecting small loss changes. Changes of 0.1 dB/km were easily revealed. This is clearly illustrated in figure 6 which shows different plots of the relative backscatter function $\Delta I(z)$. The curves, calculated by using equation (4), represent temperature induced loss change along the fiber length. The slope of the curves corresponds to the change in attenuation coefficient. In cases where temperature induced loss variations occurred, the loss change was found to be essentially linear w th length.

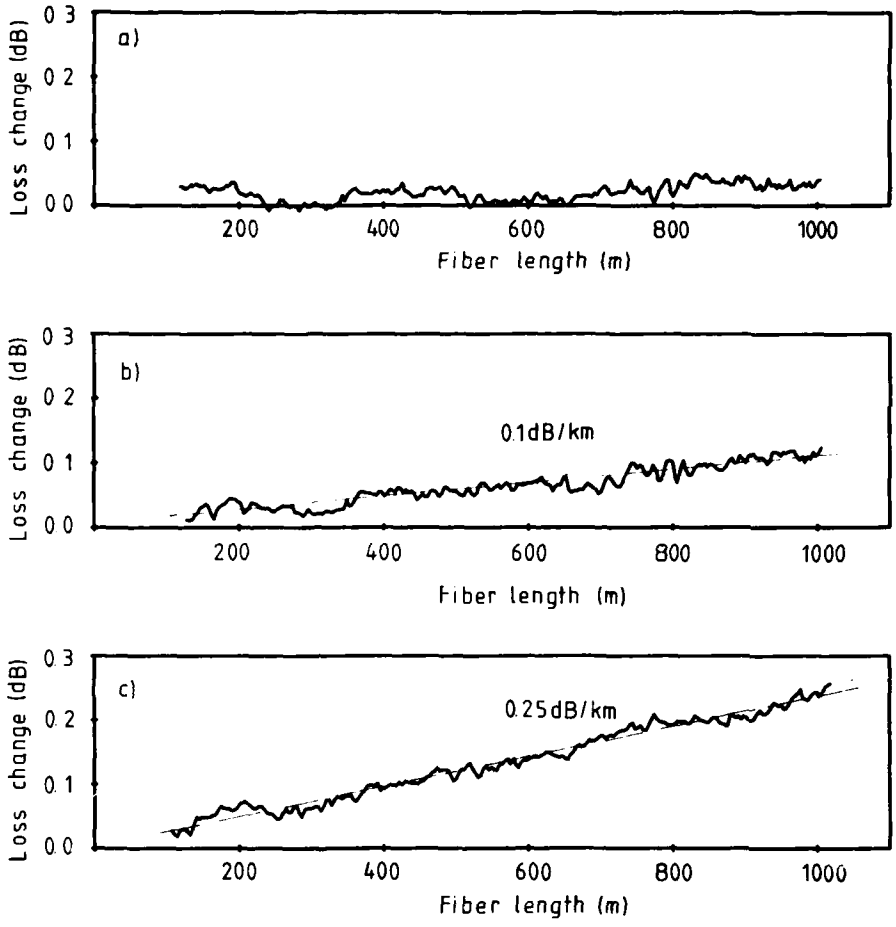



Figure 6. Changes of temperature induced cable loss measured with tne backscattering technique.

a) one of the fibers at -20°C

b) same fiber at room temperature after the temperature test was completed

c) another fiber at room temperature after the temperature test was completed

All curves are referred to the initial loss at room temperature.

## Conclusion

It has been demonstrated that highly accurate and reliable attenuation values can be provided by the non-destructive backscattering technique. Attenuation values obtained by this technique have been shown to be in very close agreement with those obtained by the more conventional cut-back method.

With its high degree of repeatability the backscattering technique also appears to be very attractive for monitoring loss variations during cable manufacturing, testing, installation and maintenance. By introducing data storage and processing facilities, measurements made at any time can easily be compared to previous measurements.


## Acknowledgements

Thanks are due to A. Hordvik and G. Nakken for preparing all fibers used in the experiments.

The work was supported by the Norwegian Telecommunication Administration Research Establishment and the Norwegian cable company, A/S Norsk Kabelfabrik.


## References


1. M.K. Barnoski and S.M. Jensen, Appl. Opt. 15, 2112 (1976).
2. S.D. Personick, Bell Syst. Tech. J. 56, 355 (1977).
3. B. Costa, C. De Bernardi, B. Sordo, Fourth European Conference on Optical Communication, Genova, Sept. 1978.
4. B. Costa, Optical Communication Conference, Amsterdam, Sept. 1979.
5. B. Costa, S. Sordo, U. Menaglia, L. Piccari, G. Grasso, Elect. Lett. 16, 352 (1980).
6. E.-G. Neumann, AEÜ 34, 157 (1980).
7. P. DiVita, U. Rossi, Opt. Quant. Elect. 11, 17 (1980).
8. M. Eriksrud, A. Hordvik, N. Ryen, G. Nakken, Opt. Quant. Elect. 11, 517 (1979).





Morten Eriksrud graduated from the University of Trondheim in 1969 and received his Dr.ing. degree in 1976. He is presently senior research scientist at the Electronics Research Laboratory, and he has been involved in research work on optical fibers for the last five years.





Noralf Ryen joined the Electronics Research Laboratory in 1966. He is a staff engineer and has been engaged in research and development work in the field of microwave acoustics and electro-optics.





Steinar Lauritzen is an engineer at the Division of Physical Electronics, Norwegian Institute of Technology. He graduated in 1978 from Trondheim Technical College and is presently working on evaluation of optical fibers and cables.

# Design and Practical Consideration for Manufacturing A Non-Metallic Fiber Optic Cable for Aerial Application

M. M. Rahman, H. K. Eastwood, P. Rivett, M. Herrera

Canstar, Division of Canada Wire and Cable Ltd.
Montreal, Quebec, Canada

## SUMMARY

The optimum performance and life of a fiber optic cable depends on the stress-free condition of the fiber in the final cable. In an aerial cable, the cable strains due to thermal, ice-loading and vibration are severe and it is necessary to decouple the fiber from these strains. The loose buffer tube design gives the greatest degree of decoupling, however, precise control of fiber excess length is required during cabling. A method of accurately measuring fiber excess length is presented and its use is demonstrated by optimizing the fiber performance in an aerial cable design.

## INTRODUCTION

Since the breakthrough in manufacturing low loss fibers in the early 70's, fiber optic cables have evolved from laboratory tests to carefully controlled field trials and finally to routine field installations. Each advance into more hostile environmental applications has required cable designers to develop the cable to the state where it isolates the delicate glass filaments from external stresses. Duct, buried, and aerial cables are now being constructed to withstand the strains of normal installation and operating procedures and operate without degradation over a wide temperature range.

The best way to decouple the optical fibers from the cable strain is to place them in individual tubes having an inside diameter large enough for them to move freely.[1] The tube, once helically stranded around a core, provides the fiber with an operating window where the effects of relative elongation and contraction will not be felt. The width of the window dictates the range of temperature-tensile performance and is affected by the expansion coefficient of the materials, their tensile modulii, and the range of excess fiber slack in the tubes. The critical temperature and tension are determined by the minimum and maximum levels of fiber slack.[2,3]

This paper consists of two parts; in the first a mechanical method of determining fiber excess length is described. The second section discusses the design and practical consideration of a non-metallic cable designed for the rigors of aerial installation and operation over a temperature range of $-40^{0}C$ to $50^{0}C$.

## EXCESS LENGTH MEASUREMENT
(Cable Geometry Considerations)

A fiber in a buffer tube suffers microbending losses when it is forced against the inside of the tube. The radial forces occur when the fiber is under tension or axial compression. The parameters that determine the presence of microbending inducing forces are two:

- The dimensions and curvature of the tube
- The quantity of fiber slack in the tube

The excess loss in a cable constructed of buffer tubes is governed by the effects of cabling and the environment on these two parameters. Excess length is the common term for expressing (as a percentage) the ratio of fiber slack to the length of the straight tube containing it. Negative excess length means the fiber is shorter than the tube.

Figures 1, 2 and 3 show how zero, positive, and negative excess length is accomodated in tubes of different curvature. Clearly, the higher the curvature (the smaller the bending radius) of the tube, the less sensitive the system is to excess length. In actual cables, the length of the tubes is affected by cable tension and thermal expansion and contraction, therefore, the cable must be designed to safely accomodate a certain amount of both positive and negative excess length. The tube curvature in a cable is a function of stranding diameter and pitch, but cannot be increased boundlessly. Not only is stranding speed reduced

with increased curvature, but the optical fiber experiences radiation losses at radii less than about 10 cm.[4] Furthermore, with planetary stranding, axial torsion on the fiber increases with stranding curvature. Although the affect of torsion on optical transmission has not been clearly documented, it is another source of fiber stress. Fiber optic cable design, therefore, is the art of balancing the cable geometry within the constraints imposed by having a distribution of excess length in the buffer tubes, and by having a range of tensile and thermal expansion and contraction requirements imposed by the cable application.

In process development, it is important to precisely measure the excess length in buffer tubes. One method involves temperature cycling the tubed fiber while monitoring its optical transmission. Unfortunately, this procedure is very slow because the rate of temperature change must be low for the tube to maintain thermal equilibrium. Also, the accuracy of the measurement depends on accurate knowledge of the thermal expansion coefficient; although this property can be accurately measured, it is a function of processing conditions and would have to be constantly monitored. An alternative method achieves the same effect mechanically using an expanding drum.

Microbending effects caused by incorrect excess length are mangified if the buffer tube is tested with a bending radius much higher than will be used in the stranded cable. Figure 4a depicts the typical situation when a tube containing a positive excess length is wound onto an expanding drum. Initially, the optical transmission is low due to microbending loss. Figures 4b, c, and d illustrate the consequences of expanding the drum. The tube stretches relieving the initial stresses; the optical transmission, which is continuously monitored, increases. When the tube is stretched to the point where its largest inside circumference is equal to the fiber length, the optical transmission reaches its peak and remains stable until further stretching brings the smallest inside circumference equal to the fiber length, thereby causing the transmission to drop. The transmission decreases sharply with continued stretching until the test is stopped.

This test was developed to test long lengths of tubed fibers, which are accomodated in a single layer on large diameter, long traverse, drum. A long length will naturally contain a distribution of excess length. During the test, the transmission will increase until the last of the buckling has been relieved; the transmission will stabilize at this point and the maximum excess length can be calculated. Similarly, the section where the excess length is minimum will be the first to suffer the associated loss in transmission. The point where the optical transmission drops indicates the minimum excess length in the tube. Figure 5 illustrates a typical transmission curve.

The upper and lower excess length limits in a buffer tube can be accurately determined by measurements of the drum circumference. Once the excess length is known, the temperature performance of the cable can be calculated. Helically stranded buffer tubes have constant curvature given by:

$$K = {}^{1}/_{r} = \frac{2\pi\ {}^{2}D}{p^{2} + \pi^{2}\ D^{2}}$$

where K is the curvature and r is the bending radius;
D is the helix diameter and p is the pitch.

Consequently, thermal expansion and contraction of the buffer tubes creates an effect analogous to the expanding drum test. As the cable contracts with cooling the region of maximum excess length will be the first to cause loss of light; areas of minimum excess length will be the first to attenuate the signal when the cable expands at higher temperatures or experiences tensile loading. Once the thermal expansion coefficients and the tensile modulii of the cable components are known, and the excess length limits are known, the temperature and tensile limits can be calculated. Between these limits, the fiber is stress-free and experiences no temperature or strain dependant loss.

The level of excess length can change dramatically during stranding and jacketing due to differential relaxation of processing tensions. For example, to maintain the same excess length during stranding, the tension of the tube let-offs must be adjusted to provide the same elongation as the central strength member so that, when the composite structure is relaxed, the tubes will have no residual stresses and hence, no relative change in length. If unbalanced, this effect can be a source of excess loss, however, on occasion it may be desirable to change the excess length in all the tubes. In such a situation, unbalanced elongations can be used to advantage.

During process development, it is useful to know the excess length in the cable after stranding and after jacketing. A method similar to the expanding drum test is used to make such a measurement. A length of cable is stretched in a straight line until the transmission begins to drop. The elongation at this point will, in conjunction with the stranding geometry, determine the minimum excess length in the sample. Using the previously measured excess length range in each buffer tube, the maximum excess length for the cable can be calculated. Alternatively, the maximum excess length can be measured by monitoring the transmission while cooling the cable.

The excess length can be accurately measured for each buffer tube prior to stranding using the expanding drum technique. In the stranded form, the excess length can also be determined by cable stretching. In all cases the total elongation is less than 0.5% which is well within the elastic

limit of the materials. By balancing, or deliberately unbalancing, the elongations of components during stranding and jacketing, it is possible to maintain, or trim and adjust, the excess length at each stage of the process. By remeasuring the excess length, the process objectives can be validated. A cable can be reliably produced to achieve optimum properties without having to screen buffer tubes for a specific excess length.

## CABLE DESIGN AND MANUFACTURING

Microbending losses in optical cables during normal operation are caused by differential expansion and contraction between the glass fibers and the cable body. The thermal expansion coefficient of glass is an order of magnitude less than conventional components comprising the cable structure. In a lashed aerial cable the variations in cable length are functions, not only of temperature, but of cable-messenger weight, wind effects, and ice loading. Table I below shows the cable strain as a function of the full range of environmental stresses[5] assuming the cable is tightly lashed to an 8mm diameter stranded steel messenger wire.

TABLE I

CALCULATED STRAIN FOR LASHED AERIAL CABLE

A. Design Parameters

| | Messenger Wire | Fiber Optic Cable |
|---|---|---|
| Diameter (mm) | 8 | 12 |
| Weight (Kg/km) | 76 | 110 |
| Tensile Modulus A·E (N) | $1.65 \times 10^6$ | $0.67 \times 10^6$ |
| Thermal Expansion Coefficient ($^0C^{-1}$) | $1.3 \times 10^{-5}$ | $2.2 \times 10^{-5}$ |
| Initial Tension (N) | 3120 | - |
| Span Length (m) | 90 | - |

B. Operating Conditions

| | Temp. $^0C$ | Cable Sag % of Span | Cable Strain % |
|---|---|---|---|
| Installed | 15 | 1.2 | 0.016 |
| Maximum Temp. | 50 | 1.5 | 0.036 |
| Max. Temp & Wind* | 50 | 1.9 | 0.079 |
| Max. Ice Load** | 0 | 1.9 | 0.078 |
| Max. Ice** & Wind* | 0 | 2.2 | 0.106 |
| Min. Temperature & Installed | -40 | 0.8 | -0.005 |
| Min. Temperature, no tension | -40 | - | -0.14 |

* $190N/m^2$ wind pressure
**12.7mm radial ice thickness

A six fiber cable (Figure 6) was designed for aerial application operating between -40 and $+50^0C$, while lashed to a stranded steel messenger wire with 90m spans. The cable was required to be non-metallic. The buffer tubes were stranded around a central member, which was strong enough to support the stranding, but was not designed to bear the full cable tensile load. A reinforced jacket incorporating rigid fiberglass filaments was designed to withstand 5000N tension without risk of fiber breakage.

For actual manufacturing, buffered fibers were selected to have fiber excess length between 0.45 and -0.08%. After stranding and first jacketing operation, fiber excess length was determined from attenuation versus temperature and tensile-elongation characteristics. In this case, we found that the maximum value of excess length to be 0.49% which was slightly higher than the design value. In subsequent processing, it was possible to reduce this value by elongating the cable core by 0.08%. This reduced value was locked into the structure by the fiberglass reinforcing elements. The ultimate value of excess length determined after the final jacketing shows that this was accomplished and was within the design values (Table II).

TABLE II

EXCESS LENGTH DURING PROCESSING

| DESCRIPTION | MAXIMUM EXCESS LENGTH IN % | MINIMUM EXCESS LENGTH IN % |
|---|---|---|
| Designed excess length range | +0.45 | -0.08 |
| Excess length on buffered fibers measured on sample basis | +0.43 | +0.09 |
| Excess length range after the first jacket determined from temperature cycling and elongation test | +0.49 | +0.32 |
| Excess length range of the final cable determined from temperature cycling and elongation test | +0.44 | +0.24 |

The tensile and temperature performance of the cable is shown in Figures 7 and 8. A tensile load of 1300N at an elongation of 0.24% and 100% transmission was obtained in the final cable. Regarding temperature performance, the worst fiber had a 0.5 dB/Km increase at $-40^0C$. The physical properties of the finished cable are summarized in Table III.

TABLE III

PHYSICAL PROPERTIES

| | |
|---|---|
| Bend radius (-50°C to 60°C) -no damage to cable or fibers | 100mm |
| Coefficient of expansion for cable | 22 x $10^{-6}$/°C |
| Crush load on 100mm length | 1580N |
| Flexure, without fiber breakage | 3500 cycles at 50mm radius |
| Impact -no damage to cable or fiber | 1.5Nm, 200 cycles with 10mm radius hammer |
| Tensile strength without fiber breakage - 15m gauge length | 5000N |
| Maximum safe operating tension | 1500N |

CONCLUSIONS

1. A method to accurately measure fiber excess length has been developed.
2. A technique to adjust the fiber excess length during cable processing has been demonstrated.
3. An aerial cable has been manufactured to operate in a full range of temperatures and tensile stresses without stressing the fiber.
4. The cable has been installed and is performing well within the desired specification.

REFERENCES:

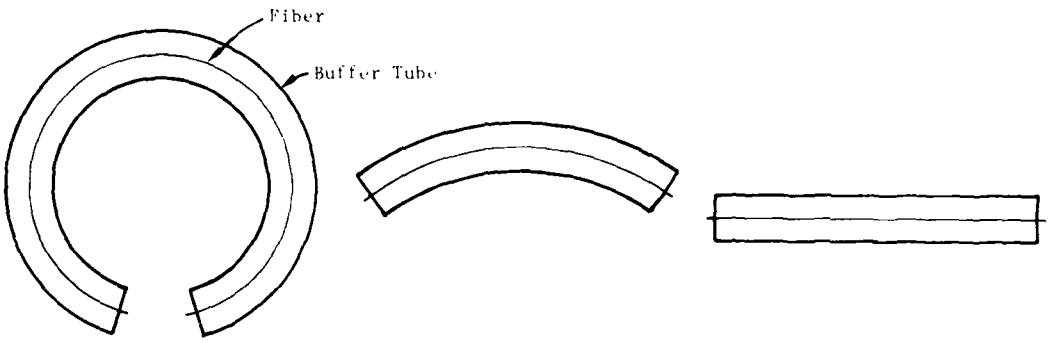

1. High Quality Optical Fiber Cable for Telecommunications
   G. Grasso, M. Pizzorno, A. Portinari
   Industrie Pirellie SpA Milan, Italy
   27th IWCS 1978

2. Fiber Optic Cable Design, Testing and Installation Experiences
   P. Bark (Siecor Opt.Cables, Horsehead, N.Y.)
   U. Oestreich, G. Zeidler (Siemens AG, Munich)
   27th IWCS 1978

3. Stress-Strain Behaviour of Optical Fiber Cable
   P. Bark (Siecor Opt.Cables, Horsehead, N.Y.)
   U. Oestreich, G. Zeidler (Siemens AG, Munich)
   28th IWCS 1979

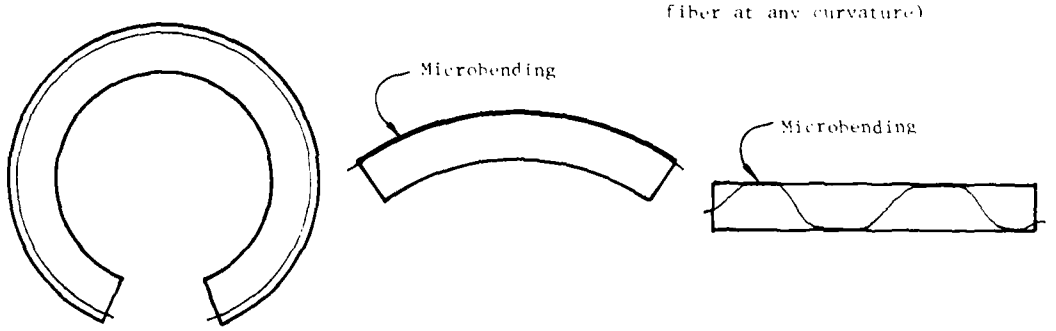
4. Bending Loss in Multimode Fibers with Graded and Ungraded Core Index
   D. Gloge
   Bell Telephone Labs., Holmdel, N.J.
   Applied Optics, Vol. 11, No. 11, Nov. 1972

5. Stress Analysis of CATV Al-Sheathed Cables Lashed to Hanging Steel Strand
   E. Winston
   Jerrold Electronic Corporation
   IEEE Trans. CATV, Vol. CATV-1, No. 1, Oct. 1976



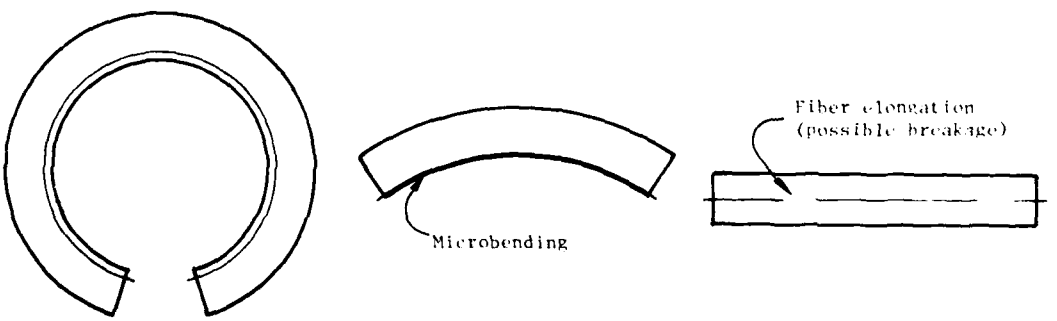

1a Large Curvature 1b Small Curvature 1c Zero Curvature

FIGURE 1 ZERO EXCESS LENGTH - i.e. fiber is the same length as the tube. (No stress on the fiber at any curvature)



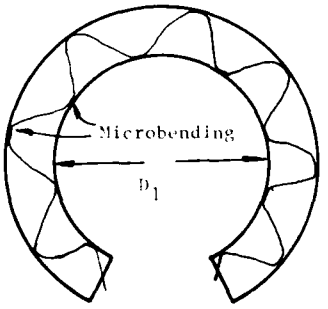

2a Large Curvature 2b Small Curvature 2c Zero Curvature

FIGURE 2 POSITIVE EXCESS LENGTH (Stress and microbending get worse as curvature decreases)

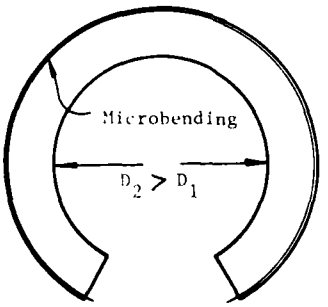



3a Large Curvature 3b Small Curvature 3c Zero Curvature

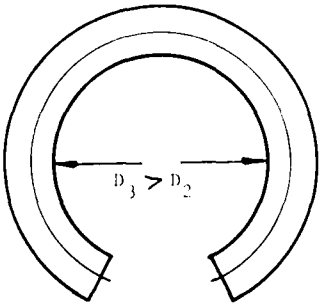
FIGURE 3 NEGATIVE EXCESS LENGTH (Stress and microbending get worse as curvature decreases)



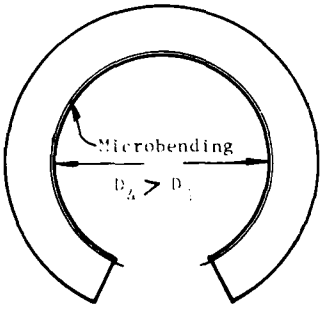

4a Fiber stressed transmission is low




4b Limit where stresses are relieved




4c Fiber is unstressed Transmission is maximum




4d Limit where fiber is stressed again

FIGURE 4 FIBER INSIDE THE BUFFER TUBE ON THE EXPANDING DRUM

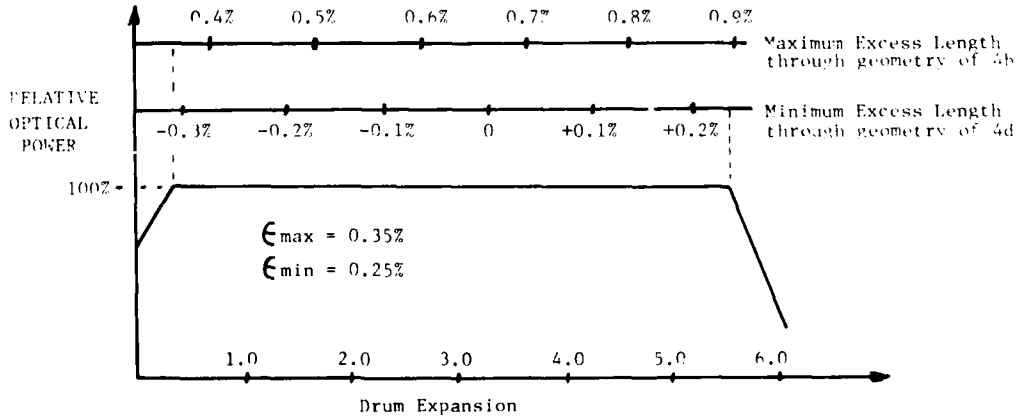



FIGURE 5 TRANSMISSION - EXPANSION CURVE

Maximum and minimum excess length scales are related to the drum expansion through the geometry of figures 4b and 4d.

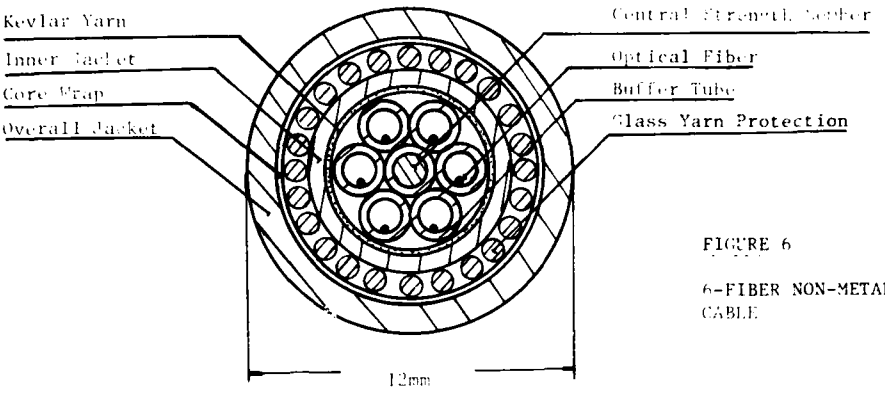



FIGURE 6

6-FIBER NON-METALLIC CABLE

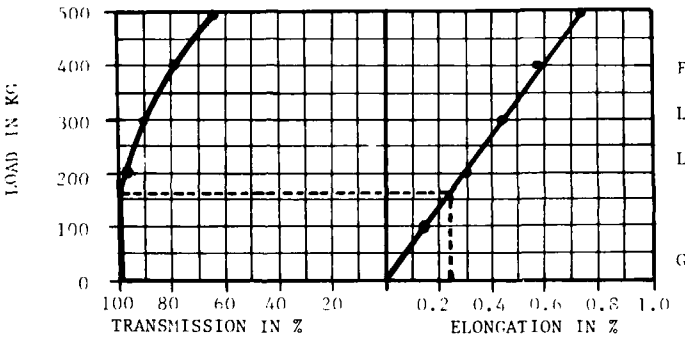



FIGURE 7

LOAD VS TRANSMISSION

LOAD VS ELONGATION

Gauge Length: 15.5m

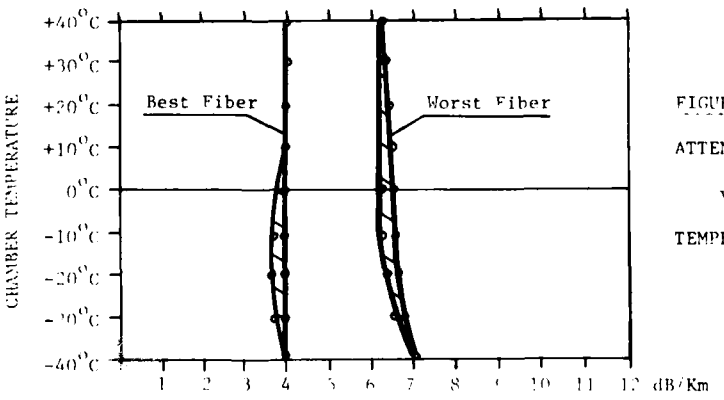



FIGURE 8

ATTENUATION

vs

TEMPERATURE



Mir Mujibar Rahman studied mechanical engineering in Bangladesh and graduated in 1973. After working one year with KSB Pumps & Co. in Dacca, he went to West Germany and completed his Masters (Dipl.-Ing.) from Technical University of Darmstadt. He worked in the Technical University of Berlin as a research assistant for a year and joined Siemens A.G., West Germany, in their R & D for telecommunication cables in 1968. In 1971, he was transferred to Siemens, Austria and worked in Vienna cable factories until 1976. Since 1977, he has been working with Canstar Fiber Optics in Montreal. At present, he is Manager - Cable Production and Development.



H. K. Eastwood received his doctorate in Physics from McMaster University in 1964. His association with Canada Wire and Cable stems from 1972 when he was manager of materials research for an affiliate company, Multi-State Devices Ltd. In 1976 he joined the fiber optics program as Group Leader for Systems and Components. Currently, he is Manager of Product Development for Canada Wire, Optical Fiber Product Division.



Paul Rivett graduated from the University of British Columbia with a degree in Engineering-Physics. In 1979 he joined the Fiber Optic Development Group at Canstar, a division of Canada Wire & Cable Ltd., where he worked on the analysis of excess length, its measurement and its effect on low temperature cable performance. Mr. Rivett has recently joined the Glass Technology Group at Canada Wire where he will be playing a leading role in the development of fiber optic components.



Manuel Herrera received a B.S. degree in Mechanical and Electrical Engineering from the Technological Institute of Monterrey (Mexico) in 1973. From 1973 to 1975 he worked for Conductores Montevreg/Canada Wire and Cable as a process engineer. From 1975 to 1979 he was employed at Northern Telecom as an R & D member in charge of communications cable design and process development. He is presently a Project Engineer with Canada Wire and Cable in charge of process development and cable design for the manufacture of fiber optic cables.

# FIBER OPTIC CABLE FOR AERIAL APPLICATION

Mr. Ulrich Oestreich, Dr. Gunter Zeidler
Siemens AG, Munich, West Germany

Dr. Peter R. Bark, Mr. Derek O. Lawrence
Siecor Optical Cables, Inc., Hickory, N. C.

## I. ABSTRACT

This paper discusses design considerations for fiber optic cables to be installed aerially. The determining criteria of an aerial cable plant are stability of transmission parameters, for a 30-to-40 year lifetime, and high reliability. It will be described how broad operating temperature range, wind and ice loading, pole distances and sag allowances have to be considered. The following cable designs will be discussed: self-supporting cable, Figure-8 cable and cable to be lashed to a messenger wire.

## II. INTRODUCTION

In general, aerial cables experience much higher mechanical and thermal variations than underground cable. Sections of duct and plow-in cable types are exposed to higher longitudinal and bending stresses for only a short time during installation. Assuming correct installation conditions and no other extrinsic failures such as damage through backhows, rodents or soil shifts, the remaining long term stresses and temperature variations in underground cables are considerably smaller than those in aerial cable plants.

In conventional aerial cable, for given loading conditions, long term cable strain values around 1% are very common. Because of the relatively large elastic region of copper no additional structural strength members are required. In fiber optic aerial cables, however, the allowable long term fiber strain determines, for a given life time and failure rate, the maximum total cable strain. In the following, design considerations for reliable fiber optic cable will be discussed together with the limiting parameters for given loading conditions.

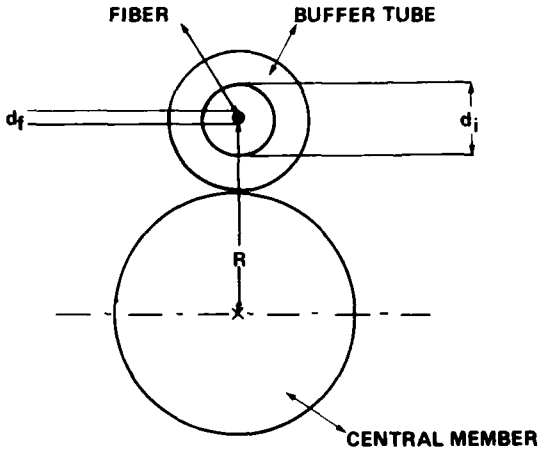
## III. CABLE DESIGN PARAMETERS

Because of its statistical nature, it is very difficult to extrapolate the results from short length, short term fiber breaking strength tests to predict allowable long term fiber stress levels. Long length, long term fiber stress test results under different load levels are not available. The only available design parameter is the fiber screen test level during fiber manufacturing. After application of a protective plastic coating, large volume commercially available fibers are screen tested over the entire fiber length with stress levels between 350 N/mm$^2$ and 700 N/mm$^2$ (50 to 100 kpsi) for approximately 1 second. Corresponding short term fiber strain values are 0.5% to 1% assuming a Young's modulus of approximately 70,000 N/mm$^2$ for silica or similar types of doped silica. By using the complex WEIBULL statistics, it is possible to extrapolate to long term fiber strain values which are in the range of 1/3 to 1/6 of the above mentioned short term fiber strain figures. This extrapolation, however, seems to be very doubtful because it has not been proven if the exponents of the WEIBULL distribution are constant over the entire range and how to take into consideration long fiber length (several kilometers), long life times (30 to 40 years) and high relative humidity levels.

Because of these uncertainties and unreliabilities - at least at this stage of the development - we assume cable designs where the optical fibers are under almost zero longitudinal stress for all loading conditions over the entire cable life time.

The compression layer of the outer fiber cladding guarantees a minimum long term stress level of approximately 80 N/mm$^2$ which corresponds to 0.11 % fiber strain. This value is sufficient to cover the bending strain required for stranding the fiber within a cable core. For fibers with an O.D. of 125 µm the limiting bending radius is approximately 60 mm.

In order to minimize fiber fatigue a cable concept using loosely buffered fibers has been developed (See Figure 1).




$d_f$ - fiber O.D.

$d_i$ - tube I.D.

R - radius of pitch circle

FIGURE 1. Geometry of Fiber Movement In A Loose Tube Design

Design details are described elsewhere[2]. For a strain free fiber the maximum strain $\frac{\Delta \ell}{\ell}$ of a stranded cable core is determined by:

$$\frac{\Delta \ell}{\ell} = -1 + \left[1 + \frac{4\Pi^2 R^2}{S^2}\left(\frac{d_i - d_f}{R} - \frac{(d_i - d_f)^2}{4R^2}\right)\right]^{\frac{1}{2}} \quad (1)$$

with -

$\ell$ = length of cable core

$\Delta \ell$ = change of length

$d_i$ = I.D. of buffer tube

$d_f$ = O.D. of fiber

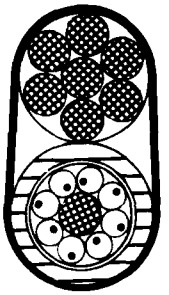
R = pitch circle radius

S = pitch

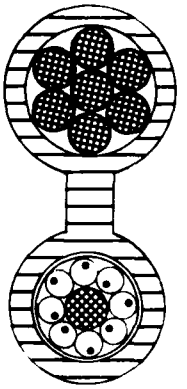
The operating "window" of this cable can be determined by variation of pitch, pitch circle radius and $d_i - d_f$, the free movement of fiber inside the buffer tube. The additional basic design parameter is the product of cross-section and Young's modulus of the longitudinal strength member. Preferred materials are extra high strength steel wires and stranded steel wire ropes or aramid yarns (Kevlar 49) for metal free designs.

## IV. SUPPORT ELEMENTS

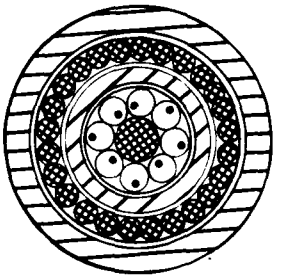
This section describes the different design options for the support element of aerial cable. The support element is generally one of three types (Figure 2):



1. Messenger Wire



2. Figure-8 Design



3. Self-Supporting Design

FIGURE 2. Types of Aerial Cable Designs

### 1. Messenger Wire

This is the most common type used in the field of telecommunications cable installations. The advantage of the messenger wire is that it can be installed prior to the cable and therefore allows the correct tensioning for expected loading conditions or creep and plastic deformation.

The most common messenger wires are extra high strength (EHS) stranded steel ropes 6 mm to 13 mm in diameter. The Young's Modulus for these materials is around $2 \times 10^5$ N/mm$^2$, the breaking strength approximately 2000 N/mm$^2$. Utility grade messenger wires consist of a lower grade, softer steel; the breaking strength is in the order of 1000 N/mm$^2$. Plastic deformation after initial installation in the order of 0.1% and unavoidable long term creep of 0.1% are typical figures to consider for the strain calculations described in Section V.

For all-dielectric requirements, ropes made of Kevlar 49 can be used. A higher safety margin for creep, plastic strain and construction stretch have to be considered. Because the Young's modulus is

lower than that of steel ($1.2 \times 10^5$ N/mm$^2$) approximately 60% more Kevlar 49 (by cross section) is required for the same strength level.

In both cases a lashing wire ties the fiber optic cable to the messenger wire.

2. Figure-8 Design

In this configuration the support element and the cable are held together by a common outer PE jacket. Designs of this type very often are used for aerial CATV cables. On one hand the installation time is reduced to approximately 50%, on the other hand Figure-8 cables are larger in diameter and shorter lengths per reel can be handled. The initial plastic strain of the support element during installation - either steel or Kevlar rope is directly transferred to the fiber optic cable.

3. Self-Supporting Design

In this technique, the support elements are integrated into the cable design. Two different design principles are possible:

- -Support element is located in the center of the cable core. This design is straightforward and provides the least overall diameter. However, installation of the cable, which requires anchoring the central element, becomes very complex and offsets any other advantages this design has.

- -Support element is located under or over the outer cable jacket. This design eliminates the installation disadvantages as described above. The cable core, however, has to be very strong and resistant against lateral forces exerted by the outer support wires or Kevlar yarns. Optimisation between the pitch length of the support elements with respect to cable flexibility and crushing of the core under extreme loading conditions is difficult.

In summary one can conclude that the self-supporting designs provide the least overall cross-section for cable and support member. This is significant when the effect of ice and wind loading is considered. Transfer of initial strain to the cable core is unavoidable in the case of both self supporting and Figure 8 designs. The most suitable aerial cable type which is simple to handle and whose performance is relatively easy to predict for the various loading conditions is the dedicated messenger/lashed cable combination.

## V. CALCULATIONS

1. Catenary Equation

Having determined the exact behavior of the cable when subjected to change of stress and temperature, it becomes necessary to determine the actual arc lengths and tensions corresponding to any definite span and sag. For this purpose the catenary equation is used.[3] Figures 3 and 4 show two cases for poles being at the same level (symmetric case) and at different levels (assymetric case). For the following calculations we use the more common assymetric case. The catenary equation describes the following relationship:

$$Y = Y_0 \,\mathrm{COSH}\,\left(\frac{x}{y_0}\right) \tag{2a}$$

$$Y_1 - Y_2 = Y_0 \left\{ \mathrm{COSH}\,\left(\frac{x_1}{y_0}\right) - \mathrm{COSH}\,\left(\frac{x_2}{y_0}\right) \right\} \tag{2b}$$

with -

$$Y_0 = \frac{F_0}{G} \tag{3}$$

The sag is described by:

$$Y' = Y_0 \left\{ \mathrm{COSH}\,\left(\frac{x}{y_0}\right) - 1 \right\} \tag{4}$$

The cable tension at any point in the span becomes:

$$F = Y \cdot G \tag{5a}$$

$$F_1 = Y_1 \cdot G_1 \tag{5b}$$

$$F_2 = Y_2 \cdot G_2 \tag{5c}$$

The length of the cable is:

$$L = 2 \cdot \frac{F_0}{G} \cdot \mathrm{SINH}\,\left(\frac{x}{y_0}\right) \tag{6}$$

The following simplifications have been made:

- -stiffness of cable and support element do not lead to any deviation from the catenary,

- -load distribution along the span length is homogeneous,

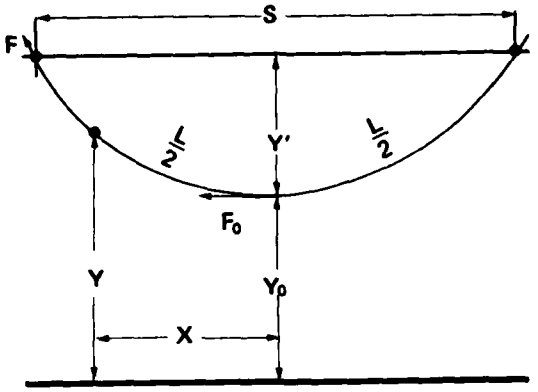
- -the cable strain behavior is determined by the support element

- -the temperature along the span is constant.

Within a span $F_0$, the horizontal tension, is constant. The highest tension within a span is at the highest support point, i.e., $F_1$ (see Figure 4). For a given highest tension $F_1$ an acceptable elastic cable strain $\varepsilon_{elastic}$ can be calculated

for the specific Young's modulus E and the cross-section A of the support element.

$$F_1 = \varepsilon_{elastic} \cdot E \cdot A \qquad (7)$$




S = Span Length

L = Cable Length

F = Cable Tension at Support

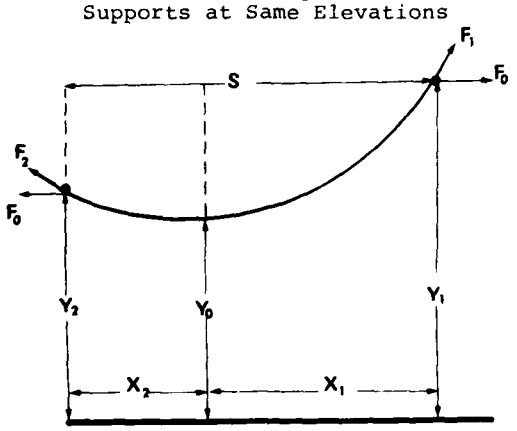
$F_0$ = Cable Tension at Center of Span

G = Resultant Weight per Length of Cable

Y' = Sag

X/Y = Coordinates of any Point of Cable from Origin

FIGURE 3. Catenary Diagram For Supports at Same Elevations




$F_0$ = Horizontal Cable Tension

$F_1$, $F_2$ = Cable Tensions at Coordinates $X_1/Y_1$ and $X_2/Y_2$ (Support Points)

$S = X_1 + X_2$ = Span Length

FIGURE 4. Catenary Diagram for Supports at Different Elevations

The following additional data of the support element have to be available:

- -Temperature coefficient of linear expansion,
- -creep coefficient,
- -deviation from the linear elastic stress-strain behavior.

The customer usually defines:

- -Pole distances,
- -difference in elevation of supporting poles,
- -maximum allowable sag,
- -operating temperature range,
- -maximum loading conditions (ice and wind).

With these assumptions and the above given equations, the following parameters can be calculated when using a special computer program:

- $-F_x$ - cable tension at any point in the span.
- $-F_0$ - horizontal tension.
- $-\varepsilon_x$ - cable strain at any point in the span and the total strain.
- $-L_1$ - arc length of cable in the load free condition.
- -Y' - the cable sag(s).

The total specific cable strain is given by the difference between maximum cable length $L_{max}$ under maximum load and initial cable length $L_0$ after installation under no load:

$$L_{max} = L_0 (1 + \varepsilon_{total}) \qquad (8)$$

The total specific strain $\varepsilon_{total}$ of an aerial cable (including support element) consists of the following strain components:

- -elastic cable strain $\varepsilon_{elastic} = \frac{F}{E \cdot A}$ (see equation 7)
- -temperature strain

$$\varepsilon_{temperature} = \alpha (T_2 - T_1) \qquad (9)$$

- -plastic strain $\varepsilon_{plastic}$, resulting from plastic deformation and construction stretch
- -creep $\varepsilon_{creep}$, plastic deformation due to creep within the material of the support elements.

$$\varepsilon_{total} = \frac{F}{E \cdot A} + \alpha (T_2 - T_1) + \varepsilon_{plastic} + \varepsilon_{creep} \qquad (10)$$

To determine the worst case conditions, the effect of a radial ice load per unit length around the cable and messenger is considered. If ice and wind loadings have to be considered the components have to be added vectorially (ice vertical, wind horizontal). The table below shows typical loading conditions for the United States.

| | LOADING DISTRICT | | |
|---|---|---|---|
| | Heavy | Medium | Light |
| Radial thickness of ice | 13 | 6 | 0(mm) |
| Horizontal wind pressure | 200 | 200 | 425 Pa |
| Resultant wind force | 65 | 65 | 95kmph |
| Temperature | -18 | -10 | -1 C° |

TABLE 1: Typical Loading Conditions for the United States[5]

As a result, in heavy loading districts effective cable weights can be 5 to 10 times their actual weight.

2. Parabolic Equation

For sag tension calculations with support poles on the same or slightly different levels, the cables are assumed to take the form of a parabola instead of their actual form of a catenary. The error is negligible and the computations are much simplified. The equation used in calculating sags is[4]:

$$Y_x = \frac{G \cdot L}{8 \cdot F_x} \qquad (11)$$

All other assumptions on loading, cable strain and support element characteristics are handled in the same way as in the previous paragraph.

Typical Examples

Figures 5 and 6 show as a function of pole distance, the variation of cable tension, strain and sag. The fiber optic cable is lashed to a messenger wire system where the support poles are on the same level. In these examples a 10 fiber cable was assumed having a weight of 100 kg/km and an O.D. of 10 mm. In Figure 5 the pulling tension for installing the messenger wire varies as a function of pole distance, in Figure 6 this pulling tension is constant along the pole line as in the practical situation. In both cases the maximum allowable sag is 1.5 m for a maximum radial ice thickness of 25 mm. Parameters are wind (65, 95 kmph) and temperature (-30°C to +60°C).

Assuming 2000 N/mm$^2$ maximum long term stress (equal to 1/3 of breaking tension) for the 6.4 mm O.D. EHS messenger wire, 15000 N is the maximum tolerable long term tension. In both examples the limiting pole distance lies between 60 to 70 m. Including 0.1% for plastic strain and 0.1% for creep of the messenger wire, the total specific strain reaches approximately 0.6% for 60 to 70 m pole distances. Stress and strain figures are drastically lower for 13 mm radial ice loading and easily allow to span pole distances up to 80 to 90 m.

## VII. INSTALLATION EXPERIENCES

Within the past 3 years Siecor has successfully installed a series of aerial cable plants (See Table 2). Some of these installations contain aerial sections as part of the total passive transmission subsystem. In all cases the optical cable was lashed to a 6.4 mm (1/4") EHS or 9.6 mm (3/8") utility grade messenger wire.

It has been proven that these cables are easy to install by normal installation crews using conventional tools and techniques. In addition, the ease of handling allows the cable to be installed faster. Exposure to several winters of ice loading on these cables as well as wind storms did not cause any measureable change of the cable performance.

## VIII. SUMMARY

It has been demonstrated that fiber optic cables for aerial installations can be designed for different types of environmental conditions. Reliability and long term stability can be achieved in cable structures using a loose tube fiber buffering technique. The most common and successful type of installation is lashing the optical cable to a dedicated messenger wire. The practice has proven that fiber optic cables can be handled more easily than copper cables.

## ACKNOWLEDGEMENT

The authors wish to thank Mr. W. Lindig at Siemens AG for suggestions made on the computer program for calculating the results under different loading conditions.

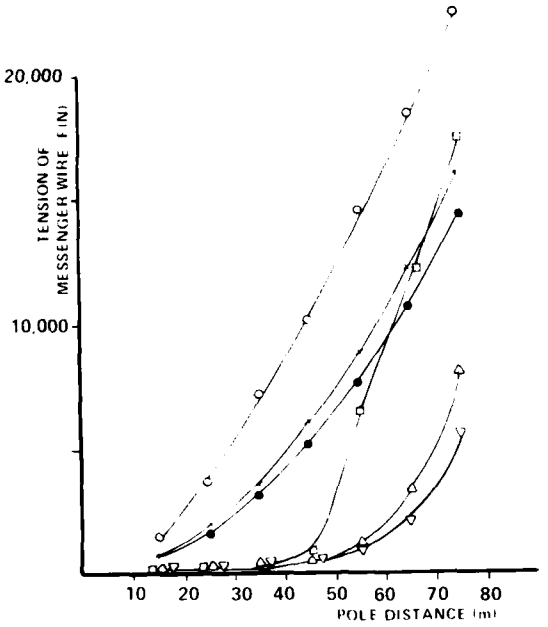



FIGURE 5a.

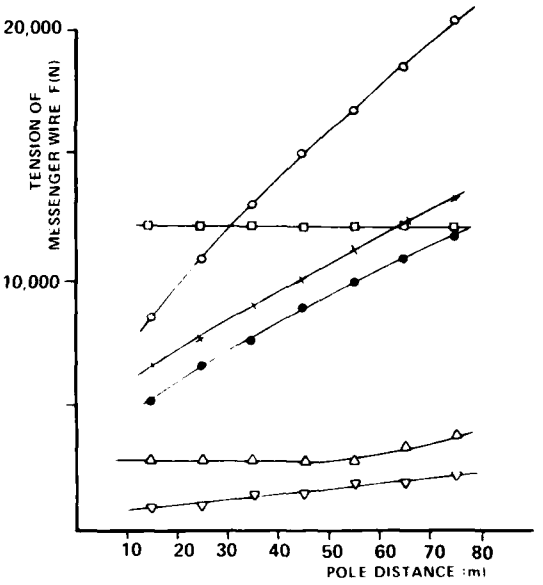



FIGURE 6a.

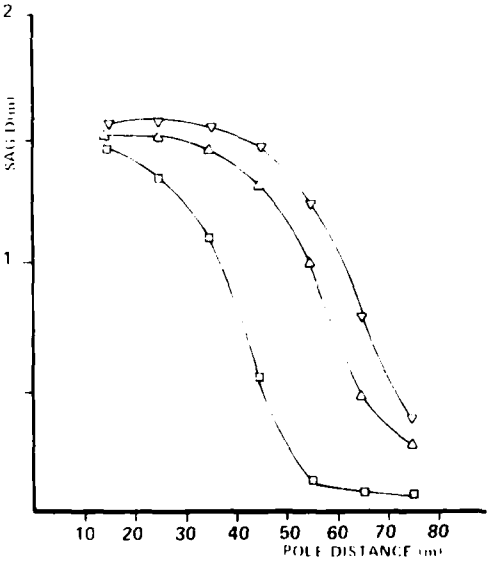



FIGURE 5b.

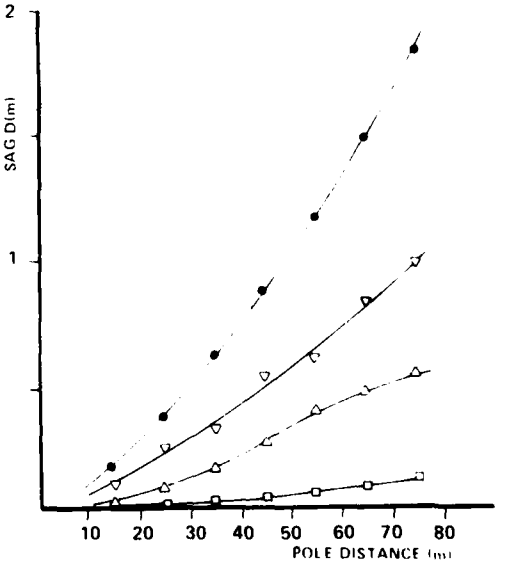



FIGURE 6b.

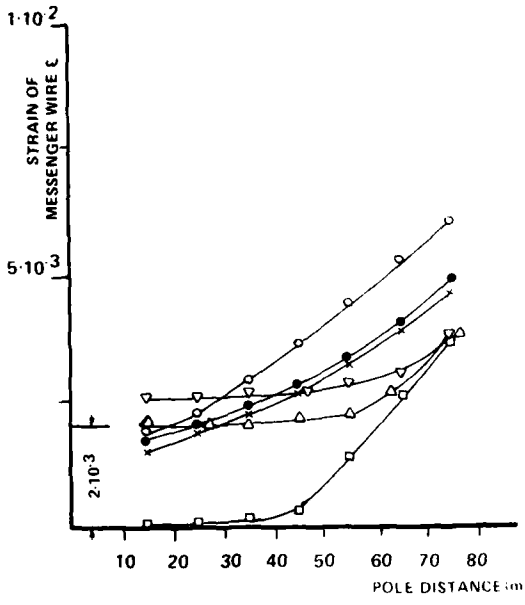



FIGURE 5c.

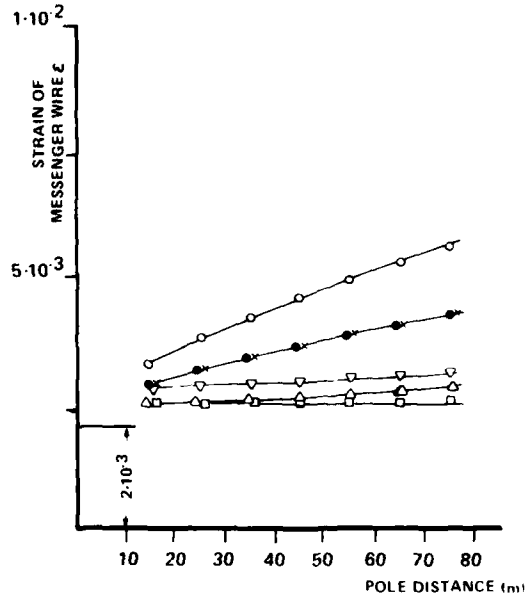



FIGURE 6c.

- ● 25 mm ice, -5°C, no wind
- x 25 mm ice, -30°C, 65 kmph wind
- ◦ 25 mm ice, -30°C, 130 kmph wind
- Δ No ice, 15°C, no wind
- ∇ No ice, 60°C, no wind
- ◻ Installation of messenger wire at 15°C (without plastic strain)

Tension, strain and sag for cable and messenger combination as a function of pole distance for various temperatures, ice and wind loading conditions.

FIGURE 5. Messenger Stringing
Tension Varying with Pole Distance

FIGURE 6. Messenger Stringing
Tension Constant

TABLE 2. SIECOR AERIAL CABLE INSTALLATIONS

| YEAR | PROGRAM | LOCATION | LOADING DISTRICT | MESSENGER WIRE | LENGTH (km) | REMARKS |
|---|---|---|---|---|---|---|
| 1978 | CATV | Missouri | heavy | 6.4mm (1/4") EHS | 6 | Hybrid cable |
| 1978 | T3 | Pennsylvania | heavy | 6.4mm (1/4") EHS | 7.5 | All-dielectric partly over-lashed |
| 1979 | T3 | Pennsylvania | heavy | 6.4mm (1/4") EHS | 10 | ---- |
| 1980 | Data | California | light | 9.6mm (3/8") UG | <1 | Hybrid cable overlashed |
| 1980 | T3 | Georgia | medium | 6.4mm (1/4") EHS | 3 | ---- |
| 1980 | Data | New York | heavy | 9.6mm (3/8") UG | 11 | All-dielectric |
| 1980 | Test | Massachusetts | heavy | 9.6mm (3/8") UG | 1 | All-dielectric Layered Design |

REFERENCES

[1] P. R. Bark, U. Oestreich, G.H. Zeidler: Fiber Optic Cable Design, Testing and Installation Experiences; Proceedings of 27th International Wire & Cable Symposium, Cherry Hill, November 1978, p. 379-384.

[2] P. R. Bark, U. Oestreich, G.H. Zeidler: Stress-Strain Behavior of Optical Fiber Cables; Proceedings of 28th International Wire & Cable Symposium, Cherry Hill, November 1979, P. 385-390.

[3] ALCOA Aluminum Overhead Conductor Engineering Data #8: Graphic Method for Sag-Tension on Calculations for ACSR and Other Conductors. Alcoa, Rome Cable Division, copyright 1961.

[4] E. Brandt, R. Thomas: Der Einfluss der bleibenden Seil-Dehung auf das Durchhangs-Verhalten von Freileitungen, Elektrizitaetswirtschaft Jg. 78 (1979), Heft 8, p. 262-268.

The Lineman's and Cableman's handbook: Fundamentals of Line Design, p. 8-15 5th edition, McGraw Hill Book Co., 1976.





Ulrich Oestreich

Siemens AG
Telecommunication Cables

Munich, West Germany


Ulrich Oestreich was born in 1928 in Berlin. He received a Dipl.-Ing degree in electrical engineering at the Technical University in Berlin. In 1953, he joined the Siemens-Cabel-Works in Berlin and was involved in the development of high-voltage and telecommunication cables. Since 1974, he has been with the telecommunication cable department in Munich, where he holds a managing position for developing and manufacturing of fiber optic cables.




Peter R. Bark

Siecor Optical Cables, Inc.

Hickory, North Carolina 28601


Peter Bark holds a bachelor of science degree from the Technical University at Munich. He also received his doctorate in engineering from the same institution in the field of molecular beam physics. He has been employed by Siemens AG in Munich, West Germany since 1971, in several positions in the telecommunications cable field. His principal assignments were in the field of developing optical cables, interconnecting hardware and subsystems. Since 1977 Peter Bark has been vice presidnet for engineering at Siecor Optical Cables, Inc.




Gunter Zeidler

Siemens AG
Telecommunication Cables

Munich, West Germany


Gunter Zeidler holds a Dipl.-Ing degree in electrical engineering and a PhD in Physics. In 1965, he joined the Central Labs of Siemens AG, in Munich, working in the laser field. In 1972 he changed to the Research Labs holding a managing position in the field of fiber and integrated optics. Since 1976, he has been with the telecommunication cable department in Munich and is responsible for the development and manufacturing of fiber optic cables and ancillary hardware.




Derek O. Lawrence

Siecor Oprical Cables, Inc.

Hickory, North Carolina 28601


Derek Lawrence graduated from the City University, London with a degree in communications engineering. Since 1970 he has held various engineering positions with leading telecommunications cable manufacturers in Great Britain, Canada and the U.S.A. His first involvement with optical communications cable was exclusively in this field. He is currently engineering manager at Siecor Optical Cables, Inc.

# OPTICAL FIBRES IN OVERHEAD POWER TRANSMISSION SYSTEMS FOR COMMUNICATION AND CONTROL.

B.J.Maddock
Central Electricity Research Laboratories, Leatherhead, Surrey, England.

K.L. Lawton
BICC Telecommunication Cables Limited
Blackley
Manchester, England.

K.H. Pickup
BICC Metals Limited
Prescot,
Merseyside,
England.

## Summary

This paper describes the development of a novel application in the United Kingdom of optical fibre technology to communication and control in electric power systems. The essential feature is the incorporation of a non-metallic induction-free optical fibre cable within conductors suitable for use in overhead power lines. The basic design considerations for the cable and the conductor are discussed. Two trials are in progress. In the first, the conductor containing the optical fibre cable has been strung as the earth wire of a high voltage test line while in the second it is smaller and is an addition to a medium voltage line on wooden poles. These new conductors are designed to have similar suspension characteristics to the existing phase conductors. Erection and test details are given. No serious problems have been encountered to date and the performance is most encouraging. A full system trial, to carry regular communications traffic on an operational line, is planned for 1981.

## 1.0 Introduction

Electric power systems need substantial communication facilities for their effective operation. These facilities are based typically on private or leased circuits, on microwave links and on power line carrier channels. Optical fibre communication is rapidly becoming an important additional technique with the special advantages of interference immunity, high capacity and freedom from radiation and frequency assignment difficulties. Furthermore, because the cable can be entirely non-metallic, it may be used in close association with high voltage equipment and to eliminate difficulties caused by rises of earth potential during power system faults. [1.2.3.]

In addition to administrative telephone traffic, channels are required for control telephony, remote control, telemetry, computer data, protection signalling (e.g. for the automatic opening of circuit breakers) and, in the future, various forms of video transmission. All these signals may be suitably coded, usually in digital form, and transmitted over optical fibre links. We are especially interested in incorporating the fibre cable within the conductors of overhead power lines, both transmission and distribution, to provide a wide range of communication facilities. [4.5.6.] Making use of the overhead lines in this way is particularly appropriate when the land beneath them is not owned by the utility or when it is unsuitable for ground laid fibre cables.

For example the Research and Transmission Division of the Central Electricity Generating Board are studying the technical and economic feasibility of a figure-of-eight ring network based on a number of its 400 kV lines in which the earth conductor would contain the optical fibre cable.[7.] This network would naturally link the major power and switching stations on it and could connect to all the principal headquarters, control centres and research laboratories from London and Bristol in the south to Manchester and Harrogate in the north. It would offer improved security and diversity of communications and provide substantial capacity for future needs.

Spurs would be needed to connect some of the centres to the power line routes and these could use optical fibre cables underground or on lower voltage lines, microwave links or post office circuits as appropriate. Some typical data for this network are given in Table 1. Because it is difficult to take a power line out of service for modification, a network of this scale would have to be installed in stages, taking advantage whenever possible of any reconductoring of existing lines, because of age or uprating, and of any construction of new lines.

TABLE 1

| | |
|---|---|
| Approximate length of ring network | 1000 km |
| Lengths between stations | 10-200 km |
| Number of channels for present telephony | 40-100 |
| Corresponding bit rate | 8 Mbits/s |
| Bit rate to cover future needs | 34 Mbits/s |
| Number of fibres | 4 - 8 |
| Repeater spacings (850/900nm wavelength) | 10-15 km |
| (1300 nm wavelength) | 20-40 km |

## 2.0 Possible Arrangements

When considering the mounting of an optical fibre cable along an overhead power transmission system consisting of wooden poles or steel towers, a number of ways appear possible. For convenience all these can be grouped under three main techniques; the cable could be suspended from the supports completely independent and separate from the line conductors, it could be fastened to one of the conductors for support or it could be mounted within a conductor. We will consider these three techniques under separate headings.

### 2.1 Self-supporting Cable

A self supporting cable in addition to carrying the fibres would need to have sufficient strength to withstand wind and ice loads and would, therefore, need to be fairly robust section. This could impose additional tower loadings which may often not be acceptable.

If the coefficient of thermal expansion is substantially different from the metal line conductors which is likely, adequate clearances may not always be available and the differences in sag with temperature could cause serious problems.

### 2.2 Fastened to a Conductor

This technique would create some difficulties such as the need for special installation equipment, increased wind and ice loadings, adverse aerodynamic effects, damage from clashing of conductors and deterioration of the fastenings by the weather.

### 2.3 Mounted Within a Conductor

By mounting the optical fibre cable within a conductor most of the above difficulties can be overcome. This assumes that the conductor used is comparable to the other line conductors and that the optical cable is light in weight. Generally speaking it will be more convenient to mount the cable in an earth or ground wire but in distribution lines at lower voltages where only the phase conductors exist these could be used.

## 3.0 Conductor and Cable Designs

In designing a conductor with an optical fibre cable within it certain primary objectives have to be achieved. So far as the conductor is concerned it must be designed to match the physical properties and dimensions of the other conductors in any given system so that it behaves similarly in terms of sags, tensions, wind and ice loadings and dynamic characteristics It must also match its companion conductors electrically in terms of current carrying capacity, including fault currents.

The optical fibre cable needs to be small in section, light, able to withstand the stresses and strains applied to it and resistant to environmental attack. It should be non-metallic to avoid additional electrical problems and must of course, fulfil the telecommunication requirements of the system.

### 3.1 Conductor Design

As already mentioned the conductor must match the physical properties and dimensions of existing conductors or earth wires, a popular type of which consists of a stranded steel core of 7 wires surrounded by 54 aluminium wires, see Fig.[1].

A basic concept of the optical cable conductor is that the fibre cable is placed in the centre of the conductor, and because of the relative delicacy of the glass fibres, as little strain as possible should be placed upon them. It is advantageous, therefore, for the cable to be free to move longitudinally within the conductor. This can be achieved in various ways but the one described and which is shown in Fig.[2] consists of the optical fibre cable in an aluminium alloy tube surrounded by 60 alloy wires. The tube is formed by extruding a suitable section, laying in the cable and closing by drawing. This tube as well as contributing to the tensile strength and current carrying capacity of the conductor, protects the cable from radial forces including those imposed by dead end and suspension fittings. Around this tube can be stranded for alternative designs, one or more layers of wires which may be aluminium, aluminium alloy or steel with various coverings or any combination of these wires. By this means the required current carrying capacity and strength to weight ratio can be achieved. The various properties of the conductors shown in Figs. [1] and [2] are given for comparison in Table 2. This example indicates that by suitable selection of aluminium tube diameter and stranding details an optical fibre cable conductor can

be produced to take the place of a standard conductor.

In addition to the geometrical design details described the optical fibre conductor must behave as well as a normal conductor and with no detriment to the fibre when subjected to typical overhead line operating conditions including creep, high temperature - about 120°C - caused by fault currents, low temperature, high strain caused by wind and ice or corrosion. Total conductor strains of the order of .25 to .35% may occur after 30 years service.

Because the optical fibre cable must continue beyond the dead end fitting, special attention needs to be paid to this feature and one type of fitting which is ideally suitable for this is the preformed aluminium alloy (or steel) helical grip dead end. Other types are currently being developed and it is considered that a modified form of compression dead end could also be used.

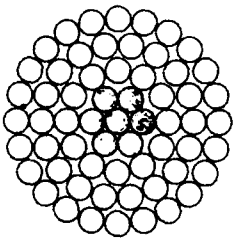


Fig.1
Zebra Conductor Section

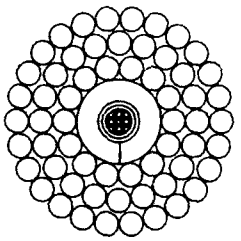


Fig.2
Zebra equivalent optical fibre conductor.

## 3.2 Optical Cable Design

The optical cable as shown in Fig. 3 comprises four fibres, each loosely housed in tubes which are helically laid up around a bundle of Kevlar filaments, a polyester tape is helically applied and finally a black polyethylene sheath brings the cable to an overall diameter of 4.6 mm. The tubes are manufactured by a technique pioneered by the British Post Office [7]. They are 1.3 mm outside diameter, 0.8 mm inside diameter polyethylene terephthalate tubes extruded under conditions such that a high degree of molecular orientation is obtained in the longitudinal direction. By this process a low coefficient of thermal expansion and a high longitudinal elastic modulus is achieved, thus avoiding problems of differential movement between fibre and tube. The plant used is shown in Fig.4.

TABLE 2

| | Zebra equivalent | Zebra |
|---|---|---|
| Material | All Aluminium Alloy | Aluminium round steel |
| Construction | 60 x 3.0 mm dia wires round 10.6 x 5.2 mm dia tube | 54 x 3.18 mm aluminium wires round 7 x 3.18 mm steel wires |
| Overall dia | 28.62 mm | 28.62 mm |
| Breaking load | 13630 kg | 13450 kg |
| Weight | 1577 kg/km | 1621 kg/km |
| Breaking length | 8.64 km | 8.3 km |
| Mod. of elast. | 5710 kg/mm$^2$ | 7040 kg/mm$^2$ |
| Coeff. of linear expansion | 23 x 10$^{-6}$/°C | 19.3 x 10$^{-6}$/°C |
| Maximum D.C. resistance at 20°C | 0.067 ohm/km | 0.0674 ohm/km |

The prime consideration in the manufacture of any optical cable is the prevention of stress and microbending caused by lateral compression. This is minimised by loosely housing the fibre in a tube, detorsioning the tube during lay-up and by the helical construction of the cable. With the fibre used in these cables, the maximum cable extension before the risk of fibre breakage occurring is about .4% . The long term situation is currently being assessed but the indications are that the maximum safe continuous extension is about 0.3% . The sources of conductor elongation which could lead to strain on the cable have already been given and if it is assumed that the composite conductor moves together under strain, i.e. no relative movement between fibres, optical cable and the conductor, then the fibres could be subject to the estimated strains given in Table 3 for a span length of 366m. The characteristics of the fibres are given in Table 4.

As the optical cable was laid in the U-section, a high melting point grease (drop point 130°C) was used to fill the annular gap around the optical cable in order to inhibit corrosion of the conductor and reduce the ingress of moisture which could affect the fibre. The laying-up operation again was undertaken with care to avoid undue stresses on the optical cable.

All these procedures resulted in only minor attenuation changes which are shown in Table 5.

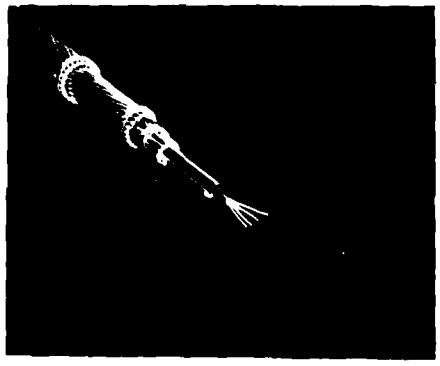


Fig 3. Optical fibre cable in an aluminium alloy conductor

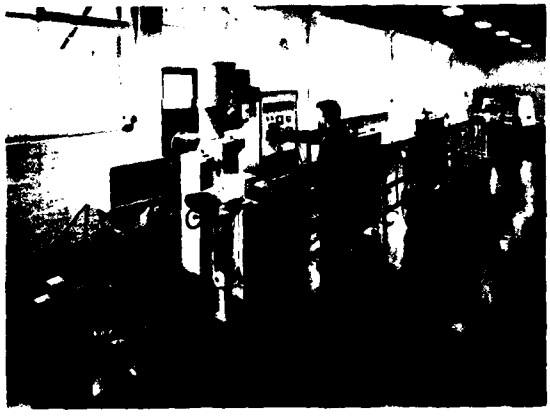


Fig 4. Manufacture of optical fibre cable.

## 4.0 Field Trials

To demonstrate the successful production and erection of the composite conductors of the type described above and to monitor their performance under varying weather conditions, two field trials are in progress.

### 4.1 CERL Trial

A conductor of the type shown in Fig. 2 was strung on 5/6 July 1979 as an earth wire on the high voltage test line at the Central Electricity Research Laboratories (Fig. 5). The total installed length is 860 m, the longest span being 366 m. Normal erection procedures and equipment, including tension running gear, were used and no special problems were encountered. Preformed helical grip tension fittings were used to avoid undue crushing of the optical fibre cable.

TABLE 3

| Operating Condition | Strain immediately after erection | Strain after 20 years service |
|---|---|---|
| Everyday stress condition 15°C conductor temperature | 0.09% | 0.12% |
| 75°C conductor temperature, still air. | 0.21% | 0.24% |
| 170°C conductor temperature still air (short circuit condition) | 0.32% | 0.35% |
| Specified maximum working load condition - 6°C 12.7 mm radial ice thickness, 380 N/m² wind load | 0.16% | 0.18% |

TABLE 4

| | |
|---|---|
| Fibre Type | Graded Index |
| Cladding diameter | 125 um |
| Core diameter | 63 um |
| Coating | laquer |
| Nominal attenuation | 5 dB/km at 820 nm |
| Nominal bandwidth | 200 MHz km |
| Numerical Aperture | 0.2 |

TABLE 5

| Attenuation, dB/km, at 900 nm | | | | |
|---|---|---|---|---|
| Fibre no. | 1 | 3 | 2 | 4 |
| Initial | 4.9 | 5.8 | 4.6 | 5.0 |
| In conductor | 5.4 | 6.0 | 4.6 | 5.5 |
| Erected | 5.3 | 6.1 | 4.3 | 5.2 |
| Spliced | 5.0 | | 5.1 | |

Measurements of the optical attenuation of the fibres were made by the cut-back technique at various stages during manufacture and erection and a summary of these is given in Table 5. Although all the results are scaled to dB/km those in the top part of the table are not strictly comparable with those at the bottom because, soon after erection, excess conductor was cut off and the four fibres spliced in pairs, at the far end of the line, to give two loops of about 1.7 km each. The changes in attenuation shown are relatively small and often of the same order as the reproduceability of this type of field measurement (about $\pm$ 0.2 dB). They arise because of changes in the small strains on the fibres and because the attenuation is not uniform along the fibres. Fig. 6 shows back-scatter traces for the two loops with the splices (a), end reflections (b) and one small fibre defect (c) indicated.

The dependence of the line attenuation on conductor temperature is being studied and preliminary results indicate that over the temperature range encountered during the observations (+5 to + 30°C) the change is small, less than $5 \times 10^{-3}$ dB/km°C and probably even lower. Excluding the first hour, the creep strain in the conductor had amounted to about 0.02% over the first year.

Various signals have been transmitted successfully over this line including camera control and television signals, the latter using a pulse position modulation system (13 MHz pulse rate). More recently 8 Mbit/s (120 channel) terminal equipment has been installed which uses LED transmitters (900 nm) and APD receivers with a 3B4B line code. Additional attenuation has been inserted in one loop to bring it up to a total of 35 dB and while feeding this from a pattern generator via one of the 2 Mbit/s tributaries in the multiplexer, bit error rates of $10^{-10}$ have been achieved.

4.2 SEEB Trial

The second trial has just been started by the South Eastern Electricity Board on a wooden pole line at Hackbridge, Surrey, England. The line consists of three Wolf conductors, 30/7/2.59 mm, running at 11 kV without an earth wire.

The optical fibre conductor is shown in Fig.7 and the existing conductors in Fig. 8, Table 6 gives their characteristics. Fig. 9 shows a photograph of the test line.

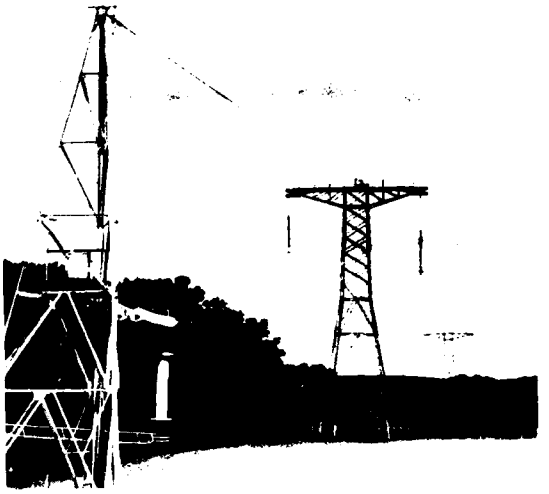


Fig.5 Test line at CERL with optical fibre earth conductor running from top of tower at left.

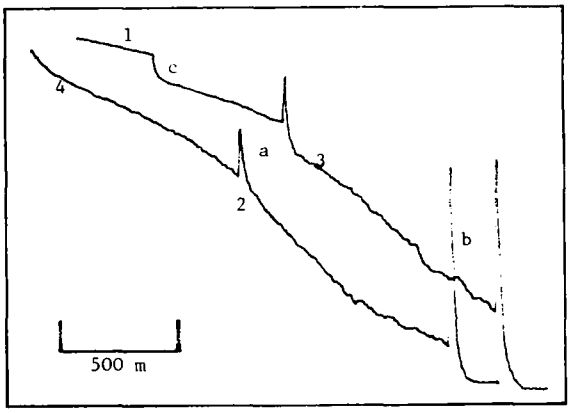



Fig.6 Back-scatter traces (offset horizontally by 200 m for clarity) for loops 1/3 and 4/2.

The conductor consists of an aluminium alloy tube with one layer of 14 wires. A 4 fibre optical cable 4.6 mm overall dia is situated inside the tube.

The line is 1151m long and consists of two sections one 677 m long having 5 spans and the other 504 m long also having 5 spans. There is an anchor pole at each end and one angle pole in the middle. Conductor fittings used are preformed aluminium alloy helical grip type, dead end and suspension. The test conductor is suspended 1m below the phase conductors. Sag and tension calculations show through a temperature range from -7°C to +50°C the test conductor should not deviate more than 130 mm from the line conductors.

A sub-station 100m from one end of the line will be used as the performance monitoring station. An underground optical fibre cable connects with the test line. Optical fibre splices are assembled at each end of the line and in the middle. Two pairs of fibres are connected together at the far end so that there are effectively 2 test fibres about 2400m long plus 340m of underground fibre.

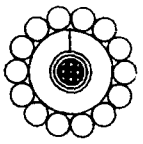


Fig 7. Optical fibre conductor

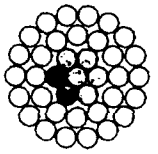


Fig 8. Wolf steel cored aluminium conductor

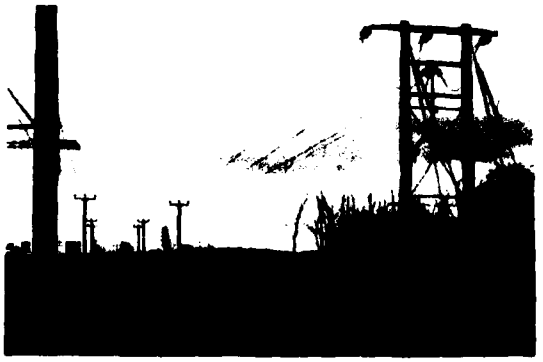


Fig 9. SEEB test line with optical fibre conductor shown furthest right

TABLE 6

| | Wolf equivalent | Wolf |
|---|---|---|
| Material | All aluminium alloy | Aluminium round steel |
| Construction | 14 x 3 mm wires round 10.6 mm x 5.2 mm dia tube | 30 x 2.59 mm aluminium wires round 7/2.59 mm steel wires |
| Overall dia | 16.6 mm | 18.13 mm |
| Breaking load | 4340 kg | 7056 kg |
| Weight | 454.3 kg/km | 726 kg/km |
| Breaking length | 9.55 km | 9.72 km |
| Mod. of elast. | 6020 kg/mm$^2$ | 8160 kg/mm$^2$ |
| Coeff. of linear expansion | 23 x 10$^{-6}$/°C | 17.8 x 10$^{-6}$/°C |
| Maximum D.C. resistance at 20°C | 0.196 ohm/km | 0.1828 ohm/km |

## 5.0 Future Work

Further designs of conductor containing fibre-optic cables are envisaged to suit a wider range of overhead power lines and work will continue on the development of fittings and joint housings. The incorporation of advanced fibres for long wavelength operation, wavelength multiplexing and monomode working will be considered.

Monitoring of the field trials already described will continue so as to build up experience of long term operation and this will be supported by laboratory investigations of the effects of short circuit currents, lightning strikes, vibration and creep. The powering of remote repeaters from local low voltage supplies, from solar panels and batteries, and by power which can be capacitively coupled to the earth wire from the phase conductors will be examined [8].

Finally a 10 to 20 km system trial on an operational 400 kV line is planned for 1981 and it is intended that live telephony and perhaps telemetry and protection signalling will be carried on the optical circuits provided.

## Conclusions

Optical fibre communication links can be integrated with overhead power transmission lines by encasing the fibre cable in the earth or one of the phase conductors. An insulating termination needs to be developed if the fibre cable is to be in a phase conductor. The use of optical fibres on power lines should allow improved telephone, control, date and protection facilities for the power system. The results of the initial field trials are encouraging: their continuation together with a range of laboratory investigations should lead to confidence in the long term reliability of such installations under all conditiona.

## 7.0 Acknowledgements

We should like to thank our many colleagues at the CERL, SEEB and BICC Limited for their contribution to this project.

This paper is published by permission of the Central Electricity Generating Board and BICC Limited.

## References

1. Gallawa, R.L., Midwinter,J.E. and Shimada, S. : 'A survey of worldwide optical waveguide systems', Topical Mtg. on Optical Fiber Comm., 1979 Washington, paper TUA1.

2. Bishop O.L. and Smith, J.C. : 'Installation of a fiber optic system in an electric power station', Proc. 27th Int. Wire and Cable Symposium, 1978, Cherry Hill, New Jersey.

3. 'All-dielectric cable strung on HV line to test remote control of sub-station', Laser Focus, Dec. 1979 p.56.

4. Jefferies, J.,Stannard-Powell,S. and Turton, P. : 'An experimental installation of optical fibre cable on the electricity grid system'. IEE Colloq., 1977 no.32 London.

5. Maddock, B.J., Hazell, N.J., Callcut,K.L., Gaylard. B., Dey.P., Slaughter, R.J. and Lawton, K. : 'Optical fibre communication using overhead transmission lines', CIGRE 1980, paper 35-01.

6. Benndorf, H., Doering,H., Dagefoerde, H.G., and Pfeiffer, T. : 'Fiber-optic system for transmission of information on high voltage overhead power lines', CIGRE 1980, paper 35-09.

7. Jackson,L.A., Reeve, M.H. and Dunn A.G., 'Optical fibre packaging in loose fitting tubes of orientated polymer', Optical and Quantum Electronics,9, 1977, 433-493.

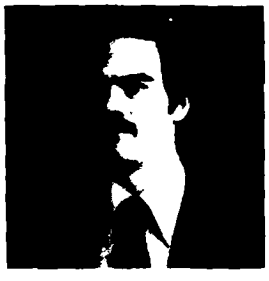
8. Berthiaume, R. and Blaise, R. : 'Microwave repeater power supply tapped from the overhead ground wire on 735 kV transmission lines' IEEE Power Engineering Society Summer Meeting 1979, Vancouver, paper F 79 730-3.



Brian J. Maddock graduated in physics at Cambridge University in 1956. He worked first on semi- conductors at Associated Electrical Industries and then joined the Central Electricity Research Laboratories (Kelvin Avenue, Leatherhead, Surrey, KT22 7SE, England) where he has done research on superconducting magnets and superconducting power cables. He is now Head of the Physics Application Section with interests in optical fibre communications, lasers, magnetic separation and novel techniques for power system measurement.



Mr.K.H.Pickup is Head of the Development Laboratory of BICC Metals Limited, P.O.Box 1, Prescot, Merseyside, L34 5SZ, and as such is responsible for Product and Process Development. He joined BICC in 1968, and previous to this was involved in research and development in the gear and friction material industries. He studied mechanical and electrical engineering, is a Chartered Engineer and a Member of the Institution of Mechanical Engineers.



Mr.K.L.Lawton is presently Senior Development Engineer in the Optical Cables Unit of BICC Telecommunication Cables Limited, Blackley, Manchester M9 3FP, England, responsible for the development and testing of optical cables. Since joining BICC in 1969 he has also been involved with cable design and process development of conventional telecommunication cables. He graduated from Salford University with A BSc. honours degree in Electrical Engineering.

# INSTALLATION OF A TRIAL OPTICAL FIBRE CABLE DESIGNED FOR TRANSOCEANIC SUBMARINE TELECOMMUNICATIONS SYSTEMS

P. Worthington

Standard Telephones and Cables Ltd.
Southampton, U.K.

*Summary*

This paper describes the development and installation of an optical fibre cable suitable for submerged telecommunication systems.

The cable manufactured for the trial is designed for long haul transoceanic applications laid in depths of up to 8 km. The optical fibres are contained within a central tube that provides them with a dry, pressure-free environment.

The trial cable is an armoured version of this deep water design for laying in shallow water regions where protection from trawling activity is required.

The cable was laid in February 1980 in a tidal loch in Scotland that provides conditions similar to cable routes across continental shelf regions. A British Post Office cable ship carried out the cable lay using conventional ship's cable handling equipment. 10 km. of cable were laid in a loop with both ends brought to a shore terminal for long term monitoring of transmission characteristics.

## 1. Introduction

Submarine telecommunication systems using coaxial cable have increased in capacity from 36 channels to over 5000 channels within the last 25 years.[1] To accommodate this increase in bandwidth, systems using large diameter cable operating with short repeater spacings have been developed.

Rapid progress has been made recently in development of low loss optical fibres operating in the wavelength range 1.2 to 1.6 μm which makes them attractive for submerged systems because of the large bandwidth and long repeater spacings potentially available in a cable of small diameter.

However, before commercial systems can be realised, it is essential that the cable for such a system has proven stability of transmission characteristics able to meet all the stringent service conditions and long life required for submarine systems.

In 1977 a design exercise was undertaken in order to determine the cable requirements for optical submerged systems. From this, a cable design was selected that would meet this outline specification and a development programme started to manufacture experimental cable for a field trial.

## 2. Cable Design Restraints

Although the first commercial systems using optical fibre cables will probably be relatively short and laid in shallow continental shelf regions requiring armoured cable for protection, the design of a deep water cable was considered to be most important for long term market requirements. Approximately 80% of cable for submarine systems is laid in depths between 2 to 6 km. which imposes several important restraints on cable design.

Cable for deep water must have a high strength to weight ratio because of the long lengths in suspension. In addition, for optical cable, the elongation at the maximum in-service tension must be minimised to avoid fibre breakage and fatigue problems. The cable is also subject to a very high hydrostatic pressure on the sea bed. This hydrostatic pressure is of little consequence with coaxial cable as the attenuation changes are small and predictable whereas pressure effects on fibres are uncertain and potentially large.

It was therefore considered necessary to provide the fibres with a dry, pressure free environment within the cable structure.

Other restraints placed on the cable design are common to conventional coaxial cable and can be summarised as follows:-

- A low resistance power feed path to provide power for repeaters
- Insulation and protection of the power feed path to allow for operation at up to 6 kV relative to the sea return
- Flex performance to be compatible with existing cable handling practice.

## 3. Cable Design

### 3.1 Basic Designs

Four basic structures (Figs. 1(a) to 1(d) were considered in some detail, characterised as follows:-

(a) Central strength member with fibres surrounding.

(b) Fibre housing adjacent to strength member.

(c) Fibres at centre, strength member surrounding.

(d) Fibres at centre, external strength member.

Design (a) was rejected primarily because of the difficulty of providing a pressure-free environment for the fibres.

Design (b) is unsymmetrical and is likely to have poor bend performance. It also requires an overall diameter some 25% greater than symmetrical designs.

(c) and (d) both offer excellent fibre protection and result in cables of about the same diameter. However, further considerations including cost of manufacture, torsional characteristics and ease of jointing and termination suggested (c) as the best overall basic structure and further development work was concentrated on this design.

### 3.2 Tensile Strength of Deep Water Cable

Having established the basic structure, the most important parameter that determines the detailed cable design is the required tensile strength.

This in turn depends on choice of strength member material as this is usually a major contribution to the weight (and hence the tensile loading) of the cable.

Following investigation of several materials, it was decided to use high tensile steel as the strength member, primarily because of its high Young's modulus and compatability with existing submarine cable manufacturing processes.

The maximum tensile loading of cable in service was calculated by summation of the static and dynamic forces acting during adverse recovery conditions when cable tensions are invariably highest.

From this, a strength requirement of about 75 kN was derived for a 25 mm. diameter cable using steel as the strength member and polyethylene as the insulant.

This gives a safety factor (defined as ratio of tensile strength to maximum tensile loading) of 1.6 which is considered to be an acceptable value for recoverable systems.

## 4. Trial Cable Design

The finalised design for the deep water cable design is shown in Fig.2.

The central optical core containing 8 fibres is housed in a thick walled aluminium tube that provides most of the pressure resistant capabilities of the cable structure.

The main cable strength member consists of 14 high tensile steel wires helically stranded around the aluminium tube. A welded copper tape formed into a tube and swaged on to the wires provides a hermetic seal for the completed composite centre conductor.

As this conductor provides the power feed path for repeaters, the conductor is insulated and protected by an extrusion coating of low density polyethylene. Table 1 summarises the mechanical characteristics of the deep water cable design.

Table 1

Deep Water Cable Characteristics

| | |
|---|---|
| Overall Diameter | 26 mm. |
| Centre conductor diameter | 12.1 mm. |
| Weight in water | 0.42 tonnes/km. |
| Tensile Strength | 92 KN |
| Safety Factor | 1.65 |
| D.C. Resistance | 0.49 Ω/km. |
| No. of Fibres | 8 x 1 mm. O/D |

The cable manufactured for the trial was an armoured version of the deep water design. Although it is unconventional to armour cable having a high tensile steel central strength member, for optical cable there are good reasons for so doing. The central strength member contributes significantly to the overall cable strength, thus minimising fibre elongation during armouring, coiling and subsequent laying.

A relatively light armouring using 18.5 mm. diameter medium tensile wires was selected for this application.

## 5. Fibre Strain In Cable Processing

The greatest hazard to the transmission path in manufacture of the submarine cable was thought to be strain imparted to the central fibre core which could occur at any of the cable process stages. To ensure fibre integrity is is important that:-

(a) The transient strains during processing do not exceed a safe figure.

(b) The residual strain in the cable after completion of manufacture is kept to a minimum.

The transient strain allowable can be established from the degree of proof test that the fibres were subjected to and the duration of the transient. Since the proof test level for submerged systems is likely to be fixed at a minimum of 1%, short term strains in the region of 0.5% should be tolerable.

The residual strain however must be kept to a very low figure. Any residual strain reduces the safe working strain in service conditions. It can also lead to failure from static fatigue over long periods of time at strains much less the original proof test level.

In order to quantify the strains of the cable processes, several experimental lengths of cable were manufactured using central cores incorporating constantan wire monofilaments coated to the same diameter as fibres. Longitudinal strain could then be determined from resistance changes of the wires at each process stage. Constantan was chosen for this purpose because of its very small temperature coefficient.

This proved to be a very sensitive method of measuring strain and the wires were subsequently incorporated into the cores of the trials cable to allow measurement at all stages through to cable laying.

## 6. 10 km Trial Cable Manufacture

### 6.1 Central Core

The cable was manufactured in 6 nominal 2 km. section lengths as this was the practical limitation on fibre lengths at the time. 5 of the sections were to be used for the laying trial, with one spare. Each central core has 6 fibres, 4 multimode graded index for operation at 0.85 μm and 2 single mode fibres for operation at longer wavelengths. In addition 2 constantan strain wires were included in each core.

The fibres were stranded around a high tensile steel strength member using a planetary strander. About 100 gms. back-tension is required on the fibres to avoid slack, which produces a short-term strain of about 0.1%. However, by applying back-tension to the strength member to give the same degree of strain, the residual fibre strain in the completed core was reduced to zero.

### 6.2 Composite Centre Conductor

At this stage the fibre core is enclosed in the aluminium pressure tube which is then drawn to size prior to entering the cable stranding machine. After the high tensile wires are stranded around the tube, the copper tube is formed around the strand and swaged to give a compacted structure. This swaging process produced some elongation of the aluminium tube, a small fraction of which was imparted to the fibre core by friction.

It was found that this elongation could be minimised by careful control of the aluminium tube diameter and minimising back tension in the aluminium during its transit through the strander. Residual elongations in the fibres of less than 0.03% were achieved for this process, although some of the earlier sections manufactured had strains in excess of 0.15% before the nature of the strain mechanisms were understood (Fig. 6).

### 6.3 Extrusion

The extrusion of the insulant (low density polyethylene) required a relatively high back tension of about 1500 lbs. to keep the cable straight during cooling. This results in a temporary strain of about 0.08% for a period of 20 minutes but produces no permanent residual strain in the fibres. However, after extrusion the cable was coiled in storage tanks which imparts one twist in the cable for each turn in the tank. This twist causes longitudinal strain to the central cable core given by:-

$$\varepsilon = \frac{\pi . Dp^2}{L.d} \cdot \frac{\overline{EAw}}{\overline{EAc}}$$

Where $Dp$ = Strength member pitch dia.
$L$ = Strength member lay length
$d$ = Coiled diameter
$\overline{EAw}$ = Strength member stiffness
$\overline{EAc}$ = Total cable stiffness

The trials cable was coiled in tanks with a 15' outer diameter and 8' inner diameter giving a calculated average strain of 0.027%.

This agreed closely with the average measured strain in the 6 sections manufactured of 0.028%.

### 6.4 Armouring

Armouring, like extrusion, imparts negligible intrinsic elongation to the fibres but again produces strain due to coiling of a structure with a helical strength member.

In this case it is the twist imparted to the armour wires that causes the whole central cable structure to be strained.

As the pitch diameter of the armouring is relatively large, strains due to this coiling could be potentially large. Accordingly, the cable after armouring was coiled into the 30' diameter final storage tanks using a much greater minimum

diameter than is used for conventional cable. (15 ft. instead of 8 ft.). Fig. 4 shows the build-up of strain versus length processed for one of the sections during armouring. This shows the rate of strain increasing as coiling approaches the centre of the storage tank and falling when coiling was at the outside of the tank.

6.5 Cable Jointing and Terminations

Following completion of armouring of the cable, 5 of the 2 km. sections were jointed to give 4 km. and 6 km. repeater sections. The joints in the fibres were made using fusion splicing and were then enclosed in a steel joint housing. The armouring was restored over the joint housing using barrel splices, selected because of the very low localised elongation that could be achieved under tensile loading.

Two of the cable ends were terminated using a specially made tail cable tube and high pressure demountable gland that enabled the fibres to be brought through the bulkheads of a repeater housing.

## 7. Laying Trial

7.1 Boat Loading

The cable sections were loaded from the factory directly to the Post Office Cable Ship Iris. As the ships tanks were smaller than the factory tanks, strains due to coiling were likely to be large. Accordingly, the cable was coiled in an anti-clockwise direction so that the strain on the central cable was negative. This direction of coiling tends to tighten the lay of the armouring making it torsionally stiffer, which can lead to handling problems. However no such problems were encountered and boat loading was completed satisfactorily. A negative strain of about 0.13% was measured on the constantan wires.

The two cable sections were coupled to the repeater housing on the ship with the fibres spliced inside to provide continuous paths for measurement.

The completed system and fibre interconnections are shown in Fig. 5.

7.2 Initial Lay (14th and 15th February 1980)

The cable was laid in a loop in Loch Fyne (Fig. 6) with both shore ends taken to a terminal repeater station. Cable strain and fibre attenuations were monitored during the lay from the shore terminal.

Following completion of lay, transmission characteristics of all fibre paths were measured.

Fig. 7 shows the attenuation changes of the single mode fibres at the two longer wavelengths (1.3 μm and 1.55 μm) through all manufacturing stages to completion of lay[2]. The only significant change occurred at the jointing and termination stages when the individual fibres were spliced together.

The fusion splices in each single mode fibre route introduced an average loss of about 0.5 dB per splice giving an overall increase on the jointed 10 km. lengths of about 0.2 dB/km.

Fig. 8 shows the multimode fibre attenuation and dispersion results averaged for all fibres. Again there is negligible change in attenuation at any process stage. There is a slight drop in attenuation per unit length after jointing the individual lengths. This is caused by the high loss, higher order modes becoming less significant when measurements are made on long fibre lengths and off-setting any small loss increase due to splicing.

The decrease in dispersion per unit length that was observed after jointing the 2 km. lengths corresponds to a $(\text{length})^{0.8}$ law, again as a result of the attenuation of higher order modes.

Fig. 9 summarises the change in strain measured on two of the cable sections through to completion of laying. The large negative strain observed after boat loading was recovered during laying leaving a nett strain in the fibres approximately equal to that existing prior to armouring. Residual strain in the 5 cable sections ranged from 0.030% to 0.150% depending on process conditions at the centre conductor stage. Monitoring of the transmission paths continued until May 1980, when the empty repeater housing was recovered and replaced by an active repeater.

7.3 Recovery and Re-Lay (May 28th and 29th 1980)

The cable was recovered by grappling a ground rope attached to the cable close to the repeater. A cable loop was successfully brought on board without kinking, although one of the terminations was subjected to a severe bend as it was manoeuvred round the bow sheave. The empty repeater housing was removed and replaced by a new housing containing 2 140 Mbit/sec. regenerators (one for each direction of transmission) which was spliced into two of the multimode paths. The existing terminations were re-used and the cable re-laid approximately 30 hours after recovery.

Fibre measurements before and after recovery show little significant change (Tables 2 and 3).

The 1 dB increase in Path 2 (single mode) at 1.55 μm is probably caused by a change in the degree of bending of the fibre in the termination tail tubes.

Path 6 shows a 1 dB drop in attenuation at all wavelengths which is consistent with an initially high loss splice being replaced by a low loss one within the repeater housing.

Since the re-lay operation the system has been powered up with error monitors connected to the repeatered fibrepaths.

Measurement of the other fibre transmission paths will continue periodically.

Table 2

Multimode Fibres (Loss At 0.85 μm)

| Fibre Path | Length km. | Post Lay 17.2.80 | Re-measure 26.3.80 | Pre-recovery 27.5.80 | Re-lay 30.5.80 |
|---|---|---|---|---|---|
| No. 3 | 9.55 | 31.7 | 31.4 | 31.3 | Repeatered |
| No. 7 | 9.55 | 30.6 | 30.1 | 30.2 | Repeatered |
| No. 4 + No. 8 Looped | 19.10 | 61.4 | 61.5 | 60.5 | 61.6 |

Table 3

Single Mode Fibres (Loss at 1.3 and 1.55 μm)

| Wavelength | Fibre Path | Length km. | Post-lay 17.3.80 | Re-measured 26.3.80 | Pre-recovery 27.5.80 | Re-lay 30.5.80 |
|---|---|---|---|---|---|---|
| λ = 1.3 μ | 2 | 9.55 | 15.4 | 15.2 | 15.2 | 15.2 |
| | 6 | 9.55 | 17.7 | 17.2 | 17.7 | 16.1 |
| λ = 1.55 μ | 2 | 9.55 | 11.9 | 11.9 | 11.9 | 12.7 |
| | 6 | 9.55 | 12.4 | 12.3 | 12.6 | 11.5 |

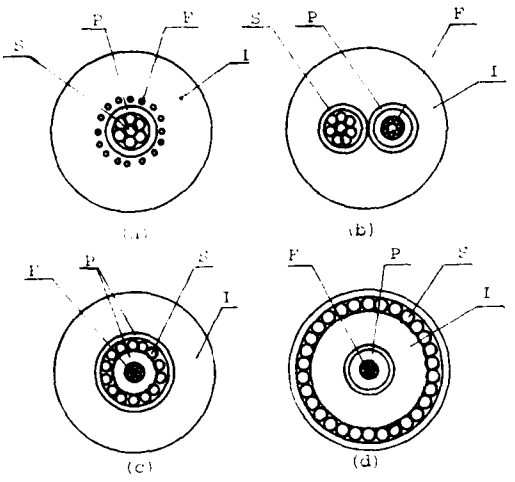
References


1. Dawidziuk, B.M. : "The Role of Submarine Systems in the Global Communications Network". IEE International Conference on Submarine Telecommunication Systems 26-27th February, 1980 London.

2. Cannell, G.J., Worthington, R., Hearne, V.C. "Evaluation of Single Mode Fibres for a Submerged Cable Laid in Loch Fyne, Scotland". Sixth European Conference on Optical Communication 16th-19th September 1980, York, U.K.



November 1980 © 1980 Standard Telephones and Cables Limited




S - Strength member

F - Fibres

P - Primary power feed

I - Insulant

FIGURE 1 - BASIC DESIGNS

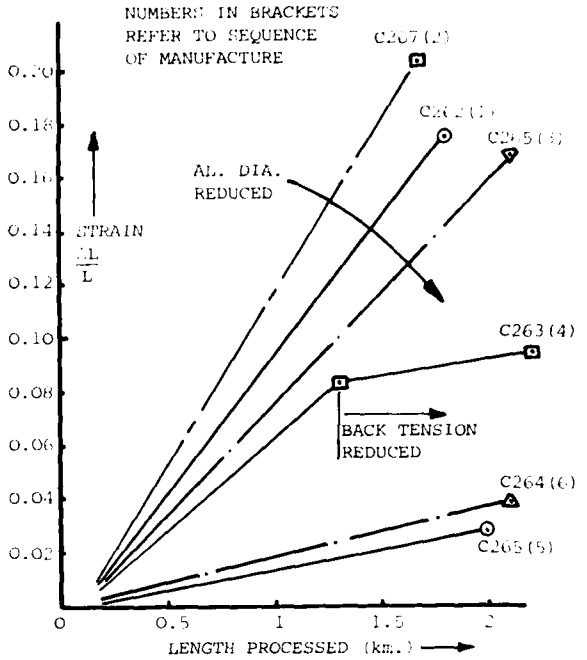
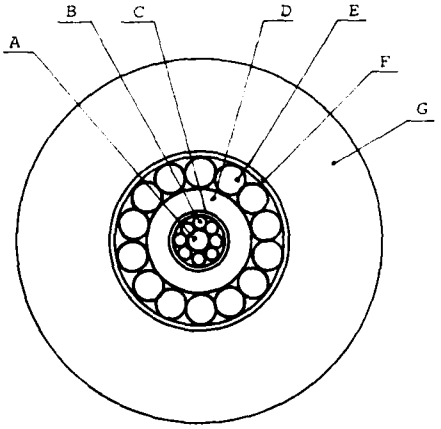



FIG. 3 STRAIN BUILD UP DURING CENTRE CONDUCTOR MANUFACTURE




A - Fibre strength member

B - Optical fibres

C - Mylar tape

D - Aluminium tube

E - High tensile wires

F - Copper tube

G - Polythene insulant

FIGURE 2 - DEEP WATER CABLE DESIGN

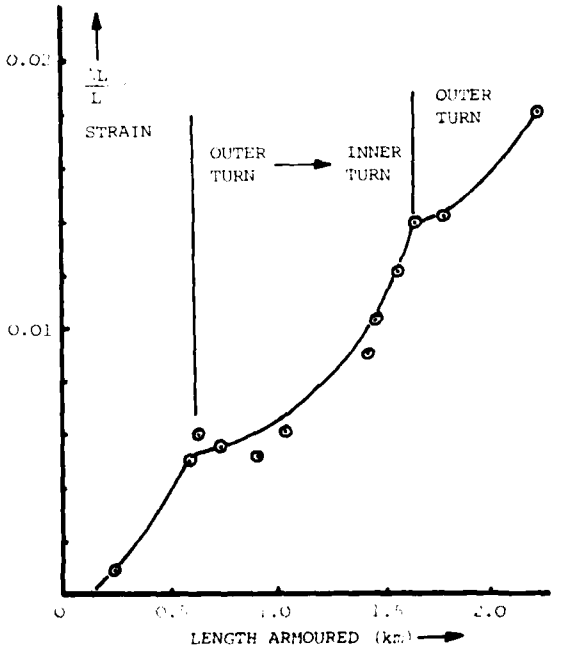
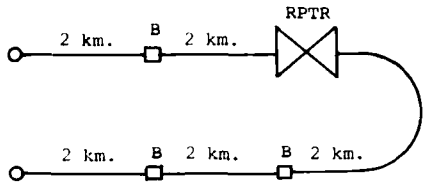
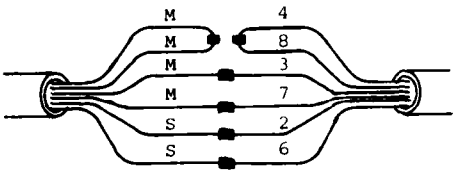



FIG. 4 STRAIN INCREASE DURING COILING AFTER ARMOURING




SYSTEM LAYOUT




M = Multimode S = Single mode

FIBRE INTERCONNECTIONS AT REPEATER

FIGURE 5 - 10 KM. TRIAL SYSTEM

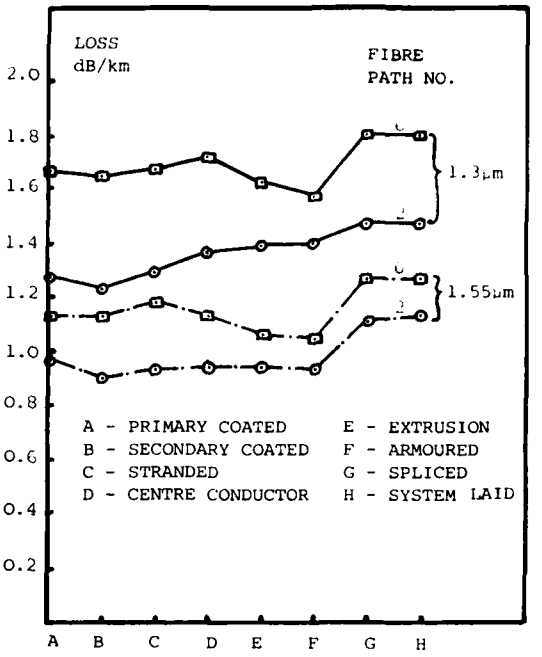



FIGURE 7 - SINGLE MODE FIBRE ATTENUATIONS

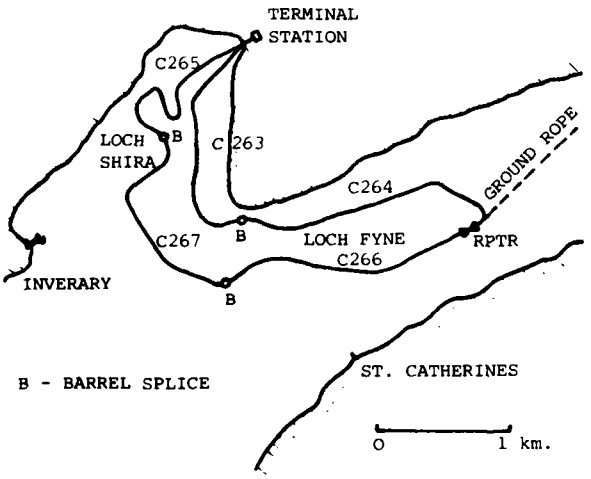



FIG.6 LOCH FYNE TRIALS LOOP

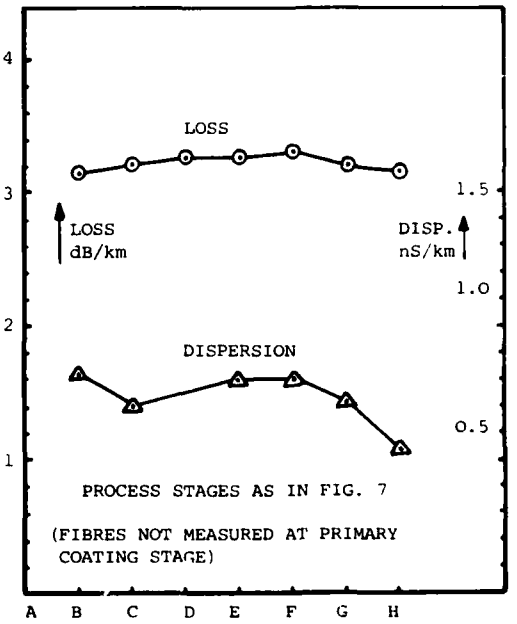



FIG. 8 MULTIMODE FIBRES ATTENUATION AND DISPERSION

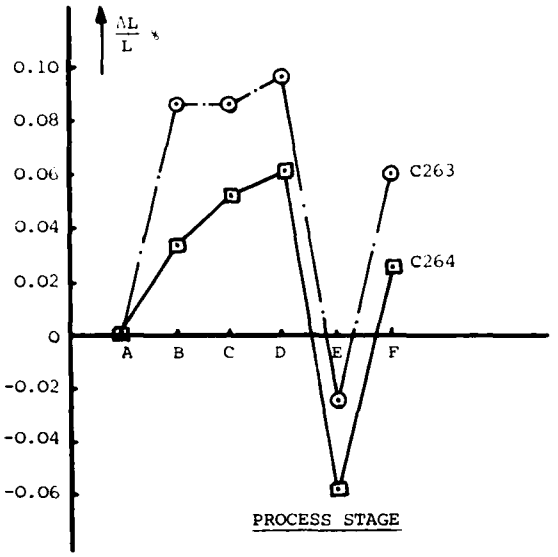



FIG. 9 FIBRE STRAIN DURING CABLING AND LAYING



Peter Worthington is a development engineer with Standard Telephones and Cables Submarine Systems Division which he joined in 1974.

He received a BSc. in Electronics and Electrical Engineering from the University of Birmingham in 1971. Since 1977 he has been involved in the development of optical cables for submarine systems.

# OPTICAL CABLE NETWORK FOR 150 SUBSCRIBERS

F. Krahn

Felten & Guilleaume Carlswerk AG, Cologne, West-Germany

## Abstract

Optical communication cables for a subscriber network have been developed, produced, installed and implemented in West Berlin for the German Post Office (Deutsche Bundespost).
150 subscribers are connected to the local exchange by two fibres. The unit-type cables for this system are composed of 1, 2, 12, 36, 108, 144 or 216 fibres. Details are given on design and properties of the complete system, the cables, the splices and connectors, the installation, the mounting and the measurements.

## Introduction

In 1978 the German Post Office (Deutsche Bundespost) prompted our company to make an offer for an optical subscriber connection system for 150 subscribers in West Berlin. The system connecting these subscribers to the local exchange, should be used in the first stage for telephone traffic via optical fibres, but the cables ought to be suited as well for broadband services. It had to be realized up to the end of 1980.

## General System Characteristics

- Each subscriber is connected to the local exchange by two fibres
- The main part of the network is designed as a fixed circuit, part of the network (for about 20 subscribers) is a combinatorial circuit for test purposes
- The optical cables do not contain any copper with the exception of the indoor 2-fibre installation cables
- Power supply is provided for a lot of 6 subscribers at the end distribution box in the building
- The telephone traffic is digital (64 kbit/s + Signalling)
- The A/D-conversion is done in the telephones
- The switching is adopted to the existing analogue switching technique
- The existing selecting test network is used.

## End Equipment

A block diagram of the end equipment at the local exchange and at the subscriber is shown in fig. 1.

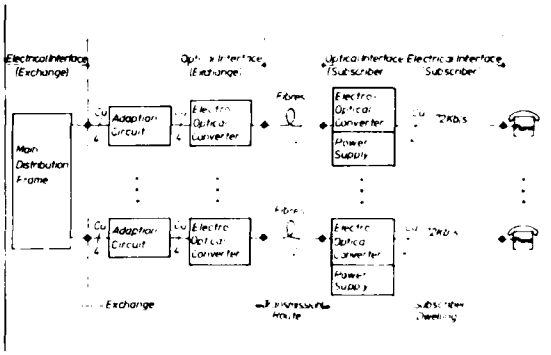



Fig. 1 Optical subscriber connection system: End equipment

For the small-band service (telephone traffic) the optical source is an LED with adapted driving circuit. The power output into the fibre is 1 nW. The optical reciever is a PIN-photodiode, a preamplifier and a clamper circuit. The minimum detectable power at a bit error rate of $10^{-9}$ is $\leq$ 1nW. A frequency dependant equalization is not necessary. The dynamic range of the reciever corresponds to 40 dB optical power, so that it is suitable for all distances in the network. Broadband services are made possible by exchanging some parts of the end equipment.

## Fibres

The graded-index fibres for the cables had been manufactured at the Philips Glass Works, Eindhoven/Netherlands, whereas the PCVD-process (1)was evolved at the Philips Research Laboratory in Aachen/Germany.
For this project fibres with the following characteristics are used:

core/outer diameter: 50/125/um
numerical aperture: 0.21 (effective)
attenuation: $<$ 6 dB/km at 850 nm
bandwidth(3dB opt.): $>$ 400 MHz · km
primary coating: Silicone
outer diameter of the coating: 250 /um

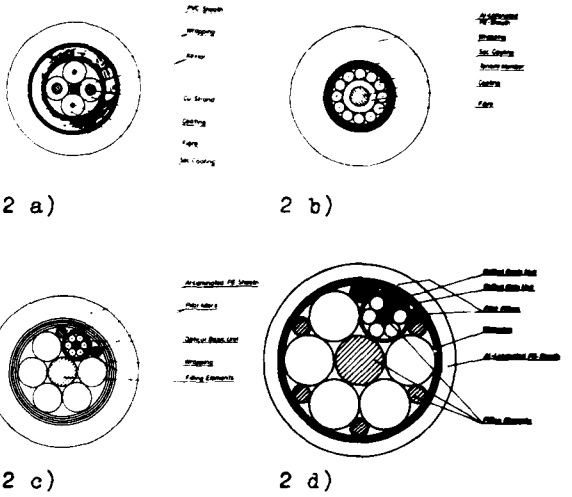
## Cables

The unit type cables contain 1, 2, 12, 36, 108, 144 or 216 tightly secondary coated fibres, 6 of which are combined to a basic unit, and 6 basic units forming a main element. Exceptions are:
- the 1 fibre cable in which the unstranded secondary coated fibre is wrapped with Kevlar
- the 2-fibre cable, the two fibres of which are stranded together with two copper strands
- the 12 fibre cable which is stranded into a single unit.

The outdoor cables are sheathed with Aluminium-laminated polyethylene, the indoor cables have a PVC jacket. The cross sections of some cables are shown in fig. 2, some of their properties are given in the following table:

| Number of fibres/cable | Weight (g/m) | Outer diameter (mm) |
|---|---|---|
| 1 | 14 | 3.5 |
| 2 | 25 | 5.2 |
| 12 | 110 | 11.0 |
| 36 | 200 | 17 |
| 108 | 580 | 30 |
| 144 | 650 | 32 |
| 216 | 900 | 38 |

Identification of the fibres in the cables is accomplished by different colours; units are marked by pilot wormings.



2 a) 2 b) 2 c) 2 d)

Fig. 2 Optical cables for the subscriber network
a) 2-fibre installation cable
b) 12-fibre cable
c) 36-fibre outdoor cable
d) 216-fibre cable

## Splices

Fixed splices were used for the jointings of cables. Splicing was done with a compact fibre welding unit (2).
To provide a good temperature behavior the splices are sheathed by a PE-tube and a shrink-on tube. Between -20°C and + 60°C no increase of splice loss could be measured. The splices are housed in thermoplastic clamping sleeves, as shown in fig. 3.

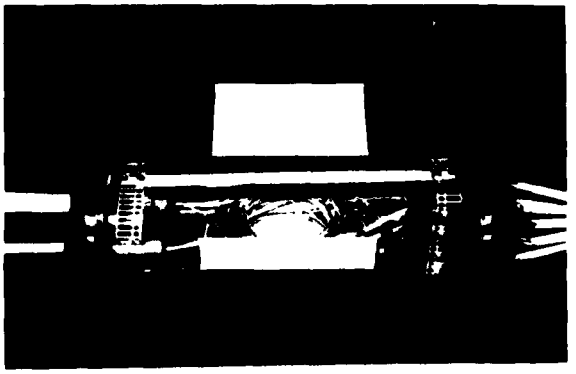


Fig. 3 Thermoplastic clamping sleeve

## Connectors

The connectors are used for the jointings between
- cable and exchange end equipment
- cable and subscriber end equipment
- cable and cable for the fibres in the combinatial network.

The connectors consist of precision plug pins which are adjusted and fixed by a new clamp mechanism (3). The principle is shown in fig. 4:

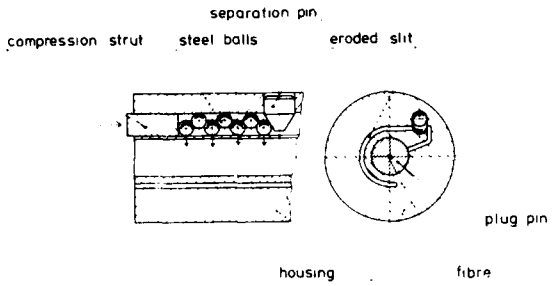



Fig. 4 Principle of the precision connector

For the inner diameter of the sleeve relatively great tolerances are permissible. As it is slit in longitudinal direction it is possible to plug-in a pin without friction and then to press the sleeve until the pin is clamped free from play.
The attenuation values, measured with a uniform light distribution on more than 700 connectors are 0.6 ± 0.2 dB per coupling (including reflection losses and losses due to mismatched fibres).
Different housings, (as to be seen in fig. 5) for the system have been realized: for a fibre-to-fibre connection, for a connection of fibres to electro-optical devices (LED or Photodiode), for a connection of the fibres of a cable to the pigtail-fibre in the end equipment, and for a plug-in-unit-connection between fibres in the end equipment.

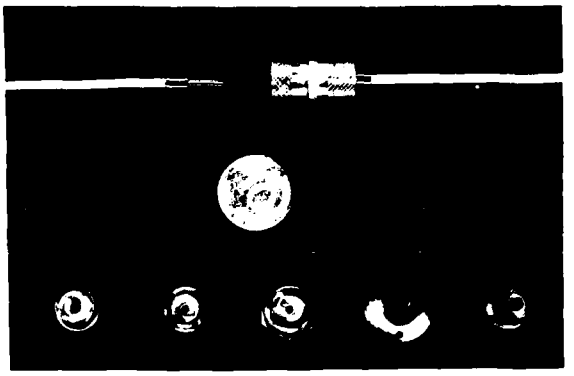


Fig. 5 View of the precision connector

## Cable Network

The scheme of the complete network is shown in fig. 6. The distance between exchange and subscriber varies between 450 and 900 m. The combinatorial network is realized in the cable distribution box connecting each of the 36 input and each of the output fibres. The connection is made by short lengths of secondary coated fibres terminated by the above mentioned connector pins. The distribution box is shown in fig. 7. The distribution terminals are located in the houses of the subscribers (see fig. 8). They contain a power supply for maximal 6 subscribers. Therefore the installation cables from the cellar to each dwelling hold not only 2 fibres but also 2 copper-wires for the power supply of the subscriber end equipment.

The installation cable ends at each subscriber in an optical connection box where the electro-optical conversion is brought about connection to the telephone is done by copper wires.

When planning the network the following optical attenuation values were assumed:

- attenuation of the cable: 8 dB/km
- splice loss: 0.5 dB/coupling
- connection loss: 1.5 dB/coupling

The resulting values for the whole system are:

| | | |
|---|---|---|
| - maximum cable attenuation (L = 900 m) | : | 7.2 dB |
| - total splice loss (maximum 6 splices) | : | 3 dB |
| - total connector loss (2 connectors) | : | 3 dB |
| - reserve: 5 splices | : | 2.5 dB |
| 200 m cables | : | 1.6 dB |
| - system reserve | : | 5 dB |
| Total | | 22.3 dB |

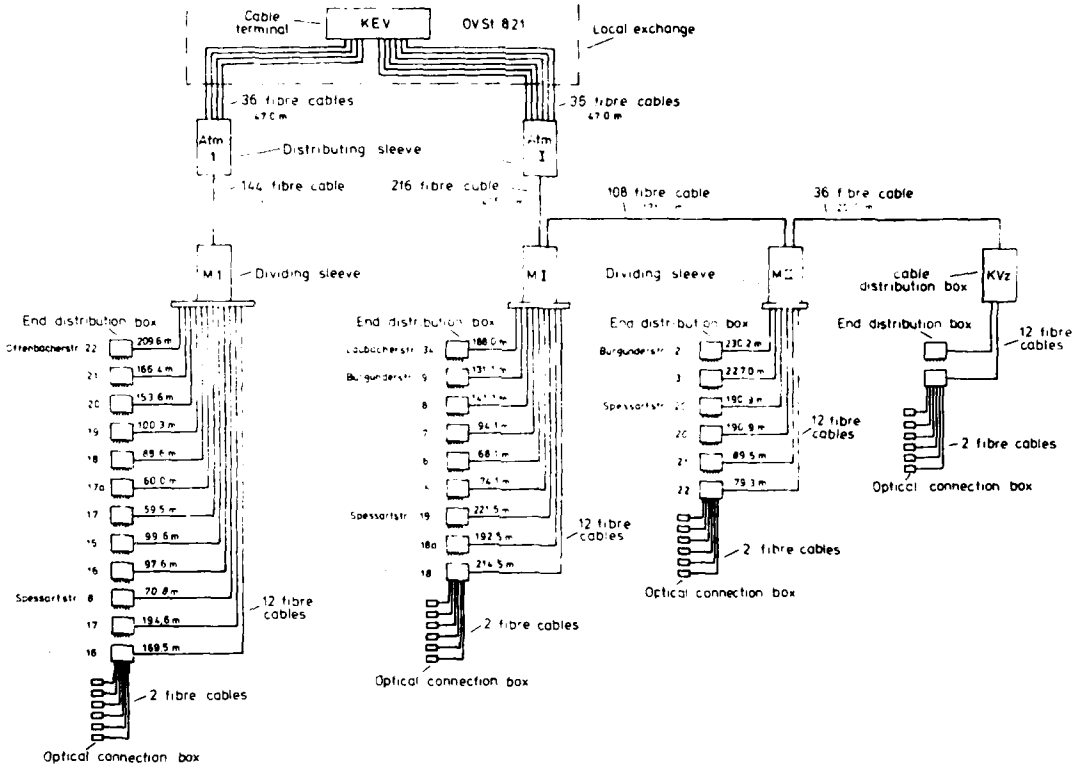



Fig. 6 Scheme of the complete network

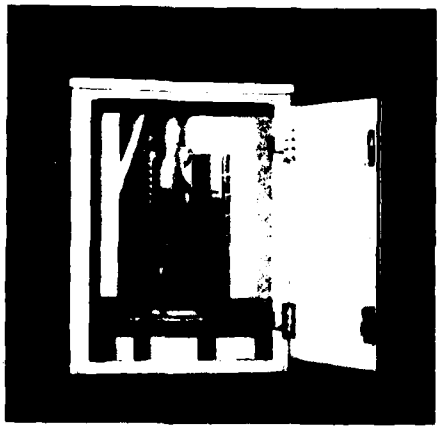


Fig. 7 Cable Distribution Box

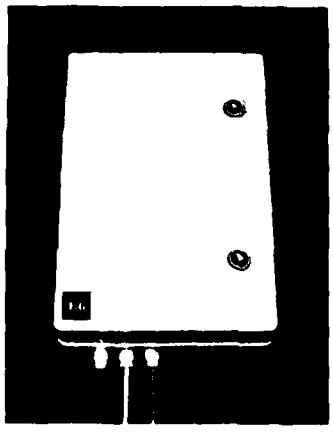


Fig. 8 Distribution Terminal

## Cable installation

The outdoor cables were drawn in existing cable ducts, the indoor cables at the subscribers were installed within the buildings by means of those conduits already used for conventional telephone wires.
The installation was done by employees of our installation department and some hired hands from a Berlin company. Although all these people were not specially trained, the cables were laid without any fibre break.

Most difficulties had been expected for the installation of the 2-fibre cables to the subscribers, because an preceding inspection had proved the existing conduits to be very narrow and partly sqeezed, and during the installation some cables required comparatively high pulling forces. But nevertheless the inspection after pulling showed no fibre break and no increase of attenuation.
The splicing and mounting of the cable sleeves were also done by our installation people; they had been trained for one week for this task.

The mounting steps were:

- Preparation of the cable sleeve and of the cable ends to be jointed
- Blocking of the cable ends for preventing water entering the cable sleeves
- Splicing the fibres by welding and protecting the splices
- Closing the sleeves.

During the splicing process the fibres were watched by a backscattering meter located at the exchange. The joints of each fibre route from the local exchange to the cellar of the subscriber were welded directly one after another.

The connectors at the cable endings at the end equipment or at the distribution box were mounted by welding the fibre pigtails of each connector pin to the fibres of the cable.

## Measurements

The following measurements were done at the cable route

- continuous supervision of the route during splicing by the backscattering meter
- looping the complete cable route at the subscriber and watching the route by the backscattering meter (4)
- measuring the attenuation of all fibres of the complete cable route terminated by connectors by using the reference method (4)
- measuring the pulse broadening for some fibres (the bandwidth of all fibres was measured before cabling to be $> 400$ MHz · km).

The following table shows typical attenuation values for a route between the local exchange and the subscribers including the fibre splices (not yet the connectors);

Route: from local exchange to Offenbacher Straße 22, Length: 514 m

| Fibre No. | attenuation (dB) |
|---|---|
| 1 | 4.3 |
| 2 | 3.9 |
| 3 | 3.4 |
| 4 | 3.3 |
| 5 | 3.5 |
| 6 | 4.2 |
| 7 | 3.6 |
| 8 | 4.3 |
| 9 | 4.0 |
| 10 | 3.7 |
| 11 | 3.9 |
| 12 | 4.6 |

The differences of the attenuation values are mainly caused by the fact that many fibres, ordered with an attenuation of $\leq 6$ dB/km, had a lower attenuation.

## Conclusion

Optical cables for a subscriber network and the corresponding accessories have been developed, produced and installed. This project was accomplished successfully, which proves and demonstrates with one more example for the fact that the future of optical communications on a commercial base has begun already.

Acknowledgement

The author wishes to express his thank to all colleagues who helped to accomplish this project, especially T. Olejak for development of the cables, B. Schmidt for development and fabrication of the connectors, P. Deußer for development and fabrication of the cable sleeves and the accessories and J. Gladenbeck for the supervision of splicing and field measurements on the cables.

References

1. Geittner, P.; Küppers, D.; Lydtin,H. "Low Loss Optical Fibres Prepared by Plasma Activated Chemical Vapor Deposition (CVD)" Appl. Phys. Letters 28 (1976) 11, pp. 645 - 646

2. Krahn, F.; Meininghaus, W.; Rittich, D.; Serapins, K.; Gladenbeck, J."Installation and Field Measurement Equipment for Optical Communication Cables" Proceedings of the 28th ICWS, 1979 pp.357-363

3. Rittich, D.; Schmidt, B. to be published

4. Rittich, D.; Meininghaus, W. "Meßgeräte für die optische Nachrichtentechnik" Frequenz 32 (1978) 12, pp. 350 - 356



Friedrich Krahn was born in 1939. He graduated from the University of Münster in 1970 with a Dr. rer. nat. in Physics. He then joined Felten & Guilleaume Carlswerk AG and was first engaged in the field of innovation and diversification. In 1973 he was appointed head of the department for fibre optics research and devolopment.

# PREVENTION OF CABLE PRESSURE DAM FAILURES

C.D. Gupta, Bell Canada, Toronto, Canada

W.P. Trumble, Bell-Northern Research, Ottawa, Canada

## ABSTRACT

Current methods of cable plugging are largely refinements of methods developed over fifty years ago. Material and technology have evolved considerably, but failures of cable plugs still occur. This paper describes an extensive study of plug failures in PIC and pulp-insulated cables and gives recommendations for improving both materials and methods.

## INTRODUCTION

Pressurization of telephone cables with dry air is a technique which was first used in the 1920s. At that time only lead sheathed toll cables were suited to this technique, but the benefits were immediately apparent. The protection of the cable core from moisture and the simplified means of monitoring sheath condition greatly reduced maintenance costs and improved reliability.

However, as Bell Canada's maintenance records show, there remains one part of the cable pressurization system which has yet to be perfected. This is the cable pressure dam, sometimes called the pressure plug. With the commonly used PIC and pulp cables, failure of the pressure dam still occurs fairly often.

Preliminary investigations demonstrated that a continuous orifice through the pressure dam of small cross-sectional area can allow considerable airflow from the pressurized side to the non-pressurized side of the cable. Figure 1 explains the relationship of airflow to cross-sectional area of the pressure dam orifice.

Bell Canada's concern with pressure dam failure led to a series of studies and laboratory experiments by Bell-Northern Research to determine the suitability of both the plugging materials and plugging methods. A detailed analysis of failure modes led to a number of surprising discoveries about both materials and methods.

## PLUGGING TECHNIQUES

The commonly used materials for plugging today are polyurethane and epoxy resin. The material is introduced into the cable through an opening made in the sheath and caused to fill all the spaces in the cable from the centre to the sheath interior surface. After curing, the plug forms a seal against the passage of air along the cable.

Because of different characteristics of PIC and pulp-insulated cable, different techniques are used for plugging each type. For PIC cables the common method is known as "Sheath Injection". For pulp-insulated cables the common method is known as "Sleeve Injection".

### Sheath Injection - PIC Cables

An opening is made in the cable sheath 100 mm (4 in.) long and 1/3 the circumference of the cable wide. A pressure fitting is installed over the opening and a measured amount of plugging compound is forced into the cable.

### Sleeve Injection - Pulp Cables

The outer cable sheath is removed for a length of 300 mm (12 in.). Then the inner sheath layers are successively removed to expose at least 40 mm (1½ in.) of each layer on each side of the opening. The conductor wrapping is removed and the conductors are separated with core pins. With the cable thus prepared, a lead sleeve is fitted over the cable and a measured amount of plugging compound is forced into the cable through a hole in the sleeve.

## FAILURE MODES

Because of differences in materials and construction, pressure dams in PIC and pulp-insulated cables tend to fail in different modes. In PIC cables, most leakage tends to develop in the interstices between the layers of the sheath or between the core wrap and the cable jacket. Some leakage occurs at the aluminum shield along the

crimped edges. In pulp-insulated cables the majority of leaks occur down the core along the wires.

One aspect that both cable types have in common is temperature dependence of plug reliability. From Bell Canada maintenance records* it was found that plug failure rates consistently follow yearly cycles, with the maxiumum failure rates occurring at the lowest temperatures and lowest rates at the highest temperatures. Spikes in the failure rate are noted to correspond to abrupt extreme temperature changes. (See Figure 2.)

## EXPERIMENTAL RESULTS - PIC CABLES

### Objective

Very little has been reported on systematic studies of pressure dam failures. Therefore the primary objective of the experiments was to generate data on failure mechanisms under controlled conditions. This would provide a sound basis for the evaluation of present techniques and materials. It would also indicate what improvements and changes are required.

### Sheath Injection Trials

To establish a baseline, a number of 2 meter lengths of cable were prepared, representing the range of sizes and types typically fitted with pressure plugs. Pressure plugs were fitted on the samples using a standard sheath injection employing a 2-part polyurethane elastomer as the plugging material with a 20-minute cure time.

After about 16 hours the samples were tested for leakage at 69 kPa. Those with a leakage rate greater than 5 cc/minute were set aside, while the others were subjected to thermal cycling. At intervals the samples were removed from the environmental chamber for testing. (Table 1 shows the results of these tests.)

In summary these baseline experiments showed the following:

- Probability of leakage increases with cable diameter,
- Wire gauge has no effect on leakage,
- The interstice between the core wrap and the inner cable jacket formed at least part of the leakage path in all cases,
- Different jacket profiles showed different tendencies to leak. In descending order of plug reliability, these are: Sealpap, Sealpeth, Alpeth, PAP.

After testing, the pressure dams were taken apart for detailed examination. The findings were as follows:

- Conductor bundles were filled for a length of at least 100 mm on each side of the injection port.
- Little material entered between the core wrap and the first cable sheath. At no point did the material encircle the cable in this interstice.
- There was good adhesion to the cable jacket sheath, particularly the aluminum shield, but not to the core wrap.
- Insufficient material entered the interstices between the cable jacket sheaths.
- Where material entered the space adjacent to the corrugated aluminum shield, it was deposited in the valleys.

### An Unexpected Finding

Since it was learned that insufficient material was entering the spaces between sheath layers, a small number of plugs were prepared using channelling pins between the layers. The objective was to increase the flow into these interstices. Otherwise the preparation followed the standard sheath injection method. In this case the specified minimum cure time of one hour was allowed.

When each of these samples was pressure tested for leakage, the initial leakage rate was low, followed by a virtual blowout. Subsequent examination of the plugs showed that the material between the sheath layers remained uncured during the allowed one hour cure time.

As a result of this finding, an experiment was devised to monitor both the flow and state of polymerization of plugging material between sheath layers in a newly formed plug. The sensors used were 750 mm lengths of pulp-insulated, 26 AWG, twisted pair wires. It is known that the insulation resistance (IR) of this type of wire changes when saturated with a polar liquid** and that the amount of change depends on the degree of polarization. Therefore, these sensors served both to detect the arrival of plugging material and also to monitor the polymerization curing process.

---

* Obtained from CCUAP (Computerized Cable Upkeep and Administrative Program)

** An organic liquid capable of conducting electrical current.

One factor which is of particular concern is the arrival of the liquid at an early stage of the cure process. Some core wrap materials such as Mylar[1] and polyethylene do not offer good adhesion in the best of circumstances. Liquid arriving at these materials after travelling a slow route would be partly cured and the probability of adhesion would be very low. Therefore, the rapid and uniform flow of material to all parts of the plug space is important.

For the flow experiment a length of 900 pair, 26 AWG PAP cable was prepared for sheath injection and instrumented with sensor wires between the sheath layers in the plug space. The plug was formed in the normal way while a recording system continuously monitored IR between the sensor pairs. Curing of the plugging compound at the sensors' location demonstrated an IR drop between the sensor pairs of $1 \times 10^6$ ohms. The IR between pairs was supposed to rise to $1 \times 10^{11}$ ohms. This rise failed to occur.

At this point an unexpected finding opened up a completely new line of investigation!

After a 4-hour cure the cable was leak tested. Like previous samples that had been given a minimum cure time, the initial leakage rate was low, followed by a sudden blow-out. In this case bits of plugging material were also blown out, ranging in consistency from gelled to liquid. Once again the compound between the sheath layers had not completely cured.

It was found by simple bench trials that a mass of material such as that in the cable core will retain the heat generated by the curing reaction and thus will cure in the specified time. On the other hand, a thin layer of material spread over a heat-conductive surface (Aluminum Shield) will rapidly lose all reaction heat and will therefore require considerably more time to cure.

## The Failure Mechanism

A number of pressure plug samples were dismantled and the plugs cut into transverse slices for examination. This revealed numerous small holes between sheath layers, particularly near constriction points. The conductor bundles were generally filled, but a few voids were noted.

It is believed that the pressure of the plugging compound in the core forces the core wrap against the cable jacket, preventing the plugging compound from adequately entering this area. In addition the space between the core wrap and the cable jacket is the last to fill. It tends to be filled with material which is in an advanced cure state due to its long residence time in the core. Because of its advanced cure state it can not adhere to the surrounding surfaces. (See Figure 3.)

## Sleeve Injection Trials

Since it appeared that the sheath injection method was not too reliable, experiments were conducted on the sleeve injection method. The first samples, prepared according to standard practice, showed minor leakage along the inter-sheath surface. Subsequent samples were prepared with a minor modification: twisted lengths of 25 mm (1 inch) wide surgical gauze were inserted between all sheath layers to ensure uniform, circumferential openings. In addition, all sheath surfaces were wiped with solvent before the sleeve was installed.

When these samples were tested the leakage through the plugs was nil. Even after 40 freeze-thaw cycles in an environmental chamber there was no detectable leakage.

A further test was made using the sleeve injection method, but this time the samples were instrumented with pairs of pulp-insulated wire. As in previous tests, the pulp-insulated pairs were used to monitor both the arrival and cure state of the plugging material in the interstices between the sheath layers. In this case, however, the monitors showed an early and uniform arrival of new material in all areas. There was no sign of reflow of earlier deposited material. (See Figure 4.)

Tests were made using compounds with 20-minute and 40-minute gel times at different field installation temperatures. It was found that 22°C (72°F) was the highest temperature at which the 20-minute material gave good adhesion with all sheath layers. The 40-minute material also gave good adhesion with all sheath layers. The 40-minute material could be used at temperatures up to 35°C (95°F) and still maintain a high degree of adhesion. Incidentally, it was realized during these and other tests that only large batches or cartridges of material should be used for plugs. The delay resulting from use of multiple small cartridges means that partially cured material is being forced into the most difficult areas to plug.

## EXPERIMENTAL RESULTS - PULP INSULATED CABLES

## Penetration Problem

From previous work it is known that the mode of failure of pressure dams in pulp-insulated cables is along the

conductors in nearly all cases. It had been suspected that the dye in the pulp insulation was in some way related to this problem. Therefore, the first step in this study was to determine what, if any, effect the dye had on the plugging material.

Accordingly an experiment was set up in which samples of plugging compound were poured through matrices of dyed and undyed pulp-insulated conductors. The cure times of the liquid collected were compared with the cure times of similar volumes of control samples. This confirmed that the dye does have an accelerating effect on the cure time, while the uncoloured insulation has only a marginal effect. Specifically, the liquid exposed to the dye gelled in 43% of the time of the control liquid.

In addition to the accelerated cure time, it was found that the pulp insulation tends to swell on exposure to plugging compound. These two factors point to a mechanism which is consistent with many examinations of failed plugs. The liquid material begins to penetrate the insulation and becomes viscous before it can reach the conductor. (See Figure 5.) The material cures and forms an outer annulus of treated pulp. At the same time the treated portion swells, forming an interface of torn and broken material through which air may flow.

Sleeve Injection Trials

To establish basic data on plug failures, a number of sample plugs were prepared. A common type of cable was used and standard practice was followed, except that silicone treated polyethylene core pins were used instead of wood dowels. One cable was left with the binder ribbons uncut, since this, in fact, is sometimes done in the field. A 20-minute gel-time material was used. Both 1200- and 3000-pair cables were tested.

Pairs of conductors were selected from different locations in the core and used as monitors to indicate the arrival and cure state of the liquid. As the plugs were formed the data from the monitors indicated poor distribution of the liquid through the core. After curing, leakage tests confirmed that all plugs in the test had failed to seal.

Subsequent examination of the plugs indicated clearly that the liquid did not penetrate to the centre of many binder groups. In addition there was evidence of swelling and numerous conductors were loose enough to be pulled out easily.

Subsequent tests were made using a 40-minute gel time material and then with a 60-minute gel time material. Results showed that the 40-minute material produced good results with the 1200-pair samples, while the 60-minute material produced good results with the 3000-pair samples. The key, it appears, is to lengthen the nominal gel-time to compensate for the accelerating effect in the cure rate caused by the dye in the pulp. This allows the material to remain in a non-viscous state long enough to penetrate to the centre of the core and to the copper of each wire. The bigger the cable, of course, the longer the penetration time.

RECOMMENDATIONS

PIC Cables

Our laboratory trials indicated that the sheath injection method of installing pressure dams is wholly inadequate. The high incidence of leakage can be directly related to the fact that movement of the core wrap can occur when a portion of the sheath is removed.

As a result of the trials the sleeve injection method is recommended. One minor change to the standard procedure is suggested. That is, a twisted length of 25 mm (1 inch) cotton gauze should be inserted circumferentially between all adjacent sheath layers. This will prevent one layer from pressing tightly against another under fluid pressure thus preventing entry of plugging material.

Pulp-Insulated Cables

The principal cause of pressure dam failure is the acceleration of the cure rate of the plugging material by the pulp dye. This inhibits the penetration of the material throughout the core. The standard method of application specified a material with a 20-minute gel time. If a plugging material of longer gel time is used (40 minutes or 60 minutes depending on the size of the cable) the incidence of pressure dam failure due to pressure loss decreases to a very low level.

Reference

Proceedings of the International Wire & Cable Symposium Atlantic City, N.J. Dec. 3-5 1974. "Economics & Performance Considerations of Telephone Cable Plugging by Francis M. Farrell III, Manual Filrets, James D. Groves & Henry K. Kappell, 3M Co. St. Paul Minn.

[1] Trademark of E.I. duPont de Nemours & Co. Inc.

*Table I*
Pressure Dam Tests on Various Sizes and Cable Configurations on Air Core PIC Cable

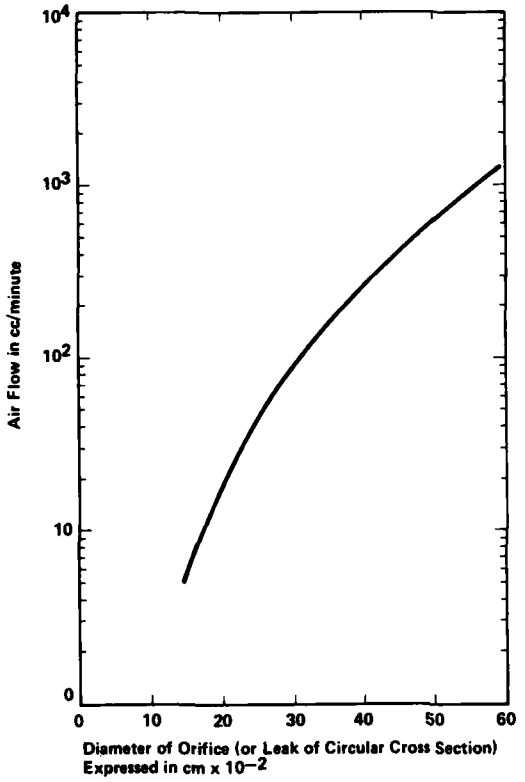
| Cable Description | Amount of Compound | Size of Air Leak | Cycle of Failure | Mode of Failure |
|---|---|---|---|---|
| 22 AWG PAP 100 pr | 260 cc | 0 cc/min | 40* | |
| 22 AWG PAP 100 pr | 255 cc | 0 cc/min | 40* | |
| 24 AWG PAP 200 pr | 165 cc | 20 cc/min | 20 | Between Metal and Outer Cable Sheath |
| 26 AWG PAP 300 pr | 145 cc | 50 cc/min | 30 | |
| 26 AWG PAP 300 pr | 140 cc | 10 cc/min | 20 | At Injection Port |
| 26 AWG PAP 600 pr | 295 cc | 500 cc/min | 0 | |
| 26 AWG PAP 600 pr | 275 cc | 500 cc/min | 0 | Between Mylar and Cable Jacket |
| 26 AWG PAP 900 pr | 450 cc | 500 cc/min | 0 | |
| 26 AWG PAP 900 pr | 475 cc | 500 cc/min | 0 | |
| 22 AWG Sealpap 100 pr | 225 cc | 0 | 40* | |
| 22 AWG Sealpap 200 pr | 300 cc | 100 | 30 | Between Mylar and Cable Jacket |
| 26 AWG Sealpap 600 pr | 325 cc | 200 | 0 | |
| 26 AWG Sealpap | 510 cc | 500 | 0 | |
| 19 AWG Sealpeth 100 pr | 300 cc | 0 cc/min | 40* | |
| 19 AWG Sealpeth 200 pr | 800 cc | 20 cc/min | 40 | Out the Injection Port |
| 19 AWG Sealpeth 200 pr | 850 cc | 0 cc/min | 40* | |

(Continued)

Table I (Continued)
Pressure Dam Tests on Various Sizes and
Cable Configurations on Air Core PIC Cable

| Cable Description | Amount of Compound | Size of Air Leak | Cycle of Failure | Mode of Failure |
|---|---|---|---|---|
| 24 AWG Sealpeth 400 pr | 150 cc | 200 cc/min | 20 | Between Mylar Wrap and Cable Sheath |
| 26 AWG Sealpeth 600 pr | 100 cc | 500 cc/min | 0 | |
| 22 AWG Alpeth 100 pr | 200 cc | 0 | 40* | |
| 22 AWG Alpeth 100 pr | 195 cc | 25 cc/min | 40 | Between Metal and Outer Sheath |
| 24 AWG Alpeth 200 pr | 115 cc | 50 cc/min | 30 | |
| 24 AWG Alpeth 300 pr | 155 cc | 250 cc/min | 5 | Between Metal and Outer Cable Sheath |
| 26 AWG Alpeth 600 pr | 180 cc | 180 cc/min | 0 | Between Mylar Wrap and Cable Jacket |
| 26 AWG Alpeth 900 pr | 480 cc | 500 cc/min | 0 | |
| 26 AWG Alpeth 900 pr | 450 cc | 500 cc/min | 0 | |

* Denotes Completion of Programmed Test Cycle




Volume of Air Lost vs Orifice Diameter

Figure I

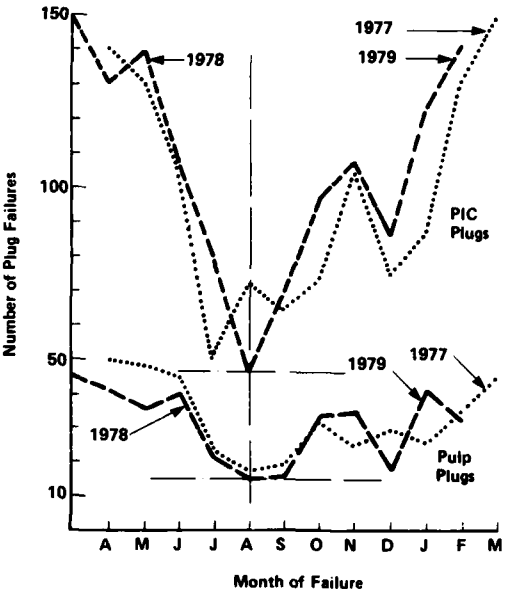



Figure II Plug Failure Record CCUAP 1977-1979

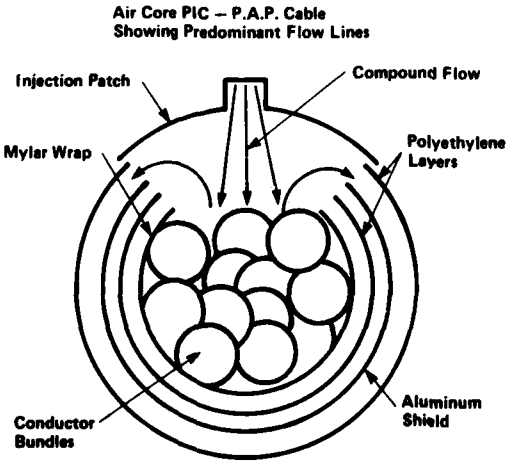



Figure III Sheath Injection Method

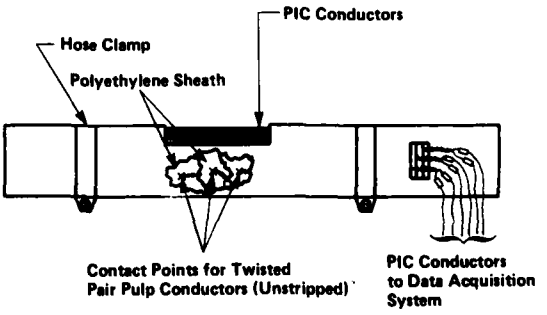



Figure IV Drawing Illustrating How the Pulp Twisted Pairs were Installed in the P.A.P. Cable Pressure Dams to Monitor Plugging Compound Flow

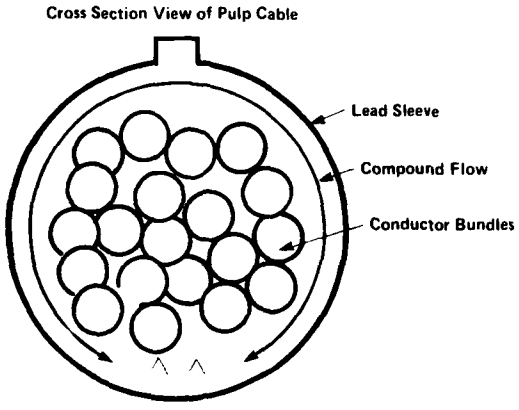



Figure V Open Sheath – Lead Sleeve Method

BIOGRAPHY



Bill Trumble graduated in 1958 from St. Ambrose College with a B.A. in Chemistry. He pursued graduate studies at St. Louis University and the University of Missouri. Bill has extensive applied plastic engineering experience based on his research activities with the polymer research groups of Emerson Electric, Brunswick, and Tremco Co. He is currently engaged as an applied plastic engineer for Bell-Northern Research.



Christopher D. Gupta graduated in May, 1974 from the University of Waterloo with Bachelor of Applied Science Degree in Electrical Engineering. He joined Bell Canada at that time. His career at Bell Canada has been in Technology Development in the Transmission System Division. Currently he is Supervising Engineer in Outside Plant for Wire Connecting, Apparatus & Closures.

# THEORETICAL ANALYSIS AND REDUCTIONAL COUNTERMEASURE OF DANCING PHENOMENA ON SELF-SUPPORTING CABLE

M. Iwazaki K. katagiri A.Sekiguchi S. Masaki

Nippon Telegraph & Telephone Public Corp.
Tokyo, Japan

## Abstract

CCP-SS Cable for overhead subscriber distribution use copes with material and manpower reduction, and improves workability and security. On the other hand, its characteristic shape easily causes vibrations. Strong wind generates self-vibration in the cable, called "dancing phenomena". In NTT, messenger wire breaking because of material fatigue was caused by vibrations. Therefore, from the result of observations on vibrations in the field during the experiment, the cable dancing locus was clarified, and the correlation between installation conditions and dancing phenomenon was analyzed. Furthermore, critical conditions of dancing occurence were explained, using the relationship between installation condition and wind velocity, resulting from numerical analysis. This paper describes theoretical analysis methods and present result obtained for vibration phenomenon on SS-cables, and an outline of new SS-cable for overhead subscriber distribution use system developed using these results.

## 1 Introduction

A Self-Supporting Cable (SS-Cable) for overhead subscriber distribution use, which has a messenger wire attached directly above the cable, copes with material and manpower reduction in overhead telephone line construction and improves workability and security, through eliminating cable hanger ring installation onto strand wires for round cables.

On the other hand, an aerodynamically nonsymmetric cross section of an SS-Cable easily causes vibrations when hit by a cross wind or a diagonal wind. Strong wind generates self-vibration in the cable, called "dancing phenomena".

Countermeasures against metal weakening, which is known as material fatigue, due to messenger wire vibration are required. However, dancing phenomena has rarely been analyzed quantitatively anywhere. So there are many unsolved problems left.

Therefore in NTT, from the result of observations on vibrations in the field during the experiment, the cable dancing locus was clarified, and the correlation between installation conditions and dancing phenomena was analyzed. Furthermore, critical conditions in regard to dancing occurence were explained, using the relationship between installation conditions and wind velocity, resulting from numerical analysis.

This paper describes theoretical analysis methods and results obtained for vibration phenomenon on SS-cables, as well as an outline of new SS-cable for overhead subscriber distribution use developed using these results.

## 2 Vibrations in Cables

### 2.1 Clasification of Vibration Phenomenon in Overhead Cables

Vibrations in overhead cables, which are generated by wind force, are segregated into self-vibrations and compulsory vibrations, depending on their occurence mechanism. (Fig. 1) Self-vibrations are generated in objects because they have aerodynamic lift characteristics, even if the wind is blowing at a constant velocity. These vibrations include galloping, pitching and dancing in SS-cables. Compulsory vibrations are the phenomenon in overhead cables compulsorily vibrated by wind force, and are strongly correlated with periodical change in wind velocity.

### 2.2 Dancing Phenomena Principle

Well known dancing phenomena principle was suggested by J. P. Den Hartog in 1932. Dancing phenomena was theorized from the point of view that objects with an aerodynamically nonsymmetric cross section, such as ice coated transmission lines and overhead cables, cause negative slope lift characteristics according to the wind striking angle force. Hartog's theory points out that vibration occurs without pitching, but vibration is recently considered to be a large factor in shifting cable movement from trembling to dancing and in keeping cables dancing for a long term.

#### 2.2.1 Dancing without Pitching

Cable with nonsymmetric cross section is hit by relative wind velocity V, as shown in Fig. 2, when it is hit by velocity U cross wind and trembles in a swing format. If the cable faces, as shown in Fig. 3, in respect to the wind direction in order that exactly transverse wind flow at relative wind velocity V would hit it,

```
Vibration Phenomena----Self-Vibration----------(due to Lift Characteristic)--------Dancing
                    '                                                    '-------Galloping
                    '
                    '---Compulsory Vibration----(due to Vortex)----------------------Karman Vibration
                                                '
                                                '---(due to Periodic Aerodynamic Force)--Buffeting
                                                                                        '-Rocking
                                                                                        '-Subspan Vibration
                                                                                        '-Wake Induced Oscillation
```

Fig. 1 Clarification of Vibration Phenomena in Overhead Cables

lift force affects the cable in the same way as air flow affects the wings of an airplane. Cable movement is accelerated in an upward motion, whose components are a resultant combination of lift and drag force. The cable keeps moving upward until the force becomes balanced with the cable's own weight, pitching moment and downward motion due to the drag on cable motion caused by pole to pole stringing tension. Thus, as the cable movement reaches the highest point, upward motion component disappears and the motion shifts downward because of the potential energy stored in the cable. When the cable has a downward velocity component, the cable is acted on by the downward suction and keeps moving until the force becomes balanced with the pitching moment and upward motion component caused by the cable pole to pole stringing tension. The amplitude of the vertical vibration at a mid-point in the cable span is amplified according to any change in wind angle in regard to the vertical motion of the cable itself.

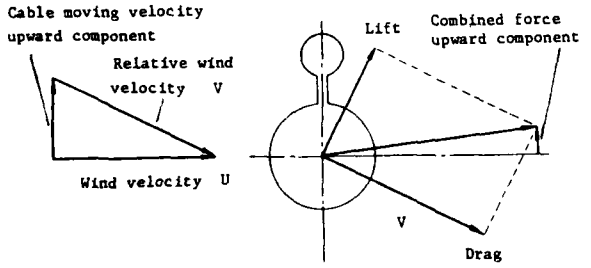



Fig. 2 Aerodynamic forces due to relative wind velocity

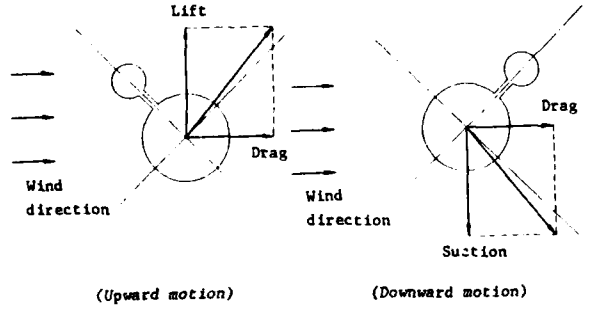



Fig. 3 Aerodynamic forces without pitching

2.2.2 Dancing with Pitching

Objects hit by wind are acted on by three forces, perpendicular lift and parallel drag to the wind, and gyrational pitching moment, as shown in Fig. 4. The strength of these forces is governed according to their shape, wind direction and wind velocity. In the case of SS-cables, the relationship between these three forces and wind strike angle is shown in Fig. 5, based on the results of wind tunnel tests. Even if wind angle is zero degree at first, the angle is increased by the pitching moment and lift strength increases. Then, the vertical motion is accelerated. Thus, once the motion of a cable has a vertical component, the motion grows into self-vibration, in the same way as represented by Hartog's theory. If vertical vibration frequency agrees with pitching vibration frequency, the cable keeps vibrating sympathetically for a long term, as shown in Fig. 6.

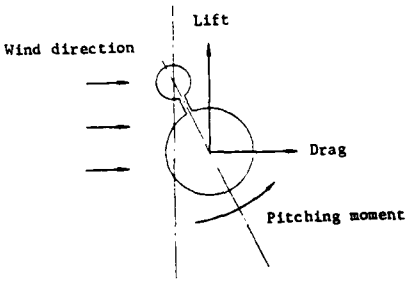



Fig. 4 Aerodynamic forces with pitching

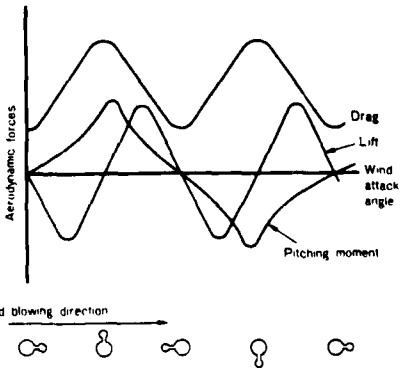



Fig. 5 Relationship between aerodynamic forces and wind attack angles

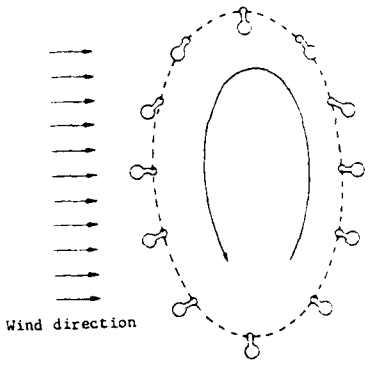



Fig. 6 Cable locus during dancing

Table 1 Relationship between Dancing Phenomenon Probability and Installation Conditions

| Installation Conditions | | Dancing Probability* |
|---|---|---|
| Cable weight | Light | ○ |
| | Heavy | × |
| Span length | Short | × |
| | Long | ○ |
| Dip | Small | × |
| | Large | ○ |
| Number of twists | Few | ○ |
| | Many | × |
| Wind direction | Parallel to cable | × |
| | Perpendicular to cable | ○ |

(* ○ :probable, × :improbable)

2.3 Observations in the Experimental Fields

Observational research on vibrations in SS-cables was carried out in Sakata experimental field for three years, from 1976 through 1978. Sakata experimental field was established in 1969. The cables installed in the field were laid out so that strong and transverse winds blew from the Sea of Japan against overhead cables installed there. Study results were useful in order to understand the environmental durability characteristics of outside plant in a stormy area.

From the results of the observations on dancing phenomenon, valuable data were obtained and used in theoretical analysis. For example, it was clarified that the cable dancing locus is elliptical, as shown in Fig. 7, and that a useful countermeasure is to twist the cable around the supporting messenger wire in one cable span and increase the cable installation tension in order to suppress the vibrating cable amplitude in respect to the relationship between dancing phenomenon and cable installation conditions, as shown in Table 1.

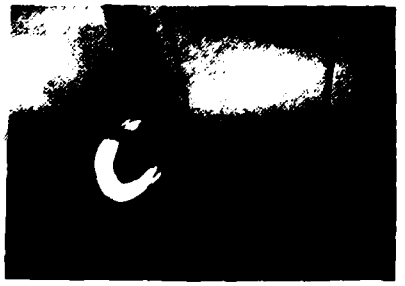


Fig. 7 Dancing phenomenon on self supporting cable

2.4 Dancing Phenomena Numerical Analysis

It is impossible to get analytical solutions from given equations on the vibrations in outside plant equipment, unless a linear approximation of aerodynamic force is taken into account, because of their unstability and nonlinearity. On the other hand, according to recent advances in computer analysis technique, various programs have been developed, which can numerically solve rather complicated equations. One of them is useful with differential approximation to analyze the equations numerically.

In this research, quantitative analysis is practiced as a part of an explanation on vibration phenomenon in SS-cables, to determine the accord between experimental results and theory, and to estimate critical wind velocity which would generate dancing in various kinds of cables under various installation conditions.

An outline of the program developed to simulate dancing phenomenon in SS-cables is shown in Fig. 8. In order to avoid the program from repeated running, Adams Bashforth's method is taken to solve the equation.

It is impossible to get an accurate representation of actual phenomenon from the solutions. If the wind conditions are assumed to be constant, it becomes possible to understand the relationship between dancing phenomenon and cable installation conditions, such as cable classification, span length, stringing tension, number of twists and so on. Natural winds have nonuniform characteristics in time and space, as shown in Fig. 9. They are approximated here using a step function wind in time as a trigger to cause dancing in a cable. A cable, which is balanced with wind at velocity V1, is hit by velocity V2 wind for time T2, then by velocity V1 wind afterwards. (Fig. 10)

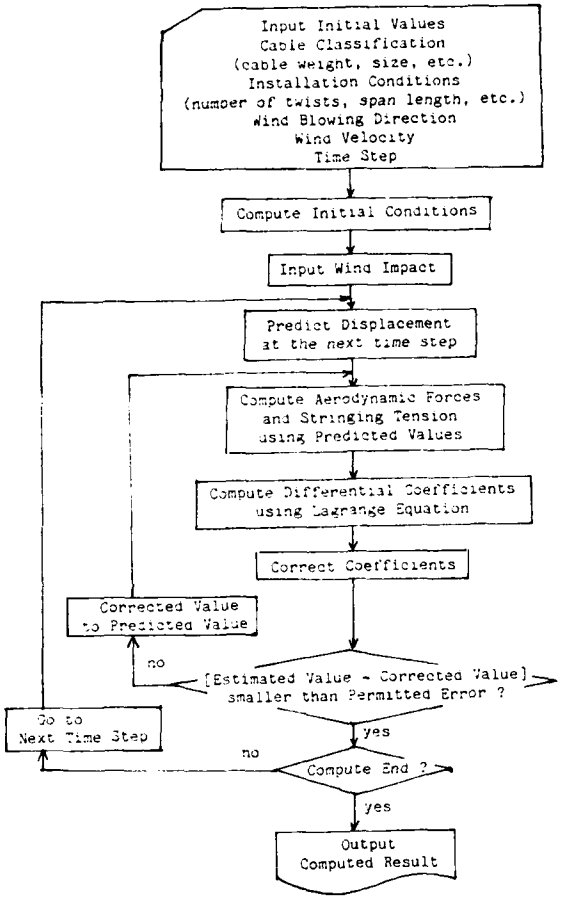



Fig. 8 Program Outline

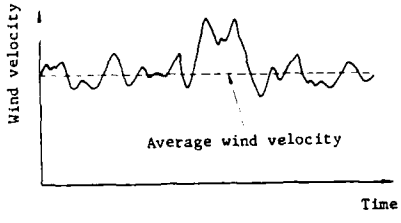



Fig. 9 Natural wind form

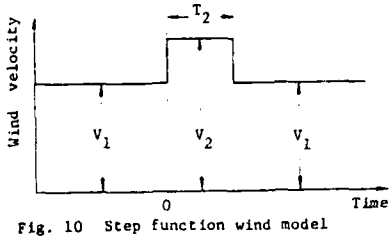



Fig. 10 Step function wind model

An example of the analysis results is shown in Fig. 11. Cable vibration locus is shown in Fig. 12.

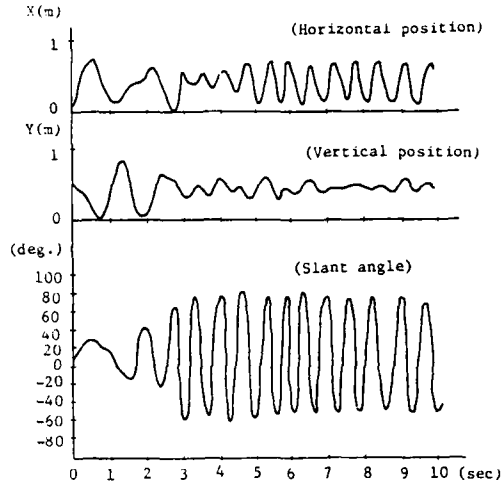



Fig.11 Dancing phenomina analysis results

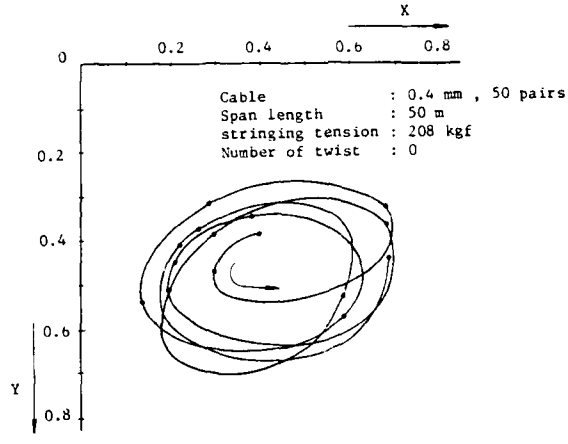



Fig. 12 Cable vibration locus

From these results, the relationship between cable classification, span length, stringing tension and critical wind velocity to generate dancing, under constant wind conditions, is shown in Fig. 13.

## 3 Reductional Countermeasures against Vibrational Strain

### 3.1 Strain Occurence Mechanism

Following six factors are considered as origins of strain around a suspension clamp used to support an overhead cable.

[1] Stress according to stringing tension
[2] Stress according to cable bending around the cable suspension clamp
[3] Distortion stress according to cable pitching

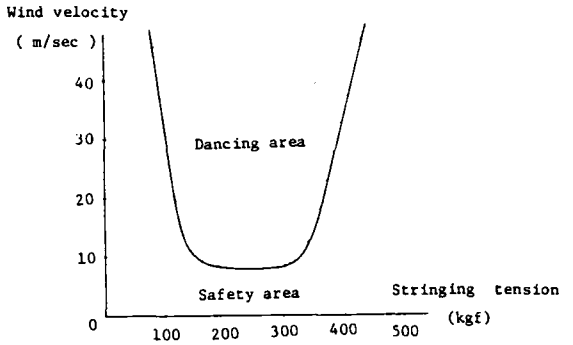



Fig. 13 Relationship between stringing tension and wind velocity

[4] Stress according to alternating additional tension because of vibration

[5] Stress according to cyclic cable bending because of vibration

[6] Stress according to cyclic cable pitching because of vibration

[1], [2] and [3] cause static strain, and [4], [5] and [6] cause dynamic strain. Bending stress is considered to be a main factor contributing to vibrational fatique.

### 3.2 Vibrational Fatique in Stranded Messenger Wire

The characteristic of vibrational fatique in stranded messenger wire is explained by the relationship between average stress calculated from stringing tension and cyclic stress according to cable bending because of vibration. Figure 14 shows endurance limit in stranded messenger wire, and maximum cyclic stress limited by total strain.

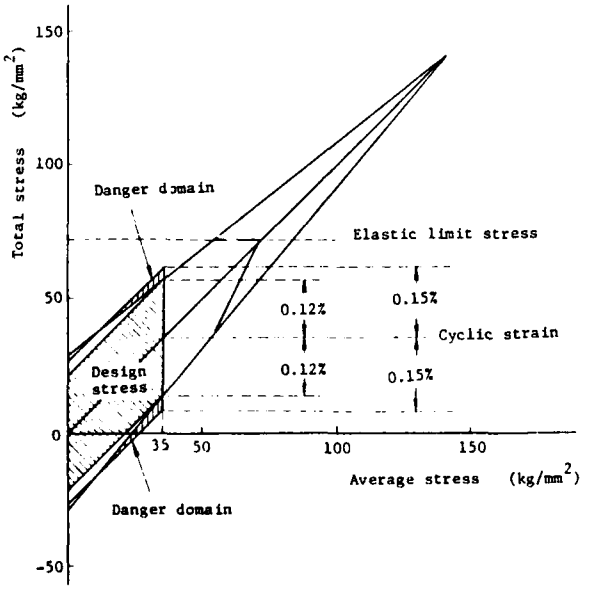



Fig. 14 Endurance limit in stranded wire

The diameter of stranded messenger wires used in present SS-cables is designed to withstand a maximum average strain of 35kgf/mm2 and a maximum vibration distortion of 0.06%, in consideration of a safety factor of 2. However the maximum bend strain happened to be about 0.15%, based on results of observations on dancing. As this strain value exceeds the safety limit of cyclic stress, there is a possibility of breakage in messenger wires.

Reduction in maximum strain because of vibration is first examined with decreasing cable dip caused by increased cable installation tension as a countermeasure against it. On the other hand, dip decrease and increased stringing tension causes some kinds of SS-cables to have higher than 35kgf/mm2 average stringing stress . Thus, cables are designed with thickened stranded messenger wire to withstand an average stress of less than 35kgf/mm2, the same as in the present construction condition.

The messenger puller and the messenger wire structure are improved to get constant stringing tension of 1000kgf, as shown in Figs. 15, 16 and 17. As a result, the maximum strain because of vibration can be about 0.09%. This strain limit satisfies cable installation safety limits.

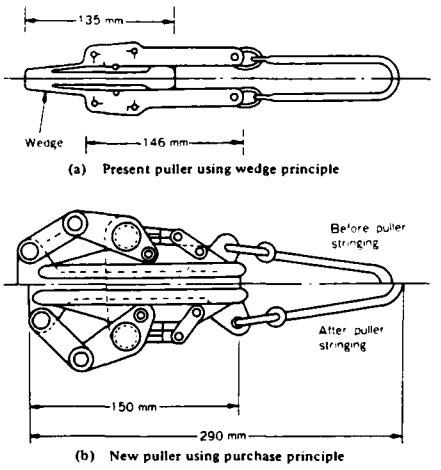



Fig. 15 Messenger puller for self supporting cable

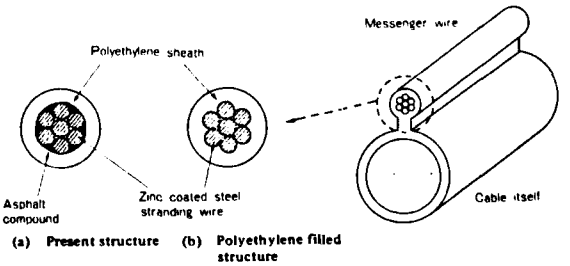



Fig. 16 Self supporting cable messenger wire structure

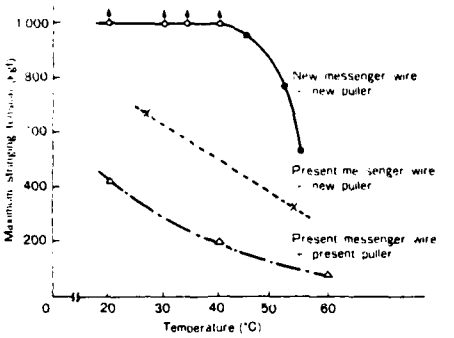



Fig. 17 Relationsnip between puller stringing tension and atmospheric temperature

In order to secure the safety factor of 2, a messenger wire protection method was developed with increased rigidity by winding a messenger guard on a messenger wire passing under the cable suspension clamp, as shown in Fig. 18. From the result of vibration test, a messenger guard, 2.15mm in diameter and 500mm long, gives the minimum strain in stranded messenger wire. This method satisfies the safety factor of 2, as shown in Figs. 19 and 20.

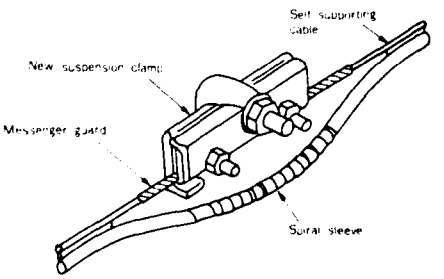



Fig. 18 New cable suspention method

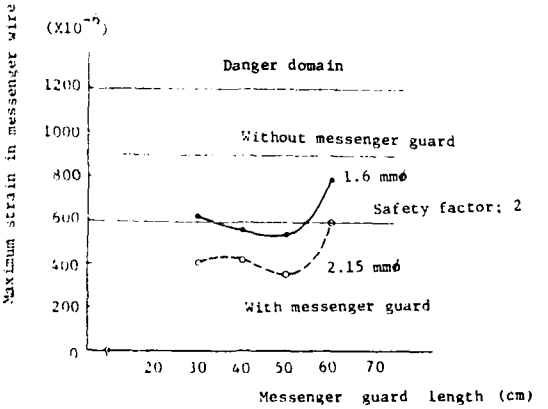



Fig. 19 Messenger guard effect

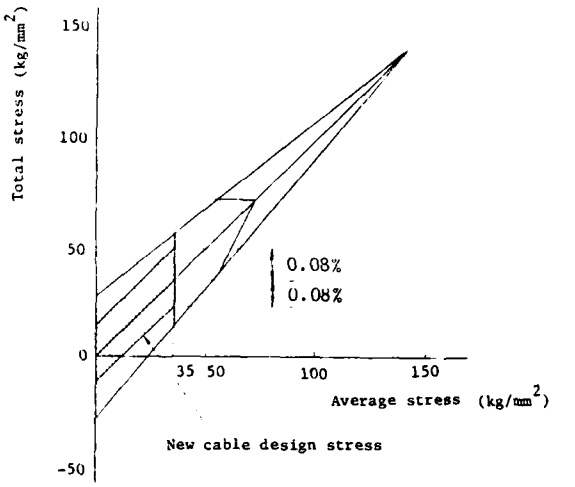



Fig. 20 New SS-cable design stress

## 4 Conclusion

Newly developed SS-cable system is considered as an effective countermeasure against vibration fatigue. It copes with material and manpower reduction and improves workability and security under the same conditions on system design, construction and maintenance, as those of round cables hung by brackets from separate messenger wires. In this developement, dancing, the inherent vibration phenomena in SS-cables, was studied as an actual motion. Vibration conditions are clarified from the observations, and are reflected in the vibration fatique test apparatus using the result of analysis. Thus, more reliable construction methods for stringing cables were developed.

Moreover, vibration conditions in this study are clarified in a particular geographical area, such as Sakata, and new cable installation system was developed theoretically, based on the results according to the vibration mechanism.

It is considered to be important to accumulate data and to build a more reliable system, as actual phenomenon in the field sometime cannot be imagined.



Masatoshi Iwazaki
Engineering Bureau, NTT
1-6, Uchisaiwai-cho
1-chome, Chiyoda-ku,
Tokyo, Japan 100

Mr. Iwazaki, Senior Staff Engineer of NTT's Engineering Bureau, is now engaged in developmental research planning on whole telecommunication outside plant, cables, telephone poles, ducts, terminal boxes and so on. He is a member of the Institute of Electronics & Communications of Japan.



Kiyoshi Katagiri
Engineering Bureau, NTT
1-6, Uchisaiwai-cho
1-chome, Chiyoda-ku,
Tokyo, Japan 100

Mr. Katagiri, Staff Engineer of NTT's Engineering Bureau, is now engaged in developmental research on underground subscriber distribution system, overhead subscriber distribution system and improvement in CCP-SS cable structure. He is a member of the Institute of Electronics & Communications of Japan.



Akiyoshi Sekiguchi
Engineering Bureau, NTT
1-6, Uchisaiwai-cho
1-chome, Chiyoda-ku,
Tokyo, Japan 100

Mr.Sekiguchi, Staff Engineer of NTT's Engineering Bureau, is now engaged in developmental research on CCP-SS cables, overhead materials, cable stringing method and is taking charge of submarine cable system. He is a member of the Institute of Electronics & Communications of Japan.



Mr. Shojiro Masaki
Engineering Bureau, NTT
1-6, Uchisaiwai-cho
1-chome, Chiyoda-ku,
Tokyo, Japan 100

Mr. masaki, Staff Engineer of NTT's Engineering Bureau, is now engaged in developmental research on CCP-SS cable stringing method and overhead telephone line construction method. He is a member of the Institute of Electronics & Communications of Japan.

# IRRADIATED POLY (VINYL CHLORIDE) INSULATED WIRE USED IN TELEPHONE EQUIPMENT

E. A. BUREK

Western Electric Co.
Omaha, Nebraska

## SUMMARY

A coordinated Western Electric-Bell Telephone Laboratories development project was initiated in the mid 1960's to develop a suitable polymeric material for use as a replacement for the composite PVC-textile-lacquer insulation used in the manufacture of approximately 5 billion conductor feet of telephone wires annually. This paper deals with the reasons for initiating the project, the development of a crosslinkable poly (vinyl chloride) compound, the development of the associated wire manufacturing facilities, the implementation of the new manufacturing process and the benefits realized.

## INTRODUCTION

A joint Western Electric - Bell Telephone Laboratories engineering task force was assembled in late 1967 as the Textile Replacement Committee. Its purpose was to replace, with a polymeric material, the composite PVC - textile - lacquer insulation used in the manufacture of some of the telephone wires. At that time, there were three composite insulations; triple textile served, PVC-textile served, and PVC-textile braided. All were coated with a fire retardant lacquer.

Over five billion conductor feet of the textile covered wires were being produced for applications where wire connections were soldered, thereby requiring insulation with good solder heat resistance characteristics. Also, uses of the wires were such that other physical characteristics such as good mechanical strength, abrasion resistance, cut through, and fire retardancy were of primary importance. The manfacturing processes for the composite textile insulating wires required the use of slow speed cotton serving, braiding and lacquering machines, and cotton purification, dyeing, and winding equipment. Substantial manufacturing savings in labor, material, and floor space could be realized if the composite insulations were replaced with a single extrudable material having comparable electrical and physical properties.

At about the same time that the Textile Replacement Task Force was formed, studies conducted by the telephone companies showed that the then increasing demand for telephones was placing a heavy burden on the central office main distributing frames. That piece of equipment in the telephone central office contains horizontal racks that hold wires referred to as Distributing Frame Wires. These wires serve as links or jumper wires between the subscribers telephone line and the switching equipment. The wire used at that time was a PVC-textile served wire. It was relatively big, with an outer diameter of .054" for the 22 gauge wire, and it had a relatively high coefficient of friction. The latter characteristic made it impossible in many instances to pull the jumper wire out of the bundle of wires in one of the frame shelves after the wire was no longer required, for example, because a subscriber moved. The large size and the problem of removing jumpers would eventually result in an overcrowded condition. A smaller wire with a lower coefficient of friction was required for more effective utilization of space in the distributing frame wire racks. Otherwise, costly building expansions would have to be made. Development efforts of the task force resulted in the development of a crosslinkable poly (vinyl chloride) compound designated as type 801 PVC. It uses a multi-functional monomer, tetraethylene glycol dimethacrylate, which acts as a PVC plasticizer during extrusion and crosslinks when bombarded with high speed electrons, forming a three dimensional molecular network. Also, the PVC matrix is incorporated into the network through a system of graft crosslinks. This converts the thermoplastic PVC into a thermoset plastic with higher tensile strength, increased abrasion and solder heat resistance, and greater thermal stability.

COMPARISON OF INSULATION CHARACTERISTICS

| | | 801 PVC | COMPOSITE INSULATION |
|---|---|---|---|
| Solder Heat Res. | (Sec.) | 1.4 | 1.6 |
| Cut Through | (Lbs.) | 8 | 11 |
| Abrasion Resistance | (Rev.) | 13 | 7 |
| Wire Diameter | (In.) | .041 | .054 |

## DEVELOPMENT OF MANUFACTURING FACILITIES

### PILOT FACILITIES

Development and initial production of the irradiated telephone wire were done on pilot wire irradiation facilities. These included two 400KeV, 50 milliampere electron beam accelerators located in a concrete block chamber. The associated wire handling supply and take-up units were located outside the chamber. The chamber was designed to allow passage of wire through the electron beam and also to properly shield the operator from the secondary X-rays generated during the irradiation process. There is no residual radioactivity associated with this process. Work done with the pilot facilities provided the data necessary for establishing requirements for the permanent facilities.

### PRODUCTION FACILITIES

Productivity studies made on the pilot irradiation facilities indicated that one 400KeV, 50 milliampere electron beam accelerator could irradiate approximately 2 billion conductor feet of wire annually at the required dose. This enabled us to determine the number of irradiation units that would be required to meet projected product demands.

The acquisition, installation, and prove-in of the permanent facilities were done in two stages. In the first stage, the PVC-textile cable and miscellaneous loose wires were replaced. In the second stage, and to some extent in the first stage, the composite textile distributing frame wires were replaced with the irradiated wire.

An irradiation facility consists of one electron beam accelerator totally enclosed by a poured concrete chamber which provides safety protection against radiation leakage during the operation of the accelerator. Within the irradiation chamber an enclosure was built around the window of the accelerator and the wires being irradiated to limit the space through which the electrons travel in air, thereby minimizing generation of ozone and other by-products (Fig. 1.) Individual wire pay-off and take-up units are located outside the chamber to simultaneously supply wires to the chamber for irradiation and to wind the irradiated wires onto individual take-up reels. A coordinated shutter and splice arrangement controls radiation dosage and permits the continuous irradiation of the multiple wires without accelerator shutdown for either a supply or take-up reel change. Design of the rewind facilities is such that lifting of the reels of wires by the operator is not required.

### UNIFORM DOSAGE

A problem of achieving uniform distribution of the dose was encountered in the initial development phase. This was due mainly to the shielding effect of the copper conductor. This was resolved by oscillating the wire as it passed through the string-up unit within the irradiation chamber. The design is such that as the wire travels from the upper to the lower pulley section of the string-up unit, it oscillates around a vertical axis, thereby achieving uniform irradiation of all surfaces. Depth dose studies were performed to determine the optimum distance for positioning wires relative to the accelerator window and the exposure time required to achieve desired energy absorption. Blue cellophane, which bleaches when exposed to radiation, was calibrated and used to determine the amount of energy absorbed. The studies showed that, as the distance from the window increased, the energy of the electrons and beam concentration decreased. Also, the electron beam has a larger width at distances farther from the accelerator window yielding an increase in exposure time. Therefore, a distance from the window can be determined which optimizes energy absorption. To determine the dosage required for maximum crosslinking, irradiated samples were immersed in hot tetrahydrofuran in which the uncrosslinked PVC and monomer are soluble. A dose was established to yield the optimum irradiation level. Any increase in dosage beyond this point did not substantially increase the percent of crosslinked PVC. (Figure 2)

### COMPOUND IMPROVEMENT

While the manufacturing facilities were being developed and installed, work on improving the processability of the crosslinkable PVC was continuing. A new compound, designated as 802 PVC was formulated. Compared to the 801 PVC, it has better extrusion characteristics with a longer time interval before gelation and, prior to irradiation, it has a higher compression rating, therefore, it is less subject to mechanical damage during processing. After irradiation it has a higher and more stable elongation value, is more flexible, and has a higher temperature rating. Development of the 802 PVC made possible the replacement of the last remaining textile served wire with the irradiated type.

# TYPICAL VAULT STRUCTURE

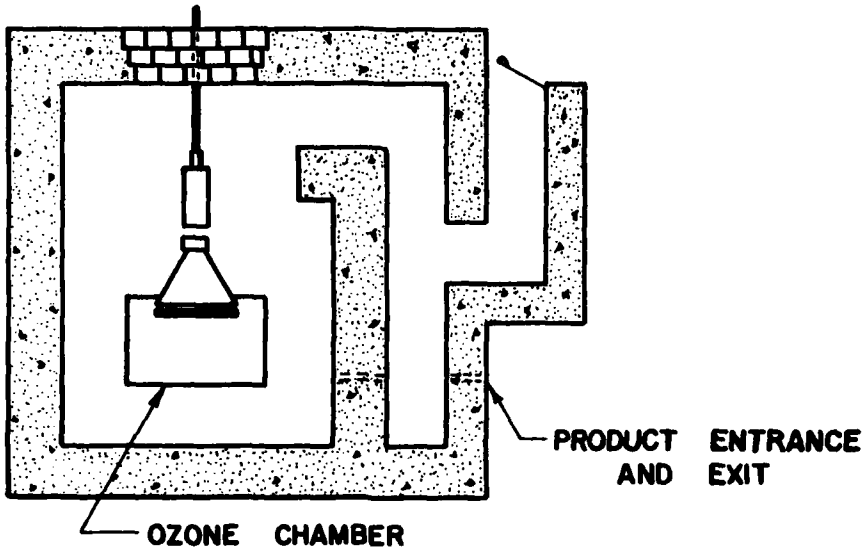
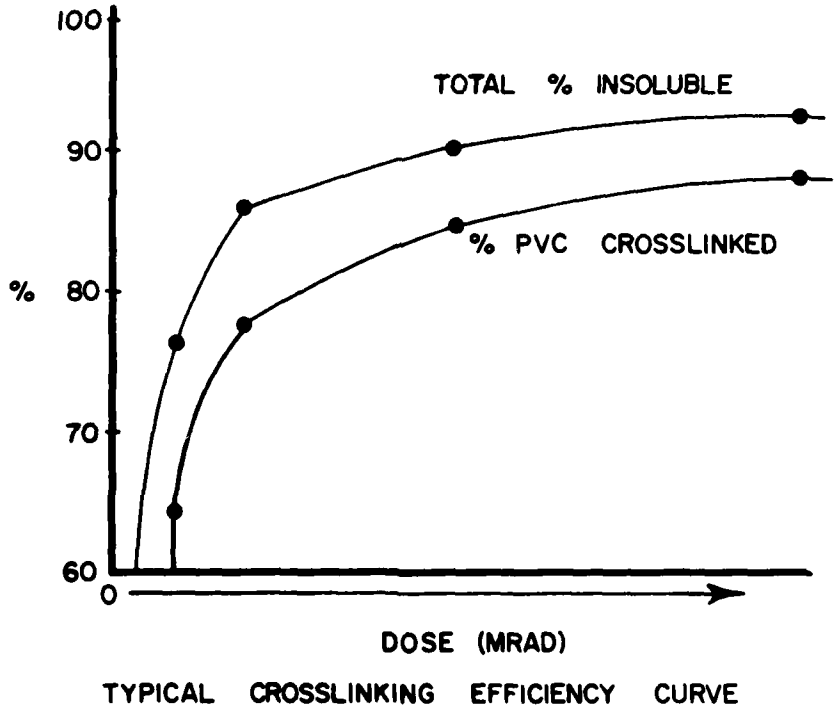



Figure 2 - Crosslinking Efficiency




TYPICAL CROSSLINKING EFFICIENCY CURVE

Figure 1 - Typical Vault Installation

## BRAIDED WIRES

Yet to be replaced are the composite PVC textile braid-lacquer coated wires used in applications where tensile strength, abrasion resistance, and cut through requirements are more stringent than for the other telephone wires. Current production levels are at approximately 200 million conductor feet per year. A total of 300 textile braiders are used in the production of these wires. The braiders are slow speed, high noise level machines and operators are required to wear ear plugs or muffs. Also, lacquering facilities are required to apply the fire retardant lacquer. Several wire designs are currently under consideration as replacements for the braided wire. It is anticipated that one of the wire designs currently under consideration will be an acceptable substitute and that braided wires will be a thing of the past, completing the work begun in 1967 by the Textile Replacement Committee.

## CONCLUSION

The systematic replacement of composite textile wires with the irradiated PVC wire has provided the following benefits:

1. Reduction by over 50% of the number of different vinyl wire codes manufactured by Western.
2. Manufacturing savings of over $4.5 million annually.
3. Cost avoidance in central office expansions.
4. Elimination of high noise level textile serving machines.
5. Reduced manufacturing floor space requirements.


## ACKNOWLEDGEMENT

The author wishes to express his appreciation to Mr. R. K. Swartz - Atlanta, PECC for his assistance in the preparation of this article and to Mr. E. Scalco - Bell Telephone Laboratories for his editing advice.


## REFERENCES


1. Mr. J. R. Austin; Mr. L. S. Dewees: A new irradiated PVC wire for Telephone Central Office Cables and Distributing Frame Wire. Proceedings of the 22nd International Wire and Cable Symposium, Atlantic City, New Jersey, December 1973.
2. Mr. R. K. Swartz: Designing an Irradiation Manufacturing Process, wire journal, September 1976.





Edward A. Burek is a Senior Engineer at the Western Electric Plant in Omaha, Nebraska. He received his B.M.E. degree from Clarkson College of Technology. He has held engineering assignments covering all facets of vinyl wire and cable products, development and manufacturing. Currently, he is the engineering coordinator for all new vinyl wire and cable products and special projects.

# PROVISION OF 30 CHANNEL PCM SYSTEMS USING TWO PRECONNECTORIZED 10 PAIR DISTRIBUTION TYPE CABLES INSTALLED IN PARALLEL

H.J.C. Spencer

British Telecom (Post Office)
Headquarters

C.E. Wilbud and B.J. Symmons

Standard Telephones & Cables Ltd.,
Cable Products Div., Gwent, U.K.

## ABSTRACT

Many Administrations are now committed to modernising their networks to provide digital transmission. If the existing cables in the network are, however, of small pair count and small conductor size, the high frequency crosstalk and attenuation characteristics may not always permit the required digital penetration to be achieved. A trial by British Telecom showed that 2 Mbit/s digital links can be economically provided by the use of two parallel 10 pr/0.6 mm "LOCAP" jelly-filled unit-type unscreened distribution cables. The paper discusses the economic and technical aspects which favour the use of this particular cable system in the UK Junction Network and further it suggests that the adaptability of such a system would be enhanced in environments where preconnectorized cable lengths and similarly terminated equipment could be simply installed over trenched or mole-ploughed routes.

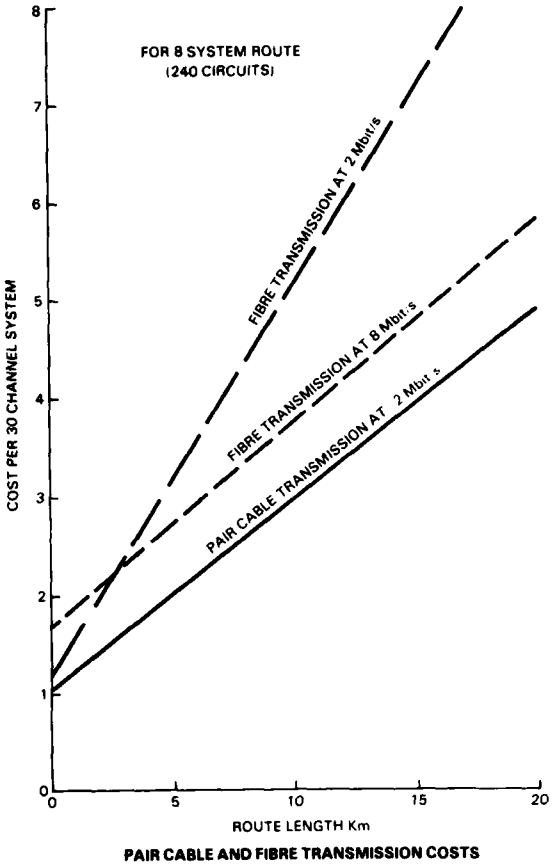
## INTRODUCTION

Most telephone administrations are now committed to policies of modernising their switching systems by the introduction of digital techniques, for reasons which are not appropriate to discussion in a paper presented to a Wire & Cable Symposium. The impact of these policies is, however, very important to cable industries because digital switching, in effectively providing the terminal multiplex equipment "free", makes the economics of using cable saving transmission systems much more attractive. Such systems are, of course, already widely used for long distance circuits. They now become viable for the short junction circuits inter-connecting local switching centres. Studies by British Telecom (BT) have shown that its programme for introducing digital switching justifies all new growth in junction network, circuit provisioning being by digital systems for distances as short as 3 km, i.e. virtually all new circuit capacity will be digital.

## SCOPE FOR SMALL PCM CABLES

BT's normal method of providing digital transmission in its junction network is to convert blocks of pairs in existing cables from audio frequency to 30 channel, 2 Mbit/s PCM working, to the limit set by cross-talk considerations. This process of further exploiting the existing plant will provide a large increase in circuit capacity without the provision of further cables. There remain, however, some locations where no cables suitable for PCM exploitation exist, and even where there are suitable cables they will eventually be exhausted. In these circumstances the provision of cables designed specifically for 100% PCM exploitation is desirable. The modern choice would seem to be optical fibre cables. BT studies suggest, however, that for routes where the increments of plant which it is operationally necessary to provide are modest, say, a few hundred circuits, optical fibre cables are not the most economic solution. The results of the studies are typified by Fig. 1 (see overleaf). This compares the cost of providing an increment of 240 circuits, eight 30 channel PCM systems, by an appropriately designed pair-type cable and by alternative 2 Mbit/s and 8 Mbit/s optical fibre systems. Clearly for this number of circuits the pair cable is much the more economic solution. It is noteworthy that the curve for the 8 Mbit/s optical fibre cables diverge from the curve for the pair cable so that there is no break-even route length. The fibre costs used in the studies was the Corning 1990 projection for a low quality fibre appropriate to 8 Mbit/s operation. The use of high order multiplexing, which would require a higher quality fibre but which would result in a lower slope for the fibre cost curves, probably yielding a break-even distance, is not appropriate because of the modest circuit requirement.

Other factors to consider in the choice between optical fibres and wire pairs for PCM bearer circuits are the small size of fibres, and the need for regeneration at relatively close spacing when wires are used. For the circuit capacities under consideration, however, the size advantage of fibres is not significant. Only 20 pairs are necessary for eight 30 channel systems, and the diameter of a single cable containing these is less than that




PAIR CABLE AND FIBRE TRANSMISSION COSTS

Fig. 1

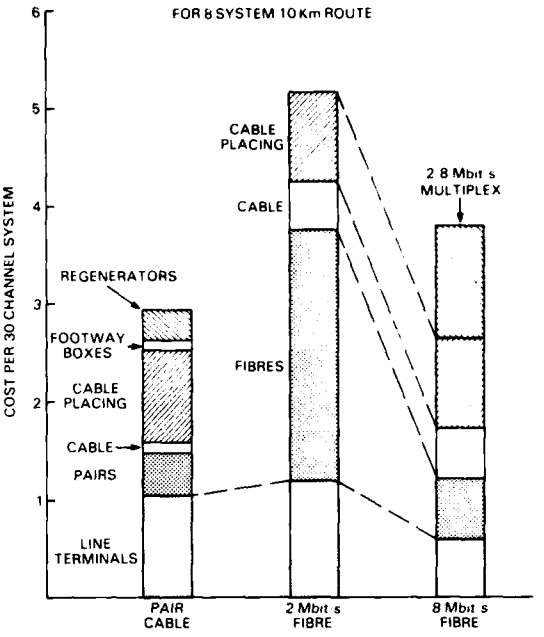



Fig. 2 TRANSMISSION COSTS BREAKDOWN

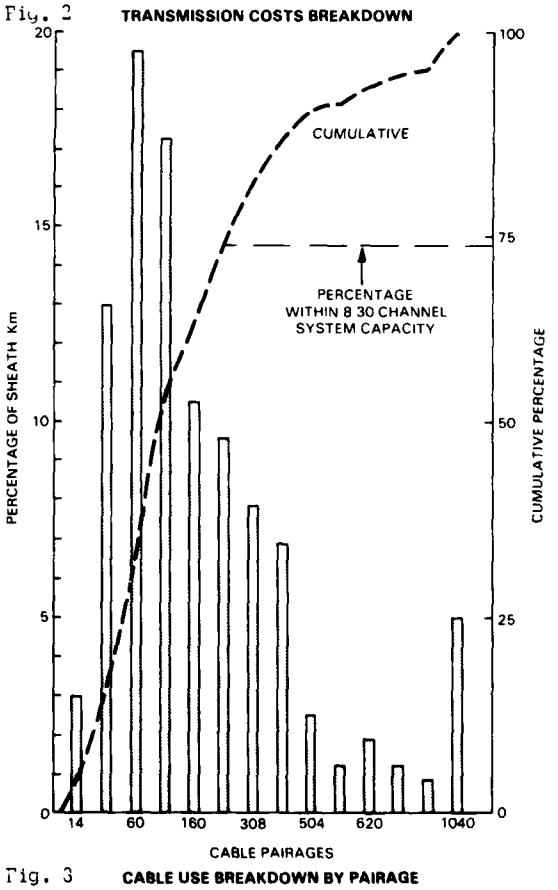



Fig. 3 CABLE USE BREAKDOWN BY PAIRAGE

of the rodding devices used to place it in ducts. No advantage can, therefore, be taken of smaller cable. The cost of regeneration has already been taken into account in Fig. 1. Its relative insignificance is emphasized by Fig. 2 which shows the component costs of the alternatives of Fig. 1 for a 10 km line length. The high cost of fibres is the dominant factor. Although capacity of only 240 circuits may seem modest, it is a very significant increment of plant when this is being provided to meet traffic growth economically. Fig. 3 indicates the break-down of cable pairage purchases by BT to satisfy growth in its Junction Network with circuits using individual pairs of wires. Over 70% of the route requirement would have been satisfied by 240 circuits. Tables 1-3 show analyses of inter-exchange links in the BT Junction Network by link length, route km and equivalent-PCM-system km. They confirm the importance of the 8-system cable increment.

TABLE 1

ANALYSIS OF JUNCTION NETWORK LINKS BY LENGTH AND CAPACITY

Percentages of Total Links:-

| Link Capacity 30 Channel Systems | Link Length km | |
|---|---|---|
| | 0 - 10 | >10 |
| 0 - 8 | 46 | 32 |
| > 8 | 18 | 4 |

TABLE 2

ANALYSIS OF JUNCTION NETWORK ROUTE LENGTH BY LINK LENGTH AND CAPACITY

Percentages of Total Route:-

| Link Capacity 30 Channel Systems | Link Length km | |
|---|---|---|
| | 0 - 10 | > 10 |
| 0 - 8 | 29 | 55 |
| > 8 | 9 | 7 |

TABLE 3

ANALYSIS OF JUNCTION NETWORK SYSTEM LENGTH BY LINK LENGTH AND CAPACITY

Percentages of Total System Length:-

| Link Capacity 30 Channel Systems | Link Length km | |
|---|---|---|
| | 0 - 10 | > 10 |
| 0 - 8 | 18 | 35 |
| > 8 | 30 | 17 |

## THE CHOICE OF CABLE CHARACTERISTICS

### Attenuation

The choice of HF attenuation of a cable for digital transmission is a trade-off between cable cost and regenerator costs. Cable material costs are roughly proportional to cross sectional area, while the attenuation is inversely proportional to the cable diameter. The trade-off is illustrated by Fig. 4. As attenuation reduces, cable material costs increase by an inverse law, but regenerator costs decrease linearly. The combined cost exhibits a minimum. Fig. 4 suggests that an attenuation of about 8 dB/km at 1 MHz is optimum. However, other factors such as trends in the relationship between the costs of electronics and cable materials, and the increase of cable size as attenuation is decreased, make it desirable to work on the high side of this, in the range 10-15 dB/km.

### Mutual Capacitance

For audio frequency cables it has been shown that for a given combination of materials the best return measured in terms of attenuation against material costs is obtained using a fixed "optimum" mutual capacitance which is independent of conductor gauge. At the high frequencies necessary for 2 Mbit/s digital transmission, however, inductance has a significant affect and resistance is affected by skin and proximity effects. Theory indicates, and measurements confirm, that for a range of conductor gauges HF attenuation is determined largely by the overall diameter of the insulated wire and is relatively insensitive to the wire diameter. In consequence, if HF transmission alone is considered, the smaller the wire diameter the better the return on material costs. It is necessary, however, to consider also the DC power requirements of PCM systems. The higher the resistance the fewer the number of regenerators which can be connected in series, and the more frequently intermediate power feed stations are required.

The power feeding requirement is particularly significant for the small capacity routes in the BT Junction Network because these are frequently greater than 20 km in length. For the attenuation range indicated as desirable previously, a copper conductor of 0.6 mm diameter would be necessary to cater for a 20 km line length. Use of this gauge in conjunction with the optimum attenuation indicates a desirable mutual capacitance in the range 35-40 nF/km.

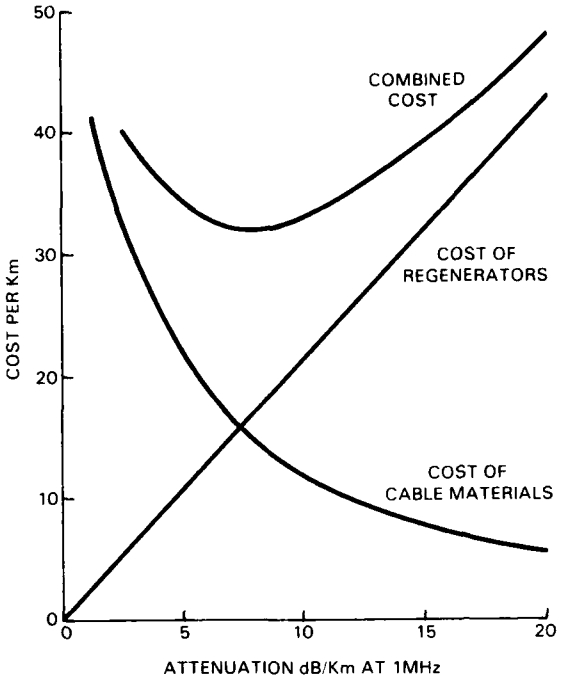



Fig. 4 **CABLE – REGENERATOR COST TRADE-OFF**

Audio Capability

It is sometimes necessary to use a cable provided for digital transmission in the audio transmission mode as an interim measure. It is, therefore, desirable that the primary characteristics chosen result in acceptable audio frequency attenuation and impedance with standard 88 mH/1830m loading.

## SUITABILITY OF AN AVAILABLE DESIGN

When the desirable characteristics of a pair-type PCM cable had been identified, it was realised that a local distribution cable recently standardised by BT had near ideal characteristics for digital transmission. The new cable has 0.6 mm copper conductors and the relatively low mutual capacitance, for a distribution cable, of 40 nF/km. These primary characteristics had been chosen for reasons outside the scope of this paper. The cable follows the normal BT practice for distribution cables in having cellular polyethylene insulation, petroleum jelly filling, and a simple polyethylene sheath without a metallic screen. The use of an already available design has the obvious attractions of eliminating the need for development work, the advantages of immediate availability and common stock holdings. It was, therefore, decided that the new local distribution cable should be adopted as a standard for a small PCM cable. Tests showed that it would permit a regenerator spacing of 2.6 km compared with 1.83 km for standard audio quad-trunk cables. Tests also showed that the cable could be used in the audio mode with standard loading and amplifying equipment.

## CROSSTALK ATTENUATION REQUIREMENTS

Satisfactory crosstalk characteristics are vital for a cable to be used for digital transmission. The most severe condition for cables with "go" and "return" circuits in one cable is near-end crosstalk (NEXT). It is impossible to achieve NEXT attenuations sufficient for acceptable regenerator spacing between closely adjacent pairs in cables. The common solution is to divide the pairs in a cable into "go" and "return" groups by layer separation or by one of the many forms of transverse screen. The transverse screen form of construction is inconvenient for very small cables and is contrary to the objective of using a common stock item as both an audio distribution cable and a digital cable. Another solution of course is to use separate cables for the two directions of transmission. For the system described in this paper the latter method has been used. It has the advantage that the first cost for two non-screened 10 pair cables is less than for a single 20 pair cable with a screen. This cost relationship, however, does not hold for cables with larger numbers of pairs. Tests have also indicated that both NEXT and FEXT attenuations are higher for the two-cable arrangement than for transversely screened cables, because there is no degradation by the proximity effects of a screen. Disadvantages are that for ducted installations two small cables take up more space than a single cable with the same number of pairs and are marginally more expensive to place. They are also likely to have a higher fault liability. On balance, however, it was considered that the lower first cost, immediate availability and common stock, favoured the twin cable solution. For greater circuit capacities, however, a transverse screen cable is preferable.

BT assesses the crosstalk performance of cables for digital transmission by using pseudo-random digital signals as interferers, and measuring noise levels at the decision point of a simulated regenerator. The results of pair-to-pair measurements of NEXT and FEXT attenuations on 2.6 km lengths of cables drawn into the same duct are shown in histogram form in Figs. 5 & 6.

The absence of metallic screens in the cable sheaths suggests the possibility of low NEXT attenuation between pairs with the same twist length when the cables are placed in the same duct and are in frequent contact. Measurements do not reveal any such tendency.

The results indicated by Figs. 5 & 6, taken in conjunction with the noise performance characteristics of the standard BT regenerator, ensures that adequate error performance is obtained when 8 pairs in each cable are carrying 2 Mbit/s 30 PCM systems over the attenuation-limited range of 2.6 km. The remaining pairs in the cables are required for alarm, control and speaker purposes.




Fig. 5

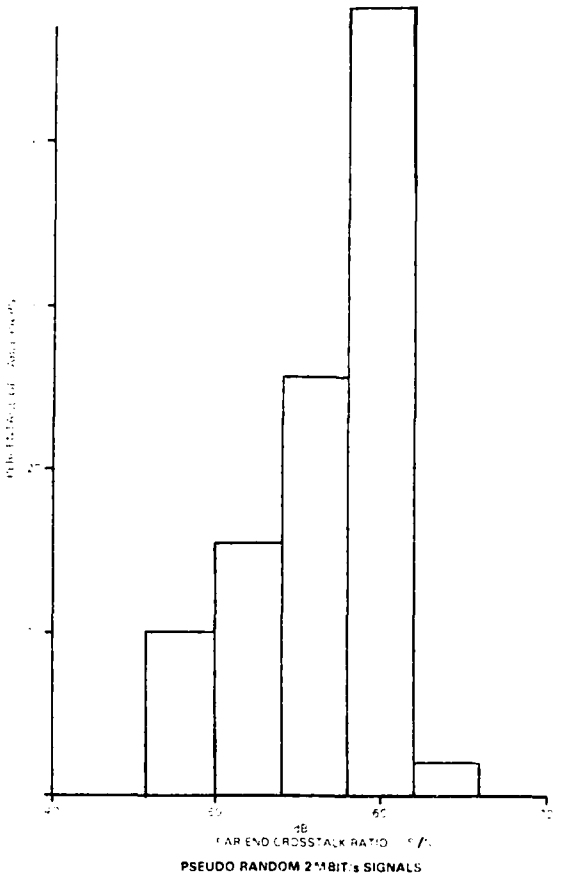



Fig. 6

## MECHANICAL CONSIDERATIONS

### Regenerator Housings

The small two-cable PCM system requires an appropriate design of regenerator housing to yield its full potential economies. The large cast-iron housings already used on high density PCM routes were not considered suitable for use in the new system. BT, therefore, developed a new generation of housing compatible with the eight system capacity of the two 10 pair cables.

The development philosophy adopted was to scale-up the already successful and proven "Sleeve 31", which, as many Administrations are aware, is a single-ended mechanical joint closure. The external appearance of the new housing is illustrated in Figure 7(see overleaf); the four separate connector-ended tail cables form an integral part of the assembly. Inside the housing a metal framework is used to give location and also mechanical stability to the regenerator equipment and is itself rigidly secured into the base of the

housing by a resin encapsulation. The resin also serves as a water block at the tail cable entry ports and secures the internal cable-form wiring connections from the tails to the equipment. An "O" ring provides an air tight seal between the removable domed cap and the lip of the base when the two mating surfaces are clamped together by the action of a three section hinged collar which is secured by a swing bolt and nut. The completed housing is tamper-proof.

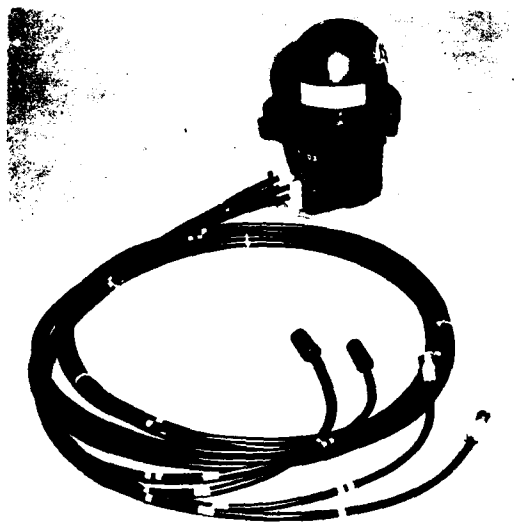


Fig. 7

Although it has been BT's practice to protect their larger cast-iron housings against moisture ingress by the use of internal static air pressure, the use of air-pressure in this instance was considered inappropriate as the cables are Petroleum Jelly filled. Instead, the new housing will contain a moisture detector located at a low point in the housing and connected to a supervisory pair in one of the cables. It is considered that this arrangement will provide protection equivalent to that of a static pressure system which, after all, only provides an alarm facility rather than afford continuous protection in the event of a seal failure. The new housing is small and light enough to be handled by one man and can be placed unobtrusively into one corner of a small underground joint box, many of which already exist on most duct routes. The fact that extensive civil works are unnecessary adds greatly to the cost effectiveness of the system. The small size of the 10 pair cables also provides some flexibility in the positioning of the housing and for ease of maintenance the regenerator housing complete with tails, if necessary, can be lifted clear of the joint box for the required work to be carried out.

Connectorisation

The advantages of connectorised jointing systems are well known. They are particularly appropriate for the small-cable PCM system described because on dedicated routes the connectors for ten pairs are small enough not to interfere with cabling operations. Added attractions are that in favourable circumstances the connectors can be factory fitted and end-to-end tests carried out before the cable is shipped. Fig. 8 shows factory tests being carried out on a drum of 10 pair connector-ended cable. Similarly, connector terminated regenerator housings, including the regenerators, can be pre-tested so that the satisfactory operation of a complete system can be assured when all the cable sections and regenerators have been plugged together.



Fig. 8

The 10 pair cables are sufficiently small for a full 2.6 km length to be supplied on one drum. It is recognised that where no duct routes exist, even more advantage can be gained by the use of a connectorized system.

It is planned to carry out field trials with direct placement of the cables by, say, mole-plough, where pre-sited footway boxes and the difficulties associated with long-length pulling into ducts are not present, but which otherwise would tend to inhibit single regenerator section length installation. A directly buried installation for example, where the cables can be placed without intermediate joints, would largely compensate for any additional fault liability which may be levelled at a

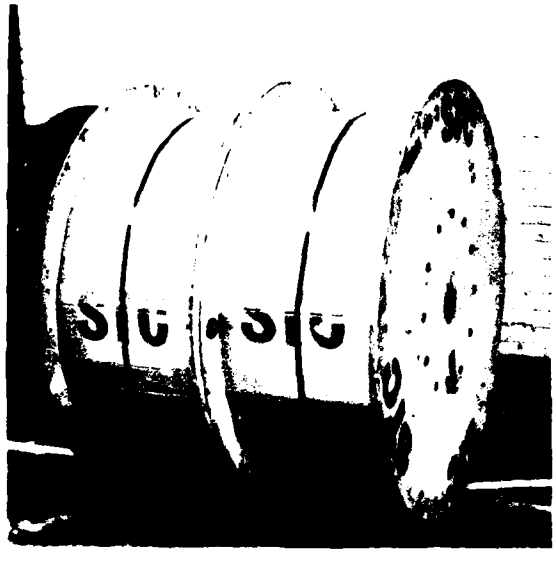
twin cable system. For provision in duct, placing of 2.6 km without intermediate joints is unlikely to be practical. The number of joints can, however, be substantially less than that required for the larger audio cables previously used in the provision of PCM circuits.

A further advantage of a plug-together system is that it makes it very easy to convert a cable initially used in the audio mode to digital transmission when digital switching is introduced. The loading coils can be assembled in housings which are interchangeable with regenerator housings. Conversion can then be effected by a simple change of housing without any wire jointing being necessary.

## WORKS PRACTICES

### Cabling

To ensure full advantage is taken of the economic possibilities of the two-cable system described, it is necessary to ensure that the cables can be placed at minimum cost. The two-cables will, therefore, be pulled-in in one operation. The cables are shipped on twin drums for mounting on a common spindle of a cable-drum trailer. Fig. 9 shows the proposed shipping arrangement.



[illegible] key control-
[illegible] be
[illegible]

see Fig. 10.



Fig. 10

It has been suggested that the connector on the inner-end of the cables could cause difficulty due to the phenomenon known as "inner-end-work-out" and that they are also vulnerable to damage in shipping and in cabling operations. To overcome this problem the cable drums are designed with a large feed-through hole in the flange for the inner-end to project through. This hole spans the barrel so that after the inner-end of the cable has been terminated on a connector, and the cable tested, the end can be sealed by a shrink-down cap and fed inside the barrel leaving no projection. The arrangement is illustrated in Fig. 11 (see overleaf).

### Jointing

Although the preferred method of joining cable lengths together is by use of pre-fitted connectors, it is not always practical. Where it is not, it is preferable to make a standard one-to-one joint using filled wire-connectors and a shrink-down sheath closure, rather than to fit connectors to the cable ends on location and then plug them together.

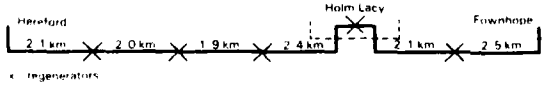
Pulling cables with connectors fitted to the leading end is, in any case, difficult and placing cables with connectors pre-fitted to both ends makes considerable demands on the accuracy of length measurements when cables are installed between joint boxes on an existing route.



Fig. 11

## TRIAL INSTALLATION

The first two-cable digital route is currently being installed in Wales and the Marches region of British Telecommunications, between Hereford and Fownhope. The route is shown in plan in Fig. 12.




LAYOUT OF HEREFORD – FOWNHOPE ROUTE

Fig. 12

It provides many challenges to the concept of quick installation with plug connections and a minimum number of joints. Experience with this pilot installation will be reported at the Symposium together with data on the overall system performance.


## ACKNOWLEDGEMENTS

The paper is published by permission of the Senior Director, Network Executive at British Telecom Headquarters and the Directors, Standard Telephones & Cables Limited.

The authors are grateful to colleagues in British Telecom and Standard Telephones & Cables Limited, for help in preparing the paper.



H.J.C. Spencer,
British Telecom NE/T8,
Lutyens House,
Finsbury Circus,
London, EC24 7LY.

Tel: 01-357-3235

Mr. Spencer is Head of Junction Planning in the Transmission Department of the British Telecom Headquarters British Post Office. He is a member of the Institution of Electrical Engineers.

C.E. Wilbud,
Manager Technical,
Cable Products Division,
Wednesbury Street,
Newport, Gwent.
NPT 0WS.

Tel: 0633-52131
Telex: 49368



Mr. Wilbud joined Standard Telephones & Cables in 1935 and has been associated with cable manufacture during the whole of this period, basically on Design and Development. Currently he is Manager Technical of the Cable Division and is a member of the Institution of Electrical Engineers.



B.J. Symmons,
Standard Telephones & Cables Ltd.,
Wednesbury Street,
Newport, Gwent.

Tel: 0633-52131
Telex: 49368

Mr. Symmons is the Senior Systems Engineer with Cable Products Division of Standard Telephones & Cables Limited, and is responsible for all aspects of cable systems design. He is a graduate of the Open University, obtaining his B.A. Degree in Pure and Applied Mathematics and is a Licentiate of the Institute of Mathematics and its Applications.

# A MEANS FOR MONITORING AND PROTECTING OUTSIDE CABLE PLANT AGAINST MOISTURE

David E. Vokey

Canada Wire and Cable Limited
Winnipeg, Manitoba

## Abstract

An electronic system has been developed for the purpose of monitoring the integrity of cable sheaths, splice closures, repeater housings, etc. in telephone cable plant. The system, which is currently being evaluated by major Canadian telcos, has a wider application scope than "Pressurization". It may be used as an alternative or as an adjunct to Pressurization and is relatively inexpensive and virtually maintenance free. Unaffected by pneumatic resistance, it may be used on filled cable or remote sections of cable plant. For greatest facility the system operates over specially designed cable which contains integrated sensors. It may, however, with somewhat less facility, be used on conventional cable plant.

## Introduction

A major and continuing concern of telephone companies is the need for constant vigilence and protection against the presence and effects of moisture in outside cable plant. For the past fifteen to twenty years, the main weapon in the battle has been "Pressurization".[1] Pressurization has proved to be invaluable; however, it is costly in its initial set-up and carries certain maintenance and nuisance burdens. For the most part, its use has been confined to large feeder and important cables and its overall efficiency has been largely dependant on the effeciency of material and physical blocking or damming.[2] Furthermore, where filled cables are interconnected with non-filled cables the use of pressurization is extremely limited if not entirely precluded. The electronic monitoring system, as described, was developed to overcome the contraints imposed by a purely physical protection system.

The system, as designed, does not prevent or retard the ingress of moisture. It does, however, react instantly to its presence and provides for pinpointing the location of entry. Except in cases of catastrophic failure, the system provides warning and facilitates remedial action before outages occur.

## Problem Definition

In approaching the problem of electrically monitoring and protecting cable plant and equipment from moisture and its effects, several design objectives were identified. Each area of concern was first addressed individually and then on an overall systems basis. It was established that the major problem areas in decreasing order of aggravation were:

1. Splice locations;
2. Repeater sites and other critical field equipment locations;
3. Cable sheaths.

Splice faults were considered to be responsible for 80-90% of outside plant outages and therefore the most critical of problem areas. Special consideration was given to this but it was decided that the solution should be applicable also to problems arising at repeaters and other interfacing locations in the field.

The matter of cable sheath breaches, and the need for detecting resultant moisture penetration was taken care of by designing and incorporating a "detection tape" in the cable construction. In effect a sensor was provided to encompass the cable core.

## System Design Objectives

In response to the defined problems, a set of design objectives were determined. In order that the solution be practical and economically viable several critera had to be met.

1. A problem must result in an immediate alarm and provision made for accurately pinpointing the fault location.
2. Splice points and other critical locations had to be uniquely identified and monitored.
3. The system had to be highly reliable and essentially maintenance free.
4. The system practices, both from a construction and from an ongoing operational standpoint, had to be compatible with existing telco practices.

5. Alarm functions had to interface directly with existing telco local and remote alarm systems.

6. The system, with a minimum number of dedicated circuits had to operate effeciently over, at least, 16 kms of cable plant.

To meet the needs, a simple and effective cable modification, and a flexible support electronic package was developed.

## Cable Design

A moisture detection tape, which would react immediately to the presence of moisture, was developed and placed under the outer jacket of the cable. (Figure 1) This detection tape has two parallel conductors laminated to an insulating polyester base. The conductors used were 22 AWG copper manufactured to the same strict tolerances as the conductors in the cable. For identification of polarity, one of the conductors was tinned and they were positioned in the substrate with a predetermined separation. The detection tape was then applied, in an open helix, over the completed cable core with the insulating substrate facing out. It was necessary to have the substrate outermost to maintain dielectric isolation from the cable shield. The complete cable core, with integrated moisture tape, was then jacketed. The finished cable thus had a moisture detection tape in an open helix located between the cable jacket, with shield, and the cable core as illustrated in Figure 2.

To facilitate location of a water breach, the tape application must follow certain design restrictions. The excess length of the moisture detecting tape in an open helix around the cable core must be of a decided value for all core and cable sizes. To achieve a fixed excess length, it is required that the angle of application of the detection tape be held constant for all core sizes. The angle of application of the detection tape in an open helix configuration is given by:

$$\text{Sec } \theta = \sqrt{1 + \left(\frac{\pi D}{L}\right)^2}$$

where L is the detection tape lay
D is the core diameter

The first production cables were manufactured with a 30° angle of application resulting in a fixed excess of 15% for all the cable sizes.

## General System Layout and Operation

The system consists basically of compact electronic modular units mounted in an equipment rack at the central office, cable plant with its detection tapes terminated on the office equipment, sensor units and disconnect units positioned in field splices and other critical locations throughout the cable plant, and appropriate termination units where required. Monitoring, scrutinizing, control and testing facilities are available from the office end. All power is provided from the office. Field sensor and disconnect units operate on selected signalling codes assigned in the lower voice frequency range. The bandwidth centred at the code frequency is $\pm$ 25 Hz. A separation guard band of 50 Hz lies between each inband code range.

The office equipment continually monitors the cable plant for the presence of moisture. Current levels are set and, barring any faults, maintained. Any deviation below the "low set" or above the "high set" current level activates an alarm indicating a system failure or a cable fault. In addition, when the alarm circuit is in the cable fault mode it will detect any splice fault signal. If a splice fault exists the splice fault indicator lights and the signal is decoded,uniquely identifying the location of the splice fault.

The alarm circuit will detect splice sensor signals to a distance of 16 kms on 26 AWG cables and 50 kms on 19 AWG cables. On one detection circuit line, up to 100 splices may be uniquely identified.

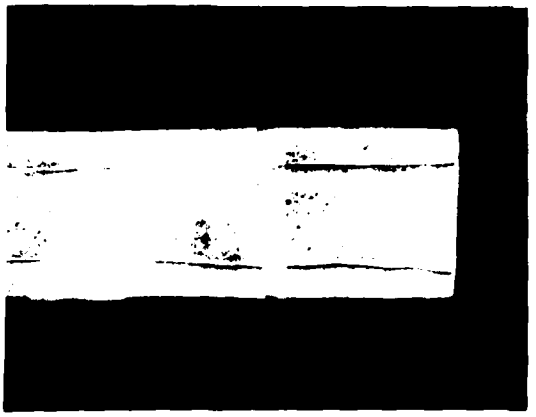


Figure 1
Detection Tape

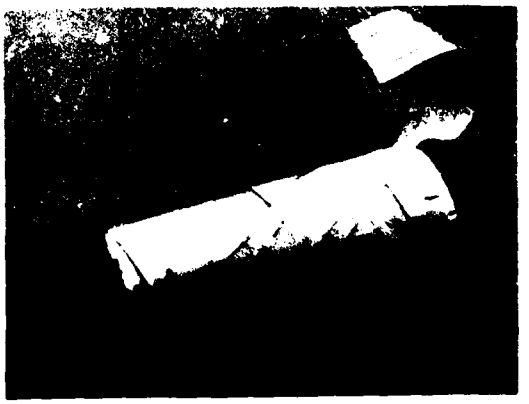


Figure 2
Cable with Detection Tape

The alarm circuit will detect deviations in the direct monitoring current of ± 50 μa and splice sensor signals over line losses up to 45 dB.

In order to sectionalize the cable plant, remote switching and disconnect units are positioned in branch and selected splices. These units are controlled fully from the Equipment Office.

## Central Office Equipment

The CO equipment is a shelf of plug-in modules, the heart of which is the alarm circuit unit (Figure 3). The incoming detection tape/pair is connected to this module and the circuitry monitors the detection line for continuity and the presence of moisture under the cable sheath and at splice points.

The alarm circuit responds to and categorizes faults as follows:

a) "Cable Fault" indicating that the detection tape/pair is shorted or partially shorting as a result of moisture vapor ingress;

b) "Line Fault" indicating that detection tape/pair, or one of the in-series connections, has become "open";

c) "Splice Fault" indicating that moisture or moisture vapour has entered and triggered the remote sensor.

The exact location of any fault is determined from the alarm circuit unit via one, or a combination, of the following:

a) Making standard bridge measurements on the detection tape/pair;

b) Operating the remote disconnect switches to isolate sections of the cable plant;

c) Operating a switch to read the decoded alarm signal from a remote sensor.

The detection circuitry which scans for remote sensor signals, has an automatic build-out capability of 45 dB thus compensating for distance and frequency-dependence of signalling levels.

## Field Equipment

The field equipment consists of remote sensor units, remote switching devices and termination units.

The remote sensor units (Figure 4) are, in effect, the nerve ends of the system. These are placed inside splice closures, repeated housings, etc., and are half-tapped onto the moisture detection tape of the cable or, in the event where the cable does not have such a tape, to a dedicated pair. A length of detection tape is tied to the input of the sensor and strategically wrapped or placed around the inside periphery of the closure or housing. (A paper-insulated pair may be substituted for the detection tape

The slightest trace of moisture on the detection tape or pair will activate the sensor electronics and a FDM coded alarm signal is transmitted back to the equipment office. At the office the alarm signal is decoded and the location of the moisture indicated.

The lower VF range of 100 to 1050 Hz is employed for signalling and up to 100 locations may be uniquely identified on a single detection line.

The sensor appears as an "open circuit" on the line unless activated, and once activated draws 7 ma line current and modulates the line with a signal level as shown in Figure 5.

FDM techniques were chosen to allow simplicity of design for the field electronics with a resultant high degree of reliability.

The remote switching devices (Figure 6) provide the means for sectionalizing the detection line at branch splices and selected junctions, thus aiding in fault locating.

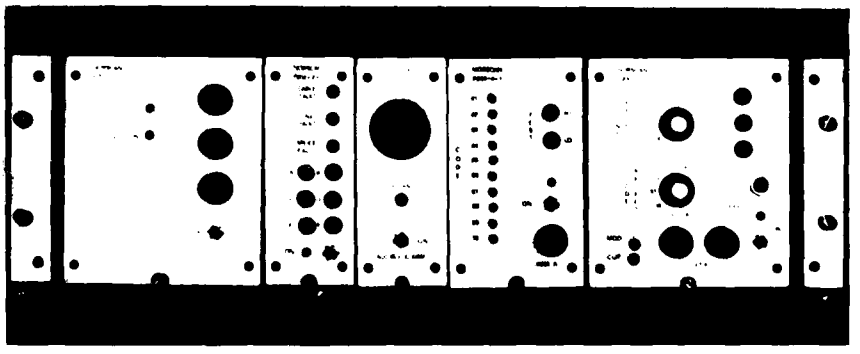


Figure 3
Central Office Equipment

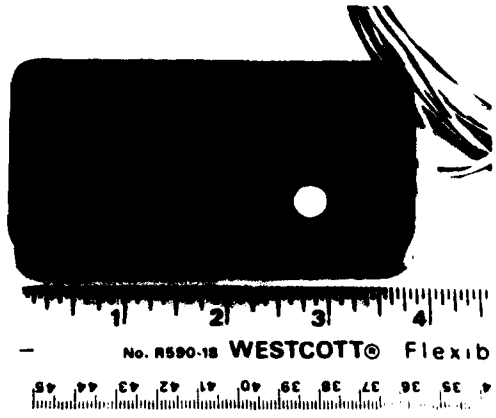



Figure 4
Remote Sensor

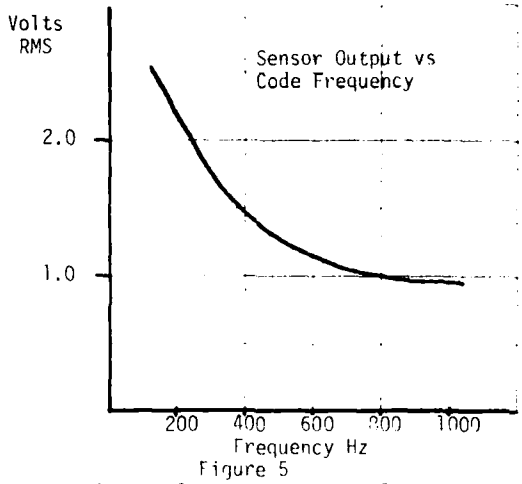



Figure 5
Remote Sensor Output Level




Figure 6
Remote Switching Device

These remote switches are powered, controlled, and signalled on a dedicated pair from the central office. They operate in the lower voice frequency range and utilize FDM techniques for signalling. The switches are series-powered and parallel-signalled and only one dedicated pair is required for the operation of several. For proper operation, they require 16 ma current at 5 volts and a signal input of 100 mu RMS.

## Laboratory Tests and Field Trial.

Laboratory tests were conducted wherein cable samples with fabricated sheath faults were placed under one metre head of water. The system alarmed and the samples were removed. In all cases longitudinal peneration of moisture did not exceed 20 cm , and the moisture had not penetrated through the core wrap to the cable core.

Office and field alarm circuits and units were laboratory cycled through fault simulation and location tests under temperature extremes ranging from $0^{o}$ to $60^{o}$C. Dc and ac signalling levels did not drift out of specification and the total system remained in proper operation.

A major feeder-cable installation in Western Canada was earmarked to evaluate the integrated system in field trials. The cables being used range from 600 pair 24 AWG to 3600 pair 26 AWG and have medium density cellular insulation. All the cables have integrated moisture detection tape under polyethylene/aluminum laminated sheaths. The installation will have two branch cable runs and 24 monitored splices. The system should be completed for acceptance into operational service in the late fall of 1980,at which time complete field testing will be carried out.

## Conclusions

In recent times, developments in the electronic industry are such that relatively complex but reliable monitoring systems can be devised and readily incorporated at relatively little cost.

This monitoring system, electrical/electronic in nature lends itself to extensive application in cable plant protection. The philosophy is to use the extensive "electronic highways" which Telcos have constructed to monitor their own physical condition, rather than to force additional, and not always compatible, physical encumberances on the cable systems.

The monitoring/protection system as described was developed to meet specific needs; it has however, as observed by Telco personnel, sufficient flexibility to lend itself to other applications. It was developed specifically to monitor cable sheaths and splices. Additional uses would be:

a) Monitoring pressure at statically - pressurized repeater housings or sites;

b) Providing alarm facilities for unauthorized entry at remote sites or equipment;

c) Monitoring the general condition of pedestals, cabinets and housings etc.;

d) Providing for multiplexing pressure transducers or other monitoring devices onto a common circuit;

e) Providing alarms on high water levels in manholes or chambers.

The sensor units may be tailored or modified to accept a great variety of transducer inputs.

FDM techniques were selected for signalling purposes to allow for simple and effective operation of all field-located equipment. To ensure a maximum system range on the detection tape or alarm pair, the lower voice frequency range was selected. More complex signalling schemes, such as digital modems are feasible and may be employed in the future.

## Acknowledgements

The author wishes to express his appreciation to the staff of the British Columbia Telephone Company and to Norscan Instruments Limited of Winnipeg for extensive input during the development of the system described herein, and to thank Mr. D. Egan for editing assistance.

## References

[1]WALTERS, J.R., KEEP, J.F., and CRAGGS, J.F. Pressurization of Telecommunication Cables, Part 1. *P.O.E.E.J.*, Vol. 55, pa. 260, Jan. 1963.

[2]MASTERSON, J.B., "Pressure Dams in Communication Cables", *Proceedings of the 18th International Wire and Cable Symposium*, 1969.



David Vokey is the Manager of the Development and Design Department, Communication Products Division, Canada Wire and Cable Limited, Winnipeg, Manitoba.

He joined Canada Wire in 1969 as an Engineering Technologist, later leaving to attend the University of Manitoba where he obtained his B.Sc.EE in 1973. Currently he is actively pursuing a Master's degree in Electrical Engineering. He is a member of APEM.

# Author Index


Abadia, V. ... 128
Allen, D. B ... 94
Amano, Y. ... 240
Asano, Y. ... 26
Avalos, J. Z. ... 128
Baden, J. L. ... 212
Bark, P. R. ... 394
Bevers, R. C. ... 1
Bopp, L. A. ... 331
Bresser, O. R. ... 290
Bro, M. I. ... 94
Burek, E. A. ... 439
Bury, J. R. ... 268
Castelli, R. ... 202
Chapman, J. E. G. ... 279
Charlebois, L. J. ... 159
Chattler, L. M. ... 350
Cheng, D. ... 279
Cronin, D. R. ... 279
Davis, L. E. ... 59
de Munck, H. ... 268
Devoldere, J. A. ... 268
DeWitt, A. ... 327
Durr, H. E. ... 1
Eastwood, H. K. ... 386
Ebrey, R. G. ... 178
Eriksrud, M. ... 380
Fech, J. ... 327
Flegal, W. M. ... 1
Furuya, S. ... 26
Gholson, N. H. ... 375
Glavas, X. G. ... 194
Goto, S. ... 151
Gupta, C. D. ... 188
Gupta, C. D. ... 424
Harbort, H. ... 263
Hardwick, N. E. ... 212
Herrera, M. ... 386
Hodge, M. ... 229
Hög, G. ... 253
Horima, H. ... 101
Huszarik, F. A. ... 159
Igarashi, M. ... 312
In't Veld, S. H. K. ... 290
Ishihara, K. ... 101
Iwamura, H. ... 312
Iwazaki, M. ... 432
Johnson, E. L. ... 48
Kalomiris, V. E. ... 194
Katagiri, K. ... 432
Kato, S. ... 26
Kaufman, S. ... 245
Kish, P. ... 117
Koch, R. O. ... 1
Koga, H. ... 363
Krahn, F. ... 418
Large, S. F. ... 221
Lauritzen, S ... 380
Lawrence, D. O. ... 394
Lawton, K. L. ... 402
LeBorgne, Y. ... 117
Lee, J. L. ... 236
Leenen, A. J. H. ... 290
Lesniewski, J. M. ... 90
Loadholt, J. T. ... 245
Maddock, B. J. ... 402
Makiyo, M. ... 151
Martin, I. E. ... 188
Masaki, S. ... 432
Mase, S. ... 151
Masterson, J. B. ... 299
Matsubara, I. ... 312
Matthews, G. B. ... 168
Mayer, H. A. ... 253
McCane, D. I. ... 94
McIntosh, D. N. ... 202
McIntyre, R. N. ... 38
Mitchell, D. M. ... 15
Moisson, M. ... 136
Mori, N. ... 312
Morikawa, G. ... 240
Motomitsu, T. ... 363
Norman, S. R. ... 202
Oestreich, U. ... 394
Ohnuma, T. ... 9
Osterfield, J. R. ... 202
Patel, N. I. ... 59
Pickup, K. H. ... 402
Pion, R. F. ... 236
Rahman, M. M. ... 386
Reed, J. C. ... 94
Refi, J. J. ... 111
Reynolds, M. R. ... 38
Rivett, P. ... 386
Rodgers, A. J. ... 202
Ryen, N. ... 380
Ryley, J. ... 229
Sabia, R. ... 15
Saito, Y. ... 26
Saito, Y. ... 312
Sammoun, S. ... 341
Satar, A. N. ... 188
Sato, N. ... 151
Scadding, P. ... 322
Schmidt, G. A. ... 331
Schneider, R. G. ... 48
Schwarz, H. F. ... 76
Sckerl, H. A. ... 178
Seaman, G. G. ... 178
Sekiguchi, A. ... 432
Sheppard, A. T. ... 145
Shmidt, W. ... 306
Simpson, W. E. ... 268
Spencer, H. J. ... 443
Sugawara, H. ... 26
Suzuki, H. ... 9
Symmons, B. J. ... 443
Taguchi, M. ... 363
Tamburello, M. ... 202
Tanaka, S. ... 101
Tewarson, A. ... 236
Thompson, R. E. ... 194
Trumble, W. P. ... 424
Tsujikawa, A. ... 9

Vokey, D. E. ..... 452
Warren, P. C. ..... 66
Wichansky, H. ..... 194
Wilbud, C. E. ..... 443
Woods, J. G. ..... 229
Worthington, P. ..... 410
Yanizeski, G. M. ..... 38
Yanizeski, G. M. ..... 48
Yasuhara, H. ..... 9
Yokoyama, J. ..... 312
Yokoyama, K. ..... 151
Yonechi, S. ..... 101
Yoshioka, K. ..... 240
Young, R. ..... 164
Zeidler, G. ..... 394
Zwick, U. ..... 306




# International Wire & Cable Symposium

**SPONSORED BY U.S. ARMY COMMUNICATIONS RESEARCH AND DEVELOPMENT COMMAND (CORADCOM)**
**17, 18 & 19 November 1981**

**Cherry Hill Hyatt House, Cherry Hill, N.J.**

Please provide in the space below a 100-500 word abstract (12 copies) of a proposed technical paper on such subjects as design, application, materials, and manufacturing of Communications and Electronics Wire & Cable of interest to the commercial and military electronics industries. Such offers should be submitted no later than 17 April 1981 to the Commanding General, U.S. Army Communications Research & Development Command, ATTN: DRDCO-COM-RM-1 (E. Godwin), Fort Monmouth, NJ 07703.

Title: _____

Authors: _____

Company: _____

Address: _____


DAT
ILM